Character deformation of the Selberg zeta function for congruence subgroups via the transfer operator

Dissertation

zur Erlangung des Grades eines Doktors
der Naturwissenschaften

vorgelegt von

Markus Szymon Fraczek

aus Mikołów / Rzeczpospolita Polska

genehmigt von der Fakultät für Natur- und Materialwissenschaften
der Technischen Universität Clausthal,
Tag der mündlichen Prüfung
23. April 2012

Vorsitzender der Promotionskommission
Prof. Dr. Peter Blöchl
Technische Universität Clausthal

Hauptberichterstatter
Prof. Dr. Dieter Mayer
Technische Universität Clausthal

Berichterstatter
Dr. Yiannis Petridis
University College London

Abstract

We introduce a method for evaluating the Selberg zeta function $Z^{(n)}(\beta,\chi^{(n)})$ for Hecke congruence subgroups $\Gamma_0(n)$ with unitary characters $\chi^{(n)} : \Gamma_0(n) \to \mathbb{C}$ and complex parameter $\beta \in \mathbb{C}$. The zeros of this function are related to the discrete eigenvalues and the resonances of the hyperbolic Laplace-Beltrami operator on the corresponding surfaces of constant negative curvature. The Selberg zeta function can be expressed in terms of Fredholm determinants of certain operators from statistical mechanics, the so-called transfer operators. We derive different forms of the transfer operator for $\Gamma_0(n)$ with $\chi^{(n)}$, one of which leads to the discovery of certain symmetries of the transfer operator. Through numerical computations we found that these symmetries are related to involutions of the eigenfunctions, the so-called Maass wave forms, of the hyperbolic Laplacian. Another form of the transfer operator we derived can be approximated by a finite matrix, which we use in numerical computations. We conjecture that this form of the transfer operator gives its analytic continuation to the entire complex β-plane.

We study certain deformations by unitary characters $\chi_\alpha^{(n)} : \Gamma_0(n) \to \mathbb{C}$ with deformation parameters $\alpha \in \mathbb{R}$, where in general these characters are non-arithmetic. The main motivation for the investigation of such character deformations of the Selberg zeta function is that by studying the deformation of its zeros we gain access to the deformation of the discrete spectrum and the resonances of the hyperbolic Laplace-Beltrami operator, both under singular and non-singular perturbations. To evaluate the Selberg zeta function we determine the spectrum of the transfer operator for $\Gamma_0(n)$ with $\chi^{(n)}$. Since there is no great hope for an analytic approach to the spectrum of the transfer operator we study its spectrum mainly by numerical methods. To carry out the numerical experiments we had to develop a comprehensive program package called Morpheus, consisting of the programs widmo and CGF. These programs can determine the necessary ingredients for computing the matrix representation of the transfer operator, its spectrum and the Selberg zeta function for any $\Gamma_0(n)$ with a character $\chi^{(n)}$. We study the curves of zeros of the Selberg zeta function for $\Gamma_0(4)$ with $\chi_\alpha^{(4)}$ and for $\Gamma_0(8)$ with $\chi_\alpha^{(8)}$, for $0 \le \alpha \le 0.5$. Our results show that for $\Re\beta \le \frac{1}{2}$ the Selberg zeta function $Z^{(4)}(\beta,\chi_\alpha^{(4)})$ behaves non-continuously in the limit $\alpha \to 0$. For $\alpha \to 0$ we found two different kinds of convergence of the zeros of $Z^{(4)}(\beta,\chi_\alpha^{(4)})$ to the zeros for $\alpha = 0$ on the line $\Re\beta = \frac{1}{2}$: zeros which belong to odd Maass wave forms under a certain involution stay on the line $\Re\beta = \frac{1}{2}$ and converge towards the zeros for $\alpha = 0$ by an infinite sequence of avoided crossings, whereas other zeros stay in general left of the line $\Re\beta = \frac{1}{2}$ and converge to zeros for $\alpha = 0$ in an infinite sequence of touching this line $\Re\beta = \frac{1}{2}$. There are also zeros on and left of the line $\Re\beta = \frac{1}{2}$ which move in pairs towards $\beta = \frac{1}{2}$ and become dense on the line $\Re\beta = \frac{1}{2}$ for $\alpha \to 0$. These zeros seem to be related to the change of the multiplicity of the continuous spectrum of the Laplacian by the singular perturbation at $\alpha = 0$. It also turns out that there is a whole family of zeros in the β-plane with $\Re\beta \to -\infty$ for $\alpha \uparrow \frac{2}{8}$ and $\alpha \downarrow \frac{2}{8}$, and which disappear for $\alpha = \frac{2}{8}$.

Finally, we apply our approximation method to the transfer operator for the Kac-Baker spin model and present results obtained from numerical experiments.

Acknowledgements

I would like to express my gratitude to my advisor Prof. Dr. Dieter Mayer for admitting me into his research group and giving me this very interesting topic to work on, as part of the project "Maass-sche Spitzenformen, die Vermutung von Phillips und Sarnak und die Transfer-Operatoren kofiniter Fuchs-scher Gruppen" supported by the Deutsche Forschungsgemeinschaft (DFG). Furthermore, I would like to thank him for the research visits to various places and for the liberty to pursue my own ideas.

I would like to thank Dr. Roelof Bruggeman and Dr. Fredrik Strömberg for their many discussions and comments on my work. I am grateful to Fredrik for sharing his expertise on Maass wave forms and numerical analysis. I would like to acknowledge the analytical work of Roelof Bruggeman, which has been very useful for the verification of certain numerical results in this thesis.

I would like to thank Prof. Dr. Peter Blöchl for his permission to use the computer clusters of his research group. To obtain the results in the numerical part of this thesis many high-performance computations were involved. It would not have been possible to carry out these numerical experiments without access to fast computational resources. In addition, I would like to thank the system administrators of his research group for providing mission-critical support. Furthermore, numerical computations were also performed on the computer clusters of the North-German Supercomputing Alliance: Norddeutscher Verbund zur Förderung des Hoch- und Höchstleistungsrechnens (HLRN), for which I am very grateful.

Also, I would like to thank Prof. Dr. Marek Kuś for his kind hospitality in Warsaw, Prof. Dr. Maciej Zworski for his kind hospitality in Berkeley, Prof. Dr. Andreas Buchleitner for his kind hospitality in Dresden and Freiburg and Dr. Tobias Mühlenbruch for many discussions. Finally, I would like to thank Dr. Yiannis Petridis for refereeing this thesis.

Dziękuję także wszystkim z mojej rodzinny za wsparcie.

Contents

List of Figures

List of Tables

Listings

Chapter 1

Introduction

This dissertation introduces a method for evaluating the Selberg zeta function $Z^{(n)}(\beta,\chi^{(n)})$ for Hecke congruence subgroups $\Gamma_0(n)$ with unitary characters $\chi^{(n)} : \Gamma_0(n) \to \mathbb{C}$ and complex parameter $\beta \in \mathbb{C}$. The zeros of this function for $\Re\beta = \frac{1}{2}$ and $\frac{1}{2} < \beta \leq 1$ are related to the discrete eigenvalues λ of the hyperbolic Laplace-Beltrami operator by $\lambda = \beta(1-\beta)$, and for $\Re\beta < \frac{1}{2}$ to its resonances. These resonances are the poles of the scattering determinant $\varphi(\beta,\chi^{(n)})$. Therefore, our method for evaluation of the Selberg zeta function provides us access to the discrete spectrum and resonances of the hyperbolic Laplacian.

The Selberg zeta function can be expressed in terms of Fredholm determinants of certain operators from statistical mechanics, the so-called transfer operators. To evaluate this function we determine the spectrum of the transfer operator for $\Gamma_0(n)$ with $\chi^{(n)}$. Since there is no great hope of an analytical approach to the spectrum of the transfer operator, we will study its spectrum mainly using numerical methods. Our strategy is as follows:

1. Define a transfer operator for $\Gamma_0(n)$ with unitary character $\chi^{(n)}$.

2. Derive a form of the transfer operator which can be approximated by a finite matrix.

3. Implement an approximation of the transfer operator in a computer program.

4. Evaluate the Selberg zeta function via the spectrum of an approximation of the transfer operator.

We use the transfer operator in this thesis to evaluate the Selberg zeta function, since the transfer operator method is one of the few methods enabling the evaluation of this function. In the introduction of [Str08] a short overview is given about numerical studies of the Selberg zeta function $Z(\beta)$ for different groups inside the critical strip $|\Re(\beta)| \leq 1/2$ so far. The main difficulty in evaluating the Selberg zeta function is that its analytic continuation to this region is required. It is surprising how few successful numerical evaluations of the Selberg zeta function exist: for the modular surface the authors in [MS91] considered a modified Selberg zeta function to overcome this difficulty. For convex co-compact Schotty groups Guillopé, Lin and Zworski used in [GLZ04] the transfer operator to obtain an explicit formula for the Fredholm determinant, which can be evaluated numerically more or less directly. In [Str08] Strömberg used the transfer operator method for the computation of the Selberg zeta function for Hecke triangle groups by approximating the operator by a finite matrix.

As an application of our implementation of the Selberg zeta function we will study certain deformations by unitary characters $\chi_\alpha^{(n)} : \Gamma_0(n) \to \mathbb{C}$ with deformation parameters $\alpha \in \mathbb{R}$, where in general these characters are non-arithmetic. The main motivation for the investigation of such character deformations of the Selberg zeta function is that by studying the deformation of its zeros we have access to the deformation of the discrete spectrum and the resonances of the hyperbolic Laplace-Beltrami operator. Such character

deformations allow us to study singular and non-singular perturbations of the hyperbolic Laplacian. Singular perturbations are perturbations for which the multiplicity of the continuous spectrum of the hyperbolic Laplacian changes. This kind of perturbation of the Laplacian is not yet very well understood and the mathematics behind it is not yet completely developed. Besides the fact that the discrete spectrum is embedded in the continuous one, which is also a problem for non-singular perturbations, several new phenomena arise for singular perturbations, which make the application of perturbation theory in this case rather doubtful. In this thesis we study both singular and non-singular perturbations by tracking the zeros of the Selberg zeta function $Z^{(n)}(\beta, \chi_\alpha^{(n)})$ in the β-plane for certain groups $\Gamma_0(n)$ with characters $\chi_\alpha^{(n)}$ for $0 \leq \alpha \leq 0.5$. To our knowledge it is the first time that such an investigation was carried out.

This thesis contains analytical results, which are necessary to derive and implement an approximation of the transfer operator for character deformations, and numerical results, obtained from an implementation of this approximation:

- In Chapter 2 we provide basic definitions and concepts. The purpose of this chapter is to state the formulas we will later use in our implementation.
- In Chapter 3 we provide a short introduction to the gamma function $\Gamma(s)$ and the incomplete gamma functions $\Gamma(s,z)$ and $\gamma(s,z)$. We present also approximation formulas for these functions, which are used in our implementation of the approximation of the transfer operator.
- In Chapter 4 we derive special representations of the Hurwitz zeta function

  $$\zeta(s,z) = \sum_{n=0}^{\infty} (z+n)^{-s}$$

  and the Lerch transcendent

  $$\Phi(\alpha, s, z) = \sum_{n=0}^{\infty} \alpha^n (z+n)^{-s},$$

  which are appropriate for their numerical evaluation. Especially the Lerch zeta function $\zeta_L(\lambda, s, z) = \Phi(\exp 2\pi i\lambda, s, z)$ is essential for our approximation of the transfer operator. To our knowledge this approximation of the Lerch zeta function is more general and precise than the one found in the literature.
- In Chapter 5 we present an algorithm to compute the complex eigenvalues of a complex matrix of typical size between 300×300 and 600×600. We discuss also the problems which arise when computing the eigenvalues of an approximation of the transfer operator. To produce an optimal algorithm with respect to accuracy and computation time we combine several different techniques, such as complex Givens rotations, Hessenberg transformations and spectral shifts.
- In Chapter 6 we discuss some properties of the groups $\mathrm{PSL}(2,\mathbb{R})$ and $\mathrm{SL}(2,\mathbb{Z})$, and its congruence subgroups $\Gamma(n)$ and $\Gamma_0(n)$. We also discuss the spectrum and the eigenfunctions of the hyperbolic Laplace-Beltrami operator for congruence subgroups Γ with a character χ. Furthermore, we give a short introduction to the Selberg zeta function and its zeros for Γ and χ. And we briefly discuss the conjecture of Phillips and Sarnak concerning Weyl's law for the hyperbolic Laplacian for certain groups. To perform character deformations of the Selberg zeta function we use a character $\chi^\Gamma_{\alpha_1,\ldots,\alpha_k}$ with deformation parameters $\alpha_j \in \mathbb{R}$ given by

  $$\chi^\Gamma_{\alpha_1,\ldots,\alpha_k}(\gamma) = \exp 2\pi i \sum_{j=1}^{k} \alpha_j \Omega_j^\Gamma(\gamma)$$

  for any freely generated group $\Gamma \subset \mathrm{SL}(2,\mathbb{Z})$ with generators $\{G_j^\Gamma\}_{1\leq j\leq k}$, where $\Omega_j^\Gamma : \Gamma \to \mathbb{Z}$ is the sum of the exponents of the generator G_j^Γ in a representation of γ. From this character we define characters

$\chi^{(4)}_{\alpha_1,\alpha_2} : \Gamma_0(4) \to \mathbb{C}$ and $\chi^{(8)}_{\alpha_1,\alpha_2,\alpha_3} : \Gamma_0(8) \to \mathbb{C}$, and discuss their properties. We derive also certain relations of the Selberg zeta functions $Z^{(4)}(\beta, \chi^{(4)}_{\alpha_1,\alpha_2})$ for $(\Gamma_0(4), \chi^{(4)}_{\alpha_1,\alpha_2})$ given by

$$\begin{aligned} Z^{(4)}\left(\beta, \chi^{(4)}_{\alpha_1,\alpha_2}\right) &= Z^{(4)}\left(\beta, \chi^{(4)}_{\alpha_1,-\alpha_2-\alpha_1}\right) \\ Z^{(4)}\left(\beta, \chi^{(4)}_{\alpha_1,\alpha_2}\right) &= Z^{(4)}\left(\beta, \chi^{(4)}_{\alpha_2,\alpha_1}\right) \\ Z^{(4)}\left(\beta, \chi^{(4)}_{\alpha_1,\alpha_2}\right) &= Z^{(4)}\left(\beta, \chi^{(4)}_{-\alpha_1,-\alpha_2}\right). \end{aligned}$$

We show that the characters $\chi^{(4)}_{\alpha_1,\alpha_2}$ and $\chi^{(8)}_{\alpha_1,\alpha_2,\alpha_3}$ are related by

$$\begin{aligned} \chi^{(4)}_{\alpha_1,\alpha_2}(\gamma) &= \chi^{(8)}_{2\alpha_2,\alpha_1,\alpha_1}(\gamma) \\ \chi^{(4)}_{\alpha_1,\alpha_2+\frac{1}{2}}(\gamma) &= \chi^{(8)}_{2\alpha_2,\alpha_1,\alpha_1}(\gamma) \end{aligned}$$

for $\gamma \in \Gamma_0(8)$. Furthermore, it follows from the functional equation of the Selberg zeta function $Z(\beta, \chi)$ for Γ with χ, that the scattering determinant $\varphi(\beta, \chi)$ can be expressed by

$$\varphi(\beta, \chi) = \eta(\beta) \frac{Z(1-\beta, \chi)}{Z(\beta, \chi)},$$

where $\eta(\beta)$ is a function which depends on the group Γ and the character χ. We derive the explicit form of $\eta(\beta)$ for $(\Gamma_0(n), \chi)$ with $4 \mid n$, and by using this result we find finally the explicit form of $\eta(\beta)$ for $\Gamma_0(4)$ and $\chi^{(4)}_{\alpha_1,0}$.

- In Chapter 7 we discuss the transfer operator method and some properties of nuclear operators. Furthermore, we present Mayer's transfer operator $\mathcal{L}_\beta$ for $\mathrm{SL}(2,\mathbb{Z})$ and its generalization by Chang to subgroups Γ of $\mathrm{SL}(2,\mathbb{Z})$ of finite index μ given by

$$\tilde{\mathcal{L}}_\beta = \begin{pmatrix} 0 & \mathcal{L}_{\beta,+1} \\ \mathcal{L}_{\beta,-1} & 0 \end{pmatrix}$$

with

$$\mathcal{L}_{\beta,\varepsilon} \vec{f}(z) = \sum_{l=1}^{\infty} (z+l)^{-2\beta} U^\Gamma\left(S T^{\varepsilon l}\right) \vec{f}\left(\frac{1}{z+l}\right), \quad \text{for } \Re\beta > \frac{1}{2},$$

with S, T the generators of $\mathrm{SL}(2,\mathbb{Z})$ and the representation U^Γ given by

$$\left[U^\Gamma(g)\right]_{i,j} = \begin{cases} 1 & \text{if } r_i^\Gamma g \left(r_j^\Gamma\right)^{-1} \in \Gamma \\ 0 & \text{else,} \end{cases}$$

where $\{r_i^\Gamma\}_{1 \le i \le \mu}$ are the right coset representatives of $\Gamma \backslash \mathrm{SL}(2,\mathbb{Z})$. The Selberg zeta function $Z(\beta)$ for Γ can then be expressed in terms of the Fredholm determinant of this operator

$$Z(\beta) = \det(1 - \tilde{\mathcal{L}}_\beta) = \det(1 - \mathcal{L}_{\beta,+1}\mathcal{L}_{\beta,-1}) = \det(1 - \mathcal{L}_{\beta,-1}\mathcal{L}_{\beta,+1}).$$

To extend this result for Selberg's zeta function $Z^{(n)}(\beta, \chi)$ for $\Gamma_0(n)$ with a character χ we define the representation $U^\chi : \mathrm{SL}(2,\mathbb{Z}) \to \mathbb{C}^{\mu_n \times \mu_n}$ by

$$\left[U^\chi(g)\right]_{i,j} = \begin{cases} \chi\left(r_i^{(n)} g \left(r_j^{(n)}\right)^{-1}\right) & \text{if } r_i^{(n)} g \left(r_j^{(n)}\right)^{-1} \in \Gamma_0(n) \\ 0 & \text{else,} \end{cases}$$

with $\{r_i^{(n)}\}_{1\le i\le\mu_n}$ the right coset representatives of $\Gamma_0(n)\backslash\mathrm{SL}(2,\mathbb{Z})$ and μ_n the index of $\Gamma_0(n)$ in $\mathrm{SL}(2,\mathbb{Z})$. We incorporate this representation into the transfer operator and derive a form of this operator where the character χ has to be evaluated only for a finite number of elements

$$\left[\mathcal{L}^{(n)}_{\beta,\varepsilon,\chi}\vec{f}(z)\right]_i = \sum_{q=0}^{\infty}\sum_{m=1}^{n}\sum_{j=1}^{\mu_n}\left[U^{\chi}\left(S\,T^{m\varepsilon}\right)\right]_{i,j}\chi\left(r_j^{(n)}T^{n\varepsilon}\left(r_j^{(n)}\right)^{-1}\right)^q(z+m+nq)^{-2\beta}f_j\left(\frac{1}{z+m+nq}\right),$$

with $1\le i\le\mu_n$ and n the level of $\Gamma_0(n)$. This form enables us to write down explicitly the transfer operator, since the representation $U^{\chi}(S\,T^{m\varepsilon})$ has to be determined only for finitely many elements for $1\le m\le n$. This leads to the discovery of intertwining operators $\mathcal{P}_k$ such that $\mathcal{P}_k\mathcal{L}^{(n)}_{\beta,+1,\chi}=\mathcal{L}^{(n)}_{\beta,-1,\chi}\mathcal{P}_k$ in Chapter 8. Furthermore, we obtain also a Mayer-type analytic continuation of the transfer operator $\mathcal{L}^{(n)}_{\beta,\varepsilon,\chi}$ given by

$$\mathcal{L}^{(n)}_{\beta,\varepsilon,\chi}\vec{f}(z)=\mathcal{N}^{(n)}_{\beta,\varepsilon,\chi,N}\vec{f}(z)+\mathcal{A}^{(n)}_{\beta,\varepsilon,\chi,N}\vec{f}(z),\quad\text{for }\Re\beta>-\frac{N}{2}\text{ with }N\in\mathbb{Z}_{>}.$$

Unfortunately, this form is not suitable to be approximated by a finite matrix, which could be used for numerical computations. However, we derive an explicit trace formula for this analytically continued transfer operator given by

$$\operatorname{tr}\mathcal{L}^{(n)}_{\beta,\varepsilon,\chi}=\operatorname{tr}\mathcal{N}^{(n)}_{\beta,\varepsilon,\chi,N}+\operatorname{tr}\mathcal{A}^{(n)}_{\beta,\varepsilon,\chi,N},$$

which is highly appropriate for numerical evaluations. We use this trace formula in our numerical experiments to compare it with the traces of other forms of transfer operators and this way get a numerical verification for our implementation. Finally, we derive the following form of the transfer operator

$$\begin{aligned}\left[\mathcal{L}^{(n)}_{\beta,\varepsilon,\chi}\vec{f}(z)\right]_i &= \sum_{k=0}^{\infty}\sum_{s=0}^{\infty}\sum_{m=1}^{n}\sum_{j=1}^{\mu_n}\left[U^{\chi}\left(S\,T^{m\varepsilon}\right)\right]_{i,j}\frac{f_j^{(k)}(1)}{k!}\sum_{t=0}^{k}\binom{k}{t}\frac{(-1)^{k-t+s}}{n^{2\beta+t+s}}\\ &\quad\frac{1}{s!}\frac{\Gamma(2\beta+t+s)}{\Gamma(2\beta+t)}\Phi\left(\chi\left(r_j^{(n)}T^{n\varepsilon}\left(r_j^{(n)}\right)^{-1}\right),2\beta+t+s,\frac{m+1}{n}\right)(z-1)^s\end{aligned}$$

with Φ being the Lerch transcendent. We conjecture that this form of the transfer operator also gives an analytic continuation to the entire complex β-plane. Moreover, this form can be approximated by a finite matrix $\mathcal{M}^{(n)}_{\beta,\varepsilon,\chi}\in\mathbb{C}^{\mu_nN\times\mu_nN}$ given by

$$\begin{aligned}\left[\left(\mathcal{M}^{(n)}_{\beta,\varepsilon,\chi}\right)_{s,k}\right]_{i,j} &= \frac{1}{s!}\sum_{t=0}^{k}\binom{k}{t}\frac{(-1)^{k-t+s}}{n^{2\beta+t+s}}\frac{\Gamma(2\beta+t+s)}{\Gamma(2\beta+t)}\sum_{m=1}^{n}\left[U^{\chi}\left(S\,T^{m\varepsilon}\right)\right]_{i,j}\\ &\quad\Phi\left(\chi\left(r_j^{(n)}T^{n\varepsilon}\left(r_j^{(n)}\right)^{-1}\right),2\beta+t+s,\frac{m+1}{n}\right)\end{aligned}$$

with $1\le i,j\le\mu_n$ and $0\le s,k<N$, $N\in\mathbb{Z}_{>}$ large.

- In Chapter 8 we present the results of our numerical experiments for the transfer operator $\mathcal{L}^{(n)}_{\beta,\varepsilon,\chi}$ and the Selberg zeta function $Z^{(n)}(\beta,\chi)$ for $\Gamma_0(n)$ with χ. We study them mainly for $\Gamma_0(4)$ with $\chi^{(4)}_{\alpha_1,\alpha_2}$ and for $\Gamma_0(8)$ with $\chi^{(8)}_{\alpha_1,\alpha_2,\alpha_3}$. We are especially interested in the curves of zeros of the Selberg zeta function $Z^{(4)}(\beta,\chi^{(4)}_{\alpha})$ with $\chi^{(4)}_{\alpha}:=\chi^{(4)}_{\alpha,0}$ for $0\le\alpha\le 0.5$. We found numerically that for $\Gamma_0(n)$ and certain χ the traces of the operators $\mathcal{L}^{(n)}_{\beta,+1,\chi}$ and $\mathcal{L}^{(n)}_{\beta,-1,\chi}$ are identical; further investigations revealed that in these cases also the spectra of these operators coincide. This indicates that the two operators are possibly conjugated. Indeed, as we mentioned above the form of the transfer operator from Chapter 7 allows

us to write down the transfer operator $\mathcal{L}^{(n)}_{\beta,\varepsilon,\chi}$ explicitly for a given $\Gamma_0(n)$ and χ. This way we found certain intertwining operators $\mathcal{P}_k$ with $1 \leq k \leq h$, which we will also call symmetries of the transfer operator, such that

$$\mathcal{P}_k \mathcal{L}^{(n)}_{\beta,+1,\chi} = \mathcal{L}^{(n)}_{\beta,-1,\chi} \mathcal{P}_k.$$

We derived an algorithm to find all symmetries $\mathcal{P}_k$ for a given $\mathcal{L}^{(n)}_{\beta,\varepsilon,\chi}$. Implementing this algorithm in our computer program allows us to automatically find these symmetries for any $\Gamma_0(n)$ and χ. By using these symmetries it can be shown that the Selberg zeta function factorises as follows

$$Z^{(n)}(\beta,\chi) = \det(1 - \mathcal{P}_k \mathcal{L}^{(n)}_{\beta,+1,\chi}) \det(1 + \mathcal{P}_k \mathcal{L}^{(n)}_{\beta,+1,\chi}).$$

Using $\Re\beta = \frac{1}{2}$ allows us to relate the eigenvalues $+1$ and -1 of the transfer operator $\mathcal{P}_k \mathcal{L}^{(n)}_{\beta,+1,\chi}$ to involutions of the eigenfunctions of the Laplacian, the so-called Maass wave forms: numerical calculations show that for $\mathcal{P}_1 \mathcal{L}^{(n)}_{\beta,+1,\chi\equiv 1}$ and the involution $jz = -\bar{z}$ we have:

$$\begin{aligned} +1 \in \sigma(\mathcal{P}_1 \mathcal{L}^{(n)}_{\beta,+1}) &\iff u(-\bar{z}) = u(z), \quad \text{i.e. } u \text{ is even} \\ -1 \in \sigma(\mathcal{P}_1 \mathcal{L}^{(n)}_{\beta,+1}) &\iff u(-\bar{z}) = -u(z), \quad \text{i.e. } u \text{ is odd.} \end{aligned}$$

where $\sigma(\mathcal{P}_1 \mathcal{L}^{(n)}_{\beta,+1})$ denotes the spectrum of the transfer operator $\mathcal{P}_1 \mathcal{L}^{(n)}_{\beta,+1}$. On the other hand, for $\Gamma_0(4)$ with $\chi^{(4)}_\alpha$ and the involution $\tau z = \frac{\bar{z}}{2\bar{z}-1}$ we found that:

$$\begin{aligned} +1 \in \sigma(\mathcal{P}_2 \mathcal{L}^{(4)}_{\beta,+1,\alpha}) &\iff u(\tau z) = u(z), \quad \text{i.e. } u \text{ is } \tau\text{-even} \\ -1 \in \sigma(\mathcal{P}_2 \mathcal{L}^{(4)}_{\beta,+1,\alpha}) &\iff u(\tau z) = -u(z), \quad \text{i.e. } u \text{ is } \tau\text{-odd.} \end{aligned}$$

Numerical experiments show that the τ-odd Maass wave forms survive the deformation by $\chi^{(4)}_\alpha$ for $0 < \alpha \leq 0.5$, while the τ-even ones exist only for discrete values α_k of α, getting destroyed as soon $\alpha \neq \alpha_k$. We find that for large $\Re\beta > \frac{1}{2}$ the spectra of the transfer operators are on concentric circles, whose radii coincide for all $\Gamma_0(n)$ and all χ. While for $\Re\beta = \frac{1}{2}$ and varying $\Im\beta$ many of the eigenvalues of the operator $\mathcal{P}_k \mathcal{L}^{(n)}_{\beta,+1,\chi}$ rotate around 0 with absolute value around 1 and pass ± 1. On the other hand, for $\Re\beta < 0$ we find for the transfer operators for $\Gamma_0(n)$ with χ besides very large eigenvalues also a lot of eigenvalues clustering around ± 1 in increasing number as $\Re\beta$ decreases. We find for the transfer operator $\mathcal{P}_2 \mathcal{L}^{(4)}_{\beta,+1,\alpha}$ for $\Gamma_0(4)$ with $\chi^{(4)}_\alpha$, that for $\Re\beta = \frac{1}{2}$ and varying $\alpha \to 0$ the eigenvalues rotate on closed orbits, whose rotation speed increases exponentially with α getting small, while one of these orbits goes through -1 with six eigenvalues rotating on it. Furthermore, we find numerically certain identities for the Selberg zeta functions for $\Gamma_0(4)$ with $\chi^{(4)}_{\alpha_1,\alpha_2}$ and $\Gamma_0(8)$ with $\chi^{(8)}_{\alpha_1,\alpha_2,\alpha_3}$, namely

$$\begin{aligned} Z^{(4)}(\beta,\chi^{(4)}_{\frac{1}{4},0}) &= Z^{(4)}(\beta,\chi^{(4)}_{\frac{1}{2},0}) \\ Z^{(8)}\left(\beta,\chi^{(8)}_{2\alpha_2,\alpha_1,\alpha_1}\right) &= Z^{(4)}\left(\beta,\chi^{(4)}_{\alpha_1,\alpha_2}\right) Z^{(4)}\left(\beta,\chi^{(4)}_{\alpha_1,\alpha_2+\frac{1}{2}}\right) \\ \text{and} \qquad Z^{(8)}\left(\beta,\chi^{(8)}_{0,\frac{1}{2},0}\right) &= Z^{(4)}\left(\beta,\chi^{(4)}_{\frac{1}{8},0}\right) Z^{(4)}\left(\beta,\chi^{(4)}_{\frac{3}{8},0}\right). \end{aligned}$$

We conjecture that the multiplicity of the zeros of the Selberg zeta function $Z^{(4)}(\beta,\chi^{(4)}_\alpha)$ is one for $0 < \alpha \leq 0.5$, and the multiplicity of the zeros of $Z^{(8)}(\beta,\chi^{(8)}_{0,\alpha,0})$ is one for $0 < \alpha < 0.5$ and two or one for $\alpha = 0.5$. Our results show that for $\Re\beta \leq \frac{1}{2}$ the Selberg zeta function $Z^{(4)}(\beta,\chi^{(4)}_\alpha)$ and the spectrum of the transfer operator $\mathcal{P}_2 \mathcal{L}^{(4)}_{\beta,+1,\alpha}$ behave non-continuously in the limes $\alpha \to 0$. Numerical experiments also revealed that for $\alpha \to 0$ there are two different kinds of convergence of the zeros of $Z^{(4)}(\beta,\chi^{(4)}_\alpha)$ to the zeros for $\alpha = 0$ on the line $\Re\beta = \frac{1}{2}$: Zeros related to the eigenvalue -1 of

$\mathcal{P}_2\mathcal{L}^{(4)}_{\beta,+1,\alpha}$ stay on the line $\Re\beta = \frac{1}{2}$ and converge towards the zeros for $\alpha = 0$ by an infinite sequence of avoided crossings, whereas the zeros related to the eigenvalue $+1$ of $\mathcal{P}_2\mathcal{L}^{(4)}_{\beta,+1,\alpha}$ are in general left of the line $\Re\beta = \frac{1}{2}$ and converge to zeros for $\alpha = 0$ by touching the line $\Re\beta = \frac{1}{2}$ infinitely many times. Furthermore, we found for $\alpha \to 0$ sequences of zeros which touch the line $\Re\beta = \frac{1}{2}$ and that these points of contact are converging towards $\frac{1}{2} + m\frac{\pi}{\ln 2}i$ with $m \in \mathbb{Z}_>$; however, these limit points are not zeros of the Selberg zeta function for $\alpha = 0$. Therefore, we call them phantom eigenvalues. There are also zeros on and left of the line $\Re\beta = \frac{1}{2}$ which move in pairs towards $\beta = \frac{1}{2}$ and become dense on the line $\Re\beta = \frac{1}{2}$ for $\alpha \to 0$. These zeros seem to be related to the change of the multiplicity of the continuous spectrum of the Laplacian by the singular perturbation around $\alpha = 0$. Finally, we found that the zero at $\beta = 1$ for $\alpha = 0$ cancels the pole of the Selberg zeta function at $\beta = \frac{1}{2}$ for $\alpha = \frac{1}{8}$ and moves to $\beta \to -\infty$ for $\alpha \to \frac{2}{8}$. Indeed, it turns out that there is a whole family of zeros in the β-plane which tend to $\Re\beta \to -\infty$ for $\alpha \uparrow \frac{2}{8}$ and $\alpha \downarrow \frac{2}{8}$, and vanish for $\alpha = \frac{2}{8}$.

- In Chapter 9 we apply our approximation method to the transfer operator $\mathcal{L}_{\beta,\lambda}$ for the Kac-Baker spin model given by

$$\mathcal{L}_{\beta,\lambda} f(z) = e^{\beta z} f(\lambda + \lambda z) + e^{-\beta z} f(-\lambda + \lambda z).$$

  We derive the following form of this transfer operator

$$\mathcal{L}_{\beta,\lambda} f(z) = \sum_{k=0}^{\infty} \sum_{l=0}^{\infty} \frac{f^{(l)}(0)}{l!} \lambda^l \left(1 + (-1)^{k+l}\right) \sum_{r=0}^{\min(k,l)} \binom{l}{r} \frac{\beta^{k-r}}{(k-r)!} z^k,$$

  which can be approximated by the finite matrix

$$\left[\mathcal{M}_{\beta,\lambda}\right]_{k,l} = \lambda^l \left(1 + (-1)^{k+l}\right) \sum_{r=0}^{\min(k,l)} \binom{l}{r} \frac{\beta^{k-r}}{(k-r)!}$$

  for $0 \le k, l \le N$ and $N \in \mathbb{Z}_>$ large. We implement this approximation in our computer program and present results obtained from numerical experiments.

- In Appendix A we give a brief introduction to our computer programs CGF and widmo that we developed to obtain the numerical results of this thesis.
  In Appendix B can be found the representatives of the rest classes of $\Gamma_0(4)$ and $\Gamma_0(8)$ in $\mathrm{SL}(2,\mathbb{Z})$ used in our numerical calculations.
  In Appendix C the explicit form of the transfer operator for $\Gamma_0(8)$ with $\chi^{(8)}_{\alpha_1,\alpha_2,\alpha_3}$ and the permutations which define the symmetries $\mathcal{P}_1$ and $\mathcal{P}_2$ are given.
  In Appendix D tables of the zeros of the Selberg zeta functions for $\Gamma_0(4)$ with $\chi^{(4)}_{\alpha}$ and $\Gamma_0(8)$ with $\chi^{(8)}_{0,\alpha,0}$ are given.

In this thesis we study numerically a character deformation for $\Gamma_0(4)$ very similar to a character deformation for the same group as was already investigated for the resonances of the Laplacian by Selberg [Sel90], and also by Phillips and Sarnak [PS94] for the eigenfunctions of the Laplacian. The main motivation for Phillips and Sarnak was to study the disappearance of these eigenfunctions under character deformations: It was proved by Selberg that the hyperbolic Laplace-Beltrami operator for congruence subgroups of $\mathrm{PSL}(2,\mathbb{Z})$ has an infinite sequence of discrete eigenvalues satisfying a Weyl law. It is an important question whether this is characteristic for congruence subgroups or whether it also holds for other cofinite Fuchsian groups. An equivalent question is to ask if the hyperbolic Laplacian on finite non-compact surfaces of constant negative curvature has infinitely many eigenfunctions, the so-called Maass wave forms, which determine its discrete spectrum. Phillips and Sarnak studied in [PS85] [PS94] the existence of Maass wave forms for general cofinite Fuchsian groups, and introduced a condition under which a Maass wave form for such a

group Γ is dissolved into a resonance by a deformation of the group in Teichmüller space, respectively a deformation of a character χ. The deformations correspond to perturbations of the hyperbolic Laplacian, where the perturbation can be singular and non-singular. They discovered that the existence of Maass cusp forms seems to be intimately tied to the arithmetic nature of (Γ, χ). According to their conjecture, for non-arithmetic (Γ, χ) the main contribution to the Weyl law should not come from the discrete spectrum.

Part of the results in this thesis are conclusions from numerical experiments. The main advantage of such experiments is that results can be obtained in areas where the theory has not yet been sufficiently developed to make good predictions. These experimental results can trigger the development of new theories and extend existing ones. Experimental mathematics and numerical mathematics are not new fields of research; famous mathematicians and physicists contributed to the development of algorithms for the numerical analysis: Newton's method, Gaussian elimination, or Euler's method are just a few of them. People like Gauss, Euler and Riemann also carried out numerical experiments with the limited resources of their time, first by "pen and paper", later using mechanical computers like the one developed by Michelson to study the Gibbs phenomenon [GS97]. Nowadays such experiments are carried out on digital computers which can be connected to form large computer clusters, providing immense computational power. During the last 50 years computational power has been growing exponentially due to new technical developments. Certainly this fact revolutionised experimental mathematics, which on the other hand also has an impact on pure mathematics, not to mention physics.

To carry out the numerical experiments we had to develop a comprehensive program package called Morpheus, consisting mainly of the programs widmo and CGF. These programs can determine the necessary ingredients for computing the matrix representation of the transfer operator, its spectrum and the Selberg zeta function for any $\Gamma_0(n)$ with a character χ. Since the source code of this program package is more then 30 000 lines long we will not include it in this thesis. The numerical experiments were carried out on computer clusters belonging to an applied theoretical physics research group at Clausthal University of Technology and the clusters of the North-German Supercomputing Alliance (HLRN) in Hanover. The numerical results so far have already initiated new theoretical work, like the already mentioned symmetries of the transfer operator and their relation to involutions of Maass wave forms [FM11]. Also a theoretical treatment of some of the phenomena we were able to obtain numerically is in progress [BFM12].

Chapter 2

Preliminaries

In this section we will recall some basic facts, which we will need later on.

2.1 Complex numbers

We can represent the complex number $z \in \mathbb{C}$ in two different ways: $z = a + ib$ with $a, b \in \mathbb{R}$ or $z = Re^{i\varphi}$ with $R, \varphi \in \mathbb{R}$, $R > 0$. The real part of z is given by $\Re z = a = R\cos\varphi$ and the imaginary part is given by $\Im z = b = R\sin\varphi$. Then the absolute value of z is given by $|z| = R = \sqrt{a^2 + b^2}$ and the argument is given by $\arg z = \varphi = \arctan_2(b, a)$, where we define $\arctan_2$ for $-\pi \leq \arg z \leq \pi$ by

$$\arctan_2(y,x) = \begin{cases} \arctan\left(\frac{y}{x}\right) & x > 0 \\ \arctan\left(\frac{y}{x}\right) + \pi & x < 0, y \geq 0 \\ \arctan\left(\frac{y}{x}\right) - \pi & x < 0, y < 0 \\ +\frac{\pi}{2} & x = 0, y > 0 \\ -\frac{\pi}{2} & x = 0, y < 0 \\ \text{undefined} & x = 0, y = 0. \end{cases} \tag{2.1}$$

For $z \in \mathbb{C}$ the complex logarithm is defined as $\ln z = \ln|z| + i\arg z$, such that for the special case $z \in \mathbb{R}$ with $z < 0$ we have $\ln z = \ln|z| + i\pi$. For $z, s \in \mathbb{C}$ the complex power z^s is given by

$$z^s = |z|^{\Re s} \exp\left(-\arg(z)\,\Im s\right)\left\{\cos\left(\ln|z|\Im s + \arg(z)\,\Re s\right) + i\sin\left(\ln|z|\Im s + \arg(z)\,\Re s\right)\right\}. \tag{2.2}$$

For the special case e^s this gives $e^s = e^{\Re s}\{\cos(\Im s) + i\sin(\Im s)\}$. Trigonometric functions for complex arguments z are defined as

$$\sin z = \sum_{n=0}^{\infty} \frac{(-1)^n}{(2n+1)!} z^{2n+1} = i\frac{e^{-iz} - e^{iz}}{2} \tag{2.3}$$

$$\cos z = \sum_{n=0}^{\infty} \frac{(-1)^n}{(2n)!} z^{2n} = \frac{e^{-iz} + e^{iz}}{2} \tag{2.4}$$

$$\tan z = \frac{\sin z}{\cos z} = i\frac{e^{-iz} - e^{iz}}{e^{-iz} + e^{iz}}. \tag{2.5}$$

2.2 The Argument Principle

The argument principle [AF03] is defined as follows: Let $f(z)$ be a meromorphic function defined on the closure of the interior of a simple closed contour C with no zeroes or poles on C. Then

$$\frac{1}{2\pi i}\oint_C \frac{f'(z)}{f(z)}dz = N - P = \frac{1}{2\pi}\left[\arg f(z)\right]_C \tag{2.6}$$

where N and P are the number of zeroes respectively poles of $f(z)$ inside C; thereby multiple zeros or poles are counted according to their multiplicity, $\arg f(z)$ is the argument of $f(z)$, that is, $f(z) = |f(z)| \exp i \arg f(z)$ and $\left[\arg f(z)\right]_C$ denotes the change in the argument of $f(z)$ along the contour C.

2.3 The Laplace method

The behavior of the integral

$$I(\lambda) = \int_a^b f(t)e^{-\lambda g(t)}dt \tag{2.7}$$

in leading order for $\lambda \to \infty$ is given by

$$I(\lambda) \sim_{\lambda\to\infty} f(c)e^{-\lambda g(c)}\sqrt{\frac{2\pi}{\lambda g''(c)}} \tag{2.8}$$

with $c \in (a, b)$, $g'(c) = 0$, $g''(c) > 0$ and $f(c) \neq 0$. Thereby a and b could possibly be infinite.

2.4 The precision of numbers

Computers have a limited memory for representing numbers; therefore, only integers and rational numbers can be represented within a limited range. The precision of rational numbers is also limited. Obviously, it is not possible in general to represent irrational numbers; they have to be approximated by a rational number or some "finite" representation has to be found for them.

We need a criterion to decide if a number is "close enough" to its real value, e.g., if we compute some infinite sum we have to find a criterion for when to stop the summation, since the result no longer changes when adding more terms. Such a criterion for a sequence $x_k \in \mathbb{R}$, $k \in \mathbb{Z}_>$, with limit $\lim_{k\to\infty} x_k = \tilde{x}$ is given by

$$\left|\frac{x_k - x_{k-1}}{x_k}\right| < \delta \tag{2.9}$$

with some small constant δ, which is usually the smallest positive non-zero number, which can be represented on the computer. For complex numbers the real and imaginary parts are checked separately. Sometimes it is useful to use the logarithmic version $\ln|x_k - x_{k-1}| - \ln|x_k| < \ln\delta$.

For technical reasons, instead of the constant δ we use the number of significant digits which can be represented on the computer. Since computers use the binary number system the size of the mantissa is given in binary digits, the so-called bits. Let P be the number of bits of the mantissa, then the number of significant digits D in the decimal number system is given by

$$D = P\frac{\ln 2}{\ln 10}.$$

We will perform the computations in this thesis with at least $P = 160$ bits, which corresponds to about $D = 48$ significant decimal digits. A good choice for δ is $\delta = 10^{-D}$; then we have $\ln|x_k| - \ln|x_k - x_{k-1}| > D$. For practical reasons we carry out the following check:

$$\text{get\_exp}(x_k) - \text{get\_exp}(x_k - x_{k-1}) > P,$$

where get_exp(x) is the exponent E of the binary floating point number x represented by $x = y \cdot 2^E$, such that $y \in [0.5, 1)$. The reason for using get_exp(x) instead of $\ln x$, is that the evaluation of the former function is much faster than the evaluation of the logarithm. For practical reasons $P' = P - I$ should be chosen instead of P in this formula, where I is some small number of bits, e.g., for $P = 160$ bits we use $I = 20$ bits.

2.5 The Newton method

We will briefly discuss Newton's method for finding zeros of complex functions. Let $F : \mathbb{C} \to \mathbb{C}$ be a function; then we can interpret this function also as $F : \mathbb{R}^2 \to \mathbb{R}^2$ with

$$F\begin{pmatrix} x \\ y \end{pmatrix} = \begin{pmatrix} \Re F(x,y) \\ \Im F(x,y) \end{pmatrix} \quad \text{for } z = x + iy \in \mathbb{C}.$$

Newton's method is an iterative method for finding the zeros of a function. It starts with some x_0, y_0 and defines iteratively

$$\begin{pmatrix} x_{n+1} \\ y_{n+1} \end{pmatrix} = \begin{pmatrix} x_n + \Delta x_n \\ y_n + \Delta y_n \end{pmatrix}.$$

To determine Δx_n and Δy_n, we need to solve the linear system of equations

$$J_F\begin{pmatrix} x_n \\ y_n \end{pmatrix}\begin{pmatrix} \Delta x_n \\ \Delta y_n \end{pmatrix} = -F\begin{pmatrix} x_n \\ y_n \end{pmatrix}$$

with the Jacobian matrix J_F given by

$$J_F\begin{pmatrix} x_n \\ y_n \end{pmatrix} = \begin{pmatrix} \partial_x \Re F(x_n,y_n) & \partial_y \Re F(x_n,y_n) \\ \partial_x \Im F(x_n,y_n) & \partial_y \Im F(x_n,y_n) \end{pmatrix}$$

with $\partial_x \Re F(x_n,y_n) = \frac{\partial}{\partial x} \Re F(x,y)\big|_{x=x_n,y=y_n}$. It is easy to show that

$$\Delta x_n = -\frac{\Re F(x_n,y_n) + \Delta y_n \partial_y \Re F(x_n,y_n)}{\partial_x \Re F(x_n,y_n)} \tag{2.10}$$

and

$$\Delta y_n = \frac{\Re F(x_n,y_n)\,\partial_x \Im F(x_n,y_n) - \Im F(x_n,y_n)\,\partial_x \Re F(x_n,y_n)}{\partial_y \Im F(x_n,y_n)\,\partial_x \Re F(x_n,y_n) - \partial_y \Re F(x_n,y_n)\,\partial_x \Im F(x_n,y_n)}. \tag{2.11}$$

Note that for a real-valued function $F : \mathbb{R} \to \mathbb{R}$ we have just $\Delta x_n = -\frac{F(x_n)}{\partial_x F(x_n)}$. Instead of looking for an exact zero of F we will stop the iterations at some n when $|F(x_n + iy_n)| < C$, where C is some small constant:

Definition 2.5.1. Define

$$N_F^C(x_0 + iy_0) := (x_e + iy_e) \tag{2.12}$$

where x_e and y_e are computed by Newton's method with starting points x_0 and y_0, such that

$$|F(N_F^C(x_0 + iy_0))| = |F(x_e + iy_e)| < C.$$

Newton's method just gives the location of a possible zero; to confirm this zero the argument principle should be used.

2.6 Numerical derivation of a function

Since we want to implement Newton's method on the computer, we need some way to compute derivatives of a function numerically. For this the function $F : \mathbb{C} \to \mathbb{C}$ has to be evaluated at several places in the complex plane. Then we have the following formulas ([AS64], pp. 883)

$$\partial_x \Re F(x,y) = \frac{\Re F(x+h,y) - \Re F(x-h,y)}{2h} \tag{2.13}$$

$$\partial_x \Im F(x,y) = \frac{\Im F(x+h,y) - \Im F(x-h,y)}{2h} \tag{2.14}$$

$$\partial_y \Re F(x,y) = \frac{\Re F(x,y+h) - \Re F(x,y-h)}{2h} \tag{2.15}$$

$$\partial_y \Im F(x,y) = \frac{\Im F(x,y+h) - \Im F(x,y-h)}{2h}. \tag{2.16}$$

To save computation time we can also use only three points to compute the derivative

$$\partial_x \Re F(x,y) = \frac{\Re F(x+h,y) - \Re F(x,y)}{h} \tag{2.17}$$

$$\partial_x \Im F(x,y) = \frac{\Im F(x+h,y) - \Im F(x,y)}{h} \tag{2.18}$$

$$\partial_y \Re F(x,y) = \frac{\Re F(x,y+h) - \Re F(x,y)}{h} \tag{2.19}$$

$$\partial_y \Im F(x,y) = \frac{\Im F(x,y+h) - \Im F(x,y)}{h}. \tag{2.20}$$

Here we choose $h = 10^{-10}$.

We want to write down Newton's method in a way that is more useful for numerical computations. For this we define $\Delta_x F(x,y) = F(x+h,y) - F(x-h,y)$ and $\Delta_y F(x,y) = F(x,y+h) - F(x,y-h)$. Using formulas (2.13) to (2.16) we finally get:

$$\Delta x_n = -2h \frac{\left(\Re F(x_n,y_n) + \Delta y'_n \Re \Delta_y F(x_n,y_n)\right)}{\Re \Delta_x F(x_n,y_n)} \tag{2.21}$$

$$\Delta y_n = 2h \Delta y'_n \tag{2.22}$$

and

$$\Delta y'_n = \frac{\Re F(x_n,y_n)\, \Im \Delta_x F(x_n,y_n) - \Im F(x_n,y_n)\, \Re \Delta_x F(x_n,y_n)}{\Im \Delta_y F(x_n,y_n) \Re \Delta_x F(x_n,y_n) - \Re \Delta_y F(x_n,y_n) \Im \Delta_x F(x_n,y_n)}. \tag{2.23}$$

Chapter 3

The Gamma and incomplete Gamma function

The gamma function is defined for $s \in \mathbb{C}$ by

$$\Gamma(s) = \int_0^\infty t^{s-1} e^{-t} dt \tag{3.1}$$

where the integral converges absolutely for $\Re s > 0$. By analytic continuation $\Gamma(s)$ can be extended to a meromorphic function defined for all $s \in \mathbb{C}$ with poles at $s = 0$ and $s \in \mathbb{Z}_<$. We can use Euler's reflection formula

$$\Gamma(s)\Gamma(1-s) = \frac{\pi}{\sin \pi s} \tag{3.2}$$

to evaluate $\Gamma(s)$ for $\Re s < 0$. The functional equation for $\Gamma(s)$ is given by

$$\Gamma(s+1) = s\Gamma(s). \tag{3.3}$$

It then follows immediately that

$$\frac{\Gamma(s+k)}{\Gamma(s)} = \prod_{p=0}^{k-1} (s+p) \tag{3.4}$$

with $k \in \mathbb{N}$ and $s \in \mathbb{C}$. In the special case of $n \in \mathbb{N}$ the gamma function is related to the factorial by

$$\Gamma(n+1) = n!\,. \tag{3.5}$$

Stirling's formula for $n \to \infty$ is given by

$$n! \sim \sqrt{2\pi} e^{-n} n^{n+\frac{1}{2}}\,. \tag{3.6}$$

A similar asymptotic formula for $s \to \infty$ is given in [AS64] for $|\arg s| < \pi$

$$\Gamma(s) \sim \sqrt{2\pi} e^{-s} s^{s-\frac{1}{2}}. \tag{3.7}$$

The upper respectively lower incomplete gamma function is defined as

$$\Gamma(s,z) = \int_z^\infty t^{s-1} e^{-t} dt \tag{3.8}$$

$$\gamma(s,z) = \int_0^z t^{s-1} e^{-t} dt. \tag{3.9}$$

Note that $\Gamma(s) = \Gamma(s,z) + \gamma(s,z)$. Their functional equations are given by

$$\Gamma(s+1,z) = s\Gamma(s,z) + z^s e^{-z} \tag{3.10}$$
$$\gamma(s+1,z) = s\gamma(s,z) - z^s e^{-z}. \tag{3.11}$$

The continued fraction expansion of $\Gamma(s,z)$ is given by

$$\Gamma(s,z) = \frac{e^{-z}z^s}{z+}\frac{1-s}{1+}\frac{1}{z+}\frac{2-s}{1+}\frac{2}{z+}\cdots. \tag{3.12}$$

According to [Tem94] (3.12) converges for all $z \neq 0$, $|\arg z| < \pi$ and any complex value of s. It converges better as the ratio $|z/s|$ increases. Formula (3.12) can also be written as

$$e^z z^{1-s}\Gamma(s,z) = \frac{1}{1+}\frac{(1-s)z^{-1}}{1+}\frac{z^{-1}}{1+}\frac{(2-s)z^{-1}}{1+}\frac{2z^{-1}}{1+}\cdots. \tag{3.13}$$

To evaluate this continued fraction, we need to approximate it by a finite continued fraction [Win03]. The partial fraction $F_{m,n}$ is given by

$$F_{m,n} = a_m + \frac{b_m}{a_{m+1}+}\frac{b_{m+1}}{a_{m+2}+}\cdots\frac{b_{n-1}}{a_n} = \frac{p_{m,n}}{q_{m,n}}.$$

One may compute the partial fractions directly $F_{m,n} = a_m + \frac{b_m}{F_{m+1,n}}$, starting from $F_{n,n} = a_n$. Instead, one may also compute the numerator $p_{m,n}$ and the denominator $q_{m,n}$ as separate sequences

$$p_{m,n} = a_m p_{m+1,n} + b_m q_{m+1,n}, \quad q_{m,n} = p_{m+1,n}$$

with $p_{n,n} = a_n$ and $q_{n,n} = 1$. Then the finite continued fraction is given by $F_{0,n} = \frac{p_{0,n}}{q_{0,n}}$. The speed of convergence, i.e. the number of terms n we need to compute to get a sufficient precise result, depends on z and s; indeed the number of terms required grows when z approaches zero.

For the lower incomplete gamma function we can use the series

$$\gamma(s,z) = \sum_{n=0}^{\infty}\frac{(-1)^n}{n!}\frac{z^{s+n}}{s+n} \tag{3.14}$$

which converges quite fast for $|z/s| < 1$, but does not converge for $s \in \mathbb{Z}_<$.

Lemma 3.0.1. *A recursive formula for the series* $\gamma(s,z) = \sum_{n=0}^{\infty}\frac{(-1)^n}{n!}\frac{z^{s+n}}{s+n}$ *is given by*

$$\gamma(s,z) = z^s\sum_{n=0}^{\infty}\frac{\alpha_n}{s+n} \tag{3.15}$$

with $\alpha_0 = 1$ *and* $\alpha_n = \alpha_{n-1}\frac{(-z)}{n}$.

Proof. We have

$$\gamma(s,z) = \sum_{n=0}^{\infty}\frac{(-1)^n}{n!}\frac{z^{s+n}}{s+n} = z^s\sum_{n=0}^{\infty}\frac{(-1)^n}{n!}\frac{z^n}{s+n} = z^s\sum_{n=0}^{\infty}\frac{\alpha_n}{s+n}$$

with $\alpha_n = \frac{(-1)^n}{n!}z^n$. We see that $\alpha_0 = 1$ and $\alpha_n = \frac{(-1)^{n-1}}{(n-1)!}z^{n-1}\frac{(-1)z}{n} = \alpha_{n-1}\frac{(-z)}{n}$. □

We compute the gamma function by an approximation from Lanczos, which gives more precise results than the more popular Stirling approximation, see [Pug04]. The Lanczos approximation is given by

$$\Gamma(z+1) = \sqrt{2\pi}\left(z+g+\frac{1}{2}\right)^{z+\frac{1}{2}} e^{-\left(z+g+\frac{1}{2}\right)}\left[b_0(g)+\sum_{i=1}^{N}\frac{b_i(g)}{z+i}\right] \tag{3.16}$$

where g is some constant such that $\Re z + g + \frac{1}{2} > 0$, N is the number of coefficients and $b_i(g)$ is defined as

$$b_i(g) = \frac{\sqrt{2}e^{g+\frac{1}{2}}}{\pi}\sum_{n=0}^{N} B_{i,n}\sum_{l=0}^{N} C_{n,l}\Gamma\left(l+\frac{1}{2}\right)\left(l+g+\frac{1}{2}\right)^{-\left(l+\frac{1}{2}\right)} e^{l} \tag{3.17}$$

with

$$B_{i,j} = \begin{cases} 0 & i > j \\ \frac{1}{2} & i = j = 0 \\ 1 & i = 0, j > 0 \\ \frac{(-1)^{j-i+1}(i+j-1)!}{(j-i)!((n-1)!)^2} & \text{else} \end{cases}$$

and

$$C_{i,j} = \begin{cases} 0 & i < j \\ 1 & i = 0, j = 0 \\ \frac{(-1)^{i-j} i (i+j)! 4^j}{(i+1)(2j)!(i-j)!} & \text{else.} \end{cases}$$

In our calculations we have chosen $N = 28$ and $g = 29.692534$.

Chapter 4

Numerical evaluation of the Hurwitz Zeta Function and the Lerch Zeta Function

In this chapter we will discuss formulas we have developed for the evaluation of certain zeta functions. We will need them later for the numerical computation of the spectrum of the transfer operator. The implementations of these zeta functions are in a sense the heart of our computations, so we need to be very careful. Unfortunately we have found approximations of these zeta functions in the literature which are quite limited; this is the case especially for the Lerch zeta function. This is understandable, since these zeta functions are special functions, which compared to others are not used so often.

To our knowledge our formulas are more general and also more precise than other approximations found in the literature; this holds in particular for the Lerch zeta function.

Let us start with the Riemann zeta function, which is given by the sum

$$\zeta_R(s) = \sum_{n=1}^{\infty} n^{-s}, \tag{4.1}$$

which converges absolutely for $\Re s > 1$. The connection between this zeta function and the prime numbers was given by Euler, namely

$$\zeta_R(s) = \prod_{p \text{ prime}} \frac{1}{1-p^{-s}} \tag{4.2}$$

for $\Re s > 1$. Its functional equation is given by

$$\zeta_R(s) = 2^s \pi^{s-1} \sin\left(\frac{\pi s}{2}\right) \Gamma(1-s)\, \zeta_R(1-s) \tag{4.3}$$

valid for all $s \in \mathbb{C}$. The famous Riemann conjecture states that the non-trivial zeros of ζ_R are all on the critical line $\Re s = \frac{1}{2}$.

4.1 The Euler-MacLaurin formula and the Bernoulli numbers

We want to use the Euler-MacLaurin formula [AS64] pp.806, given by

$$\sum_{k=a}^{b} f(k) \quad = \quad \int_a^b f(t)\, dt + \frac{f(b)+f(a)}{2} + \sum_{k=1}^{p-1} \frac{B_{2k}}{(2k)!} \left(f^{(2k-1)}(b) - f^{(2k-1)}(a) \right) + R, \tag{4.4}$$

where the remainder term R is given for some $0 < \theta < 1$, depending on $f^{(2p)}(x)$, and (a, b) by

$$R = \frac{B_{2p}}{(2p)!} \sum_{k=a}^{b-1} f^{(2p)}(k + \theta). \tag{4.5}$$

The B_j are the Bernoulli numbers, which can be computed for instance by the following formula (see [Car92]):

$$\sum_{k=0}^{m} \binom{m+1}{k} B_k = 0, \quad \text{with } B_0 = 1. \tag{4.6}$$

Euler expressed the Bernoulli numbers as

$$B_{2p} = (-1)^{n-1} \frac{2\,(2p)!}{(2\pi)^{2p}} \zeta_R(2p) \tag{4.7}$$

with ζ_R the Riemann zeta function (4.1). By using Stirling's formula (3.6) it is easy to verify that for $p \to \infty$ they behave like

$$|B_{2p}| \sim 4\sqrt{\pi p} \left(\frac{p}{e\pi}\right)^{2p}. \tag{4.8}$$

For the remainder R we get $|R| \leq \frac{2\zeta_R(2p)}{(2\pi)^{2p}} \sum_{k=a}^{b-1} |f^{(2p)}(k + \theta)|$ and have in the limit $p \to \infty$

$$|R| \sim 2\,(2\pi)^{-2p} \sum_{k=a}^{b-1} |f^{(2p)}(k + \theta)|\,.$$

4.2 The Hurwitz Zeta function

The Hurwitz zeta function [Hur82] is defined as

$$\zeta(s, z) = \sum_{n=0}^{\infty} (z + n)^{-s} \tag{4.9}$$

where the sum converges uniformly for $\Re(s) > 1$. We see that for $z = 1$ the Hurwitz zeta function coincides with the Riemann zeta function i.e. $\zeta(s, 1) = \zeta_R(s)$. Hurwitz' formula [Erd53] is given by

$$\zeta(s, z) = 2\,(2\pi)^{s-1}\,\Gamma(1 - s) \sum_{n=1}^{\infty} n^{s-1} \sin\left(2\pi n z + \frac{\pi s}{2}\right) \tag{4.10}$$

for $0 < z \leq 1$ and $\Re s < 0$.

Lemma 4.2.1. *For rational $\frac{p}{q} \in \mathbb{Q}$ with positive p and q and $p \leq q$ the following functional equation holds*

$$\zeta\left(s, \frac{p}{q}\right) = 2\,(2\pi q)^{s-1}\,\Gamma(1 - s) \sum_{m=1}^{q} \zeta\left(1 - s, \frac{m}{q}\right) \sin\left(2\pi m \frac{p}{q} + \frac{\pi s}{2}\right) \tag{4.11}$$

for all $s \in \mathbb{C}$.

Proof. Setting $n = m + ql$ the sum $\sum_{n=1}^{\infty}$ in (4.10) can be written as

$$\begin{aligned}\sum_{n=1}^{\infty} n^{s-1} \sin\left(2\pi n\frac{p}{q} + \frac{\pi s}{2}\right) &= \sum_{l=1}^{\infty}\sum_{m=1}^{q} (m+ql)^{s-1} \sin\left(2\pi\,(m+ql)\,\frac{p}{q} + \frac{\pi s}{2}\right)\\ &= q^{s-1}\sum_{l=1}^{\infty}\sum_{m=1}^{q}\left(\frac{m}{q}+l\right)^{s-1} \sin\left(2\pi m\frac{p}{q} + 2\pi lp + \frac{\pi s}{2}\right)\\ &= q^{s-1}\sum_{m=1}^{q}\zeta\left(1-s,\frac{m}{q}\right)\sin\left(2\pi m\frac{p}{q}+\frac{\pi s}{2}\right).\end{aligned}$$

This sum is valid for all $s \in \mathbb{C}$ since the Hurwitz zeta function has an analytic continuation. □

Since we want to use this functional equation for $z > 1$, we need the following lemma, which also presents some kind of functional equation for ζ:

Lemma 4.2.2. *The Hurwitz zeta function fulfills for $N \in \mathbb{N}$ and $z \in \mathbb{C}$ the relation*

$$\zeta(s, z+N) = \zeta(s,z) - \sum_{n=0}^{N-1}(z+n)^{-s}. \tag{4.12}$$

Proof. Since $\zeta(s, z+N) = \sum_{n=0}^{\infty}(z+N+n)^{-s} = \sum_{n=N}^{\infty}(z+n)^{-s} = \sum_{n=0}^{\infty}(z+n)^{-s} - \sum_{n=0}^{N-1}(z+n)^{-s}$ the lemma holds. □

Later on we will also need the derivative in z of the Hurwitz zeta function. For this we use first the following lemma:

Lemma 4.2.3. *Let $n \in \mathbb{N}$, $z, s \in \mathbb{C}$ and $p, q \in \mathbb{Z}$. The k-th derivative of $\left(\frac{z+p}{q}+n\right)^{-s}$ in z is given by*

$$\frac{\partial^k}{\partial z^k}\left(\frac{z+p}{q}+n\right)^{-s} = \frac{(-1)^k}{q^k}\frac{\Gamma(s+k)}{\Gamma(s)}\left(\frac{z+p}{q}+n\right)^{-s-k} \tag{4.13}$$

and the k-th derivative in n is given by

$$\frac{\partial^k}{\partial \eta^k}\left(\frac{z+p}{q}+\eta\right)^{-s}|_{\eta=n} = (-1)^k\frac{\Gamma(s+k)}{\Gamma(s)}\left(\frac{z+p}{q}+n\right)^{-s-k}. \tag{4.14}$$

Proof. It is enough to prove the first formula, the proof for the second one is analogous. The proof is by induction. For $k = 1$ the right hand side of formula (4.13) reads

$$\frac{(-1)}{q}\frac{\Gamma(s+1)}{\Gamma(s)}\left(\frac{z+p}{q}+n\right)^{-s-1} = \frac{(-1)}{q}\frac{s\Gamma(s)}{\Gamma(s)}\left(\frac{z+p}{q}+n\right)^{-s-1} = \frac{(-s)}{q}\left(\frac{z+p}{q}+n\right)^{-s-1}.$$

But this is just $\frac{\partial}{\partial z}\left(\frac{z+p}{q}+n\right)^{-s} = (-s)\left(\frac{z+p}{q}+n\right)^{-s-1}q^{-1}$. Next we have to prove it for $k+1$. Formula (4.13) then reads

$$\frac{(-1)^{k+1}}{q^{k+1}}\frac{\Gamma(s+k+1)}{\Gamma(s)}\left(\frac{z+p}{q}+n\right)^{-s-k-1} = \frac{(-1)^k}{q^k}\frac{\Gamma(s+k)}{\Gamma(s)}\frac{(-s-k)}{q}\left(\frac{z+p}{q}+n\right)^{-s-k-1}.$$

But $\frac{(-s-k)}{q}\left(\frac{z+p}{q}+n\right)^{-s-k-1} = \frac{\partial}{\partial z}\left(\frac{z+p}{q}+n\right)^{-s-k}$ and hence formula (4.13) for $k+1$ coincides with the derivative of formula (4.13) for k. □

4.2.1 Application of the Euler-MacLaurin formula

We will need an analytic continuation of the Hurwitz zeta function in the region $\Re s < 1$. But since even for $\Re s > 1$ the formula $\zeta(s,z) = \sum_{n=0}^{\infty}(z+n)^{-s}$ is not suitable for numerical evaluations, we will need to apply the Euler-MacLaurin formula (4.4), see also [Car92] and [Str07]. Note, that we will use a form of the Euler-MacLaurin formula different to the one by [Car92] and [Str07]. Our result is then slightly more general than the results of these authors.

Proposition 4.2.4. *By using the Euler-MacLaurin formula (4.4) the Hurwitz zeta function*

$$\zeta(s,z) = \sum_{n=0}^{\infty}(z+n)^{-s}$$

can be written for some $a, p \in \mathbb{Z}$ as

$$\zeta(s,z) = \zeta_{a,p}(s,z) + R_{a,p} \tag{4.15}$$

defined for $\Re s + 2p > 1$. The function $\zeta_{a,p}(s,z)$ is given by

$$\begin{aligned}\zeta_{a,p}(s,z) &= \sum_{n=0}^{a-1}(z+n)^{-s} + \frac{(z+a)^{1-s}}{s-1} + \frac{(z+a)^{-s}}{2} \\ &+ \frac{(z+a)^{1-s}}{\Gamma(s)}\sum_{k=1}^{p-1}\frac{B_{2k}}{(2k)!}\frac{\Gamma(s+2k-1)}{(z+a)^{2k}}.\end{aligned} \tag{4.16}$$

Then the remainder term $R_{a,p}$ is given by

$$R_{a,p} = \frac{B_{2p}}{(2p)!}\frac{\Gamma(s+2p)}{\Gamma(s)}\zeta(s+2p, z+a+\theta) \tag{4.17}$$

with some $0 < \theta < 1$ and defined for $\Re s + 2p > 1$.

Proof. We split the zeta function (4.9) into two sums

$$\zeta(s,z) = \sum_{n=0}^{a-1}(z+n)^{-s} + \lim_{b\to\infty}\sum_{n=a}^{b}(z+n)^{-s}. \tag{4.18}$$

We approximate the second sum by applying the Euler-MacLaurin formula (4.4), with $f(n) = (z+n)^{-s}$, which leads to

$$\begin{aligned}\sum_{n=a}^{b}(z+n)^{-s} &= \int_a^b (z+t)^{-s}\,dt + \frac{(z+b)^{-s} + (z+a)^{-s}}{2} \\ &+ \sum_{k=1}^{p-1}\frac{B_{2k}}{(2k)!}\left(f^{(2k-1)}(b) - f^{(2k-1)}(a)\right) + R\end{aligned} \tag{4.19}$$

The integral can be calculated explicitly

$$\int_a^b (z+t)^{-s}\,dt = \frac{(z+b)^{-s+1}}{-s+1} - \frac{(z+a)^{-s+1}}{-s+1}. \tag{4.20}$$

In the sum over k we apply formula (4.14) to get

$$\begin{aligned}&\sum_{k=1}^{p-1}\frac{B_{2k}}{(2k)!}(-1)^{2k-1}\frac{\Gamma(s+2k-1)}{\Gamma(s)}\left((z+b)^{-s-2k+1} - (z+a)^{-s-2k+1}\right) = \\ &\sum_{k=1}^{p-1}\frac{B_{2k}}{(2k)!}\frac{\Gamma(s+2k-1)}{\Gamma(s)}\left((z+a)^{-s-2k+1} - (z+b)^{-s-2k+1}\right)\end{aligned} \tag{4.21}$$

since $(-1)^{2k-1} = -1$.

In the limit $b \to \infty$ we see with (4.20) and (4.21), that the right-hand side of (4.19) converges for $\Re s > 1$ and is given as

$$\begin{aligned}\sum_{n=a}^{\infty}(z+n)^{-s} &= \frac{(z+a)^{1-s}}{s-1}+\frac{(z+a)^{-s}}{2}\\ &+ \frac{(z+a)^{1-s}}{\Gamma(s)}\sum_{k=1}^{p-1}\frac{B_{2k}}{(2k)!}\frac{\Gamma(s+2k-1)}{(z+a)^{2k}}\\ &+ R\end{aligned}$$

Define next $\zeta_{a,p}$ by

$$\begin{aligned}\zeta_{a,p}(s,z) &= \sum_{n=0}^{a-1}(z+n)^{-s}+\frac{(z+a)^{1-s}}{s-1}+\frac{(z+a)^{-s}}{2}\\ &+ \frac{(z+a)^{1-s}}{\Gamma(s)}\sum_{k=1}^{p-1}\frac{B_{2k}}{(2k)!}\frac{\Gamma(s+2k-1)}{(z+a)^{2k}}.\end{aligned} \tag{4.22}$$

By using formula (4.5) we get for the remainder term R

$$\begin{aligned}R &= \frac{B_{2p}}{(2p)!}\sum_{k=a}^{b-1}(-1)^{2p}\frac{\Gamma(s+2p)}{\Gamma(s)}(z+k+\theta)^{-s-2p}\\ &= \frac{B_{2p}}{(2p)!}\frac{\Gamma(s+2p)}{\Gamma(s)}\left(\sum_{k=a}^{\infty}(z+k+\theta)^{-s-2p}-\sum_{k=b}^{\infty}(z+k+\theta)^{-s-2p}\right)\\ &= \frac{B_{2p}}{(2p)!}\frac{\Gamma(s+2p)}{\Gamma(s)}\left(\zeta(s+2p,z+a+\theta)-\zeta(s+2p,z+b+\theta)\right).\end{aligned}$$

We see that R is well defined for $\Re s + 2p > 1$. Define $R_{a,p} := \lim_{b\to\infty} R$, then one has

$$R_{a,p} = \frac{B_{2p}}{(2p)!}\frac{\Gamma(s+2p)}{\Gamma(s)}\zeta(s+2p,z+a+\theta) \tag{4.23}$$

for some $0 < \theta < 1$. □

The function $\zeta_{a,p}$ in (4.16) can be determined through a recursion relation as follows:

Lemma 4.2.5. *The expression*

$$\frac{(z+a)^{1-s}}{\Gamma(s)}\sum_{k=1}^{p-1}\frac{B_{2k}}{(2k)!}\frac{\Gamma(s+2k-1)}{(z+a)^{2k}}$$

can be written as

$$\frac{s(z+a)^{-1-s}}{2}\left(B_2+\rho_4\left(B_4+\cdots+\rho_{2(p-2)}\left(B_{2(p-2)}+\rho_{2(p-1)}B_{2(p-1)}\right)\right)\right)$$

with

$$\rho_{2k} = \frac{(s+2k-2)(s+2k-3)}{2k(2k-1)}(z+a)^{-2}.$$

Proof. Rewriting $\sum_{k=1}^{p-1} \frac{B_{2k}}{(2k)!} \frac{\Gamma(s+2k-1)}{(z+a)^{2k}} = \sum_{k=1}^{p-1} B_{2k} a_{2k}$, with $a_{2k} = \frac{\Gamma(s+2k-1)}{(z+a)^{2k}(2k)!}$ we get

$$\begin{aligned} a_{2(k-1)} &= \frac{\Gamma(s+2k-2-1)}{(z+a)^{2k-2}(2k-2)!} \\ &= \frac{\Gamma(s+2k-3)\,2k\,(2k-1)}{(z+a)^{2k}(2k)!\,(z+a)^{-2}} \\ &= \frac{\Gamma(s+2k-1)\,2k\,(2k-1)}{(z+a)^{2k}(2k)!\,(z+a)^{-2}\,(s+2k-3)\,(s+2k-2)} \\ &= a_{2k}\frac{2k\,(2k-1)}{(z+a)^{-2}\,(s+2k-3)\,(s+2k-2)} \end{aligned}$$

Next define

$$\rho_{2k} = \frac{a_{2k}}{a_{2(k-1)}} = \frac{(s+2k-3)\,(s+2k-2)}{(z+a)^2\,2k\,(2k-1)}.$$

Then $\sum_{k=1}^{p-1} B_{2k} a_{2k} = a_2\left(B_2 + \rho_4\left(B_4 + \cdots + \rho_{2(p-2)}\left(B_{2(p-2)} + \rho_{2(p-1)} B_{2(p-1)}\right)\right)\right)$ with $a_2 = \frac{\Gamma(s+2-1)}{(z+a)^2(2)!} = \frac{\Gamma(s+1)}{(z+a)^2 2} = \frac{s\Gamma(s)}{(z+a)^2 2}$. This concludes our proof. □

Next we want to investigate $R_{a,p}$ with respect to its dependence on a and p. First of all, it may be a little surprising that the Hurwitz zeta function appears again in $R_{a,p}$, but since it is shifted in both arguments one can evaluate it for $\Re s + 2p > 1$. Let us assume $p \gg 1$, so that we can use for $(2p)!$ and B_{2p} the asymptotic formulas (3.6) and (4.8). Then we get for $p \to \infty$

$$\frac{\left|B_{2p}\right|}{(2p)!} \sim 2\,(2\pi)^{-2p}\,.$$

To give an idea of what $p \gg 1$ means, we set $p = 10$, then $2\,(2\pi)^{-2p} = 2.17486662381E-16$, whereas the actual value is $\frac{B_{2p}}{(2p)!} = -2.17486869855E-16$. We see that the asymptotic of $\frac{B_{2p}}{(2p)!}$ is already quite close to the actual value for a relatively small value of p. For the gamma function $\Gamma(s+2p)$ we can write according to (3.7)

$$\Gamma(s+2p) \sim \sqrt{2\pi} e^{-s-2p} (s+2p)^{s+2p-1/2}.$$

For a and p big enough we can approximate the Hurwitz zeta function by

$$\zeta(s+2p, z+a+\theta) \sim (z+a)^{-s-2p}\,.$$

So we finally get

$$\begin{aligned} |R_{a,p}| &\sim \frac{1}{\Gamma(s)} 2\,(2\pi)^{-2p}\,\sqrt{2\pi} e^{-s-2p} (s+2p)^{s+2p-1/2}\,(z+a)^{-s-2p} \\ &\sim \frac{1}{\Gamma(s)} \frac{2\sqrt{2\pi}}{(2\pi)^{2p}\sqrt{s+2p}} \left(\frac{s+2p}{e\,(z+a)}\right)^{s+2p}. \end{aligned}$$

Since we assume that p is big enough, the only problem that could appear is the term $\left(\frac{s+2p}{e(z+a)}\right)^{s+2p}$. Assuming $a \gg z$, we need the condition $\Re s + 2p < ea$ and therefore $a > \frac{\Re s+2p}{e}$. This means that when we increase p or $\Re s$, we need to increase a. Note that if we increase only p our approximation does not necessarily get better. On the other hand, because of the factor $\frac{1}{\Gamma(s)}$ the approximation gets better if we increase $\Re s$. The same holds when increasing $|z|$.

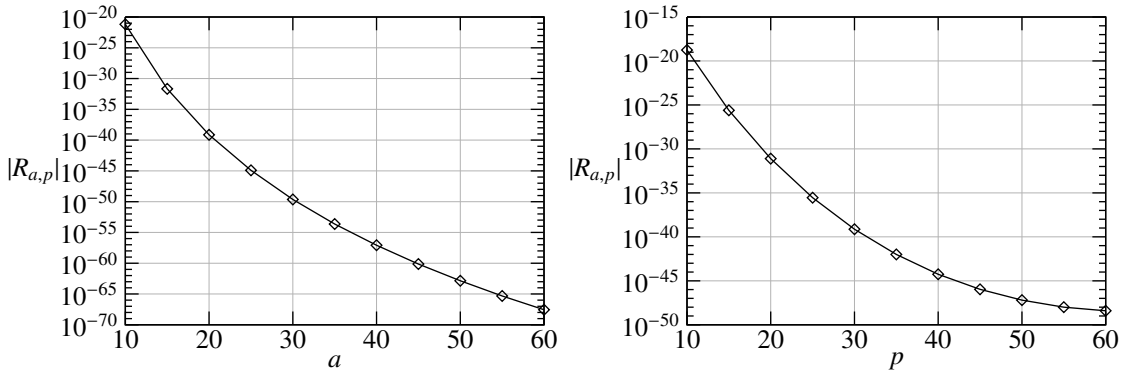

Figure 4.1: Remainder term $|R_{a,p}|$ for $p := 30$ and for $a := 20$ (Hurwitz zeta function)

Figure 4.1 shows the dependence of $|R_{a,p}|$ on a and on p. We evaluate $R_{a,p}$ using formula (4.17) with $s = 0.14 + 10i$ and $z = 1/10$. In the first plot p is set to a constant value $p = 30$, in the second plot a is set to a constant value $a = 20$. The value of the approximation $\zeta_{a,p}$ of the Hurwitz zeta function for this s and z is $0.373790681505400013 - 2.39444292468710652i$. We see that in both figures $|R_{a,p}|$ is decreasing rather fast; indeed if we increased a and p at the same time the decrease of $|R_{a,p}|$ would be even stronger.

4.2.2 The implementation of the Hurwitz zeta function for $s \in \mathbb{C}, z \in \mathbb{Q}$

We want to present the basic ideas for implementing the Hurwitz zeta function by using a pseudo code. Of course, the implementation in a real programming language is much more complicated.

We apply the functional equation (4.11), denoted by `Apply_Functional_Equation`, if we evaluate the Hurwitz zeta function for $\Re s < 0$. If the integer part of $[z] \geq 1$ we set $z_r = z - [z]$ and apply first the functional equation (4.11) for z_r, then apply equation (4.12). The function `Apply_Functional_Equation` uses `Zeta_Function_EM`, to evaluate the sum in (4.11). Also for $\Re s \geq 0$ we use the function `Zeta_Function_EM`, which tries to find the optimal values of p and a for the approximation of the Hurwitz zeta function (4.16). To do this, we choose $p = 30$ and $a = 20$, and increase a by one until the result no longer changes. Formula (4.16) is implemented in the function `compute_formula_zeta`. Obviously, when increasing the parameter a or p the evaluation of formula (4.16) in function `compute_formula_zeta` becomes rather slow. On the other hand, if too-small values of a and p are used to begin with, it might take many iterations in `Zeta_Function_EM` to find the optimal a and p. One can extend the function `Zeta_Function_EM` and also adjust p during the iterations, but this was not necessary for our computations. Since in the worst case there could be infinitely many iterations, a counter should also be implemented for the number of iterations and the program should be terminated with an error message in the case of too many iterations. For our proposes it is enough to use this implementation only for $z \in \mathbb{Q}$. For $z \in \mathbb{R}$ formula (4.16) works still very well, but unfortunately we cannot use the functional equation (4.11) anymore. So instead of using this functional equation p has to be increased to evaluate the Hurwitz zeta function for $\Re s < 0$.

4.2.3 Test of the implementation

To test our implementation we compared it first with other implementations, e.g., those of Strömberg [Str07], Maple and Mathematica (the last one only for real-valued arguments).

Another good way to check our implementation is to see if it fulfills the functional equation (4.11). For $\Re s > 1$ we can compare our implementation with the original definition (4.9). Of course, the evaluation of formula (4.9) is much slower than our implementations, but here it does not matter. Below we present some

Listing 4.1: Hurwitz zeta function

```
Zeta_Hurwitz(s,z):
        if Real_Part(s) < 0
                N = IntegerPart(z)
                zr = z - N
                zeta = Apply_Functional_Equation(s,zr)
                if N not equal 0
                        zeta = zeta - Sum_N(s,zr,N)
        else
                zeta = Zeta_Function_EM(s,z)
        return zeta

Zeta_Function_EM(s,z):
        a = 20
        p = 30
        last = 0
        repeat:
                result = compute_formula_zeta(s,z,a,p)
                if |last - result| < delta
                        return result
                a = a + 1
                last = result
```

of our results for arguments that we will use in our later computations. EM denotes our implementation of formula (4.16), FE is the functional equation (4.11) and Sum the definition (4.9). The time is the average of 100 runs.

4.3 The Lerch transcendent and the Lerch zeta function

The Lerch transcendent [Ler87] is defined as

$$\Phi(\alpha, s, z) = \sum_{n=0}^{\infty} \alpha^n (z+n)^{-s} \tag{4.24}$$

with $|\alpha| < 1$, $z \neq 0$, $z \notin \mathbb{Z}_<$ and $s \in \mathbb{C}$. An integral representation [Erd53] is given by

$$\Phi(\alpha, s, z) = \frac{1}{\Gamma(s)} \int_0^{\infty} \frac{t^{s-1} e^{-zt}}{1 - \alpha e^{-t}} dt \tag{4.25}$$

for $\Re z > 0$ and either $|\alpha| \leq 1$, $\alpha \neq 1$, $\Re s > 0$ or $\alpha = 1$, $\Re s > 1$. For $|\alpha| = 1$ we set $\alpha = \exp 2\pi i\lambda$ then the function (4.24) becomes the Lerch zeta function

$$\zeta_L(\lambda, s, z) = \sum_{n=0}^{\infty} e^{2\pi i \lambda n} (z+n)^{-s}. \tag{4.26}$$

It converges absolutely either for $\lambda \in \mathbb{R} \setminus \mathbb{Z}$ and $\Re s > 0$ or $\lambda \in \mathbb{Z}$ and $\Re s > 1$. Note that for $\lambda \in \mathbb{Z}$ the function $\zeta_L(\lambda, s, z)$ is the Hurwitz zeta function $\zeta(s, z)$.

Table 4.1: Performance and accuracy of the approximation of the Hurwitz zeta function

args.	impl.		time
s=0.95+10I	EM	-1.008766737050193084+8.377693345938255443E-1I	1.98ms
z=3/4	FE	-1.008766737050193084+8.377693345938255443E-1I	9.33ms
	|EM-FE|	4.338090584480014223E-42	
	Sum	—	—
	|EM-Sum|	—	—
s=9.2+0.5I	EM	1.030324268162233376E8+1.754153327256336148E8I	1.72ms
z=1/8	FE	1.030324268162233376E8+1.754153327256336148E8I	83.11ms
	|EM-FE|	2.229884573489399883E-23	
	Sum	1.030324268162233376E8+1.754153327256336148E8I	386.34ms
	|EM-Sum|	6.436406490650466801E-32	
s=68.3+5.2I	EM	9.594951948969788693E-8-2.204893913820418093E-7I	2.53ms
z=5/4	FE	—	—
	|EM-FE|	—	
	Sum	9.594951948969788693E-8-2.204893913820418093E-7I	3.74ms
	|EM-Sum|	0	
s=0.5+14.3I	EM	3.293795504174408752E-1+2.499637152889994613I	2.74ms
z=1/4	FE	3.293795504174408752E-1+2.499637152889994613I	10.92ms
	|EM-FE|	4.992194978284140561E-40	
	Sum	—	—
	|EM-Sum|	—	
s=-8.5+4.8I	EM	-6.99742914948200166E-1+1.5767621216266489171	41.07ms
z=6/8	FE	-6.99742914948200166E-1+1.5767621216266489171	7.67ms
	|EM-FE|	2.612739201181641559E-29	
	Sum	—	—
	|EM-Sum|	—	
s=1.7	EM	4.62011510535879058	1.84ms
z=1/2	FE	4.62011510535879058	4.17ms
	|EM-FE|	2.62360294512064383E-44	
	Sum	—	—
	|EM-Sum|	—	

Results from widmo version *5.1.5*. Precision 160 bits (49 digits).

Lemma 4.3.1. *Since $\zeta_L(\lambda+N,s,z)=\zeta_L(\lambda,s,z)$ for $N\in\mathbb{Z}$ the parameter λ can be restricted to $-\frac{1}{2}<\lambda\leq\frac{1}{2}$, $\lambda\neq 0$.*

Proof. Since $e^{2\pi i(\lambda+N)}=e^{2\pi i\lambda}$ for $N\in\mathbb{Z}$, we have $\zeta_L(\lambda+N,s,z)=\zeta_L(\lambda,s,z)$, so we see that we can restrict λ to $0<\lambda<1$, or choosing a different branch $-\frac{1}{2}<\lambda\leq\frac{1}{2}$ with $\lambda\neq 0$. □

The Lerch transcendent (4.24) fulfills the following transformation formula [Erd53]:

$$\begin{aligned}\Phi(\alpha,s,z) &= \frac{i\alpha^{-z}}{(2\pi)^{1-s}}\Gamma(1-s)\left\{\exp\left(-i\pi\frac{s}{2}\right)\Phi\left(e^{-2\pi iz},1-s,\frac{\ln\alpha}{2\pi i}\right)\right.\\ &- \left.\exp\left(i\pi\left(\frac{s}{2}+2z\right)\right)\Phi\left(e^{2\pi iz},1-s,1-\frac{\ln\alpha}{2\pi i}\right)\right\}\end{aligned}\tag{4.27}$$

for $0<z\leq 1$. Since we want to use this formula for $z>1$, we need the following lemma:

Lemma 4.3.2. *The Lerch transcendent fulfills for $z+N$, with $N\in\mathbb{Z}$ positive and $z\in\mathbb{C}$, the equation*

$$\Phi(\alpha,s,z+N)=\alpha^{-N}\left(\Phi(\alpha,s,z)-\sum_{n=0}^{N-1}\alpha^n(z+n)^{-s}\right).\tag{4.28}$$

Proof. By definition we get $\Phi(\alpha,s,z+N)=\sum_{n=0}^{\infty}\alpha^n(z+N+n)^{-s}=\sum_{n=N}^{\infty}\alpha^{n-N}(z+n)^{-s}=\alpha^{-N}\sum_{n=0}^{\infty}\alpha^n(z+n)^{-s}-\alpha^{-N}\sum_{n=0}^{N-1}\alpha^n(z+n)^{-s}$. □

Following an idea by Strömberg we have:

Lemma 4.3.3. *The Lerch zeta function for $\lambda=\frac{p}{q}\in\mathbb{Q}$ can be written as*

$$\zeta_L\left(\frac{p}{q},s,z\right)=\sum_{m=0}^{q-1}\frac{e^{2\pi i\frac{p}{q}m}}{q^s}\zeta\left(s,\frac{z+m}{q}\right)\tag{4.29}$$

with ζ the Hurwitz zeta function.

Proof. The Lerch zeta function is given by $\zeta_L(\lambda,s,z)=\sum_{n=0}^{\infty}e^{2\pi i\lambda n}(z+n)^{-s}$. Setting $n=m+rl$ the sum $\sum_{n=0}^{\infty}$ can be written as

$$\begin{aligned}\sum_{n=0}^{\infty}e^{2\pi i\lambda n}(z+n)^{-s} &= \sum_{m=0}^{r-1}\sum_{l=0}^{\infty}e^{2\pi i\lambda(m+rl)}(z+m+rl)^{-s}\\ &= \sum_{m=0}^{r-1}e^{2\pi i\lambda m}\sum_{l=0}^{\infty}e^{2\pi i\lambda rl}(z+m+rl)^{-s}\\ &= \sum_{m=0}^{r-1}\frac{e^{2\pi i\lambda m}}{r^s}\sum_{l=0}^{\infty}e^{2\pi i\lambda rl}\left(\frac{z+m}{r}+l\right)^{-s}\\ &= \sum_{m=0}^{r-1}\frac{e^{2\pi i\lambda m}}{r^s}\zeta_L\left(\lambda r,s,\frac{z+m}{r}\right).\end{aligned}$$

Now assume $\lambda=\frac{p}{q}\in\mathbb{Q}$ and set $r=q$. Then $\zeta_L\left(\lambda q,s,\frac{z+m}{r}\right)=\zeta_L\left(p,s,\frac{z+m}{r}\right)$, and since $p\in\mathbb{Z}$ this is equal to $\zeta\left(s,\frac{z+m}{r}\right)$. So we get finally for $\lambda=\frac{p}{q}\in\mathbb{Q}$:

$$\zeta_L\left(\frac{p}{q},s,z\right)=\sum_{m=0}^{q-1}\frac{e^{2\pi i\frac{p}{q}m}}{q^s}\zeta\left(s,\frac{z+m}{q}\right).$$ □

We want to mention that Mühlenbruch uses another method to compute the Lerch zeta function in terms of theta functions in [Müh03].

4.3.1 Application of the Euler-MacLaurin formula

We want to apply the Euler-MacLaurin formula (4.4) to the Lerch transcendent

$$\Phi(\alpha, s, z) = \sum_{n=0}^{\infty} \alpha^n (z+n)^{-s}.$$

For this we need the following lemma:

Lemma 4.3.4. *Let $n \in \mathbb{N}$, $z, s \in \mathbb{C}$ and $\alpha \in \mathbb{C}$ with $|\alpha| \leq 1$. The k-th derivative $\frac{\partial^k}{\partial \eta^k} \alpha^\eta (z+\eta)^{-s}|_{\eta=n}$ is given by*

$$\frac{\partial^k}{\partial \eta^k} \alpha^\eta (z+\eta)^{-s}|_{\eta=n} = \alpha^n \sum_{l=0}^{k} \binom{k}{l} (\ln \alpha)^{k-l} (-1)^l \frac{\Gamma(s+l)}{\Gamma(s)} (z+n)^{-s-l} \tag{4.30}$$

Note that $\frac{\partial^k}{\partial \eta^k} \alpha^\eta (z+\eta)^{-s} = \alpha^{\eta-z} \frac{\partial^k}{\partial z^k} \alpha^z (z+\eta)^{-s}$.

Proof. By using the generalized product rule we get

$$\frac{\partial^k}{\partial \eta^k} \alpha^\eta (z+\eta)^{-s} = \sum_{l=0}^{k} \binom{k}{l} \left(\frac{\partial^{k-l}}{\partial \eta^{k-l}} \alpha^\eta \right) \left(\frac{\partial^l}{\partial \eta^l} (z+\eta)^{-s} \right).$$

With $\frac{\partial^k}{\partial \eta^k} \alpha^\eta|_{\eta=n} = (\ln \alpha)^k \alpha^n$ and lemma 4.2.3 the proof follows. □

Lemma 4.3.5. *For $z, s \in \mathbb{C}$ and $\alpha \in \mathbb{C}$ with $|\alpha| \leq 1$ and $\alpha \neq 1$ one has*

$$\int_a^b \alpha^t (z+t)^{-s} dt = \alpha^{-z} (-\ln \alpha)^{s-1} \left\{ \Gamma(1-s, -(z+a)\ln \alpha) - \Gamma(1-s, -(z+b)\ln \alpha) \right\} \tag{4.31}$$

with $\Gamma(s,z)$ the incomplete gamma function. For $b \to \infty$ and $\Re s > 0$ we get

$$\int_a^\infty \alpha^t (z+t)^{-s} dt = \alpha^{-z} (-\ln \alpha)^{s-1} \Gamma(1-s, -(z+a)\ln \alpha). \tag{4.32}$$

Proof. In the integral $\int_a^b \alpha^t (z+t)^{-s} dt$ we substitute k for $z+t$ and get $\int_{z+a}^{z+b} \alpha^{k-z} k^{-s} dk$. Setting $k = -u(\ln \alpha)^{-1}$ leads to

$$\int_a^b \alpha^t (z+t)^{-s} dt = \alpha^{-z} (-\ln \alpha)^{s-1} \int_{-(z+a)\ln \alpha}^{-(z+b)\ln \alpha} e^{-u} u^{-s} du.$$

Hence we can write the integral as the difference of two lower incomplete gamma functions γ

$$\int_{-(z+a)\ln \alpha}^{-(z+b)\ln \alpha} e^{-u} u^{-s} du = \gamma(1-s, -(z+b)\ln \alpha) - \gamma(1-s, -(z+a)\ln \alpha),$$

but since $\gamma(s,x) = \Gamma(s) - \Gamma(s,x)$

$$\int_{-(z+a)\ln \alpha}^{-(z+b)\ln \alpha} e^{-u} u^{-s} du = \Gamma(1-s, -(z+a)\ln \alpha) - \Gamma(1-s, -(z+b)\ln \alpha).$$

We now want to consider the limit $b \to \infty$. We claim that $\Gamma(1-s, -(z+b)\ln \alpha)$ vanishes in this limit. Since $b \gg z$ we have $-(z+b)\ln \alpha \sim -b \ln \alpha$. From (3.12) we get

$$\Gamma(1-s, -b\ln \alpha) = \frac{e^{b\ln \alpha} (-b\ln \alpha)^{1-s}}{-b\ln \alpha +} \frac{s}{1+} \frac{1}{-b\ln \alpha +} \frac{1+s}{1+} \frac{2}{-b\ln \alpha +} \cdots \sim e^{b\ln \alpha} (-b\ln \alpha)^{-s}$$

Since $|\alpha| \leq 1$ we have $|\Gamma(1-s, -b\ln \alpha)| \sim |b|^{-s} |\ln \alpha|^{-s} \sim |b|^{-s} \to 0$ for $\Re s > 0$. □

Proposition 4.3.6. *By using the Euler-MacLaurin formula (4.4) the Lerch transcendent*

$$\Phi(\alpha, s, z) = \sum_{n=0}^{\infty} \alpha^n (z+n)^{-s}$$

can be written for some $a, p \in \mathbb{Z}$ as

$$\Phi(\alpha, s, z) = \Phi_{a,p}(\alpha, s, z) + R_{a,p} \tag{4.33}$$

defined for $\Re s > 0$ and $|\arg \alpha| < \pi$. The function $\Phi_{a,p}(\alpha, s, z)$ is given by

$$\begin{aligned} \Phi_{a,p}(\alpha, s, z) &= \sum_{n=0}^{a-1} \alpha^n (z+n)^{-s} + \alpha^{-z} (-\ln \alpha)^{s-1} \Gamma(1-s, -(z+a)\ln\alpha) \\ &+ \frac{\alpha^a (z+a)^{-s}}{2} \\ &+ \alpha^a \sum_{k=1}^{p-1} \frac{B_{2k}}{(2k)!} \sum_{l=0}^{2k-1} \binom{2k-1}{l} (\ln\alpha)^{2k-1-l} (-1)^{l+1} \frac{\Gamma(s+l)}{\Gamma(s)} (z+a)^{-s-l}. \end{aligned} \tag{4.34}$$

Then the remainder term $R_{a,p}$ is given by

$$R_{a,p} = \frac{B_{2p}}{(2p)!} \sum_{l=0}^{2p} \binom{2p}{l} (\ln\alpha)^{2p-l} (-1)^l \frac{\Gamma(s+l)}{\Gamma(s)} \Phi(\alpha, s+l, z+a+\theta) \tag{4.35}$$

with some $0 < \theta < 1$ and defined for $\Re s > 0$.

Note that contrary to the case of the Hurwitz zeta function, this approximation is only valid for $\Re s > 0$. For smaller values of $\Re s$ one has to use the functional equation.

Proof. We split the Lerch transcendent into two sums

$$\Phi(\alpha, s, z) = \sum_{n=0}^{a-1} \alpha^n (z+n)^{-s} + \lim_{b\to\infty} \sum_{n=a}^{b} \alpha^n (z+n)^{-s}.$$

We approximate the second sum by applying the Euler-MacLaurin formula (4.4), with $f(n) = \alpha^n (z+n)^{-s}$. This leads to

$$\begin{aligned} \sum_{n=a}^{b} \alpha^n (z+n)^{-s} &= \int_a^b \alpha^t (z+t)^{-s}\, dt + \frac{\alpha^b (z+b)^{-s} + \alpha^a (z+a)^{-s}}{2} \\ &+ \sum_{k=1}^{p-1} \frac{B_{2k}}{(2k)!} \left(f^{(2k-1)}(b) - f^{(2k-1)}(a) \right) + R \end{aligned} \tag{4.36}$$

with R the remainder term. From lemma 4.3.5 we get for the integral

$$\begin{aligned} &\int_a^b \alpha^t (z+t)^{-s}\, dt = \\ &\alpha^{-z} (-\ln\alpha)^{s-1} \left\{ \Gamma(1-s, -(z+a)\ln\alpha) - \Gamma(1-s, -(z+b)\ln\alpha) \right\}. \end{aligned}$$

The sum over k we can rewrite by using lemma 4.3.4, as

$$\begin{aligned} &\sum_{k=1}^{p-1} \frac{B_{2k}}{(2k)!} \sum_{l=0}^{2k-1} \binom{2k-1}{l} (\ln\alpha)^{2k-1-l} (-1)^l \frac{\Gamma(s+l)}{\Gamma(s)} \\ &\left(\alpha^b (z+b)^{-s-l} - \alpha^a (z+a)^{-s-l} \right). \end{aligned}$$

In the limit $b \to \infty$, the right-hand side of (4.36) converges for $\Re s > 1$ to give

$$\begin{aligned}\sum_{n=a}^{\infty} \alpha^n (z+n)^{-s} &= \alpha^{-z} (-\ln\alpha)^{s-1} \Gamma(1-s, -(z+a)\ln\alpha) \\ &+ \frac{\alpha^a (z+a)^{-s}}{2} \\ &+ \sum_{k=1}^{p-1} \frac{B_{2k}}{(2k)!} \sum_{l=0}^{2k-1} \binom{2k-1}{l} (\ln\alpha)^{2k-1-l} (-1)^{l+1} \frac{\Gamma(s+l)}{\Gamma(s)} \alpha^a (z+a)^{-s-l} \\ &+ R.\end{aligned}$$

Next we define $\Phi_{a,p}$ as

$$\begin{aligned}\Phi_{a,p}(\alpha, s, z) &= \sum_{n=0}^{a-1} \alpha^n (z+n)^{-s} + \alpha^{-z} (-\ln\alpha)^{s-1} \Gamma(1-s, -(z+a)\ln\alpha) \\ &+ \frac{\alpha^a (z+a)^{-s}}{2} \\ &+ \sum_{k=1}^{p-1} \frac{B_{2k}}{(2k)!} \sum_{l=0}^{2k-1} \binom{2k-1}{l} (\ln\alpha)^{2k-1-l} (-1)^{l+1} \frac{\Gamma(s+l)}{\Gamma(s)} \alpha^a (z+a)^{-s-l}.\end{aligned}$$

By using formula (4.5) we get for R

$$\begin{aligned}R &= \frac{B_{2p}}{(2p)!} \sum_{k=a}^{b-1} \alpha^{k+\theta} \sum_{l=0}^{2p} \binom{2p}{l} (\ln\alpha)^{2p-l} (-1)^l \frac{\Gamma(s+l)}{\Gamma(s)} (z+k+\theta)^{-s-l} \\ &= \frac{B_{2p}}{(2p)!} \alpha^\theta \sum_{l=0}^{2p} \binom{2p}{l} (\ln\alpha)^{2p-l} (-1)^l \frac{\Gamma(s+l)}{\Gamma(s)} \\ &\quad \times \left(\sum_{k=a}^{\infty} \alpha^k (z+k+\theta)^{-s-l} - \sum_{k=b}^{\infty} \alpha^k (z+k+\theta)^{-s-l} \right) \\ &= \frac{B_{2p}}{(2p)!} \alpha^\theta \sum_{l=0}^{2p} \binom{2p}{l} (\ln\alpha)^{2p-l} (-1)^l \frac{\Gamma(s+l)}{\Gamma(s)} \\ &\quad \times (\Phi(\alpha, s+l, z+a+\theta) - \Phi(\alpha, s+l, z+b+\theta)).\end{aligned}$$

We see that this is well defined for $\Re s > 1$. For $b \to \infty$ we get for $R_{a,p} = \lim_{b\to\infty} R$

$$R_{a,p} = \frac{B_{2p}}{(2p)!} \sum_{l=0}^{2p} \binom{2p}{l} (\ln\alpha)^{2p-l} (-1)^l \frac{\Gamma(s+l)}{\Gamma(s)} \Phi(\alpha, s+l, z+a+\theta).$$

Now we can finally write $\Phi(\alpha, s, z) = \Phi_{a,p}(\alpha, s, z) + R_{a,p}$. □

Now we want to write down a recursion formula for the sum in the last term in (4.34):

Lemma 4.3.7. *The following identity holds:*

$$\begin{aligned}&\sum_{l=0}^{2k-1} \binom{2k-1}{l} (\ln\alpha)^{2k-1-l} (-1)^{l+1} \frac{\Gamma(s+l)}{\Gamma(s)} (z+a)^{-s-l} = \\ &-(\ln\alpha)^{2k-1} (z+a)^{-s} (1+\rho_1 (1+\rho_2 (1+\cdots+\rho_{2k-2} (1+\rho_{2k-1}))))\end{aligned}$$

with

$$\rho_l = -\frac{(2k-l)\,(s+l-1)}{l\,(\ln\alpha)\,(z+a)}.$$

Proof. Put $a_l := \binom{2k-1}{l}(\ln\alpha)^{2k-1-l}(-1)^{l+1}\frac{\Gamma(s+l)}{\Gamma(s)}(z+a)^{-s-l}$. Then we get for a_{l-1}

$$\begin{aligned}
a_{l-1} &= \binom{2k-1}{l-1}(\ln\alpha)^{2k-1-l+1}(-1)^{l-1+1}\frac{\Gamma(s+l-1)}{\Gamma(s)}(z+a)^{-s-l+1} \\
&= -\frac{(2k-1)!}{l!\,(2k-1-l)!}\frac{l}{(2k-l)}(\ln\alpha)^{2k-1-l}(\ln\alpha)(-1)^{l-1} \\
&\quad \frac{\Gamma(s+l)}{\Gamma(s)}(s+l-1)^{-1}(z+a)^{-s-l}(z+a) \\
&= -\binom{2k-1}{l}(\ln\alpha)^{2k-1-l}(-1)^{l+1}\frac{\Gamma(s+l)}{\Gamma(s)}(z+a)^{-s-l}\frac{l\,(\ln\alpha)\,(z+a)}{(2k-l)\,(s+l-1)} \\
&= -a_l\frac{l\,(\ln\alpha)\,(z+a)}{(2k-l)\,(s+l-1)}.
\end{aligned}$$

Define next

$$\rho_l := \frac{a_l}{a_{l-1}} = -\frac{(2k-l)\,(s+l-1)}{l\,(\ln\alpha)\,(z+a)}.$$

Then $\sum_{l=0}^{2k-1} a_l = a_0\,(1+\rho_1\,(1+\rho_2\,(1+\cdots+\rho_{2k-2}\,(1+\rho_{2k-1}))))$ for $a_0 = -(\ln\alpha)^{2k-1}(z+a)^{-s}$. This concludes our proof. □

Now we want to discuss $R_{a,p}$. Using the integral representation (4.25) we get

$$\begin{aligned}
R_{a,p} &= \frac{B_{2p}}{(2p)!}\sum_{l=0}^{2p}\binom{2p}{l}(\ln\alpha)^{2p-l}(-1)^l\frac{\Gamma(s+l)}{\Gamma(s)}\frac{1}{\Gamma(s+l)}\int_0^\infty\frac{t^{s+l-1}e^{-(z+a+\theta)t}}{1-\alpha e^{-t}}dt \\
&= \frac{B_{2p}}{(2p)!}\frac{1}{\Gamma(s)}\int_0^\infty\frac{t^{s-1}e^{-(z+a+\theta)t}}{1-\alpha e^{-t}}\sum_{l=0}^{2p}\binom{2p}{l}(\ln\alpha)^{2p-l}(-1)^l t^l dt \\
&= \frac{B_{2p}}{(2p)!}\frac{1}{\Gamma(s)}\int_0^\infty\frac{t^{s-1}e^{-(z+a+\theta)t}}{1-\alpha e^{-t}}(\ln\alpha-t)^{2p}\,dt.
\end{aligned}$$

We can also write this as

$$\begin{aligned}
R_{a,p} &= \frac{B_{2p}}{(2p)!}\frac{1}{\Gamma(s)}\int_0^\infty\frac{t^{s-1}}{1-\alpha e^{-t}}e^{-2p\left(\frac{(z+a+\theta)t}{2p}-\ln(\ln\alpha-t)\right)}dt \\
&= \frac{B_{2p}}{(2p)!}\frac{2p}{\Gamma(s)}\int_0^\infty\frac{(2pu)^{s-1}}{1-\alpha e^{-2pu}}e^{-2p((z+a+\theta)u-\ln(\ln\alpha-2pu))}du.
\end{aligned}$$

In the limit $2p\to\infty$ we get

$$\begin{aligned}
R_{a,p} &\sim_{2p\to\infty} \frac{B_{2p}}{(2p)!}\frac{(2p)^s}{\Gamma(s)}\int_0^\infty u^{s-1}e^{-2p((z+a+\theta)u-\ln(-2pu))}du \\
&= \frac{B_{2p}}{(2p)!}\frac{(2p)^s}{\Gamma(s)}\int_0^\infty u^{s-1}e^{-2p((z+a+\theta)u-\ln(2pu)-i\pi)}du \\
&= \frac{B_{2p}}{(2p)!}\frac{(2p)^{s+2p}\,e^{2\pi ip}}{\Gamma(s)}\int_0^\infty u^{s-1}e^{-2p((z+a+\theta)u-\ln u)}du.
\end{aligned}$$

To apply Laplace's method (2.8) we set $f(u) = u^{s-1}$ and $g(u) = (z + a + \theta)\, u - \ln u$. Then we have $g'(u) = z + a + \theta - \frac{1}{u}$ and $g''(u) = \frac{1}{u^2}$. The zero of $g'(c) = 0$ is given by $c = \frac{1}{z+a+\theta}$ and we have finally

$$R_{a,p} \quad \sim_{2p\to\infty} \quad \frac{B_{2p}}{(2p)!}\frac{(2p)^{s+2p}\, e^{2\pi i p}}{\Gamma(s)}(z + a + \theta)^{1-s}\, e^{-2p(1+\ln(z+a+\theta))}\sqrt{\frac{2\pi}{2p(z + a + \theta)^2}}.$$

We use $\frac{|B_{2p}|}{(2p)!} \sim_{2p\to\infty} 2\,(2\pi)^{-2p}$ from our discussion of the remainder term in the Hurwitz zeta function in the foregoing section and get

$$\begin{aligned}
|R_{a,p}| \quad &\sim_{2p\to\infty} \quad 2\,(2\pi)^{-2p+\frac{1}{2}}\,\frac{(2p)^{s+2p-\frac{1}{2}}}{|\Gamma(s)|}\,|z + a + \theta|^{-s}\, e^{-2p(1+\ln(z+a+\theta))} \\
&\sim_{2p\to\infty} \quad 2\,(2\pi)^{-2p}\,\frac{(2p)^{2p}}{|\Gamma(s)|}\,|z + a + \theta|^{-s}\, e^{-2p(1+\ln(z+a+\theta))} \\
&\sim_{2p\to\infty} \quad \frac{2}{(2\pi)^{2p}\,|\Gamma(s)|\,|z + a + \theta|^{s}} e^{-2p(1+\ln(z+a+\theta)-\ln(2p))}.
\end{aligned}$$

We can assume that $a \gg |z| + \theta$ and therefore

$$|R_{a,p}| \quad \sim_{2p\to\infty,a\to\infty} \quad \frac{2}{(2\pi)^{2p}\,|\Gamma(s)|\,|a|^{s}} e^{-2p(1+\ln(a)-\ln(2p))}. \tag{4.37}$$

Now we see that the term $e^{-2p(1+\ln(a)-\ln(2p))}$ is mainly responsible of the decrease of $R_{a,p}$ for $a \to \infty$ and $p \to \infty$. We need the condition $1 + \ln\frac{a}{2p} > 0$, and hence $a > \frac{2p}{e}$. This condition is almost the same as the one we found in the case of the Hurwitz zeta function. The problem is that this is a rather rough estimate of $R_{a,p}$ when we first let $2p \to \infty$ and afterwards $a \to \infty$; we would probably get a better estimate if we let both variables go to infinity at the same time.

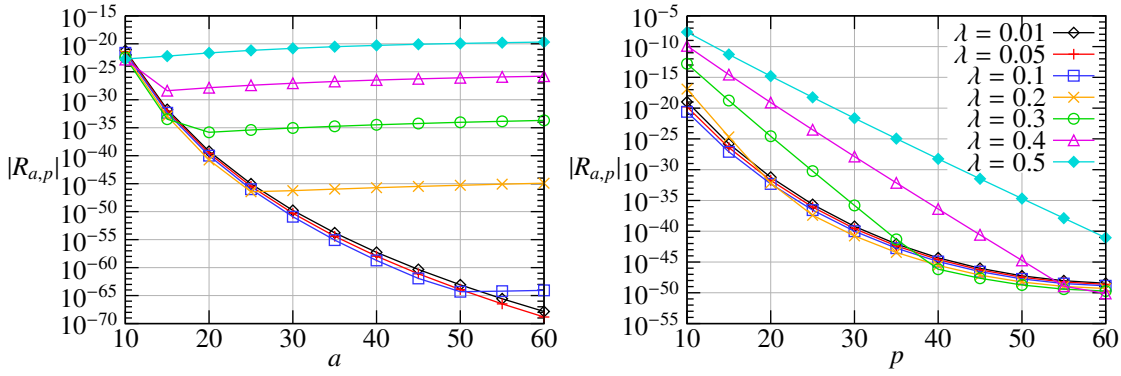

Figure 4.2: Remainder term $|R_{a,p}|$ for $p := 30$ and for $a := 20$ (Lerch zeta function)

Figure 4.2 shows the dependence of $|R_{a,p}|$ on a and p when evaluating formula (4.35). We choose $\beta = 0.14 + 10i$, $z = \frac{1}{10}$ and $\alpha = \exp 2\pi i\lambda$, and did calculations for different values of λ. In the first plot p is set to a constant value $p = 30$ and in the second plot a is set to a constant value $a = 20$. We see that $R_{a,p}$ depends on λ: when λ grows, one has to increase p to make $|R_{a,p}|$ sufficiently small. We see also, that increasing a helps only up to a certain value, after which $|R_{a,p}|$ stays almost constant. Unfortunately, we can not see this dependence on λ in our approximation (4.37) of $|R_{a,p}|$.

4.3.2 The Implementation of the Lerch zeta function for $s \in \mathbb{C}$, $z \in \mathbb{Q}$ and $\lambda \in \mathbb{R}$

As in the case of the Hurwitz zeta function we want to present the basic ideas for the implementation of the Lerch zeta function by using a pseudo code. The implementation in a real programming language is again much more complicated.

We have implemented the Lerch zeta function, i.e. the Lerch transcendent for the value $\alpha = \exp 2\pi i\lambda$. The function `Zeta_Lerch` chooses which implementation to use to compute the Lerch zeta function: For $\lambda \in \mathbb{Z}$ it uses the implementation `Zeta_Hurwitz` of the Hurwitz zeta function, which is given in listing 4.1. If $0 < \Re s < 1$ and the parameter `use_functional_equation` is set to a non-zero value then it checks if $\lambda \in \mathbb{Q}$ and the denominator of λ is smaller than some constant `MaxQ`; if so it then computes the value of the zeta function by using the sum over Hurwitz zeta functions given in (4.29). This formula is implemented in the function `Sum_Over_Hurwitz_Zeta` which also uses the implementation `Zeta_Hurwitz`. Otherwise if $\Re s < 1$ and the parameter `use_functional_equation` is set to a non-zero value, the Lerch zeta function is computed by the functional equation (4.27) denoted by `Apply_Functional_Equation`. If the integer part $[z] \geq 1$ we set $z_r = z - [z]$ and apply first the functional equation (4.27) for z_r and then apply equation (4.28), which is implemented in `Apply_Formula_Sum_N`. If $\Re s \geq 1$ or the parameter `use_functional_equation` is set to zero, it again checks if $\lambda \in \mathbb{Q}$ and the denominator of λ is smaller than `MaxQ`; if this is the case it computes the Lerch zeta function by formula (4.29). Otherwise it uses the function `Zeta_Function_EM`, which tries to find the optimal values of p and a for the approximation of the Lerch zeta function (4.34). To do this it sets $a = 15$ and $p = 40$ as initial values. The `while` statements at the beginning of `Zeta_Function_EM` make sure that λ is between -0.5 and 0.5, see lemma 4.3.1 for details. The functions `Choose_a` and `Choose_p` choose initial values for a and p depending on the values of s, z and λ; we implemented this by using a look-up table. Then the parameter a is increased until the result no longer changes. The formula (4.34) is implemented in the function `compute_formula_zeta`. Care must be taken about the initial values of the parameters a and p; it took us a long time to find the optimal values as s, z and λ change. It is useful to use a counter for the iterations and terminate the program with an error message in case there are too many iterations. The value of p can also be increased during the iterations, but this was not necessary for our computations. The only problem, which could occur if we extended this implementation to $z \in \mathbb{R}$, is in the function `Sum_Over_Hurwitz_Zeta`, since this function uses the implementation of the Hurwitz zeta function, for which we only have a functional equation if $z \in \mathbb{Q}$. The speed of the implementations must be compared and a decision made regarding which one to use - see also the next section. Among other things this has impact on the value of `MaxQ`.

4.3.3 Test of the implementation

To our knowledge only very few successful implementations of the Lerch zeta functions exist. Unfortunately there are also implementations which give incorrect results[1], and other implementations are limited in their arguments, e.g., they are restricted to only real numbers etc.

Indeed, we did not find any implementation with which we could compare the results of our implementation. Fortunately, as we mentioned in this chapter, there are several ways to compute the Lerch zeta function. We check if our implementation fulfills the functional equation (4.27). For $\Re s > 1$ we can also use the definition (4.24) of the Lerch transcendent with $\alpha = \exp 2\pi i\lambda$, and for $\lambda \in \mathbb{Q}$ we can perform the sum over the Hurwitz zeta functions (4.29). In the next table, we present some of the results, EM denotes formula (4.34), FE is the functional equation (4.27), Sum is the definition of the Lerch zeta function (4.24) and HSum is the sum over the Hurwitz zeta functions (4.29). The time is average of 100 runs.

[1] The implementation in *Mathematica* of the Lerch zeta transcendent, is actually an implementation of the function $\sum_{n=0}^{\infty} \alpha^n ((z+n)^2)^{-s/2}$. And the implementation of the Hurwitz zeta function is analog. See http://functions.wolfram.com/ZetaFunctionsandPolylogarithms/LerchPhi/02/ and http://functions.wolfram.com/ZetaFunctionsandPolylogarithms/Zeta2/02/

Listing 4.2: Lerch zeta function

```
Zeta_Lerch(s,z,l,use_functional_equation):
        if l is integer
                zeta = Zeta_Hurwitz(s,z)
        else if Real_Part(s) < 1 and use_functional_equation
                if Real_Part(s) > 0 and l is rational
                   and Denominator(l) < MaxQ
                        zeta = Sum_Over_Hurwitz_Zeta(s,z,l)
                else
                        N = IntegerPart(z)
                        zr = z - N
                        zeta = Apply_Functional_Equation(s,zr,l)
                        if N not equal 0
                                zeta = Apply_Formula_Sum_N(zeta,s,zr,N)
        else if l is rational and Denominator(l) < MaxQ
                zeta = Sum_Over_Hurwitz_Zeta(s,z,l)
        else
                zeta = Zeta_Function_EM(s,z,l)
        return zeta

Zeta_Function_EM(s,z,l):
        a = 15
        p = 40

        while l > 0.5
                l = l - 1
        while l < -0.5
                l = l + 1
        a = Choose_a(s,z,l,a)
        p = Choose_p(s,z,l,p)
        last = 0
        repeat:
                result = compute_formula_zeta(s,z,l,a,p)
                if |last - result| < delta
                        return result
                a = a + 1
                last = result
```

Table 4.2: Performance and accuracy of the approximation of the Lerch zeta function

args .	impl.		time
s=0.95+10I	EM	-2.3164668711303766+1.5541812187737106E-1I	13.96ms
z=3/4	FE	-2.3164668711303766+1.5541812187737106E-1I	17.04ms
λ=0.25	|EM-FE|	7.734575210145233412E-42	
	Sum	—	
	|EM-Sum|	—	
	HSum	-2.3164668711303766+1.5541812187737106E-1I	7.28ms
	|EM-HSum|	1.491154962942613231E-44	
s=9.2+0.5I	EM	1.0303242681622333E8+1.7541533272563361E8I	8.44ms
z=1/8	FE	1.0303242681622333E8+1.7541533272563361E8I	189.48ms
λ=1E-20	|EM-FE|	4.553587053810249377E-22	
	Sum	1.0303242681622333E8+1.7541533272563361E8I	421.97ms
	|EM-Sum|	6.436406491643562289E-32	
	HSum	—	
	|EM-HSum|	—	
s=68.3+5.2I	EM	9.5949519489697887E-8-2.2048939138204181E-7I	28.49ms
z=5/4	FE	—	
λ=0.5	|EM-FE|	—	
	Sum	9.5949519489697887E-8-2.2048939138204181E-7I	3.65ms
	|EM-Sum|	0	
	HSum	9.5949519489697887E-8-2.2048939138204181E-7I	4.66ms
	|EM-HSum|	5.938116698505301196E-55	
s=0.5+14.3I	EM	1.1172710992950803E-1-1.68929893972105451	33.18ms
z=1/4	FE	1.1172710992950803E-1-1.68929893972105451	19.90ms
λ=0.125	|EM-FE|	3.352513059023154153E-40	
	Sum	—	
	|EM-Sum|	—	
	HSum	1.1172710992950803E-1-1.68929893972105451	19.26ms
	|EM-HSum|	3.6870042329205334445E-44	
s=-3.5+4.8I	EM	1.3480786436245563E1+8.3255733157977006E1I	45.10ms
z=6/8	FE	1.3480786436245563E1+8.3255733157977006E1I	12.81ms
λ=0.32	|EM-FE|	4.776054091671447469E-41	
	Sum	—	
	|EM-Sum|	—	
	HSum	1.3480786436245563E1+8.3255733157977006E1I	3306.4ms
	|EM-HSum|	4.716842635938552509E-41	
s=1.7	EM	2.9845656566026281+3.0545751112348827E-1I	11.81ms
z=1/2	FE	2.9845656566026281+3.0545751112348827E-1I	3.76ms
λ=0.32	|EM-FE|	1.719803767083806330E-44	
	Sum	—	
	|EM-Sum|	—	
	HSum	2.9845656566026281+3.0545751112348827E-1I	19.05ms
	|EM-HSum|	2.736911063134408341E-48	

Results from widmo version *6.1.0*. Precision 160 bits (49 digits).

Chapter 5

Algorithm for computing the spectrum of large complex matrices

One of the critical points in our numerical investigation of the transfer operator is the computation of its eigenvalues. In this section we want to describe briefly what problems arise when computing the eigenvalues of the transfer operator and how we can overcome these problems. To get the best results, both with respect to accuracy and computation time, we had to combine several techniques to produce an optimal algorithm.

- The algorithm should be able to handle large matrices; indeed the typical size of a matrix for $\Gamma_0(4)$ is 300×300 and for $\Gamma_0(8)$ it is already 600×600. To reduce the computation time of matrix operations like multiplication, we use a transformation to the Hessenberg form [Sch97] prior to the computation of the eigenvalues. These matrices have only zero entries below their subdiagonal. In the algorithm which computes the eigenvalues, we use a specific kind of unitary transformations, so-called Givens rotations [BDKM02], which can very efficiently transform Hessenberg matrices. Also, we will use a technique called deflation, which breaks down the eigenvalue problem of a matrix to several smaller matrices [GL96]. Finally, we use spectral shifts in the algorithm to reduce the computation time further [GL96].

- The range of eigenvalues varies quite a lot. Usually we are looking for the eigenvalues which are one or near to one, but the matrix approximating the transfer operator can also have eigenvalues larger by several decimal places. This poses two problems: First, some algorithms compute the eigenvalues with a fixed precision given by $r \cdot 10^{-D}$, where $r = \max_i |\lambda_i|$ is the spectral radius and D some precision constant. Hence if r is greater then 10^D we are no longer able to find the eigenvalues which are near to one. The second problem are round-off errors during the computation of small eigenvalues in the presence of large eigenvalues. To avoid these kinds of problems we use Givens rotations [BDKM02] since they produce fewer round-off errors compared to other methods like Householder reflections, see also [GL96].

- To use the eigenvalues for computing the Fredholm determinant, they need to be computed with high precision. We performed our computations with a precision of at least 160Bits (which corresponds to a precision of about 50 digits). To achieve this we use the *mpfr* program library [MPF09] for multiple-precision floating-point computations. Also the above-mentioned Givens rotations help us to achieve a high precision in the eigenvalues.

- Most algorithms we found in the literature are only for real matrices and usually also real eigenvalues. In general, the matrix which approximates the transfer operator has complex entries and complex

eigenvalues. Hence we had to generalize parts of the algorithm to be able to compute the (complex) eigenvalues of such complex matrices.

- Since we want to compute the spectrum of the transfer operator for many different parameters, the computations have to be rather fast. The high precision we are using is obviously contradicting this, but results obtained by using a lower precision would not be reliable enough. Also, the size of the matrices obviously poses problems, but we cannot do anything about this. Again, the Hessenberg form, the Givens rotations, deflation and spectral shifts are the best choices for fast computations. To increase the performance of our computation we have to optimize the software and the hardware. To reduce the computation time we optimize our implementation by analysing the runtime with tools like *gprof*. Our program can run on a normal PC with a UNIX-based OS, but we use also high-performance hardware, like a large computer cluster using up to several thousand CPUs.

Existing implementations like, e.g., MuPAD or LAPACK do not fit all the requirements we need, thereby the speed of computation and the precision of the results are the main problems.

5.1 Eigenvalues of a matrix

We want to recall some of the properties of the spectrum of a matrix, for more details see, e.g., [GL96]. The eigenvalues of a matrix $M \in \mathbb{C}^{d\times d}$ are the d roots of its characteristic polynomial

$$p(\lambda) = \det(\lambda I - M).$$

The set of these roots is called the spectrum of M and is denoted by $\sigma(M) = \{\lambda_i : 1 \le i \le d\}$. Then the trace of M given by $\operatorname{tr} M = \sum_{i=1}^{d} M_{i,i}$ is also given by $\operatorname{tr} M = \sum_{i=1}^{d} \lambda_i$ and the determinant of M is given by $\det(M) = \prod_{i=1}^{d} \lambda_i$. The non-zero vectors $x \in \mathbb{C}^d$ are called eigenvectors if $Mx = \lambda x$, for $\lambda \in \sigma(M)$.

For $B \in \mathbb{C}^{d\times d}$ and $X \in \mathbb{C}^{d\times d}$, with $MX = XB$ and X non-singular, i.e. the inverse X^{-1} of X exists, $\sigma(M) = \sigma(B)$. If $By = \lambda y$ then $MXy = X\lambda y = M(Xy) = \lambda(Xy)$. We say that M and $B = X^{-1}MX$ are similar and X is called a similarity transformation.

If the matrix $M \in \mathbb{C}^{d\times d}$ has the form

$$M = \begin{pmatrix} T_{1,1} & T_{1,2} \\ 0 & T_{2,2} \end{pmatrix} \tag{5.1}$$

where $T_{1,1} \in \mathbb{C}^{p\times p}$, $T_{1,2} \in \mathbb{C}^{p\times q}$ and $T_{2,2} \in \mathbb{C}^{q\times q}$, with $p + q = d$, then $\sigma(M) = \sigma(T_{1,1}) \cup \sigma(T_{2,2})$. The eigenvalue equation is given by

$$Mx = \begin{pmatrix} T_{1,1} & T_{1,2} \\ 0 & T_{2,2} \end{pmatrix} \begin{pmatrix} x_1 \\ x_2 \end{pmatrix} = \lambda \begin{pmatrix} x_1 \\ x_2 \end{pmatrix}$$

where $x_1 \in \mathbb{C}^p$ and $x_2 \in \mathbb{C}^q$. If $x_2 \neq 0$, then $T_{2,2}x_2 = \lambda x_2$, i.e. $\lambda \in \sigma(T_{2,2})$. If $x_2 = 0$, then $T_{1,1}x_1 = \lambda x_1$, i.e. $\lambda \in \sigma(T_{1,1})$. It follows that $\sigma(M) \subset \sigma(T_{1,1}) \cup \sigma(T_{2,2})$, but since the sets $\sigma(M)$ and $\sigma(T_{1,1}) \cup \sigma(T_{2,2})$ have the same size, they are equal. To get the spectrum of M we have to find the spectrum of $T_{1,1}$ and $T_{2,2}$. Obviously, this can lower the computation time, since we are dealing with smaller matrices. The breaking down of an eigenvalue problem into several smaller problems is called decoupling. It is also obvious that the eigenvalues of an upper triangular matrix are the diagonal entries of this matrix.

5.1.1 Schur decomposition

For any matrix $M \in \mathbb{C}^{d\times d}$ there exists a unitary matrix $U \in \mathbb{C}^{d\times d}$ which leads to the so-called Schur decomposition [GL96] of M given by

$$UMU^{\dagger} = T = D + N, \tag{5.2}$$

where $D = \operatorname{diag}(\lambda_1, \ldots, \lambda_d)$ and $N \in \mathbb{C}^{d\times d}$ is strictly upper triangular.

Usually one cannot find U explicitly. Instead, we will use an iterative process of unitary transformations to find the Schur decomposition of M. Actually, to obtain the eigenvalues we do not need to find an upper triangular matrix; it is enough to find a quasi-triangular one, given by

$$UMU^\dagger = \begin{pmatrix} R_{1,1} & R_{1,2} & R_{1,3} & \cdots & R_{1,n} \\ 0 & R_{2,2} & R_{2,3} & \cdots & R_{2,n} \\ 0 & 0 & R_{3,3} & \cdots & R_{3,n} \\ \vdots & \vdots & \vdots & \ddots & \vdots \\ 0 & 0 & 0 & \cdots & R_{n,n} \end{pmatrix}. \tag{5.3}$$

Thereby each $R_{i,i}$ for $1 \leq i \leq n$ is either in $\mathbb{C}$ or in $\mathbb{C}^{2\times 2}$. If $R_{i,i} \in \mathbb{C}$, it is an eigenvalue of M. Otherwise if $R_{i,i} = \begin{pmatrix} a & b \\ c & d \end{pmatrix} \in \mathbb{C}^{2\times 2}$, we obtain two eigenvalues of M by the usual formula

$$\lambda_{1,2} = \frac{a+b}{2} \pm \sqrt{\frac{(a-b)^2}{4} + bc}. \tag{5.4}$$

5.2 Complex Givens Rotations

To compute the eigenvalues of a matrix we need to perform some unitary transformations. One possible way to do this is to apply Givens rotations [Giv58]. We will briefly describe the complex version of Givens rotations, see also [GL96] and [BDKM02]. The Givens rotation is a unitary matrix $R(p,q,c,s) \in \mathbb{C}^{d\times d}$ defined by

$$[R(p,q,c,s)]_{i,j} = \begin{cases} c & \text{for } i = p, j = p \\ s & \text{for } i = p, j = q \\ -\overline{s} & \text{for } i = q, j = p \\ \overline{c} & \text{for } i = q, j = q \\ \delta_{i,j} & \text{else} \end{cases} \tag{5.5}$$

for $c, s \in \mathbb{C}$. Since $R(p,q,c,s)$ is unitary, this implies that $|c|^2 + |s|^2 = 1$ (for this compute $R(p,q,c,s)$ $R(p,q,c,s)^\dagger = I$). We want to use the conjugate $R(p,q,c,s)MR(p,q,c,s)^\dagger$ of the matrix $M \in \mathbb{C}^{d\times d}$. For computing $R(p,q,c,s)M$, there are three cases to consider:

$$\begin{aligned} [R(p,q,c,s)M]_{i,j} &= \sum_{n=1}^{d} R(p,q,c,s)_{i,n} M_{n,j} = \sum_{n=1}^{d} \delta_{i,n} M_{n,j} = M_{i,j} \quad \text{for } i \neq p, i \neq q \\ [R(p,q,c,s)M]_{p,j} &= \sum_{n=1}^{d} R(p,q,c,s)_{p,n} M_{n,j} = R(p,q,c,s)_{p,p} M_{p,j} + R(p,q,c,s)_{p,q} M_{q,j} \\ &= cM_{p,j} + sM_{q,j} \quad \text{for all } 1 \leq j \leq d \qquad (5.6) \\ [R(p,q,c,s)M]_{q,j} &= \sum_{n=1}^{d} R(p,q,c,s)_{q,n} M_{n,j} = R(p,q,c,s)_{q,p} M_{p,j} + R(p,q,c,s)_{q,q} M_{q,j} \\ &= -\overline{s}M_{p,j} + \overline{c}M_{q,j} \quad \text{for all } 1 \leq j \leq d \qquad (5.7) \end{aligned}$$

We see that this transformation changes only the two rows p and q of the matrix M. To compute $MR(p,q,c,s)^\dagger$, with $R(p,q,c,s)^\dagger_{i,j} = \overline{R(p,q,c,s)}_{j,i}$, we have again three cases to consider:

$$\begin{aligned}
\left[MR(p,q,c,s)^\dagger\right]_{i,j} &= \sum_{n=1}^{d} M_{i,n}\overline{R(p,q,c,s)}_{j,n} = \sum_{n=1}^{d} M_{i,n}\delta_{j,n} = M_{i,j} \quad \text{for } j \neq p, j \neq q \\
\left[MR(p,q,c,s)^\dagger\right]_{i,p} &= \sum_{n=1}^{d} M_{i,n}\overline{R(p,q,c,s)}_{p,n} = \overline{c}M_{i,p} + \overline{s}M_{i,q} \quad \text{for all } 1 \leq i \leq d \qquad (5.8) \\
\left[MR(p,q,c,s)^\dagger\right]_{i,q} &= \sum_{n=1}^{d} M_{i,n}\overline{R(p,q,c,s)}_{q,n} = -sM_{i,p} + cM_{i,q} \quad \text{for all } 1 \leq i \leq d \qquad (5.9)
\end{aligned}$$

We see that this transformation changes only the two columns p and q.

We want to apply this kind of unitary transformation $R(p,q,c,s)MR(p,q,c,s)^\dagger = M'$ to transform the matrix M to a matrix M' with a special form. Usually we want to have zeros in some entries of the matrix $R(p,q,c,s)M$. The transformation by the matrix $R(p,q,c,s)$ leads to one vanishing entry of the matrix $R(p,q,c,s)M$. If we want to have more zeros, we have to apply a sequence of such transformations. To get the entry $[R(p,q,c,s)M]_{q,k}$ to vanish we have to choose c and s such that

$$[R(p,q,c,s)M]_{q,k} = -\overline{s}M_{p,k} + \overline{c}M_{q,k} = 0.$$

To complete the multiplication $R(p,q,c,s)M$ we also have to transform the rows p and q according to (5.6) and (5.7). All other entries of $R(p,q,c,s)M$ are the same as for M. Finally we have to multiply $R(p,q,c,s)M$ with $R(p,q,c,s)^\dagger$. We see that the choice of c and s depends on the elements $M_{p,k}$ and $M_{q,k}$. Since there is some freedom in this choice, we want to chose c and s such that we reduce the computational effort. Indeed, we use [BDKM02]:

$$c\left(M_{p,k}, M_{q,k}\right) = \begin{cases} 1 & \text{for } M_{q,k} = 0 \\ 0 & \text{for } M_{p,k} = 0 \text{ and } M_{q,k} \neq 0 \\ \frac{|M_{p,k}|}{\sqrt{|M_{p,k}|^2+|M_{q,k}|^2}} & \text{else} \end{cases} \qquad (5.10)$$

$$s\left(M_{p,k}, M_{q,k}\right) = \begin{cases} 0 & \text{for } M_{q,k} = 0 \\ \frac{\overline{M}_{q,k}}{|M_{q,k}|} & \text{for } M_{p,k} = 0 \text{ and } M_{q,k} \neq 0 \\ \frac{M_{p,k}}{|M_{p,k}|}\frac{\overline{M}_{q,k}}{\sqrt{|M_{p,k}|^2+|M_{q,k}|^2}} & \text{else.} \end{cases} \qquad (5.11)$$

Note that $c\left(M_{p,k}, M_{q,k}\right)$ is real. Then the entry $[R(p,q,c,s)M]_{p,k}$ is given by

$$[R(p,q,c,s)M]_{p,k} = \begin{cases} M_{p,k} & \text{for } M_{q,k} = 0 \\ |M_{q,k}| & \text{for } M_{p,k} = 0 \text{ and } M_{q,k} \neq 0 \\ \frac{M_{p,k}}{|M_{p,k}|}\sqrt{|M_{p,k}|^2 + |M_{q,k}|^2} & \text{else.} \end{cases} \qquad (5.12)$$

The algorithm in listing 5.1 describes the transformation $R(p,q,c,s)MR(p,q,c,s)^\dagger$ by using the Givens rotation $R(p,q,c,s)$. Instead of computing the matrix $R(p,q,c,s)$ explicitly we compute only c and s by using (5.10) and (5.11) respectively. The function `compute_c_s` returns besides c and s also a variable r which is given by (5.12). Instead of creating a new matrix, we replace the entries in the matrix M which are changed by the transformation $R(p,q,c,s)MR(p,q,c,s)^\dagger$. This reduces the use of the memory and the computation time. First we use the function `rotation_left` to replace the matrix M by the matrix $R(p,q,c,s)M$, by using (5.6) and (5.7). Then we use the function `rotation_right` to replace the matrix M by $MR(p,q,c,s)^\dagger$, by using (5.8) and (5.9). The functions `rotation_left` and `rotation_right` have two extra parameters `min`

Listing 5.1: complex Givens rotations

```
compute_c_s(f,g)
        if g is equal zero
                c = 1
                s = 0
                r = f
        else if f is equal zero
                c = 0
                s = sign(compl_conjugate(g))
                r = abs(g)
        else
                t = sqrt(abs(f)^2+abs(g)^2)
                c = abs(f) / t
                s = sign(f) * compl_conjugate(g) / t
                r = sign(f) * t
        return (c,s,r)

rotation_left(M,p,q,c,s,min,max)
        for j=min,...,max
                h = c * M[p,j]  + s * M[q,j]
                M[q,j] = - compl_conjugate(s) * M[p,j] ...
                           + compl_conjugate(c) * M[q,j]
                M[p,j] = h

rotation_right(M,p,q,c,s,min,max)
        for j=min,...,max
                h = compl_conjugate(c) * M[j,p] ...
                    + compl_conjugate(s) * M[j,q]
                M[j,q] = - s * M[j,p] + c * M[j,q]
                M[j,p] = h
```

and `max`. They restrict relations (5.6) and (5.7) resp. (5.8) and (5.9) to certain columns resp. rows. One reason is that we want to apply these transformations sometimes only to submatrices of M. Another reason is that we usually apply a series of such transformations in an order, such that we know already that the next transformation will change only certain entries of the matrix. This procedure reduces the computation time a lot; we will see this later in the algorithm for the Hessenberg transformation and QR algorithm.

5.3 Hessenberg form

A square matrix $H \in \mathbb{C}^{d\times d}$ which only has zeros below the subdiagonal is called a Hessenberg matrix, i.e. $H_{i,j} = 0 \quad \text{for } i > j+1$. We call a Hessenberg matrix unreduced if all entries in its subdiagonal are non-zero.

As we will see, the computation of the eigenvalues of a Hessenberg matrix is much faster than that of an arbitrary matrix. According to [Sch97] and [GL96] we can transform any matrix $M \in \mathbb{C}^{d\times d}$ with an unitary matrix $U \in \mathbb{C}^{d\times d}$ to a Hessenberg matrix $H_M \in \mathbb{C}^{d\times d}$ by $UMU^\dagger = H_M$. Instead of applying U directly to M, we will apply a sequence of complex Givens rotations, which transform one entry at a time to zero in the matrix M until it has the Hessenberg form. We have to transform the entries $M_{i,j}$ with

Listing 5.2: Hessenberg reduction

```
Hessenberg_Reduction(M)
        d = number_of_rows(M)
        for j=1,...,d-2
                for i=j+2,...,d
                        if M[i][j] not equal zero
                                (c,s,r) = ...
                                  compute_c_s(M[j+1][j],M[i][j])
                                M[j+1][j] = r
                                M[i][j] = 0
                                 rotation_left(M,j+1,i,c,s,j+1,d)
                                 rotation_right(M,j+1,i,c,s,1,d)
```

$1 \leq j \leq d-2$ and $j+2 \leq i \leq d$ to obtain the Hessenberg form. To do this we choose for the Givens rotation $R(p,q,c,s) \in \mathbb{C}^{d\times d}$ the parameter $p = j+1$, and c and s such that $[R(j+1,i,c,s)M]_{i,j} = 0$. The choice of $p = j+1$ ensures that the multiplication with $R(j+1,i,c,s)^\dagger$ does not destroy this zero entry, i.e. $\left[R(j+1,i,c,s)MR(j+1,i,c,s)^\dagger\right]_{i,j} = 0$. Instead of creating a new matrix $M' = R(j+1,i,c,s)MR(j+1,i,c,s)^\dagger$ we replace the matrix M by $R(j+1,i,c,s)MR(j+1,i,c,s)^\dagger$ at each iteration. This algorithm is given in listing 5.2. We transform the entries in the matrix M to zero in such an order that we reduce the computation time: when we set the entry $M_{i,j}$ to zero we apply the Givens rotation $R(j+1,i,c,s)$ to M in the function `rotation_left` only to those entries $M_{j+1,k}$ and $M_{i,k}$ where $j+1 \leq k \leq d$, since the entries for $1 \leq k \leq j-1$ have already been transformed to zero by the previous Givens rotations.

5.4 The QR algorithm for complex matrices

We want to compute the eigenvalues of the matrix $M \in \mathbb{C}^{d\times d}$ using the QR algorithm, see [Fr61] and [Fr62]. The basic idea of the QR algorithm is to find a unitary matrix $Q \in \mathbb{C}^{d\times d}$ and an upper triangular matrix $R \in \mathbb{C}^{d\times d}$ such that $M = QR$. Next we set $M_1 = RQ$ and look for another Q_1 and R_1 such that $M_1 = Q_1R_1$. Again, we set $M_2 = R_1Q_1$ and look for Q_2 and R_2 with $M_2 = Q_2R_2$ and so on. Any of the matrices M_i have the same spectrum as M since the matrices are similar (see section 5.1): $M_i = R_{i-1}Q_{i-1} = Q_{i-1}^\dagger Q_{i-1}R_{i-1}Q_{i-1} = Q_{i-1}^\dagger M_{i-1}Q_{i-1}$ and by induction we get

$$M_i = Q_{i-1}^\dagger Q_{i-2}^\dagger \cdots Q_1^\dagger Q^\dagger MQQ_1 \cdots Q_{i-2}Q_{i-1}.$$

The crucial point is that the sequence $\{M_i\}_{i\in\mathbb{Z}_>}$ almost always converges to an upper triangular matrix $T = \lim_{i\to\infty} M_i$, which is the Schur decomposition (5.2) of M, see [Fr61]. The eigenvalues of M are just the diagonal entries of T. Note that in the case $M \in \mathbb{R}^{d\times d}$, $Q \in \mathbb{R}^{d\times d}$ and M having complex eigenvalues, $\lim_{i\to\infty} M_i = T$ will never converge to the triangular form. In this case the matrix T can only have the quasi-triangular form (5.3).

This basic QR algorithm is given in listing 5.3, the function `QR_basic` takes a matrix $M \in \mathbb{C}^{d\times d}$ as argument and returns an upper triangular matrix. In this algorithm we just assume that a function `decompose` is given, which decomposes M_i in Q_i and R_i. The QR algorithm presents just the basic idea; for practical computations we will use a modified and optimized version.

Listing 5.3: Basic QR algorithm

```
QR_basic(M)
        M_0 = M
        i = 1
        repeat
                (Q_(i-1),R_(i-1)) = decompose(M_(i-1))
                ( such that Q_(i-1)*R_(i-1) are equal M_(i-1) )
                M_i = R_(i-1) * Q_(i-1)
                if M_i is upper triangular
                        return M_i
                i = i + 1
```

5.4.1 Deflation

Assume $M \in \mathbb{C}^{d\times d}$ to be a Hessenberg matrix. If M has just one zero subdiagonal entry $M_{p+1,p} = 0$, then the eigenvalue problem decouples (5.1) into two smaller problems involving matrices $T_{1,1} \in \mathbb{C}^{p\times p}$ and $T_{2,2} \in \mathbb{C}^{q\times q}$ (with $q = d - p$). Note that $T_{1,1}$ and $T_{2,2}$ are unreduced Hessenberg matrices. This is also called deflation, and usually $T_{2,2} \in \mathbb{C}^{2\times 2}$ or $T_{2,2} \in \mathbb{C}$.

To speed up the deflation of the matrix M we declare the entry $M_{p+1,p}$ to be zero if it is suitably small

$$|M_{p+1,p}| < \delta\left(|M_{p,p}| + |M_{p+1,p+1}|\right). \tag{5.13}$$

Where δ is some small constant. A good choice for δ is the smallest positive number, which can be represented by the computer such that $1 + \delta \neq 1$. See [GL96] for more details and a justification of this procedure with respect to the numerical error.

5.4.2 The shifted QR iteration

Assume $M \in \mathbb{C}^{d\times d}$ to be a Hessenberg matrix. Instead of decomposing the matrix $M \in \mathbb{C}^{d\times d}$ into $Q \in \mathbb{C}^{d\times d}$ and $R \in \mathbb{C}^{d\times d}$ we decompose the matrix $(M - \mu I)$ with $\mu \in \mathbb{C}$. Then the QR iteration is given by setting the matrix $M_i = R_{i-1}Q_{i-1} + \mu I$ and looking for Q_i and R_i such that $M_i - \mu I = Q_i R_i$. Each matrix M_i is similar to M, since $M_i = R_{i-1}Q_{i-1} + \mu I = Q_{i-1}^{\dagger}Q_{i-1}R_{i-1}Q_{i-1} + \mu I = Q_{i-1}^{\dagger}\left(M_{i-1} - \mu I\right)Q_{i-1} + \mu I = Q_{i-1}^{\dagger}M_{i-1}Q_{i-1}$. Of course, we can choose a different $\mu \in \mathbb{C}$ at each iteration. Then we set

$$M_i = R_{i-1}Q_{i-1} + \mu_{i-1}I, \tag{5.14}$$

with μ_{i-1} from the decomposition $M_{i-1} - \mu_{i-1}I = Q_{i-1}R_{i-1}$ and choose a new μ_i and look for Q_i and R_i such that

$$M_i - \mu_i I = Q_i R_i. \tag{5.15}$$

This kind of shift increases the rate of convergence to zero of entries in the subdiagonal of M_i during the QR iterations [GL96]. If μ is much closer to the eigenvalue λ_d than to other eigenvalues, then the vanishing of the entry $[M_i]_{d,d-1}$ is rapid. To accelerate the deflation of the matrix M_i we choose $\mu_i \in \mathbb{C}$ is such a way that the entry $[M_i]_{d,d-1}$ converges to zero as fast as possible. The best approximation for the eigenvalue λ_d is given by the entry $[M_i]_{d,d}$. Indeed, if we set $\mu_i = [M_i]_{d,d}$ during the iterations, then, in case the entry $[M_i]_{d,d-1}$ converges to zero, it is likely to do so at a quadratic rate [GL96].

5.4.3 The final QR algorithm

Applying the function `QR_algorithm` in listing 5.4 transforms the matrix $M \in \mathbb{C}^{d\times d}$ into the quasi-triangular form (5.3). Before we start with the QR iteration we transform the matrix M into Hessenberg form by using the function `Hessenberg_Reduction` in listing 5.2. In the function `Decoupling` we set the subdiagonal entries of M equal zero if they satisfy relation (5.13). This may break down the eigenvalue problem to smaller submatrices of M. Using the function `get_submatrix` we try to find the largest $q \in \mathbb{Z}$ and smallest $p \in \mathbb{Z}$ such that

$$M = \begin{pmatrix} T_{1,1} & T_{1,2} & T_{1,3} \\ 0 & T_{2,2} & T_{2,3} \\ 0 & 0 & T_{3,3} \end{pmatrix},$$

where $T_{1,1} \in \mathbb{C}^{p\times p}$, $T_{3,3} \in \mathbb{C}^{q\times q}$ is upper quasi-triangular and $T_{2,2} \in \mathbb{C}^{r\times r}$ has an unreduced Hessenberg form, with $r = d - p - q$. If the function `get_submatrix` can find such a decomposition of M then it returns $e \in \mathbb{Z}$ and $s \in \mathbb{Z}$ such that $M_{s:e,s:e} = T_{2,2}$, where by $M_{s:e,s:e}$ we denote a submatrix of M formed by rows s to e and columns s to e. The QR algorithm is terminated if the function `get_submatrix` returns $e = 0$, which indicates that the entire matrix M is upper quasi-triangular. Otherwise, we compute the eigenvalues $\lambda'_{1,2}$ of the 2×2 submatrix $M_{e-1:e,e-1:e}$ by equation (5.4) and perform two shifted QR steps on the submatrix $M_{s:e,s:e}$, with the shifts $\mu_1 = \lambda'_1$ and $\mu_2 = \lambda'_2$. Instead we could perform just one shifted QR step, with the shift $\mu = M_{e,e}$, but the former procedure turns out to be the fastest way of computing the eigenvalues of M.

Unlike in the basic QR algorithm in listing 5.3 we will not create a new matrix M_i at every QR iteration. Instead, using the function `QR_Step` we decompose the matrix $M_{s:e,s:e} \in \mathbb{C}^{r\times r}$ into $Q \in \mathbb{C}^{r\times r}$ and $R \in \mathbb{C}^{r\times r}$ with the shift μ according to (5.15), such that $M_{s:e,s:e} - \mu I = QR$. Afterwards we replace the matrix $M_{s:e,s:e}$ by (5.14), i.e. $RQ+\mu I$. To compute R we set $Q^\dagger(M_{s:e,s:e}-\mu I) = R$, since R is upper triangular and $M_{s:e,s:e}-\mu I$ is an unreduced Hessenberg matrix, then $Q^\dagger$ must transform the subdiagonal entries in $M_{s:e,s:e} - \mu I$ to zero. Like in the Hessenberg transformation, we do not apply the unitary transformation $Q^\dagger$ on $M_{s:e,s:e}-\mu I$ directly, instead we will apply a sequence of complex Givens rotations, which transform one subdiagonal entry of the matrix $M_{s:e,s:e} - \mu I$ at a time until it is upper triangular. To transform the entry $[M_{s:e,s:e}]_{j+1,j}$ we choose a Givens rotation $R(p, q, c, s) \in \mathbb{C}^{r\times r}$, with $p = j$, and $c = c_j$ and $s = s_j$ such that $\left[R(j, j+1, c_j, s_j)M_{s:e,s:e}\right]_{j+1,j} = 0$. This transformation has to be performed for all $1 \le j \le r - 1$:

$$Q^\dagger(M_{s:e,s:e} - \mu I) = R(r-1, r, c_{r-1}, s_{r-1}) \cdots R(1, 2, s_1, c_1)(M_{s:e,s:e} - \mu I) = R.$$

Instead of computing R explicitly we finish the QR iteration by replacing the $M_{s:e,s:e}$ with the matrix (5.14); the new matrix is given by

$$R(r-1, r, c_{r-1}, s_{r-1}) \cdots R(1, 2, s_1, c_1)(M_{s:e,s:e} - \mu I)R(1, 2, s_1, c_1)^\dagger \cdots R(r-1, r, c_{r-1}, s_{r-1})^\dagger + \mu I.$$

The order in which we apply the Givens rotations is very important; this way we can reduce the use of memory and the computation time [Sch97]: First we apply the Givens rotations $R(2, 3, s_2, c_2)R(1, 2, s_1, c_1)$ on $M_{s:e,s:e} - \mu I$. Remember that we replace the original matrix $M_{s:e,s:e} - \mu I$ by the transformed matrix every time. After these rotations the matrix $M_{s:e,s:e} - \mu I$ will have two zeros in the first and second subdiagonal entry. Further rotations from the left will not change the first and second rows and columns. Next, we apply $R(1, 2, s_1, c_1)^\dagger$ from the right, which changes the first and second column. We have to apply this transformation only for $[M_{s:e,s:e} - \mu I]_{k,1}$ and $[M_{s:e,s:e} - \mu I]_{k,2}$ with $1 \le k \le 2$, since we know that all other entries in these columns are zeros. Then we apply $R(3, 4, s_3, c_3)$ from the left only to $[M_{s:e,s:e} - \mu I]_{3,k}$ and $[M_{s:e,s:e} - \mu I]_{4,k}$ with $3 \le k \le r$, since all the other entries in these rows are zero. Again, we apply a rotation from the right and then from the left and so on. At the end we have to apply two rotations from the right $R(r-2, r-1, s_{r-1}, c_{r-1})^\dagger R(r-1, r, s_r, c_r)^\dagger$.

Listing 5.4: QR algorithm

```
QR_algorithm(M)
        Hessenberg_Reduction(M)
        repeat
                Decoupling(M)
                (s,e)=get_submatrix(M)
                if e is zero
                        return
                (l1,l2)=eigenvalue(M[e-1:e,e-1:e])
                QR_Step(M,s,e,l1)
                QR_Step(M,s,e,l2)

Decoupling(M)
        d = number_of_rows(M)
        for j = 1,...,d-1
                if M[j+1][j] is not zero
                        if abs(M[j+1][j]) < delta * (abs(M[j][j]) ...
                                                    + abs(M[j+1][j+1]))
                                M[j+1][j] = 0


get_submatrix(M)
        d = number_of_rows(M)
        e=0
        s=1
        for j = d-1,...,2
                if M[j+1][j] is not zero
                        if M[j][j-1] is not zero
                                e = j + 1
                                end iteration over j
                        else
                                j = j - 2
        for j = e,...,2 (only if e > 2)
                if M[j][j-1] is zero
                        s = j
                        end iteration over j
        return (s,e)


QR_Step(M,s,e,m)
        for j = s,...,e
                M[j][j] = M[j][j] - m
        for j = s,...,e
                if j < e
                        (c,s,r) = compute_c_s(M[j][j],M[j+1][j])
                        M[j][j] = r
                        M[j+1][j] = 0
                        rotation_left(M,j,j+1,c,s,j+1,e)
                if j > s
```

```
                    rotation_right(M,j-1,j,ct,st,s,j)
            ct = c
            st = s
    for j = s,...,e
        M[j][j] = M[j][j] + m
```

Some remarks: This algorithm is optimized to compute the spectrum of the matrix, which approximates the transfer operator, i.e. a complex matrix with complex eigenvalues and a typical size of 300×300 and 600×600. For real-valued matrices with complex eigenvalues the implicit double-shift QR algorithm is more useful, see [Sch97] and [GL96]. There are also more advanced techniques, like the multishift QR algorithm, see [BBM02]. For a general introduction to the QR algorithm see also [Wat08].

5.5 A verification of the implementation

We implemented the algorithm in our computer program package Morpheus. To verify our implementation we compared the eigenvalues computed by our computer program widmo with the eigenvalues obtained from the computer algebra system *MuPAD* version 3.1.1. The matrices M we used are actually approximations of the transfer operator, to be introduced in later chapters, which were computed by our program widmo. In Table 5.1 we present the Fredholm determinants of the matrices M computed by the formula $\prod_{i=1}^{d}(1-\lambda_i)$, with $\lambda_i \in \sigma(M)$. As we can see, both implementations give almost the same results.

Further verifications of this algorithm are the results in Chapter 8 where we verify the implementation of approximation of the transfer operator, since we are using this algorithm to compute the spectrum of this approximation.

Table 5.1: Performance and accuracy of an algorithm for computing eigenvalues

size	n	β	α	impl.	Fredholm determinant	time
300×300	4	0.5+2.4I	0	widmo	1.13503748+3.53447240E-1I	2m18.177s
				MuPAD	1.13503748+3.53447240E-1I	18m18.609s
				diff	4.55943266E-43	
300×300	4	0.42+8.3I	0.324	widmo	-1.05350645E-1+3.05266212I	2m30.716s
				MuPAD	-1.05350645E-1+3.05266212I	16m41.451s
				diff	2.23389197E-39	
50×50	1	0.32+8.1I	0	widmo	8.25940857E-1+1.23329171I	1.062s
				MuPAD	8.25940857E-1+1.23329171I	8.200s
				diff	1.11119709E-40	
300×300	4	-1.3+2.7I	0	widmo	-9.84006194+9.48032598I	2m33.736s
				MuPAD	-9.84006194+9.48032598I	18m25.026s
				diff	2.35957613E-39	
150×150	2	1	0	widmo	5.05575814E-17+1.41188802E-64I	12.731s
				MuPAD	5.05575814E-17+1.15288611E-73I	1m33.908s
				diff	1.51299335E-44	
200×200	3	-5.3+1.4I	0	widmo	5.72428102E-11+1.98458200E-10I	43.999s
				MuPAD	5.72428102E-11+1.98458200E-10I	7m8.979s
				diff	1.36268923E-37	

Results from widmo version 6.1.1 and *MuPAD* version 3.1.1. Precision 160 bits (49 digits).

Note, that the result for $n = 2$ and $\beta = 1$ should be zero, but we see that the result is roughly $5.1E-17$. This is a problem connected with our approximation of the transfer operator, not with the computation of the

eigenvalues, since we see that both programs give the same result. To get a result which is closer to zero one has to increase the precision and use more Taylor coefficients in the approximation of the transfer operator.

Chapter 6

The hyperbolic Laplace-Beltrami operator

In this chapter we will introduce some basic concepts of hyperbolic geometry and automorphic forms, for more details see [Hej76], [Hej83], [Iwa02], [Bru94] and [Bum98]. We denote the upper half plane by

$$\mathbb{H} = \{x + iy \in \mathbb{C} : y > 0\}.$$

The hyperbolic metric and the hyperbolic area element are given by

$$ds^2 = \frac{dx^2 + dy^2}{y^2} \quad \text{and} \quad d\mu = \frac{dxdy}{y^2}.$$

The Laplace-Beltrami operator Δ related to this metric is given by

$$\Delta = y^2\left(\frac{\partial^2}{\partial x^2} + \frac{\partial^2}{\partial y^2}\right). \tag{6.1}$$

6.1 The group $\mathrm{PSL}(2,\mathbb{R})$ and congruence subgroups

The group $\mathrm{GL}(2,\mathbb{R})$ acts on $\mathbb{H}$ by Möbius transformations given by

$$\begin{pmatrix} a & b \\ c & d \end{pmatrix} : z \mapsto \frac{az+b}{cz+d}, \quad \text{with } a,b,c,d \in \mathbb{R} \text{ and } ad-bc = 1$$

$$\text{respectively} \qquad \begin{pmatrix} a & b \\ c & d \end{pmatrix} : z \mapsto \overline{\frac{az+b}{cz+d}}, \quad \text{with } a,b,c,d \in \mathbb{R} \text{ and } ad-bc = -1.$$

They are mappings, which preserve distances and areas in the upper half plane, and hence are isometries. The group of all orientation-preserving isometries is $\mathrm{PSL}(2,\mathbb{R})$, which is the group of Möbius transformations with $ad - bc = 1$. A different way to look at $\mathrm{PSL}(2,\mathbb{R})$ is like the group of 2×2 matrices with real entries and determinant equal to one, where the matrix γ is identified with $-\gamma$. We are interested in discrete subgroups of $\mathrm{PSL}(2,\mathbb{R})$, the so-called Fuchsian groups. An example of such a group is the modular group $\mathrm{PSL}(2,\mathbb{Z}) \subset \mathrm{PSL}(2,\mathbb{R})$, which has integer entries. The group $\mathrm{SL}(2,\mathbb{Z})$ is defined by

$$\mathrm{SL}(2,\mathbb{Z}) = \left\{ \begin{pmatrix} a & b \\ c & d \end{pmatrix} : a,b,c,d \in \mathbb{Z}, ad-bc = 1 \right\},$$

it is related to $\mathrm{PSL}(2,\mathbb{Z})$ by $\mathrm{PSL}(2,\mathbb{Z}) = \mathrm{SL}(2,\mathbb{Z})/\{\pm I\}$, with I the identity element in $\mathrm{SL}(2,\mathbb{Z})$. A system of generators of $\mathrm{SL}(2,\mathbb{Z})$ is $T = \begin{pmatrix} 1 & 1 \\ 0 & 1 \end{pmatrix}$ and $S = \begin{pmatrix} 0 & -1 \\ 1 & 0 \end{pmatrix}$. As can be easily seen, the Möbius transformation on the upper half plane associated to $\gamma \in \mathrm{SL}(2,\mathbb{Z})$ is the same as that determined by $-\gamma \in \mathrm{SL}(2,\mathbb{Z})$, so that $\mathrm{PSL}(2,\mathbb{Z})$ and $\mathrm{SL}(2,\mathbb{Z})$ have the same effect on the upper half plane. A strict fundamental domain of a group Γ is a connected set $F_\Gamma \subseteq \mathbb{H}$ such that

- $\bigcup_{\gamma\in\Gamma} \gamma F_\Gamma = \mathbb{H}$
- $\gamma \,\mathrm{int}\,(F_\Gamma) \cap \gamma' \,\mathrm{int}\,(F_\Gamma) = \emptyset$, for all $\gamma, \gamma' \in \Gamma$ with $\gamma \neq \gamma'$, where $\mathrm{int}\,(F_\Gamma)$ denotes the interior of F_Γ.

The quotient space $\mathrm{SL}(2,\mathbb{Z})\backslash\mathbb{H} = \{\mathrm{SL}(2,\mathbb{Z})z : z \in \mathbb{H}\}$ defines the modular surface. The standard fundamental domain of $\mathrm{SL}(2,\mathbb{Z})$ is

$$F_{\mathrm{SL}(2,\mathbb{Z})} = \left\{ z \in \mathbb{H} : |z| \geq 1, |\Re z| \leq \frac{1}{2} \right\}.$$

The Iwasawa decomposition of $\mathrm{SL}(2,\mathbb{R})$ is given by $\mathrm{SL}(2,\mathbb{R}) = NAK$

$$\begin{aligned} K &= \left\{ \begin{pmatrix} \cos\theta & \sin\theta \\ -\sin\theta & \cos\theta \end{pmatrix} : \theta \in \mathbb{R} \right\} \\ A &= \left\{ \begin{pmatrix} 1 & x \\ 0 & 1 \end{pmatrix} : x \in \mathbb{R} \right\} \\ N &= \left\{ \begin{pmatrix} a & 0 \\ 0 & a^{-1} \end{pmatrix} : a \in \mathbb{R}^+ \right\}. \end{aligned}$$

Every $\gamma \in \mathrm{SL}(2,\mathbb{R})$ has a unique factorization $\gamma = nak, \quad n \in N, a \in A, k \in K$. We call $z \in \mathbb{C}$ a fixed point of $\gamma \in \mathrm{SL}(2,\mathbb{R})$, if $\gamma z = z$. An element $\gamma = \begin{pmatrix} a & b \\ c & d \end{pmatrix} \in \mathrm{SL}(2,\mathbb{R})$, with $\gamma \neq \pm I$ is

1. parabolic, iff $|a+d| = 2 \quad \Leftrightarrow \quad$ it has exactly one fixed point on $\hat{\mathbb{R}}$
2. hyperbolic iff $|a+d| > 2 \quad \Leftrightarrow \quad$ it has two distinct fixed points on $\hat{\mathbb{R}}$
3. elliptic iff $|a+d| < 2 \quad \Leftrightarrow \quad$ it has one fixed point in $\mathbb{H}$ and one in $\bar{\mathbb{H}}$,

with $\hat{\mathbb{R}} = \mathbb{R} \cup \{\infty\}$ and $\bar{\mathbb{H}}$ the lower half plane. The elements in $\pm A$ are parabolic, in $\pm N$ hyperbolic and in K elliptic. The stabilizer group $\Gamma_z \subseteq \Gamma$ of a point $z \in \mathbb{H} \cup \mathbb{R} \cup \{\infty\}$ is defined by

$$\Gamma_z = \{\gamma \in \Gamma : \gamma z = z\}.$$

We are interested in certain subgroups of $\mathrm{SL}(2,\mathbb{Z})$. The principal congruence subgroup $\Gamma(n) \subset \mathrm{SL}(2,\mathbb{Z})$ of level $n \in \mathbb{Z}_>$ is defined by

$$\Gamma(n) = \left\{ \begin{pmatrix} a & b \\ c & d \end{pmatrix} \in \mathrm{SL}(2,\mathbb{Z}) : a \equiv d \equiv 1 \mod n, \quad b \equiv c \equiv 0 \mod n \right\}.$$

Note that $\Gamma(n)$ is a normal subgroup of $\mathrm{SL}(2,\mathbb{Z})$, i.e. invariant under conjugation: for all $\gamma \in \Gamma(n)$ and all $g \in \mathrm{SL}(2,\mathbb{Z})$ we have $g\gamma g^{-1} \in \Gamma(n)$. A subgroup of $\mathrm{SL}(2,\mathbb{Z})$ is called a congruence subgroup if it contains $\Gamma(n)$ for some n. Examples of such groups are the Hecke congruence subgroups $\Gamma_0(n) \subset \mathrm{SL}(2,\mathbb{Z})$ of level $n \in \mathbb{Z}_>$ defined by

$$\Gamma_0(n) = \left\{ \begin{pmatrix} a & b \\ c & d \end{pmatrix} \in \mathrm{SL}(2,\mathbb{Z}) : c \equiv 0 \mod n \right\}.$$

The right cosets of Γ in $\mathrm{SL}(2,\mathbb{Z})$ are given by $\Gamma g = \{\gamma g : \gamma \in \Gamma\}$ with $g \in \mathrm{SL}(2,\mathbb{Z})$. For $g, g' \in \mathrm{SL}(2,\mathbb{Z})$ we have either $\Gamma g \cap \Gamma g' = \emptyset$ or $\Gamma g = \Gamma g'$. The cardinal number of $\Gamma\backslash\mathrm{SL}(2,\mathbb{Z}) = \{\Gamma g : g \in \mathrm{SL}(2,\mathbb{Z})\}$ is called the index μ_Γ of Γ in $\mathrm{SL}(2,\mathbb{Z})$. The index μ_n of $\Gamma_0(n)$ in $\mathrm{SL}(2,\mathbb{Z})$ is given by [Iwa02]

$$\mu_n = [\,\mathrm{SL}(2,\mathbb{Z}) : \Gamma_0(n)\,] = n \prod_{p|n} \left(1 + \frac{1}{p}\right) < \infty, \quad p \text{ prime.}$$

A system of representatives $\left\{r_i^\Gamma \in \mathrm{SL}(2,\mathbb{Z})\right\}_{1 \le i \le \mu_\Gamma}$ of the right cosets $\Gamma\backslash\mathrm{SL}(2,\mathbb{Z})$ satisfies

$$\bigsqcup_{i=1}^{\mu_\Gamma} \Gamma\, r_i^\Gamma = \mathrm{SL}(2,\mathbb{Z})$$

where $\bigsqcup$ denotes a disjoint union. We denote a system of right coset representatives of $\Gamma_0(n)$ in $\mathrm{SL}(2,\mathbb{Z})$ by $\{r_i^{(n)}\}_{1 \le i \le \mu_n}$. We have

$$\Gamma\backslash\mathrm{SL}(2,\mathbb{Z}) = \left\{\Gamma\, r_i^\Gamma : 1 \le i \le \mu_\Gamma\right\}.$$

A fundamental domain $F_\Gamma \subset \mathbb{H}$ of Γ is then given by

$$F_\Gamma = \bigcup_{i=1}^{\mu_\Gamma} r_i^\Gamma F_{\mathrm{SL}(2,\mathbb{Z})}.$$

The area of $F_{\mathrm{SL}(2,\mathbb{Z})}$ is $\mu(F_{\mathrm{SL}(2,\mathbb{Z})}) = \frac{\pi}{3}$, see [Iwa02] for a general formula to compute the area. For subgroups Γ of $\mathrm{SL}(2,\mathbb{Z})$ with finite index μ_Γ the area of the fundamental domain is given by

$$\mu(F_\Gamma) = \mu(F_{\mathrm{SL}(2,\mathbb{Z})}) \cdot \mu_\Gamma.$$

Assume, F_Γ has h Γ-inequivalent cuspidal points $\kappa_i \in \mathbb{Q} \cup \{\infty\}$, with $1 \le i \le h$. For $\sigma_i \in \mathrm{PSL}(2,\mathbb{R})$ such that $\sigma_i \kappa_i = \infty$ the stabilizer $\Gamma_i = \{\gamma \in \Gamma : \gamma\kappa_i = \kappa_i\}$ of κ_i is given by $\sigma_i \Gamma_i \sigma_i^{-1} = \left\{\begin{pmatrix} 1 & n \\ 0 & 1 \end{pmatrix} : n \in \mathbb{Z}\right\}$.

6.2 The spectrum of the hyperbolic Laplace-Beltrami operator

A *Maass wave form* u with eigenvalue λ for a congruence subgroup $\Gamma \subset \mathrm{SL}(2,\mathbb{Z})$ and a unitary character $\chi : \Gamma \to \mathbb{C}$ is a real-analytic function $u : \mathbb{H} \to \mathbb{C}$ which is:

1. Γ-automorphic: $u(\gamma z) = \chi(\gamma)\, u(z)$ for all $\gamma \in \Gamma$ and $z \in \mathbb{H}$
2. an eigenfunction of Δ: $\Delta u + \lambda u = 0$, with $\lambda \ge 0$
3. square integrable on the Riemann surface $\Gamma\backslash\mathbb{H}$: $\int_{\Gamma\backslash\mathbb{H}} |u(z)|^2\, d\mu(z) < \infty$.

A conjecture of Selberg (see [Iwa02]) says that for congruence subgroups $\lambda \ge \frac{1}{4}$, except $\lambda = 0$ for the constant function. Eigenvalues $\lambda \in \left(0, \frac{1}{4}\right]$ are called exceptional. Usually we write $\lambda = \beta(1-\beta)$, with $\beta \in \mathbb{C}$ and $\Re\beta = \frac{1}{2}$ or $\beta \in [0,1]$, and call β the *spectral parameter*. We can write the eigenvalue as $\lambda = \frac{1}{4} + (\Im\beta)^2$ for $\Re\beta = \frac{1}{2}$, with $\Im\beta \in [0,\infty)$. We denote the space of Maass wave forms for (Γ,χ) with spectral parameter β by $\mathcal{S}(\Gamma,\chi,\beta)$. A linear operator $B : \mathcal{S}(\Gamma,\chi,\beta) \to \mathcal{S}(\Gamma,\chi,\beta)$ is called an involution if $B^2 u(z) = u(z)$ for any $u \in \mathcal{S}(\Gamma,\chi,\beta)$. An example of such an involution for $\Gamma_0(n)$ is $Ju(z) := u(jz)$ with $j = \begin{pmatrix} 1 & 0 \\ 0 & -1 \end{pmatrix} \in \mathrm{GL}(2,\mathbb{Z})$ and $jz = -\bar{z}$. The wave form u is said to be even if $Ju(z) = u(z)$ and odd if $Ju(z) = -u(z)$. We can split the space $\mathcal{S}(\Gamma,\chi,\beta)$ into a direct sum of even and odd Maass wave forms:

$\mathcal{S}(\Gamma,\chi,\beta) = \mathcal{S}_{\text{even}}(\Gamma,\chi,\beta) \oplus \mathcal{S}_{\text{odd}}(\Gamma,\chi,\beta)$. In general there may exist more involutions: let τ be another involution, then we use the notation τ-even respectively τ-odd.

The Maass wave forms determine the discrete spectrum of Δ. The continuous spectrum of Δ is determined by the so-called Eisenstein series. Note that the discrete spectrum $\{\lambda_i = \beta_i(1-\beta_i) : \beta_i \in \frac{1}{2} + i\mathbb{R}\}$ is embedded in the continuous spectrum $\{\lambda = \beta(1-\beta) : \beta \in \frac{1}{2} + i\mathbb{R}\} = [\frac{1}{4}, \infty)$. Let $T_i \in \Gamma$ be a primitive parabolic element such that $T_i\kappa_i = \kappa_i$. We say χ is singular in the cusp κ_i if $\chi(T_i) = 1$ and χ is non-singular if $\chi(T_i) \neq 1$. If χ is non-singular in a cusp then this cusp is said to be *closed* and it does not contribute to the continuous spectrum of Δ. The multiplicity h_0 of the continuous spectrum is given by the number of open cusps

$$h_0 = \#\{\chi(T_i) = 1 : 1 \leq i \leq h\}.$$

The Eisenstein series ([Hej83], p. 280) for the inequivalent open cusps κ_i of Γ with $1 \leq i \leq h_0$ are given by

$$E_i(z,\beta,\chi) = \sum_{\gamma \in \Gamma_i \backslash \Gamma} \chi\left(\gamma^{-1}\right) (\Im \sigma_i \gamma z)^\beta .$$

This series is absolutely convergent for $\Re\beta > 1$ and it has a meromorphic continuation to $\mathbb{C}$. The automorphic scattering matrix is given by [Sel90]

$$[\Theta(\beta,\chi)]_{i,j} = \sqrt{\pi}\frac{\Gamma(\beta - \frac{1}{2})}{\Gamma(\beta)} L_{i,j}(\beta,\chi)$$

for $1 \leq i, j \leq h_0$ and $L_{i,j}(\beta,\chi)$ some Dirichlet L-series. The functional equation for the Eisenstein series is given by

$$E_i(z,\beta,\chi) = \sum_{j=1}^{h_0} [\Theta(\beta,\chi)]_{i,j} E_j(z, 1-\beta,\chi) \quad 1 \leq i \leq h_0.$$

The determinant $\varphi(\beta,\chi)$ of $\Theta(\beta,\chi)$ has the form

$$\varphi(\beta,\chi) = \det\Theta(\beta,\chi) = \left(\sqrt{\pi}\frac{\Gamma(\beta - \frac{1}{2})}{\Gamma(\beta)}\right)^{h_0} L(\beta,\chi),$$

where $L(\beta,\chi)$ is a Dirichlet L-series. It satisfies the functional equation

$$\varphi(\beta,\chi)\varphi(1-\beta,\chi) = 1.$$

Furthermore, on the critical line $\Re\beta = \frac{1}{2}$ we have

$$\left|\varphi\left(\frac{1}{2} + i\Im\beta,\chi\right)\right| = 1.$$

$\varphi(\beta,\chi)$ has possibly a finite number of poles in $\frac{1}{2} < \beta \leq 1$ and infinite many poles for $\Re\beta < \frac{1}{2}$. The poles for $\Re\beta < \frac{1}{2}$ correspond to zeros of $\varphi(\beta,\chi)$ in the region $\Re\beta > \frac{1}{2}$. Some of the poles of $\varphi(\beta,\chi)$ are located at the zeros of some Dirichlet L-series $\tilde{L}$. For a congruence subgroup Γ these poles are at $\tilde{L}(2\beta,\chi) = 0$ [Hux84]. According to the generalized Riemann hypothesis they should be located on the line $\Re\beta = \frac{1}{4}$ if χ is a Dirichlet character. For $\chi \equiv 1$ these poles are located on $\zeta_R(2\beta) = 0$ (according to the Riemann hypothesis they are hence on the line $\Re\beta = \frac{1}{4}$). Note that for a Dirichlet character χ respectively $\chi \equiv 1$ there can be other lines on which the poles of $\varphi(\beta,\chi)$ are located.

6.3 The Selberg zeta function

The Selberg zeta function [Sel56] (see also [Hej83], p. 496) for (Γ,χ) is given by

$$Z(\beta,\chi)=\prod_{\{P_0\}\text{primitive}}\prod_{k=0}^{\infty}\left(1-\chi(P_0)\,\mathcal{N}(P_0)^{-\beta-k}\right)\quad\text{for }\Re\beta>1 \tag{6.2}$$

where "$\{P_0\}$ primitive" is a primitive hyperbolic conjugacy class in Γ, i.e. no P exists such that $P_0=P^k$ with $k\geq 2$, and $\{P_0\}=\left\{\tau P_0\tau^{-1}:\tau\in\mathrm{PSL}(2,\mathbb{R})\right\}$. The norm $\mathcal{N}(P_0)$ of a representative P_0 of the class $\{P_0\}$ is given by $\mathrm{tr}\,(P_0)=\mathcal{N}(P_0)^{\frac{1}{2}}+\mathcal{N}(P_0)^{-\frac{1}{2}}$. For cofinite Fuchsian groups Sinai realized that this function can be related to the Ruelle-Smale zeta function for the geodesic flow $\Phi_t:SM_\Gamma\to SM_\Gamma$ on the unit tangent bundle SM_Γ of the corresponding surface $M_\Gamma=\Gamma\backslash\mathbb{H}$. Then one can write the Selberg zeta function as

$$Z(\beta,\chi)=\prod_{\gamma}\prod_{k=0}^{\infty}\left(1-\chi\left(g_\gamma\right)e^{-(\beta+k)l(\gamma)}\right)\quad\text{for }\Re\beta>1 \tag{6.3}$$

with $\gamma=\{\Phi_t(x):t\in\mathbb{R}\}$ a primitive closed orbit of the geodesic flow Φ_t on $\Gamma\setminus\mathbb{H}$ with prime period $l(\gamma)=\ln\mathcal{N}(g_\gamma)$ (i.e. $\Phi_{l(\gamma)}(x)=x$) and the hyperbolic elements $g_\gamma\in\Gamma$ such that $g_\gamma\gamma=\gamma$. We denote the Selberg zeta function for the Hecke congruence subgroups $\Gamma_0(n)$ by $Z^{(n)}(\beta,\chi)$.

It is surprising, that there are only very few successful numerical evaluations of the Selberg zeta function see [MS91], [GLZ04] and [Str08]. The main difficulty for evaluating this function is to find an analytic continuation for $\Re\beta\leq\frac{1}{2}$. Another problem is to compute the product $\prod_{\{P_0\}\text{primitive}}$ respectively $\prod_\gamma$. Later we will evaluate the Selberg zeta function for $(\Gamma_0(n),\chi)$ by using the Fredholm determinant of an approximation of the transfer operator. See Chapter 7 for more details on this method.

The zeros and poles of the Selberg zeta function are related through the Selberg trace formula to the hyperbolic Laplacian (see also [Hej83], p. 498):

- The zeros on the line $\Re\beta=\frac{1}{2}$ are related to the discrete spectrum of the hyperbolic Laplacian Δ, where β is related to the eigenvalue $\lambda=\beta(1-\beta)$. The multiplicity of these zeros is given by the multiplicity of the eigenvalues.
- The zeros in the interval $\beta\in[0,1]$ correspond to small eigenvalues related to the residues of the poles of the analytically continued Eisenstein series respectively to cusp forms [Iwa02].
- The zeros in $\Re\beta<\frac{1}{2}$, $\Im\beta>0$ are related to the resonances, i.e. the poles of the determinant $\varphi(\beta,\chi)$ of the scattering matrix. The multiplicity of these zeros is given by the order of the poles of $\varphi(\beta,\chi)$.
- The trivial zeros or poles at $\beta\in\mathbb{Z}_{\leq}$, which have different multiplicities.
- The zeros or poles at $\beta\in\frac{1}{2}+\mathbb{Z}_{\leq}$. The order of the pole at $\beta=\frac{1}{2}$ is given by the number of open cusps h_0 minus twice the dimension of the $\lambda=1/4$-eigenspace [Iwa02].

In [Hej76] Chapter 2 some properties of the Selberg zeta function $Z(\beta)$ for the trivial character $\chi\equiv 1$ are given: there it was proved that for $\Re\beta\geq 2$ we have

$$Z(\beta)=1+O\left(m(\Gamma)^{-\Re\beta}\right) \tag{6.4}$$

where $1<m(\Gamma)<\infty$ is given by $m(\Gamma)=\inf\{\mathcal{N}(P):P\text{ hyperbolic}\in\Gamma\}$;
for $-1\leq\Re\beta\leq 2$ we have

$$|Z(\beta)|\leq\exp\left(O\left((\Im\beta)^2\right)\right), \tag{6.5}$$

and for $\Re\beta\leq -1$ we have

$$|Z(\beta)|\leq\exp\left(O\left(|\beta|^2\right)\right). \tag{6.6}$$

The functional equation for the Selberg zeta function is given by ([Hej83], p. 499)

$$\varphi(\beta,\chi)\,Z(\beta,\chi) = \eta(\beta)\,Z(1-\beta,\chi) \tag{6.7}$$

with

$$\eta(\beta) = \eta\left(\frac{1}{2}\right)\exp\int_{\frac{1}{2}}^{\beta} C(u)\,du \tag{6.8}$$

and $\eta\left(\frac{1}{2}\right) = \pm 1$. Furthermore, we have

$$\eta(\beta)\,\eta(1-\beta) = 1.$$

Note that if the number h_0 of open cusps vanishes then $\varphi(\beta,\chi)$ is absent in (6.7). The function $C(u)$ depends on the properties of the group Γ (see [Hej83], p. 499 for details). Later we need the following lemma:

Lemma 6.3.1. *For $(\Gamma_0(n),\chi)$ with $4\,|\,n$ the function $\eta(\beta)$ is given by*

$$\eta(\beta) = \eta\left(\frac{1}{2}\right)\left(2^{2\beta-1}\frac{\Gamma\left(\frac{1}{2}+\beta\right)}{\Gamma\left(\frac{3}{2}-\beta\right)}\right)^{h_0}\exp\left\{\frac{\pi}{3}\mu_n\int_0^{\beta-\frac{1}{2}}\tau\tan(\pi\tau)d\tau\right\}\prod_{\chi(T_i)\neq 1}|1-\chi(T_i)|^{2\beta-1}, \tag{6.9}$$

where μ_n is the index of $\Gamma_0(n)$ in $\mathrm{SL}(2,\mathbb{Z})$, $\prod_{\chi(T_i)\neq 1}$ is the product over all closed cusps κ_i with $T_i\kappa_i = \kappa_i$, and h_0 the number of open cusps of $(\Gamma_0(n),\chi)$.

Proof. The function C in (6.8) is given in [Hej83], p. 499, for general groups Γ. For $(\Gamma_0(n),\chi)$ with $4\,|\,n$ where there are no elliptic points (see [Miy06], p. 108), we have

$$C(u) = \mu(F_{\Gamma_0(n)})\left(u-\frac{1}{2}\right)\frac{\sin\left(2\pi\left(u-\frac{1}{2}\right)\right)}{\cos\left(2\pi\left(u-\frac{1}{2}\right)\right)+1} + 2\sum_{\chi(T_i)\neq 1}\ln|1-\chi(T_i)| + 2h_0\ln 2 + h_0\left(\psi\left(\frac{1}{2}+u\right)+\psi\left(\frac{3}{2}-u\right)\right)$$

where $\mu(F_{\Gamma_0(n)})$ is the area of the fundamental domain of $\Gamma_0(n)$ and $\psi(s) = \frac{\Gamma'(s)}{\Gamma(s)} = \frac{d}{ds}\ln\Gamma(s)$. In this case we have

$$\begin{aligned}\eta(\beta) &= \eta\left(\frac{1}{2}\right)\exp\left\{\mu(F_{\Gamma_0(n)})\int_{\frac{1}{2}}^{\beta}\left(u-\frac{1}{2}\right)\frac{\sin\left(2\pi\left(u-\frac{1}{2}\right)\right)}{\cos\left(2\pi\left(u-\frac{1}{2}\right)\right)+1}du\right.\\ &+ (2\beta-1)\left(\sum_{\chi(T_i)\neq 1}\ln|1-\chi(T_i)| + h_0\ln 2\right)\\ &+ \left. h_0\int_{\frac{1}{2}}^{\beta}\psi\left(\frac{1}{2}+u\right)+\psi\left(\frac{3}{2}-u\right)du\right\},\end{aligned} \tag{6.10}$$

where $\mu(F_{\Gamma_0(n)})$ is given by $\mu(F_{\Gamma_0(n)}) = \mu(F_{\mathrm{SL}(2,\mathbb{Z})})\,\mu_n = \frac{\pi}{3}\,\mu_n$. By setting $\tau = u-\frac{1}{2}$, and using $\sin(2z) = 2\sin(z)\cos(z)$ and $\cos(2z) = 2\cos^2(z)-1$ (see [AS64], p. 72) we get

$$\int_{\frac{1}{2}}^{\beta}\left(u-\frac{1}{2}\right)\frac{\sin\left(2\pi\left(u-\frac{1}{2}\right)\right)}{\cos\left(2\pi\left(u-\frac{1}{2}\right)\right)+1}du = \int_0^{\beta-\frac{1}{2}}\tau\tan(\pi\tau)d\tau.$$

The second integral in (6.10) can be calculated explicitly

$$\int_{\frac{1}{2}}^{\beta}\psi\left(\frac{1}{2}+u\right)+\psi\left(\frac{3}{2}-u\right)du = \int_{\frac{1}{2}}^{\beta}\frac{d}{du}\ln\Gamma\left(\frac{1}{2}+u\right)-\frac{d}{du}\ln\Gamma\left(\frac{3}{2}-u\right)du = \ln\Gamma\left(\frac{1}{2}+\beta\right)-\ln\Gamma\left(\frac{3}{2}-\beta\right).$$

□

6.4 The conjecture of Phillips and Sarnak

In a series of papers [PS85], [PS91] and [PS94] Phillips and Sarnak studied the problem of whether Maass cusp forms exist for general groups or only for a certain kind of groups. They introduced a condition under which a Maass cusp form for Γ is dissolved into a resonance by a perturbation of the group Γ in Teichmüller space, respectively a character perturbation. This condition is expressed in terms of the so-called *Fermi's golden rule*; for more recent developments on this problem see also [PR10]. See also [Wol94] and [Jud95]. Note that a perturbation of the spectrum is rather complicated in this case, since the corresponding discrete spectrum is embedded in the continuous spectrum. Also, some of the perturbations like the character perturbation in [PS94] are singular. See also Chapter 8 for more details and results for singular and non-singular perturbations.

It was conjectured by Sarnak and Phillips [PS94] that the existence of Maass cusp forms is intimately tied to the arithmetic nature of (Γ, χ), see also [DIPS85]. In particular, for non-arithmetic (Γ, χ) there should exist at most a finite number of cusp forms. For a character χ and a congruence subgroup $\Gamma \subset \mathrm{SL}(2, \mathbb{Z})$ arithmetic means that the kernel $\ker \chi = \{\gamma \in \Gamma : \chi(\gamma) = 1\}$ of χ is again a congruence subgroup.

Obviously, the question about the existence of Maass cusps forms is closely related to the validity of a Weyl law for the discrete spectrum: The counting function for the eigenvalues λ_i in the discrete spectrum is defined as [Iwa02]

$$N_\Gamma(R) = \#\left\{\lambda_i = \frac{1}{4} + R_i^2 : R_i \leq R\right\}, \tag{6.11}$$

whereas the contribution of the continuous spectrum is given by

$$M_\Gamma(R) = -\frac{1}{4\pi}\int_{-R}^{R} \frac{\varphi'}{\varphi}\left(\frac{1}{2} + ir, \chi\right) dr \tag{6.12}$$

which counts the winding of the determinant φ. The Weyl law is then

$$N_\Gamma(R) + M_\Gamma(R) \sim \frac{\mu(F_\Gamma)}{4\pi} R^2, \quad R \to \infty \tag{6.13}$$

where $\mu(F_\Gamma)$ denotes the area of the fundamental domain F_Γ of Γ. It is an essential problem to determine which of $N_\Gamma(R)$ and $M_\Gamma(R)$ makes the main contribution to the spectrum. Indeed, one motivation of Selberg for introducing the trace formula was to establish a Weyl law [Sel89]. Thereby he proved that for congruence subgroups Γ and trivial character $\chi \equiv 1$ the primary term is N_Γ, i.e.

$$N_\Gamma(R) \sim \frac{\mu(F_\Gamma)}{4\pi} R^2, \quad R \to \infty. \tag{6.14}$$

Following the convention of Sarnak and Phillips [PS94] we say that (Γ, χ) is *essentially cuspidal* if (6.14) holds for (Γ, χ). It is a fundamental question if (6.14) is characteristic for congruence subgroups or it may also hold for some general subgroups $\Gamma \subset \mathrm{SL}(2, \mathbb{Z})$. According to the conjecture of Phillips and Sarnak non-arithmetic (Γ, χ) should not be essentially cuspidal.

Several numerical experiments have been carried out to verify the conjecture of Phillips and Sarnak: Winkler [Win88] and Hejhal [Hej92] found in the case of Hecke triangle groups only for the arithmetic ones even Maass cusp forms, which confirms this conjecture. More recent computations have been concerned with the deformation of the group $\Gamma_0(5)$ in Teichmüller space: Farmer and Lemurell studied in [FL05] the survival or destruction of Maass cusp forms for $\Gamma_0(5)$. They found that every Maass cusp form has a deformation path, along which it is not destroyed. They tracked several Maass cusp forms along such paths in a two-parameter deformation. When a Maass cups form is destroyed a resonance is created; these resonances manifest themselves as poles of the determinant of the scattering matrix very close to the critical line $\Re\beta = \frac{1}{2}$. In [Ave07] Avelin tracks how these poles move as the group $\Gamma_0(5)$ is deformed in Techmüller space, finding second- and fourth-order contact of the poles with the critical line $\Re\beta = \frac{1}{2}$. In principle it

should be also possible to use other techniques like the cut-off Laplacian [PS94] or the scattering determinant using L-series [Sel90] to track eigenvalues and resonances under singular perturbation.

Instead of studying the Maass wave forms and Eisenstein series directly, we will track the zeros of the Selberg zeta function $Z^{(n)}(\beta,\chi_\alpha)$ for $\Gamma_0(4)$ and $\Gamma_0(8)$ along a character deformation χ_α introduced in the next section. Since the zeros of this function on the line $\Re\beta = \frac{1}{2}$ correspond to eigenvalues of the Laplacian determined by cusp forms and the zeros in $\Re\beta < \frac{1}{2}$, $\Im\beta > 0$ correspond to poles of the determinant of the scattering matrix we are able to study both the eigenvalues and resonances at the same time. When a zero leaves the critical line $\Re\beta = \frac{1}{2}$ a Maass wave form is destroyed and a resonance is created. And when a zero moves from $\Re\beta < \frac{1}{2}$ to the critical line a resonance vanishes and a Maass cusp form is created. Note also that we do not have to deal with the problem of embedded eigenvalues, since the continuous spectrum does not appear in the Selberg zeta function.

6.5 Character deformations

Let $\left\{G_i^\Gamma\right\}_{1\le i\le k}$ be a system of generators of a freely generated group $\Gamma \subset \mathrm{SL}(2,\mathbb{Z})$. We can represent any element $\gamma \in \Gamma$ as

$$\gamma = \prod_{j=1}^{N} (G_1^\Gamma)^{n_{1,j}} (G_2^\Gamma)^{n_{2,j}} \cdots (G_k^\Gamma)^{n_{k,j}} \tag{6.15}$$

with $n_{i,j} = n_{i,j}(\gamma) \in \mathbb{Z}$ and $N = N(\gamma) \in \mathbb{Z}_>$. Hereby $\prod$ we mean multiplication from the right, i.e. $\prod_{j=1}^N g_j = g_1 g_2 \cdots g_N$. Note that by setting some of the $n_{i,j}$ to zero, we can construct any possible combination of the G_i^Γ in any possible order.

Definition 6.5.1. A character $\chi^\Gamma_{\alpha_1,\ldots,\alpha_k} : \Gamma \to \mathbb{C}$ for a freely generated group Γ is given by

$$\chi^\Gamma_{\alpha_1,\ldots,\alpha_k}(\gamma) = \exp 2\pi i \sum_{i=1}^{k} \alpha_i \Omega_i^\Gamma(\gamma) \tag{6.16}$$

where k is the number of generators of Γ, $0 \le \alpha_i \le 1$, and $\Omega_i^\Gamma : \Gamma \to \mathbb{Z}$ is given by

$$\Omega_i^\Gamma(\gamma) = \sum_{j=1}^{N} n_{i,j}, \tag{6.17}$$

where $N = N(\gamma)$ and $n_{i,j} = n_{i,j}(\gamma)$ are given by (6.15).

For numerical computations the complicated part is to evaluate the function $\Omega_i^\Gamma(\gamma)$, since a decomposition of γ needs to be found in the generators. Usually this has to be done by *brute force*; unfortunately this kind of computation is rather slow. Of course, for a finite number of elements in Γ one can compute their character in advance and re-use the results. We will later use this character for the transfer operator for $\Gamma_0(n)$. As we will see later, we have been able to find a form of the transfer operator for these groups, where the evaluation of the character is limited to a small number of elements, see Chapter 7.

Next we define the characters for $\Gamma_0(4)$ and $\Gamma_0(8)$ which we will later use in our numerical investigations of the Selberg zeta function. We use the same system of generators of $\Gamma_0(4)$ as Selberg in [Sel90]:

$$G_1^{(4)} = \begin{pmatrix} 1 & 1 \\ 0 & 1 \end{pmatrix} = T \quad \text{and} \quad G_2^{(4)} = \begin{pmatrix} 1 & 0 \\ -4 & 1 \end{pmatrix} = S T^4 S. \tag{6.18}$$

Note that $\Gamma_0(4)$ is freely generated by $G_1^{(4)}$ and $G_2^{(4)}$, i.e. there are no relations for the generators. The group $\Gamma_0(4)$ has three inequivalent cusps at $\kappa_1 = \infty$, $\kappa_2 = 0$ and $\kappa_3 = \frac{1}{2}$, which are the fixed points of $T_1 = G_1^{(4)}$,

$T_2 = G_2^{(4)}$ and $T_3 = (G_2^{(4)})^{-1}(G_1^{(4)})^{-1}$ respectively. We define the character $\chi^{(4)}_{\alpha_1,\alpha_2} : \Gamma_0(4) \to \mathbb{C}$ by

$$\chi^{(4)}_{\alpha_1,\alpha_2}(\gamma) = \exp 2\pi i(\alpha_1\Omega_1^{(4)}(\gamma) + \alpha_2\Omega_2^{(4)}(\gamma)), \tag{6.19}$$

with $0 \leq \alpha_1, \alpha_2 \leq 1$ and $\Omega_i^{(4)} : \Gamma_0(4) \to \mathbb{Z}$ given by (6.17). Obviously, the character $\chi^{(4)}_{\alpha_1,\alpha_2}$ is given on the generators $G_i^{(4)}$'s respectively T_i's by

$$\chi^{(4)}_{\alpha_1,\alpha_2}\left(G_1^{(4)}\right) = \exp 2\pi i\alpha_1 \tag{6.20}$$

$$\chi^{(4)}_{\alpha_1,\alpha_2}\left(G_2^{(4)}\right) = \exp 2\pi i\alpha_2 \tag{6.21}$$

$$\chi^{(4)}_{\alpha_1,\alpha_2}\left((G_2^{(4)})^{-1}(G_1^{(4)})^{-1}\right) = \exp 2\pi i(-\alpha_1 - \alpha_2). \tag{6.22}$$

The character used by Selberg in [Sel90] to study a deformation of the Eisenstein series corresponds to our character $\chi^{(4)}_{0,\frac{\alpha}{2\pi}}$. For $\alpha_1 \notin \mathbb{Z}$ the cusp at $\kappa_1 = \infty$ is closed, for $\alpha_2 \notin \mathbb{Z}$ the cusp at $\kappa_2 = 0$ is closed and for $\alpha_1 + \alpha_2 \notin \mathbb{Z}$ the cusp at $\kappa_3 = \frac{1}{2}$ is closed. Obviously, a deformation by $\chi^{(4)}_{0,\alpha}$ respectively $\chi^{(4)}_{\alpha,0}$ closes two cusps for $\alpha \notin \mathbb{Z}$. We also see that such a deformation is singular since at the moment when α is "turned on", i.e. set to a non-integer value, the multiplicity of the continuous spectrum changes from three to one. See also Chapter 8 for more details on other problems arising from such character perturbations.

A similar character was also used by Phillips and Sarnak in [PS94] to study the spectrum of the hyperbolic Laplacian under a character deformation for $\Gamma(2)$. The group $\Gamma(2)$ is conjugate to $\Gamma_0(4)$ through $K^{-1}\Gamma(2)K = \Gamma_0(4)$ with $K = \begin{pmatrix} 2 & 0 \\ 0 & 1 \end{pmatrix}$. The generators of $\Gamma(2)$ are the conjugate generators of $\Gamma_0(4)$ and given by

$$G_1^{\Gamma(2)} = KG_1^{(4)}K^{-1} = \begin{pmatrix} 1 & 2 \\ 0 & 1 \end{pmatrix} = T^2 \quad \text{and} \quad G_2^{\Gamma(2)} = KG_2^{(4)}K^{-1} = \begin{pmatrix} 1 & 0 \\ -2 & 1 \end{pmatrix} = STS.$$

Our character $\chi^{(4)}_{\alpha_1,\alpha_2}$ is related to the character $\hat{\chi}_{\alpha_1,\alpha_2}$ of Sarnak and Phillips by

$$\hat{\chi}_{\alpha_1,\alpha_2}\left(K\gamma K^{-1}\right) = \chi^{(4)}_{\alpha_1,\alpha_2}(\gamma) \quad \gamma \in \Gamma_0(4).$$

Since these groups are conjugate their Selberg zeta functions coincide

$$Z^{\Gamma(2)}(\beta, \hat{\chi}_{\alpha_1,\alpha_2}) = Z^{(4)}\left(\beta, \chi^{(4)}_{\alpha_1,\alpha_2}\right). \tag{6.23}$$

Phillips and Sarnak proved in [PS91] that the character $\hat{\chi}_{0,\alpha}$ (respectively $\chi_{0,\alpha}$) is arithmetic (i.e. $\ker\chi^{(4)}_{0,\alpha}$ is a congruence subgroup) iff $\alpha \in \left\{0, \frac{1}{8}, \frac{2}{8}, \frac{3}{8}, \frac{4}{8}\right\}$. The conjecture of Sarnak and Phillips says that only for these α values $(\Gamma(2), \hat{\chi}_{0,\alpha})$ is essentially cuspidal. The following lemma shows that a deformation by $\chi^{(4)}_{0,\alpha}$ is the same as by $\chi^{(4)}_{\alpha,0}$:

Lemma 6.5.2. *For the Selberg zeta function for* $(\Gamma_0(4), \chi^{(4)}_{\alpha_1,\alpha_2})$ *we have the following relations*

$$Z^{(4)}\left(\beta, \chi^{(4)}_{\alpha_1,\alpha_2}\right) = Z^{(4)}\left(\beta, \chi^{(4)}_{\alpha_1,-\alpha_2-\alpha_1}\right) \tag{6.24}$$

$$Z^{(4)}\left(\beta, \chi^{(4)}_{\alpha_1,\alpha_2}\right) = Z^{(4)}\left(\beta, \chi^{(4)}_{\alpha_2,\alpha_1}\right) \tag{6.25}$$

$$Z^{(4)}\left(\beta, \chi^{(4)}_{\alpha_1,\alpha_2}\right) = Z^{(4)}\left(\beta, \chi^{(4)}_{-\alpha_1,-\alpha_2}\right). \tag{6.26}$$

Proof. Conjugation of the group $\Gamma(2)$ by $g \in \mathrm{GL}(2,\mathbb{Z})$ gives the same Selberg zeta function with the conjugate character $\hat{\chi}_{\alpha_1,\alpha_2}\left(g\gamma g^{-1}\right)$. Conjugating the generators of $\Gamma(2)$ by $T = \begin{pmatrix} 1 & 1 \\ 0 & 1 \end{pmatrix}$ leads to the character

$$\hat{\chi}_{\alpha_1,\alpha_2}(TG_1^{\Gamma(2)}T^{-1}) = \hat{\chi}_{\alpha_1,\alpha_2}(TT^2T^{-1}) = \hat{\chi}_{\alpha_1,\alpha_2}(G_1^{\Gamma(2)})$$

$$\hat{\chi}_{\alpha_1,\alpha_2}(TG_2^{\Gamma(2)}T^{-1}) = \hat{\chi}_{\alpha_1,\alpha_2}(TSTSTS^{-1}) = \hat{\chi}_{\alpha_1,\alpha_2}((G_2^{\Gamma(2)})^{-1}(G_1^{\Gamma(2)})^{-1}).$$

Conjugating the generators of $\Gamma(2)$ by $S = \begin{pmatrix} 0 & -1 \\ 1 & 0 \end{pmatrix}$ leads to the character

$$\begin{aligned} \hat{\chi}_{\alpha_1,\alpha_2}(S G_1^{\Gamma(2)} S^{-1}) &= \hat{\chi}_{\alpha_1,\alpha_2}(S T^2 S) = \hat{\chi}_{\alpha_1,\alpha_2}(G_2^{\Gamma(2)}) \\ \hat{\chi}_{\alpha_1,\alpha_2}(S G_2^{\Gamma(2)} S) &= \hat{\chi}_{\alpha_1,\alpha_2}(S S T^2 S S) = \hat{\chi}_{\alpha_1,\alpha_2}(G_1^{\Gamma(2)}) \end{aligned}$$

and by $J = \begin{pmatrix} -1 & 0 \\ 0 & 1 \end{pmatrix}$ leads to

$$\begin{aligned} \hat{\chi}_{\alpha_1,\alpha_2}(J G_1^{\Gamma(2)} J^{-1}) &= \hat{\chi}_{\alpha_1,\alpha_2}(J T^2 J) = \hat{\chi}_{\alpha_1,\alpha_2}((G_1^{\Gamma(2)})^{-1}) \\ \hat{\chi}_{\alpha_1,\alpha_2}(J G_2^{\Gamma(2)} J) &= \hat{\chi}_{\alpha_1,\alpha_2}(J S T^2 S J) = \hat{\chi}_{\alpha_1,\alpha_2}((G_2^{\Gamma(2)})^{-1}). \end{aligned}$$

Finally, we see that these conjugations for the character $\hat{\chi}_{\alpha_1,\alpha_2}$ can be written as

$$\begin{aligned} \hat{\chi}_{\alpha_1,\alpha_2}(T\gamma T^{-1}) &= \hat{\chi}_{\alpha_1,-\alpha_2-\alpha_1}(\gamma) \\ \hat{\chi}_{\alpha_1,\alpha_2}(S\gamma S) &= \hat{\chi}_{\alpha_2,\alpha_1}(\gamma) \\ \hat{\chi}_{\alpha_1,\alpha_2}(J\gamma J) &= \hat{\chi}_{-\alpha_1,-\alpha_2}(\gamma) \end{aligned}$$

for $\gamma \in \Gamma(2)$, and therefore

$$\begin{aligned} Z^{\Gamma(2)}(\beta, \hat{\chi}_{\alpha_1,\alpha_2}) &= Z^{\Gamma(2)}(\beta, \hat{\chi}_{\alpha_1,-\alpha_2-\alpha_1}) \\ Z^{\Gamma(2)}(\beta, \hat{\chi}_{\alpha_1,\alpha_2}) &= Z^{\Gamma(2)}(\beta, \hat{\chi}_{\alpha_2,\alpha_1}) \\ Z^{\Gamma(2)}(\beta, \hat{\chi}_{\alpha_1,\alpha_2}) &= Z^{\Gamma(2)}(\beta, \hat{\chi}_{-\alpha_1,-\alpha_2}). \end{aligned}$$

Using these relations and relation (6.23) concludes the proof. □

Note that relation (6.26) just says that the Selberg zeta functions with a character and with the complex conjugated character are the same. Indeed, according to [Hej08] this is the case for all $(\Gamma_0(n), \chi)$. It is more convenient for us to study the deformation of $\Gamma_0(4)$ by the character $\chi^{(4)}_{\alpha,0}$, which is singular in the cusp at $\kappa_2 = 0$, and which closes the cusps at $\kappa_1 = \infty$ and $\kappa_3 = \frac{1}{2}$. We hence define the character $\chi^{(4)}_{\alpha}$ by

$$\chi^{(4)}_{\alpha} := \chi^{(4)}_{\alpha,0}. \tag{6.27}$$

Obviously, from (6.25) it follows that the deformation Phillips and Sarnak studied for $(\Gamma(2), \hat{\chi}_{0,\alpha})$ corresponds exactly to our deformation $(\Gamma_0(4), \chi^{(4)}_{\alpha,0})$. As we will see later, deformation under this character preserves a new kind of symmetry of the transfer operator, which is destroyed under the deformation of $\chi^{(4)}_{0,\alpha}$, see Chapter 8. Using this symmetry helps us a great deal with our numerical computations, since the computations can be performed faster and it is possible to obtain additional information about the eigenvalues and resonances of the hyperbolic Laplacian.

To compute the functional equation (6.7) of the Selberg zeta function we need to evaluate the function $\eta(\beta)$ in (6.9):

Lemma 6.5.3. *For $(\Gamma_0(4), \chi \equiv 1)$ the function $\eta(\beta)$ is given by*

$$\eta(\beta) = \eta\left(\frac{1}{2}\right)\left(2^{2\beta-1}\frac{\Gamma\left(\frac{1}{2}+\beta\right)}{\Gamma\left(\frac{3}{2}-\beta\right)}\right)^3 \exp\left\{2\pi\int_0^{\beta-\frac{1}{2}} \tau\tan(\pi\tau)d\tau\right\} \tag{6.28}$$

and for $(\Gamma_0(4), \chi_\alpha^{(4)})$ *by*

$$\eta(\beta) = \eta\left(\frac{1}{2}\right) 2^{2\beta-1} \frac{\Gamma\left(\frac{1}{2}+\beta\right)}{\Gamma\left(\frac{3}{2}-\beta\right)} \exp\left\{2\pi \int_0^{\beta-\frac{1}{2}} \tau \tan(\pi\tau) d\tau\right\} \left(|1-e^{2\pi i\alpha}|\,|1-e^{-2\pi i\alpha}|\right)^{2\beta-1}. \tag{6.29}$$

Proof. The index μ_4 of $\Gamma_0(4)$ in $\mathrm{SL}(2,\mathbb{Z})$ is $\mu_4 = 6$. For $(\Gamma_0(4), \chi \equiv 1)$ the number of open cusps is $h_0 = 3$. For $(\Gamma_0(4), \chi_\alpha^{(4)})$ the number of open cusps is $h_0 = 1$ and the character $\chi_\alpha^{(4)}$ on the T_i's is given by (6.20) - (6.22): $\chi_\alpha^{(4)}(T_1) = \exp 2\pi i\alpha, \chi_\alpha^{(4)}(T_2) = 1$ and $\chi_\alpha^{(4)}(T_3) = \exp -2\pi i\alpha$. Inserting these results in (6.9) concludes the proof. □

Another group we want to study is the freely generated group $\Gamma_0(8)$, which is a subgroup of $\Gamma_0(4)$. We use for $\Gamma_0(8)$ the system of generators given by

$$\begin{aligned}
G_1^{(8)} &= \begin{pmatrix} 1 & 0 \\ -8 & 1 \end{pmatrix} = ST^8S = (G_2^{(4)})^2 \\
G_2^{(8)} &= \begin{pmatrix} -3 & 1 \\ -16 & 5 \end{pmatrix} = ST^{-4}STST^4S = (G_2^{(4)})^{-1} G_1^{(4)} G_2^{(4)} \\
G_3^{(8)} &= \begin{pmatrix} 1 & 1 \\ 0 & 1 \end{pmatrix} = T = G_1^{(4)},
\end{aligned}$$

with the generators $G_i^{(4)}$ of $\Gamma_0(4)$ given in (6.18). The inequivalent cusps are $\kappa_1 = 0, \kappa_2 = \frac{1}{4}, \kappa_3 = \infty, \kappa_4 = \frac{1}{2}$, which are fixed points of $T_1 = G_1^{(8)}$, $T_2 = G_2^{(8)}$, $T_3 = G_3^{(8)}$ and $T_4 = G_1^{(8)} G_2^{(8)}$ respectively. We define the character $\chi_{\alpha_1,\alpha_2,\alpha_3}^{(8)} : \Gamma_0(8) \to \mathbb{C}$ following (6.16) as

$$\chi_{\alpha_1,\alpha_2,\alpha_3}^{(8)}(\gamma) = \exp 2\pi i(\alpha_1 \Omega_1^{(8)}(\gamma) + \alpha_2 \Omega_2^{(8)}(\gamma) + \alpha_3 \Omega_3^{(8)}(\gamma)) \tag{6.30}$$

with $0 \le \alpha_1, \alpha_2, \alpha_3 \le 1$ and $\Omega_i^{(8)} : \Gamma_0(8) \to \mathbb{Z}$ given by (6.17). This character is given for the $G_i^{(8)}$'s respectively T_i's by

$$\begin{aligned}
\chi_{\alpha_1,\alpha_2,\alpha_3}^{(8)}\left(G_1^{(8)}\right) &= \exp 2\pi i\alpha_1 \\
\chi_{\alpha_1,\alpha_2,\alpha_3}^{(8)}\left(G_2^{(8)}\right) &= \exp 2\pi i\alpha_2 \\
\chi_{\alpha_1,\alpha_2,\alpha_3}^{(8)}\left(G_3^{(8)}\right) &= \exp 2\pi i\alpha_3 \\
\chi_{\alpha_1,\alpha_2,\alpha_3}^{(8)}\left(G_1^{(8)} G_2^{(8)}\right) &= \exp 2\pi i\,(\alpha_1+\alpha_2).
\end{aligned}$$

The character we will use for the deformation is given by

$$\chi_\alpha^{(8)}(\gamma) := \chi_{0,\alpha,0}^{(8)}(\gamma) = \exp 2\pi i\alpha \Omega_2^{(8)}(\gamma). \tag{6.31}$$

It is singular in the cups $\kappa_1 = 0$ and $\kappa_3 = \infty$ and closes the other two cusps. Since $\Gamma_0(8) \subset \Gamma_0(4)$ the character $\chi_{\alpha_1,\alpha_2}^{(4)}$ can also be defined for $\Gamma_0(8)$:

Lemma 6.5.4. *The character* $\chi_{\alpha_1,\alpha_2}^{(4)}$ *for* $\Gamma_0(4)$ *restricted to* $\Gamma_0(8)$ *is related to the character* $\chi_{\alpha_1,\alpha_2,\alpha_3}^{(8)}$ *for* $\Gamma_0(8)$ *by*

$$\chi_{\alpha_1,\alpha_2}^{(4)}(\gamma) = \chi_{2\alpha_2,\alpha_1,\alpha_1}^{(8)}(\gamma) \quad \textit{and} \tag{6.32}$$

$$\chi_{\alpha_1,\alpha_2+\frac{1}{2}}^{(4)}(\gamma) = \chi_{2\alpha_2,\alpha_1,\alpha_1}^{(8)}(\gamma) \tag{6.33}$$

for $\gamma \in \Gamma_0(8)$.

Proof. The generators of the groups $\Gamma_0(4)$ and $\Gamma_0(8)$ are related by $G_1^{(8)} = G_2^{(4)} G_2^{(4)}$, $G_2^{(8)} = (G_2^{(4)})^{-1} G_1^{(4)} G_2^{(4)}$ and $G_3^{(8)} = G_1^{(4)}$. The character $\chi^{(4)}_{\alpha_1,\alpha_2}$ on the generators of $\Gamma_0(8)$ is given by

$$\begin{aligned}
\chi^{(4)}_{\alpha_1,\alpha_2}\left(G_1^{(8)}\right) &= \exp 2\pi i \alpha_2 2 \\
\chi^{(4)}_{\alpha_1,\alpha_2}\left(G_2^{(8)}\right) &= \exp 2\pi i \alpha_1 \\
\chi^{(4)}_{\alpha_1,\alpha_2}\left(G_3^{(8)}\right) &= \exp 2\pi i \alpha_1 \\
\chi^{(4)}_{\alpha_1,\alpha_2}\left(G_1^{(8)} G_2^{(8)}\right) &= \exp 2\pi i \left(\alpha_2 2 + \alpha_1\right).
\end{aligned}$$

Comparing it to the character $\chi^{(8)}_{\alpha_1,\alpha_2,\alpha_3}$ on the generators $G_i^{(8)}$ concludes the proof. □

Chapter 7

The transfer operator for the geodesic flow on hyperbolic surfaces

The transfer operator method plays a central role in this thesis; therefore, we want to briefly describe its origins and historical development. Later we will present the transfer operator for the geodesic flow on hyperbolic surfaces and discuss how to incorporate a character into this transfer operator. Finally, we will introduce a form of the transfer operator which is appropriate for numerical computations.

Statistical mechanics is the science of macroscopic behavior of physical systems, which consist of a large number n of subunits, the limit $n \to \infty$ is called the *thermodynamic limit*. Statistical properties of a system in thermodynamic equilibrium can be encoded in the so-called partition function from statistical mechanics (see, e.g., [DGLR94]), which is usually a kind of exponential sum over energy levels of all possible states of a system. There are several types of partition functions, which correspond to different kinds of statistical ensembles. It is possible to obtain properties of a physical system from a partition function and its derivatives. These may be thermodynamical properties like, e.g., free energy, entropy and pressure, but it is also possible to obtain other properties depending on the type of physical system.

One of the essential parts of thermodynamic is the study of phase transitions. Real physical systems exist in the three-dimensional world, but it is usually not possible to solve the equations which describe such systems. Instead, one tries to describe the properties of these systems by models which have fewer than three dimensions, sometimes even only one. One hopes that by solving such models results can be obtained, which allow make statements about the real system. For more on one-dimensional models in mathematical physics see [LM66]. When studying a one-dimensional model of ferromagnetism, Ising introduced in [Isi25] a transfer matrix to calculate the partition functions of this model, which are given by the traces of this transfer matrix. This model is now known as the one-dimensional Ising model, which was actually invented by Lenz in [Len20], who was Ising's PhD advisor. The one-dimensional Ising model has no phase transition. On the other hand, Onsager found an exact solution for the two-dimensional Ising model in [Ons44] by using also a transfer matrix. He showed that this model indeed has a phase transition. Van Hove introduced an integral operator in [Hov50] to compute the partition functions of a certain one-dimensional gas model with nearest neighbour interactions and has shown that no phase transition can occur. Another integral operator was introduced by Kac [Kac59] to calculate the partition functions of a model of a one-dimensional gas with long range interactions, see also Chapter 9.

Obviously, the results from one-dimensional systems are somehow limited and unfortunately, often not very relevant to a real three-dimensional physical system. On the other hand, since time is one-dimensional, the methods which are used to study one-dimensional systems can also be applied to describe the time behavior of some abstract systems, so-called dynamical systems [Dev03], [ER85]. The development of the ergodic theory of dynamical systems [Sin77] was motivated by problems in statistical physics. This theory

deals with the long-term behavior of dynamical systems. It turned out that the formalism used in thermodynamics can also be applied to other fields besides dynamical systems. The application of methods of statistical mechanics to dynamical systems is known as the *Thermodynamic Formalism*, which was introduced by Bowen [Bow08], Ruelle [Rue04] and Sinai. One can define generalized partition functions for dynamical systems in an abstract mathematical way: Let X be for instance some metric space and $\tau : X \to X$ a continuous map. Denote the set of fix points of τ with period n by $\mathrm{Fix}\,\tau^n = \{x \in X : \tau^n(x) = x\}$ for $n \in \mathbb{Z}_>$. If $A : X \to \mathbb{C}$ is a function on X, then the generalized partition functions Z_n are given by

$$Z_n(A) = \sum_{x \in \mathrm{Fix}\,\tau^n} \exp \sum_{k=0}^{n-1} A\left(\tau^k(x)\right). \tag{7.1}$$

The physical interpretation of a dynamical system is that the map τ describes the time development of the states of the system in the phase space X. Note that the ergodic properties of a system are determined by the expanding part of such a map. Furthermore, A can be interpreted as an observable, which usually is a real-valued function. Sinai realized that a special role is played for smooth dynamical systems by the observable

$$A(x) = -\beta \ln |D\tau(x)| \tag{7.2}$$

where $D\tau(x)$ is the Jacobian determinant of $\tau(x)$. The factor $\beta \in \mathbb{C}$ is also called the "inverse temperature", since in physics it is usually defined as $\beta = (k_B T)^{-1}$, with the Boltzmann constant k_B and the absolute temperature T. One can also define a pressure when the mapping τ meets certain conditions (see [Rue04] section 7.19). The so-called topological pressure is given by

$$P(A) = \lim_{n \to \infty} \frac{1}{n} \ln Z_n(A), \tag{7.3}$$

where the limit $n \to \infty$ corresponds to the thermodynamic limit. Ruelle introduced a dynamical zeta function in [Rue76a] given by

$$Z_R(z, A) = \exp \sum_{n=1}^{\infty} \frac{z^n}{n} Z_n(A) \tag{7.4}$$

which is an elegant way to combine the partitions functions $Z_n(A)$ for all $n \in \mathbb{Z}_>$. The series over n converges for $|z| < e^{-P(A)}$. This zeta function can obviously be interpreted as a generating function for the partition functions $Z_n(A)$. An evident question is then if one can also find an operator to calculate the partition functions $Z_n(A)$, like in the case of Ising's transfer matrix, Van Hove's operator or the operator of Kac. For this, Ruelle's transfer operator [May80b], [Bal00] should be considered defined by

$$\mathcal{L}_A f(x) = \sum_{y \in \tau^{-1}(x)} \exp(A(y))\, f(y) \tag{7.5}$$

with $\tau^{-1}(x) = \{y : \tau(y) = x\}$, which is acting on some Banach space [Ban32] of functions f. In special cases this transfer operator is indeed related to the partition functions by its traces and to the dynamical zeta function by its Fredholm determinant. Examples for which this holds are the transfer operator for the geodesic flow on hyperbolic surfaces, which we discuss in this chapter, and the transfer operator for the Kac-Baker model in Chapter 9. Unfortunately, in general there is no such connection between the transfer operator and partition functions. The main problem is that this kind of operator generally does not have a well-defined trace or a well-defined Fredholm determinant. It is not easy in general to find an appropriate Banach space on which this operator is trace class; the choice of a such space clearly depends on τ and A. Furthermore, if the chosen space is too large then the transfer operator will not reveal much interesting information about the dynamical system under investigation. The transfer operator can be regarded as a generalized Perron-Frobenius operator well known from the ergodic theory of dynamical systems [LM94]. Indeed, in the special case where A is given by (7.2) and β is set to one, the transfer operator is exactly the

Perron-Frobenius operator. The Perron-Frobenius operator describes the time development of states in phase space; its eigenfunctions with the eigenvalue one are the equilibrium states in the phase space, i.e. states of maximum entropy. This operator can be thought of as a discrete version of the well-known Liouville operator from classical mechanics. For a more detailed discussion of the transfer operator and the Perron-Frobenius operator see also [May91a] and the survey [Fra05].

7.1 Nuclear operators

The definition of nuclear operators and trace-class operators well known in Hilbert spaces has been extended by Ruston [Rus51] and Grothendieck [Gro55], [Gro56] to general Banach spaces. A general treatment of nuclear operators is given by Pietsch in [Pie86] which we follow here. Let B be a Banach space and B^* its dual space. Let $0 < p \leq 1$, an operator $A : B \to B$ is said to be p-nuclear if there exists a so-called p-nuclear representation

$$A = \sum_{i=1}^{\infty} a_i^* \otimes a_i \quad \text{with} \sum_{i=1}^{\infty} \|a_i^*\|^p \cdot \|a_i\|^p < \infty \tag{7.6}$$

where $a_i \in B$ and $a_i^* \in B^*$. Note, that in general a nuclear operator can have more then one such representation. The infimum of p such that (7.6) holds is called the order of A. A set of axioms for an abstract trace of operators on Banach spaces is given in section 4.2.1 of [Pie86]. The absolutely convergent series $\sum_{i=1}^{\infty} a_i^*(a_i)$ fulfills these axioms. Unfortunately, usually this sum depends on the representation (7.6) of the operator A. If this is not the case, then

$$\operatorname{tr} A = \sum_{i=1}^{\infty} a_i^*(a_i) \tag{7.7}$$

is called the trace of A. On the other hand, it was proved in [Whi96] that if the sum over the eigenvalues $\lambda_i = \lambda_i(A) \in \sigma(A)$ of A is absolutely convergent, then there exists a spectral trace of A, denoted by

$$\operatorname{tr}_\sigma A = \sum_{i \in I_\sigma} \lambda_i \tag{7.8}$$

where the set I_σ counts the eigenvalues according to their multiplicity.

There are several conditions for Banach spaces such that the traces (7.7) and (7.8) exist and are equal, (see also [Kön80], [Pie91] and [Fri86]). Note that for nuclear operators on Hilbert spaces the nuclear trace always coincides with the spectral one [Lid59]. It was already proven by Grothendieck [Gro52] that for a p-nuclear operator A with $0 < p \leq \frac{2}{3}$ the rhs of (7.7) does not depend on the representation (7.6) of A and that the sum over the eigenvalues of A converges absolutely, i.e. the trace (7.7) of A exists and coincides with the spectral trace (7.8). Furthermore, in this case the Fredholm determinant of A is given by

$$\det(1 - zA) = \prod_{i \in I_\sigma} (1 - z\lambda_i) \quad \text{with } \lambda_i \in \sigma(A) \tag{7.9}$$

and defines a holomorphic function. In [Gro55] Grothendieck also proved the following identity for nuclear operators of order zero

$$\det(1 - zA) = \exp \operatorname{tr} \ln(1 - zA) \tag{7.10}$$

where ln is given by $\ln(1 - zA) = -\sum_{m=1}^{\infty} \frac{(zA)^m}{m}$.

All nuclear operators can be approximated by operators of finite rank, see [Pie91] and [Fri96]. Indeed, this property is very useful for our numerical investigations since it allows us to approximate certain transfer operators by a finite matrix.

A more extensive introduction of nuclear operators if given in [CS99]. For an overview of Grothendieck's results see also the appendix in [May91a].

7.2 The transfer operator as a sum of composition operators

Now we want to discuss systems where the transfer operator belongs to the class of nuclear operators of order zero. We restrict ourselves to $\dim X = 1$, for the more general case see [Rue76b] and [Bal00]. We define intervals $U_i \subset X$ such that $X = \cup_{i\in I} U_i$ and $\operatorname{int} U_i \cap \operatorname{int} U_j = \emptyset$ for $i \neq j$. The map $\tau : U \to U$ restricted to the interval U_i is denoted by $\tau_i = \tau|_{U_i}$. We choose U_i such that the map τ_i is monotone. Then the transfer operator (7.5) is given by

$$\mathcal{L}_A f(x) = \sum_{i\in I} \delta_{\tau(U_i)}(x) \exp\left(A\left(\tau_i^{-1}(x)\right)\right) f\left(\tau_i^{-1}(x)\right)$$

where $\delta_{\tau(U_i)}(x)$ is one if $x \in \tau(U_i)$ and else zero. By setting $\Phi_i(x) = \delta_{\tau(U_i)}(x) \exp A\left(\tau_i^{-1}(x)\right)$ and $\psi_i(x) = \tau_i^{-1}(x)$ we can write this operator in a more abstract way as a sum of composition operators

$$\mathcal{L} f(x) = \sum_{i\in I} \Phi_i(x)\, f \circ \psi_i(x) = \sum_{i\in I} \mathcal{L}_i f(x) \tag{7.11}$$

where $\mathcal{L}_i f(x) = \Phi_i(x)\, f \circ \psi_i(x)$. Now assume we can extend X to some complex disk D, and assume that ψ_i is holomorphic in a neighborhood of $\bar{D}$ and contracting, i.e. $\psi_i\left(\bar{D}\right) \subset D$ for all i. It was proved in [EH70] that ψ_i has exactly one fixed point z_i^* such that $\psi_i\left(z_i^*\right) = z_i^*$ and $\|\psi_i'\left(z_i^*\right)\| < 1$, where $\psi_i'\left(z_i^*\right) = \frac{\partial}{\partial x}\psi_i(x)|_{x=z_i^*}$. Ruelle [Rue76b] and Mayer [May76] noticed that under certain conditions the sum of composition operators in (7.11) is itself nuclear of order zero, i.e. the operator $\mathcal{L}$ has a trace which is also spectral. We will present here the trace formula for the transfer operator introduced by Chang [Cha99], which is a generalization of Mayer's formula [May80a], based on some ideas in [Kam75]. Ruelle derived also the trace formula for such a transfer operator in [Rue76b] by evaluating an integral kernel for $\mathcal{L}$. Let $\mathcal{L}$ resp. $\mathcal{L}_i$ act on vector-valued functions $f \in E$, where the Banach space E is given as a direct sum $E = \bigoplus_{i=1}^N B(D)$ of the Banach space $B(D)$ and $\Phi_i(x) \in \mathbb{C}^{N\times N}$, for some finite $N \in \mathbb{Z}_>$. Then the spectrum of $\mathcal{L}_i$ is given by $\sigma(\mathcal{L}_i) = \left\{\rho(\psi_i'\left(z_i^*\right))^n : n \in \mathbb{Z}_\geq, \rho \in \sigma(\Phi_i\left(z_i^*\right))\right\}$ and the spectral trace of $\mathcal{L}_i$ is a geometric series which can be written explicitly as $\frac{\operatorname{tr}\Phi_i(z_i^*)}{1-\psi_i'(z_i^*)}$. The trace of $\mathcal{L}$ is then given by

$$\operatorname{tr}\mathcal{L} = \sum_{i\in I} \operatorname{tr}\mathcal{L}_i = \sum_{i\in I} \frac{\operatorname{tr}\Phi_i\left(z_i^*\right)}{1-\psi_i'\left(z_i^*\right)}. \tag{7.12}$$

Obviously this formula is quite useful not only for the transfer operator, but also for general composition operators. A similar trace formula was also given by Fried in [Fri86]. Note also that this trace formula can also be obtained by using the Atiyah-Bott fixed point formula.

7.3 The transfer operator for the geodesic flow

So-called symbolic dynamics was introduced by Hadamard [Had98], whereby he created a correspondence between geodesics on a surface of negative curvature and certain symbolic sequences, see also [Bow73]. Artin [Art24] noticed that there is a connection between geodesics on the modular surface $\mathrm{SL}(2,\mathbb{Z})\backslash\mathbb{H}$ and continued fractions. Sinai realized that the Selberg zeta function [Sel56] can be interpreted dynamically as a product over the closed orbits of the geodesic flow on $\Gamma\backslash\mathbb{H}$, where Γ denotes a Fuchsian group. Smale [Sma67] generalized the flows on manifolds of negative curvature to so-called Axiom A flows, for which Bowen [Bow73] developed a symbolic dynamics. On the other hand, Ruelle [Rue04], [Rue76b] noticed the connection of zeta functions for Axiom A flows and certain partition functions for the discrete dynamical system defined by the Poincaré map of the flow, see also [Fri86]. In [BS79] Bowen and Series constructed

symbolic dynamics for the geodesic flow on surfaces of constant negative curvature defined by finitely generated discrete subgroups of $\mathrm{SL}(2,\mathbb{R})$.

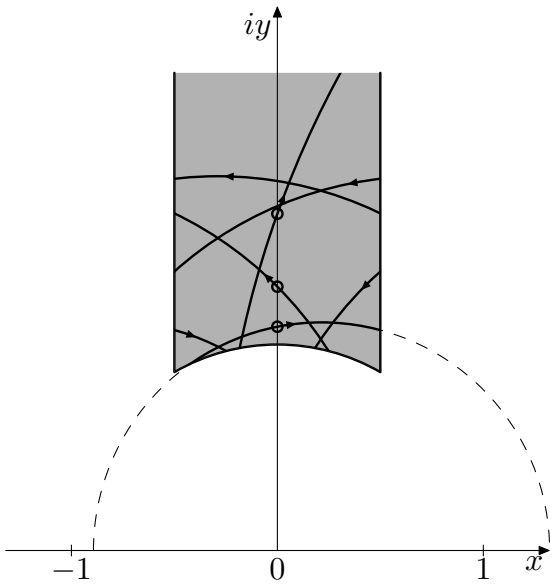

Figure 7.1: Geodesic flow on $\mathrm{SL}(2,\mathbb{Z})\backslash\mathbb{H}$ (fragment of an orbit)

For co-compact groups nuclear transfer operators can be constructed by using the symbolic dynamics of Bowen and Series, and the Selberg zeta function can be expressed in terms of Fredholm determinants of these operators [Pol91]. Nuclear transfer operators for general co-finite groups have been constructed in [Mor97]. For $\mathrm{SL}(2,\mathbb{Z})$ a different symbolic dynamics has been found in [AF84] and [Ser85]. It turns out that its dynamics can be described by the continued fraction map, also called the Gauss map $T_G : [0,1] \to [0,1]$, defined by

$$T_G(x) = \frac{1}{x} - \left[\frac{1}{x}\right] \quad \text{and} \quad T_G(0) = 0 \tag{7.13}$$

with $[\,\cdot\,]$ denoting the integer part, see also Fig. 7.2.

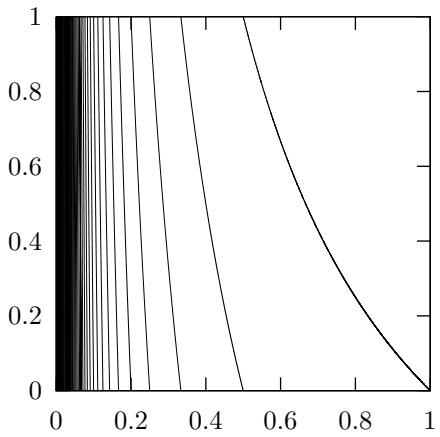

Figure 7.2: The Gauss map on the unit interval

The transfer operator for the Gauss map was studied by Mayer in [May90]. In [May91b] the Selberg zeta function for $\mathrm{SL}(2,\mathbb{Z})$ was expressed by the Fredholm determinant of this transfer operator, see also [May91a]. For a more detailed introduction to Series' symbolic dynamics and its relation to Mayer's transfer operator see also [Fra06]. In [Fri96] Fried generalized the results of Mayer to finite index subgroups of triangle groups. About the same time Chang [Cha99] extended Mayer's transfer operator to finite index subgroups Γ of $\mathrm{SL}(2,\mathbb{Z})$. Using Series' results [Ser85] Chang found that the symbolic dynamics of the geodesic flow on $\Gamma\backslash\mathbb{H}$ can be described by the Poincaré map

$$P_\Gamma : [0,1]\times[0,1]\times\{+1,-1\}\times\Gamma\backslash\mathrm{SL}(2,\mathbb{Z}) \to [0,1]\times[0,1]\times\{+1,-1\}\times\Gamma\backslash\mathrm{SL}(2,\mathbb{Z})$$

given by

$$P_\Gamma(x,y,\varepsilon,\Gamma g) = \left(T_G(x), \left(y+\left[\frac{1}{x}\right]\right)^{-1}, -\varepsilon, \Gamma g T^{\varepsilon[\frac{1}{x}]} S\right). \tag{7.14}$$

The expanding part of this map determining the ergodic properties, is given by

$$P_{\Gamma,\mathrm{ex.}}(x,\varepsilon,\Gamma g) = \left(T_G(x), -\varepsilon, \Gamma g T^{\varepsilon[\frac{1}{x}]} S\right).$$

To construct the transfer operator we need the inverse branches of this map, given by

$$P^{-1}_{\Gamma,\mathrm{ex.}}(x,\varepsilon,\Gamma g) = \left\{\left(\frac{1}{x+l}, -\varepsilon, \Gamma g S T^{\varepsilon l}\right) : l\in\mathbb{Z}_>\right\}.$$

The transfer operator for the geodesic flow on $\Gamma\backslash\mathbb{H}$ introduced in [Cha99] has the form

$$\tilde{\mathcal{L}}_\beta = \begin{pmatrix} 0 & \mathcal{L}_{\beta,+1} \\ \mathcal{L}_{\beta,-1} & 0 \end{pmatrix}, \tag{7.15}$$

where $\mathcal{L}_{\beta,\varepsilon} : \bigoplus_{i=1}^{\mu} B(D) \to \bigoplus_{i=1}^{\mu} B(D)$ is given by

$$\mathcal{L}_{\beta,\varepsilon}\vec{f}(z) = \sum_{l=1}^{\infty} (z+l)^{-2\beta} U^\Gamma\left(S T^{\varepsilon l}\right)\vec{f}\left(\frac{1}{z+l}\right), \quad \text{for } \Re\beta > \frac{1}{2} \tag{7.16}$$

with $\vec{f}(z) = (f_i(z))_{1\le i\le\mu}$, and $\mu = [\mathrm{SL}(2,\mathbb{Z}) : \Gamma]$ the index of Γ in $\mathrm{SL}(2,\mathbb{Z})$. For the disk

$$D = \left\{z\in\mathbb{C} : |z-1| < \frac{3}{2}\right\}$$

the Banach space $B(D)$ is defined by

$$B(D) = \left\{ f : D \to \mathbb{C} : f \text{ holomorphic and continuous on } \bar{D} \right\}, \tag{7.17}$$

with the supremum norm $\|f\| = \sup_{z \in D} |f(z)|$. Note that one has to choose the disk D such that $\psi_l(z) = \frac{1}{z+l}$ maps it strictly inside D for all $l \in \mathbb{Z}_>$, and $-1 \notin D$, otherwise the operator would become singular. The induced representation $U^\Gamma : \mathrm{SL}(2,\mathbb{Z}) \to \mathbb{R}^{\mu \times \mu}$ is defined as

$$\left[U^\Gamma(g) \right]_{i,j} = \delta_\Gamma \left(r_i^\Gamma g \left(r_j^\Gamma \right)^{-1} \right) \tag{7.18}$$

with $\left\{ r_i^\Gamma \right\}_{1 \le i \le \mu}$ the right coset representatives of $\Gamma \backslash \mathrm{SL}(2,\mathbb{Z})$ and $\delta_\Gamma : \mathrm{SL}(2,\mathbb{Z}) \to \{0,1\}$ the characteristic function of Γ given by

$$\delta_\Gamma(g) = \begin{cases} 1 & \text{if } g \in \Gamma \\ 0 & \text{else.} \end{cases} \tag{7.19}$$

Chang proved that this transfer operator is nuclear of order zero, see also the results of Fried in [Fri96]. By using formula (7.12) we can write the trace of $\mathcal{L}_{\beta,\varepsilon}$ as

$$\operatorname{tr} \mathcal{L}_{\beta,\varepsilon} = \sum_{l=1}^{\infty} \frac{\left(z_l^* + l \right)^{-2\beta}}{1 + \left(z_l^* + l \right)^{-2}} \operatorname{tr} \left(U^\Gamma \left(S T^{\varepsilon l} \right) \right) \tag{7.20}$$

with $z_l^* = -\frac{l}{2} \pm \sqrt{\left(\frac{l}{2}\right)^2 + 1}$ and $z_l^* \in [0,1]$, i.e. $z_l^* = -\frac{l}{2} + \sqrt{\left(\frac{l}{2}\right)^2 + 1}$.

Mayer [May91a] found an analytic continuation of the transfer operator for $\mathrm{SL}(2,\mathbb{Z})$ into the entire complex β-plane. Following Mayer's ideas Chang [Cha99] determined an analytic continuation of the transfer operator for $\Gamma \subset \mathrm{SL}(2,\mathbb{Z})$; unfortunately this analytic continuation is only valid for representations U^Γ which are induced from the trivial representation of Γ. Furthermore, Fried [Fri96] generalized Mayer's analytical continuation for finite index subgroups of triangle groups. His analytic continuation is valid for any representation. We will later discuss an analytic continuation, which is useful for our proposes.

In [May91b] Mayer established a connection of the transfer operator for $\mathrm{SL}(2,\mathbb{Z})$ and the Selberg zeta function for this group. A generalization of his results to subgroups of $\mathrm{SL}(2,\mathbb{Z})$ was achieved by Chang in [Cha99], where he showed that the Selberg zeta function for Γ can be written as

$$Z(\beta) = \det\left(1 - \tilde{\mathcal{L}}_\beta\right) = \det\left(1 - \mathcal{L}_{\beta,+1}\mathcal{L}_{\beta,-1}\right) = \det\left(1 - \mathcal{L}_{\beta,-1}\mathcal{L}_{\beta,+1}\right). \tag{7.21}$$

Although Chang established this formula for subgroups Γ of $\mathrm{SL}(2,\mathbb{Z})$ only for the trivial character, his results also remain valid for the case when the representation U^Γ is induced by a non-trivial character, see also remark 1 in [Str08]. Since the discrete spectrum of the hyperbolic Laplacian (6.1) for modular groups is given by $\beta(1-\beta)$, where β are the zeros of $Z(\beta)$ on the line $\Re\beta = \frac{1}{2}$, formula (7.21) relates the spectrum of the hyperbolic Laplacian to β values with the eigenvalue one of the transfer operator $\tilde{\mathcal{L}}_\beta$. This gives in principle a new approach to the theory of quantum chaos, where one tries to understand the relation between a quantum system and its classical limit: the transfer operator describes a classical chaotic system, namely the geodesic flow on surfaces with constant negative curvature, that means a particle moving freely on such a surface with constant velocity. On the other hand, the hyperbolic Laplacian is the Schrödinger operator of the quantized version of the geodesic flow.

For $\mathrm{SL}(2,\mathbb{Z})$ $\mathcal{L}_{\beta,+1} = \mathcal{L}_{\beta,-1} = \mathcal{L}_\beta$ is found, and Mayer observed that in this case the Fredholm determinant factorizes in $Z(\beta) = \det\left(1 - \mathcal{L}_\beta\right)\det\left(1 + \mathcal{L}_\beta\right)$. Obviously in this case the Selberg zeta function becomes zero if the transfer operator has the eigenvalue ± 1. Efrat [Efr93] proved that eigenvalues $+1$ of the transfer operator are related to the even symmetry $u(-\bar{z}) = u(z)$ and eigenvalues -1 of the transfer operator are related to the odd symmetry $u(-\bar{z}) = -u(z)$ of Maass wave forms u for $\mathrm{SL}(2,\mathbb{Z})$. Later we will show a

similar factorization of the Fredholm determinant of the transfer operator for $\Gamma_0(n)$, by introducing a new kind of symmetry. In [FM11] we proved that these symmetries are again related to involutions of the Maass wave forms. Similar factorizations for some groups were given in [Cha99]. It turns out that these are just cases where our symmetries are trivial. Another transfer operator was introduced by Manin and Marcolli in [MM02], which always leads to a factorisation of the Selberg zeta function. This operator is conjugated to our transfer operator for one of the above symmetries.

Obviously, the transfer operator method opens a new access to the Selberg zeta function and its zeros. This operator even has the potential to solve the Riemann hypothesis if the values of β could be determined for which it has the eigenvalue one. Unfortunately, apart from some special cases we cannot say much about the exact spectrum of this transfer operator. The transfer operator is a rather difficult object to handle analytically. On the other hand, in recent years it became clear that the transfer operator method is one of the few methods which allows the Selberg zeta function to be evaluated numerically. Indeed, besides the transfer operator method, which can be applied to a large number of different groups, the other methods to compute the Selberg zeta function are only valid for very special cases. The main difficulty is in finding an analytic continuation of the Selberg zeta function for $\Re\beta \leq \frac{1}{2}$. In [MS91] Matthies and Steiner considered a modified Selberg zeta function for the modular group to overcome this difficulty. For convex co-compact Schotty groups Guillopé, Lin and Zworski in [GLZ04] used the transfer operator to obtain an explicit formula for the Fredholm determinant, which can be evaluated numerically more or less directly. In [Str08] Strömberg used the transfer operator method [MS08], [MMS11] for the computation of the Selberg zeta function for Hecke triangle groups, by approximating the transfer operator by a finite matrix.

Since there is no obvious method to determine the spectrum of the transfer operator analytically, we will study this operator numerically instead. Indeed, this method seems to be quite promising to obtain information about this operator, which can help in understanding it better. The numerical results so far have already initiated new theoretical work, like the already mentioned symmetries of the transfer operator [FM11]. Also a theoretical treatment of some of the phenomena we were able to obtain numerically is in progress [BFM12].

There is also a direct connection between the eigenfunctions of the hyperbolic Laplacian and the eigenfunctions of the transfer operator with eigenvalue one. This relation is also very important with regard to quantum chaos, since in contrast to other methods the transfer operator approach enables us not only to relate the spectrum of a quantum system to a classical system, but also its eigenstates. The connection between Maass wave forms and so-called period functions for the modular group was established in [LZ01] by an integral transform and generalized to congruence subgroups in [Müh03]. It turns out that the eigenfunctions of the transfer operator to the eigenvalue one coincide with these period functions [CM99]. Also the Hecke operators, well known for Maass wave forms [AL70], can be defined on period functions [Müh06]. They coincide with the Hecke-*like* operators introduced in [HMM05], which are acting on the eigenfunctions of the transfer operator to the eigenvalue one [FMM07]. For this, the exact relation is used between the period functions and the eigenfunctions of the transfer operator to the eigenvalue one in [Fra06]. Also the Fricke element acting on Maass wave forms has been transferred to the space of period functions in [Fra06].

7.4 The transfer operator for a character deformation

In this section we discuss the transfer operator $\mathcal{L}^{(n)}_{\beta,\varepsilon,\chi}$ for $\Gamma_0(n) \subset \mathrm{SL}(2,\mathbb{Z})$ with the representation U^χ induced from a non-trivial character χ. This is a generalization of the transfer operator (7.16) for finite index subgroups Γ of $\mathrm{SL}(2,\mathbb{Z})$ with a representation U^Γ induced from the trivial character.

We define the representation U^χ and show that it has a special form for some elements. This form is useful for simplifying the transfer operator with the representation U^χ. Then we write down an analytic continuation of this transfer operator and a trace formula for this operator. Finally, we derive a form of the transfer operator which is suitable for numerical computations, since it can be approximated by a finite rank operator, and write down the matrix which we will use to approximate this transfer operator numerically.

Although we will define the transfer operator with the representation U^χ only for Hecke congruence subgroups $\Gamma_0(n)$, the results remain valid also for other congruence subgroups of $\mathrm{SL}(2,\mathbb{Z})$. In the next chapter we will investigate the spectrum of the transfer operator, which we will also use to evaluate the Selberg zeta function. We are especially interested in a character deformation when the representation U^χ is induced by a special character χ_α with a deformation parameter $\alpha \in \mathbb{R}$, introduced in section 6.5.

7.4.1 The induced representation U^χ

To define the representation U^χ we need the following lemma:

Lemma 7.4.1. *For every right coset representative $r_i^{(n)}$ and $g_1, g_2 \in \mathrm{SL}(2,\mathbb{Z})$ there exist unique $d, j \in \{1,\ldots,\mu_n\}$ such that $r_i^{(n)} g_1 \left(r_d^{(n)}\right)^{-1} \in \Gamma_0(n)$ and $r_d^{(n)} g_2 \left(r_j^{(n)}\right)^{-1} \in \Gamma_0(n)$ iff $r_i^{(n)} g_1 g_2 \left(r_j^{(n)}\right)^{-1} \in \Gamma_0(n)$.*

Proof. There exists j with $r_i^{(n)} g_1 g_2 \left(r_j^{(n)}\right)^{-1} = g \in \Gamma_0(n)$. Hence $r_i^{(n)} g_1 = g r_j^{(n)} g_2^{-1}$. We can also find $d \in \{1,\ldots,\mu_n\}$ such that $r_j^{(n)} g_2^{-1} \left(r_d^{(n)}\right)^{-1} \in \Gamma_0(n)$. Hence $r_i^{(n)} g_1 \left(r_d^{(n)}\right)^{-1} \in \Gamma_0(n)$ iff $g \in \Gamma_0(n)$. □

Proposition 7.4.2. *The map $U^\chi : \mathrm{SL}(2,\mathbb{Z}) \to \mathbb{C}^{\mu_n \times \mu_n}$ defined by*

$$[U^\chi(g)]_{i,j} = \delta_{\Gamma_0(n)}\left(r_i^{(n)} g \left(r_j^{(n)}\right)^{-1}\right) \chi\left(r_i^{(n)} g \left(r_j^{(n)}\right)^{-1}\right) \tag{7.22}$$

is a representation of $\mathrm{SL}(2,\mathbb{Z})$ for $\chi : \Gamma_0(n) \to \mathbb{C}$ a non-trivial unitary 1-dim representation of $\Gamma_0(n)$ and $\delta_{\Gamma_0(n)}$ the characteristic function (7.19).

Proof. Since $\delta_{\Gamma_0(n)}\left(r_i^{(n)} g \left(r_j^{(n)}\right)^{-1}\right) \neq 0$ only for $r_i^{(n)} g \left(r_j^{(n)}\right)^{-1} \in \Gamma_0(n)$

$$[U^\chi(g)]_{i,j} = \delta_{\Gamma_0(n)}\left(r_i^{(n)} g \left(r_j^{(n)}\right)^{-1}\right) \chi\left(r_i^{(n)} g \left(r_j^{(n)}\right)^{-1}\right)$$

is well defined. We want to show that U^χ is indeed a representation. From lemma 7.4.1 we see that there exist unique j and d' such that $r_i^{(n)} g_1 g_2 \left(r_j^{(n)}\right)^{-1} \in \Gamma_0(n)$ iff $r_i^{(n)} g_1 \left(r_{d'}^{(n)}\right)^{-1} \in \Gamma_0(n)$ and $r_{d'}^{(n)} g_2 \left(r_j^{(n)}\right)^{-1} \in \Gamma_0(n)$. Therefore

$$\begin{aligned}
\chi\left(r_i^{(n)} g_1 g_2 \left(r_j^{(n)}\right)^{-1}\right) &= \chi\left(r_i^{(n)} g_1 \left(r_{d'}^{(n)}\right)^{-1} r_{d'}^{(n)} g_2 \left(r_j^{(n)}\right)^{-1}\right) \\
&= \chi\left(r_i^{(n)} g_1 \left(r_{d'}^{(n)}\right)^{-1}\right) \chi\left(r_{d'}^{(n)} g_2 \left(r_j^{(n)}\right)^{-1}\right).
\end{aligned}$$

We finally get

$$\begin{aligned}
[U^\chi(g_1 g_2)]_{i,j} &= \textstyle\sum_{d=1}^{\mu_n} \delta_{\Gamma_0(n)}\left(r_i^{(n)} g_1 \left(r_d^{(n)}\right)^{-1}\right) \chi\left(r_i^{(n)} g_1 \left(r_d^{(n)}\right)^{-1}\right) \\
&\qquad \delta_{\Gamma_0(n)}\left(r_d^{(n)} g_2 \left(r_j^{(n)}\right)^{-1}\right) \chi\left(r_d^{(n)} g_2 \left(r_j^{(n)}\right)^{-1}\right) \\
[U^\chi(g_1 g_2)]_{i,j} &= [U^\chi(g_1)\, U^\chi(g_2)]_{i,j}\,.
\end{aligned}$$

The representation $U^\chi\begin{pmatrix} 1 & 0 \\ 0 & 1 \end{pmatrix}$ is diagonal since $\delta_{\Gamma_0(n)}\left(r_i^{(n)}\left(r_j^{(n)}\right)^{-1}\right)$ is non-zero iff $i = j$, and all diagonal entries are given by $\chi\begin{pmatrix} 1 & 0 \\ 0 & 1 \end{pmatrix} = 1$. We see that U^χ is a representation. □

Next we will show that the representation $U^\chi(T^l)$ of the elements $T^l \in \mathrm{SL}(2,\mathbb{Z})$ for certain $l \in \mathbb{Z}$ has a special form, which will help us later to simplify the form of the transfer operator for the groups $\Gamma_0(n)$.

Lemma 7.4.3. *The representation $U^\chi\left(T^{nl}\right)$ of $T^{nl} \in \Gamma_0(n)$ is a diagonal matrix for $l \in \mathbb{Z}$ and n the level of $\Gamma_0(n)$. Indeed, the representation $U^\chi\left(T^{nl}\right)^q$ for $q \in \mathbb{Z}$ is given by*

$$\left[U^\chi\left(T^{nl}\right)^q\right]_{i,j} = \delta_{i,j} \cdot \left(\chi\left(r_i^{(n)} T^{nl} \left(r_j^{(n)}\right)^{-1}\right)\right)^q \tag{7.23}$$

with $\delta_{i,j} = 1$ if $i = j$ and $\delta_{i,j} = 0$ if $i \neq j$.

Corollary 7.4.4. *Lemma 7.4.3 is also true for any representation U^χ which is induced by any one-dimensional representation χ of $\Gamma(n)$ or any other congruence subgroup of $\mathrm{SL}(2,\mathbb{Z})$.*

Proof. Obviously $T^{nl} = \begin{pmatrix} 1 & nl \\ 0 & 1 \end{pmatrix}$ is also an element in $\Gamma(n)$. $\Gamma(n)$ is a normal subgroup of $\mathrm{SL}(2,\mathbb{Z})$, therefore $r_i^{(n)} T^{nl} \left(r_i^{(n)}\right)^{-1} \in \Gamma(n)$ for $1 \leq i \leq \mu_n$. Also $r_i^{(n)} T^{nl} \left(r_i^{(n)}\right)^{-1} \in \Gamma_0(n)$ since $\Gamma(n) \subset \Gamma_0(n)$. By the definition of the representatives of $\Gamma_0(n)$ in $\mathrm{SL}(2,\mathbb{Z})$ we know that

$$\delta_{\Gamma_0(n)}\left(r_i^{(n)} T^{nl} \left(r_j^{(n)}\right)^{-1}\right) = \delta_{i,j},$$

with $\delta_{i,j} = 1$ if $i = j$ and $\delta_{i,j} = 0$ if $i \neq j$. Hence $U^\chi\left(T^{nl}\right)$ is a diagonal matrix and

$$\left[U^\chi\left(T^{nl}\right)^q\right]_{i,j} = \left(\left[U^\chi\left(T^{nl}\right)\right]_{i,j}\right)^q = \delta_{i,j} \cdot \left(\chi\left(r_i^{(n)} T^{nl} \left(r_j^{(n)}\right)^{-1}\right)\right)^q$$

for $q \in \mathbb{Z}$. The corollary follows from the fact that every congruence subgroup of $\mathrm{SL}(2,\mathbb{Z})$ contains some $\Gamma(n)$. □

To give an impression of how the representation (7.22) looks, we present the example of the representation $U^\chi(ST^3)$ for a character of $\Gamma_0(4)$. The definition of the character $\chi = \chi^{(4)}_{\alpha_1,\alpha_2}$ and the system of representatives $r_i^{(4)}$ are given in Appendix B. The following data were generated by our computer program CGF:

---

the index μ_4 of $\Gamma_0(4)$ in $\mathrm{SL}(2,\mathbb{Z})$ is given by

$$\mu_4 = [\,\mathrm{SL}(2,\mathbb{Z}) : \Gamma_0(4)\,] = 6$$

The non-zero entries of the representation $\left[U^{\chi^{(4)}_{\alpha_1,\alpha_2}}\begin{pmatrix} 0 & -1 \\ 1 & 3 \end{pmatrix}\right]_{i,j}$ of $ST^3 \in \mathrm{SL}(2,\mathbb{Z})$ induced by the 1-dim representation $\chi^{(4)}_{\alpha_1,\alpha_2}$ of $\Gamma_0(4)$, with $\gamma_{i,j} = r_i^{(4)}\begin{pmatrix} 0 & -1 \\ 1 & 3 \end{pmatrix}\left(r_j^{(4)}\right)^{-1}$, are

i,j	$\gamma_{i,j}$	$\chi^{(4)}_{\alpha_1,\alpha_2}\left(\gamma_{i,j}\right)$
1,5	$\begin{pmatrix} 1 & 0 \\ 0 & 1 \end{pmatrix}$	1
2,1	$\begin{pmatrix} -1 & -3 \\ 0 & -1 \end{pmatrix} = T^3 = \left(G_1^{(4)}\right)^2 G_1^{(4)}$	$\exp 2\pi i\,(3\alpha_1)$
3,4	$\begin{pmatrix} 1 & -1 \\ 0 & 1 \end{pmatrix} = STST = S = \left(G_1^{(4)}\right)^{-1}$	$\exp 2\pi i\,(-\alpha_1)$
4,6	$\begin{pmatrix} 7 & 3 \\ -12 & -5 \end{pmatrix} = ST^2ST^3 = ST^{-2}S = \left(G_1^{(4)}\right)^{-1}\left(G_2^{(4)}\right)^{-1} = \left(G_1^{(4)}\right)^{-1}\left(G_2^{(4)}\right)^{-1} = \left(G_1^{(4)}\right)^{-1}\left(G_2^{(4)}\right)^{-1}$	$\exp 2\pi i\,(-3\alpha_1 - 3\alpha_2)$

5,2	$\begin{pmatrix} 3 & -1 \\ -8 & 3 \end{pmatrix}$	=	ST^3ST^3	=	$G_2^{(4)}G_1^{(4)}$	$\exp 2\pi i\,(\alpha_1+2\alpha_2)$
			S		$G_2^{(4)}$	
6,3	$\begin{pmatrix} -1 & 0 \\ 4 & -1 \end{pmatrix}$	=	ST^4S	=	$G_2^{(4)}$	$\exp 2\pi i\,(\alpha_2)$

with $G_1^{(4)} = \begin{pmatrix} 1 & 1 \\ 0 & 1 \end{pmatrix}$ and $G_2^{(4)} = \begin{pmatrix} 1 & 0 \\ -4 & 1 \end{pmatrix}$ the generators of $\Gamma_0(4)$, and $S = \begin{pmatrix} 0 & -1 \\ 1 & 0 \end{pmatrix}$ and $T = \begin{pmatrix} 1 & 1 \\ 0 & 1 \end{pmatrix}$.

7.4.2 The transfer operator $\mathcal{L}^{(n)}_{\beta,\varepsilon,\chi}$ with the representation U^χ

We want to write the transfer operator in such a way that it depends only on the representation U^χ of a finite number of elements in $\mathrm{SL}(2,\mathbb{Z})$. This allows us to give a rather explicit form of the transfer operator for certain congruence subgroups. Indeed, we will be able to determine the matrix defining the representation U^χ explicitly, which enables us to study the structure of the transfer operator directly. This form is also the first step to making the transfer operator suitable for numerical investigations.

Consider the i-th component of the function $\mathcal{L}^{(n)}_{\beta,\varepsilon,\chi}\vec{f}(z)$ with the transfer operator $\mathcal{L}^{(n)}_{\beta,\varepsilon,\chi}$ given for $\Re\beta > \frac{1}{2}$ in (7.16):

$$\begin{aligned}\left[\mathcal{L}^{(n)}_{\beta,\varepsilon,\chi}\vec{f}(z)\right]_i &= \sum_{l=1}^{\infty}(z+l)^{-2\beta}\sum_{j=1}^{\mu_n}\left[U^\chi\left(ST^{l\varepsilon}\right)\right]_{i,j} f_j\left(\frac{1}{z+l}\right)\\ &= \sum_{l=1}^{\infty}\sum_{j=1}^{\mu_n}\left[U^\chi\left(ST^{l\varepsilon}\right)\right]_{i,j} f_j|_{2\beta}\tilde{S}T^l z,\end{aligned}$$

with $\tilde{S} = \begin{pmatrix} 0 & 1 \\ 1 & 0 \end{pmatrix}$ and the slash action $f|_s g$ defined as $f|_s\begin{pmatrix} a & b \\ c & d \end{pmatrix} z = (cz+d)^{-s} f\left(\frac{az+b}{cz+d}\right)$.

Lemma 7.4.5. *The action of the transfer operator applied to $\vec{f} \in \bigoplus_{i=1}^{\mu_n} B(D)$, given for $\Re\beta > \frac{1}{2}$ by*

$$\left[\mathcal{L}^{(n)}_{\beta,\varepsilon,\chi}\vec{f}(z)\right]_i = \sum_{l=1}^{\infty}\sum_{j=1}^{\mu_n}\left[U^\chi\left(ST^{l\varepsilon}\right)\right]_{i,j} f_j|_{2\beta}\tilde{S}T^l z$$

can be written as

$$\left[\mathcal{L}^{(n)}_{\beta,\varepsilon,\chi}\vec{f}(z)\right]_i = \sum_{q=0}^{\infty}\sum_{m=1}^{n}\sum_{j=1}^{\mu_n}\left[U^\chi\left(ST^{m\varepsilon}\right)\right]_{i,j}\chi\left(r_j^{(n)}T^{n\varepsilon}\left(r_j^{(n)}\right)^{-1}\right)^q f_j|_{2\beta}\tilde{S}T^{m+nq}z$$

with n the level of $\Gamma_0(n)$.

Proof. Splitting the sum $\sum_{l=1}^{\infty}$ into $\sum_{q=0}^{\infty}\sum_{m=1}^{n}$ with $l = m+nq$ gives

$$\sum_{l=1}^{\infty}\sum_{j=1}^{\mu_n}\left[U^\chi\left(ST^{l\varepsilon}\right)\right]_{i,j} f_j|_{2\beta}\tilde{S}T^l z = \sum_{q=0}^{\infty}\sum_{m=1}^{n}\sum_{j=1}^{\mu_n}\left[U^\chi\left(ST^{(m+nq)\varepsilon}\right)\right]_{i,j} f_j|_{2\beta}\tilde{S}T^{m+nq}z =$$

$$\sum_{q=0}^{\infty}\sum_{m=1}^{n}\sum_{j=1}^{\mu_n}\sum_{k=1}^{\mu_n}\left[U^\chi\left(ST^{m\varepsilon}\right)\right]_{i,k}\left[U^\chi\left(T^{nq\varepsilon}\right)\right]_{k,j} f_j|_{2\beta}\tilde{S}T^{m+nq}z.$$

Since U^χ is a representation we have $U^\chi(T^{nq\varepsilon}) = U^\chi(T^{n\varepsilon})^q$. From lemma 7.4.3 we know that $[U^\chi(T^{n\varepsilon})^q]_{k,j} = \delta_{k,j}\chi\left(r_k^{(n)} T^{n\varepsilon}\left(r_j^{(n)}\right)^{-1}\right)^q$ and therefore

$$\sum_{q=0}^{\infty}\sum_{m=1}^{n}\sum_{j=1}^{\mu_n}\sum_{k=1}^{\mu_n}\left[U^\chi(S T^{m\varepsilon})\right]_{i,k}\delta_{k,j}\chi\left(r_k^{(n)} T^{n\varepsilon}\left(r_j^{(n)}\right)^{-1}\right)^q f_j|_{2\beta}\tilde{S}T^{m+nq}z =$$
$$\sum_{q=0}^{\infty}\sum_{m=1}^{n}\sum_{j=1}^{\mu_n}\left[U^\chi(S T^{m\varepsilon})\right]_{i,j}\chi\left(r_j^{(n)} T^{n\varepsilon}\left(r_j^{(n)}\right)^{-1}\right)^q f_j|_{2\beta}\tilde{S}T^{m+nq}z. \qquad \square$$

The form of the transfer operator in lemma 7.4.5 looks more complicated at first glance. However, since U^χ has the structure of a permutation matrix, the sum $\sum_{j=1}^{\mu_n}$ has only one non-vanishing term and since U^χ has to be determined only for the finite number of elements $ST^{m\varepsilon}$, $1 \le m \le n$, we can write it down explicitly for every m. Indeed, this form also enables us to find symmetries of the transfer operator which we will introduce later. In [FM11] we discuss the relation of these symmetries to symmetries of the Maass wave forms. Another advantage of this form of the transfer operator is that we have to evaluate the character χ only for a finite number of elements. Indeed, it was this form that made numerical computations possible at all. It might be surprising that evaluating the character χ is such a complicated task, but the decomposition of every element into the generators of the group $\Gamma_0(n)$ is needed to evaluate its character, see also section 6.5. To find such a decomposition is not easy; usually it has to be done more or less with *brute force*, which can be quite time consuming. As an example we present the transfer operator $\mathcal{L}^{(4)}_{\beta,\varepsilon,\chi^{(4)}_{\alpha_1,\alpha_2}} = \mathcal{L}^{(4)}_{\beta,\varepsilon,\alpha_1,\alpha_2}$ for $\Gamma_0(4)$ in lemma 7.4.5 and the character $\chi^{(4)}_{\alpha_1,\alpha_2}$ introduced in section 6.5. We also mention two symmetry operators $\mathcal{P}_i : \bigoplus_{j=1}^{\mu_4} B(D) \to \bigoplus_{j=1}^{\mu_4} B(D)$ with $i = 1, 2$, defined as $\left[\mathcal{P}_i\vec{f}(z)\right]_j = f_{p_i(j)}(z)$, with $p_i : \{1,\dots,\mu_4\} \to \{1,\dots,\mu_4\}$ such that $\mathcal{P}_i\mathcal{L}^{(4)}_{\beta,+1,\alpha_1,\alpha_2} = \mathcal{L}^{(4)}_{\beta,-1,\alpha_1,\alpha_2}\mathcal{P}_i$ and $\mathcal{P}_i = \mathcal{P}_i^{-1}$. Note that the symmetry $\mathcal{P}_1$ exists only for the trivial character $\chi^{(4)}_{0,0}$, whereas the symmetry $\mathcal{P}_2$ also exists in the case $\chi^{(4)}_{\alpha,0}$. The following data were generated by our computer program CGF:

The transfer operator for $\Gamma_0(4)$ reads as

$$\begin{aligned}
\left[\mathcal{L}^{\Gamma_0(4)}_{\beta,+1}\vec{f}\right]_1 &= \sum_{q=0}^{\infty} e^{2\pi i(q\alpha_2)} f_3|_\beta\tilde{S}T^{1+4q} + e^{2\pi i(q\alpha_2)} f_4|_\beta\tilde{S}T^{2+4q} \\
&\quad + e^{2\pi i(q\alpha_2)} f_5|_\beta\tilde{S}T^{3+4q} + e^{2\pi i((1+q)\alpha_2)} f_2|_\beta\tilde{S}T^{4+4q} \\
\left[\mathcal{L}^{\Gamma_0(4)}_{\beta,+1}\vec{f}\right]_2 &= \sum_{q=0}^{\infty} e^{2\pi i((1+4q)\alpha_1)} f_1|_\beta\tilde{S}T^{1+4q} + e^{2\pi i((2+4q)\alpha_1)} f_1|_\beta\tilde{S}T^{2+4q} \\
&\quad + e^{2\pi i((3+4q)\alpha_1)} f_1|_\beta\tilde{S}T^{3+4q} + e^{2\pi i((4+4q)\alpha_1)} f_1|_\beta\tilde{S}T^{4+4q} \\
\left[\mathcal{L}^{\Gamma_0(4)}_{\beta,+1}\vec{f}\right]_3 &= \sum_{q=0}^{\infty} e^{2\pi i(-\alpha_1+q\alpha_2)} f_2|_\beta\tilde{S}T^{1+4q} + e^{2\pi i(-\alpha_1+q\alpha_2)} f_3|_\beta\tilde{S}T^{2+4q} \\
&\quad + e^{2\pi i(-\alpha_1+q\alpha_2)} f_4|_\beta\tilde{S}T^{3+4q} + e^{2\pi i(-\alpha_1+q\alpha_2)} f_5|_\beta\tilde{S}T^{4+4q} \\
\left[\mathcal{L}^{\Gamma_0(4)}_{\beta,+1}\vec{f}\right]_4 &= \sum_{q=0}^{\infty} e^{2\pi i((-1-4q)\alpha_1+(-1-4q)\alpha_2)} f_6|_\beta\tilde{S}T^{1+4q} + e^{2\pi i((-2-4q)\alpha_1+(-2-4q)\alpha_2)} f_6|_\beta\tilde{S}T^{2+4q} \\
&\quad + e^{2\pi i((-3-4q)\alpha_1+(-3-4q)\alpha_2)} f_6|_\beta\tilde{S}T^{3+4q} + e^{2\pi i((-4-4q)\alpha_1+(-4-4q)\alpha_2)} f_6|_\beta\tilde{S}T^{4+4q} \\
\left[\mathcal{L}^{\Gamma_0(4)}_{\beta,+1}\vec{f}\right]_5 &= \sum_{q=0}^{\infty} e^{2\pi i(\alpha_1+(1+q)\alpha_2)} f_4|_\beta\tilde{S}T^{1+4q} + e^{2\pi i(\alpha_1+(1+q)\alpha_2)} f_5|_\beta\tilde{S}T^{2+4q}
\end{aligned}$$

$$
\begin{aligned}
&+ \quad e^{2\pi i(\alpha_1+(2+q)\alpha_2)} f_2|_\beta \tilde{S} T^{3+4q} \quad + \quad e^{2\pi i(\alpha_1+(2+q)\alpha_2)} f_3|_\beta \tilde{S} T^{4+4q} \\
\left[\mathcal{L}^{\Gamma_0(4)}_{\beta,+1} \vec{f}\right]_6 &= \sum_{q=0}^{\infty} \quad e^{2\pi i(q\alpha_2)} f_5|_\beta \tilde{S} T^{1+4q} \quad + \quad e^{2\pi i((1+q)\alpha_2)} f_2|_\beta \tilde{S} T^{2+4q} \\
&+ \quad e^{2\pi i((1+q)\alpha_2)} f_3|_\beta \tilde{S} T^{3+4q} \quad + \quad e^{2\pi i((1+q)\alpha_2)} f_4|_\beta \tilde{S} T^{4+4q} \\
\left[\mathcal{L}^{\Gamma_0(4)}_{\beta,-1} \vec{f}\right]_1 &= \sum_{q=0}^{\infty} \quad e^{2\pi i((-1-q)\alpha_2)} f_5|_\beta \tilde{S} T^{1+4q} \quad + \quad e^{2\pi i((-1-q)\alpha_2)} f_4|_\beta \tilde{S} T^{2+4q} \\
&+ \quad e^{2\pi i((-1-q)\alpha_2)} f_3|_\beta \tilde{S} T^{3+4q} \quad + \quad e^{2\pi i((-1-q)\alpha_2)} f_2|_\beta \tilde{S} T^{4+4q} \\
\left[\mathcal{L}^{\Gamma_0(4)}_{\beta,-1} \vec{f}\right]_2 &= \sum_{q=0}^{\infty} \quad e^{2\pi i((-1-4q)\alpha_1)} f_1|_\beta \tilde{S} T^{1+4q} \quad + \quad e^{2\pi i((-2-4q)\alpha_1)} f_1|_\beta \tilde{S} T^{2+4q} \\
&+ \quad e^{2\pi i((-3-4q)\alpha_1)} f_1|_\beta \tilde{S} T^{3+4q} \quad + \quad e^{2\pi i((-4-4q)\alpha_1)} f_1|_\beta \tilde{S} T^{4+4q} \\
\left[\mathcal{L}^{\Gamma_0(4)}_{\beta,-1} \vec{f}\right]_3 &= \sum_{q=0}^{\infty} \quad e^{2\pi i(-\alpha_1+(-1-q)\alpha_2)} f_4|_\beta \tilde{S} T^{1+4q} \quad + \quad e^{2\pi i(-\alpha_1+(-1-q)\alpha_2)} f_3|_\beta \tilde{S} T^{2+4q} \\
&+ \quad e^{2\pi i(-\alpha_1+(-1-q)\alpha_2)} f_2|_\beta \tilde{S} T^{3+4q} \quad + \quad e^{2\pi i(-\alpha_1+(-2-q)\alpha_2)} f_5|_\beta \tilde{S} T^{4+4q} \\
\left[\mathcal{L}^{\Gamma_0(4)}_{\beta,-1} \vec{f}\right]_4 &= \sum_{q=0}^{\infty} \quad e^{2\pi i((1+4q)\alpha_1+(1+4q)\alpha_2)} f_6|_\beta \tilde{S} T^{1+4q} \quad + \quad e^{2\pi i((2+4q)\alpha_1+(2+4q)\alpha_2)} f_6|_\beta \tilde{S} T^{2+4q} \\
&+ \quad e^{2\pi i((3+4q)\alpha_1+(3+4q)\alpha_2)} f_6|_\beta \tilde{S} T^{3+4q} \quad + \quad e^{2\pi i((4+4q)\alpha_1+(4+4q)\alpha_2)} f_6|_\beta \tilde{S} T^{4+4q} \\
\left[\mathcal{L}^{\Gamma_0(4)}_{\beta,-1} \vec{f}\right]_5 &= \sum_{q=0}^{\infty} \quad e^{2\pi i(\alpha_1+(1-q)\alpha_2)} f_2|_\beta \tilde{S} T^{1+4q} \quad + \quad e^{2\pi i(\alpha_1-q\alpha_2)} f_5|_\beta \tilde{S} T^{2+4q} \\
&+ \quad e^{2\pi i(\alpha_1-q\alpha_2)} f_4|_\beta \tilde{S} T^{3+4q} \quad + \quad e^{2\pi i(\alpha_1-q\alpha_2)} f_3|_\beta \tilde{S} T^{4+4q} \\
\left[\mathcal{L}^{\Gamma_0(4)}_{\beta,-1} \vec{f}\right]_6 &= \sum_{q=0}^{\infty} \quad e^{2\pi i(-q\alpha_2)} f_3|_\beta \tilde{S} T^{1+4q} \quad + \quad e^{2\pi i(-q\alpha_2)} f_2|_\beta \tilde{S} T^{2+4q} \\
&+ \quad e^{2\pi i((-1-q)\alpha_2)} f_5|_\beta \tilde{S} T^{3+4q} \quad + \quad e^{2\pi i((-1-q)\alpha_2)} f_4|_\beta \tilde{S} T^{4+4q}
\end{aligned}
$$

i	1	2	3	4	5	6
$p_1(i)$	1	2	5	4	3	6

i	1	2	3	4	5	6
$p_2(i)$	6	4	3	2	5	1

The symmetries $\mathcal{P}_1$ and $\mathcal{P}_2$ commute since $p_1 \circ p_2(i) = p_2 \circ p_1(i)$ for $1 \leq i \leq 6$.

7.4.3 An analytic continuation of the transfer operator

Following the ideas in [May91a] we derive an analytic continuation of the transfer operator with the representation U^χ. A similar analytic continuation was also given by Chang in [Cha99], but his analytic continuation is only valid for the representation U^Γ induced from the trivial representation. An analytic continuation of the transfer operator for triangle groups with an arbitrary representation was given by Fried in [Fri96].

Lemma 7.4.6. *The analytic continuation of the transfer operator in lemma 7.4.5 is given for $\Re\beta > -\frac{N}{2}$, $N \in \mathbb{Z}_>$, by*

$$\left[\mathcal{L}^{(n)}_{\beta,\varepsilon,\chi}\vec{f}(z)\right]_i = \left[\mathcal{N}^{(n)}_{\beta,\varepsilon,\chi,N}\vec{f}(z)\right]_i + \left[\mathcal{A}^{(n)}_{\beta,\varepsilon,\chi,N}\vec{f}(z)\right]_i$$

where

$$\begin{aligned}\left[\mathcal{N}^{(n)}_{\beta,\varepsilon,\chi,N}\vec{f}(z)\right]_i &= \sum_{q=0}^{\infty}\sum_{m=1}^{n}\sum_{j=1}^{\mu_n}\left[U^\chi\left(ST^{m\varepsilon}\right)\right]_{i,j}\chi\left(r_j^{(n)}T^{n\varepsilon}\left(r_j^{(n)}\right)^{-1}\right)^q \\ &\quad \left[(z+m+nq)^{-2\beta}f_j\left(\frac{1}{z+m+nq}\right) - \sum_{k=0}^{N}(z+m+nq)^{-2\beta-k}\frac{f_j^{(k)}(0)}{k!}\right] \\ &\quad \textit{and} \\ \left[\mathcal{A}^{(n)}_{\beta,\varepsilon,\chi,N}\vec{f}(z)\right]_i &= \sum_{m=1}^{n}\sum_{j=1}^{\mu_n}\left[U^\chi\left(ST^{m\varepsilon}\right)\right]_{i,j}\sum_{k=0}^{N}\frac{f_j^{(k)}(0)}{k!}\frac{1}{n^{2\beta+k}} \\ &\quad \Phi\left(\chi\left(r_j^{(n)}T^{n\varepsilon}\left(r_j^{(n)}\right)^{-1}\right), 2\beta+k, \frac{z+m}{n}\right).\end{aligned}$$

Thereby n denotes the level of $\Gamma_0(n)$, and Φ the Lerch transcendent. $\mathcal{N}^{(n)}_{\beta,\varepsilon,\chi,N}$ is holomorphic in β for $\Re\beta > -\frac{N}{2}$ and $\mathcal{A}^{(n)}_{\beta,\varepsilon,\chi,N}$ is meromorphic in $\beta \in \mathbb{C}$ with possible poles at $\beta = \frac{1-k}{2}$ for $0 \le k \le N$. Hence the transfer operator $\mathcal{L}^{(n)}_{\beta,\varepsilon,\chi}$ defines a meromorphic family of nuclear operators for $\Re\beta > -\frac{N}{2}$ with possible poles at $\beta = \frac{1-k}{2}$ for $0 \le k \le N$.

Proof. The transfer operator from lemma 7.4.5 can be written as

$$\begin{aligned}&\sum_{q=0}^{\infty}\sum_{m=1}^{n}\sum_{j=1}^{\mu_n}\left[U^\chi\left(ST^{m\varepsilon}\right)\right]_{i,j}\chi\left(r_j^{(n)}T^{n\varepsilon}\left(r_j^{(n)}\right)^{-1}\right)^q \\ &\left[(z+m+nq)^{-2\beta}f_j\left(\frac{1}{z+m+nq}\right) - \sum_{k=0}^{N}(z+m+nq)^{-2\beta-k}\frac{f_j^{(k)}(0)}{k!}\right] + \\ &\sum_{q=0}^{\infty}\sum_{m=1}^{n}\sum_{j=1}^{\mu_n}\left[U^\chi\left(ST^{m\varepsilon}\right)\right]_{i,j}\chi\left(r_j^{(n)}T^{n\varepsilon}\left(r_j^{(n)}\right)^{-1}\right)^q\sum_{k=0}^{N}(z+m+nq)^{-2\beta-k}\frac{f_j^{(k)}(0)}{k!} = \\ &\sum_{q=0}^{\infty}\sum_{m=1}^{n}\sum_{j=1}^{\mu_n}\left[U^\chi\left(ST^{m\varepsilon}\right)\right]_{i,j}\chi\left(r_j^{(n)}T^{n\varepsilon}\left(r_j^{(n)}\right)^{-1}\right)^q \\ &\left[(z+m+nq)^{-2\beta}f_j\left(\frac{1}{z+m+nq}\right) - \sum_{k=0}^{N}(z+m+nq)^{-2\beta-k}\frac{f_j^{(k)}(0)}{k!}\right] + \\ &\sum_{m=1}^{n}\sum_{j=1}^{\mu_n}\left[U^\chi\left(ST^{m\varepsilon}\right)\right]_{i,j}\sum_{k=0}^{N}\frac{f_j^{(k)}(0)}{k!}\frac{1}{n^{2\beta+k}}\sum_{q=0}^{\infty}\frac{\chi\left(r_j^{(n)}T^{n\varepsilon}\left(r_j^{(n)}\right)^{-1}\right)^q}{\left(\frac{z+m}{n}+q\right)^{2\beta+k}}\end{aligned}$$

The last sum $\sum_{q=0}^{\infty}$ can be performed and leads to the Lerch transcendent

$$\Phi\left(\chi\left(r_j^{(n)}T^{n\varepsilon}\left(r_j^{(n)}\right)^{-1}\right),2\beta+k,\frac{z+m}{n}\right)=\sum_{q=0}^{\infty}\frac{\chi\left(r_j^{(n)}T^{n\varepsilon}\left(r_j^{(n)}\right)^{-1}\right)^q}{\left(\frac{z+m}{n}+q\right)^{2\beta+k}}.$$

It was shown in [Fri96] that Φ can be extended to $2\beta+k\in\mathbb{C}$ with a possible pole at $2\beta+k=1$. On the other hand, the first sum over q converges absolutely for $2\Re\beta+N+1>1$, see [Fri96]. The operator

$$\begin{aligned}\left[\mathcal{A}^{(n)}_{\beta,\varepsilon,\chi,N}\vec{f}(z)\right]_i &= \sum_{m=1}^{n}\sum_{j=1}^{\mu_n}\left[U^{\chi}\left(ST^{m\varepsilon}\right)\right]_{i,j}\sum_{k=0}^{N}\frac{f_j^{(k)}(0)}{k!}\frac{1}{n^{2\beta+k}}\\ &\quad\Phi\left(\chi\left(r_j^{(n)}T^{n\varepsilon}\left(r_j^{(n)}\right)^{-1}\right),2\beta+k,\frac{z+m}{n}\right)\end{aligned}$$

is a finite rank operator and therefore a nuclear operator. We use the basis $\{\vec{e}_i\}_{1\le i\le\mu_n}$ of $\mathbb{C}^{\mu_n}$ given by $[\vec{e}]_j=\delta_{i,j}$ to write the operator $\mathcal{N}^{(n)}_{\beta,\varepsilon,\chi,N}$ as

$$\begin{aligned}\mathcal{N}^{(n)}_{\beta,\varepsilon,\chi,N}\vec{f}(z) &= \sum_{q=0}^{\infty}\sum_{m=1}^{n}\sum_{i=1}^{\mu_n}\sum_{j=1}^{\mu_n}\left[U^{\chi}\left(ST^{m\varepsilon}\right)\right]_{i,j}\chi\left(r_j^{(n)}T^{n\varepsilon}\left(r_j^{(n)}\right)^{-1}\right)^q\\ &\quad\left[(z+m+nq)^{-2\beta}f_j\left(\frac{1}{z+m+nq}\right)-\sum_{k=0}^{N}(z+m+nq)^{-2\beta-k}\frac{f_j^{(k)}(0)}{k!}\right]\vec{e}_i\\ &= \sum_{m=1}^{n}\sum_{i=1}^{\mu_n}\sum_{j=1}^{\mu_n}\left[U^{\chi}\left(ST^{m\varepsilon}\right)\right]_{i,j}\vec{e}_i\sum_{q=0}^{\infty}\chi\left(r_j^{(n)}T^{n\varepsilon}\left(r_j^{(n)}\right)^{-1}\right)^q\\ &\quad\left[(z+m+nq)^{-2\beta}f_j\left(\frac{1}{z+m+nq}\right)-\sum_{k=0}^{N}(z+m+nq)^{-2\beta-k}\frac{f_j^{(k)}(0)}{k!}\right].\end{aligned}$$

We see that this is a multiplication (resp. tensor product) of two operators, where the first one is $U^{\chi}\left(ST^{m\varepsilon}\right)$ acting on $\vec{e}_i$, while the second operator is given by

$$\begin{aligned}N^{(m,j)}_{\beta,\varepsilon,\chi,N}f_j(z) &= \sum_{q=0}^{\infty}\chi\left(r_j^{(n)}T^{n\varepsilon}\left(r_j^{(n)}\right)^{-1}\right)^q\\ &\quad\left[(z+m+nq)^{-2\beta}f_j\left(\frac{1}{z+m+nq}\right)-\sum_{k=0}^{N}(z+m+nq)^{-2\beta-k}\frac{f_j^{(k)}(0)}{k!}\right].\end{aligned}$$

Since $|\chi(\gamma)|=1$ for all $\gamma\in\Gamma_0(n)$ we can use the result in [May90] (page 327) that this operator is a nuclear operator of order zero. □

The trace formula (7.20) is valid only for the transfer operator in the region $\Re\beta>\frac{1}{2}$. Next we want to determine the trace of the analytically continued transfer operator for $\Re\beta>-\frac{N}{2}$:

Proposition 7.4.7. *The trace of the analytic continuation of $\mathcal{L}^{(n)}_{\beta,\varepsilon,\chi}$ for $\Re\beta>-\frac{N}{2}$, $N\in\mathbb{Z}_{>}$, is given by*

$$tr\,\mathcal{L}^{(n)}_{\beta,\varepsilon,\chi}=tr\,\mathcal{N}^{(n)}_{\beta,\varepsilon,\chi,N}+tr\,\mathcal{A}^{(n)}_{\beta,\varepsilon,\chi,N},$$

where the traces of the operators $\mathcal{N}^{(n)}_{\beta,\varepsilon,\chi,N}$ and $\mathcal{A}^{(n)}_{\beta,\varepsilon,\chi,N}$ are given by the formulas

$$\begin{aligned} tr\,\mathcal{N}^{(n)}_{\beta,\varepsilon,\chi,N} &= \sum_{q=0}^{\infty}\sum_{m=1}^{n}\sum_{i=1}^{\mu_n}\left[U^{\chi}\left(ST^{m\varepsilon}\right)\right]_{i,i}\chi\left(r_i^{(n)}T^{n\varepsilon}\left(r_i^{(n)}\right)^{-1}\right)^{q} \\ &\quad \left(\frac{\left(z^*_{q,m}+m+nq\right)^{-2\beta}}{1+\left(z^*_{q,m}+m+nq\right)^{-2}} - \sum_{k=0}^{N}\frac{(-1)^k}{k!}\frac{\Gamma(2\beta+2k)}{\Gamma(2\beta+k)}(m+nq)^{-2\beta-2k}\right) \\ &\text{and} \\ tr\,\mathcal{A}^{(n)}_{\beta,\varepsilon,\chi,N} &= \sum_{k=0}^{N}\sum_{m=1}^{n}\sum_{i=1}^{\mu_n}\left[U^{\chi}\left(ST^{m\varepsilon}\right)\right]_{i,i}\frac{(-1)^k}{n^{2\beta+2k}k!}\frac{\Gamma(2\beta+2k)}{\Gamma(2\beta+k)} \\ &\quad \Phi\left(\chi\left(r_i^{(n)}T^{n\varepsilon}\left(r_i^{(n)}\right)^{-1}\right),2\beta+2k,\frac{m}{n}\right) \end{aligned}$$

with $z^*_{q,m} = -\frac{m+nq}{2} + \sqrt{\left(\frac{m+nq}{2}\right)^2+1}$.

Proof. We write the operator $\mathcal{N}^{(n)}_{\beta,\varepsilon,\chi,N}$ as a sum of two series of operators:

$$\left[\mathcal{N}^{(n)}_{\beta,\varepsilon,\chi,N}\vec{f}(z)\right]_i = \sum_{q=0}^{\infty}\sum_{m=1}^{n}\left(\left[\Lambda^{(q,m)}_{\beta,\varepsilon}\vec{f}(z)\right]_i - \left[\Xi^{(q,m)}_{\beta,\varepsilon,N}\vec{f}(z)\right]_i\right)$$

with

$$\begin{aligned} \left[\Lambda^{(q,m)}_{\beta,\varepsilon}\vec{f}(z)\right]_i &= \sum_{j=1}^{\mu_n}\left[U^{\chi}\left(ST^{m\varepsilon}\right)\right]_{i,j}\chi\left(r_j^{(n)}T^{n\varepsilon}\left(r_j^{(n)}\right)^{-1}\right)^{q} \\ &\quad (z+m+nq)^{-2\beta}f_j\left(\frac{1}{z+m+nq}\right) \\ \left[\Xi^{(q,m)}_{\beta,\varepsilon,N}\vec{f}(z)\right]_i &= \sum_{j=1}^{\mu_n}\left[U^{\chi}\left(ST^{m\varepsilon}\right)\right]_{i,j}\chi\left(r_j^{(n)}T^{n\varepsilon}\left(r_j^{(n)}\right)^{-1}\right)^{q} \\ &\quad \sum_{k=0}^{N}(z+m+nq)^{-2\beta-k}\frac{f_j^{(k)}(0)}{k!}. \end{aligned}$$

Obviously $\Lambda^{(q,m)}_{\beta,\varepsilon}$ is just a composition operator and its trace is given according to (7.12) by

$$\mathrm{tr}_{\sigma}\,\Lambda^{(q,m)}_{\beta,\varepsilon} = \frac{\left(z^*_{q,m}+m+nq\right)^{-2\beta}}{1+\left(z^*_{q,m}+m+nq\right)^{-2}}\sum_{i=1}^{\mu_n}\left[U^{\chi}\left(ST^{m\varepsilon}\right)\right]_{i,i}\chi\left(r_i^{(n)}T^{n\varepsilon}\left(r_i^{(n)}\right)^{-1}\right)^{q} \tag{7.24}$$

with $z^*_{q,m} = -\frac{m+nq}{2} + \sqrt{\left(\frac{m+nq}{2}\right)^2+1}$. We denote this trace by tr_{σ} since the trace formula (7.12) is the spectral trace of $\Lambda^{(q,m)}_{\beta,\varepsilon}$. We can write the operator $\Lambda^{(q,m)}_{\beta,\varepsilon}$ also as

$$\begin{aligned} \Lambda^{(q,m)}_{\beta,\varepsilon}\vec{f}(z) &= \sum_{i=1}^{\mu_n}\sum_{j=1}^{\mu_n}\left[U^{\chi}\left(ST^{m\varepsilon}\right)\right]_{i,j}\chi\left(r_j^{(n)}T^{n\varepsilon}\left(r_j^{(n)}\right)^{-1}\right)^{q} \\ &\quad (z+m+nq)^{-2\beta}f_j\left(\frac{1}{z+m+nq}\right)\vec{e}_i \end{aligned}$$

with $\{\vec{e}_i\}_{1\le i\le\mu_n}$ the basis of $\mathbb{C}^{\mu_n}$ given by $[\vec{e}_i]_j = \delta_{i,j}$. Next we expand f_j in a Taylor series around $z = 0$

$$f_j\left(\frac{1}{z+m+nq}\right) = \sum_{k=0}^{\infty} \frac{f_j^{(k)}(0)}{k!} (z+m+nq)^{-k}.$$

This series does not converge uniformly for every $z \in D$, (see also section 7.4.4). With this expansion the nuclear representation (7.6) of $\Lambda_{\beta,\varepsilon}^{(q,m)}$ is given by

$$\Lambda_{\beta,\varepsilon}^{(q,m)} = \sum_{i=1}^{\mu_n}\sum_{j=1}^{\mu_n}\sum_{k=0}^{\infty} [U^\chi (S T^{m\varepsilon})]_{i,j} \chi\left(r_j^{(n)} T^{n\varepsilon}\left(r_j^{(n)}\right)^{-1}\right)^q \frac{(z+m+nq)^{-2\beta-k}}{k!} \left[\frac{\partial^k}{\partial z^k}(\,\cdot\,)|_{z=0}\right]_j \vec{e}_i.$$

Then the trace of the nuclear representation of $\Lambda_{\beta,\varepsilon}^{(q,m)}$ is given by (7.7), i.e.

$$\begin{aligned}
\operatorname{tr}\Lambda_{\beta,\varepsilon}^{(q,m)} &= \sum_{i=1}^{\mu_n}\sum_{j=1}^{\mu_n}\sum_{k=0}^{\infty}\left[\frac{\partial^k}{\partial z^k}\left([U^\chi (S T^{m\varepsilon})]_{i,j}\chi\left(r_j^{(n)}T^{n\varepsilon}\left(r_j^{(n)}\right)^{-1}\right)^q \frac{(z+m+nq)^{-2\beta-k}}{k!}\vec{e}_i\right)|_{z=0}\right]_j \\
&= \sum_{i=1}^{\mu_n}\sum_{j=1}^{\mu_n}\sum_{k=0}^{\infty}[U^\chi (S T^{m\varepsilon})]_{i,j}\chi\left(r_j^{(n)}T^{n\varepsilon}\left(r_j^{(n)}\right)^{-1}\right)^q \frac{\partial^k}{\partial z^k}\left(\frac{(z+m+nq)^{-2\beta-k}}{k!}\right)|_{z=0}[\vec{e}_i]_j \\
&= \sum_{i=1}^{\mu_n}\sum_{j=1}^{\mu_n}\sum_{k=0}^{\infty}[U^\chi (S T^{m\varepsilon})]_{i,j}\chi\left(r_j^{(n)}T^{n\varepsilon}\left(r_j^{(n)}\right)^{-1}\right)^q \frac{(-1)^k}{k!}\frac{\Gamma(2\beta+2k)}{\Gamma(2\beta+k)}(z+m+nq)^{-2\beta-2k}|_{z=0}\delta_{i,j} \\
&= \sum_{i=1}^{\mu_n}\sum_{k=0}^{\infty}[U^\chi (S T^{m\varepsilon})]_{i,i}\chi\left(r_i^{(n)}T^{n\varepsilon}\left(r_i^{(n)}\right)^{-1}\right)^q \frac{(-1)^k}{k!}\frac{\Gamma(2\beta+2k)}{\Gamma(2\beta+k)}(m+nq)^{-2\beta-2k}. \qquad (7.25)
\end{aligned}$$

The infinite sum over k does not converge for every m and q. We are using (3.6) and (3.7) to show that this sum is only convergent for $m + nq \ge 3$, since

$$\begin{aligned}
&\lim_{k\to\infty}\frac{(-1)^k}{k!}\frac{\Gamma(2\beta+2k)}{\Gamma(2\beta+k)}(m+nq)^{-2\beta-2k} \\
\sim\ &\frac{(-1)^k}{\sqrt{2\pi}e^{-k}k^{k+1/2}}\frac{\sqrt{2\pi}e^{-2\beta-2k}(2\beta+2k)^{2\beta+2k-1/2}}{\sqrt{2\pi}e^{-2\beta-k}(2\beta+k)^{2\beta+k-1/2}}(m+nq)^{-2\beta-2k} \\
=\ &\frac{(-1)^k}{\sqrt{2\pi}k^{k+1/2}}\frac{(2\beta+2k)^{2\beta+2k-1/2}}{(2\beta+k)^{2\beta+k-1/2}}(m+nq)^{-2\beta-2k} \\
\sim\ &\frac{(-1)^k}{\sqrt{2\pi}k^{k+1/2}}\frac{(2k)^{2\beta+2k-1/2}}{k^{2\beta+k-1/2}}(m+nq)^{-2\beta-2k} = \frac{(-1)^k}{2\sqrt{\pi k}}\left(\frac{2}{m+nq}\right)^{2\beta+2k}.
\end{aligned}$$

Hence, the sum $\sum_{k=0}^{\infty}$ in the trace $\operatorname{tr}\Lambda_{\beta,\varepsilon}^{(q,m)}$ converges absolutely for $m+nq > 2$ and it diverges for $m+nq = 1$. In the case $m + nq = 2$ we have just $\frac{(-1)^k}{2\sqrt{\pi k}}$, according to the Leibniz test the sum $\sum_{k=0}^{\infty}$ converges only if $\frac{1}{\sqrt{k}}$ converges to 0 monotonically, which is the case.

On the other hand, we see that $\Xi_{\beta,\varepsilon,N}^{(q,m)}$ is of finite rank and hence a nuclear operator of order zero in the sense of Grothendieck. Its nuclear representation (7.6) has the form

$$\Xi_{\beta,\varepsilon,N}^{(q,m)} = \sum_{i=1}^{\mu_n}\sum_{j=1}^{\mu_n}\sum_{k=0}^{N}[U^\chi (S T^{m\varepsilon})]_{i,j}\chi\left(r_j^{(n)}T^{n\varepsilon}\left(r_j^{(n)}\right)^{-1}\right)^q \frac{(z+m+nq)^{-2\beta-k}}{k!}\left[\frac{\partial^k}{\partial z^k}(\,\cdot\,)|_{z=0}\right]_j \vec{e}_i$$

and the trace of $\Xi_{\beta,\varepsilon,N}^{(q,m)}$ is given by (7.7), i.e.

$$\operatorname{tr}\Xi_{\beta,\varepsilon,N}^{(q,m)} = \sum_{i=1}^{\mu_n}\sum_{k=0}^{N}[U^\chi (S T^{m\varepsilon})]_{i,i}\chi\left(r_i^{(n)}T^{n\varepsilon}\left(r_i^{(n)}\right)^{-1}\right)^q \frac{(-1)^k}{k!}\frac{\Gamma(2\beta+2k)}{\Gamma(2\beta+k)}(m+nq)^{-2\beta-2k}.$$

Next we show that $\operatorname{tr} \mathcal{N}^{(n)}_{\beta,\varepsilon,\chi,N} = \sum_{q=0}^{\infty}\sum_{m=1}^{n}\left(\operatorname{tr}_\sigma \Lambda^{(q,m)}_{\beta,\varepsilon} - \operatorname{tr} \Xi^{(q,m)}_{\beta,\varepsilon,N}\right)$ is well defined for $\Re\beta > -\frac{N}{2}$. We write this sum as

$$\sum_{q=0}^{1}\sum_{m=1}^{n}\left(\operatorname{tr}_\sigma \Lambda^{(q,m)}_{\beta,\varepsilon} - \operatorname{tr} \Xi^{(q,m)}_{\beta,\varepsilon,N}\right) + \sum_{q=2}^{\infty}\sum_{m=1}^{n}\left(\operatorname{tr}_\sigma \Lambda^{(q,m)}_{\beta,\varepsilon} - \operatorname{tr} \Xi^{(q,m)}_{\beta,\varepsilon,N}\right).$$

The finite sum $\sum_{q=0}^{1}\sum_{m=1}^{n}$ is well defined where $\operatorname{tr}_\sigma \Lambda^{(q,m)}_{\beta,\varepsilon}$ is given by (7.24). For the sum $\sum_{q=2}^{\infty}\sum_{m=1}^{n}$ we have $m+nq \geq 3$ and trace $\operatorname{tr} \Lambda^{(q,m)}_{\beta,\varepsilon}$ in (7.25) converges absolutely. According to Grothendieck $\operatorname{tr}_\sigma \Lambda^{(q,m)}_{\beta,\varepsilon} = \operatorname{tr} \Lambda^{(q,m)}_{\beta,\varepsilon}$, and therefore

$$\begin{aligned}
&\sum_{q=2}^{\infty}\sum_{m=1}^{n}\left(\operatorname{tr}_\sigma \Lambda^{(q,m)}_{\beta,\varepsilon} - \operatorname{tr} \Xi^{(q,m)}_{\beta,\varepsilon,N}\right) = \sum_{q=2}^{\infty}\sum_{m=1}^{n}\left(\operatorname{tr} \Lambda^{(q,m)}_{\beta,\varepsilon} - \operatorname{tr} \Xi^{(q,m)}_{\beta,\varepsilon,N}\right)\\
&= \sum_{q=2}^{\infty}\sum_{m=1}^{n}\sum_{i=1}^{\mu_n}\sum_{k=N+1}^{\infty}\left[U^\chi\left(S T^{m\varepsilon}\right)\right]_{i,i}\chi\left(r_i^{(n)}T^{n\varepsilon}\left(r_i^{(n)}\right)^{-1}\right)^q \frac{(-1)^k}{k!}\frac{\Gamma(2\beta+2k)}{\Gamma(2\beta+k)}(m+nq)^{-2\beta-2k}.
\end{aligned}$$

We see that the sum over $\sum_{q=2}^{\infty}$ converges absolutely in the region $\Re\beta > -\frac{N}{2}$, since $\sum_{q=2}^{\infty}\sum_{m=1}^{n}|m+nq|^{-2\beta-2(N+1)}$ converges for $2\Re\beta + 2(N+1) > 1$.

The operator $\mathcal{A}^{(n)}_{\beta,\varepsilon,\chi,N}$ is of finite rank and hence a nuclear operator with the nuclear representation

$$\begin{aligned}
\mathcal{A}^{(n)}_{\beta,\varepsilon,\chi,N} \quad = \quad & \sum_{i=1}^{\mu_n}\sum_{m=1}^{n}\sum_{j=1}^{\mu_n}\sum_{k=0}^{N}\left[U^\chi\left(S T^{m\varepsilon}\right)\right]_{i,j}\frac{1}{n^{2\beta+k}k!}\Phi\left(\chi\left(r_j^{(n)}T^{n\varepsilon}\left(r_j^{(n)}\right)^{-1}\right), 2\beta+k, \frac{z+m}{n}\right)\\
& \left[\frac{\partial^k}{\partial z^k}(\,\cdot\,)|_{z=0}\right]_j \vec{e}_i.
\end{aligned}$$

And its trace is given by

$$\begin{aligned}
\operatorname{tr} \mathcal{A}^{(n)}_{\beta,\varepsilon,\chi,N} \quad = \quad & \sum_{i=1}^{\mu_n}\sum_{m=1}^{n}\sum_{j=1}^{\mu_n}\sum_{k=0}^{N}\left[\frac{\partial^k}{\partial z^k}\left(\left[U^\chi\left(S T^{m\varepsilon}\right)\right]_{i,j}\frac{1}{n^{2\beta+k}k!}\right.\right.\\
& \left.\left.\Phi\left(\chi\left(r_j^{(n)}T^{n\varepsilon}\left(r_j^{(n)}\right)^{-1}\right), 2\beta+k, \frac{z+m}{n}\right)\vec{e}_i\right)|_{z=0}\right]_j\\
= \quad & \sum_{i=1}^{\mu_n}\sum_{m=1}^{n}\sum_{j=1}^{\mu_n}\sum_{k=0}^{N}\left[U^\chi\left(S T^{m\varepsilon}\right)\right]_{i,j}\frac{1}{n^{2\beta+k}k!}\\
& \frac{\partial^k}{\partial z^k}\left(\Phi\left(\chi\left(r_j^{(n)}T^{n\varepsilon}\left(r_j^{(n)}\right)^{-1}\right), 2\beta+k, \frac{z+m}{n}\right)\right)|_{z=0}\left[\vec{e}_i\right]_j\\
= \quad & \sum_{i=1}^{\mu_n}\sum_{m=1}^{n}\sum_{j=1}^{\mu_n}\sum_{k=0}^{N}\left[U^\chi\left(S T^{m\varepsilon}\right)\right]_{i,j}\frac{1}{n^{2\beta+k}k!}\\
& \frac{(-1)^k}{n^k}\frac{\Gamma(2\beta+2k)}{\Gamma(2\beta+k)}\Phi\left(\chi\left(r_j^{(n)}T^{n\varepsilon}\left(r_j^{(n)}\right)^{-1}\right), 2\beta+2k, \frac{z+m}{n}\right)|_{z=0}\delta_{i,j}\\
= \quad & \sum_{i=1}^{\mu_n}\sum_{m=1}^{n}\sum_{k=0}^{N}\left[U^\chi\left(S T^{m\varepsilon}\right)\right]_{i,i}\frac{(-1)^k}{n^{2\beta+2k}k!}\frac{\Gamma(2\beta+2k)}{\Gamma(2\beta+k)}\Phi\left(\chi\left(r_i^{(n)}T^{n\varepsilon}\left(r_i^{(n)}\right)^{-1}\right), 2\beta+2k, \frac{m}{n}\right).\square
\end{aligned}$$

The trace formula for $\mathcal{L}^{(n)}_{\beta,\varepsilon,\chi}$ in proposition 7.4.7 is very appropriate for numerical computations, since the infinite sum $\sum_{q=0}^{\infty}$ converges exponentially. The only problem which arises is that the traces of $\mathcal{A}^{(n)}_{\beta,\varepsilon,\chi,N}$

and $\mathcal{N}^{(n)}_{\beta,\varepsilon,\chi,N}$ diverge for $N \to \infty$. A similar calculation like in the proof of proposition 7.4.7 shows that for large N the leading term of $\operatorname{tr} \mathcal{N}^{(n)}_{\beta,\varepsilon,\chi,N}$ is given by

$$-\frac{(-1)^N}{2\sqrt{\pi N}} 2^{2\beta+2N}$$

which is obviously divergent for $N \to \infty$. Using $\Phi(\alpha, s, z) \sim (z)^{-s}$ for $\Re s \to \infty$ one shows that the leading term of $\operatorname{tr} \mathcal{A}^{(n)}_{\beta,\varepsilon,\chi,N}$ is given by

$$\frac{(-1)^N}{2\sqrt{\pi N}} 2^{2\beta+2N}$$

which diverges also for $N \to \infty$. We see that the values of the traces of $\mathcal{N}^{(n)}_{\beta,\varepsilon,\chi,N}$ and $\mathcal{A}^{(n)}_{\beta,\varepsilon,\chi,N}$ grow exponentially with N. On the other hand, for a fixed $\beta \in \mathbb{C}$ with $\Re\beta > -\frac{N}{2}$ the value of the sum of $\operatorname{tr} \mathcal{N}^{(n)}_{\beta,\varepsilon,\chi,N}$ and $\operatorname{tr} \mathcal{A}^{(n)}_{\beta,\varepsilon,\chi,N}$ remains constant when N grows, since these traces are growing in different directions, therfore the value of the trace of $\mathcal{L}^{(n)}_{\beta,\varepsilon,\chi}$ remains constant when N grows. We implemented the trace formula in proposition 7.4.7 and the trace formula (7.20) for U^χ in our computer program package Morpheus. We compared the results of these formulas in the region $\Re\beta > \frac{1}{2}$. As always when computing an infinite sum, we add up terms of this sum until the result does not change within the precision we are working, usually 160 bits. Both formulas give the same result, but their computation times differ extremely. The trace formula in proposition 7.4.7 converges within milliseconds; on the other hand, the computation time for the trace formula (7.20) is several days in the worst case. In principle it was already noticed in [MR87] that the formula (7.20) is not well suited for numerical computations, since its convergence is rather slow.

Of course, one would like to use the analytic continuation of the transfer operator in lemma 7.4.6 also for numerical computations. Unfortunately, the main problem is to find a form of the operator $\mathcal{N}^{(n)}_{\beta,\varepsilon,\chi,N}$ which can be approximated by a finite matrix. In [Str08] Strömberg numerically treated the transfer operator for Hecke triangle groups by approximating an operator, which corresponds to our operator $\mathcal{A}^{(n)}_{\beta,\varepsilon,\chi,N}$, and presented an algorithm to determine the spectrum of the transfer operator and its Fredholm determinant. The main idea is to find a matrix representation $\mathcal{A}_{\beta,\varepsilon,(N,N)}$ of $\mathcal{A}^{(n)}_{\beta,\varepsilon,\chi,N}$ by using some finite Taylor expansions. The eigenvalues of $\mathcal{A}_{\beta,\varepsilon,(N_1,N_1)}$ and $\mathcal{A}_{\beta,\varepsilon,(N_2,N_2)}$ are computed with $N_2 > N_1$. Then one assumes that those eigenvalues of $\mathcal{A}_{\beta,\varepsilon,(N_1,N_1)}$ and $\mathcal{A}_{\beta,\varepsilon,(N_2,N_2)}$ which coincide within a certain limit give approximate eigenvalues of the transfer operator. We denote the set of these approximating eigenvalues by σ_{N_1,N_2}. His method is based on certain claims of how the spectrum of $\mathcal{A}_{\beta,\varepsilon,(N,N)}$ approximates the spectrum of the transfer operator, which he did not prove.

Unfortunately, in our case this procedure does not work very well. A simple test by comparing the sum over the approximating eigenvalues in σ_{N_1,N_2}, with the trace formula in proposition 7.4.7 shows that in all cases we tested for different values N_1 and N_2 the best result was that only the order of magnitude coincides. It it possible that the claims made in [Str08] about the spectrum of $\mathcal{A}_{\beta,\varepsilon,(N,N)}$ do not hold in our case. Note that it is obvious that $\operatorname{tr} \mathcal{A}^{(n)}_{\beta,\varepsilon,\chi,N} \neq \operatorname{tr} \mathcal{L}^{(n)}_{\beta,\varepsilon,\chi}$ for $\Re\beta > -\frac{N}{2}$, and the hope that we can approximate $\mathcal{L}^{(n)}_{\beta,\varepsilon,\chi}$ by $\mathcal{A}^{(n)}_{\beta,\varepsilon,\chi,N}$ for N large is destroyed. On the other hand, even if it is not possible to approximate the spectrum of $\mathcal{L}^{(n)}_{\beta,\varepsilon,\chi}$ by σ_{N_1,N_2}, numerical calculations indicate that we can still obtain the zeros of the Fredholm determinant of $\mathcal{L}^{(n)}_{\beta,\varepsilon,\chi}$ by the function $\prod_{\lambda\in\sigma_{N_1,N_2}}(1-\lambda)$. Indeed, comparing the zeros of $\prod_{\lambda\in\sigma_{N_1,N_2}}(1-\lambda)$ on the critical line $\Re\beta = \frac{1}{2}$ with well-known values of the eigenvalues $\lambda = \frac{1}{4} + R^2$ of the hyperbolic Laplacian [Str09b] for $\Gamma_0(n)$ with $1 \leq n \leq 10$ and $R \leq 10$, obtained by completely different methods [Str04], shows that we can find these values with rather high precision.

In the next sections we present a better way to approximate the transfer operator.

7.4.4 A nuclear representation of the transfer operator

The next step is to expand f_j in a Taylor series. An important question is at which point we should make this expansion. Indeed, it is known (see the proof of lemma 4 in [CM99]) that $f_j(z) = \sum_{k=0}^{\infty} \frac{f_j^{(k)}(1)}{k!}(z-1)^k$ converges uniformly and absolutely in every compactum in D and absolutely on the boundary of D.[1] We will need this property since we will interchange the summation of the Taylor series and the infinite sum in the transfer operator, which we can only do if both infinite sums converge uniformly.

Lemma 7.4.8. *The transfer operator acting on $\vec{f}$ is given for $\Re\beta > \frac{1}{2}$ by*

$$\begin{aligned}\left[\mathcal{L}^{(n)}_{\beta,\varepsilon,\chi}\vec{f}(z)\right]_i &= \sum_{k=0}^{\infty}\sum_{m=1}^{n}\sum_{j=1}^{\mu_n}\left[U^{\chi}\left(ST^{m\varepsilon}\right)\right]_{i,j}\frac{f_j^{(k)}(1)}{k!} \\ &\quad \sum_{t=0}^{k}\binom{k}{t}\frac{(-1)^{k-t}}{n^{2\beta+t}}\Phi\left(\chi\left(r_j^{(n)}T^{n\varepsilon}\left(r_j^{(n)}\right)^{-1}\right), 2\beta+t, \frac{z+m}{n}\right)\end{aligned}$$

with Φ the Lerch transcendent and n the level of $\Gamma_0(n)$.

Proof. First consider the term $f_j|_{2\beta}\tilde{S}T^{m+nq}z = (z+m+nq)^{-2\beta}f_j\left(\frac{1}{z+m+nq}\right)$. Using the Taylor expansion of f_j at point 1 we get

$$\begin{aligned}f_j\left(\frac{1}{z+m+nq}\right) &= \sum_{k=0}^{\infty}\frac{f_j^{(k)}(1)}{k!}\left(\frac{1}{z+m+nq}-1\right)^k \\ &= \sum_{k=0}^{\infty}\frac{f_j^{(k)}(1)}{k!}\sum_{t=0}^{k}\binom{k}{t}\left(\frac{1}{z+m+nq}\right)^t(-1)^{k-t}\end{aligned}$$

which converges uniformly for $z \in \bar{D}$. We insert this expansion into the transfer operator in lemma 7.4.5 to get

$$\sum_{q=0}^{\infty}\sum_{m=1}^{n}\sum_{j=1}^{\mu_n}\left[U^{\chi}\left(ST^{m\varepsilon}\right)\right]_{i,j}\chi\left(r_j^{(n)}T^{n\varepsilon}\left(r_j^{(n)}\right)^{-1}\right)^q\sum_{k=0}^{\infty}\frac{f_j^{(k)}(1)}{k!}\sum_{t=0}^{k}\binom{k}{t}(z+m+nq)^{-2\beta-t}(-1)^{k-t}.$$

Since for $\Re\beta > \frac{1}{2}$ the sum $\sum_{q=0}^{\infty}$ converges uniformly, we can interchange it with the sum $\sum_{k=0}^{\infty}$ and therefore get

$$\begin{aligned}&\sum_{k=0}^{\infty}\sum_{m=1}^{n}\sum_{j=1}^{\mu_n}\left[U^{\chi}\left(ST^{m\varepsilon}\right)\right]_{i,j}\frac{f_j^{(k)}(1)}{k!}\sum_{t=0}^{k}\binom{k}{t}(-1)^{k-t}\sum_{q=0}^{\infty}\frac{\chi\left(r_j^{(n)}T^{n\varepsilon}\left(r_j^{(n)}\right)^{-1}\right)^q}{(z+m+nq)^{2\beta+t}} = \\ &\sum_{k=0}^{\infty}\sum_{m=1}^{n}\sum_{j=1}^{\mu_n}\left[U^{\chi}\left(ST^{m\varepsilon}\right)\right]_{i,j}\frac{f_j^{(k)}(1)}{k!}\sum_{t=0}^{k}\binom{k}{t}\frac{(-1)^{k-t}}{n^{2\beta+t}}\sum_{q=0}^{\infty}\frac{\chi\left(r_j^{(n)}T^{n\varepsilon}\left(r_j^{(n)}\right)^{-1}\right)^q}{\left(\frac{z+m}{n}+q\right)^{2\beta+t}}\end{aligned}$$

We see now that the last sum $\sum_{q=0}^{\infty}$ defines the Lerch transcendent

$$\Phi\left(\chi\left(r_j^{(n)}T^{n\varepsilon}\left(r_j^{(n)}\right)^{-1}\right), 2\beta+t, \frac{z+m}{n}\right) = \sum_{q=0}^{\infty}\frac{\chi\left(r_j^{(n)}T^{n\varepsilon}\left(r_j^{(n)}\right)^{-1}\right)^q}{\left(\frac{z+m}{n}+q\right)^{2\beta+t}}.$$

□

[1] We would like to thank Oscar Bandtlow for reminding us about this fact.

To find a form of the transfer operator, which can be approximated by a finite matrix we need the following proposition:

Proposition 7.4.9. *The transfer operator has for $\Re\beta > \frac{1}{2}$ the following form*

$$\begin{aligned}\left[\mathcal{L}^{(n)}_{\beta,\varepsilon,\chi}\vec{f}(z)\right]_i &= \sum_{k=0}^{\infty}\sum_{s=0}^{\infty}\sum_{m=1}^{n}\sum_{j=1}^{\mu_n}\left[U^{\chi}\left(S\,T^{m\varepsilon}\right)\right]_{i,j}\frac{f_j^{(k)}(1)}{k!}\sum_{t=0}^{k}\binom{k}{t}\frac{(-1)^{k-t+s}}{n^{2\beta+t+s}}\\ &\quad \frac{1}{s!}\frac{\Gamma(2\beta+t+s)}{\Gamma(2\beta+t)}\Phi\left(\chi\left(r_j^{(n)}T^{n\varepsilon}\left(r_j^{(n)}\right)^{-1}\right),2\beta+t+s,\frac{m+1}{n}\right)(z-1)^s\end{aligned}$$

with Φ the Lerch transcendent and n the level of $\Gamma_0(n)$.

Proof. By using lemma 4.2.3 we can write down the Taylor expansion of $\Phi(\alpha,\nu,z) = \sum_{q=0}^{\infty}\alpha^q(z+q)^{-\nu}$ as follows

$$\begin{aligned}\Phi(\alpha,\nu,z) &= \sum_{s=0}^{\infty}\frac{\Phi^{(s)}(\alpha,\nu,z_0)}{s!}(z-z_0)^s\\ &= \sum_{s=0}^{\infty}\sum_{q=0}^{\infty}\alpha^q\frac{\partial^s}{\partial z^s}(z+q)^{-\nu}|_{z=z_0}\frac{1}{s!}(z-z_0)^s\\ &= \sum_{s=0}^{\infty}\sum_{q=0}^{\infty}\alpha^q(-1)^s\frac{\Gamma(\nu+s)}{\Gamma(\nu)}(z_0+q)^{-\nu-s}\frac{1}{s!}(z-z_0)^s.\end{aligned}$$

Obviously the sum $\sum_{q=0}^{\infty}$ exists, since it is just $\Phi(\alpha,\nu+s,z_0)$. To show that the sum $\sum_{s=0}^{\infty}$ converges uniformly we use the Weierstrass M-Test. We have to find an M_s such that

$$\left|(-1)^s\frac{\Gamma(\nu+s)}{s!}\frac{(z-z_0)^s}{(z_0+q)^{\nu+s}}\right| \le M_s \quad \text{and} \quad \sum_{s=0}^{\infty}M_s < \infty.$$

Obviously we can choose

$$M_s = \frac{|\Gamma(\nu+s)|}{s!}\frac{|z-z_0|^s}{|z_0|^{\nu+s}}.$$

To show that $\sum_{s=0}^{\infty}M_s$ is convergent we use d'Alembert's ratio test

$$\lim_{s\to\infty}\frac{M_{s+1}}{M_s} = \lim_{s\to\infty}\frac{\frac{|\Gamma(\nu+s+1)|}{(s+1)!}\frac{|z-z_0|^{s+1}}{|z_0|^{\nu+s+1}}}{\frac{|\Gamma(\nu+s)|}{(s)!}\frac{|z-z_0|^{s}}{|z_0|^{\nu+s}}} = \frac{|z-z_0|}{|z_0|}.$$

Finally we see that the sum over $\sum_{s=0}^{\infty}$ is only uniformly convergent if $|z-z_0| < |z_0|$. Hence we set $z_0 = \frac{m+1}{n}$ and $z = \frac{z'+m}{n}$, with $z' \in D$. We see that $|z-z_0| = |\frac{z'-1}{n}| \le \frac{3/2}{n}$, since the center of the disk D is at 1 and its radius is $3/2$. On the other hand, since $m \ge 1$ we have $|z_0| = |\frac{m+1}{n}| \ge \frac{2}{n}$ and finally $|z-z_0| \le \frac{3/2}{n} < \frac{2}{n} \le |z_0|$. Therefore

$$\begin{aligned}&\Phi\left(\chi\left(r_j^{(n)}T^{n\varepsilon}\left(r_j^{(n)}\right)^{-1}\right),2\beta+t,\frac{z'+m}{n}\right) =\\ &\sum_{s=0}^{\infty}\frac{(-1)^s}{s!}\frac{\Gamma(2\beta+t+s)}{\Gamma(2\beta+t)}\Phi\left(\chi\left(r_j^{(n)}T^{n\varepsilon}\left(r_j^{(n)}\right)^{-1}\right),2\beta+t+s,\frac{m+1}{n}\right)\left(\frac{z'-1}{n}\right)^s.\end{aligned}$$

Inserting this result into the transfer operator in lemma 7.4.8 concludes the proof. □

Conjecture 7.4.10. *Numerical results suggest that the transfer operator in proposition 7.4.9 is also well defined for $\Re\beta \le \frac{1}{2}$. Indeed, we conjecture that it is an analytic continuation of the transfer operator in $\beta \in \mathbb{C}$.*

7.4.5 An approximation of the transfer operator

It is known that one can approximate a nuclear operator like the transfer operator $\mathcal{L}^{(n)}_{\beta,\varepsilon,\chi}$ by operators of finite rank, see, e.g., [Fri96]. In this section we write the transfer operator $\mathcal{L}^{(n)}_{\beta,\varepsilon,\chi}$ in terms of a matrix $\mathcal{M}^{(n)}_{\beta,\varepsilon,\chi}$ which is suitable for computations. The main difficulty is to show that this approximation is also valid for $\Re\beta < \frac{1}{2}$, since we can only approximate the transfer operator in proposition 7.4.9 and not the analytic continuation of the transfer operator in lemma 7.4.6. The second problem is to proof that the spectrum of $\mathcal{M}^{(n)}_{\beta,\varepsilon,\chi}$ is an approximation of the spectrum of $\mathcal{L}^{(n)}_{\beta,\varepsilon,\chi}$, see also [BH99] and [Str08]. We will present in later chapters several arguments which show that our approximation leads to correct results when compared to known facts. Indeed, also some properties of the spectrum of the Laplacian under a character deformation, which have been found numerically by this procedure have been proven to be true, see [BFM12]. We are very confident that our approximation is the correct one.

In a first step we write the transfer operator in the basis $\{\vec{e}_i\}_{1\le i\le \mu_n}$ of $\mathbb{C}^{\mu_n}$, with $[\vec{e}_i]_j = \delta_{i,j}$. The transfer operator in proposition 7.4.9 can then be written as

$$\begin{aligned}
\mathcal{L}^{(n)}_{\beta,\varepsilon,\chi}\vec{f}(z) &= \sum_{i=1}^{\mu_n}\left[\mathcal{L}^{(n)}_{\beta,\varepsilon,\chi}\vec{f}(z)\right]_i \vec{e}_i \\
&= \sum_{k=0}^{\infty}\sum_{s=0}^{\infty}\sum_{i=1}^{\mu_n}\sum_{j=1}^{\mu_n}\sum_{m=1}^{n}\left[U^\chi\left(S\,T^{m\varepsilon}\right)\right]_{i,j}\sum_{t=0}^{k}\binom{k}{t}\frac{(-1)^{k-t+s}}{n^{2\beta+t+s}}\frac{1}{s!}\frac{\Gamma(2\beta+t+s)}{\Gamma(2\beta+t)} \\
&\quad \Phi\left(\chi\left(r^{(n)}_j T^{n\varepsilon}\left(r^{(n)}_j\right)^{-1}\right), 2\beta+t+s, \frac{m+1}{n}\right)\frac{f^{(k)}_j(1)}{k!}(z-1)^s\,\vec{e}_i. \qquad (7.26)
\end{aligned}$$

Next we consider the eigenvalue equation for the transfer operator and expand f_i in a Taylor series

$$\begin{aligned}
\mathcal{L}^{(n)}_{\beta,\varepsilon,\chi}\vec{f}(z) &= \lambda\vec{f}(z) \\
&= \lambda\sum_{r=1}^{\mu_n} f_r(z)\,\vec{e}_r \\
&= \lambda\sum_{r=1}^{\mu_n}\sum_{q=0}^{\infty}\frac{f^{(q)}_r(1)}{q!}(z-1)^q\,\vec{e}_r \qquad (7.27)
\end{aligned}$$

To determine the coefficients $\frac{f^{(q)}_r(1)}{q!}$ in the Taylor expansion, we have to compare the rhs of (7.27) with the rhs of (7.26). This leads to

$$\begin{aligned}
\lambda\frac{f^{(s)}_i(1)}{s!} &= \sum_{k=0}^{\infty}\sum_{j=1}^{\mu_n}\frac{1}{s!}\sum_{t=0}^{k}\binom{k}{t}\frac{(-1)^{k-t+s}}{n^{2\beta+t+s}}\frac{\Gamma(2\beta+t+s)}{\Gamma(2\beta+t)} \\
&\quad \sum_{m=1}^{n}\left[U^\chi\left(S\,T^{m\varepsilon}\right)\right]_{i,j}\Phi\left(\chi\left(r^{(n)}_j T^{n\varepsilon}\left(r^{(n)}_j\right)^{-1}\right), 2\beta+t+s, \frac{m+1}{n}\right)\frac{f^{(k)}_j(1)}{k!}.
\end{aligned}$$

Next we define the matrix $\mathcal{M}^{(n)}_{\beta,\varepsilon,\chi}$ by

$$\begin{aligned}
\left[\left(\mathcal{M}^{(n)}_{\beta,\varepsilon,\chi}\right)_{s,k}\right]_{i,j} &= \frac{1}{s!}\sum_{t=0}^{k}\binom{k}{t}\frac{(-1)^{k-t+s}}{n^{2\beta+t+s}}\frac{\Gamma(2\beta+t+s)}{\Gamma(2\beta+t)} \\
&\quad \sum_{m=1}^{n}\left[U^\chi\left(S\,T^{m\varepsilon}\right)\right]_{i,j}\Phi\left(\chi\left(r^{(n)}_j T^{n\varepsilon}\left(r^{(n)}_j\right)^{-1}\right), 2\beta+t+s, \frac{m+1}{n}\right).
\end{aligned}$$

The eigenvalue equation then reads in terms of this matrix

$$\lambda \frac{f_i^{(s)}(1)}{s!} = \sum_{k=0}^{\infty} \sum_{j=1}^{\mu_n} \left[\left(\mathcal{M}^{(n)}_{\beta,\varepsilon,\chi} \right)_{s,k} \right]_{i,j} \frac{f_j^{(k)}(1)}{k!}.$$

with $1 \leq i, j \leq \mu_n$ and $0 \leq s, k < \infty$. Obviously the dimension of this matrix is infinite, so that for numerical computations we have to truncate the Taylor expansion such that $0 \leq s, k < N$. Summarizing, we can state the following proposition:

Proposition 7.4.11. *The transfer operator $\mathcal{L}^{(n)}_{\beta,\varepsilon,\chi}$ in proposition 7.4.9 can be approximated for $\Re\beta > \frac{1}{2}$ in the weak sense by the matrix $\mathcal{M}^{(n)}_{\beta,\varepsilon,\chi} \in \mathbb{C}^{\mu_n N \times \mu_n N}$ given by*

$$\begin{aligned} \left[\left(\mathcal{M}^{(n)}_{\beta,\varepsilon,\chi} \right)_{s,k} \right]_{i,j} &= \frac{1}{s!} \sum_{t=0}^{k} \binom{k}{t} \frac{(-1)^{k-t+s}}{n^{2\beta+t+s}} \frac{\Gamma(2\beta+t+s)}{\Gamma(2\beta+t)} \sum_{m=1}^{n} \left[U^{\chi}\left(S T^{m\varepsilon}\right) \right]_{i,j} \\ &\quad \Phi\left(\chi\left(r_j^{(n)} T^{n\varepsilon} \left(r_j^{(n)} \right)^{-1} \right), 2\beta+t+s, \frac{m+1}{n} \right) \end{aligned} \tag{7.28}$$

with $1 \leq i, j \leq \mu_n$ and $0 \leq s, k < N$, in the limit of large $N \in \mathbb{Z}_{>}$ and n the level of $\Gamma_0(n)$.

Proof. We have already shown that $\left[\left(\mathcal{M}^{(n)}_{\beta,\varepsilon,\chi} \right)_{s,k} \right]_{i,j}$ for $0 \leq s, k < N$ corresponds to a finite matrix representation of $\mathcal{L}^{(n)}_{\beta,\varepsilon,\chi}$. Now we have to show that

$$\lim_{N\to\infty} \sum_{s=0}^{N-1} \sum_{k=0}^{N-1} \sum_{i=1}^{\mu_n} \sum_{j=1}^{\mu_n} \left[\left(\mathcal{M}^{(n)}_{\beta,\varepsilon,\chi} \right)_{s,k} \right]_{i,j} \frac{f^{(k)}(1)}{k!} (z-1)^s \vec{e}_i = \mathcal{L}^{(n)}_{\beta,\varepsilon,\chi} \vec{f}(z)$$

exists, but this follows immediately from both the sums $\sum_{s=0}^{\infty}$ and $\sum_{k=0}^{\infty}$ converging uniformly, which was shown in proposition 7.4.9 and lemma 7.4.8. □

Corollary 7.4.12. *An approximation of the transfer operator with the representation U^{χ_α} induced by the charater $\chi_\alpha(\gamma) = \exp 2\pi i \alpha \Omega(\gamma)$ defined in section 6.5 is given by*

$$\begin{aligned} \left[\left(\mathcal{M}^{(n)}_{\beta,\varepsilon,\chi} \right)_{s,k} \right]_{i,j} &= \frac{1}{s!} \sum_{t=0}^{k} \binom{k}{t} \frac{(-1)^{k-t+s}}{n^{2\beta+t+s}} \frac{\Gamma(2\beta+t+s)}{\Gamma(2\beta+t)} \sum_{m=1}^{n} \left[U^{\chi_\alpha}\left(S T^{m\varepsilon}\right) \right]_{i,j} \\ &\quad \zeta_L\left(\alpha\Omega\left(r_j^{(n)} T^{n\varepsilon} \left(r_j^{(n)} \right)^{-1} \right), 2\beta+t+s, \frac{m+1}{n} \right) \end{aligned} \tag{7.29}$$

where $\alpha \in \mathbb{R}$ is the deformation parameter and ζ_L the Lerch zeta function. This result can be extended to the more general character $\chi_{\alpha_1,\ldots,\alpha_\kappa}(\gamma) = \exp 2\pi i \sum_{q=1}^{\kappa} \alpha_q \Omega_q(\gamma)$ defined in (6.16) in an obvious way.

One can approximate also $\tilde{\mathcal{L}}^{(n)}_{\beta,\chi} = \begin{pmatrix} 0 & \mathcal{L}^{(n)}_{\beta,+1,\chi} \\ \mathcal{L}^{(n)}_{\beta,-1,\chi} & 0 \end{pmatrix}$ by $\begin{pmatrix} 0 & \mathcal{M}^{(n)}_{\beta,+1,\chi} \\ \mathcal{M}^{(n)}_{\beta,-1,\chi} & 0 \end{pmatrix}$. Since the Selberg zeta function is given by $Z^{(n)}(\beta,\chi) = \det\left(1 - \tilde{\mathcal{L}}^{(n)}_{\beta,\chi}\right) = \det\left(1 - \mathcal{L}^{(n)}_{\beta,+1,\chi} \mathcal{L}^{(n)}_{\beta,-1,\chi}\right)$ it is enough to compute the spectrum of $(\mathcal{M}^{(n)}_{\beta,+1,\chi} \mathcal{M}^{(n)}_{\beta,-1,\chi})$. Later we will introduce symmetries which allow us to factorize this Fredholm determinant, see also [FM11]. This approximation should also be valid for the transfer operators for $\Gamma(n)$ and all congruence subgroups of $\mathrm{SL}(2,\mathbb{Z})$. To find such an approximation for other groups one needs to find a form of the representation U^{χ} similar to that in lemma 7.4.3; otherwise one has to evaluate a matrix-valued Lerch zeta function, like the one in the analytic continuation of the transfer operator in [Fri96]. Also, the

Taylor expansion of $\vec{f}$ has to be performed around the center of the disk D, which can be different from $z = 1$ for other groups. According to conjecture 7.4.10 the matrix $\mathcal{M}^{(n)}_{\beta,\varepsilon,\chi}$ in proposition 7.4.11 is also an approximation of the transfer operator for $\Re\beta \leq \frac{1}{2}$. To support this conjecture, later we will present numerical results for $\Re\beta \leq \frac{1}{2}$, which can be proven to be true.

In [BH99] Baladi and Holschneider showed that under certain conditions a subset of the spectra $\sigma(\mathcal{L}_N)$ of a sequence of approximations $\mathcal{L}_N$ of the transfer operator $\mathcal{L}$ is converging to the spectrum $\sigma(\mathcal{L})$ of the transfer operator with N. In [Str08] Strömberg constructed an approximation of the transfer operator for Hecke triangle groups which fulfills these conditions. The problem is that some of the eigenvalues $\lambda_{i,N} \in \sigma(\mathcal{L}_N)$ of the approximation $\mathcal{L}_N$ may not be related to the spectrum $\sigma(\mathcal{L})$ of the transfer operator $\mathcal{L}$. Also, it is not clear if all the eigenvalues λ_{i_j,N_j} of such a sequence of approximations which are converging to some stable value $\lambda_{i_j,N_j} \to_j \lambda$ belong to the spectrum of the transfer operator, i.e. if $\lambda \in \sigma(\mathcal{L})$. Even if we knew the subset $\left\{\lambda_{i_j,N}\right\}_{1\leq j\leq K}$ of the eigenvalues of $\mathcal{L}_N$ which are approximating the eigenvalues of $\mathcal{L}$, ordered by decreasing absolute value i.e. $|\lambda_{i_j,N}| \geq |\lambda_{i_l,N}|$ for $j < l$, then another issue is that one cannot prove that $\left\{\lambda_{i_j,N}\right\}_{1\leq j\leq k}$ approximates all of the eigenvalues of $\mathcal{L}$ with absolute value greater or equal to $|\lambda_{i_K,N}|$.

On the other hand, numerical results indicate that all problems mentioned above do not occur in our approximation in proposition 7.4.11 of the transfer operator $\mathcal{L}^{(n)}_{\beta,\varepsilon,\chi}$. All eigenvalues of this approximation seem to approximate eigenvalues of the transfer operator $\mathcal{L}^{(n)}_{\beta,\varepsilon,\chi}$. Furthermore, it seems that the spectrum of the approximation contains all the eigenvalues of the transfer operator with absolute value greater than the smallest in absolute value of the eigenvalues of the approximation. It was proved in [BJ08] that the eigenvalues λ_j of the transfer operator decrease exponentially

$$|\lambda_j| \leq Ae^{-c\,j}$$

for all $j \in \mathbb{Z}_>$, and with some constant $A, c > 0$. Since we are interested in the Fredholm determinant and its zeros, it is enough to approximate the eigenvalues with the leading absolute value and the eigenvalues around one. Since they are decreasing exponentially, an excellent test to make sure if we have got all the significant eigenvalues is to compare the sum of the eigenvalues of the approximation to the trace formula in proposition 7.4.7. In the next chapter we will present some results by comparing the trace formula with the spectrum of $\mathcal{M}^{(n)}_{\beta,\varepsilon,\chi}$ and also other results to support our claims. We should mention that also the spectrum of the approximation of the transfer operator for the Kac-Baker model in Chapter 9 shows this nice behavior.

We have also made an approximation of the transfer operator by using Chebyshev polynomials instead of the Taylor expansion. Unfortunately, the computation time increases dramatically and the results themselves are not very accurate. On the other hand, according to Strömberg [Str09a] the approximation of the transfer operator for Hecke triangle groups improves a lot by using Chebyshev polynomials.

One should also try to obtain results by applying perturbation theory in α for the transfer operator with these deformation by the character χ_α from section 6.5. It would be interesting to compare these results to our numerical results for $\Gamma_0(4)$ and $\Gamma_0(8)$.

Chapter 8

Numerical investigations of Selberg zeta functions under character deformations

> "I think that it is a relatively good approximation to truth – which is much too complicated to allow anything but approximations – that mathematical ideas originate in empirics"
>
> — John von Neumann

In this chapter we present the numerical results we obtained using our computer program package Morpheus for the transfer operators $\mathcal{L}^{(n)}_{\beta,\varepsilon,\chi}$ in section 7.4 and the Selberg zeta function $Z^{(n)}(\beta,\chi)$ for $\Gamma_0(n)$ and character χ given by

$$Z^{(n)}(\beta,\chi) = \det\left(1-\tilde{\mathcal{L}}^{(n)}_{\beta,\chi}\right) = \det\left(1-\mathcal{L}^{(n)}_{\beta,+1,\chi}\mathcal{L}^{(n)}_{\beta,-1,\chi}\right) = \det\left(1-\mathcal{L}^{(n)}_{\beta,-1,\chi}\mathcal{L}^{(n)}_{\beta,+1,\chi}\right).$$

The main focus of our investigations is on the character deformation by $\chi^{(4)}_{\alpha_1,\alpha_2}$ of the transfer operator

$$\mathcal{L}^{(4)}_{\beta,\varepsilon,(\alpha_1,\alpha_2)} := \mathcal{L}^{(4)}_{\beta,\varepsilon,\chi^{(4)}_{\alpha_1,\alpha_2}}$$

for $\Gamma_0(4)$ and the character deformation by $\chi^{(8)}_{\alpha_1,\alpha_2,\alpha_3}$ of the transfer operator

$$\mathcal{L}^{(8)}_{\beta,\varepsilon,(\alpha_1,\alpha_2,\alpha_3)} := \mathcal{L}^{(8)}_{\beta,\varepsilon,\chi^{(8)}_{\alpha_1,\alpha_2,\alpha_3}}$$

for $\Gamma_0(8)$. The definitions of the characters $\chi^{(4)}_{\alpha_1,\alpha_2}$ and $\chi^{(8)}_{\alpha_1,\alpha_2,\alpha_3}$ are given in section 6.5:

$$\begin{aligned}\chi^{(4)}_{\alpha_1,\alpha_2}(\gamma) &= \exp 2\pi i\left(\alpha_1\Omega^{(4)}_1(\gamma)+\alpha_2\Omega^{(4)}_2(\gamma)\right)\\ \chi^{(8)}_{\alpha_1,\alpha_2,\alpha_3}(\gamma) &= \exp 2\pi i\left(\alpha_1\Omega^{(8)}_1(\gamma)+\alpha_2\Omega^{(8)}_2(\gamma)+\alpha_3\Omega^{(8)}_3(\gamma)\right),\end{aligned}$$

where the functions $\Omega^{(4)}_i : \Gamma_0(4) \to \mathbb{Z}$ and $\Omega^{(8)}_i : \Gamma_0(8) \to \mathbb{Z}$ are defined by (6.17). We are especially interested in the character deformation of the transfer operator and the Selberg zeta function by $\chi^{(4)}_\alpha := \chi^{(4)}_{\alpha,0}$ for $\Gamma_0(4)$ and the deformation by $\chi^{(8)}_\alpha := \chi^{(8)}_{0,\alpha,0}$ for $\Gamma_0(8)$. We denote the corresponding transfer operators by $\mathcal{L}^{(4)}_{\beta,\varepsilon,\alpha} := \mathcal{L}^{(4)}_{\beta,\varepsilon,(\alpha,0)}$, $\mathcal{L}^{(8)}_{\beta,\varepsilon,\alpha} := \mathcal{L}^{(8)}_{\beta,\varepsilon,(0,\alpha,0)}$ respectively for $(\Gamma_0(n),\chi\equiv 1)$ by $\mathcal{L}^{(n)}_{\beta,\varepsilon} := \mathcal{L}^{(n)}_{\beta,\varepsilon,\chi\equiv 1}$.

All the results we present in this chapter are based on numerical calculations by our computer programs widmo and CGF which are part of our computer program packages Morpheus, see Appendix A. Unfortunately, most of these results cannot be proven yet. A practical problem that arises is how to present our results, since the data sets are extremely large so that we cannot include them in this thesis. Instead, we will

describe our results and our conclusions; when necessary we will include figures and tables obtained from our data to clarify them. We use the term *Experimental Observation* to describe results from our numerical experiments and the term *Conclusion* for general predictions based on numerical experiments we believe to be true. For some results we use the term *Conjecture*.

8.1 Numerical results for the transfer operator

To evaluate the Selberg zeta function $Z^{(n)}(\beta,\chi)$ one needs the spectrum of $\tilde{\mathcal{L}}^{(n)}_{\beta,\chi} = \begin{pmatrix} 0 & \mathcal{L}^{(n)}_{\beta,+1,\chi} \\ \mathcal{L}^{(n)}_{\beta,-1,\chi} & 0 \end{pmatrix}$ or $\mathcal{L}^{(n)}_{\beta,+1,\chi}\mathcal{L}^{(n)}_{\beta,-1,\chi}$ (resp. $\mathcal{L}^{(n)}_{\beta,-1,\chi}\mathcal{L}^{(n)}_{\beta,+1,\chi}$). To obtain a numerical approximation of the spectrum of the transfer operator $\mathcal{L}^{(n)}_{\beta,\varepsilon,\chi}$ in proposition 7.4.9

$$\begin{aligned}\left[\mathcal{L}^{(n)}_{\beta,\varepsilon,\chi}\vec{f}(z)\right]_i &= \sum_{k=0}^{\infty}\sum_{s=0}^{\infty}\sum_{m=1}^{n}\sum_{j=1}^{\mu_n}\left[U^{\chi}\left(ST^{m\varepsilon}\right)\right]_{i,j}\frac{f_j^{(k)}(1)}{k!}\sum_{t=0}^{k}\binom{k}{t}\frac{(-1)^{k-t+s}}{n^{2\beta+t+s}} \\ &\quad \frac{1}{s!}\frac{\Gamma(2\beta+t+s)}{\Gamma(2\beta+t)}\Phi\left(\chi\left(r_j^{(n)}T^{n\varepsilon}\left(r_j^{(n)}\right)^{-1}\right),2\beta+t+s,\frac{m+1}{n}\right)(z-1)^s,\end{aligned}$$

we approximate this operator by the matrix $\mathcal{M}^{(n)}_{\beta,\varepsilon,\chi}$ in proposition 7.4.11

$$\begin{aligned}\left[\left(\mathcal{M}^{(n)}_{\beta,\varepsilon,\chi}\right)_{s,k}\right]_{i,j} &= \frac{1}{s!}\sum_{t=0}^{k}\binom{k}{t}\frac{(-1)^{k-t+s}}{n^{2\beta+t+s}}\frac{\Gamma(2\beta+t+s)}{\Gamma(2\beta+t)}\sum_{m=1}^{n}\left[U^{\chi}\left(ST^{m\varepsilon}\right)\right]_{i,j} \\ &\quad \Phi\left(\chi\left(r_j^{(n)}T^{n\varepsilon}\left(r_j^{(n)}\right)^{-1}\right),2\beta+t+s,\frac{m+1}{n}\right)\end{aligned}$$

and compute its spectrum. This leads to the approximation of the Selberg zeta function

$$Z^{(n)}_{\mathcal{M}}(\beta,\chi) = \det(1-\mathcal{M}^{(n)}_{\beta,+1,\chi}\mathcal{M}^{(n)}_{\beta,-1,\chi}) = \det(1-\mathcal{M}^{(n)}_{\beta,-1,\chi}\mathcal{M}^{(n)}_{\beta,+1,\chi}).$$

Note that we cannot use the analytic continuation of the transfer operator in lemma 7.4.6

$$\left[\mathcal{L}^{(n)}_{\beta,\varepsilon,\chi}\vec{f}(z)\right]_i = \left[\mathcal{N}^{(n)}_{\beta,\varepsilon,\chi,N}\vec{f}(z)\right]_i + \left[\mathcal{A}^{(n)}_{\beta,\varepsilon,\chi,N}\vec{f}(z)\right]_i$$

for numerical computations. On the other hand, we can compute numerically the trace of its analytic continuation by the trace formula in proposition 7.4.7

$$\operatorname{tr}\mathcal{L}^{(n)}_{\beta,\varepsilon,\chi} = \operatorname{tr}\mathcal{N}^{(n)}_{\beta,\varepsilon,\chi,N} + \operatorname{tr}\mathcal{A}^{(n)}_{\beta,\varepsilon,\chi,N}.$$

From conjecture 7.4.10 we expect that the transfer operator $\mathcal{L}^{(n)}_{\beta,\varepsilon,\chi}$ in proposition 7.4.9, which we are using for numerical computations by approximating it by a finite matrix $\mathcal{M}^{(n)}_{\beta,\varepsilon,\chi}$, is also well defined for $\Re\beta \leq \frac{1}{2}$. We checked this conjecture numerically by comparing the traces of the approximating matrix $\mathcal{M}^{(n)}_{\beta,\varepsilon,\chi}$ and the analytic continuation of the transfer operator given by the trace formula in proposition 7.4.7. Indeed, we found in all cases that both traces are practically identical, which supports our conjecture 7.4.10 and also indicates that the transfer operator in proposition 7.4.9 is indeed an analytical continuation.

Furthermore, we found numerically that for $(\Gamma_0(n),\chi \equiv 1)$ and $(\Gamma_0(4),\chi^{(4)}_{\alpha})$ the traces of the operators $\mathcal{L}^{(n)}_{\beta,+1,\chi}$ and $\mathcal{L}^{(n)}_{\beta,-1,\chi}$ coincide. Further numerical investigations revealed that in these cases the spectra of $\mathcal{L}^{(n)}_{\beta,+1,\chi}$ and $\mathcal{L}^{(n)}_{\beta,-1,\chi}$ are also identical. This indicates that there should exist a symmetry between the operators

$\mathcal{L}^{(n)}_{\beta,+1,\chi}$ and $\mathcal{L}^{(n)}_{\beta,-1,\chi}$. Indeed, for $(\Gamma_0(n), \chi \equiv 1)$ and $(\Gamma_0(4), \chi^{(4)}_\alpha)$ we found such symmetries by using the form of theses operators given in lemma 7.4.5:

$$\left[\mathcal{L}^{(n)}_{\beta,\varepsilon,\chi}\vec{f}(z)\right]_i = \sum_{q=0}^{\infty}\sum_{m=1}^{n}\sum_{j=1}^{\mu_n}\left[U^\chi\left(ST^{m\varepsilon}\right)\right]_{i,j}\chi\left(r_j^{(n)}T^{n\varepsilon}\left(r_j^{(n)}\right)^{-1}\right)^q f_j|_{2\beta}\tilde{S}T^{m+nq}z.$$

It allows explicit expressions for every component of $\mathcal{L}^{(n)}_{\beta,+1,\chi}\vec{f}(z)$ and $\mathcal{L}^{(n)}_{\beta,-1,\chi}\vec{f}(z)$, see section 7.4.2 for the transfer operator for $\Gamma_0(4)$ and Appendix C for the transfer operator for $\Gamma_0(8)$. Comparing these components of $\mathcal{L}^{(n)}_{\beta,+1,\chi}\vec{f}(z)$ and $\mathcal{L}^{(n)}_{\beta,-1,\chi}\vec{f}(z)$ showed the existence of operators $\mathcal{P}_k : \bigoplus_{j=1}^{\mu_n} B(D) \to \bigoplus_{j=1}^{\mu_n} B(D)$ given by $\left[\mathcal{P}_k\vec{f}(z)\right]_j = f_{p_k(j)}(z)$, with $p_k : \{1,\ldots,\mu_n\} \to \{1,\ldots,\mu_n\}$ a permutation such that $\mathcal{P}_k = \mathcal{P}_k^{-1}$ and

$$\mathcal{P}_k\mathcal{L}^{(n)}_{\beta,+1,\chi} = \mathcal{L}^{(n)}_{\beta,-1,\chi}\mathcal{P}_k.$$

These operators $\mathcal{P}_k$ define a new kind of symmetries $\tilde{\mathcal{P}}_k = \begin{pmatrix} 0 & \mathcal{P}_k \\ \mathcal{P}_k & 0 \end{pmatrix}$ of the transfer operator such that

$$\begin{aligned} \tilde{\mathcal{P}}_k\tilde{\mathcal{L}}^{(n)}_{\beta,\chi} &= \tilde{\mathcal{L}}^{(n)}_{\beta,\chi}\tilde{\mathcal{P}}_k \\ \begin{pmatrix} 0 & \mathcal{P}_k \\ \mathcal{P}_k & 0 \end{pmatrix}\begin{pmatrix} 0 & \mathcal{L}^{(n)}_{\beta,+1,\chi} \\ \mathcal{L}^{(n)}_{\beta,-1,\chi} & 0 \end{pmatrix} &= \begin{pmatrix} 0 & \mathcal{L}^{(n)}_{\beta,+1,\chi} \\ \mathcal{L}^{(n)}_{\beta,-1,\chi} & 0 \end{pmatrix}\begin{pmatrix} 0 & \mathcal{P}_k \\ \mathcal{P}_k & 0 \end{pmatrix}. \end{aligned}$$

In the following we will call also the operators $\mathcal{P}_k$ symmetries. Then the Selberg zeta function is given by

$$Z^{(n)}(\beta,\chi) = \det\left(1 - \mathcal{P}_k\mathcal{L}^{(n)}_{\beta,+1,\chi}\right)\det\left(1 + \mathcal{P}_k\mathcal{L}^{(n)}_{\beta,+1,\chi}\right).$$

For $\mathrm{SL}(2,\mathbb{Z})$ such a factorization of the Selberg zeta function in terms of a transfer operator $\mathcal{L}^{(1)}_\beta$ is well known [May91b]: Here $Z^{(1)}(\beta) = \det(1 - \mathcal{L}^{(1)}_\beta)\det(1 + \mathcal{L}^{(1)}_\beta)$. In [Efr93] it was proved that the eigenvalues ± 1 of the transfer operator $\mathcal{L}^{(1)}_\beta$ for $\mathrm{SL}(2,\mathbb{Z})$ are related to the even / odd symmetry of the Maass wave forms u for $\mathrm{SL}(2,\mathbb{Z})$ under the involution $u(-\bar{z}) = \pm u(z)$. A similar relation of the symmetries $\mathcal{P}_k$ to involutions of the Maass wave forms for $\Gamma_0(n)$ for $\chi \equiv 1$ and $\Gamma_0(4)$ for $\chi^{(4)}_\alpha$ was found by us numerically. Note that for the character deformation of $\Gamma_0(4)$ we will use the operator $\mathcal{P}_2\mathcal{L}^{(4)}_{\beta,+1,\alpha}$, with $\mathcal{P}_2$ the only remaining symmetry for $\alpha \notin \mathbb{Z}$ which is defined by the permutation $p_2(i)$ given in section 7.4.2. While for $\Gamma_0(8)$ we have to use the operator $\mathcal{L}^{(8)}_{\beta,+1,\chi}\mathcal{L}^{(8)}_{\beta,-1,\chi}$, since symmetries for a non-trivial character $\chi^{(8)}_\alpha$ for $\Gamma_0(8)$ do not exist.

Finally, at the end of this section we show the results of our numerical experiments we performed to investigate the spectrum of the transfer operator $\mathcal{L}^{(n)}_{\beta,\varepsilon,\chi}$ for $(\Gamma_0(n), \chi \equiv 1)$, $(\Gamma_0(4), \chi^{(4)}_\alpha)$ and $(\Gamma_0(8), \chi^{(8)}_\alpha)$, with and without using the symmetries $\mathcal{P}_k$. We were able to obtain new results for the spectrum and we verified our approximation by comparing them with several known properties.

8.1.1 A numerical verification of the approximation matrix $\mathcal{M}^{(n)}_{\beta,\varepsilon,\chi}$ by the trace of the transfer operator $\mathcal{L}^{(n)}_{\beta,\varepsilon,\chi}$

In section 7.4.5 we formulated the claim that the spectrum of the transfer operator $\mathcal{L}^{(n)}_{\beta,\varepsilon,\chi}$ in proposition 7.4.9 can be approximated by the spectrum of the matrix $\mathcal{M}^{(n)}_{\beta,\varepsilon,\chi}$ in proposition 7.4.11, namely

1. Every eigenvalue of $\mathcal{M}^{(n)}_{\beta,\varepsilon,\chi}$ approximates an eigenvalue of $\mathcal{L}^{(n)}_{\beta,\varepsilon,\chi}$.
2. All eigenvalues of $\mathcal{L}^{(n)}_{\beta,\varepsilon,\chi}$ with absolute value larger than or equal to $|\lambda_{\min}|$ are approximated by eigenvalues of $\mathcal{M}^{(n)}_{\beta,\varepsilon,\chi}$, where $\lambda_{\min}$ denotes the eigenvalue of $\mathcal{M}^{(n)}_{\beta,\varepsilon,\chi}$ for an appropriately chosen N with the smallest absolute value.

Unfortunately, we cannot prove these claims, (see also section 7.4.5, [BH99] and [Str08]). On the other hand, it was proved in [BH99] that under certain conditions a subset of the spectrum of an approximation of a transfer operator approximates the spectrum of this transfer operator. Thus, we can assume that at least part of the spectrum of $\mathcal{M}^{(n)}_{\beta,\varepsilon,\chi}$ approximates the spectrum of the transfer operator $\mathcal{L}^{(n)}_{\beta,\varepsilon,\chi}$ in proposition 7.4.9. In [BJ08] it was proved that the eigenvalues of the transfer operator decrease exponentially. Since we want to evaluate the Selberg zeta function by the Fredholm determinant of the transfer operator, it is hence enough to approximate the eigenvalues with leading absolute values.

The best way to verify our claims about the spectrum of $\mathcal{M}^{(n)}_{\beta,\varepsilon,\chi}$ and the implementation of the computation of the matrix $\mathcal{M}^{(n)}_{\beta,\varepsilon,\chi}$ would be to compare the spectrum of $\mathcal{M}^{(n)}_{\beta,\varepsilon,\chi}$ with the spectrum of the transfer operator $\mathcal{L}^{(n)}_{\beta,\varepsilon,\chi}$. Unfortunately, we cannot do this, since neither analytical nor independent numerical results for the spectra of the transfer operator exist. Instead, we compare the traces of the approximation matrix $\mathcal{M}^{(n)}_{\beta,\varepsilon,\chi}$ and the analytic continued transfer operator $\mathcal{L}^{(n)}_{\beta,\varepsilon,\chi}$ using the trace formula in proposition 7.4.7. Both traces are determined numerically by independent methods, and thus one can expect that the traces will only coincide if both implementations are indeed correct. This way we verify whether our implementation of the computation of the matrix $\mathcal{M}^{(n)}_{\beta,\varepsilon,\chi}$ and its eigenvalues is correct, and at the same time we also check all the technical ingredients of this implementation like our approximation of certain special functions and the computation of the eigenvalues. Furthermore, by comparing the traces of $\mathcal{M}^{(n)}_{\beta,\varepsilon,\chi}$ with the trace formula in proposition 7.4.7 for the analytic continued transfer operator for $\Re\beta \leq \frac{1}{2}$ we also verify our conjecture 7.4.10, namely that the transfer operator in proposition 7.4.9 is an analytical continuation and hence our approximation is also valid for $\Re\beta \leq \frac{1}{2}$. Note that we performed most of our numerical experiments presented in later sections of this chapter for $\Re\beta \leq \frac{1}{2}$; all these numerical results for the transfer operator and the Selberg zeta function also support conjecture 7.4.10. So far we did not find any contradiction between the numerical and analytical results. From the results in [BH99] it follows that at least part of the spectrum of the matrix $\mathcal{M}^{(n)}_{\beta,\varepsilon,\chi}$ approximates the spectrum of the transfer operator $\mathcal{L}^{(n)}_{\beta,\varepsilon,\chi}$, and from the identity of the traces of $\mathcal{M}^{(n)}_{\beta,\varepsilon,\chi}$ and $\mathcal{L}^{(n)}_{\beta,\varepsilon,\chi}$ we conclude that at least the largest (in absolute value) eigenvalues of $\mathcal{M}^{(n)}_{\beta,\varepsilon,\chi}$ are approximating the largest (in absolute value) eigenvalues of $\mathcal{L}^{(n)}_{\beta,\varepsilon,\chi}$. This conclusion is based on the expectation that, if some large (in absolute value) eigenvalues of $\mathcal{M}^{(n)}_{\beta,\varepsilon,\chi}$ do not approximate the eigenvalues of $\mathcal{L}^{(n)}_{\beta,\varepsilon,\chi}$, then these eigenvalues should not be related to $\mathcal{L}^{(n)}_{\beta,\varepsilon,\chi}$ in any form, and thereby will not lead to the same trace. An argument supporting this assumption is the following: We also approximated the analytic continuation of the transfer operator in lemma 7.4.6 given by $\mathcal{L}^{(n)}_{\beta,\varepsilon,\chi}\vec{f}(z) = \mathcal{N}^{(n)}_{\beta,\varepsilon,\chi,N}\vec{f}(z) + \mathcal{A}^{(n)}_{\beta,\varepsilon,\chi,N}\vec{f}(z)$ by a matrix representation $\mathcal{A}^{(n)}_{\beta,\varepsilon,\chi,(N,N)}$ of $\mathcal{A}^{(n)}_{\beta,\varepsilon,\chi,N}$. This approximation is equivalent to the approximation used in [Str08] and to the matrix representation of the transfer operator for $\mathrm{SL}(2,\mathbb{Z})$ in [May90]. We found that even for large N there are always eigenvalues of $\mathcal{A}^{(n)}_{\beta,\varepsilon,\chi,(N,N)}$ which depend on N, which indicates that they are not part of the spectrum of the transfer operator $\mathcal{L}^{(n)}_{\beta,\varepsilon,\chi}$. The traces of $\mathcal{A}^{(n)}_{\beta,\varepsilon,\chi,(N,N)}$ and $\mathcal{L}^{(n)}_{\beta,\varepsilon,\chi}$ were never identical; indeed, the trace of $\mathcal{A}^{(n)}_{\beta,\varepsilon,\chi,(N,N)}$ diverges for N becoming large. However, from other numerical observations we know that part of the spectrum of $\mathcal{A}^{(n)}_{\beta,\varepsilon,\chi,(N,N)}$ approximates the spectrum of $\mathcal{L}^{(n)}_{\beta,\varepsilon,\chi}$. See section 7.4.3 for further details on an approximation of the transfer operator by $\mathcal{A}^{(n)}_{\beta,\varepsilon,\chi,(N,N)}$. This lets us conclude that, if the eigenvalues of an approximation of the transfer operator do not change with N and its traces are equal or are converging to the traces of the transfer operator $\mathcal{L}^{(n)}_{\beta,\varepsilon,\chi}$ given by the trace formula in proposition 7.4.7, then all of its largest (in absolute value) eigenvalues should approximate the corresponding eigenvalues of the transfer operator. This seems to be the case for the approximation matrix $\mathcal{M}^{(n)}_{\beta,\varepsilon,\chi}$: The largest (in absolute value) eigenvalues of $\mathcal{M}^{(n)}_{\beta,\varepsilon,\chi}$ do not change with the number of Taylor coefficients N in the approximation, and the trace is converging with N exponentially to the trace of the transfer operator $\mathcal{L}^{(n)}_{\beta,\varepsilon,\chi}$. Obviously, it could happen that some eigenvalues of $\mathcal{M}^{(n)}_{\beta,\varepsilon,\chi}$ cancel each other, and thus the trace of $\mathcal{M}^{(n)}_{\beta,\varepsilon,\chi}$ would be equal to the trace of $\mathcal{L}^{(n)}_{\beta,\varepsilon,\chi}$ even with different eigenvalues. If this occurred we could see numerically that the sum

over part of the eigenvalues $\mathcal{M}^{(n)}_{\beta,\varepsilon,\chi}$ is zero, but we never saw such behavior of the spectrum.

We denote by

$$\operatorname{tr} \mathcal{M}^{(n)}_{\beta,\varepsilon,\chi} = \sum_{i=1}^{\mu_n} \sum_{k=0}^{N-1} \left[\left(\mathcal{M}^{(n)}_{\beta,\varepsilon,\chi} \right)_{k,k} \right]_{i,i}$$

the trace of the matrix $\mathcal{M}^{(n)}_{\beta,\varepsilon,\chi}$ when determined by the sum of its diagonal elements, with N the number of Taylor coefficients in the approximation matrix $\mathcal{M}^{(n)}_{\beta,\varepsilon,\chi}$. And by

$$\operatorname{tr}_\sigma \mathcal{M}^{(n)}_{\beta,\varepsilon,\chi} = \sum_{i=1}^{\mu_n N} \lambda_i$$

we denote the trace of $\mathcal{M}^{(n)}_{\beta,\varepsilon,\chi}$ when determined by the sum of its eigenvalues $\lambda_i = \lambda_i(\beta) \in \sigma\left(\mathcal{M}^{(n)}_{\beta,\varepsilon,\chi}\right)$. The trace of $\mathcal{L}^{(n)}_{\beta,\varepsilon,\chi}$ is given by

$$\operatorname{tr} \mathcal{L}^{(n)}_{\beta,\varepsilon,\chi} = \operatorname{tr} \mathcal{N}^{(n)}_{\beta,\varepsilon,\chi,\tilde{N}} + \operatorname{tr} \mathcal{A}^{(n)}_{\beta,\varepsilon,\chi,\tilde{N}}$$

where $\operatorname{tr} \mathcal{N}^{(n)}_{\beta,\varepsilon,\chi,\tilde{N}}$ and $\operatorname{tr} \mathcal{A}^{(n)}_{\beta,\varepsilon,\chi,\tilde{N}}$ are given in proposition 7.4.7, with $\tilde{N}$ the number of terms in the analytic continuation of the transfer operator $\mathcal{L}^{(n)}_{\beta,\varepsilon,\chi} = \mathcal{N}^{(n)}_{\beta,\varepsilon,\chi,\tilde{N}} + \mathcal{A}^{(n)}_{\beta,\varepsilon,\chi,\tilde{N}}$ in lemma 7.4.6.

We computed these traces for several hundred random values of $\beta \in \mathbb{C}$ for $-2.0 \leq \Re\beta \leq 10.0$ and $0 \leq \Im\beta \leq 10.0$, for $(\Gamma_0(n), \chi \equiv 1)$ with $1 \leq n \leq 10$. We restricted β to these values since it is the region of the β-plane where we performed most of our computations. On the other hand, we also computed these traces for several other non-random values of β in a much larger region. For $\Gamma_0(4)$ and $\Gamma_0(8)$ we did these computations also for the non-trivial characters $\chi^{(4)}_{\alpha_1,\alpha_2}$ respectively $\chi^{(8)}_{\alpha_1,\alpha_2,\alpha_3}$. In most cases we used $N = 50$ Taylor coefficients in the approximation matrix $\mathcal{M}^{(n)}_{\beta,\varepsilon,\chi}$ and a fixed precision of 160 bits, which is about 50 decimal places. Our choice of the number of terms $\tilde{N}$ in the trace formula for the analytic continuation of the transfer operator depends on $\Re\beta$ with $\Re\beta > -\frac{\tilde{N}}{2}$ and $\tilde{N} \geq 10$. We present some of the results in Table 8.1; in all cases considered, the absolute value of the difference between the traces of $\mathcal{M}^{(n)}_{\beta,\varepsilon,\chi}$ and $\mathcal{L}^{(n)}_{\beta,\varepsilon,\chi}$ is very small, which indicates that our computations are indeed correct: The size of the matrix $\mathcal{M}^{(n)}_{\beta,\varepsilon,\chi}$ and the time needed to compute this matrix and its eigenvalues are specified in the right column of Table 8.1. Note that for $\Gamma_0(4)$ and $\Gamma_0(8)$ the difference between the traces of $\mathcal{L}^{(n)}_{\beta,\varepsilon,\chi}$ and $\mathcal{M}^{(n)}_{\beta,\varepsilon,\chi}$ is about 10^{-20}. In these cases we computed 300, respectively 600 eigenvalues. If we take into account that computation of the eigenvalues involves many complicated transformations of the matrix $\mathcal{M}^{(n)}_{\beta,\varepsilon,\chi}$, it is quite remarkable that summing up that many eigenvalues gives such a high-precision result. This indicates that the eigenvalues are computed with a rather high precision.

Figure 8.1 shows how the absolute value of these traces depends on the number N of Taylor coefficients for $\mathcal{M}^{(n)}_{\beta,\varepsilon,\chi}$ respectively the number $\tilde{N}$ in $\mathcal{N}^{(n)}_{\beta,\varepsilon,\chi,\tilde{N}}$ and $\mathcal{A}^{(n)}_{\beta,\varepsilon,\chi,\tilde{N}}$. As expected theoretically the traces of $\mathcal{N}^{(n)}_{\beta,\varepsilon,\chi,\tilde{N}}$ and $\mathcal{A}^{(n)}_{\beta,\varepsilon,\chi,\tilde{N}}$ are growing exponentially with $\tilde{N}$ but with opposite signs, see section 7.4.3. On the other hand, the trace of $\mathcal{L}^{(n)}_{\beta,\varepsilon,\chi}$ remains practically constant when $\tilde{N}$ changes. We see also that $\operatorname{tr}_\sigma \mathcal{M}^{(n)}_{\beta,\varepsilon,\chi}$ approaches $\operatorname{tr} \mathcal{L}^{(n)}_{\beta,\varepsilon,\chi}$ exponentially.

Next we want to discuss how our approximation matrix $\mathcal{M}^{(n)}_{\beta,\varepsilon,\chi}$ depends on $\beta \in \mathbb{C}$ and χ for different numbers N of Taylor coefficients and for different precision p. For this we have compared the spectral trace of $\mathcal{M}^{(n)}_{\beta,\varepsilon,\chi}$ with the trace of $\mathcal{L}^{(n)}_{\beta,\varepsilon,\chi}$ given by the trace formula in proposition 7.4.7. Some of the results are shown in Table 8.2. As can be seen the approximation gets better for larger $\Re\beta$ and small $\Im\beta$. It turns out that for $0 < \Re\beta$ and $0 \leq \Im\beta < 20$ the choice $N = 50$ and $p = 160$ bits (about 50 decimal places) gives the best compromise between precision of the results and computation time. For $\Gamma_0(4)$ and $\Gamma_0(8)$ we get satisfactory results even for $\Im\beta < 30$ for this choice of N and p. On the other hand, for $\mathrm{SL}(2,\mathbb{Z})$ one has to increase N to 80 already for $\Im\beta > 15$. For $\Re\beta < 0$ it seems that some of the eigenvalues of $\mathcal{M}^{(n)}_{\beta,\varepsilon,\chi}$ are

Table 8.1: The traces of $\mathcal{L}^{(n)}_{\beta,+1,\chi}$, $\mathcal{N}^{(n)}_{\beta,+1,\chi,\tilde{N}}$, $\mathcal{A}^{(n)}_{\beta,+1,\chi,\tilde{N}}$ and $\mathcal{M}^{(n)}_{\beta,+1,\chi}$

		trace	size/time
$\Gamma_0(1)$	$\operatorname{tr} \mathcal{M}^{(1)}_{\beta,+1}$	-4.227028353626E-2+4.455218795216E-1I	50×50
$N = 50$	$\operatorname{tr}_\sigma \mathcal{M}^{(1)}_{\beta,+1}$	-4.227028353626E-2+4.455218795216E-1I	1.411s
$\Re\beta = 0.26$	$\operatorname{tr} \mathcal{L}^{(1)}_{\beta,+1}$	-4.227028353614E-2+4.455218795215E-1I	
$\Im\beta = 5.4$	$\lvert\operatorname{tr}_\sigma \mathcal{M}^{(1)}_{\beta,+1} - \operatorname{tr} \mathcal{L}^{(1)}_{\beta,+1}\rvert$	1.247000590087E-13	
	$\operatorname{tr} \mathcal{N}^{(1)}_{\beta,+1,\chi\equiv 1,\tilde{N}}$	-4.289363590638E28-9.312957622600E28I	
	$\operatorname{tr} \mathcal{A}^{(1)}_{\beta,+1,\chi\equiv 1,\tilde{N}}$	4.289363590638E28+9.312957622600E28I	
$\Gamma_0(4)$	$\operatorname{tr} \mathcal{M}^{(4)}_{\beta,+1,\alpha}$	2.050716998092E-1-1.258411878665E-1I	300×300
$N = 50$	$\operatorname{tr}_\sigma \mathcal{M}^{(4)}_{\beta,+1,\alpha}$	2.050716998092E-1-1.258411878665E-1I	55.523s
$\Re\beta = 0.48$	$\operatorname{tr} \mathcal{L}^{(4)}_{\beta,+1,\alpha}$	2.050716998092E-1-1.258411878665E-1I	
$\Im\beta = 3.8$	$\lvert\operatorname{tr}_\sigma \mathcal{M}^{(4)}_{\beta,+1,\alpha} - \operatorname{tr} \mathcal{L}^{(4)}_{\beta,+1,\alpha}\rvert$	1.990457255498E-23	
$\alpha = 0.21$	$\operatorname{tr} \mathcal{N}^{(4)}_{\beta,+1,\alpha,\tilde{N}}$	-1.301435887632E-2+7.210076263399E-4I	
	$\operatorname{tr} \mathcal{A}^{(4)}_{\beta,+1,\alpha,\tilde{N}}$	2.180860586855E-1-1.265621954928E-1I	
$\Gamma_0(4)$	$\operatorname{tr} \mathcal{M}^{(4)}_{\beta,+1,\alpha}$	-1.06641469043352	300×300
$N = 50$	$\operatorname{tr}_\sigma \mathcal{M}^{(4)}_{\beta,+1,\alpha}$	-1.06641469043352+2.815261247199E-48I	59.972s
$\Re\beta = 0.33$	$\operatorname{tr} \mathcal{L}^{(4)}_{\beta,+1,\alpha}$	-1.06641469043352	
$\Im\beta = 0$	$\lvert\operatorname{tr}_\sigma \mathcal{M}^{(4)}_{\beta,+1,\alpha} - \operatorname{tr} \mathcal{L}^{(4)}_{\beta,+1,\alpha}\rvert$	7.03612680791353E-26	
$\alpha = 0.12$	$\operatorname{tr} \mathcal{N}^{(4)}_{\beta,+1,\alpha,\tilde{N}}$	-2.88967534836905E-2	
	$\operatorname{tr} \mathcal{A}^{(4)}_{\beta,+1,\alpha,\tilde{N}}$	-1.03751793694983	
$\Gamma_0(8)$	$\operatorname{tr} \mathcal{M}^{(8)}_{\beta,+1}$	-7.195525313235E-7-2.299836221857E-7I	600×600
$N = 50$	$\operatorname{tr}_\sigma \mathcal{M}^{(8)}_{\beta,+1}$	-7.195525313235E-7-2.299836221857E-7I	5m49.569s
$\Re\beta = 8.3$	$\operatorname{tr} \mathcal{L}^{(8)}_{\beta,+1}$	-7.195525313235E-7-2.299836221857E-7I	
$\Im\beta = 12.3$	$\lvert\operatorname{tr}_\sigma \mathcal{M}^{(8)}_{\beta,+1} - \operatorname{tr} \mathcal{L}^{(8)}_{\beta,+1}\rvert$	1.229683523547E-21	
	$\operatorname{tr} \mathcal{N}^{(8)}_{\beta,+1,\alpha=0,\tilde{N}}$	7.930376514800E-2-3.226857346122E-2I	
	$\operatorname{tr} \mathcal{A}^{(8)}_{\beta,+1,\alpha=0,\tilde{N}}$	-7.930448470053E-2+3.226834347760E-2I	
$\Gamma_0(9)$	$\operatorname{tr} \mathcal{M}^{(9)}_{\beta,+1}$	-2.194153145324+1.430181958910I	600×600
$N = 50$	$\operatorname{tr}_\sigma \mathcal{M}^{(9)}_{\beta,+1}$	-2.194153145324+1.430181958910I	5m57.805s
$\Re\beta = 0.15$	$\operatorname{tr} \mathcal{L}^{(9)}_{\beta,+1}$	-2.194153145324+1.430181958910I	
$\Im\beta = 2.23$	$\lvert\operatorname{tr}_\sigma \mathcal{M}^{(9)}_{\beta,+1} - \operatorname{tr} \mathcal{L}^{(9)}_{\beta,+1}\rvert$	1.05648873794731E-23	
	$\operatorname{tr} \mathcal{N}^{(9)}_{\beta,+1,\chi\equiv 1,\tilde{N}}$	-6.604538703511E-2-2.826804747E-4I	
	$\operatorname{tr} \mathcal{A}^{(9)}_{\beta,+1,\chi\equiv 1,\tilde{N}}$	-2.128107758289+1.430464639385I	

Results from widmo version *6.4.6*. Precision 160 bits (49 digits). CPU: Intel Core i7, 2.66 GHz

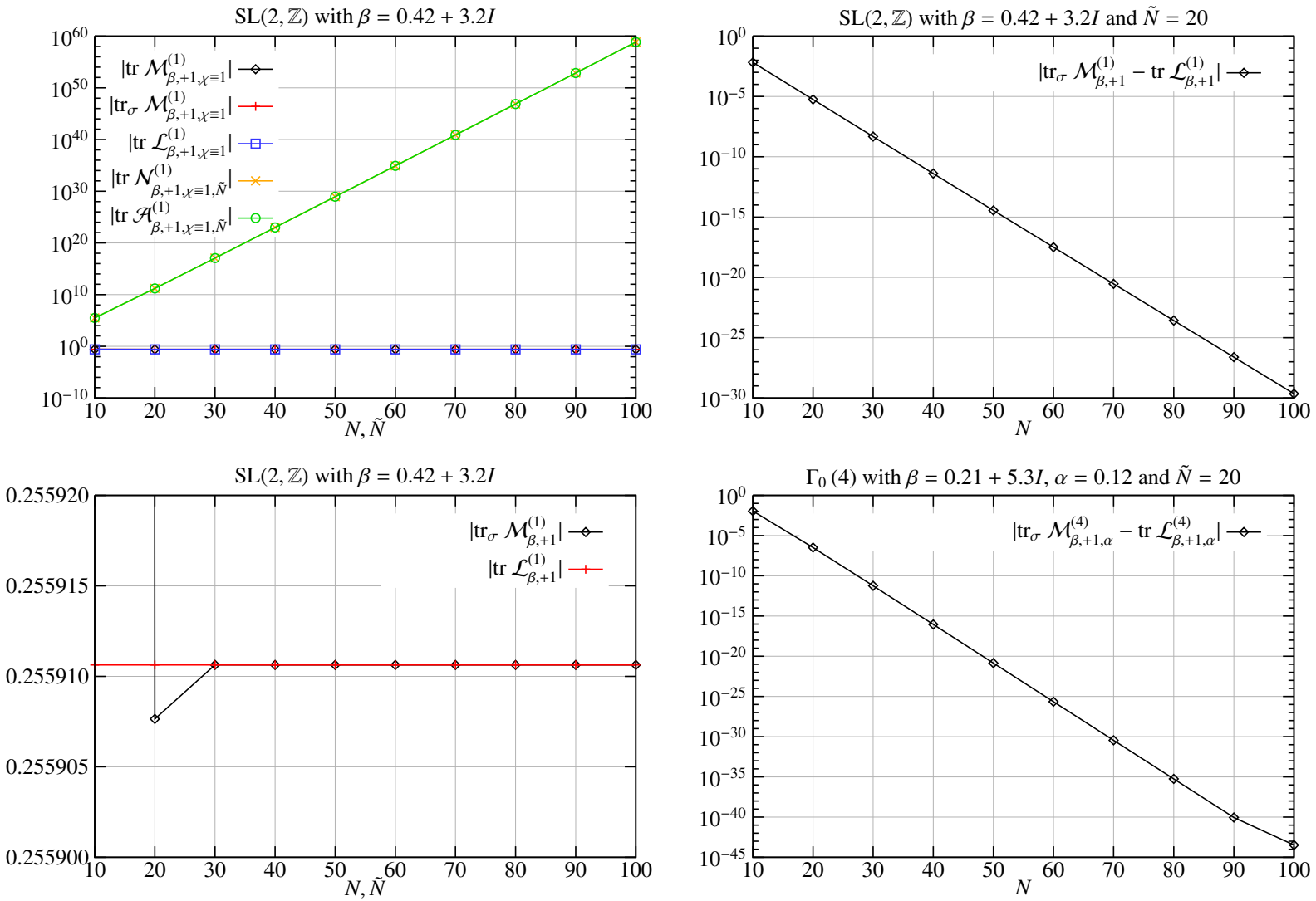

Figure 8.1: Dependence of $|\mathrm{tr}\,\mathcal{L}^{(n)}_{\beta,+1,\chi}|$, $|\mathrm{tr}\,\mathcal{N}^{(n)}_{\beta,+1,\chi,\tilde{N}}|$ and $|\mathrm{tr}\,\mathcal{A}^{(n)}_{\beta,+1,\chi,\tilde{N}}|$ on $\tilde{N}$, and $|\mathrm{tr}_\sigma\,\mathcal{M}^{(n)}_{\beta,+1,\chi}|$ on N

growing exponentially with $\Re\beta$ getting negative; we will investigate this issue in more detail in section 8.1.4. We can also see that for $\Gamma_0(4)$ and $\Gamma_0(8)$ the quality of approximation does not depend on the deformation parameters α_i.

Table 8.1 and Table 8.2 show that the computation time for the matrix $\mathcal{M}^{(n)}_{\beta,\varepsilon,\chi}$ and its eigenvalues scales with the size of the matrix, for $\Gamma_0(4)$ it is about 60 seconds and for $\Gamma_0(8)$ already 6 times longer. This is one of the reasons we obtained most of our results for $(\Gamma_0(4),\chi^{(4)}_\alpha)$, which was still very time consuming since this matrix and its eigenvalues have to be computed usually several ten thousand times to obtain one data set for $0 \le \alpha \le 0.5$.

The first new result was that for $(\Gamma_0(n),\chi \equiv 1)$ respectively $(\Gamma_0(4),\chi^{(4)}_\alpha)$ the traces of $\mathcal{L}^{(n)}_{\beta,+1,\chi}$ and $\mathcal{L}^{(n)}_{\beta,-1,\chi}$ are identical. We compared the traces of these operators for many different values of $\beta \in \mathbb{C}$ and for different groups $\Gamma_0(n)$. We present some of the results in Table 8.3. The size of the matrix $\mathcal{M}^{(n)}_{\beta,\varepsilon,\chi}$ and the time needed to compute this matrix and its eigenvalues are specified in the right column. As one can see, the traces of $\mathcal{L}^{(n)}_{\beta,+1,\chi}$ and $\mathcal{L}^{(n)}_{\beta,-1,\chi}$ for $\Gamma_0(4)$ coincide also for the non-trivial character $\chi^{(4)}_\alpha$; note, that this is no longer true for $\Gamma_0(8)$ with a non-trivial character.

Conclusion 8.1.1. *For $(\Gamma_0(n),\chi \equiv 1)$ and $(\Gamma_0(4),\chi^{(4)}_\alpha)$ with $\beta \in \mathbb{C}$ the traces of $\mathcal{L}^{(n)}_{\beta,+1,\chi}$ and $\mathcal{L}^{(n)}_{\beta,-1,\chi}$ are equal.*

Indeed, as we will see in the next section, in all cases where these traces are equal, also the spectra of $\mathcal{L}^{(n)}_{\beta,+1,\chi}$ and $\mathcal{L}^{(n)}_{\beta,-1,\chi}$ coincide. This was the first indication that the operators $\mathcal{L}^{(n)}_{\beta,+1,\chi}$ and $\mathcal{L}^{(n)}_{\beta,-1,\chi}$ must be closely related.

8.1.2 The equality of the spectra of $\mathcal{L}^{(n)}_{\beta,+1,\chi}$ and $\mathcal{L}^{(n)}_{\beta,-1,\chi}$

From our numerical results we concluded in the last section that the traces of $\mathcal{L}^{(n)}_{\beta,+1,\chi}$ and $\mathcal{L}^{(n)}_{\beta,-1,\chi}$ are equal for $\Gamma_0(n)$ with a trivial character $\chi \equiv 1$ and $\Gamma_0(4)$ with the character $\chi^{(4)}_\alpha$. It was important to see if even the spectra of $\mathcal{L}^{(n)}_{\beta,+1,\chi}$ and $\mathcal{L}^{(n)}_{\beta,-1,\chi}$ are equal, since this indicates that these operators could be conjugate. Obviously, $\mathcal{L}^{(n)}_{\beta,+1,\chi}$ and $\mathcal{L}^{(n)}_{\beta,-1,\chi}$ are in general different operators, which means that a relation between their spectra cannot be trivial.

We computed the spectrum of the approximation matrices $\mathcal{M}^{(n)}_{\beta,+1,\chi}$ and $\mathcal{M}^{(n)}_{\beta,-1,\chi}$ for different groups $(\Gamma_0(n),\chi \equiv 1)$ with $1 \le n \le 25$, and random values of $\beta \in \mathbb{C}$ with $0 \le \Re\beta \le 1$ and $0 \le \Im\beta \le 10$. We also did computations for $(\Gamma_0(4),\chi^{(4)}_{\alpha_1,\alpha_2})$ and $(\Gamma_0(8),\chi^{(8)}_{\alpha_1,\alpha_2,\alpha_3})$ with $0 \le \alpha_1,\alpha_2,\alpha_3, \le 0.5$. To compare the eigenvalues $\{\lambda_i(\beta,+1)\}_{1\le i\le \mu_n N}$ of the matrix $\mathcal{M}^{(n)}_{\beta,+1,\chi}$ with the eigenvalues $\{\lambda_i(\beta,-1)\}_{1\le i\le \mu_n N}$ of the matrix $\mathcal{M}^{(n)}_{\beta,-1,\chi}$, we order the eigenvalues in both sets such that $\Re\lambda_i \le \Re\lambda_{i+1}$ and if $\Re\lambda_i = \Re\lambda_{i+1}$ then $\Im\lambda_i \le \Im\lambda_{i+1}$. This way we ensure that eigenvalues which should be equal have the same index i in both sets. We define

$$d_\beta = \max_{1\le i\le \mu_n N} \left| \frac{\lambda_i(\beta,+1) - \lambda_i(\beta,-1)}{\lambda_i(\beta,+1)} \right|. \tag{8.1}$$

Obviously, d_β is the greatest relative difference between the eigenvalues of $\mathcal{M}^{(n)}_{\beta,+1,\chi}$ and $\mathcal{M}^{(n)}_{\beta,-1,\chi}$. If the spectra of $\mathcal{L}^{(n)}_{\beta,+1,\chi}$ and $\mathcal{L}^{(n)}_{\beta,-1,\chi}$ coincide we expect that d_β is a very small number. In Table 8.4 we present some of the results, where the size of the matrix $\mathcal{M}^{(n)}_{\beta,+1,\chi}$, its computation time and the computation time of its eigenvalues are given. Furthermore, this table also includes the eigenvalues $\lambda_{\min}$ and $\lambda_{\max}$ of $\mathcal{M}^{(n)}_{\beta,+1,\chi}$ of smallest respectively largest absolute value. We also computed the absolute difference $|\operatorname{tr}\mathcal{L}^{(n)}_{\beta,+1,\chi} - \operatorname{tr}\mathcal{L}^{(n)}_{\beta,-1,\chi}|$ of the traces of $\mathcal{L}^{(n)}_{\beta,+1,\chi}$ and $\mathcal{L}^{(n)}_{\beta,-1,\chi}$, which can only be zero if the spectra of $\mathcal{L}^{(n)}_{\beta,+1,\chi}$ and $\mathcal{L}^{(n)}_{\beta,-1,\chi}$ coincide, i.e. if d_β is a small number. The trace of the transfer operator $\mathcal{L}^{(n)}_{\beta,\varepsilon,\chi}$ was computed by the trace formula given in proposition 7.4.7. As in the forgoing section, we also checked if the trace of the approximation matrix $\mathcal{M}^{(n)}_{\beta,+1,\chi}$ coincides with the trace of the transfer operator $\mathcal{L}^{(n)}_{\beta,+1,\chi}$ by computing the absolute difference of both traces $|\operatorname{tr}\mathcal{L}^{(n)}_{\beta,+1,\chi} - \operatorname{tr}_\sigma \mathcal{M}^{(n)}_{\beta,+1,\chi}|$, which should also be a small number if the approximation is correct. The

Table 8.2: Dependence of the approximation matrix $\mathcal{M}^{(n)}_{\beta,+1,\chi}$ of $\mathcal{L}^{(n)}_{\beta,+1,\chi}$ on $\beta \in \mathbb{C}$

$\Gamma_0(n)$	N	p	β	α_1	α_2	α_3	$\lvert\mathrm{tr}\,\mathcal{L}^{(n)}_{\beta,+1,\chi} - \mathrm{tr}_\sigma\,\mathcal{M}^{(n)}_{\beta,+1,\chi}\rvert$	size	time
$\Gamma_0(1)$	50	160	10				5.3913E-20	50×50	1.263s
$\Gamma_0(1)$	50	160	10+10I				8.1886E-15	50×50	3.233s
$\Gamma_0(1)$	50	160	0.5+10I				9.8636E-11	50×50	3.158s
$\Gamma_0(1)$	80	160	0.25+30I				2.1024E-7	80×80	17.556s
$\Gamma_0(1)$	50	160	-10+10I				2.9808E-5	50×50	3.258s
$\Gamma_0(1)$	50	160	-15.2				1.1556E-7	50×50	1.727s
$\Gamma_0(4)$	50	160	10				5.0166E-31	300×300	56.978s
$\Gamma_0(4)$	50	160	10+10I				3.6616E-24	300×300	1m55s
$\Gamma_0(4)$	50	160	0.5+10I				6.4408E-18	300×300	1m59s
$\Gamma_0(4)$	50	160	0.5+10I	0.3	0.12		4.1055E-18	300×300	2m54s
$\Gamma_0(4)$	20	32	0.25+10I				2.627E-3	120×120	5.894s
$\Gamma_0(4)$	20	64	0.25+10I				4.9124E-4	120×120	6.368s
$\Gamma_0(4)$	20	160	0.25+10I				4.9124E-4	120×120	8.486s
$\Gamma_0(4)$	30	32	0.25+10I				2.780E-3	180×180	20.803s
$\Gamma_0(4)$	30	64	0.25+10I				2.0585E-8	180×180	20.396s
$\Gamma_0(4)$	30	160	0.25+10I				2.0586E-8	180×180	25.365s
$\Gamma_0(4)$	50	32	0.25+10I				2.792E-3	300×300	1m21s
$\Gamma_0(4)$	50	64	0.25+10I				4.2604E-13	300×300	1m28s
$\Gamma_0(4)$	50	128	0.25+10I				9.6409E-18	300×300	1m44s
$\Gamma_0(4)$	50	160	0.25+10I				9.6409E-18	300×300	1m45s
$\Gamma_0(4)$	80	64	0.25+10I				4.2590E-13	480×480	5m45s
$\Gamma_0(4)$	80	128	0.25+10I				5.9366E-32	480×480	6m38s
$\Gamma_0(4)$	80	160	0.25+10I				4.9396E-32	480×480	6m46s
$\Gamma_0(4)$	80	192	0.25+10I				4.9396E-32	480×480	7m21s
$\Gamma_0(4)$	50	160	0.25+30I				6.8676E-5	300×300	2m1s
$\Gamma_0(4)$	80	160	0.25+30I				2.4139E-17	480×480	8m39s
$\Gamma_0(4)$	80	160	0.25+30I	0.15	0.21		7.5823E-19	480×480	2h52m
$\Gamma_0(4)$	35	128	-3.1+4.2I				7.6075E-13	210×210	39.601s
$\Gamma_0(4)$	35	160	-3.1+4.2I				5.7711E-13	210×210	42.643s
$\Gamma_0(4)$	50	128	-3.1+4.2I				1.8427E-13	300×300	1m45s
$\Gamma_0(4)$	50	160	-3.1+4.2I				7.6988E-20	300×300	1m51s
$\Gamma_0(4)$	65	128	-3.1+4.2I				1.8427E-13	390×390	3m39s
$\Gamma_0(4)$	65	160	-3.1+4.2I				5.9730E-20	390×390	3m51s
$\Gamma_0(8)$	50	160	10				5.0166E-31	600×600	6m58s
$\Gamma_0(8)$	50	160	10+10I				3.6616E-24	600×600	15m10s
$\Gamma_0(8)$	50	160	0.5+10I				6.4408E-18	600×600	15m25s
$\Gamma_0(8)$	50	160	0.25+30I				6.8676E-5	600×600	15m39s
$\Gamma_0(8)$	80	160	0.25+30I				2.4139E-17	960×960	1h07m
$\Gamma_0(8)$	80	160	0.25+30I	0.15	0.21	0.32	2.2712E-17	960×960	1h29m
$\Gamma_0(8)$	50	160	-3.1+4.2I				6.9388E-20	600×600	12m58s

Results from widmo version *6.4.8*. Precision 160 bits (49 digits). CPU: AMD Opteron 2350, 2.00 GHz

trace $\mathrm{tr}_\sigma\, \mathcal{M}^{(n)}_{\beta,+1,\chi}$ is given by the sum of the eigenvalues of $\mathcal{M}^{(n)}_{\beta,+1,\chi}$. As expected from the results in the last section, the only cases for which the spectra coincide are $(\Gamma_0(n), \chi \equiv 1)$ and $(\Gamma_0(4), \chi^{(4)}_{\alpha_1,0})$:

Conclusion 8.1.2. *For* $(\Gamma_0(n), \chi \equiv 1)$ *and* $(\Gamma_0(4), \chi^{(4)}_\alpha)$ *with* $\beta \in \mathbb{C}$ *the spectra of* $\mathcal{L}^{(n)}_{\beta,+1,\chi}$ *and* $\mathcal{L}^{(n)}_{\beta,-1,\chi}$ *are equal.*

In all cases for which the spectra of $\mathcal{M}^{(n)}_{\beta,+1,\chi}$ and $\mathcal{M}^{(n)}_{\beta,-1,\chi}$ are equal, the largest relative difference d_β is quite small, which means that even the smallest eigenvalues coincide with at least about 12 decimal places, where the smallest absolute value of the eigenvalues is around 10^{-40}. This shows that the spectra of $\mathcal{M}^{(n)}_{\beta,+1,\chi}$ and $\mathcal{M}^{(n)}_{\beta,-1,\chi}$ are computed with a rather high precision. We conclude that the matrices $\mathcal{M}^{(n)}_{\beta,+1,\chi}$ and $\mathcal{M}^{(n)}_{\beta,-1,\chi}$ are similar, i.e. $\mathcal{M}^{(n)}_{\beta,+1,\chi} = X^{-1}\mathcal{M}^{(n)}_{\beta,-1,\chi}X$ with a non-singular matrix $X \in \mathbb{C}^{\mu_n N \times \mu_n N}$, see also Chapter 5. In the next section we show a similar relation between the operators $\mathcal{L}^{(n)}_{\beta,+1,\chi}$ and $\mathcal{L}^{(n)}_{\beta,-1,\chi}$.

8.1.3 Symmetries of the transfer operator $\mathcal{L}^{(n)}_{\beta,\varepsilon,\chi}$ and the operators $\mathcal{P}_k$

In the foregoing sections we concluded from numerical experiments that for $(\Gamma_0(n), \chi \equiv 1)$ and $(\Gamma_0(4), \chi^{(4)}_\alpha)$ the traces of $\mathcal{L}^{(n)}_{\beta,+1,\chi}$ and $\mathcal{L}^{(n)}_{\beta,-1,\chi}$ respectively the spectra of $\mathcal{L}^{(n)}_{\beta,+1,\chi}$ and $\mathcal{L}^{(n)}_{\beta,-1,\chi}$ are presumably identical. This also indicates that the transfer operators $\mathcal{L}^{(n)}_{\beta,+1,\chi}$ and $\mathcal{L}^{(n)}_{\beta,-1,\chi}$ could be conjugate. In this section we want to show that there indeed exist operators $\mathcal{P}_k$ conjugating these transfer operators. We start with the transfer operator from lemma 7.4.5:

$$\left[\mathcal{L}^{(n)}_{\beta,\varepsilon,\chi}\vec{f}(z)\right]_i = \sum_{q=0}^{\infty}\sum_{m=1}^{n}\sum_{j=1}^{\mu_n}\left[U^\chi(ST^{m\varepsilon})\right]_{i,j}\chi\left(r^{(n)}_j T^{n\varepsilon}\left(r^{(n)}_j\right)^{-1}\right)^q f_j|_{2\beta}\tilde{S}T^{m+nq}z.$$

Since U^χ has the structure of a permutation matrix, in the sum $\sum_{j=1}^{\mu_n}$ there is only one non-vanishing term for the index j such that $r^{(n)}_i ST^{m\varepsilon}\left(r^{(n)}_j\right)^{-1} \in \Gamma_0(n)$. Obviously, this specific j depends on i and $ST^{m\varepsilon}$. We define the permutation map $u_{m,\varepsilon} : \{1,\dots,\mu_n\} \to \{1,\dots,\mu_n\}$, such that $r^{(n)}_i ST^{m\varepsilon}\left(r^{(n)}_{u_{m,\varepsilon}(i)}\right)^{-1} \in \Gamma_0(n)$ for every $1 \le i \le \mu_n$. Then the representation U^χ in (7.22) is given by

$$\left[U^\chi(ST^{m\varepsilon})\right]_{i,j} = \delta_{u_{m,\varepsilon}(i),j}\,\chi\left(r^{(n)}_i ST^{m\varepsilon}\left(r^{(n)}_j\right)^{-1}\right)$$

with $\delta_{u_{m,\varepsilon}(i),j} = 0$ if $u_{m,\varepsilon}(i) \neq j$ and $\delta_{u_{m,\varepsilon}(i),j} = 1$ if $u_{m,\varepsilon}(i) = j$. The transfer operator in lemma 7.4.5 can hence be written

$$\left[\mathcal{L}^{(n)}_{\beta,\varepsilon,\chi}\vec{f}(z)\right]_i = \sum_{m=1}^{n}\chi\left(r^{(n)}_i ST^{m\varepsilon}\left(r^{(n)}_{u_{m,\varepsilon}(i)}\right)^{-1}\right)\sum_{q=0}^{\infty}\chi\left(r^{(n)}_{u_{m,\varepsilon}(i)}T^{n\varepsilon}\left(r^{(n)}_{u_{m,\varepsilon}(i)}\right)^{-1}\right)^q f_{u_{m,\varepsilon}(i)}|_{2\beta}\tilde{S}T^{m+nq}z.$$

We have to show that there exist operators $\mathcal{P}_k$ with

$$\mathcal{P}_k\mathcal{L}^{(n)}_{\beta,+1,\chi}\vec{f}(z) = \mathcal{L}^{(n)}_{\beta,-1,\chi}\mathcal{P}_k\vec{f}(z), \tag{8.2}$$

which intertwine the transfer operators $\mathcal{L}^{(n)}_{\beta,+1,\chi}$ and $\mathcal{L}^{(n)}_{\beta,-1,\chi}$. Let $\tilde{\mathcal{P}}_k = \begin{pmatrix} 0 & \mathcal{P}_k \\ \mathcal{P}_k & 0 \end{pmatrix}$, then this operator commutes with $\tilde{\mathcal{L}}^{(n)}_{\beta,\chi}$, and hence defines a symmetry of the transfer operator. Indeed

$$\begin{aligned}\tilde{\mathcal{P}}_k\tilde{\mathcal{L}}^{(n)}_{\beta,\chi} &= \begin{pmatrix} 0 & \mathcal{P}_k \\ \mathcal{P}_k & 0 \end{pmatrix}\begin{pmatrix} 0 & \mathcal{L}^{(n)}_{\beta,+1,\chi} \\ \mathcal{L}^{(n)}_{\beta,-1,\chi} & 0 \end{pmatrix} = \begin{pmatrix} \mathcal{P}_k\mathcal{L}^{(n)}_{\beta,-1,\chi} & 0 \\ 0 & \mathcal{P}_k\mathcal{L}^{(n)}_{\beta,+1,\chi} \end{pmatrix} \\ &= \begin{pmatrix} \mathcal{L}^{(n)}_{\beta,+1,\chi}\mathcal{P}_k & 0 \\ 0 & \mathcal{L}^{(n)}_{\beta,-1,\chi}\mathcal{P}_k \end{pmatrix} = \begin{pmatrix} 0 & \mathcal{L}^{(n)}_{\beta,+1,\chi} \\ \mathcal{L}^{(n)}_{\beta,-1,\chi} & 0 \end{pmatrix}\begin{pmatrix} 0 & \mathcal{P}_k \\ \mathcal{P}_k & 0 \end{pmatrix} = \tilde{\mathcal{L}}^{(n)}_{\beta,\chi}\tilde{\mathcal{P}}_k.\end{aligned}$$

Table 8.3: Comparison of the traces of $\mathcal{L}^{(n)}_{\beta,+1,\mathcal{X}}$ and $\mathcal{L}^{(n)}_{\beta,-1,\mathcal{X}}$

		trace	size/time
$\Gamma_0\,(3)$	$\mathrm{tr}_\sigma\,\mathcal{M}^{(3)}_{\beta,+1}$	2.303999131384-9.635738819609I	200×200
$N=50$	$\mathrm{tr}\,\mathcal{L}^{(3)}_{\beta,+1}$	2.303999131375-9.635738819624I	17.942s
$\Re\beta=-0.4$	$\lvert\mathrm{tr}_\sigma\,\mathcal{M}^{(3)}_{\beta,+1}-\mathrm{tr}\,\mathcal{L}^{(3)}_{\beta,+1}\rvert$	1.725103776940E-11	
$\Im\beta=8.2$	$\mathrm{tr}\,\mathcal{L}^{(3)}_{\beta,-1}$	2.303999131375-9.635738819624I	
	$\lvert\mathrm{tr}\,\mathcal{L}^{(3)}_{\beta,+1}-\mathrm{tr}\,\mathcal{L}^{(3)}_{\beta,-1}\rvert$	0	
$\Gamma_0\,(4)$	$\mathrm{tr}_\sigma\,\mathcal{M}^{(4)}_{\beta,+1}$	7.490877543575E-1+1.1887684613221	300×300
$N=50$	$\mathrm{tr}\,\mathcal{L}^{(4)}_{\beta,+1}$	7.490877543575E-1+1.1887684613221	53.276s
$\Re\beta=0.28$	$\lvert\mathrm{tr}_\sigma\,\mathcal{M}^{(4)}_{\beta,+1}-\mathrm{tr}\,\mathcal{L}^{(4)}_{\beta,+1}\rvert$	2.757558790286E-23	
$\Im\beta=3.1$	$\mathrm{tr}\,\mathcal{L}^{(4)}_{\beta,-1}$	7.490877543575E-1+1.1887684613221	
	$\lvert\mathrm{tr}\,\mathcal{L}^{(4)}_{\beta,+1}-\mathrm{tr}\,\mathcal{L}^{(4)}_{\beta,-1}\rvert$	0	
$\Gamma_0\,(4)$	$\mathrm{tr}_\sigma\,\mathcal{M}^{(4)}_{\beta,+1,\alpha}$	6.005144889805E-1-9.398788536393E-2I	300×300
$N=50$	$\mathrm{tr}\,\mathcal{L}^{(4)}_{\beta,+1,\alpha}$	6.005144889805E-1-9.398788536393E-2I	1m03.915s
$\Re\beta=0.48$	$\lvert\mathrm{tr}_\sigma\,\mathcal{M}^{(4)}_{\beta,+1,\alpha}-\mathrm{tr}\,\mathcal{L}^{(4)}_{\beta,+1,\alpha}\rvert$	2.945934829898E-21	
$\Im\beta=5.8$	$\mathrm{tr}\,\mathcal{L}^{(4)}_{\beta,-1,\alpha}$	6.005144889805E-1-9.398788536393E-2I	
$\alpha=0.42$	$\lvert\mathrm{tr}\,\mathcal{L}^{(4)}_{\beta,+1,\alpha}-\mathrm{tr}\,\mathcal{L}^{(4)}_{\beta,-1,\alpha}\rvert$	0	
$\Gamma_0\,(8)$	$\mathrm{tr}_\sigma\,\mathcal{M}^{(8)}_{\beta,+1}$	-2.82059589099E-1+3.57051311710E-1I	600×600
$N=50$	$\mathrm{tr}\,\mathcal{L}^{(8)}_{\beta,+1}$	-2.82059589099E-1+3.57051311710E-1I	6m15.288s
$\Re\beta=0.75$	$\lvert\mathrm{tr}_\sigma\,\mathcal{M}^{(8)}_{\beta,+1}-\mathrm{tr}\,\mathcal{L}^{(8)}_{\beta,+1}\rvert$	4.048880641894E-24	
$\Im\beta=2.4$	$\mathrm{tr}\,\mathcal{L}^{(8)}_{\beta,-1}$	-2.82059589099E-1+3.57051311710E-1I	
	$\lvert\mathrm{tr}\,\mathcal{L}^{(8)}_{\beta,+1}-\mathrm{tr}\,\mathcal{L}^{(8)}_{\beta,-1}\rvert$	0	
$\Gamma_0\,(8)$	$\mathrm{tr}_\sigma\,\mathcal{M}^{(8)}_{\beta,+1,\alpha}$	1.43133706999E-1+2.22391408029E-1I	600×600
$N=50$	$\mathrm{tr}\,\mathcal{L}^{(8)}_{\beta,+1,\alpha}$	1.43133706999E-1+2.22391408029E-1I	6m54.583s
$\Re\beta=0.75$	$\lvert\mathrm{tr}_\sigma\,\mathcal{M}^{(8)}_{\beta,+1,\alpha}-\mathrm{tr}\,\mathcal{L}^{(8)}_{\beta,+1,\alpha}\rvert$	2.6775728097643E-24	
$\Im\beta=2.4$	$\mathrm{tr}\,\mathcal{L}^{(8)}_{\beta,-1,\alpha}$	-3.89841855740E-1+8.99095082357E-2I	
$\alpha=0.27$	$\lvert\mathrm{tr}\,\mathcal{L}^{(8)}_{\beta,+1,\alpha}-\mathrm{tr}\,\mathcal{L}^{(8)}_{\beta,-1,\alpha}\rvert$	5.49194322850E-1	
$\Gamma_0\,(15)$	$\mathrm{tr}_\sigma\,\mathcal{M}^{(15)}_{\beta,+1}$	-1.381465471088+2.653545098043E-48I	1200×1200
$N=50$	$\mathrm{tr}\,\mathcal{L}^{(15)}_{\beta,+1}$	-1.38146547108808	22m54.302s
$\Re\beta=0.29$	$\lvert\mathrm{tr}_\sigma\,\mathcal{M}^{(15)}_{\beta,+1}-\mathrm{tr}\,\mathcal{L}^{(15)}_{\beta,+1}\rvert$	5.42304897881949E-26	
$\Im\beta=0$	$\mathrm{tr}\,\mathcal{L}^{(15)}_{\beta,-1}$	-1.38146547108808	
	$\lvert\mathrm{tr}\,\mathcal{L}^{(15)}_{\beta,+1}-\mathrm{tr}\,\mathcal{L}^{(15)}_{\beta,-1}\rvert$	0	

Results from widmo version *6.4.6*. Precision 160 bits (49 digits). CPU: Intel Core i7, 2.66 GHz

Table 8.4: Comparison of the spectra of $\mathcal{M}^{(n)}_{\beta,+1,\chi}$ and $\mathcal{M}^{(n)}_{\beta,-1,\chi}$

$\Gamma_0(n)$	N	β	α_1	α_2	α_3	d_β	$\lambda_{\min}$ $\lambda_{\max}$	$\lvert\mathrm{tr}\,\mathcal{L}^{(n)}_{\beta,+1,\chi} - \mathrm{tr}\,\mathcal{L}^{(n)}_{\beta,-1,\chi}\rvert$ $\lvert\mathrm{tr}\,\mathcal{L}^{(n)}_{\beta,+1,\chi} - \mathrm{tr}_\sigma\,\mathcal{M}^{(n)}_{\beta,+1,\chi}\rvert$	size time
$\Gamma_0(3)$	50	0.14+9.3I				2.6001E-12	2.37E-40-3.28E-39I 2.26+9.37E-1I	0 5.1480E-11	200×200 19.049s
$\Gamma_0(4)$	50	0.55+4.3I				4.8705E-14	-4.90E-41-6.93E-41I -1.00E-1-6.70E-1I	0 1.8655E-22	300×300 56.723s
$\Gamma_0(4)$	50	0.55+4.3I	0.24			5.1170E-14	-5.96E-43+4.59E-41I -8.24E-1-5.09E-1I	0 1.1713E-23	300×300 1m6.200s
$\Gamma_0(4)$	50	0.25+7.8I		0.33		2.7417	1.68E-40+2.543I -1.05+2.48I	2.2469 9.4704E-20	300×300 2m15.860s†
$\Gamma_0(4)$	50	0.42+3.7I	0.12	0.34		1.9902	4.36E-41+5.64E-41I 2.75E-1-1.40I	0.5349 1.7836E-23	300×300 1m10.640s
$\Gamma_0(8)$	50	0.5+3.5I				2.5101E-14	1.80E-41+3.73E-41I 1.00+3.57E-1I	0 4.4288E-23	600×600 7m34.424s
$\Gamma_0(8)$	50	0.5+3.5I		0.47		1.9748	9.71E-42+2.72E-41I 1.52E-1-1.18I	0.03387 4.1679E-24	600×600 6m15.442s
$\Gamma_0(8)$	50	0.32+8.6I	0.24			3.2238	1.41E-40+6.25E-40I -1.77E-1+1.84I	1.3295 7.1090E-19	600×600 13m37.635s†
$\Gamma_0(8)$	50	0.54+3.6I			0.02	2.9219	-5.88E-41-7.60E-42I 9.47E-1+1.85E-1I	0.0362 5.0658E-23	600×600 13m17.320s†
$\Gamma_0(8)$	50	0.43+1.2I	0.34	0.11		3.4864	6.82E-42+3.00E-42I -1.33E-1-1.68I	1.2093 5.7229E-25	600×600 13m49.341s†
$\Gamma_0(8)$	50	0.3+0.5I	0.23		0.26	2.6869	5.35E-43+1.63E-41I -5.33E-1-1.38I	0.8028 1.3010E-25	600×600 13m34.861s†
$\Gamma_0(8)$	50	0.3+5.5I		0.42	0.05	2.9661	3.64E-41+5.56E-41I 1.07-1.28I	0.4521 9.8590E-22	600×600 13m3.281s†
$\Gamma_0(8)$	50	0.12+3.7I	0.12	0.04	0.23	3.6709	7.88E-41-7.91E-42I 3.53+6.80I	6.8789 8.8002E-23	600×600 7m0.8924s
$\Gamma_0(24)$	50	0.43+7.5I				1.3941E-12	5.76E-40-2.24E-40I 7.85E-1+1.09I	0 8.2075E-20	2400×2400 14h28m †

Results from widmo version *6.4.7*. Precision 160 bits (49 digits). CPU: Intel Core i7-620M, 2.66 GHz, † AMD Opteron 2350, 2.00 GHz

For convenience we also call the intertwining operators $\mathcal{P}_k$ symmetries. Assume the operator $\mathcal{P}_k : \bigoplus_{j=1}^{\mu_n} B(D) \to \bigoplus_{j=1}^{\mu_n} B(D)$ is a permutation matrix $\mathcal{P}_k \in \mathbb{C}^{\mu_n \times \mu_n}$ defined by a permutation $p_k : \{1,\dots,\mu_n\} \to \{1,\dots,\mu_n\}$ such that

$$[\mathcal{P}_k]_{i,j} = \delta_{p_k(i),j} \quad \text{and} \quad \left[\mathcal{P}_k \vec{f}(z)\right]_i = f_{p_k(i)}(z). \tag{8.3}$$

Then the operators $\mathcal{P}_k \mathcal{L}^{(n)}_{\beta,\varepsilon,\chi} \vec{f}(z)$ and $\mathcal{L}^{(n)}_{\beta,\varepsilon,\chi} \mathcal{P}_k \vec{f}(z)$ have the form

$$\begin{aligned}\left[\mathcal{P}_k \mathcal{L}^{(n)}_{\beta,\varepsilon,\chi} \vec{f}(z)\right]_i &= \left[\mathcal{L}^{(n)}_{\beta,\varepsilon,\chi} \vec{f}(z)\right]_{p_k(i)} \\ &= \sum_{m=1}^{n} \chi\left(r^{(n)}_{p_k(i)} S T^{m\varepsilon} \left(r^{(n)}_{u_{m,\varepsilon}(p_k(i))}\right)^{-1}\right) \sum_{q=0}^{\infty} \chi\left(r^{(n)}_{u_{m,\varepsilon}(p_k(i))} T^{n\varepsilon} \left(r^{(n)}_{u_{m,\varepsilon}(p_k(i))}\right)^{-1}\right)^q f_{u_{m,\varepsilon}(p_k(i))}|_{2\beta} \tilde{S} T^{m+nq} z\end{aligned}$$

respectively

$$\left[\mathcal{L}^{(n)}_{\beta,\varepsilon,\chi} \mathcal{P}_k \vec{f}(z)\right]_i = \sum_{m=1}^{n} \chi\left(r^{(n)}_i S T^{m\varepsilon} \left(r^{(n)}_{u_{m,\varepsilon}(i)}\right)^{-1}\right) \sum_{q=0}^{\infty} \chi\left(r^{(n)}_{u_{m,\varepsilon}(i)} T^{n\varepsilon} \left(r^{(n)}_{u_{m,\varepsilon}(i)}\right)^{-1}\right)^q f_{p_k(u_{m,\varepsilon}(i))}|_{2\beta} \tilde{S} T^{m+nq} z.$$

For $\mathcal{P}_k \mathcal{L}^{(n)}_{\beta,+1,\chi} \vec{f}(z)$ and $\mathcal{L}^{(n)}_{\beta,-1,\chi} \mathcal{P}_k \vec{f}(z)$ to be equal the terms in the sums $\sum_{m=1}^{n}$ and $\sum_{q=0}^{\infty}$ have to be identical. Hence the following conditions have to be satisfied for all $1 \le m \le n$ and all $1 \le i \le \mu_n$:

1. $\chi\left(r^{(n)}_{p_k(i)} S T^{+m} \left(r^{(n)}_{u_{m,+1}(p_k(i))}\right)^{-1}\right) = \chi\left(r^{(n)}_i S T^{-m} \left(r^{(n)}_{u_{m,-1}(i)}\right)^{-1}\right)$
2. $\chi\left(r^{(n)}_{u_{m,+1}(p_k(i))} T^{+n} \left(r^{(n)}_{u_{m,+1}(p_k(i))}\right)^{-1}\right) = \chi\left(r^{(n)}_{u_{m,-1}(i)} T^{-n} \left(r^{(n)}_{u_{m,-1}(i)}\right)^{-1}\right)$
3. $u_{m,+1}(p_k(i)) = p_k(u_{m,-1}(i))$

For a trivial character $\chi \equiv 1$ only condition 3 remains. To determine the maps $p_k : \{1,\dots,\mu_n\} \to \{1,\dots,\mu_n\}$ the following lemma is useful:

Lemma 8.1.3. *For the right coset representatives* $\left\{r^{(n)}_i\right\}_{1 \le i \le \mu_n}$ *of* $\Gamma_0(n)$ *in* $\mathrm{SL}(2,\mathbb{Z})$ *with* $r^{(n)}_1 = \begin{pmatrix} 1 & 0 \\ 0 & 1 \end{pmatrix}$ *and* $r^{(n)}_2 = S = \begin{pmatrix} 0 & -1 \\ 1 & 0 \end{pmatrix}$ *the second component of the transfer operator* $\mathcal{L}^{(n)}_{\beta,\varepsilon,\chi}$ *for* $(\Gamma_0(n),\chi)$ *is given by*

$$\left[\mathcal{L}^{(n)}_{\beta,\varepsilon,\chi} \vec{f}(z)\right]_2 = \sum_{m=1}^{n} \chi(T^{m\varepsilon}) \sum_{q=0}^{\infty} \chi(T^{n\varepsilon})^q f_1|_{2\beta} \tilde{S} T^{m+nq} z.$$

Proof. Obviously one can choose $r^{(n)}_1 = I$ and $r^{(n)}_2 = S$ for every $\Gamma_0(n)$. Then the second component of $\mathcal{L}^{(n)}_{\beta,\varepsilon,\chi} \vec{f}(z)$ is given by

$$\left[\mathcal{L}^{(n)}_{\beta,\varepsilon,\chi} \vec{f}(z)\right]_2 = \sum_{m=1}^{n} \chi\left(r^{(n)}_2 S T^{m\varepsilon} \left(r^{(n)}_{u_{m,\varepsilon}(2)}\right)^{-1}\right) \sum_{q=0}^{\infty} \chi\left(r^{(n)}_{u_{m,\varepsilon}(2)} T^{n\varepsilon} \left(r^{(n)}_{u_{m,\varepsilon}(2)}\right)^{-1}\right)^q f_{u_{m,\varepsilon}(2)}|_{2\beta} \tilde{S} T^{m+nq} z.$$

Since $r^{(n)}_2 = S$ we have $r^{(n)}_2 S T^{m\varepsilon} \left(r^{(n)}_{u_{m,\varepsilon}(2)}\right)^{-1} = S S T^{m\varepsilon} \left(r^{(n)}_{u_{m,\varepsilon}(2)}\right)^{-1} = T^{m\varepsilon} \left(r^{(n)}_{u_{m,\varepsilon}(2)}\right)^{-1} \in \Gamma_0(n)$. But $T^{m\varepsilon} \in \Gamma_0(n)$ for all $1 \le m \le n$, thus $\left(r^{(n)}_{u_{m,\varepsilon}(2)}\right)^{-1}$ must be $\begin{pmatrix} 1 & 0 \\ 0 & 1 \end{pmatrix}$, i.e. $u_{m,\varepsilon}(2) = 1$ for all m. □

This lemma shows that there is at least one component of the transfer operators $\mathcal{L}^{(n)}_{\beta,+1,\chi}$ and $\mathcal{L}^{(n)}_{\beta,-1,\chi}$, which has the same component of $\vec{f}$ appearing in all terms in the sums $\sum_{m=1}^{n}$ and $\sum_{q=0}^{\infty}$. We will use this fact to find

the operators $\mathcal{P}_k$ in the case of a trivial character $\chi \equiv 1$. In listing 8.1 we present an algorithm to find all these operators $\mathcal{P}_k$ for a given $\Gamma_0(n)$ with trivial character $\chi \equiv 1$: The function `find_symmetries` takes $u_{m,+1}$ and $u_{m,-1}$ as argument and returns a set $S_p = \{p_k\}_{1\leq k\leq h_n}$ of permutations such that $u_{m,+1}(p_k(i)) = p_k(u_{m,-1}(i))$ for all $1 \leq m \leq n$ and $1 \leq i \leq \mu_n$. The first step is to find all $i \in \{1,\dots,\mu_n\}$ for which $u_{m,\varepsilon}(i) = u_{m',\varepsilon}(i)$ for all $1 \leq m, m' \leq n$, which corresponds to finding all components of the transfer operator where the sum over m and q contains only one component of $\vec{f}$: The maps $u_{m,+1}$ and $u_{m,-1}$ are determined by the representation $U^\chi(ST^{+m})$ respectively $U^\chi(ST^{-m})$, and the function `find_components_with_one_index_in_terms` takes $u_{m,+1}$ or $u_{m,-1}$ as an argument and returns a set $X_\pm = \{i : u_{1,\pm1}(i) = u_{m,\pm1}(i) \text{ for all } 1 \leq m \leq n\}$. To define the map $p : \{1,\dots,\mu_n\} \to \{1,\dots,\mu_n\}$ we first set $p(y_+) := y_-$ and $p(u_{m,-1}(y_+)) := u_{m,+1}(p(y_+))$ for $1 \leq m \leq n$, one pair $y_+ \in X_+$ and $y_- \in X_-$. To define the map $p(i)$ for all $1 \leq i \leq \mu_n$ we use the relation $p(u_{m,-1}(i)) := u_{m,+1}(p(i))$ for the $p(i)$ already defined and for all $1 \leq m \leq n$. As soon as the map $p : \{1,\dots,\mu_n\} \to \{1,\dots,\mu_n\}$ is defined we check in the function `is_consistent` if it satisfies $p(u_{m,-1}(i)) = u_{m,+1}(p(i))$ for every $1 \leq m \leq n$ and $1 \leq i \leq \mu_n$. This check is necessary, even if p was defined using this relation, which can still be violated for some combinations of $1 \leq m \leq n$ and $1 \leq i \leq \mu_n$. If the map p fulfills all the conditions and is not already contained in the set S_p we add it to $S_p := S_p \cup \{p\}$. By repeating this procedure for every combination of $y_+ \in X_+$ and $y_- \in X_-$ we find all possible permutations p_k.

Listing 8.1: Symmetries of the transfer operator

```
index_in_terms_equal(u,i)
        for m=2,...,n
                if u(1,i) is not equal u(m,i)
                        return False
        return True

find_components_with_one_index_in_terms(u)
        X = empty_set()
        for i=1,...,mu_n
                if index_in_terms_equal(u,i) is True
                        X = add_to_set(X,i)
        return X

is_defined(p)
        for i=1,...,mu_n
                if p(i) is not defined
                        return False
        return True

set_map(p,u+,u-)
        for i=1,...,mu_n
                if p(i) is defined
                        for m=1,...,n
                                if p(u-(m,i)) is not defined
                                        p(u-(m,i)) = u+(m,p(i))

is_consistent(p,u+,u-)
        for i=1,...,mu_n
                for m=1,...,n
                        if p(u-(m,i)) is not equal u+(m,p(i))
                                return False
        return True
```

```
33
34 find_symmetries(u+,u-)
35         X+ = find_components_with_one_index_in_terms(u+)
36         X- = find_components_with_one_index_in_terms(u-)
37         p_set = empty_set()
38         for all elements y+ in X+
39                 for all elemets y- in X-
40                         p(y+) = y-
41                         p(u-(1,y+)) = u+(1,p(y+))
42                         while is_defined(p) is False
43                                 set_map(p,u+,u-)
44                         if is_consistent(p,u+,u-) is True ...
45                            and if p not in p_set
46                                 p_set = add_to_set(p_set,p)
47         return p_set
```

By implementing this algorithm in our computer program CGF, we are able to find all operators $\mathcal{P}_k$ for any group $\Gamma_0(n)$. Table 8.5 shows the index μ_n and the number of symmetries h_n for $\Gamma_0(n)$ for $1 \le n \le 100$. Indeed, we found numerically that there is always at least one symmetry $\mathcal{P}_1$ for every $(\Gamma_0(n), \chi \equiv 1)$. This symmetry $\mathcal{P}_1$ is defined by a permutation $p_1 : \{1, \ldots, \mu_n\} \to \{1, \ldots, \mu_n\}$ with $p_1(1) = 1$ and $p_1(2) = 2$, which is in agreement with lemma 8.1.3. Furthermore, $p_k(i) = p_k^{-1}(i)$ for all $1 \le i \le \mu_n$, thus $\mathcal{P}_k = \mathcal{P}_k^{-1}$. By using these symmetries one can show that the Selberg zeta function factorises as follows

$$\begin{aligned} Z^{(n)}(\beta,\chi) &= \det\left(1 - \tilde{\mathcal{L}}^{(n)}_{\beta,\chi}\right) = \det\left(1 - \mathcal{L}^{(n)}_{\beta,-1,\chi}\mathcal{L}^{(n)}_{\beta,+1,\chi}\right) = \det\left(1 - \mathcal{L}^{(n)}_{\beta,-1,\chi}\mathcal{P}_k\mathcal{P}_k\mathcal{L}^{(n)}_{\beta,+1,\chi}\right) \\ &= \det\left(1 - \mathcal{P}_k\mathcal{L}^{(n)}_{\beta,+1,\chi}\mathcal{P}_k\mathcal{L}^{(n)}_{\beta,+1,\chi}\right) = \det\left(1 - \mathcal{P}_k\mathcal{L}^{(n)}_{\beta,+1,\chi}\right)\det\left(1 + \mathcal{P}_k\mathcal{L}^{(n)}_{\beta,+1,\chi}\right). \end{aligned} \tag{8.4}$$

Such a factorization for $\mathrm{SL}(2,\mathbb{Z})$ was found in [May91b]. As we see, the Selberg zeta function is vanishing if $\mathcal{P}_k\mathcal{L}^{(n)}_{\beta,+1,\chi}$ has an eigenvalue $+1$ or -1. For $\mathrm{SL}(2,\mathbb{Z})$ it is known [Efr93] that for $\Re\beta = \frac{1}{2}$ the eigenvalue $+1$ of the transfer operator is related to an even Maass wave form $u(-\bar{z}) = u(z)$ and -1 to an odd Maass wave form $u(-\bar{z}) = -u(z)$. Numerical calculations for $(\Gamma_0(n), \chi \equiv 1)$ and comparison with even/odd symmetries of Maass wave forms given in [Str09b] indicate this also holds for the operator $\mathcal{P}_1\mathcal{L}^{(n)}_{\beta,+1}$:

Conclusion 8.1.4. *For $(\Gamma_0(n), \chi \equiv 1)$ the involution $jz = -\bar{z}$ for Maass wave forms $u(z)$ with the spectral parameter $\beta \in \mathbb{C}$, i.e. $\Delta u(z) = \beta(1-\beta)u(z)$, and the operator $\mathcal{P}_1$, which intertwines the transfer operators $\mathcal{L}^{(n)}_{\beta,+1}$ and $\mathcal{L}^{(n)}_{\beta,-1}$, i.e. $\mathcal{P}_1\mathcal{L}^{(n)}_{\beta,+1} = \mathcal{L}^{(n)}_{\beta,-1}\mathcal{P}_1$, are related by:*

$$\begin{aligned} +1 \in \sigma(\mathcal{P}_1\mathcal{L}^{(n)}_{\beta,+1}) &\iff u(-\bar{z}) = u(z), \quad \textit{i.e. } u \textit{ is even} \\ -1 \in \sigma(\mathcal{P}_1\mathcal{L}^{(n)}_{\beta,+1}) &\iff u(-\bar{z}) = -u(z), \quad \textit{i.e. } u \textit{ is odd.} \end{aligned}$$

For a non-trivial character the symmetries $\mathcal{P}_k$ are usually destroyed. Lemma 8.1.3 indicates that for the transfer operator $\mathcal{L}^{(n)}_{\beta,\varepsilon,\chi}$ with a character χ the only possible relation is given by $\mathcal{P}_1\mathcal{L}^{(n)}_{\beta,+1,\chi} = \mathcal{L}^{(n)}_{\beta,-1,\chi^{-1}}\mathcal{P}_1$. An output from our program CGF of the transfer operator for $\Gamma_0(4)$ with the character $\chi^{(4)}_{\alpha_1,\alpha_2}$ and the operators $\mathcal{P}_1$ and $\mathcal{P}_2$ are given in section 7.4.2:

Conclusion 8.1.5. *For $(\Gamma_0(4), \chi^{(4)}_{\alpha_1,\alpha_2})$ and $\beta \in \mathbb{C}$ the operators $\mathcal{P}_1$ and $\mathcal{P}_2$ relate the transfer operators $\mathcal{L}^{(4)}_{\beta,\pm1,(\alpha_1,\alpha_2)} := \mathcal{L}^{(4)}_{\beta,\pm1,\chi^{(4)}_{\alpha_1,\alpha_2}}$ as follows*

$$\begin{aligned} \mathcal{P}_1\mathcal{L}^{(4)}_{\beta,+1,(\alpha_1,0)} &= \mathcal{L}^{(4)}_{\beta,-1,(-\alpha_1,0)}\mathcal{P}_1 \\ \mathcal{P}_2\mathcal{L}^{(4)}_{\beta,+1,(\alpha_1,0)} &= \mathcal{L}^{(4)}_{\beta,-1,(\alpha_1,0)}\mathcal{P}_2. \end{aligned}$$

Table 8.5: Index μ_n of $\Gamma_0(n)$ in $\mathrm{SL}(2,\mathbb{Z})$ and the number h_n of symmetries $\{\mathcal{P}_k\}_{1\le k\le h_n}$

$\Gamma_0(n)$	μ_n	h_n	$\Gamma_0(n)$	μ_n	h_n	$\Gamma_0(n)$	μ_n	h_n	$\Gamma_0(n)$	μ_n	h_n
$\Gamma_0(1)$	1	1	$\Gamma_0(26)$	42	1	$\Gamma_0(51)$	72	1	$\Gamma_0(76)$	120	2
$\Gamma_0(2)$	3	1	$\Gamma_0(27)$	36	3	$\Gamma_0(52)$	84	2	$\Gamma_0(77)$	96	1
$\Gamma_0(3)$	4	1	$\Gamma_0(28)$	48	2	$\Gamma_0(53)$	54	1	$\Gamma_0(78)$	168	1
$\Gamma_0(4)$	6	2	$\Gamma_0(29)$	30	1	$\Gamma_0(54)$	108	3	$\Gamma_0(79)$	80	1
$\Gamma_0(5)$	6	1	$\Gamma_0(30)$	72	1	$\Gamma_0(55)$	72	1	$\Gamma_0(80)$	144	4
$\Gamma_0(6)$	12	1	$\Gamma_0(31)$	32	1	$\Gamma_0(56)$	96	2	$\Gamma_0(81)$	108	3
$\Gamma_0(7)$	8	1	$\Gamma_0(32)$	48	4	$\Gamma_0(57)$	80	1	$\Gamma_0(82)$	126	1
$\Gamma_0(8)$	12	2	$\Gamma_0(33)$	48	1	$\Gamma_0(58)$	90	1	$\Gamma_0(83)$	84	1
$\Gamma_0(9)$	12	3	$\Gamma_0(34)$	54	1	$\Gamma_0(59)$	60	1	$\Gamma_0(84)$	192	2
$\Gamma_0(10)$	18	1	$\Gamma_0(35)$	48	1	$\Gamma_0(60)$	144	2	$\Gamma_0(85)$	108	1
$\Gamma_0(11)$	12	1	$\Gamma_0(36)$	72	6	$\Gamma_0(61)$	62	1	$\Gamma_0(86)$	132	1
$\Gamma_0(12)$	24	2	$\Gamma_0(37)$	38	1	$\Gamma_0(62)$	96	1	$\Gamma_0(87)$	120	1
$\Gamma_0(13)$	14	1	$\Gamma_0(38)$	60	1	$\Gamma_0(63)$	96	3	$\Gamma_0(88)$	144	2
$\Gamma_0(14)$	24	1	$\Gamma_0(39)$	56	1	$\Gamma_0(64)$	96	8	$\Gamma_0(89)$	90	1
$\Gamma_0(15)$	24	1	$\Gamma_0(40)$	72	2	$\Gamma_0(65)$	84	1	$\Gamma_0(90)$	216	3
$\Gamma_0(16)$	24	4	$\Gamma_0(41)$	42	1	$\Gamma_0(66)$	144	1	$\Gamma_0(91)$	112	1
$\Gamma_0(17)$	18	1	$\Gamma_0(42)$	96	1	$\Gamma_0(67)$	68	1	$\Gamma_0(92)$	144	2
$\Gamma_0(18)$	36	3	$\Gamma_0(43)$	44	1	$\Gamma_0(68)$	108	2	$\Gamma_0(93)$	128	1
$\Gamma_0(19)$	20	1	$\Gamma_0(44)$	72	2	$\Gamma_0(69)$	96	1	$\Gamma_0(94)$	144	1
$\Gamma_0(20)$	36	2	$\Gamma_0(45)$	72	3	$\Gamma_0(70)$	144	1	$\Gamma_0(95)$	120	1
$\Gamma_0(21)$	32	1	$\Gamma_0(46)$	72	1	$\Gamma_0(71)$	72	1	$\Gamma_0(96)$	192	4
$\Gamma_0(22)$	36	1	$\Gamma_0(47)$	48	1	$\Gamma_0(72)$	144	6	$\Gamma_0(97)$	98	1
$\Gamma_0(23)$	24	1	$\Gamma_0(48)$	96	4	$\Gamma_0(73)$	74	1	$\Gamma_0(98)$	168	1
$\Gamma_0(24)$	48	2	$\Gamma_0(49)$	56	1	$\Gamma_0(74)$	114	1	$\Gamma_0(99)$	144	3
$\Gamma_0(25)$	30	1	$\Gamma_0(50)$	90	1	$\Gamma_0(75)$	120	1	$\Gamma_0(100)$	180	2

Results from CGF version *2.3.1*.

Obviously, the factorization of the Selberg zeta function in (8.4) exists only for $\mathcal{P}_2\mathcal{L}^{(4)}_{\beta,+1,(\alpha_1,0)}$. It might be surprising that for $\chi^{(4)}_{0,\alpha_2}$ such an operator does not exist, since we saw in section 6.5 that the Selberg zeta function for $\chi^{(4)}_{\alpha,0}$ is the same as for $\chi^{(4)}_{0,\alpha}$. After we found the operators $\mathcal{P}_k$ we used the transfer operator $\mathcal{P}_2\mathcal{L}^{(4)}_{\beta,+1,\alpha}$ for further numerical investigations of the character deformation with $\chi^{(4)}_{\alpha,0}$ for $\Gamma_0(4)$. This obviously reduces the computation time, since we need to compute only the operator $\mathcal{L}^{(4)}_{\beta,+1,\alpha}$ and $\mathcal{P}_2$. In [PS94] it was shown that all Maass wave forms which are odd with respect to the involution $\tau z = \frac{\bar{z}}{2\bar{z}-1}$ survive the deformation by $\chi^{(4)}_{0,\alpha}$, and only the even ones can be destroyed. As we will see later, our numerical computations show that the eigenvalues $+1$ of $\mathcal{P}_2\mathcal{L}^{(4)}_{\beta,+1,\alpha}$ are related to the zeros of the Selberg zeta function which leave the critical line $\Re\beta = \frac{1}{2}$ under the deformation by α and that the eigenvalues -1 are related to the zeros which stay on the critical line for every α. This indicates already that the symmetry corresponding to the operator $\mathcal{P}_2$ is related to the involution τ. Indeed, since the involution τ is preserved throughout the deformation by $\chi^{(4)}_{\alpha}$, see [PS94], and $\mathcal{P}_2$ is the only operator defining a symmetry of the transfer operator for this deformation we conclude that:

Conclusion 8.1.6. *For $(\Gamma_0(4),\chi^{(4)}_{\alpha})$ the involution $\tau z = \frac{\bar{z}}{2\bar{z}-1}$ for Maass wave forms $u(z)$ with the spectral parameter $\beta \in \mathbb{C}$, i.e. $\Delta u(z) = \beta(1-\beta)u(z)$, and the operator $\mathcal{P}_2$, which intertwines the transfer operator*

$\mathcal{L}^{(4)}_{\beta,+1,\alpha}$ *and* $\mathcal{L}^{(4)}_{\beta,-1,\alpha}$, *i.e.* $\mathcal{P}_2\mathcal{L}^{(4)}_{\beta,+1,\alpha} = \mathcal{L}^{(4)}_{\beta,-1,\alpha}\mathcal{P}_2$, *are related by:*

$$\begin{aligned} +1 \in \sigma(\mathcal{P}_2\mathcal{L}^{(4)}_{\beta,+1,\alpha}) &\iff u(\tau z) = u(z), \quad \textit{i.e. } u \textit{ is } \tau\textit{-even} \\ -1 \in \sigma(\mathcal{P}_2\mathcal{L}^{(4)}_{\beta,+1,\alpha}) &\iff u(\tau z) = -u(z), \quad \textit{i.e. } u \textit{ is } \tau\textit{-odd.} \end{aligned}$$

The form of the transfer operator $\mathcal{L}^{(8)}_{\beta,\varepsilon,(\alpha_1,\alpha_2,\alpha_3)} := \mathcal{L}^{(8)}_{\beta,\varepsilon,\chi^{(8)}_{\alpha_1,\alpha_2,\alpha_3}}$ for $\Gamma_0(8)$ with character $\chi^{(8)}_{\alpha_1,\alpha_2,\alpha_3}$ is given in Appendix C. For this operator we have

Conclusion 8.1.7. *For* $(\Gamma_0(8), \chi^{(8)}_{\alpha_1,\alpha_2,\alpha_3})$ *the operators* $\mathcal{P}_1$ *and* $\mathcal{P}_2$ *relate* $\mathcal{L}^{(8)}_{\beta,+1,(\alpha_1,\alpha_2,\alpha_3)}$ *and* $\mathcal{L}^{(8)}_{\beta,-1,(\alpha_1,\alpha_2,\alpha_3)}$ *by*

$$\begin{aligned} \mathcal{P}_1\mathcal{L}^{(8)}_{\beta,+1,(0,\alpha_2,\alpha_3)} &= \mathcal{L}^{(8)}_{\beta,-1,(0,-\alpha_2,-\alpha_3)}\mathcal{P}_1 \\ \mathcal{P}_2\mathcal{L}^{(8)}_{\beta,+1,(0,0,0)} &= \mathcal{L}^{(8)}_{\beta,-1,(0,0,0)}\mathcal{P}_2. \end{aligned}$$

Unfortunately, for $\Gamma_0(8)$ all symmetries are destroyed for a non-trivial character, and therefore we have to use the operator $\mathcal{L}^{(8)}_{\beta,+1,\alpha}\mathcal{L}^{(8)}_{\beta,-1,\alpha}$ to study the character deformation by $\chi^{(8)}_{\alpha}$.

We conclude from the numerical observations in this section that:

Conclusion 8.1.8. *For* $(\Gamma_0(n), \chi \equiv 1)$ *with* $\beta \in \mathbb{C}$ *at least one operator* $\mathcal{P}_k$ *exists such that* $\mathcal{P}_k\mathcal{L}^{(n)}_{\beta,+1} = \mathcal{L}^{(n)}_{\beta,-1}\mathcal{P}_k$; *for* $(\Gamma_0(4), \chi^{(4)}_{\alpha})$ *only one operator* $\mathcal{P}_2$ *exists such that* $\mathcal{P}_2\mathcal{L}^{(4)}_{\beta,+1,\alpha} = \mathcal{L}^{(4)}_{\beta,-1,\alpha}\mathcal{P}_2$. *The symmetries corresponding to the* $\mathcal{P}_k$*'s are related to the involutions for Maass wave forms.*

The existence of the operators $\mathcal{P}_k$ confirms our numerical observations in the previous sections concerning the equality of the traces of $\mathcal{L}^{(n)}_{\beta,+1,\chi}$ and $\mathcal{L}^{(n)}_{\beta,-1,\chi}$ and the spectra $\mathcal{L}^{(n)}_{\beta,+1,\chi}$ and $\mathcal{L}^{(n)}_{\beta,-1,\chi}$ for $(\Gamma_0(n), \chi \equiv 1)$ and $(\Gamma_0(4), \chi^{(4)}_{\alpha_1,0})$, respectively the difference of these traces and spectra for $(\Gamma_0(4), \chi^{(4)}_{\alpha_1,\alpha_2})$ and $(\Gamma_0(8), \chi^{(8)}_{\alpha_1,\alpha_2,\alpha_3})$. The symmetries defined by the operators $\mathcal{P}_k$ were obtained by symbolic computations using the program CGF, while the results in the previous sections were obtained by numerical analysis using the program widmo. Note that the two methods are completely different, and therefore these results provide further verification for the computations performed by our computer programs widmo and CGF.

We have explicitly determined in [FM11] the symmetries corresponding to the operators $\mathcal{P}_k$ for $(\Gamma_0(n), \chi \equiv 1)$ and $(\Gamma_0(4), \chi^{(4)}_{\alpha})$. We also showed that the operator $\mathcal{P}_1$ corresponds to the involution $z \to -\bar{z}$ of the Maass wave forms. These results confirm our numerical observations of the operators $\mathcal{P}_k$, and hence are an analytic verification of our numerical computations. Note also that the transfer operator for $\Gamma_0(n)$ of Manin and Marcolli in [MM02], which always leads to a factorisation of the Selberg zeta function for these groups, is conjugate to our transfer operator with the operator $\mathcal{P}_1$ corresponding to the involution $z \to -\bar{z}$.

8.1.4 The spectra and traces of the transfer operator

To evaluate the Selberg zeta function we need to compute the spectra of $\mathcal{L}^{(n)}_{\beta,+1,\chi}\mathcal{L}^{(n)}_{\beta,-1,\chi}$ respectively $\mathcal{P}_k\mathcal{L}^{(n)}_{\beta,\varepsilon,\chi}$. The operator $\mathcal{L}^{(n)}_{\beta,+1,\chi}\mathcal{L}^{(n)}_{\beta,-1,\chi}$ can be approximated by

$$\mathcal{M}^{(n)}_{\beta,+1,\chi}\mathcal{M}^{(n)}_{\beta,-1,\chi}$$

which is just the product of the matrices $\mathcal{M}^{(n)}_{\beta,+1,\chi}$ and $\mathcal{M}^{(n)}_{\beta,-1,\chi}$ in proposition 7.4.11. On the other hand, the operator $\mathcal{P}_k\mathcal{L}^{(n)}_{\beta,\varepsilon,\chi}$ can be approximated by the matrix $\mathcal{P}_k\mathcal{M}^{(n)}_{\beta,\varepsilon,\chi}$ with $\mathcal{M}^{(n)}_{\beta,\varepsilon,\chi}$ given in proposition 7.4.11 and $\mathcal{P}_k$ determined by the permutation p_k in (8.3):

$$\begin{aligned} \left[\left(\mathcal{P}_k\mathcal{M}^{(n)}_{\beta,\varepsilon,\chi}\right)_{s,k}\right]_{i,j} &= \frac{1}{s!}\sum_{t=0}^{k}\binom{k}{t}\frac{(-1)^{k-t+s}}{n^{2\beta+t+s}}\frac{\Gamma(2\beta+t+s)}{\Gamma(2\beta+t)}\sum_{m=1}^{n}\left[\mathcal{P}_k U^{\chi}\left(S T^{m\varepsilon}\right)\right]_{i,j} \\ &\quad \Phi\left(\chi\left(r^{(n)}_j T^{n\varepsilon}\left(r^{(n)}_j\right)^{-1}\right), 2\beta+t+s, \frac{m+1}{n}\right) \end{aligned} \tag{8.5}$$

where $[\mathcal{P}_k U^\chi(ST^{m\varepsilon})]_{i,j} = [U^\chi(ST^{m\varepsilon})]_{p_k(i),j}$. In this section we want to investigate the spectra of $\mathcal{L}^{(n)}_{\beta,\varepsilon,\chi}$, $\mathcal{P}_k\mathcal{L}^{(n)}_{\beta,\varepsilon,\chi}$ and $\mathcal{L}^{(n)}_{\beta,+1,\chi}\mathcal{L}^{(n)}_{\beta,-1,\chi}$. To verify our numerical results for the spectrum of the approximation of the transfer operator we compare them with known properties: As theoretically expected, for $\beta = 1$ the matrices $\mathcal{M}^{(n)}_{\beta,+1}\mathcal{M}^{(n)}_{\beta,-1}$ and $\mathcal{P}_1\mathcal{M}^{(n)}_{\beta,\varepsilon}$ have the eigenvalue 1 for $(\Gamma_0(n), \chi \equiv 1)$. We also found that $\mathcal{M}^{(n)}_{\beta,\varepsilon}$ for $(\Gamma_0(n), \chi \equiv 1)$ has an eigenvalue $\lambda = 1$ for $\beta = 1$, which is also in agreement with theoretical considerations since the eigenfunction of the transfer operator $\mathcal{L}^{(n)}_{\beta,\varepsilon}$ for $\beta = 1$ and $\lambda = 1$ is $f_i(z) = \frac{1}{z+1}$ for all $1 \le i \le \mu_n$. Since the Selberg zeta function for $(\Gamma_0(n), \chi \equiv 1)$ has a pole at $\beta = 0.5$ one should expect that near this value some of the eigenvalues of $\mathcal{M}^{(n)}_{\beta,+1}\mathcal{M}^{(n)}_{\beta,-1}$ and $\mathcal{P}_1\mathcal{M}^{(n)}_{\beta,\varepsilon}$ become very large, which we can also see in our numerical computations. In all cases, we investigated for $(\Gamma_0(n), \chi)$ and $\beta \in \mathbb{C}$, most of the eigenvalues of $\mathcal{M}^{(n)}_{\beta,\varepsilon,\chi}$, $\mathcal{M}^{(n)}_{\beta,+1,\chi}\mathcal{M}^{(n)}_{\beta,-1,\chi}$, and $\mathcal{P}_k\mathcal{M}^{(n)}_{\beta,\varepsilon,\chi}$ are accumulating near zero, which corresponds to the fact that the eigenvalues of the transfer operator decrease exponentially, see [BJ08]. It was proved in [May90] that the transfer operator $\mathcal{L}^{(1)}_\beta$ for $\mathrm{SL}(2,\mathbb{Z})$ with $\beta \in \mathbb{R}$ has a real spectrum for $\beta > 0.5$. Our numerical results show that (see Figure 8.2 top left):

Experimental Observation 8.1.9. *For* $\mathrm{SL}(2,\mathbb{Z})$ *and* $\beta \in \mathbb{R}$ *the spectrum of the transfer operator* $\mathcal{L}^{(1)}_\beta$ *is real for* $\beta > C_{\mathrm{ev}}$ *and for* $\beta \le C_{\mathrm{ev}}$ *the spectrum contains a pair of complex conjugate eigenvalues; all other eigenvalues are real. Numerically we obtained* $C_{\mathrm{ev}} \approx 0.390908820806\ldots$. *As a consequence the trace of* $\mathcal{L}^{(1)}_\beta$ *is real for all* $\beta \in \mathbb{R}$.

The results for the spectrum of $\mathcal{L}^{(1)}_\beta$ for the special values $\beta = \frac{1-k}{2}$ with $k \in \mathbb{Z}_>$ in [CM99] agree with our observations, see also Corollary 2 in [CM99]. We also computed the spectrum of the transfer operators $\mathcal{L}^{(4)}_{\beta,\varepsilon,\alpha}$ and $\mathcal{P}_k\mathcal{L}^{(4)}_{\beta,\varepsilon,\alpha}$ for $(\Gamma_0(4), \chi^{(4)}_\alpha)$ with $\beta \in \mathbb{R}$ (see Figures 8.2 and 8.3):

Experimental Observation 8.1.10. *For* $(\Gamma_0(4), \chi^{(4)}_\alpha)$ *and* $\beta \in \mathbb{R}$ *the spectra of the transfer operators* $\mathcal{L}^{(4)}_{\beta,\varepsilon,\alpha}$ *and* $\mathcal{P}_k\mathcal{L}^{(4)}_{\beta,\varepsilon,\alpha}$ *contain finitely many pairs of complex conjugate eigenvalues; all other eigenvalues are real. The traces of these operators are real for all* $\beta \in \mathbb{R}$.

We also conducted a few experiments for other groups $\Gamma_0(n)$ and trivial character for $\beta \in \mathbb{R}$. It seems that like in observation 8.1.10 the traces are always real and there are a few complex conjugate eigenvalues. The observations in 8.1.9 and 8.1.10 concerning reality of the traces agree with the fact that the Selberg zeta function for $\Gamma_0(n)$ and unitary χ is real on the real axis $\beta \in \mathbb{R}$, which follows from the product definition (6.2). On the other hand, for the characters $\chi^{(4)}_{\alpha_1,\alpha_2}$ and $\chi^{(4)}_{0,\alpha_2}$ we found that:

Experimental Observation 8.1.11. *For* $(\Gamma_0(4), \chi^{(4)}_{0,\alpha_2})$ *and* $(\Gamma_0(4), \chi^{(4)}_{\alpha_1,\alpha_2})$, $\beta \in \mathbb{R}$ *and* $\alpha_1, \alpha_2 \notin \mathbb{Z}$ *the spectra of the transfer operators* $\mathcal{L}^{(4)}_{\beta,\varepsilon,\chi}$ *and* $\mathcal{P}_k\mathcal{L}^{(4)}_{\beta,\varepsilon,\chi}$ *are complex, and also the traces of these operators are complex.*

This observation shows that the Selberg zeta function cannot be expressed by the Fredholm determinants of these operators, since the Fredholm determinant is not real valued for these characters. This confirms our observation in the foregoing section that only for a trivial character and the character $\chi^{(4)}_\alpha$ the operator $\mathcal{P}_2$ leads to a factorization of the Selberg zeta function. The observation in 8.1.10 that the trace of the operator $\mathcal{L}^{(4)}_{\beta,\varepsilon,\alpha}$ is real for $\beta \in \mathbb{R}$ indicates that its Fredholm determinant might be related to the Selberg zeta function. Indeed, we found numerically that for $(\Gamma_0(4), \chi \equiv 1)$ and $\beta \in \mathbb{C}$ the Fredholm determinant $\det(1 + \mathcal{L}^{(4)}_{\beta,\varepsilon})\det(1 - \mathcal{L}^{(4)}_{\beta,\varepsilon})$ with $\varepsilon = \pm 1$ is the Selberg zeta function. From further numerical investigations we are led to:

Conclusion 8.1.12. *For* $(\Gamma_0(4), \chi \equiv 1)$ *and* $\beta \in \mathbb{C}$ *the spectra of* $\mathcal{L}^{(4)}_{\beta,\varepsilon}$ *and* $\mathcal{P}_2\mathcal{L}^{(4)}_{\beta,\varepsilon}$ *are equal.*

For a non-trivial character χ the spectra of $\mathcal{L}^{(4)}_{\beta,\varepsilon,\chi}$ and $\mathcal{P}_2\mathcal{L}^{(4)}_{\beta,\varepsilon,\chi}$ are different, but we have found that:

Conclusion 8.1.13. *For* $(\Gamma_0(4), \chi^{(4)}_\alpha)$ *and* $\beta \in \mathbb{C}$ *the traces of* $\mathcal{L}^{(4)}_{\beta,\varepsilon,\alpha}$ *and* $\mathcal{P}_2\mathcal{L}^{(4)}_{\beta,\varepsilon,\alpha}$ *are equal.*

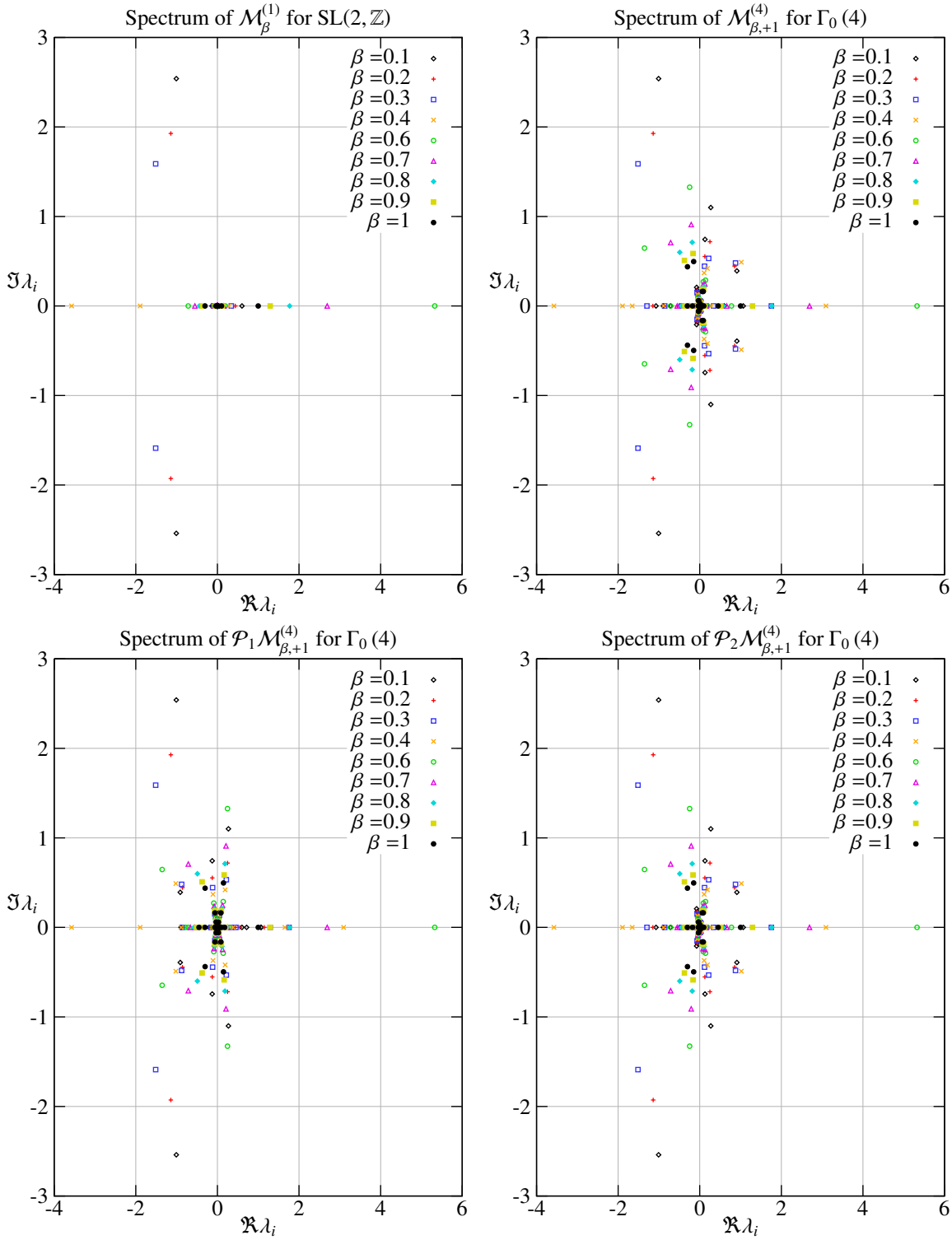

Figure 8.2: Spectrum $\{\lambda_i\}$ of $\mathcal{M}_{\beta,\varepsilon}^{(1)}$, $\mathcal{M}_{\beta,\varepsilon}^{(4)}$, $\mathcal{P}_1\mathcal{M}_{\beta,\varepsilon}^{(4)}$ and $\mathcal{P}_2\mathcal{M}_{\beta,\varepsilon}^{(4)}$ on the real line $\beta \in \mathbb{R}$

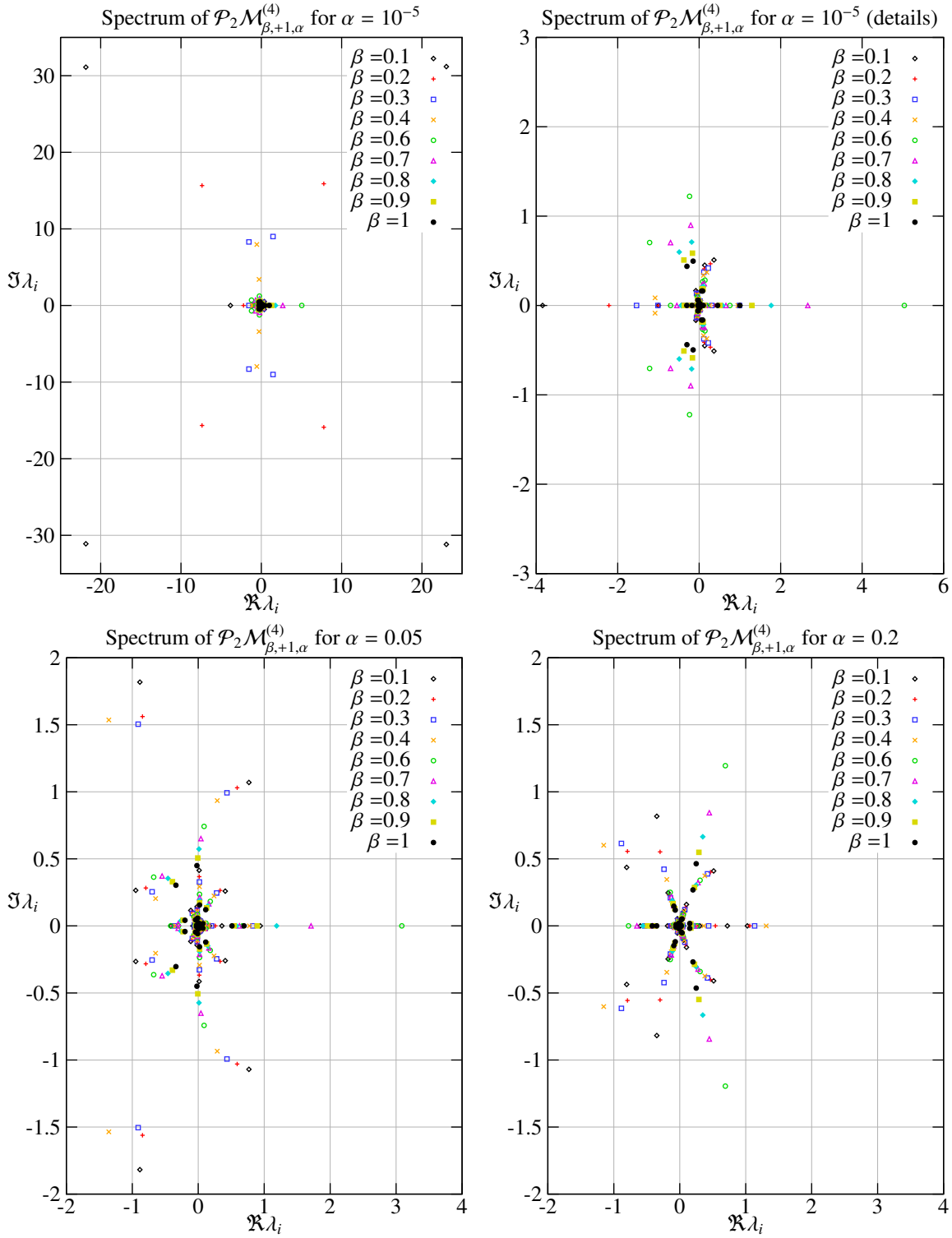

Figure 8.3: Spectrum $\{\lambda_i\}$ of $\mathcal{P}_2\mathcal{M}^{(4)}_{\beta,\varepsilon,\alpha}$ on the real line $\beta \in \mathbb{R}$ for $\alpha \in \{10^{-5}, 0.05, 0.2\}$

We have been able to prove in [FM11] that for $(\Gamma_0(4), \chi \equiv 1)$ the Fredholm determinants of $\mathcal{L}^{(4)}_{\beta,\varepsilon}$ and $\mathcal{P}_2\mathcal{L}^{(4)}_{\beta,\varepsilon}$ are equal, which agrees with conclusion 8.1.12. Numerical investigations also show that the traces of the transfer operators for $(\Gamma_0(4), \chi \equiv 1)$ and $(\Gamma_0(8), \chi \equiv 1)$ are equal:

Conclusion 8.1.14. *For* $(\Gamma_0(4), \chi \equiv 1)$ *and* $(\Gamma_0(8), \chi \equiv 1)$ *the traces of* $\mathcal{L}^{(4)}_{\beta,\varepsilon}$ *and* $\mathcal{L}^{(8)}_{\beta,\varepsilon}$ *are equal for* $\beta \in \mathbb{C}$.

On the other hand, the spectra of $\mathcal{L}^{(4)}_{\beta,\varepsilon}$ and $\mathcal{L}^{(8)}_{\beta,\varepsilon}$ are different. We also checked for other groups $(\Gamma_0(n), \chi \equiv 1)$ with $1 \leq n \leq 12$ if their traces coincide, but this does not seem to be the case. This result indicates that there is some special relation between the transfer operators for the groups $(\Gamma_0(4), \chi \equiv 1)$ and $(\Gamma_0(8), \chi \equiv 1)$. During our numerical investigations of the trace of $\mathcal{L}^{(4)}_{\beta,\varepsilon,\alpha}$ for $(\Gamma_0(4), \chi^{(4)}_\alpha)$ we found that it vanishes for $\alpha = \frac{1}{4}$ and every $\beta \in \mathbb{C}$. By further numerical experiments we also found that the traces of the operators $\mathcal{P}_1\mathcal{L}^{(4)}_{\beta,\varepsilon,\frac{1}{4}}$ and $\mathcal{P}_2\mathcal{L}^{(4)}_{\beta,\varepsilon,\frac{1}{4}}$ vanish for every $\beta \in \mathbb{C}$:

Conclusion 8.1.15. *For* $(\Gamma_0(4), \chi^{(4)}_\alpha)$ *with* $\alpha = \frac{1}{4}$ *the traces of* $\mathcal{L}^{(4)}_{\beta,\varepsilon,\frac{1}{4}}$, $\mathcal{P}_1\mathcal{L}^{(4)}_{\beta,\varepsilon,\frac{1}{4}}$ *and* $\mathcal{P}_2\mathcal{L}^{(4)}_{\beta,\varepsilon,\frac{1}{4}}$ *are vanishing for* $\beta \in \mathbb{C}$.

Note, that we did not find any other value of α where this happens also. Indeed, we found numerically an explanation why the trace of $\mathcal{P}_1\mathcal{L}^{(4)}_{\beta,\varepsilon,\frac{1}{4}}$ must be zero:

Experimental Observation 8.1.16. *For* $(\Gamma_0(4), \chi^{(4)}_\alpha)$ *with* $\alpha = \frac{1}{4}$ *for every eigenvalue* λ *of* $\mathcal{P}_1\mathcal{L}^{(4)}_{\beta,\varepsilon,\frac{1}{4}}$ *there is an eigenvalue* $-\lambda$ *of this operator for* $\beta \in \mathbb{C}$.

The spectra of the operators $\mathcal{L}^{(4)}_{\beta,\varepsilon,\frac{1}{4}}$ and $\mathcal{P}_2\mathcal{L}^{(4)}_{\beta,\varepsilon,\frac{1}{4}}$ do not have this property. However, we found another relation between the spectra of these two operators:

Experimental Observation 8.1.17. *For* $(\Gamma_0(4), \chi^{(4)}_\alpha)$ *with* $\alpha = \frac{1}{4}$, λ *is an eigenvalue of* $\mathcal{L}^{(4)}_{\beta,\varepsilon,\frac{1}{4}}$ *iff* $-\lambda$ *is an eigenvalue of* $\mathcal{P}_2\mathcal{L}^{(4)}_{\beta,\varepsilon,\frac{1}{4}}$ *for* $\beta \in \mathbb{C}$.

For values of $\alpha \in \{0, \frac{1}{8}, \frac{3}{8}, \frac{4}{8}\}$ with $\chi^{(4)}_\alpha$ arithmetic the traces of $\mathcal{L}^{(4)}_{\beta,\varepsilon,\alpha}$, $\mathcal{P}_1\mathcal{L}^{(4)}_{\beta,\varepsilon,\alpha}$ and $\mathcal{P}_2\mathcal{L}^{(4)}_{\beta,\varepsilon,\alpha}$ do not vanish, but we found relations between the traces of $\mathcal{P}_2\mathcal{L}^{(4)}_{\beta,\varepsilon,\alpha}$ for different values of α:

Conclusion 8.1.18. *For* $(\Gamma_0(4), \chi^{(4)}_\alpha)$ *the following relations hold for* $\beta \in \mathbb{C}$

$$\begin{aligned} tr\,\mathcal{P}_2\mathcal{L}^{(4)}_{\beta,\varepsilon,0} + tr\,\mathcal{P}_2\mathcal{L}^{(4)}_{\beta,\varepsilon,\frac{1}{2}} &= 0 \\ tr\,\mathcal{P}_2\mathcal{L}^{(4)}_{\beta,\varepsilon,\frac{1}{8}} + tr\,\mathcal{P}_2\mathcal{L}^{(4)}_{\beta,\varepsilon,\frac{3}{8}} &= 0. \end{aligned}$$

The spectra of these operators are different, and also eigenvalues λ of one operator do not just correspond to eigenvalues $-\lambda$ of the other operator. The following observations 8.1.19 and 8.1.20 are trivial, but we include them anyway as a verification of our numerical calculations:

Experimental Observation 8.1.19. *For* $(\Gamma_0(n), \chi \equiv 1)$, $1 \leq n \leq 12$, *and* $(\Gamma_0(4), \chi^{(4)}_\alpha)$ *we have:* λ *is an eigenvalue of* $\mathcal{L}^{(n)}_{\beta,\varepsilon}$ *for* $\beta \in \mathbb{C}$ *iff* $\bar{\lambda}$ *is an eigenvalue of* $\mathcal{L}^{(n)}_{\bar{\beta},\varepsilon}$ *for* $\bar{\beta}$. *This holds also for* $\mathcal{P}_1\mathcal{L}^{(n)}_{\beta,\varepsilon}$ *and* $\mathcal{P}_1\mathcal{L}^{(n)}_{\bar{\beta},\varepsilon}$, *respectively for* $\mathcal{P}_k\mathcal{L}^{(4)}_{\beta,\varepsilon,\alpha}$ *and* $\mathcal{P}_k\mathcal{L}^{(4)}_{\bar{\beta},\varepsilon,\alpha}$.

Experimental Observation 8.1.20. *For* $(\Gamma_0(n), \chi \equiv 1)$ *and* $(\Gamma_0(mn) \subset \Gamma_0(n), \chi \equiv 1)$, $1 \leq mn \leq 12$, *the spectrum of* $\mathcal{L}^{(n)}_{\beta,\varepsilon}$ *is contained in the spectrum of* $\mathcal{L}^{(mn)}_{\beta,\varepsilon}$ *for all* $\beta \in \mathbb{C}$, *and the spectrum of* $\mathcal{P}_1\mathcal{L}^{(n)}_{\beta,\varepsilon}$ *is contained in the one of* $\mathcal{P}_1\mathcal{L}^{(mn)}_{\beta,\varepsilon}$, *i.e* $\sigma(\mathcal{L}^{(n)}_{\beta,\varepsilon}) \subset \sigma(\mathcal{L}^{(mn)}_{\beta,\varepsilon})$ *and* $\sigma(\mathcal{P}_1\mathcal{L}^{(n)}_{\beta,\varepsilon}) \subset \sigma(\mathcal{P}_1\mathcal{L}^{(mn)}_{\beta,\varepsilon})$. *Furthermore,* $\sigma(\mathcal{P}_1\mathcal{L}^{(4)}_{\beta,\varepsilon}) \subset \sigma(\mathcal{P}_k\mathcal{L}^{(8)}_{\beta,\varepsilon})$ *for* $k = 1, 2$.

We also investigated how the spectra of $\mathcal{L}^{(n)}_{\beta,\varepsilon,\chi}$ and $\mathcal{P}_k\mathcal{L}^{(n)}_{\beta,\varepsilon,\chi}$ for $(\Gamma_0(n),\chi\equiv 1)$ and $(\Gamma_0(4),\chi^{(4)}_\alpha)$ depend on $\beta\in\mathbb{C}$ and $\alpha\in[0,0.5]$.

Experimental Observation 8.1.21. *For $(\Gamma_0(n),\chi\equiv 1)$, $1\leq n\leq 12$, respectively $(\Gamma_0(4),\chi^{(4)}_\alpha)$ we have for $\mathcal{L}^{(n)}_{\beta,\varepsilon}$, $\mathcal{P}_k\mathcal{L}^{(n)}_{\beta,\varepsilon}$ respectively $\mathcal{P}_2\mathcal{L}^{(4)}_{\beta,\varepsilon,\alpha}$ for $\beta\in\mathbb{C}$ and fixed α:*

- *For $\Re\beta>\frac{1}{2}$ the eigenvalues are decreasing exponentially with increasing $\Re\beta$. For $\Re\beta$ large enough, the eigenvalues lay on concentric circles, whose radii coincide for all $(\Gamma_0(n),\chi)$ (see Figure 8.4 on the top left). For fixed $\Re\beta$ and $\Im\beta$ varying the eigenvalues rotate on these circles. As $\Re\beta$ approaches $\frac{1}{2}$ the circles grow and get deformed depending on β and $(\Gamma_0(n),\chi)$.*
- *For $\Re\beta=\frac{1}{2}$ a few eigenvalues are growing exponentially with increasing $\Im\beta$. For $\Im\beta$ varying the eigenvalues of $\mathcal{P}_k\mathcal{L}^{(n)}_{\beta,\varepsilon,\chi}$ rotate around 0 (see Figure 8.5 lower left), many of these eigenvalues rotate with absolute value $|\lambda_i|\approx 1$ and passing through ±1 (see Figure 8.5 top left).*
- *For $0\leq\Re\beta<\frac{1}{2}$ the eigenvalues are growing for decreasing $\Re\beta$. For fixed $\Re\beta$ a few eigenvalues are growing exponentially with increasing $\Im\beta$. It seems that for every one of these large eigenvalues λ there is another large eigenvalue $-\lambda$ (see Figure 8.4 top right); this is not the case for the other eigenvalues (see Figure 8.4 lower right).*
- *For $\Re\beta<0$ and fixed $\Im\beta$ the eigenvalues are increasing exponentially for $\Re\beta$ decreasing. For fixed $\Re\beta$ the eigenvalues grow exponentially with increasing $\Im\beta$. A lot of eigenvalues cluster around ±1 (see Figure 8.4 lower left), whose number increases as $\Re\beta$ decreases.*

We expect these observations to be true for all $(\Gamma_0(n),\chi\equiv 1)$. In section 8.1.1 we noticed that our approximation is getting worse for large $\Im\beta$ and negative $\Re\beta$; this seems to be related to the appearance of large eigenvalues. To obtain reliable results for the smaller eigenvalues we have to increase the precision p of the numbers we are using for the computations and also the number N of Taylor coefficients in the approximation. This is also the reason why we performed most of our calculations for $0\leq\Im\beta\leq 10$ and $0\leq\Re\beta\leq 1$, since increasing the precision p or the number N of Taylor coefficients increases the computation time quite a lot.

It would be nice to find an explanation for the eigenvalues which cluster around ±1 for $\Re\beta<0$, obviously these eigenvalues create a lot of very small terms when computing the Selberg zeta function. On the other hand, we also see very large eigenvalues for $\Re\beta<0$, which create very large terms in the Selberg zeta function. These large terms should cancel at least some of the very small terms from the eigenvalues around ±1. Numerically this situation creates some problems, since care should be taken regarding which order to multiply the terms. The eigenvalues for $\Re\beta=\frac{1}{2}$ which rotate around 0 and pass ±1 when $\Im\beta$ varies, correspond to zeros of the Selberg zeta function and therefore to the eigenvalues of the hyperbolic Laplacian. Unfortunately, not much is known analytically about the spectrum of the transfer operator, so we cannot compare the observations in 8.1.21 to any known facts. Instead, we will compare our observations to known properties of the Selberg zeta function, see (6.4) - (6.6) in section 6.3: in [Hej76] it is shown that the Selberg zeta function behaves for $\Re\beta\geq 2$ as $Z(\beta)=1+O\left(m(\Gamma)^{-\Re\beta}\right)$; this corresponds to our observation that the eigenvalues of the transfer operator decrease with $\Re\beta$ exponentially for $\Re\beta>\frac{1}{2}$. For $-1\leq\Re\beta\leq 2$ the Selberg zeta function behaves like $|Z(\beta)|\leq\exp\left(O\left((\Im\beta)^2\right)\right)$, which corresponds to our observation that the eigenvalues are increasing with $\Im\beta$ for $0\leq\Re\beta\leq\frac{1}{2}$. Also the behavior of the Selberg zeta function for $\Re\beta\leq-1$ as $|Z(\beta)|\leq\exp\left(O\left(|\beta|^2\right)\right)$ corresponds to our observation that for $\Re\beta<0$ the eigenvalues increase exponentially for decreasing $\Re\beta<0$ and growing $\Im\beta$.

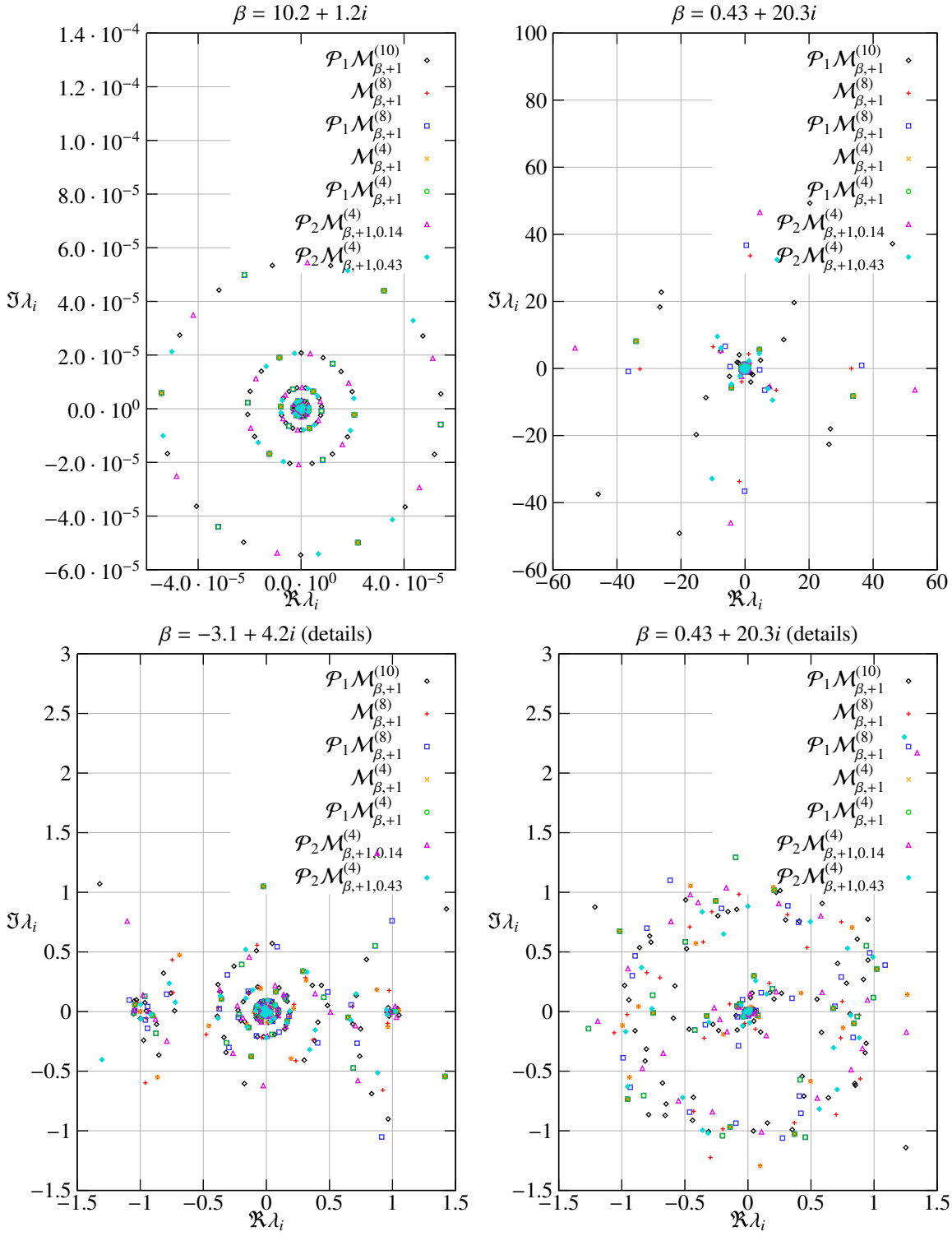

Figure 8.4: Spectrum $\{\lambda_i\}$ of $\mathcal{M}^{(n)}_{\beta,\varepsilon}$, $\mathcal{P}_1\mathcal{M}^{(n)}_{\beta,\varepsilon}$ and $\mathcal{P}_2\mathcal{M}^{(4)}_{\beta,\varepsilon,\alpha}$ in the β-plane

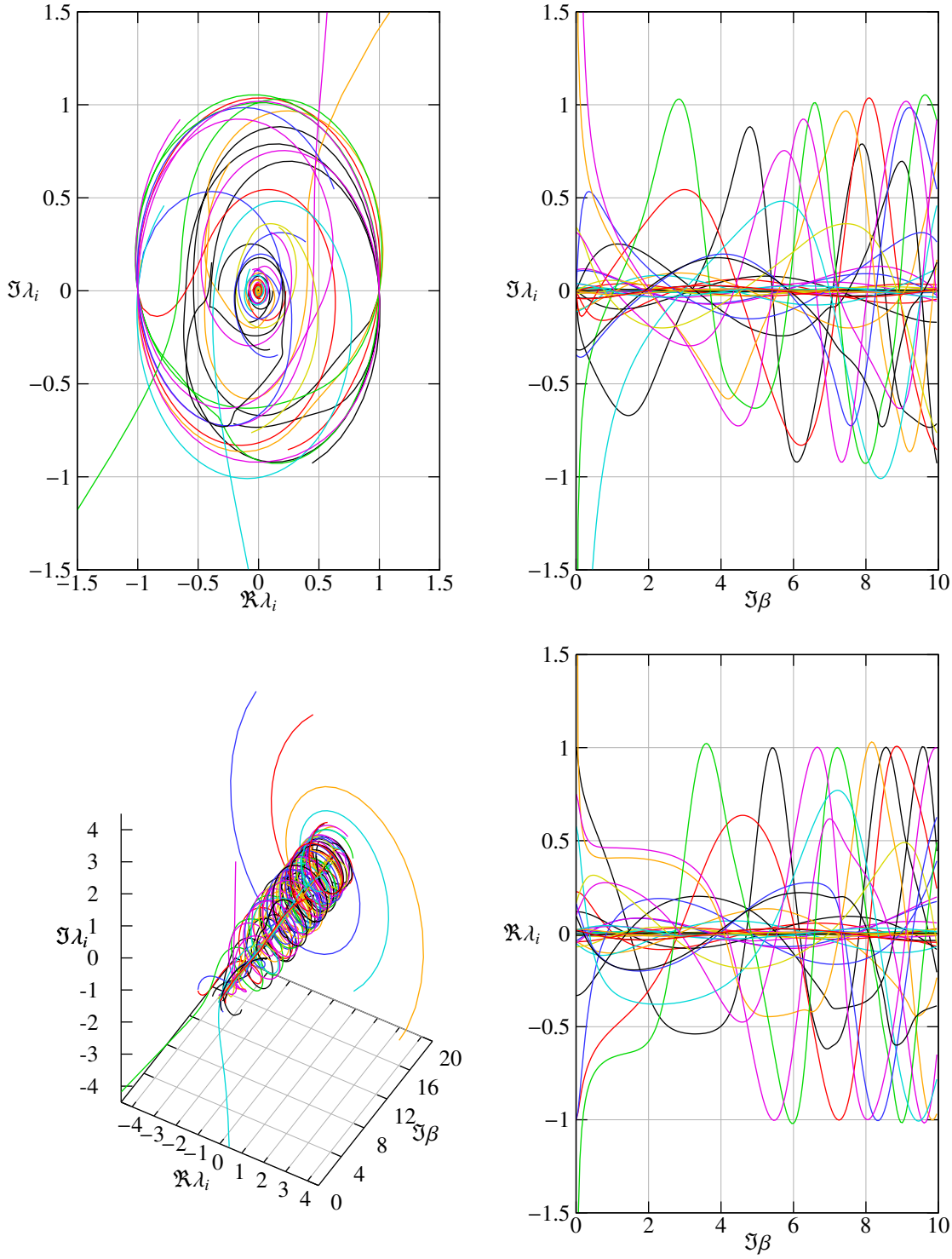

Figure 8.5: Spectrum $\{\lambda_i\}$ of $\mathcal{P}_2\mathcal{M}^{(4)}_{\beta,+1}$ for $\beta = 0.5 + i\Im\beta$ and $0.005 \leq \Im\beta \leq 10$

We investigated also the spectrum of the transfer operator for $(\Gamma_0(4), \chi_\alpha^{(4)})$ when α changes, especially the case when $\alpha \to 0$:

Experimental Observation 8.1.22. *For $(\Gamma_0(4), \chi_\alpha^{(4)})$, $\alpha \in [0, \frac{1}{2}]$ we have for $\mathcal{P}_2\mathcal{L}^{(4)}_{\beta,\varepsilon,\alpha}$ and $\beta \in \mathbb{C}$:*

- *For $\Re\beta > \frac{1}{2}$ and fixed β the eigenvalues rotate on some curves around 0 as α changes. The curves of the eigenvalues of $\mathcal{P}_2\mathcal{L}^{(4)}_{\beta,\varepsilon,\alpha}$ converge to the eigenvalues of $\mathcal{P}_2\mathcal{L}^{(4)}_{\beta,\varepsilon,0}$ for $\alpha \to 0$.*
- *For $\Re\beta = \frac{1}{2}$ and fixed β the eigenvalues of $\mathcal{P}_2\mathcal{L}^{(4)}_{\beta,\varepsilon,\alpha}$ move on more or less straight lines for $0 \ll \alpha \leq 0.5$ (see Figure 8.6). For fixed β the situation changes dramatically as $\alpha \to 0$ (see Figure 8.7): the eigenvalues are rotating on constant closed orbits when α changes; the speed of the rotation grows exponentially with α getting smaller. One of these orbits passes -1 and close to $+0.75$; six eigenvalues are located on this orbit (see Figure 8.7 top left). Increasing $\Im\beta$ changes the shape of these orbits and the rotation speed increases exponentially with $\Im\beta$, but the orbits remain closed and there is always one orbit which goes through -1. Obviously, the eigenvalues of $\mathcal{P}_2\mathcal{L}^{(4)}_{\beta,\varepsilon,\alpha}$ have no limit points for $\alpha \to 0$, i.e. the spectrum of the transfer operator $\mathcal{P}_2\mathcal{L}^{(4)}_{\beta,\varepsilon,\alpha}$ does not converge to the spectrum of the operator $\mathcal{P}_2\mathcal{L}^{(4)}_{\beta,\varepsilon,0}$ for $\alpha \to 0$.*
- *For $\Re\beta < \frac{1}{2}$ and fixed β the eigenvalues of $\mathcal{P}_2\mathcal{L}^{(4)}_{\beta,\varepsilon,\alpha}$ grow exponentially as $\alpha \to 0$. The eigenvalues of $\mathcal{P}_2\mathcal{L}^{(4)}_{\beta,\varepsilon,\alpha}$ have no limit points for $\alpha \to 0$, i.e. the spectrum of the transfer operator $\mathcal{P}_2\mathcal{L}^{(4)}_{\beta,\varepsilon,\alpha}$ does not converge to the spectrum of the operator $\mathcal{P}_2\mathcal{L}^{(4)}_{\beta,\varepsilon,0}$ for $\alpha \to 0$.*

From these results we see that for $\beta \leq \frac{1}{2}$ the spectrum of $\mathcal{P}_2\mathcal{L}^{(4)}_{\beta,\varepsilon,\alpha}$ changes completely as soon as we "turn on" the parameter α, i.e. α is set to a non-integer value. This result corresponds to the fact that the perturbation by $\chi_\alpha^{(4)}$ in $\alpha = 0$ is singular, since two cusps are closed when α is set to a non-integer value. We see also that since there are eigenvalues of $\mathcal{P}_2\mathcal{L}^{(4)}_{\beta,\varepsilon,\alpha}$ on closed orbits passing through -1 for $\Re\beta = \frac{1}{2}$ and $\alpha \to 0$, we can find a zero of the Selberg zeta function at every $\Im\beta > 0$ for some small α, which means also that there is an eigenvalue of the hyperbolic Laplacian. We will investigate this issue in the next section when we study the Selberg zeta function on $\Re\beta = \frac{1}{2}$ for $\alpha \to 0$.

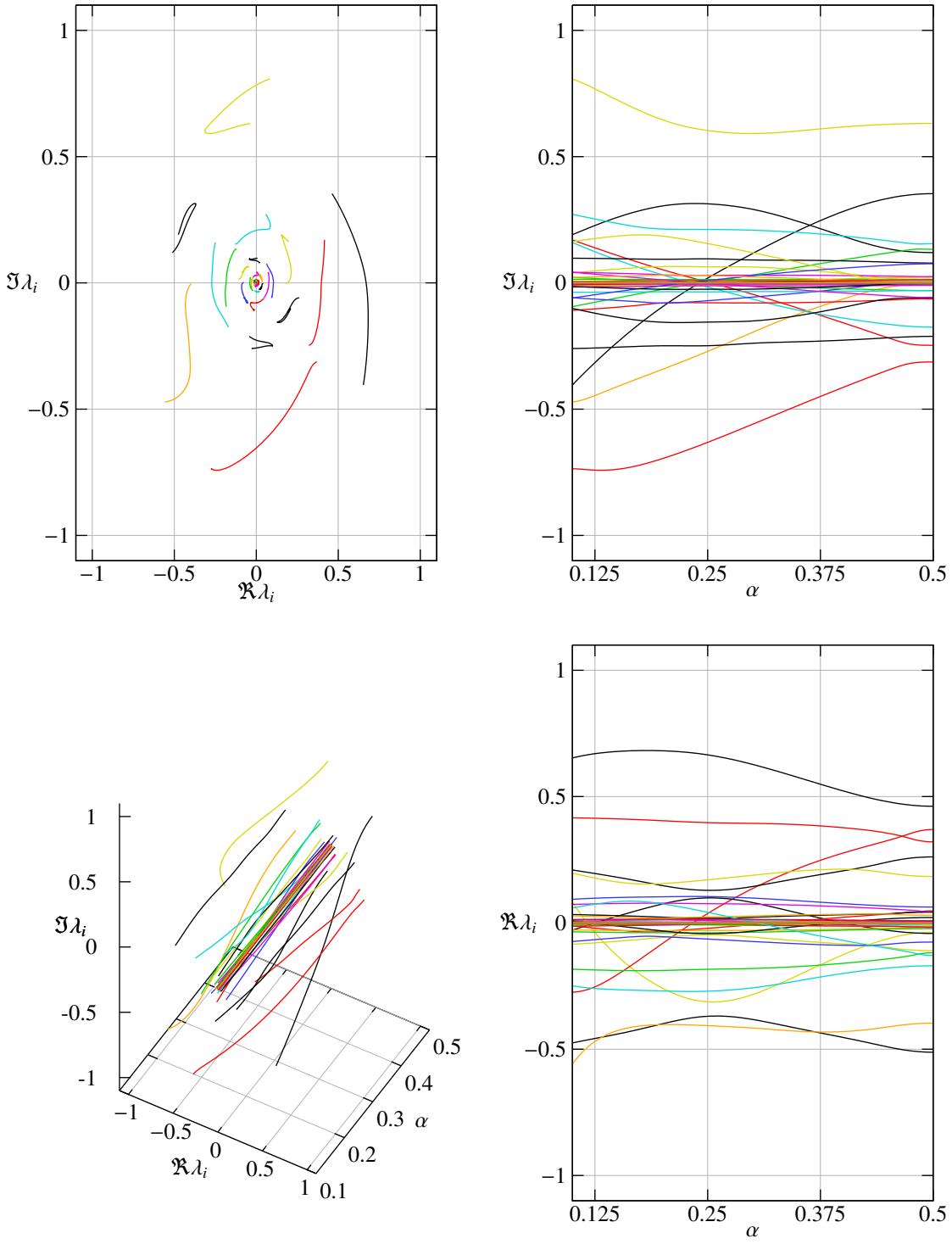

Figure 8.6: Spectrum $\{\lambda_i\}$ of $\mathcal{P}_2\mathcal{M}^{(4)}_{\beta,+1,\alpha}$ for $\beta = 0.5 + 1i$ and $0.1 \leq \alpha \leq 0.5$

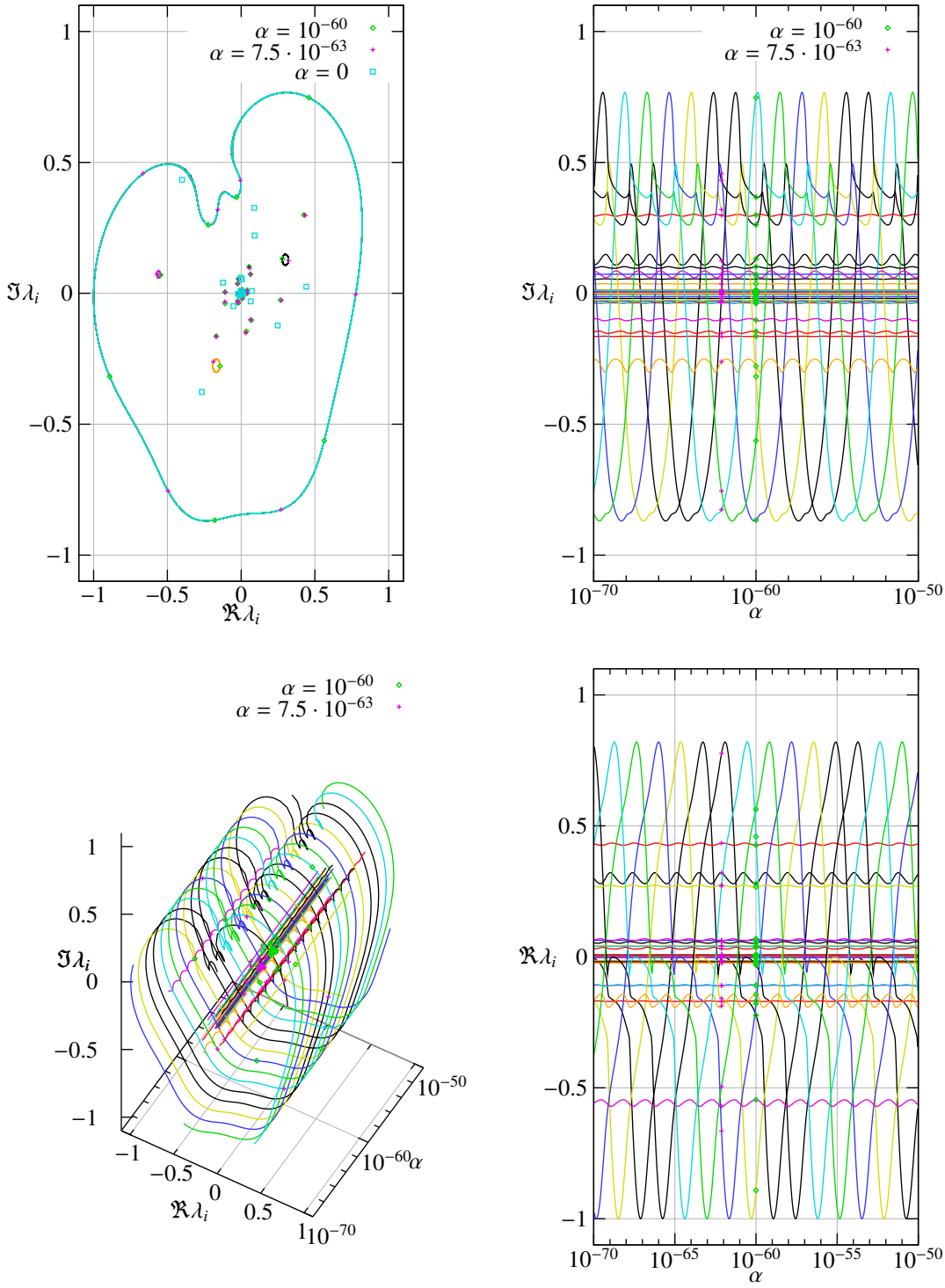

Figure 8.7: Spectrum $\{\lambda_i\}$ of $\mathcal{P}_2\mathcal{M}^{(4)}_{\beta,+1,\alpha}$ for $\beta = 0.5 + 1i$ and $10^{-70} \leq \alpha \leq 10^{-50}$

8.2 Numerical results for the Selberg zeta function and its zeros

In this section we present the results from our numerical investigations of the Selberg zeta function $Z^{(n)}(\beta,\chi)$ for $(\Gamma_0(n),\chi)$ and its zeros. The Selberg zeta function $Z^{(n)}(\beta,\chi) = \det(1-\mathcal{L}^{(n)}_{\beta,+1,\chi}\mathcal{L}^{(n)}_{\beta,-1,\chi})$ can be approximated by

$$Z^{(n)}_{\mathcal{M}}(\beta,\chi) = \det(1-\mathcal{M}^{(n)}_{\beta,+1,\chi}\mathcal{M}^{(n)}_{\beta,-1,\chi}) = \prod_{i=1}^{\mu_n N}(1-\lambda_i) \tag{8.6}$$

with the matrix $\mathcal{M}^{(n)}_{\beta,\varepsilon,\chi}$ defined in proposition 7.4.11, and $\lambda_i \in \sigma(\mathcal{M}^{(n)}_{\beta,+1,\chi}\mathcal{M}^{(n)}_{\beta,-1,\chi})$. Using the operators $\{\mathcal{P}_k\}_{1\le k\le h_n}$ in section 8.1.3 the Selberg zeta function is given by $Z^{(n)}(\beta,\chi) = \det(1-\mathcal{P}_k\mathcal{L}^{(n)}_{\beta,\varepsilon,\chi})\det(1+\mathcal{P}_k\mathcal{L}^{(n)}_{\beta,\varepsilon,\chi})$, which can be approximated by

$$Z^{(n)}_{\mathcal{M}}(\beta,\chi) = \det(1-\mathcal{P}_k\mathcal{M}^{(n)}_{\beta,+1,\chi})\det(1+\mathcal{P}_k\mathcal{M}^{(n)}_{\beta,+1,\chi}) = \prod_{i=1}^{\mu_n N}(1-\lambda_i)\,(1+\lambda_i) \tag{8.7}$$

with $\lambda_i \in \sigma(\mathcal{P}_k\mathcal{M}^{(n)}_{\beta,+1,\chi})$. We investigated the Selberg zeta functions $Z^{(4)}(\beta,\chi^{(4)}_{\alpha_1,\alpha_2})$ and $Z^{(8)}(\beta,\chi^{(8)}_{\alpha_1,\alpha_2,\alpha_3})$ under the character deformations of section 6.5. We have mainly studied the zeros of the Selberg zeta functions $Z^{(4)}(\beta,\chi^{(4)}_{\alpha}) = Z^{(4)}(\beta,\chi^{(4)}_{\alpha,0})$ and $Z^{(8)}(\beta,\chi^{(8)}_{\alpha}) = Z^{(8)}(\beta,\chi^{(8)}_{0,\alpha,0})$ for $0 \le \alpha \le 0.5$. Since the operators $\mathcal{P}_k$ exist only for $(\Gamma_0(n),\chi\equiv 1)$ and $(\Gamma_0(4),\chi^{(4)}_{\alpha})$ we have used formula (8.7) only in these cases, otherwise we had to use formula (8.6).

We denote the set of zeros of the Selberg zeta function $Z^{(n)}(\beta,\chi)$ in the β-plane for fixed $(\Gamma_0(n),\chi)$ and counted according to their multiplicity by

$$\mathcal{Z}^{(n)}_{\chi} = \left\{\beta\in\mathbb{C} : Z^{(n)}(\beta,\chi) = 0\right\} \tag{8.8}$$

and put

$$\mathcal{Z}^{(n)}_{\alpha} := \mathcal{Z}^{(n)}_{\chi^{(n)}_{\alpha}}.$$

For $(\Gamma_0(4),\chi^{(4)}_{\alpha})$ one can determine when a zero in $\mathcal{Z}^{(4)}_{\alpha}$ comes from the eigenvalue $+1$ or -1 of $\mathcal{P}_2\mathcal{L}^{(4)}_{\beta,\varepsilon,\alpha}$: we define $\mathcal{Z}^{(4)}_{\alpha,+1}$ respectively $\mathcal{Z}^{(4)}_{\alpha,-1}$ to be the corresponding subsets of $\mathcal{Z}^{(4)}_{\alpha}$

$$\mathcal{Z}^{(4)}_{\alpha,\pm 1} = \left\{\beta\in\mathcal{Z}^{(4)}_{\alpha} : \pm 1 \in \sigma(\mathcal{P}_2\mathcal{L}^{(4)}_{\beta,\varepsilon,\alpha})\right\}. \tag{8.9}$$

Note that $\mathcal{P}_2\mathcal{L}^{(4)}_{\beta,+1,\alpha}$ and $\mathcal{P}_2\mathcal{L}^{(4)}_{\beta,-1,\alpha}$ have the same spectrum, see section 8.1.3. Obviously

$$\mathcal{Z}^{(4)}_{\alpha} = \mathcal{Z}^{(4)}_{\alpha,+1}\cup\mathcal{Z}^{(4)}_{\alpha,-1}.$$

As mentioned in section 6.3 the zeros of the Selberg zeta function $Z^{(n)}(\beta,\chi)$ on the critical line $\Re\beta = \frac{1}{2}$ are related to the eigenvalues λ of the hyperbolic Laplacian through $\lambda = \beta(1-\beta)$, while the zeros of $Z^{(n)}(\beta,\chi)$ in $\Re\beta < \frac{1}{2}$, $\Im\beta > 0$ are related to the poles of the determinant $\varphi(\beta,\chi)$ of the scattering matrix. This obviously allows us to study a perturbation of the hyperbolic Laplacian by a character deformation $\chi^{(4)}_{\alpha}$ for $\Gamma_0(4)$ and $\chi^{(8)}_{\alpha}$ for $\Gamma_0(8)$. It was proved in [PS91] that $(\Gamma_0(4),\chi^{(4)}_{\alpha})$ is arithmetic only for the special values $\alpha\in\{0,\frac{1}{8},\frac{2}{8},\frac{3}{8},\frac{4}{8}\}$, and according to their conjecture in [PS94] only for these values $(\Gamma_0(4),\chi^{(4)}_{\alpha})$ should be essentially cuspidal, see also section 6.4. The perturbations by $\chi^{(4)}_{\alpha}$ and $\chi^{(8)}_{\alpha}$ are singular around $\alpha\in\mathbb{Z}$, since setting α to a non-integer value closes cusps and thus the multiplicity of the continuous spectrum changes suddenly. In case of $\Gamma_0(4)$ the multiplicity changes from three to one and for $\Gamma_0(8)$ from four to two. The deformation at the values $\alpha\in\{\frac{1}{8},\frac{2}{8},\frac{3}{8},\frac{4}{8}\}$ for $\Gamma_0(4)$ corresponds then to a non-singular perturbation of the Laplacian for arithmetic $(\Gamma_0(4),\chi^{(4)}_{\alpha})$, while the deformation at $\alpha = 0$ corresponds to a singular one.

Our numerical results for $(\Gamma_0(8),\chi_\alpha^{(8)})$ show that the character $\chi_\alpha^{(8)}$ is arithmetic only for $\alpha \in \{0,\frac{1}{2}\}$. A perturbation of the Laplacian for arithmetic $(\Gamma_0(8),\chi_\alpha^{(8)})$ at $\alpha = \frac{1}{2}$ is non-singular and at $\alpha = 0$ is singular. By studying $0 \le \alpha \le 0.5$ we have hence investigated both singular and non-singular perturbations for $\Gamma_0(4)$ and $\Gamma_0(8)$. Besides the usual problems arising with a singular perturbation, see [Kat80], there are several other difficulties: The discrete spectrum of the hyperbolic Laplacian is embedded in its continuous spectrum and some of the discrete eigenvalues are degenerate, which makes it hard in any case to apply perturbation theory in this case. Also, a phenomenon which was predicted for $\Gamma_0(4)$ by Selberg in [Sel90] Theorem 3, and which we will call the "Selberg phenomenon", says that

> "Given a T_0 and an $\varepsilon > 0$, there exists a $\delta = \delta(\varepsilon, T_0) > 0$, such that for $0 < |\alpha| < \delta$, $\varphi(\beta,\chi_{0,\frac{\alpha}{2\pi}}^{(4)})$ always has a zero in $|\beta - \beta_0| < \varepsilon$ where $\beta_0 = \frac{1}{2} + it_0$, $|t_0| \le T_0$."

Thereby φ is the determinant of the scattering matrix for $(\Gamma_0(4),\chi_{0,\frac{\alpha}{2\pi}}^{(4)})$. The zeros of $\varphi(\beta,\chi)$ in the region $\Re\beta > \frac{1}{2}$ correspond to poles of φ for $\Re\beta < \frac{1}{2}$, see also section 6.2, and hence are also the zeros of the Selberg zeta function $Z^{(n)}(\beta,\chi)$ in $\Re\beta < \frac{1}{2}$. As we have shown in section 6.5 the Selberg zeta function for the character $\chi_{0,\alpha}^{(4)}$ is the same as the one for the character $\chi_\alpha^{(4)} := \chi_{\alpha,0}^{(4)}$, thus the zeros related to the Selberg phenomenon manifest themselves also as zeros of the Selberg zeta function for the deformation by the character $\chi_\alpha^{(4)}$ which we have studied . We call "Selberg zeros" the zeros of the Selberg zeta function related to the Selberg phenomenon. We found numerically that for $\alpha \to 0$ these zeros are moving down towards $\beta = \frac{1}{2}$ and are getting dense very near to the left of the critical line $\Re\beta = \frac{1}{2}$. And we found numerically a similar phenomenon also for $(\Gamma_0(8),\chi_\alpha^{(8)})$ as $\alpha \to 0$. As we will see later, the situation for $\Gamma_0(4)$ is even more complicated since we found for $\alpha \to 0$ also zeros on the critical line, whose behavior is similar to the zeros from the Selberg phenomenon, namely moving towards $\beta = \frac{1}{2}$ and getting dense on the critical line $\Re\beta = \frac{1}{2}$. Obviously, this makes perturbation theory for the Laplacian very difficult if not impossible. An advantage of our method is that we are able to study the whole range of the deformation parameter $0 \le \alpha \le 0.5$, whereas theoretical methods are usually limited to some small neighborhood $\alpha_0 - \delta < \alpha < \alpha_0 + \delta$. This makes it possible to start the deformation at $\alpha = 0.5$ and to change α in small steps until α becommes very small. Indeed, we are not only able to see the Selberg phenomenon but also where the corresponding zeros of the Selberg zeta function come from. As we will see later, there are other interesting phenomena concerning the behavior of the zeros of the Selberg zeta function for $\alpha \to 0$.

To verify our implementation of the Selberg zeta function we compared our numerical results with known theoretical and numerical facts. For a verification of the poles and zeros of the Selberg zeta function see section 8.2.2. Unfortunately, to our knowledge no other implementations of the Selberg zeta function with character deformations exist, so we cannot compare them directly. The following verifications of our implementation of the Selberg zeta function $Z^{(n)}(\beta,\chi)$ in this section were performed for $(\Gamma_0(n),\chi \equiv 1)$, and $1 \le n \le 10$, $(\Gamma_0(4),\chi_{\alpha_1,\alpha_2}^{(4)})$ respectively $(\Gamma_0(8),\chi_{\alpha_1,\alpha_2,\alpha_3}^{(8)})$ for random $\beta \in \mathbb{C}$ and random $0 \le \alpha_i \le 0.5$.

As expected, we found numerically that the Selberg zeta function for $(\Gamma_0(n),\chi)$ is real for $\beta \in \mathbb{R}$, which follows from the product definition (6.2). Furthermore, numerical computations show that also the relation

$$Z^{(n)}(\beta,\chi) = Z^{(n)}(\beta,\bar{\chi}) \tag{8.10}$$

holds, which is known to be true [Hej08]. Because of (8.10) we can restrict the parameter α in the characters $\chi_\alpha^{(4)}$ and $\chi_\alpha^{(8)}$ to $0 \le \alpha \le 0.5$. Another relation which follows from ([Hej83], p. 499, (5.5)) and (8.10) is given by

$$Z^{(n)}(\beta,\chi) = \overline{Z^{(n)}(\bar{\beta},\chi)},$$

which we verified numerically as well.

The functional equation (6.7) of the Selberg zeta function can be used to compute the determinant of the scattering matrix as

$$\varphi(\beta,\chi) = \eta(\beta)\frac{Z^{(n)}(1-\beta,\chi)}{Z^{(n)}(\beta,\chi)}.$$

For this we implemented the function $\eta(\beta)$ in (6.8) for $(\Gamma_0(4), \chi \equiv 1)$ and $(\Gamma_0(4), \chi_\alpha^{(4)})$, given in (6.28) and (6.29) in section 6.5 to compute the determinant of the scattering matrix. Since not much is known about the determinant of the scattering matrix for non-arithmetic χ, we cannot compare it in this case to theoretical results. We checked if it fulfills the formulas from section 6.2, i.e. the functional equation $\varphi(\beta,\chi)\varphi(1-\beta,\chi) = 1$ and if $|\varphi(\frac{1}{2} + i\Im\beta,\chi)| = 1$. Our calculations confirm both formulas.

We checked for $(\Gamma_0(n), \chi \equiv 1)$ if properties (6.4) - (6.6) in section 6.3 of the Selberg zeta function $Z^{(n)}(\beta) := Z^{(n)}(\beta, \chi \equiv 1)$ are satisfied, namely

$$\begin{aligned} Z^{(n)}(\beta) &= 1 + O\left(m(\Gamma)^{-\Re\beta}\right) && \text{for } \Re\beta \geq 2, \text{ where } 1 < m(\Gamma) < \infty \\ \left|Z^{(n)}(\beta)\right| &\leq \exp\left(O\left((\Im\beta)^2\right)\right) && \text{for } -1 \leq \Re\beta \leq 2 \\ \left|Z^{(n)}(\beta)\right| &\leq \exp\left(O\left(|\beta|^2\right)\right) && \text{for } \Re\beta \leq -1, \end{aligned}$$

Indeed, we found them to be true. Further numerical experiments showed that:

Experimental Observation 8.2.1. *For $(\Gamma_0(n), \chi \equiv 1)$, $1 \leq n \leq 10$, and $(\Gamma_0(4), \chi_\alpha^{(4)})$ we have for $\beta \in \mathbb{C}$ and fixed α:*

- *For $\Re\beta > \frac{1}{2}$ there are practically no oscillations of the real and imaginary parts of the Selberg zeta function $Z^{(n)}(\beta,\chi)$ in the β-plane.*
- *For $0 \leq \Re\beta \leq \frac{1}{2}$ the absolute value of $Z^{(n)}(\beta,\chi)$ increases with $\Im\beta$. Also oscillations of the real and imaginary parts of $Z^{(n)}(\beta,\chi)$ appear in the β-plane, which are getting stronger with increasing $\Im\beta$.*
- *For $\Re\beta < 0$ the absolute value of $Z^{(n)}(\beta,\chi)$ increases both with $\Re\beta$ and $\Im\beta$. Strong oscillations of the real and imaginary parts of $Z^{(n)}(\beta,\chi)$ can be found everywhere in the β-plane, getting stronger with $|\beta|$ increasing.*

We expect this observation to be true for all $(\Gamma_0(n), \chi \equiv 1)$. Note that these oscillations make tracking of the zeros of the Selberg zeta function in the region $\Re\beta \leq \frac{1}{2}$ very difficult. Indeed, this is one of the reasons we restricted our computations in most cases to $-5 \leq \Re\beta \leq 1$ and $\Im\beta < 10$. On the other hand, the dependence of the Selberg zeta functions $Z^{(4)}(\beta,\chi_\alpha^{(4)})$ and $Z^{(8)}(\beta,\chi_\alpha^{(8)})$ on α is quite complicated. Analogous to our observation 8.1.22 for the spectrum of the transfer operator we found for the Selberg zeta function that:

Experimental Observation 8.2.2. *For $(\Gamma_0(4), \chi_\alpha^{(4)})$ we have for $\beta \in \mathbb{C}$ and $\alpha \in [0, \frac{1}{2}]$:*

- *For $\Re\beta > \frac{1}{2}$ and fixed β as $\alpha \to 0$ the Selberg zeta function $Z^{(4)}(\beta,\chi_\alpha^{(4)})$ converges to $Z^{(4)}(\beta,\chi_0^{(4)})$, i.e. $\lim_{\alpha\to 0} Z^{(4)}(\beta,\chi_\alpha^{(4)})$ exists.*
- *For $\Re\beta = \frac{1}{2}$ and fixed β as $\alpha \to 0$ the real and imaginary parts of $Z^{(4)}(\beta,\chi_\alpha^{(4)})$ oscillates very fast; therefore $\lim_{\alpha\to 0} Z^{(4)}(\beta,\chi_\alpha^{(4)})$ does not exist.*
- *For $\Re\beta < \frac{1}{2}$ and fixed β the absolute value of $Z^{(4)}(\beta,\chi_\alpha^{(4)})$ grows exponentially as $\alpha \to 0$ and at the same time also strong oscillations of the real and imaginary parts of $Z^{(4)}(\beta,\chi_\alpha^{(4)})$ appear, $\lim_{\alpha\to 0} Z^{(4)}(\beta,\chi_\alpha^{(4)})$ does not exist.*

In principle this observation says that the functions $Z^{(4)}(\beta,\chi_\alpha^{(4)})$, $\alpha \neq 0$ and $Z^{(4)}(\beta,\chi_0^{(4)})$ are completely different, and that $Z^{(4)}(\beta,\chi_\alpha^{(4)})$ is non-analytic in $\alpha = 0$. This observation describes just the general behavior; later we will explain in more detail what happens to the zeros of $Z^{(4)}(\beta,\chi_\alpha^{(4)})$ as $\alpha \to 0$. To visualise the dramatic change from $Z^{(4)}(\beta,\chi_0^{(4)})$ to $Z^{(4)}(\beta,\chi_\alpha^{(4)})$ even for infinitesimal $\alpha \neq 0$, we plot both functions in the β-plane for $\alpha = 0$ and $\alpha = 10^{-15}$, see Figure 8.8. The positive values of $\Re Z^{(4)}(\beta,\chi_\alpha^{(4)})$ and $\Im Z^{(4)}(\beta,\chi_\alpha^{(4)})$ are colored yellow-orange, while the negative ones are colored blue-turquoise. The border line between the

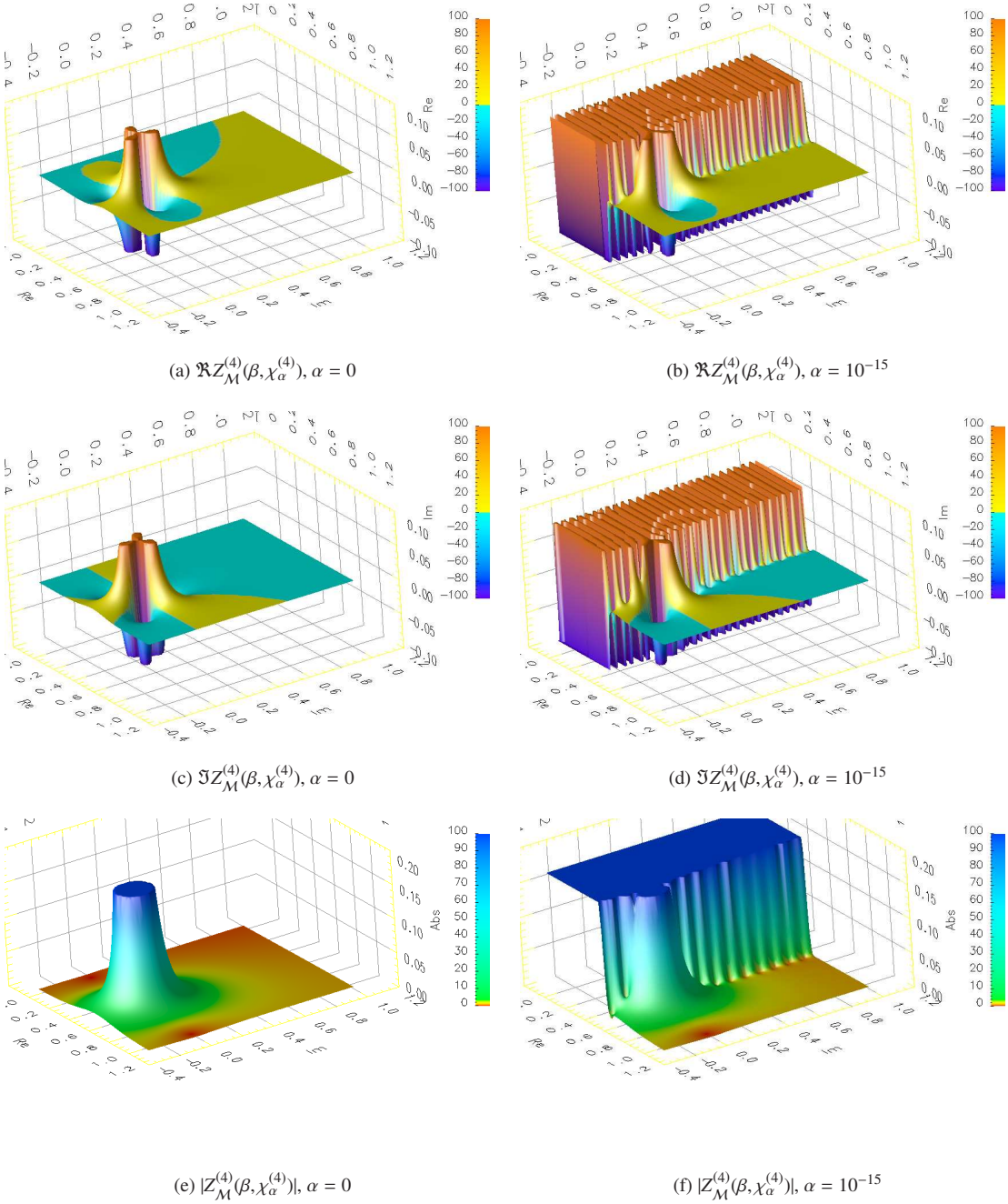

(a) $\Re Z_{\mathcal{M}}^{(4)}(\beta,\chi_\alpha^{(4)})$, $\alpha = 0$

(b) $\Re Z_{\mathcal{M}}^{(4)}(\beta,\chi_\alpha^{(4)})$, $\alpha = 10^{-15}$

(c) $\Im Z_{\mathcal{M}}^{(4)}(\beta,\chi_\alpha^{(4)})$, $\alpha = 0$

(d) $\Im Z_{\mathcal{M}}^{(4)}(\beta,\chi_\alpha^{(4)})$, $\alpha = 10^{-15}$

(e) $|Z_{\mathcal{M}}^{(4)}(\beta,\chi_\alpha^{(4)})|$, $\alpha = 0$

(f) $|Z_{\mathcal{M}}^{(4)}(\beta,\chi_\alpha^{(4)})|$, $\alpha = 10^{-15}$

Figure 8.8: Selberg zeta function $Z_{\mathcal{M}}^{(4)}(\beta,\chi_\alpha^{(4)})$ for $-0.05 \leq \Re\beta \leq 1.05$ and $-0.306 \leq \Im\beta \leq 1.0$

colors blue and yellow is where the value of the Selberg zeta function is zero. For the absolute value of the Selberg zeta function we colored the values near to zero red, as expected we see for $\alpha = 0$ zeros at $\beta = 0$ and $\beta = 1$. We can see in this figure that for $\Re\beta \leq \frac{1}{2}$ both functions are completely different, with lots of zeros on and near the critical line for $\alpha = 10^{-15}$, see Figure (f). Note also the strong oscillations for $\Re\beta < \frac{1}{2}$ and $\alpha = 10^{-15}$. For $\Re\beta > \frac{1}{2}$ both functions appear practically the same.

In lemma 6.5.2 we found the following relations for the Selberg zeta function $Z^{(4)}(\beta, \chi^{(4)}_{\alpha_1,\alpha_2})$:

$$\begin{aligned} Z^{(4)}(\beta,\chi^{(4)}_{\alpha_1,\alpha_2}) &= Z^{(4)}(\beta,\chi^{(4)}_{\alpha_1,-\alpha_2-\alpha_1}) \\ Z^{(4)}(\beta,\chi^{(4)}_{\alpha_1,\alpha_2}) &= Z^{(4)}(\beta,\chi^{(4)}_{\alpha_2,\alpha_1}) \\ Z^{(4)}(\beta,\chi^{(4)}_{\alpha_1,\alpha_2}) &= Z^{(4)}(\beta,\chi^{(4)}_{-\alpha_1,-\alpha_2}). \end{aligned}$$

To verify our implementation we tested these relations for random values of $\beta \in \mathbb{C}$ and $0 \leq \alpha_1, \alpha_2 \leq 0.5$. Indeed, we found that in all cases these relations hold. For the character $\chi^{(4)}_\alpha := \chi^{(4)}_{\alpha,0}$ we found numerically another identity for the Selberg zeta function:

Conclusion 8.2.3. *For* $(\Gamma_0(4), \chi^{(4)}_\alpha)$ *the following identity holds for* $\beta \in \mathbb{C}$

$$Z^{(4)}(\beta,\chi^{(4)}_{\frac{1}{4}}) = Z^{(4)}(\beta,\chi^{(4)}_{\frac{1}{2}}). \tag{8.11}$$

Note that we did not find any other values of α for which such an identity holds. When α moves away from $\frac{1}{4}$ respectively $\frac{1}{2}$ the functions become different and their zeros move in different directions. Also, the spectra of the transfer operators $\mathcal{P}_2\mathcal{L}^{(4)}_{\beta,\varepsilon,\frac{1}{4}}$ and $\mathcal{P}_2\mathcal{L}^{(4)}_{\beta,\varepsilon,\frac{1}{2}}$ are different, indeed even the eigenvalues ± 1 of $\mathcal{P}_2\mathcal{L}^{(4)}_{\beta,\varepsilon,\frac{1}{4}}$ and $\mathcal{P}_2\mathcal{L}^{(4)}_{\beta,\varepsilon,\frac{1}{2}}$ which correspond to the same zero β can be different, i.e. $\mathcal{Z}^{(4)}_{\frac{1}{4}} = \mathcal{Z}^{(4)}_{\frac{1}{2}}$ but $\mathcal{Z}^{(4)}_{\frac{1}{4},\pm 1} \neq \mathcal{Z}^{(4)}_{\frac{1}{2},\pm 1}$. Also, formula (7.10) suggests that the traces of the powers of the transfer operators $\mathcal{P}_2\mathcal{L}^{(4)}_{\beta,\varepsilon,\frac{1}{4}}$ and $\mathcal{P}_2\mathcal{L}^{(4)}_{\beta,\varepsilon,\frac{1}{2}}$ might be equal. But we found that already the traces of $\mathcal{P}_2\mathcal{L}^{(4)}_{\beta,\varepsilon,\frac{1}{4}}$ and $\mathcal{P}_2\mathcal{L}^{(4)}_{\beta,\varepsilon,\frac{1}{2}}$ are different. Indeed, we expect from our numerical results that the trace of $\mathcal{P}_2\mathcal{L}^{(4)}_{\beta,\varepsilon,\frac{1}{4}}$ vanishes for every $\beta \in \mathbb{C}$, see conclusion 8.1.15. On the other hand, the trace of $\mathcal{P}_2\mathcal{L}^{(4)}_{\beta,\varepsilon,\frac{1}{2}}$ changes with $\beta \in \mathbb{C}$. For other arithmetic $\chi^{(4)}_\alpha$, with $\alpha \in \{0, \frac{1}{8}, \frac{3}{8}\}$, the Selberg zeta functions do not coincide, we found however in these cases that the set of zeros of the Selberg zeta function for one α is contained in the set of zeros for another α, see conclusion 8.2.7.

In lemma 6.5.4 we showed relations between the characters $\chi^{(4)}_{\alpha_1,\alpha_2}$ restricted to $\Gamma_0(8)$ and $\chi^{(8)}_{\alpha_1,\alpha_2,\alpha_3}$, namely $\chi^{(4)}_{\alpha_1,\alpha_2} = \chi^{(8)}_{2\alpha_2,\alpha_1,\alpha_1}$ and $\chi^{(4)}_{\alpha_1,\alpha_2+\frac{1}{2}} = \chi^{(8)}_{2\alpha_2,\alpha_1,\alpha_1}$. They suggest that also the Selberg zeta functions for $(\Gamma_0(4), \chi^{(4)}_{\alpha_1,\alpha_2})$ and $(\Gamma_0(8), \chi^{(8)}_{\alpha_1,\alpha_2,\alpha_3})$ might be related. Indeed, we found numerically such a relation:

Conclusion 8.2.4. *For* $(\Gamma_0(4), \chi^{(4)}_{\alpha_1,\alpha_2})$ *and* $(\Gamma_0(8), \chi^{(8)}_{\alpha_1,\alpha_2,\alpha_3})$ *the following identity holds for* $\beta \in \mathbb{C}$

$$Z^{(8)}\left(\beta,\chi^{(8)}_{2\alpha_2,\alpha_1,\alpha_1}\right) = Z^{(4)}\left(\beta,\chi^{(4)}_{\alpha_1,\alpha_2}\right) Z^{(4)}\left(\beta,\chi^{(4)}_{\alpha_1,\alpha_2+\frac{1}{2}}\right). \tag{8.12}$$

Obviously, for the characters $\chi^{(4)}_\alpha := \chi^{(4)}_{\alpha,0}$ and $\chi^{(8)}_\alpha := \chi^{(8)}_{0,\alpha,0}$ formula (8.12) can be applied only for $\alpha = 0$, i.e.

$$Z^{(8)}\left(\beta,\chi^{(8)}_0\right) = Z^{(4)}\left(\beta,\chi^{(4)}_0\right) Z^{(4)}\left(\beta,\chi^{(4)}_{\frac{1}{2}}\right). \tag{8.13}$$

Note, that we used $Z^{(4)}(\beta,\chi^{(4)}_{0,\frac{1}{2}}) = Z^{(4)}(\beta,\chi^{(4)}_{\frac{1}{2},0})$ here, see (6.25). Obviously, because of (8.11) we can write (8.13) also as $Z^{(8)}\left(\beta,\chi^{(8)}_0\right) = Z^{(4)}\left(\beta,\chi^{(4)}_0\right) Z^{(4)}\left(\beta,\chi^{(4)}_{\frac{1}{4}}\right)$. We found numerically another factorization, which cannot be explained by the factorization (8.12):

Conclusion 8.2.5. *For* $(\Gamma_0(4), \chi_\alpha^{(4)})$ *and* $(\Gamma_0(8), \chi_\alpha^{(8)})$ *the following identity holds for* $\beta \in \mathbb{C}$

$$Z^{(8)}\left(\beta, \chi^{(8)}_{\frac{1}{2}}\right) = Z^{(4)}\left(\beta, \chi^{(4)}_{\frac{1}{8}}\right) Z^{(4)}\left(\beta, \chi^{(4)}_{\frac{3}{8}}\right). \tag{8.14}$$

Relations (8.13) and (8.14) connect the Selberg zeta functions for arithmetic $(\Gamma_0(8), \chi_\alpha^{(8)})$ to the one for arithmetic $(\Gamma_0(4), \chi_\alpha^{(4)})$. We also checked if the traces of the corresponding transfer operators for the Selberg zeta functions for $(\Gamma_0(8), \chi_\alpha^{(8)})$ on the lhs of (8.13) and (8.14) coincide with the sum of the traces of the corresponding transfer operators for the Selberg zeta functions for $(\Gamma_0(4), \chi_\alpha^{(4)})$ on the rhs, but this does not seem to be the case. Indeed, we expect from our numerical computations that $\operatorname{tr} \mathcal{P}_2 \mathcal{L}^{(4)}_{\beta,\varepsilon,0} + \operatorname{tr} \mathcal{P}_2 \mathcal{L}^{(4)}_{\beta,\varepsilon,\frac{1}{2}}$ and $\operatorname{tr} \mathcal{P}_2 \mathcal{L}^{(4)}_{\beta,\varepsilon,\frac{1}{8}} + \operatorname{tr} \mathcal{P}_2 \mathcal{L}^{(4)}_{\beta,\varepsilon,\frac{3}{8}}$ vanish for every $\beta \in \mathbb{C}$, see conclusion 8.1.18. On the other hand, the traces of the transfer operators for $(\Gamma_0(8), \chi_\alpha^{(8)})$ for $\alpha = 0$ and $\alpha = \frac{1}{2}$ depend on $\beta \in \mathbb{C}$. According to [May11] formula (8.12) can be proven by using the factorization formula in [CM01] for a subgroup of another subgroup of the modular group. Relation (8.14), on the other hand, remains unproven.

8.2.1 Tracking of the zeros of the Selberg zeta function in the β-plane for $\alpha \in [0, 0.5]$

The main focus of the numerical part of this thesis is the tracking of the zeros of the Selberg zeta function $Z^{(n)}(\beta, \chi_\alpha^{(n)})$ for $(\Gamma_0(4), \chi_\alpha^{(4)})$ and $(\Gamma_0(8), \chi_\alpha^{(8)})$. All zeros $\mathcal{Z}_\alpha^{(n)}$ of $Z^{(n)}(\beta, \chi_\alpha^{(n)})$ in the (β, α)-plane are given by

$$\mathcal{W}^{(n)} = \left\{(\beta, \alpha) : \beta \in \mathcal{Z}_\alpha^{(n)}, \alpha \in [0, \frac{1}{2}]\right\}. \tag{8.15}$$

Let $(\beta_i, \alpha_i) \in \mathcal{W}^{(n)}$ be a zero of the Selberg zeta function i.e. $Z^{(n)}(\beta_i, \chi^{(n)}_{\alpha_i}) = 0$, with multiplicity one; let $\psi_i^{(n)}$ be a continuous map

$$\psi_i^{(n)} : A_i \to \mathcal{Z}_\cdot^{(n)} \tag{8.16}$$

on some interval $A_i \subseteq [0, \frac{1}{2}]$ such that $\psi_i^{(n)}(\alpha_i) = \beta_i$ and $(\psi_i^{(n)}(\alpha), \alpha) \in \mathcal{W}^{(n)}$ for all $\alpha \in A_i$, and

$$\psi_i^{(n)}(\alpha) \neq \psi_j^{(n)}(\alpha) \quad \text{for } i \neq j \text{ and all } \alpha \in A_i \cap A_j,$$

except for possible discrete points $\alpha_s \in A_i \cap A_j$ with $\psi_i^{(n)}(\alpha_s) = \psi_j^{(n)}(\alpha_s)$. The set of all points on a path $\psi_i^{(n)}$ is given by

$$\mathcal{V}_i^{(n)} = \left\{(\beta, \alpha) : \beta = \psi_i^{(n)}(\alpha), \alpha \in A_i\right\}. \tag{8.17}$$

For $(\Gamma_0(4), \chi_\alpha^{(4)})$ we can define $\mathcal{W}^{(4)}_{\pm 1}$, $\psi^{(4)}_{i,\pm 1}$ and $\mathcal{V}^{(4)}_{i,\pm 1}$ corresponding to the eigenvalues $+1$ and -1 of the transfer operator $\mathcal{P}_2 \mathcal{L}^{(4)}_{\beta,\varepsilon,\alpha}$, as

$$\mathcal{W}^{(4)}_{\pm 1} = \left\{(\beta, \alpha) : \beta \in \mathcal{Z}^{(4)}_{\alpha,\pm 1}, \alpha \in [0, \frac{1}{2}]\right\}, \tag{8.18}$$

$$\psi^{(4)}_{i,\pm 1} : A_{i,\pm 1} \to \mathcal{Z}^{(4)}_{\cdot,\pm 1} \tag{8.19}$$

and

$$\mathcal{V}^{(4)}_{i,\pm 1} = \left\{(\beta, \alpha) : \beta = \psi^{(4)}_{i,\pm 1}(\alpha), \alpha \in A_{i,\pm 1}\right\}. \tag{8.20}$$

Our aim is to find the $\mathcal{V}_j^{(n)}$ in the (β, α)-plane. We define the distance function d in an obvious way

$$d\left((\beta_1, \alpha_1), (\beta_2, \alpha_2)\right) = \sqrt{(\Re\beta_1 - \Re\beta_2)^2 + (\Im\beta_1 - \Im\beta_2)^2 + (\alpha_1 - \alpha_2)^2}. \tag{8.21}$$

Obviously, we can compute only discrete points $(\beta_i, \alpha_i) \in \mathcal{V}_j^{(n)}$ on such curves with our implementation of the Selberg zeta function. We will compute these points with a small distance such that

$$d((\beta_i, \alpha_i), (\beta_{i-1}, \alpha_{i-1})) \leq C_d, \tag{8.22}$$

where we usually choose $C_d = 10^{-3}$. Even if we compute the points $\{(\beta_i, \alpha_i)\}$ with such small distances, it is possible that we accidentally jump over from one curve $\mathcal{V}_j^{(n)}$ to another $\mathcal{V}_k^{(n)}$ if both curves are very close to each other. Fortunately, since we are computing the Selberg zeta function via the transfer operator $\mathcal{P}_2\mathcal{L}^{(4)}_{\beta,\varepsilon,\alpha}$ for $(\Gamma_0(4), \chi_\alpha^{(4)})$ respectively $\mathcal{L}^{(8)}_{\beta,+1,\alpha}\mathcal{L}^{(8)}_{\beta,-1,\alpha}$ for $(\Gamma_0(8), \chi_\alpha^{(8)})$, we can search in the spectrum of these transfer operators for a given $(\beta_i, \alpha_i) \in \mathcal{V}_j^{(n)}$ for eigenvalues which are near to ± 1 for $\Gamma_0(4)$ respectively $+1$ for $\Gamma_0(8)$. If we find an eigenvalue λ_i of the transfer operator close to ± 1 respectively $+1$ besides the one which corresponds to the zero at $(\beta_i, \alpha_i) \in \mathcal{V}_j^{(n)}$ of the Selberg zeta function which we are tracking, we can conclude that another zero of the Selberg zeta function is close by. Let $(\beta', \alpha') \in \mathcal{V}_k^{(n)}$ be a zero on the curve $\mathcal{V}_k^{(n)}$ which is close to $(\beta_i, \alpha_i) \in \mathcal{V}_j^{(n)}$. Assuming that $|\lambda_i - 1|$ respectively $|\lambda_i + 1|$ is proportional to the distance $d((\beta_i, \alpha_i), (\beta', \alpha'))$, we define

$$\begin{aligned} d_\lambda^i &= |1 - \lambda_i| \quad \text{if } \lambda_i \text{ is close to } +1 \\ d_\lambda^i &= |1 + \lambda_i| \quad \text{if } \lambda_i \text{ is close to } -1. \end{aligned}$$

Obviously, if d_λ^i is small it tells us that possibly an eigenvalue ± 1 and therefore a zero of the Selberg zeta function is nearby in the β-plane, but it does not tell us where it is or if this zero really exists. Obviously, this definition of d_λ^i is only useful if the multiplicity of the zero at (β_i, α_i) is one, i.e. there is no other eigenvalue ± 1, (as we will see later, we found numerically that the multiplicity of the zeros of the Selberg zeta function can be different to one only for certain values of α, i.e. in the case $(\Gamma_0(4), \chi_\alpha^{(4)})$ for $\alpha = 0$ and in the case $(\Gamma_0(8), \chi_\alpha^{(8)})$ for $\alpha \in \{0, \frac{1}{2}\}$). If d_λ^i is below a certain threshold we reduce the distance between the points $\{(\beta_i, \alpha_i)\}$, and replace equation (8.22) by

$$d((\beta_{i+1}, \alpha_{i+1}), (\beta_i, \alpha_i)) \leq C_d^{i+1}, \tag{8.23}$$

where C_d^{i+1} is given by

$$C_d^{i+1} = \begin{cases} C_d \cdot d_\lambda^i \cdot 10 & \text{if } d_\lambda^i < 0.1 \\ C_d & \text{else.} \end{cases} \tag{8.24}$$

The basic idea for how to determine the next point $(\beta_{i+1}, \alpha_{i+1}) \in \mathcal{V}_j^{(n)}$ after the point $(\beta_i, \alpha_i) \in \mathcal{V}_j^{(n)}$ is to increase α_i by some small constant $\delta\alpha$, such that $\alpha_{i+1} = \alpha_i + \delta\alpha$, and finally use Newton's method to find the zero β_{i+1} of the Selberg zeta function for α_{i+1}. Instead of choosing a fixed constant $\delta\alpha$ we will use an adaptive algorithm, which tries to determine the optimal $\delta\alpha_{i+1}$ with

$$\alpha_{i+1} = \alpha_i + \delta\alpha_{i+1},$$

such that the point $(\beta_{i+1}, \alpha_{i+1})$ is not too far away from (β_i, α_i); therefore satisfying (8.23). On the other hand, $\delta\alpha_{i+1}$ also has to be chosen in such a way that $d((\beta_{i+1}, \alpha_{i+1}), (\beta_i, \alpha_i))$ is not too small, since otherwise the computation of the curves of zeros would take too long. An adequate choice of $\delta\alpha_{i+1}$ is such that $d((\beta_{i+1}, \alpha_{i+1}), (\beta_i, \alpha_i)) \approx C_d^{i+1}/(1.05)$. Since $d((\beta_{i+1}, \alpha_{i+1}), (\beta_i, \alpha_i)) \ll 1$ and usually $|\beta_{i+1} - \beta_i| \gg |\alpha_{i+1} - \alpha_i|$ we assume that the distance $d((\beta_{i+1}, \alpha_{i+1}), (\beta_i, \alpha_i))$ is more or less proportional to $\delta\alpha_{i+1}$. Thus, we determine $\delta\alpha_{i+1}$ based on $\delta\alpha_i$ and the distance between the last two computed points (β_i, α_i) and $(\beta_{i-1}, \alpha_{i-1})$ according to

$$\delta\alpha_{i+1} = \begin{cases} \delta\alpha_i & \text{if } i = 0 \\ \delta\alpha_i \frac{C_d^{i+1}/(1.05)}{d((\beta_i, \alpha_i), (\beta_{i-1}, \alpha_{i-1}))} & \text{else.} \end{cases} \tag{8.25}$$

Obviously, if the distance between the last two points is smaller than $C_d^{i+1}/(1.05)$, $\delta\alpha_{i+1}$ will be larger than $\delta\alpha_i$, i.e. the step size will be increased, and if the distance was larger then $C_d^{i+1}/(1.05)$, $\delta\alpha_{i+1}$ will be smaller then $\delta\alpha_i$, i.e. the step size will be reduced. We usually choose for the initial value $\delta\alpha_0 = 10^{-4}$.

Next we have to locate the zero β_{i+1} of the Selberg zeta function in the β-plane for a given α_{i+1}. We can do this by using Newton's method from section 2.5. Obviously, the outcome and the number of iterations of Newton's method depends mostly on the initial value β_{i+1}^0, which should be as close as possible to the zero β_{i+1}. Since $d((\beta_i,\alpha_i),(\beta_{i-1},\alpha_{i-1}))$ is very small we will use the last two points (β_i,α_i) and $(\beta_{i-1},\alpha_{i-1})$ for a linear extrapolation to get the initial point β_{i+1}^0 which should be near to the zero β_{i+1} for small $d((\beta_{i+1},\alpha_{i+1}),(\beta_i,\alpha_i))$. We hence define

$$\Re\beta_{i+1}^0 = \begin{cases} \Re\beta_i & \text{if } i=0 \\ \Re\beta_i + \delta\alpha_{i+1}\frac{\Re\beta_i-\Re\beta_{i-1}}{\alpha_i-\alpha_{i-1}} & \text{else} \end{cases} \tag{8.26}$$

$$\Im\beta_{i+1}^0 = \begin{cases} \Im\beta_i & \text{if } i=0 \\ \Im\beta_i + \delta\alpha_{i+1}\frac{\Im\beta_i-\Im\beta_{i-1}}{\alpha_i-\alpha_{i-1}} & \text{else.} \end{cases} \tag{8.27}$$

Newton's method

$$N_{\alpha_{i+1}}^{C_Z}(\beta_{i+1}^0) := N_{Z_{\mathcal{M}}^{(n)}(\cdot,\chi_{\alpha_{i+1}}^{(n)})}^{C_Z}(\beta_{i+1}^0) \tag{8.28}$$

as defined in (2.12) then gives

$$\left|Z_{\mathcal{M}}^{(n)}\left(N_{\alpha_{i+1}}^{C_Z}(\beta_{i+1}^0),\chi_{\alpha_{i+1}}^{(n)}\right)\right| = \left|Z_{\mathcal{M}}^{(n)}\left(\beta_{i+1},\chi_{\alpha_{i+1}}^{(n)}\right)\right| < C_Z,$$

with $\beta_{i+1} = N_{\alpha_{i+1}}^{C_Z}(\beta_{i+1}^0)$, and C_Z a small constant, for which we usually choose $C_Z = 10^{-10}$. By Newton's method we get a point in the β-plane where the absolute value of the Selberg zeta function is smaller than C_Z. Even if we choose C_Z very small we cannot be sure that this is really a zero of the Selberg zeta function. To check if a supposed zero is a true zero one would have to use the argument principle, but it is impractical to check every single point, since the computation time would greatly increase. Instead, we check only several points on a curve by the argument principle.

In case the new computed zero at $(\beta_{i+1},\alpha_{i+1})$ is too far away from the last one (β_i,α_i), i.e.

$$d((\beta_{i+1},\alpha_{i+1}),(\beta_i,\alpha_i)) > C_d^{i+1},$$

we disregard $(\beta_{i+1},\alpha_{i+1})$, re-define $\delta\alpha_{i+1}$ based on the distance between $(\beta_{i+1},\alpha_{i+1})$ and (β_i,α_i) with

$$\delta\alpha'_{i+1} = \delta\alpha_{i+1}\frac{C_d^{i+1}/(1.05)}{d((\beta_{i+1},\alpha_{i+1}),(\beta_i,\alpha_i))}, \quad \delta\alpha_{i+1} := \delta\alpha'_{i+1}$$

and re-compute $(\beta_{i+1},\alpha_{i+1})$.

Finally we get a sequence of points

$$\begin{aligned} S\left((\beta_0,\alpha_0),\delta\alpha_0,\alpha_{\text{end}},C_Z,C_d\right) = \{(\beta_i,\alpha_i) \quad : \quad & 0\le i\le N, \alpha_i\in[\alpha_0,\alpha_{\text{end}}], \left|Z^{(n)}(\beta_i,\chi_{\alpha_i}^{(n)})\right| < C_Z, \\ & d\left((\beta_{i+1},\alpha_{i+1}),(\beta_i,\alpha_i)\right) \le C_d\}, \end{aligned}$$

which depends on the initial point (β_0,α_0), the initial step size $\delta\alpha_0$, the final value of α given by α_{end}, the maximal absolute value C_Z of the Selberg zeta function at (β_i,α_i) and the maximal distance between two points C_d. We usually choose $\delta\alpha_0 = 10^{-4}$, $C_Z = 10^{-10}$ and $C_d = 10^{-3}$. For (β_0,α_0) we usually take a zero on one of the lines $\Re\beta\in\{0,\frac{1}{4},\frac{1}{2}\}$ when $\chi_{\alpha_0}^{(n)}$ is arithmetic. In most cases it is not possible to compute all the points (β_i,α_i) on a curve for $0\le\alpha_i\le 0.5$ by a single computation; instead we compute subintervals of a curve with different parameters given by

$$S_l = S\left(\left(\beta_0^l,\alpha_0^l\right),\delta\alpha_0^l,\alpha_{\text{end}}^l,C_Z^l,C_d^l\right).$$

As the initial point (β_0^l,α_0^l) we take the last point of the last sequence $(\beta_N^{l-1},\alpha_N^{l-1}=\alpha_{\text{end}}^{l-1})$. Then the union of these sets contains computed points which belong to a single curve. For practical reasons we have denoted

the curves of zeros of the Selberg zeta function in the (β,α)-plane by the letter "S" followed by a positive integer:

$$\mathrm{S}\,r = \bigcup_{l=1}^{M} S_l = \{(\beta_i,\alpha_i) : \beta_i \in \mathcal{Z}^{(n)}_{\alpha_i}, \text{ ordered by } \alpha_i \text{ ascending}\}, \quad r \in \mathbb{Z}_{>},$$

with $S_l = S_l(r)$ and $M = M(r)$. For $(\Gamma_0(4),\chi^{(4)}_\alpha)$ we have the collection of these sets $\{\mathrm{S}\,r\}_{1\le r\le 46}$ and for $(\Gamma_0(8),\chi^{(8)}_\alpha)$ the collection $\{\mathrm{S}\,r\}_{1\le r\le 8}$. We save these sets with additional information, like the eigenvalue $+1$ or -1 of the transfer operator to which this zero corresponds and possible other eigenvalues ±1 nearby, in files named by "n4-deform-S r.data" for $(\Gamma_0(4),\chi^{(4)}_\alpha)$ resp. "n8-deform-S r.data" for $(\Gamma_0(8),\chi^{(8)}_\alpha)$. The files contain usually between 1 000 and 40 000 points, depending on the kind of zeros we are tracking. The typical computation time for one set usually takes between 2 and 4 months for $(\Gamma_0(4),\chi^{(4)}_\alpha)$. The set of points $\mathrm{S}\,r$ for $(\Gamma_0(n),\chi^{(n)}_\alpha)$ should approximate discrete points (β_i,α_i) on a curve $\mathcal{V}^{(n)}_r$.

In certain cases we want to see how the zeros (β,α) of the Selberg zeta function left of the critical line $\Re\beta = \frac{1}{2}$ approach this line for $\Re\beta \to \frac{1}{2}$, and in case they touch the critical line $\Re\beta = \frac{1}{2}$ we want to compute the corresponding values of β and α. A simple but effective way to study the zeros for $\Re\beta \to \frac{1}{2}$ is to reduce the distance between the points (β_i,α_i) by reducing the constant C_d^{i+1} in (8.23) as soon as a zero (β_i,α_i) is close to the critical line. We can do this by re-defining C_d^{i+1} in the following way

$$\begin{aligned} C'^{i+1}_d &= \begin{cases} (\frac{1}{2} - \Re\beta_i)\cdot 0.9 & \text{if } C_d^{i+1} > (\frac{1}{2} - \Re\beta_i)\cdot 0.9 \\ C_d^{i+1} & \text{else} \end{cases} \\ C_d^{i+1} &:= C'^{i+1}_d. \end{aligned}$$

Since we are reducing C_d^{i+1} depending on the distance of a zero β_i to the critical line $\Re\beta = \frac{1}{2}$, this zero will never reach the critical line $\Re\beta = \frac{1}{2}$, but approaches it in smaller and smaller steps.

To compute the exact value α for which the path $\psi^{(n)}_j(\alpha)$ touches the critical line $\Re\beta = \frac{1}{2}$ we have to determine the zero of the function

$$F(\alpha) = 0.5 - \Re(\psi^{(n)}_j(\alpha)).$$

For this we will again use Newton's method, with

$$\alpha_{i+1} = \alpha_i - \frac{F(\alpha_i)}{\partial_\alpha F(\alpha_i)},$$

such that $\lim_{i\to\infty} F(\alpha_i) = 0$. The actual implementation is a bit tricky since we do not have a continuous path $\psi^{(n)}_j(\alpha)$, but we can compute the point β_i on it for a given α_i. We define the function

$$F_{\beta_i^0}(\alpha_i) = 0.5 - \Re N^{C_Z}_{\alpha_i}(\beta_i^0), \tag{8.29}$$

where $N^{C_Z}_{\alpha_i}(\beta_i^0) = \beta_i$ is given by Newton's method (8.28) to compute the zero β_i of the Selberg zeta function for α_i near to the initial value β_i^0. Since we only have a discrete set of points we will use the numerical derivation in section 2.6, given by

$$\partial_\alpha F_{\beta_i^0}(\alpha_i) = \frac{F_{\beta_i^0}(\alpha_i + h) - F_{\beta_i^0}(\alpha_i - h)}{2h}$$

where h is a small constant. The iteration of Newton's method to find the zero of (8.29) then gives

$$\beta_i^0 = \begin{cases} \beta_0 & \text{if } i = 0 \\ N^{C_Z}_{\alpha_{i-1}}(\beta^0_{i-1}) & \text{else} \end{cases} \tag{8.30}$$

$$\alpha_{i+1} = \alpha_i - 2h\frac{F_{\beta_i^0}(\alpha_i)}{F_{\beta_i^0}(\alpha_i + h) - F_{\beta_i^0}(\alpha_i - h)}. \tag{8.31}$$

We will stop the iterations if $|F_{\beta_i^0}(\alpha_i)| < C_R$, where C_R is a small constant, or if $F_{\beta_i^0}(\alpha_i + h) - F_{\beta_i^0}(\alpha_i - h) = 0$. For this computation we have to provide (β_0, α_0) which has to be as near as possible to a zero of the Selberg zeta function on the critical line $\Re\beta = \frac{1}{2}$.

For tracking the zeros on the curves $\mathcal{V}_j^{(n)}$ we need initial points (β_0, α_0): for this we determined the zeros of the Selberg zeta function on the lines $\Re\beta \in \{0, \frac{1}{4}, \frac{1}{2}\}$ for arithmetic $(\Gamma_0(4), \chi_\alpha^{(4)})$ and on the line $\Re\beta = \frac{1}{2}$ for arithmetic $(\Gamma_0(8), \chi_\alpha^{(8)})$, see Appendix D. As mentioned already we cannot use the zeros for $\alpha = 0$ as initial points, since a huge number of zeros appear on and near to the critical line $\Re\beta = \frac{1}{2}$ for a small change in α, which makes tracking these zeros impossible. Instead, we will use for $(\Gamma_0(4), \chi_\alpha^{(4)})$ the zeros for $\alpha = \frac{1}{8}$ and $\alpha = \frac{4}{8}$ as initial points and for $(\Gamma_0(8), \chi_\alpha^{(8)})$ the zeros for $\alpha = \frac{1}{2}$, and change α in small steps to arrive at $\alpha \to 0$. The zeros of the Selberg zeta function of $(\Gamma_0(8), \chi_\alpha^{(8)})$ for $\alpha = \frac{1}{2}$ can have multiplicities higher than one. In this case we will change α by a small constant h, to $\alpha = \frac{1}{2} - h$, such that the zeros split in the β-plane but do not move too far away. We can find these zeros in the β-plane and use them as initial points for our computation.

8.2.2 Zeros of the Selberg zeta function for $\Gamma_0(4)$ and $\Gamma_0(8)$

Before we discuss the curves of zeros of the Selberg zeta function $Z^{(n)}(\beta, \chi_\alpha^{(n)})$ in the (β, α)-plane for $(\Gamma_0(4), \chi_\alpha^{(4)})$ and $(\Gamma_0(8), \chi_\alpha^{(8)})$ we want to discuss some verifications of our computations. We have computed the Selberg zeta function in several regions of the β-plane for $(\Gamma_0(1), \chi \equiv 1)$, $(\Gamma_0(4), \chi_\alpha^{(4)})$ and $(\Gamma_0(8), \chi_\alpha^{(8)})$. This gave us an overview where the zeros and poles of the Selberg zeta function are located. As theoretically expected for $\Im\beta > 0$ we found zeros for $(\Gamma_0(1), \chi \equiv 1)$ only on the lines $\Re\beta \in \{\frac{1}{4}, \frac{1}{2}\}$ and for arithmetic $(\Gamma_0(4), \chi_\alpha^{(4)})$, i.e. $\alpha \in \{0, \frac{1}{8}, \frac{2}{8}, \frac{3}{8}, \frac{4}{8}\}$, only on the lines $\Re\beta \in \{0, \frac{1}{4}, \frac{1}{2}\}$. For non-arithmetic $(\Gamma_0(4), \chi_\alpha^{(4)})$ we found that the zeros for $\Im\beta > 0$ can be located at any point in $\Re\beta \leq \frac{1}{2}$, and that it never happens that all zeros are on some lines parallel to the imaginary axis. The result for $(\Gamma_0(4), \chi_\alpha^{(4)})$ agrees with the conjecture of Phillips and Sarnak, since they proved that $(\Gamma_0(4), \chi_\alpha^{(4)})$ is arithmetic only for the values of $\alpha \in \{0, \frac{1}{8}, \frac{2}{8}, \frac{3}{8}, \frac{4}{8}\}$ and conjectured that only then $(\Gamma_0(4), \chi_\alpha^{(4)})$ is essentially cuspidal (see section 6.4). For $(\Gamma_0(8), \chi_\alpha^{(8)})$ we found only two values for α where all zeros in $\Im\beta > 0$ are on lines $\Re\beta \in \{\frac{1}{4}, \frac{1}{2}\}$. We are led from our results together with the conjecture of Sarnak and Phillips to:

Conclusion 8.2.6. $(\Gamma_0(8), \chi_\alpha^{(8)})$ *is arithmetic only for* $\alpha \in \{0, \frac{1}{2}\}$.

Since the scattering matrix for $(\Gamma_0(n), \chi)$ with unitary character χ does not have poles in $\Re\beta > \frac{1}{2}$ except for a finite number on the interval $\frac{1}{2} < \beta \leq 1$, (see e.g. [Sel90]), it is clear that the zeros of the Selberg zeta function cannot be located in $\Re\beta > \frac{1}{2}$, $\Im\beta > 0$ and $\beta > 1$. Indeed, our numerical computations for the Selberg zeta function in the β-plane and our computations for tracking the zeros of the Selberg zeta function for $0 \leq \alpha \leq 0.5$ never showed any zero in the region $\Re\beta > \frac{1}{2}$, $\Im\beta > 0$ and $\beta > 1$ of the β-plane.

Now we want to take a closer look at the zeros and poles of the Selberg zeta function for $(\Gamma_0(1), \chi \equiv 1)$, and $(\Gamma_0(4), \chi_\alpha^{(4)})$ respectively $(\Gamma_0(8), \chi_\alpha^{(8)})$ arithmetic. The existence and the multiplicity of the zeros and poles were determined by numerical computations using the argument principle. The exact locations of these zeros were computed by Newton's method. In Appendix D we present tables with the zeros and poles of the Selberg zeta function for arithmetic $(\Gamma_0(4), \chi_\alpha^{(4)})$ with $\alpha \in \{0, \frac{1}{8}, \frac{2}{8}, \frac{3}{8}, \frac{4}{8}\}$ in the region $0 \leq \Re\beta \leq 1$, $0 \leq \Im\beta \leq 10$ and for arithmetic $(\Gamma_0(8), \chi_\alpha^{(8)})$ with $\alpha \in \{0, \frac{1}{2}\}$ on the critical line $\Re\beta = \frac{1}{2}$, $0 < \Im\beta \leq 10$. Unfortunately, we cannot verify the exact locations of the zeros of the Selberg zeta function on the lines $\Re\beta \in \{0, \frac{1}{4}, \frac{1}{2}\}$ as given in the tables in Appendix D for $(\Gamma_0(4), \chi_\alpha^{(4)})$ with $\alpha \in \{\frac{1}{8}, \frac{2}{8}, \frac{3}{8}, \frac{4}{8}\}$ and $(\Gamma_0(8), \chi_\alpha^{(8)})$ for $\alpha = \frac{1}{2}$ since no theoretical or independent numerical results exist. We compared the zeros of the Selberg zeta function for $\Gamma_0(4)$ and $\Gamma_0(8)$ for the trivial character, i.e. $\alpha = 0$, on the critical line $\Re\beta = \frac{1}{2}$ to the ones in [Str09b], it turns out that not only the values of $\Im\beta$ and the multiplicity of the zeros agree, but also the eigenvalues $+1$ and -1 of $\mathcal{P}_1 \mathcal{L}_{\beta,+1,\alpha}^{(n)}$ correspond exactly to the even $u(-\bar{z}) = u(z)$ and odd $u(-\bar{z}) = u(z)$

symmetries of the Maass wave forms $u(z)$. The results in [Str09b] were obtained numerically by a completely different approach by Strömberg, namely by computation of the eigenvalues of the hyperbolic Laplacian. Indeed, we have even found new zeros which were later confirmed by Strömberg and included in his list [Str09b]. For $(\Gamma_0(1),\chi \equiv 1)$, $(\Gamma_0(4),\chi_\alpha^{(4)})$ and $(\Gamma_0(8),\chi_\alpha^{(8)})$, with $\alpha = 0$ the zeros on the line $\Re\beta = \frac{1}{4}$ are as expected at the same locations as the zeros of the Riemann zeta function $\zeta_R(2\beta)$. For $(\Gamma_0(4),\chi_\alpha^{(4)})$ with $\alpha \in \{\frac{1}{8},\frac{2}{8},\frac{3}{8},\frac{4}{8}\}$ and $(\Gamma_0(8),\chi_\alpha^{(8)})$ with $\alpha = \frac{1}{2}$ some zeros of the Selberg zeta function are also on the line $\Re\beta = \frac{1}{4}$, which is in agreement with the generalized Riemann hypothesis (see also section 6.3). Furthermore, the multiplicity of the pole at $\beta = \frac{1}{2}$ and the multiplicity of the zeros on the line $\Re\beta = \frac{1}{4}$ of the Selberg zeta function for $(\Gamma_0(4),\chi_\alpha^{(4)})$ with $\alpha = 0$ is three, in agreement with the presence of three open cusps, and it changes to one for $\alpha \notin \mathbb{Z}$, which corresponds to the fact that two cusps are closed, (see also section 6.5). For $\alpha = \frac{1}{8}$ there is no pole of the Selberg zeta function at $\beta = \frac{1}{2}$, it is canceled by a zero which moves to $\beta = 1$ for $\alpha = 0$. In [BFM12] the scattering matrix for $(\Gamma_0(4),\chi \equiv 1)$ is given; it has a factor $(2^{2\beta}-1)^{-1}$, which obviously creates poles of the determinant of the scattering matrix at $\beta = \frac{i\pi m}{\ln 2}$, for all $m \in \mathbb{Z}$. Indeed, these are exactly the locations of the zeros of the Selberg zeta function for $\Gamma_0(4)$ and $\alpha = 0$ we have found on the line $\Re\beta = 0$. We found these zeros on the line $\Re\beta = 0$ also for $\Gamma_0(4)$ and $\alpha \in \{\frac{2}{8},\frac{4}{8}\}$. Furthermore, as expected we found for $(\Gamma_0(1),\chi \equiv 1)$, $(\Gamma_0(4),\chi_\alpha^{(4)})$ respectively $(\Gamma_0(8),\chi_\alpha^{(8)})$ and $\alpha = 0$ a zero of the Selberg zeta function at $\beta = 1$. There is no such zero at $\beta = 1$ for $(\Gamma_0(4),\chi_\alpha^{(4)})$ and $(\Gamma_0(8),\chi_\alpha^{(8)})$ with $\alpha \notin \mathbb{Z}$.

We already mentioned in conclusion 8.2.3 that the Selberg zeta functions for $(\Gamma_0(4),\chi_{\frac{1}{4}}^{(4)})$ and $(\Gamma_0(4),\chi_{\frac{1}{2}}^{(4)})$ coincide. We did not find for any other values of $\alpha \in \{0,\frac{1}{8},\frac{3}{8}\}$ such a relation, but as can be seen in the tables D.1 - D.5 in Appendix D, some zeros of the Selberg zeta function for $(\Gamma_0(4),\chi_\alpha^{(4)})$ coincide for different values of α:

Conclusion 8.2.7. *For arithmetic $(\Gamma_0(4),\chi_\alpha^{(4)})$ the following relations between the zeros $\mathcal{Z}_\alpha^{(4)}$ of the Selberg zeta function $Z^{(4)}(\beta,\chi_\alpha^{(4)})$ hold:*

- *The zeros $\mathcal{Z}_{\frac{3}{8}}^{(4)}$ of the Selberg zeta function $Z^{(4)}(\beta,\chi_{\frac{3}{8}}^{(4)})$ belong to the zeros $\mathcal{Z}_{\frac{1}{8}}^{(4)}$ of the Selberg zeta function $Z^{(4)}(\beta,\chi_{\frac{1}{8}}^{(4)})$ with the same multiplicity. i.e. $\mathcal{Z}_{\frac{3}{8}}^{(4)} \subset \mathcal{Z}_{\frac{1}{8}}^{(4)}$.*
- *The zeros $\mathcal{Z}_0^{(4)}$ of the Selberg zeta function $Z^{(4)}(\beta,\chi_0^{(4)})$ belong to the zeros $\mathcal{Z}_{\frac{2}{8}}^{(4)}$ of the Selberg zeta function $Z^{(4)}(\beta,\chi_{\frac{2}{8}}^{(4)})$ with different multiplicities. The same is true for the zeros $\mathcal{Z}_0^{(4)}$ and $\mathcal{Z}_{\frac{4}{8}}^{(4)}$, since $Z^{(4)}(\beta,\chi_{\frac{2}{8}}^{(4)}) = Z^{(4)}(\beta,\chi_{\frac{4}{8}}^{(4)})$, (see conclusion 8.2.3).*

This conclusion holds only for these values of α, when α is changing the coinciding zeros move in different directions. It also seems that the eigenvalues ± 1 of the transfer operators $\mathcal{P}_2\mathcal{L}_{\beta,\varepsilon,\frac{3}{8}}^{(4)}$ and $\mathcal{P}_2\mathcal{L}_{\beta,\varepsilon,\frac{1}{8}}^{(4)}$ which correspond to the same zero β of the Selberg zeta function always coincide, therefore

$$\mathcal{Z}_{\frac{3}{8},\pm 1}^{(4)} \subset \mathcal{Z}_{\frac{1}{8},\pm 1}^{(4)}.$$

Such a relation doesn't hold for the eigenvalues ± 1 of $\mathcal{P}_2\mathcal{L}_{\beta,\varepsilon,0}^{(4)}$ and $\mathcal{P}_2\mathcal{L}_{\beta,\varepsilon,\frac{2}{8}}^{(4)}$ respectively $\mathcal{P}_2\mathcal{L}_{\beta,\varepsilon,0}^{(4)}$ and $\mathcal{P}_2\mathcal{L}_{\beta,\varepsilon,\frac{4}{8}}^{(4)}$.

We investigated for arithmetic $(\Gamma_0(4),\chi_{\alpha_0}^{(4)})$ and arithmetic $(\Gamma_0(8),\chi_{\alpha_0}^{(8)})$ the order d_i of contact of the zeros of the Selberg zeta function $Z^{(n)}(\beta,\chi_\alpha^{(n)})$ to the critical line $\Re\beta = \frac{1}{2}$ for $\alpha \to \alpha_0$, given by

$$\frac{1}{2} - \Re(\psi_i^{(n)}(\alpha)) \sim C_i\,(\alpha-\alpha_0)^{d_i}\,, \tag{8.32}$$

with $\psi_i^{(n)}$ the path in (8.16) of a zero in the β-plane parametrised by α. The constants C_i and d_i obviously depend on the zero we are tracking. It turned out that the constant C_i is different for every path $\psi_i^{(n)}$, while

the d_i coincide for different paths. The results for $(\Gamma_0(4), \chi^{(4)}_{\alpha_0})$ with $\alpha_0 \in \{\frac{1}{8}, \frac{2}{8}, \frac{3}{8}, \frac{4}{8}\}$ are given in Tables D.2 - D.5 and the ones for $(\Gamma_0(8), \chi^{(8)}_{\alpha_0})$ with $\alpha_0 = \frac{1}{2}$ are given in Table D.7; in the column "O" the order d_i is given and the letter "E" instead of a number indicates that the corresponding zero stays on the critical line.

Experimental Observation 8.2.8. *For $(\Gamma_0(4), \chi^{(4)}_{\alpha_0})$ with $\alpha_0 \in \{\frac{1}{8}, \frac{2}{8}, \frac{3}{8}, \frac{4}{8}\}$ and $0 < \Im\beta \leq 10$, respectively for $(\Gamma_0(8), \chi^{(8)}_{\alpha_0})$ with $\alpha_0 = \frac{1}{2}$ and $0 < \Im\beta < 4.53$ we have for the order d_i of contact in (8.32) for $\alpha \to \alpha_0$:*

- *For $(\Gamma_0(4), \chi^{(4)}_{\alpha_0})$ and $\alpha_0 \in \{\frac{1}{8}, \frac{2}{8}, \frac{3}{8}\}$ the order of contact d_i is 2.*
- *For $(\Gamma_0(4), \chi^{(4)}_{\alpha_0})$ respectively $(\Gamma_0(8), \chi^{(8)}_{\alpha_0})$ and $\alpha_0 = \frac{4}{8} = \frac{1}{2}$ the order of contact d_i is 2 or 4.*

For $(\Gamma_0(4), \chi^{(4)}_{\alpha_0})$ respectively $(\Gamma_0(8), \chi^{(8)}_{\alpha_0})$ and $\alpha_0 = 0$ it is not possible to determine the order d_i. We will discuss later a new phenomenon how the zeros for $\alpha \to 0$ are converging towards the critical line, which is related to the fact that the perturbation is singular in this case. A fourth-order contact has been found numerically in [Ave07] for a deformation of the determinant of the scattering matrix in Teichmüller space, and in [PR10] such higher-order dissolving conditions for Maass wave forms are discussed. In conclusion 8.2.7 we mentioned that all zeros of the Selberg zeta function for $(\Gamma_0(4), \chi^{(4)}_0)$ are contained in the zeros of the Selberg zeta function for $(\Gamma_0(4), \chi^{(4)}_{\frac{4}{8}})$. We found that all zeros of the Selberg zeta function for $(\Gamma_0(4), \chi^{(4)}_{\frac{4}{8}})$ with $d_i = 4$ are also zeros of this function for $(\Gamma_0(4), \chi^{(4)}_0)$. Unfortunately, we do not have enough results to predict if this is a characteristic of these zeros or just a pure coincidence.

We see also from the results in Tables D.2 - D.5, that the zeros of the Selberg zeta function for $(\Gamma_0(4), \chi^{(4)}_\alpha)$ which leave the critical line are related to eigenvalue $+1$ of $\mathcal{P}_2\mathcal{M}^{(4)}_{\beta,+1,\alpha}$ and the ones which stay on the critical line to eigenvalues -1 of $\mathcal{P}_2\mathcal{M}^{(4)}_{\beta,+1,\alpha}$:

Conclusion 8.2.9. *For $(\Gamma_0(4), \chi^{(4)}_\alpha)$ and $0 < \alpha \leq \frac{1}{2}$ we find for the zeros $\mathcal{Z}^{(4)}_\alpha = \mathcal{Z}^{(4)}_{\alpha,+1} \cup \mathcal{Z}^{(4)}_{\alpha,-1}$ of the Selberg zeta function $Z^{(4)}\left(\beta, \chi^{(4)}_\alpha\right)$ in $\Im\beta > 0$:*

- *All zeros $\mathcal{Z}^{(4)}_{\alpha,-1}$ which correspond to eigenvalues -1 of the transfer operator $\mathcal{P}_2\mathcal{L}^{(4)}_{\beta,\varepsilon,\alpha}$ are on the critical line $\Re\beta = \frac{1}{2}$.*
- *All zeros $\mathcal{Z}^{(4)}_{\alpha,+1}$ which correspond to eigenvalues $+1$ of the transfer operator $\mathcal{P}_2\mathcal{L}^{(4)}_{\beta,\varepsilon,\alpha}$ are possibly on the critical line $\Re\beta = \frac{1}{2}$ only for certain discrete values of α and stay otherwise in $\Re\beta < \frac{1}{2}$.*

This conclusion indicates that the paths $\psi^{(n)}_i$ of these zeros are analytic for $0 < \alpha \leq \frac{1}{2}$. The zeros related to the eigenvalue $+1$ can be on the critical line $\Re\beta = \frac{1}{2}$ also for non-arithmetic $\chi^{(4)}_\alpha$. Conclusion 8.2.9 does not hold for $\alpha = 0$. Indeed, for $\alpha = 0$ there are zeros on $\Re\beta = \frac{1}{4}$ and $\Re\beta = 0$ related to the eigenvalue -1, see Table D.1. These zeros seem to exist only for $\alpha = 0$, they vanish immediately as soon as one changes α. Conclusion 8.2.9 does not hold also for $\Im\beta = 0$, since there are zeros on the real line at $\beta \in \mathbb{Z}_{\leq}$ for which it cannot be determined if they are related to the eigenvalue $+1$ or -1 of the transfer operator $\mathcal{P}_2\mathcal{L}^{(4)}_{\beta,\varepsilon,\alpha}$; since one cannot evaluate the spectrum of the transfer operator at these values of β. Instead we compute the spectrum in a point nearby, e.g., for a value of β very near to 0 we found that the transfer operator $\mathcal{P}_2\mathcal{L}^{(4)}_{\beta,\varepsilon,\alpha}$ has eigenvalues very near to $+1$ and -1, but the result from the argument principle shows that there is only one zero of the Selberg zeta function at $\beta = 0$. It seems very likely that one of the zeros which corresponds to the eigenvalues either $+1$ or -1 is canceled by a pole at $\beta = 0$, but it is not possible to determine which one is canceled.

In [PS94] it was shown that for $(\Gamma_0(4), \chi^{(4)}_\alpha)$ all Maass wave forms, which are odd with respect to the involution $\tau z = \frac{\bar{z}}{2\bar{z}-1}$ survive a character deformation and only the even ones can be destroyed. Since the symmetry corresponding to the operator $\mathcal{P}_2$ of the transfer operator $\mathcal{L}^{(4)}_{\beta,\varepsilon,\alpha}$ is the only symmetry which exists for $\alpha \neq 0$ and since our numerical experiments show that the zeros $\mathcal{Z}^{(4)}_{\alpha,-1}$ of the Selberg zeta function

$Z^{(4)}\left(\beta,\chi_\alpha^{(4)}\right)$ which correspond to the eigenvalue -1 of the transfer operator $\mathcal{P}_2\mathcal{L}^{(4)}_{\beta,\varepsilon,\alpha}$ stay on the critical line $\Re\beta=\frac{1}{2}$ (see conclusion 8.2.9), we concluded in 8.1.6 that the τ-odd Maass wave forms are related to the eigenvalue -1 of the operator $\mathcal{P}_2\mathcal{L}^{(4)}_{\beta,\varepsilon,\alpha}$. And since the zeros $\mathcal{Z}^{(4)}_{\alpha,+1}$ leave the critical line $\Re\beta=\frac{1}{2}$ we concluded that the eigenvalue $+1$ of the transfer operator $\mathcal{P}_2\mathcal{L}^{(4)}_{\beta,\varepsilon,\alpha}$ is related to τ-even Maass wave forms. Therefore, from our conclusions in 8.2.9 concerning the zeros $\mathcal{Z}^{(4)}_{\alpha,+1}$ we conjecture that:

Conjecture 8.2.10. *For $(\Gamma_0(4),\chi_\alpha^{(4)})$ and $\alpha\in[0,\frac{1}{2}]$ Maass wave forms $u(z)$ which are even with respect to $\tau z=\frac{\bar{z}}{2\bar{z}-1}$, i.e. $u(\tau z)=u(z)$, exist only for discrete values of α and are destroyed under the smallest infinitesimal change of the value of α.*

Obviously, τ-even Maass wave forms exist for all arithmetic $(\Gamma_0(4),\chi_\alpha^{(4)})$, i.e. $\alpha\in\{0,\frac{1}{8},\frac{2}{8},\frac{3}{8},\frac{4}{8}\}$, but they may also exist for non-arithmetic $(\Gamma_0(4),\chi_\alpha^{(4)})$. In case $(\Gamma_0(4),\chi_\alpha^{(4)})$ is non-arithmetic the value of α for which a τ-even Maass wave form exists is different for every τ-even Maass wave form, it seems that at most only finitely many τ-even Maass wave forms exist for a given α what therefore does not contradict the conjecture of Phillips and Sarnak. We see also from the results in Tables D.2 - D.5, that the multiplicity of the zeros of the Selberg zeta function for $(\Gamma_0(4),\chi_\alpha^{(4)})$ with $\alpha\in\{\frac{1}{8},\frac{2}{8},\frac{3}{8},\frac{4}{8}\}$ is always one. Indeed, we found that curves $\mathcal{V}_i^{(4)}$ of zeros in the (β,α)-plane never cross or even touch each other:

Conjecture 8.2.11. *For $(\Gamma_0(4),\chi_\alpha^{(4)})$ and $0<\alpha\leq\frac{1}{2}$ the multiplicity of the zeros $\mathcal{Z}^{(4)}_\alpha$ of the Selberg zeta function $Z^{(4)}(\beta,\chi_\alpha^{(4)})$ in $\Im\beta>0$ is always one.*

Obviously, this conjecture does not hold for $\alpha=0$. Also, it does not hold for the zeros on the real line $\beta\in\mathbb{R}$, e.g. the multiplicity of the zero $(\beta=1,\alpha=0)$ which moves on $\mathbb{R}$ for $0\leq\alpha\leq\frac{1}{2}$ changes when it crosses the pole at $\beta=\frac{1}{2}$, or the zeros and poles at $\beta\in\mathbb{Z}_{\leq}$ and at $\beta\in\frac{1}{2}+\mathbb{Z}_{\leq}$.

Based on numerical experiments for the Selberg zeta function for $(\Gamma_0(8),\chi_\alpha^{(8)})$ we formulate:

Conjecture 8.2.12. *For $(\Gamma_0(8),\chi_\alpha^{(8)})$ the multiplicity of the zeros $\mathcal{Z}^{(8)}_\alpha$ of the Selberg zeta function $Z^{(8)}(\beta,\chi_\alpha^{(8)})$ in $\Im\beta>0$:*

- *for $0<\alpha<\frac{1}{2}$ is always one,*
- *for $\alpha=\frac{1}{2}$ is either one or two.*

The zeros which have multiplicity two for $\alpha=\frac{1}{2}$ split up in the β-plane as soon α is changed. The following numerical results support conjecture 8.2.12 for $\alpha=\frac{1}{2}$: From numerical experiments we concluded formula (8.14), namely that the Selberg zeta function $Z^{(8)}(\beta,\chi_\alpha^{(8)})$ for $\alpha=\frac{1}{2}$ can be expressed as $Z^{(8)}\left(\beta,\chi^{(8)}_{\frac{1}{2}}\right)=Z^{(4)}\left(\beta,\chi^{(4)}_{\frac{1}{8}}\right)Z^{(4)}\left(\beta,\chi^{(4)}_{\frac{3}{8}}\right)$. Since our conclusion 8.2.7 says that all the zeros of $Z^{(4)}\left(\beta,\chi^{(4)}_{\frac{3}{8}}\right)$ are also zeros of $Z^{(4)}\left(\beta,\chi^{(4)}_{\frac{1}{8}}\right)$ and we conjectured in 8.2.11 that all zeros of $Z^{(4)}(\beta,\chi_\alpha)$ with $0<\alpha\leq\frac{1}{2}$ have multiplicity one, it is clear that the zeros of $Z^{(8)}\left(\beta,\chi^{(8)}_{\frac{1}{2}}\right)$ can only have multiplicity of either one or two, which is in agreement with conjecture 8.2.12.

On the other hand, for $\alpha=0$ we found formula (8.13), namely $Z^{(8)}\left(\beta,\chi_0^{(8)}\right)=Z^{(4)}\left(\beta,\chi_0^{(4)}\right)Z^{(4)}\left(\beta,\chi^{(4)}_{\frac{1}{2}}\right)$. Conclusion 8.2.7 and conjecture 8.2.11 then show that a zero of $Z^{(8)}\left(\beta,\chi_0^{(8)}\right)$ can have either multiplicity one or the multiplicity of the zero of $Z^{(4)}\left(\beta,\chi_0^{(4)}\right)$ plus one.

8.2.3 The zeros $\mathcal{Z}^{(4)}_{\alpha,-1}$ of the Selberg zeta function $Z^{(4)}\left(\beta,\chi_\alpha^{(4)}\right)$

Here we will discuss in detail the zeros $\mathcal{Z}^{(4)}_{\alpha,-1}$ of the Selberg zeta function $Z^{(4)}\left(\beta,\chi_\alpha^{(4)}\right)$ which correspond to eigenvalues -1 of the transfer operator $\mathcal{P}_2\mathcal{L}^{(4)}_{\beta,\varepsilon,\alpha}$ for $(\Gamma_0(4),\chi_\alpha^{(4)})$ and the paths $\psi^{(4)}_{i,-1}$ in (8.19) of these zeros

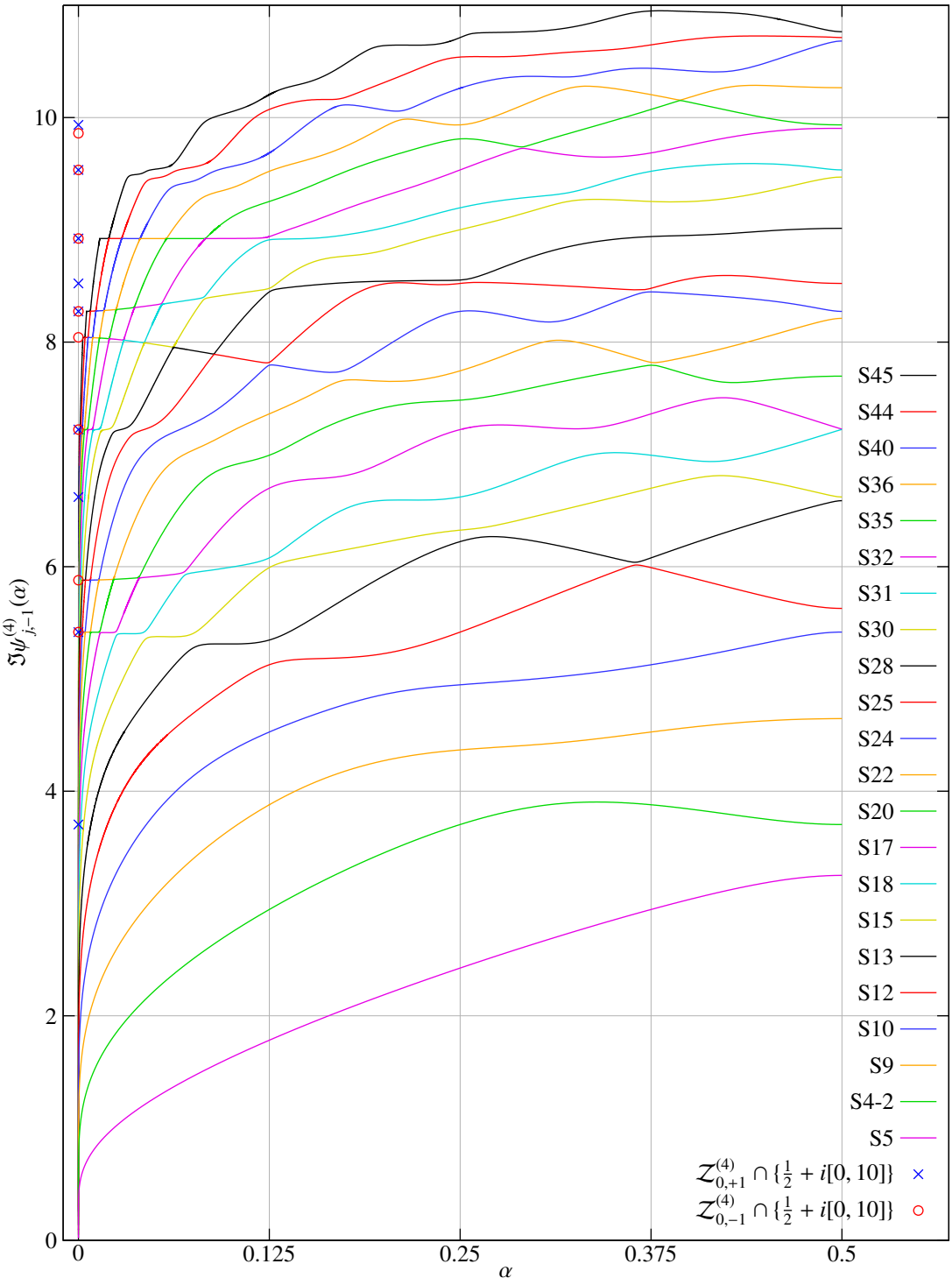

Figure 8.9: The zeros $\mathcal{Z}^{(4)}_{\alpha,-1}$ of the Selberg zeta function $Z^{(4)}\left(\beta, \chi^{(4)}_{\alpha}\right)$ on $\Re\beta = \frac{1}{2}$ for $\alpha \in (0, \frac{1}{2}]$

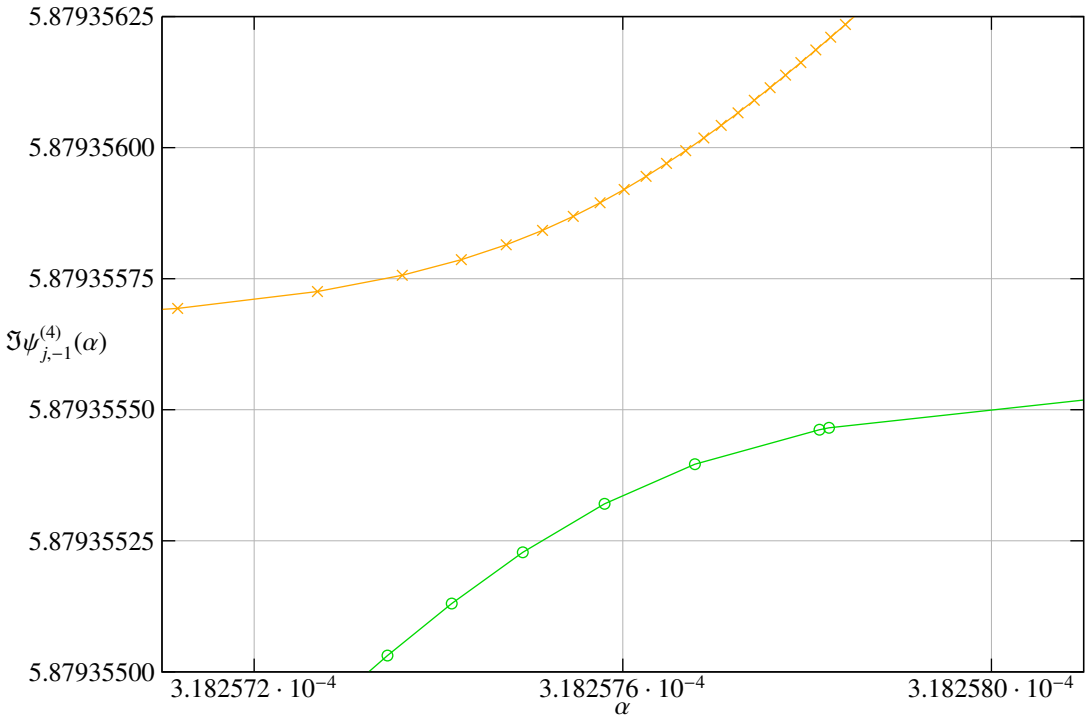

Figure 8.10: Avoided crossing of two zeros $\mathcal{Z}^{(4)}_{\alpha,-1}$ of the Selberg zeta function $Z^{(4)}\left(\beta,\chi^{(4)}_{\alpha}\right)$ on $\Re\beta = \frac{1}{2}$

in the β-plane parametrized by $\alpha \in (0, \frac{1}{2}]$. These paths $\psi^{(4)}_{i,-1}$ define the sets $\mathcal{V}^{(4)}_{i,-1}$ in (8.20) of the zeros in the (β,α)-plane of the Selberg zeta function $Z^{(4)}\left(\beta,\chi^{(4)}_{\alpha}\right)$ corresponding to eigenvalue -1 of the transfer operator $\mathcal{P}_2\mathcal{L}^{(4)}_{\beta,\varepsilon,\alpha}$. In the figures shown in the present section we denote the computed curves of zeros in the (β,α)-plane by $\mathrm{S}\,r$, with $r \in \mathbb{Z}_{>}$. As mentioned in section 8.2.1 the points in a set $\mathrm{S}\,r$ approximate discrete points on a curve $\mathcal{V}^{(4)}_{r,-1}$. In Figure 8.9 the first 22 curves $\mathrm{S}\,r$ of zeros are shown, which correspond to the eigenvalue -1 of the transfer operator $\mathcal{P}_2\mathcal{L}^{(4)}_{\beta,\varepsilon,\alpha}$ for $\alpha \in (0, \frac{1}{2}]$ respectively the zeros $\mathcal{Z}^{(4)}_{\alpha,\pm1}$ for $\alpha = 0$ on the critical line $\Re\beta = \frac{1}{2}$. We summarise our results for $\mathcal{Z}^{(4)}_{\alpha,-1}$ mentioned already in previous sections:

- Conclusion 8.2.9: for $\alpha \in (0, \frac{1}{2}]$ all zeros $\mathcal{Z}^{(4)}_{\alpha,-1}$ are on the critical line $\Re\beta = \frac{1}{2}$ for $\Im\beta > 0$.
- Conclusion 8.1.6: for $\alpha \in [0, \frac{1}{2}]$ and $\Re\beta = \frac{1}{2}$ the zeros $\beta \in \mathcal{Z}^{(4)}_{\alpha,-1}$ give eigenvalues $\beta(1-\beta)$ of the hyperbolic Laplacian Δ, and the eigenfunctions are Maass wave forms $u(z)$ which are odd with respect to the involution $\tau z = \frac{\bar{z}}{2\bar{z}-1}$.
- Conjecture 8.2.11: for $\alpha \in (0, \frac{1}{2}]$ and $\Im\beta > 0$ the zeros $\mathcal{Z}^{(4)}_{\alpha,-1}$ have multiplicity one.

For $\alpha = 0$ some zeros in $\mathcal{Z}^{(4)}_{\alpha,-1}$ are not on the critical line $\Re\beta = \frac{1}{2}$, also the multiplicity of the zeros $\mathcal{Z}^{(4)}_{\alpha,-1}$ for $\alpha = 0$ can be different from one.

We already mentioned that a perturbation of the hyperbolic Laplacian for $\Gamma_0(4)$ by the character $\chi^{(4)}_{\alpha}$ is singular at $\alpha = 0$, since two cusps are closed as soon as α is set to a non-zero value. Our computations of the Selberg zeta function $Z^{(4)}\left(\beta,\chi^{(4)}_{\alpha}\right)$ for very small values of α show a dramatic change between $Z^{(4)}\left(\beta,\chi^{(4)}_{\alpha}\right)$ for $\alpha \to 0$ and $Z^{(4)}\left(\beta,\chi^{(4)}_{0}\right)$ for $\alpha = 0$ in the region $\Re\beta \leq \frac{1}{2}$, (see observation 8.2.2 and Figure 8.8). We observed also that the curves of zeros of $Z^{(4)}\left(\beta,\chi^{(4)}_{\alpha}\right)$ at $\alpha = 0$ are non-analytic in this case:

Experimental Observation 8.2.13. *For $(\Gamma_0(4), \chi_\alpha^{(4)})$ even the smallest change of α away from zero leads to the following behavior of the zeros $\mathcal{Z}_{\alpha,-1}^{(4)}$ of the Selberg zeta function $Z^{(4)}\left(\beta, \chi_\alpha^{(4)}\right)$ corresponding to the eigenvalue -1 of the transfer operator $\mathcal{P}_2\mathcal{L}_{\beta,\varepsilon,\alpha}^{(4)}$:*

- *All zeros $\mathcal{Z}_{\alpha,-1}^{(4)}$ for $\alpha = 0$ on the lines $\Re\beta \in \{0, \frac{1}{4}\}$ disappear for a non-zero value of α.*
- *New zeros $\mathcal{Z}_{\alpha,-1}^{(4)}$ appear suddenly everywhere on the critical line $\Re\beta = \frac{1}{2}$ for a non-zero value of α: near every point $\beta_0 = \frac{1}{2} + \Im\beta_0$ on the critical line one can find a zero $\beta = \frac{1}{2} + \Im\beta$ of the Selberg zeta function, such that $|\Im\beta - \Im\beta_0| < \varepsilon$, with $\varepsilon = \varepsilon(\Im\beta_0, \alpha)$. The distance ε increases both with α and $\Im\beta_0$.*

We verified the disappearance of the zeros $\mathcal{Z}_{0,-1}^{(4)}$ on the lines $\Re\beta \in \{0, \frac{1}{4}\}$ for $\alpha \neq 0$ by using the argument principle for the Selberg zeta function $Z^{(4)}\left(\beta, \chi_\alpha^{(4)}\right)$ in the β-plane for very small values of α. It turns out that only the zeros $\mathcal{Z}_{\alpha,+1}^{(4)}$ exist very near but off the lines $\Re\beta \in \{0, \frac{1}{4}\}$ for small values of $\alpha \to 0$. Our observation 8.2.13 is one of the reasons why we believe that it is rather difficult to apply perturbation theory to study the spectrum of the hyperbolic Laplacian for perturbations at $\alpha = 0$, since for the smallest change in α instantaneously many eigenvalues of the hyperbolic Laplacian appear near to each other. This shows also clearly that it is not possible for us to track the zeros of the Selberg zeta function $\mathcal{Z}_{\alpha,-1}^{(4)}$ on the critical line $\Re\beta = \frac{1}{2}$ starting with $\alpha = 0$, since nearby to these zeros many other zeros appear for the smallest non-zero value of α. Instead, we started the computations with a value of $\alpha \neq 0$ for which $\chi_\alpha^{(4)}$ is arithmetic and tracked these zeros for $\alpha \in (0, \frac{1}{2}]$.

In Figure 8.9 it can be seen that for certain values of α the paths $\psi_{i,-1}^{(4)}$ of zeros are very close to each other, in some cases it even appears as if they would touch. However, a closer examination reveals that the zeros on these paths never touch, even if the distance between the zeros gets very small. An example of two zeros on the curves S 35 and S 36 which appear to merge is shown in a close-up in Figure 8.10. As one can see the smallest distance $|\Im\psi_{35,-1}^{(4)}(\alpha) - \Im\psi_{36,-1}^{(4)}(\alpha)|$ is about $5 \cdot 10^{-7}$. Indeed, we found cases where the distance was even smaller. We found the following phenomenon when two zeros get very close to each other in the (β, α)-plane:

Experimental Observation 8.2.14. *(Avoided Crossing) For $(\Gamma_0(4), \chi_\alpha^{(4)})$ let $(\beta_1, \alpha_1) \in \mathcal{V}_{j,-1}^{(4)}$ and $(\beta_2, \alpha_2) \in \mathcal{V}_{k,-1}^{(4)}$ be zeros of the Selberg zeta function $Z^{(4)}\left(\beta, \chi_\alpha^{(4)}\right)$ on the curves $\mathcal{V}_{j,-1}^{(4)}$ and $\mathcal{V}_{k,-1}^{(4)}$ such that $d((\beta_1, \alpha_1), (\beta_2, \alpha_2))$ is a local minimum. We found that the zeros (β_1, α_1) and (β_2, α_2) on the paths $\psi_{j,-1}^{(4)}$ and $\psi_{k,-1}^{(4)}$ deflect each other if $d((\beta_1, \alpha_1), (\beta_2, \alpha_2)) \ll 1$. The zero on the path $\psi_{j,-1}^{(4)}$ takes over the direction of the zero on the path $\psi_{k,-1}^{(4)}$ at the point of nearest approach and vice versa.*

This deflection of the zeros doesn't happen instantly: if $\alpha_c = \frac{\alpha_1+\alpha_2}{2}$ then for small $d((\beta_1, \alpha_1), (\beta_2, \alpha_2))$ we have $\alpha_c \approx \alpha_1 \approx \alpha_2$. Since the zeros (β_1, α_1) and (β_2, α_2) on the paths $\psi_{j,-1}^{(4)}$ respectively $\psi_{k,-1}^{(4)}$ do not change their directions instantly there is an interval $\alpha_c - \delta_{j,-} < \alpha < \alpha_c + \delta_{j,+}$ such that for

$$\left| \frac{d^2\psi_{j,-1}^{(4)}(\alpha)}{d\alpha^2}|_{\alpha_c-\delta_{j,-}<\alpha<\alpha_c+\delta_{j,+}} \right| = c(\alpha)$$

with $c(\alpha) > 0$, one finds $\lim_{\alpha\to\alpha_c-\delta_{j,-}} c(\alpha) = 0$ and $\lim_{\alpha\to\alpha_c+\delta_{j,+}} c(\alpha) = 0$. There is also such an interval $\alpha_c - \delta_{k,-} < \alpha < \alpha_c + \delta_{k,+}$ for the path $\psi_{k,-1}^{(4)}$. The zeros on these paths take over the direction of the other zero, that is

$$\frac{d\psi_{j,-1}^{(4)}(\alpha)}{d\alpha}|_{\alpha=\alpha_c-\delta_{j,-}} \approx \frac{d\psi_{k,-1}^{(4)}(\alpha)}{d\alpha}|_{\alpha=\alpha_c+\delta_{k,+}} \quad \text{and} \quad \frac{d\psi_{j,-1}^{(4)}(\alpha)}{d\alpha}|_{\alpha=\alpha_c+\delta_{j,+}} \approx \frac{d\psi_{k,-1}^{(4)}(\alpha)}{d\alpha}|_{\alpha=\alpha_c-\delta_{k,-}}.$$

Note that this is not a general law, since this taking over of the direction of another zero depends on the distance of both zeros during the avoided crossing and can also be influenced by a possible presence of other zeros nearby. Since we found the phenomena of avoided crossing every time when two zeros are close to each other, we conjectured in 8.2.11 that the multiplicity of the zeros $\mathcal{Z}^{(4)}_{\alpha,-1}$ for $0 < \alpha \leq \frac{1}{2}$ is always one. Therefore, the curves $\mathcal{V}^{(4)}_{i,-1}$ of the zeros of the Selberg zeta function $Z^{(4)}\left(\beta, \chi^{(4)}_\alpha\right)$ corresponding to the eigenvalue -1 of the transfer operator $\mathcal{P}_2\mathcal{L}^{(4)}_{\beta,\varepsilon,\alpha}$ never cross or even touch each other. The fact that the zeros can be very close to each other makes computations very difficult and also demands small distances between the computed points $(\beta_i, \alpha_i) \in \mathrm{S}\, r$ on the curve $\mathcal{V}^{(4)}_{r,-1}$ of a zero, since during the tracking of a zero it can easily happen that we accidentally jump from one curve $\mathcal{V}^{(4)}_{r,-1}$ to another $\mathcal{V}^{(4)}_{k,-1}$. For details on how we solved this problem and how the curves of zeros were computed see section 8.2.1. From the point of view of the hyperbolic Laplacian the observation that two zeros can be very close to each other means that some of the eigenvalues are almost degenerate for certain values of α.

In Figure 8.9 we can see that for $\alpha \to 0$ all zeros move down towards $\Im\beta = 0$. In Figure 8.11 the curves $\mathrm{S}\, r$ of zeros for $\alpha \in [10^{-60}, \frac{1}{2}]$ are shown with α in logarithmic scale, in the right plot $\Im\beta$ is also scaled logarithmically, while in the left one it is scaled linearly. We arrive therefore at:

Conclusion 8.2.15. *For $(\Gamma_0(4), \chi^{(4)}_\alpha)$ the zeros $\mathcal{Z}^{(4)}_{\alpha,-1}$ of the Selberg zeta function $Z^{(4)}\left(\beta, \chi^{(4)}_\alpha\right)$ corresponding to the eigenvalue -1 of the transfer operator $\mathcal{P}_2\mathcal{L}^{(4)}_{\beta,\varepsilon,\alpha}$ tend to $\beta = \frac{1}{2}$ for $\alpha \to 0$. For small α the distance between two zeros on the paths $\psi^{(4)}_{j,-1}$ and $\psi^{(4)}_{k,-1}$ which are next to each other with $\Im\psi^{(4)}_{j,-1}(\alpha) < \Im\psi^{(4)}_{k,-1}(\alpha)$ is given by*

$$|\psi^{(4)}_{k,-1}(\alpha) - \psi^{(4)}_{j,-1}(\alpha)| = c_j(\alpha).$$

The value of $c_j(\alpha)$ depends on j such that $c_j(\alpha) > c_l(\alpha)$ for $\Im\psi^{(4)}_{j,-1}(\alpha) > \Im\psi^{(4)}_{l,-1}(\alpha)$. $c_j(\alpha)$ decreases as α is getting smaller and the zeros $\mathcal{Z}^{(4)}_{\alpha,-1}$ are getting dense for $\alpha \to 0$, i.e. $c_j(\alpha) \to 0$ for $\alpha \to 0$.

See also conclusion 8.2.26 for the zeros $\mathcal{Z}^{(4)}_{\alpha,+1}$ to the left of the critical line $\Re\beta = \frac{1}{2}$, which form pairs with the zeros $\mathcal{Z}^{(4)}_{\alpha,-1}$ from conclusion 8.2.15. To see that the zeros $\mathcal{Z}^{(4)}_{\alpha,-1}$ are moving down and are almost equidistant for small $\Im\beta$ and α see the left plot in Figure 8.19, where the zeros $\mathcal{Z}^{(4)}_{\alpha,-1}$ are shown in the β-plane for $\alpha = 10^{-20}$ and $\alpha = 10^{-50}$. Our experimental observation 8.1.22 says that for $\Re\beta = \frac{1}{2}$, fixed $\Im\beta$ and $\alpha \to 0$ the eigenvalues of the transfer operator $\mathcal{P}_2\mathcal{L}^{(4)}_{\beta,\varepsilon,\alpha}$ rotate in closed orbits with varying α, where one of these orbits is going through -1. The rotation speed of the eigenvalues increases exponentially with $\alpha \to 0$, see Figure 8.7. This observation also supports conclusion 8.2.15 for $\alpha \to 0$, namely that the zeros $\mathcal{Z}^{(4)}_{\alpha,-1}$ of the Selberg zeta function are moving in one direction and are getting dense.

We want to discuss the relation between the zeros $\mathcal{Z}^{(4)}_{\alpha,-1}$ for $\alpha \to 0$ and the zeros $\mathcal{Z}^{(4)}_{0,-1}$ for $\alpha = 0$. From observation 8.2.13 and conclusion 8.2.15 follows:

Conclusion 8.2.16. *For $(\Gamma_0(4), \chi^{(4)}_\alpha)$ and $\alpha \to 0$ the zeros $\mathcal{Z}^{(4)}_{\alpha,-1}$ of the Selberg zeta function $Z^{(4)}\left(\beta, \chi^{(4)}_\alpha\right)$ corresponding to the eigenvalue -1 of the transfer operator $\mathcal{P}_2\mathcal{L}^{(4)}_{\beta,\varepsilon,\alpha}$ do not converge towards the zeros in $\mathcal{Z}^{(4)}_{0,-1}$.*

Surprisingly, even if there is no convergence of a single zero in $\mathcal{Z}^{(4)}_{\alpha,-1}$ for $\alpha \to 0$ towards the zeros $\mathcal{Z}^{(4)}_{0,-1}$, we found that there is nevertheless a relation between the zeros $\mathcal{Z}^{(4)}_{\alpha,-1}$ and the zeros $\mathcal{Z}^{(4)}_{0,-1}$ on the critical line $\Re\beta = \frac{1}{2}$ for $\alpha \to 0$: In Figure 8.9 one can see lines which consist of different pieces of curves $\mathcal{V}^{(4)}_{j,-1}$ of zeros converging to the zeros $\mathcal{Z}^{(4)}_{0,-1}$ (red circles in Figure 8.9) for $\alpha = 0$. Note that such lines do not exist for the zeros $\mathcal{Z}^{(4)}_{0,+1}$ (blue crosses in Figure 8.9) for $\alpha = 0$ on the critical line $\Re\beta = \frac{1}{2}$. In Figure 8.12 we can see a close-up of four of these curves, in the right plot the value of α is scaled logarithmically, which shows these lines more clearly. We arrive therefore at:

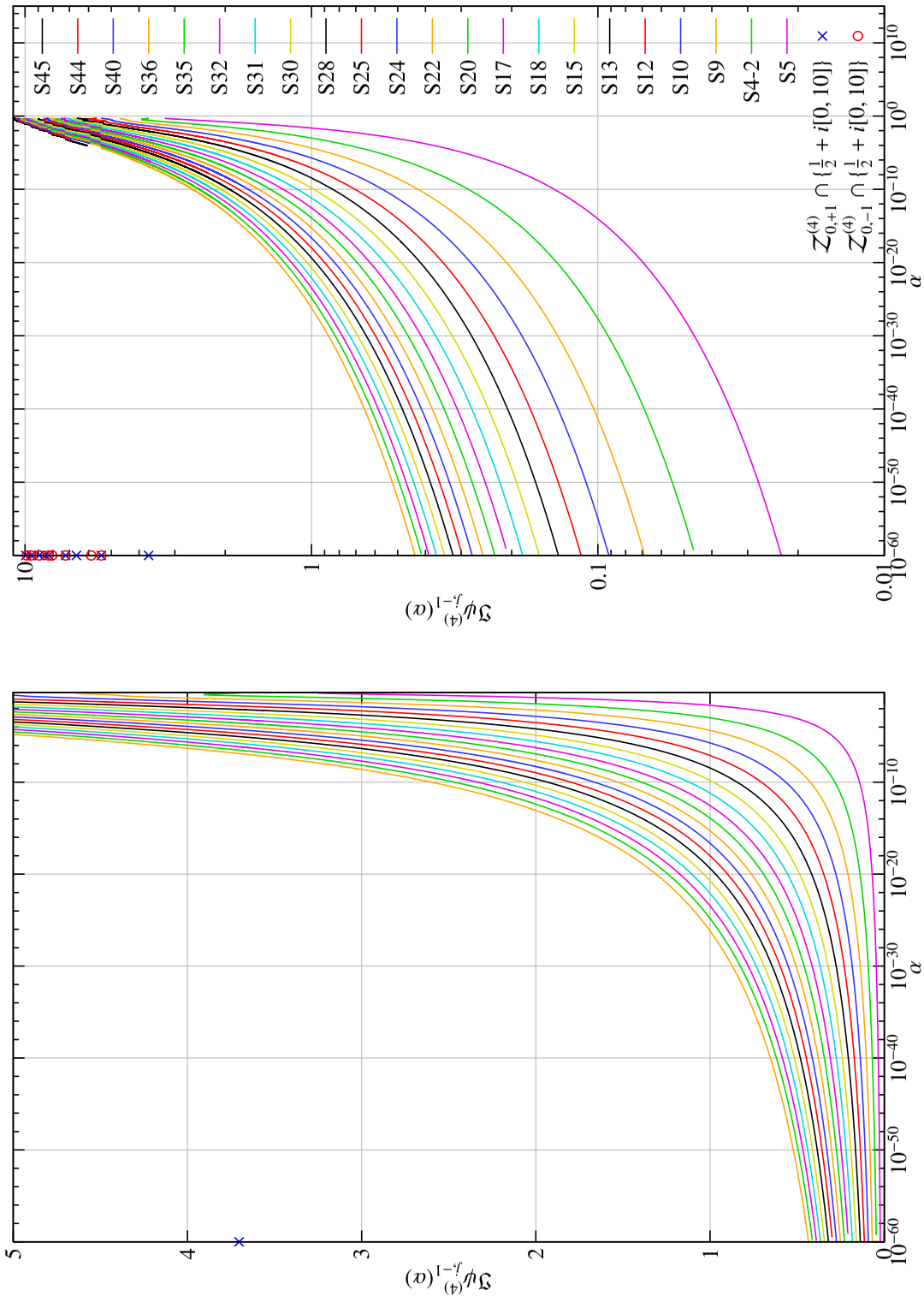

Figure 8.11: The zeros $\mathcal{Z}^{(4)}_{\alpha,-1}$ of the Selberg zeta function $Z^{(4)}\left(\beta, \chi^{(4)}_{\alpha}\right)$ on $\Re\beta = \frac{1}{2}$ for $\alpha \to 0$

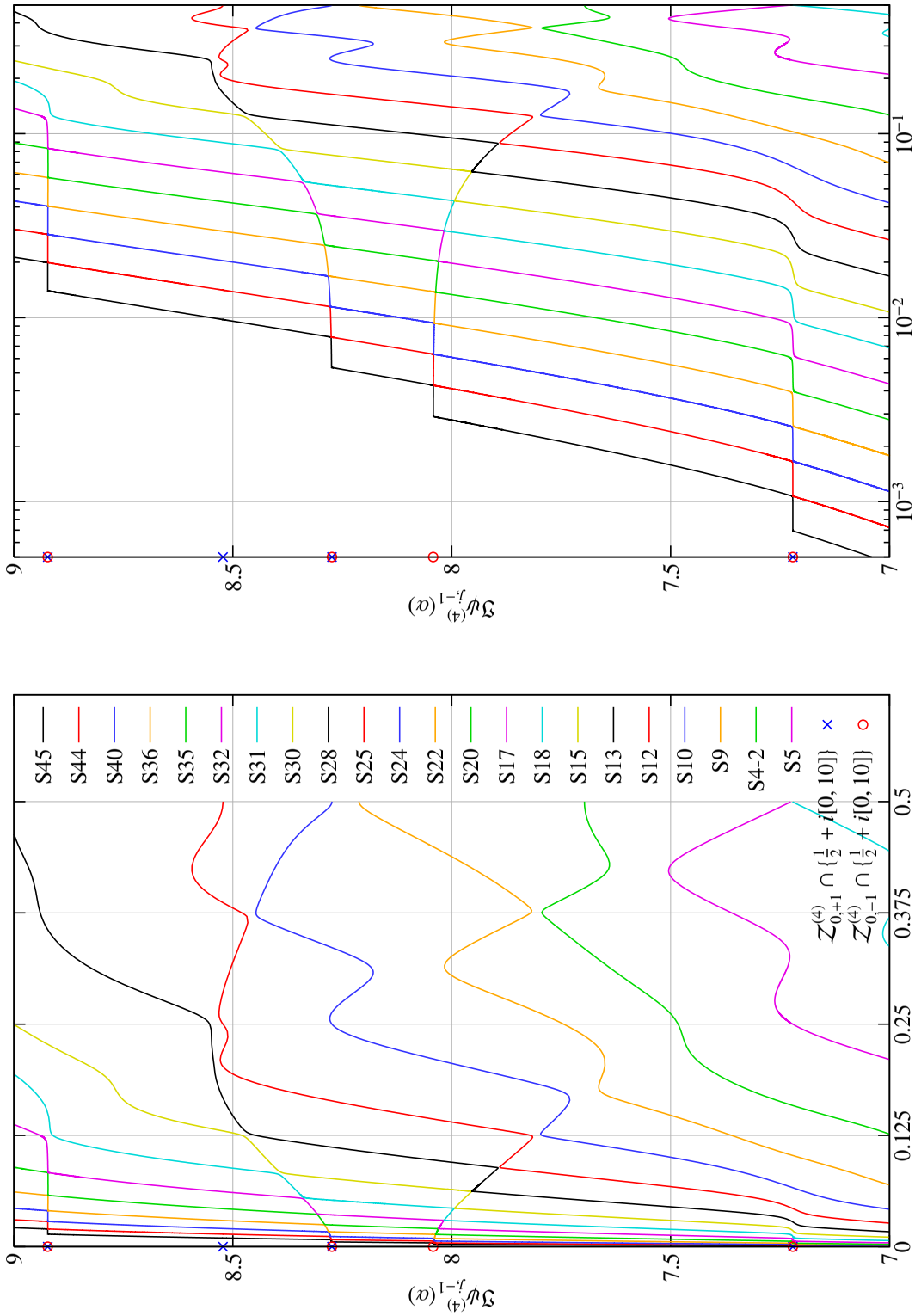

Figure 8.12: Infinite Avoided Crossing of the zeros $\mathcal{Z}^{(4)}_{\alpha,-1}$ on $\Re\beta = \frac{1}{2}$ for $\alpha \to 0$

Conclusion 8.2.17. *(Infinite Avoided Crossing) For every zero $\beta_l \in \mathcal{Z}^{(4)}_{0,-1}$ of the Selberg zeta function $Z^{(4)}\left(\beta, \chi^{(4)}_\alpha\right)$ for $(\Gamma_0(4), \chi^{(4)}_\alpha)$ and $\alpha = 0$ there are infinitely many paths $\psi^{(4)}_{m_l(i),-1} : A_{m_l(i)} \to \mathcal{Z}^{(4)}_{\cdot,-1}$ and subintervals $A^{(l)}_i = [a^{(l)}_i, b^{(l)}_i] \subset A_{m_l(i)} \subseteq (0, \frac{1}{2}]$ with $i = 1, 2, 3, \ldots$, such that a zero on a path $\psi^{(4)}_{m_l(i),-1}(A^{(l)}_i)$ tends towards β_l, where $m_l : \mathbb{Z}_> \to \mathbb{Z}_>$ maps the counting index i of the intervals $A^{(l)}_i$ to the index of the corresponding paths:*

- *The intervals $A^{(l)}_i$ are disjoint and ordered by i such that $b^{(l)}_{i+1} < a^{(l)}_i$. The length $L^{(l)}_i = b^{(l)}_i - a^{(l)}_i$ of the intervals $A^{(l)}_i$ decreases exponentially with $i \to \infty$, and $a^{(l)}_i \to 0$ for $i \to \infty$.*
- *The path $\psi^{(4)}_{m_l(i+1),-1}$ on the interval $A^{(l)}_{i+1}$ takes over the direction of the path $\psi^{(4)}_{m_l(i),-1}$ on the interval $A^{(l)}_i$ by avoided crossing.*
- *The distance between the zero $\beta_l \in \mathcal{Z}^{(4)}_{0,-1}$ and the zeros on the paths $\psi^{(4)}_{m_l(i),-1}$ on the intervals $A^{(l)}_i$ is getting smaller with i:*

$$|\Im\beta_l - \Im\psi^{(4)}_{m_l(i),-1}(\alpha)| \le \varepsilon^{(l)}_i \quad \text{for all } \alpha \in A^{(l)}_i \quad \text{and} \quad \lim_{i\to\infty} \varepsilon^{(l)}_i = 0$$

- *The zeros on the paths $\psi^{(4)}_{m_l(i),-1}$ slow down on the intervals $A^{(l)}_i$:*

$$\left|\frac{d\psi^{(4)}_{m_l(i),-1}(\alpha)}{d\alpha}\right| \le \delta^{(l)}_i \quad \text{for all } \alpha \in A^{(l)}_i \quad \text{and} \quad \lim_{i\to\infty} \delta^{(l)}_i = 0$$

  Outside of the intervals $A^{(l)}_i$ these zeros move fast towards $\Im\beta = 0$ for $\alpha \to 0$.

Obviously, we can only compute a finite number of these avoided crossings, but there are several arguments which suggest that this avoided crossing happens infinitely many times: conclusion 8.2.15 says that all zeros of the Selberg zeta function on the critical line $\Re\beta = \frac{1}{2}$ go down to $\Im\beta = 0$ for $\alpha \to 0$ and conjecture 8.2.11 says that the multiplicity of these zeros is always one; therefore, it is not possible that a zero on a path $\psi^{(4)}_{j,-1}$ will converge for $\alpha \to 0$ to a zero $\beta_l \in \mathcal{Z}^{(4)}_{0,-1}$ on the critical line. In the right Figure 8.12 the length $L^{(l)}_i$ of the intervals $A^{(l)}_i$ appears to be constant, but since α is scaled there logarithmically this means that the length $L^{(l)}_i$ decreases exponentially for $\alpha \to 0$ and that infinitely many intervals $A^{(l)}_i$ will appear.

Conclusion 8.2.17 says that the zeros on the sequence of paths $\{\psi^{(4)}_{m_l(i),-1}\}_{i\in\mathbb{Z}}$ converge towards a zero of the Selberg zeta function for $\alpha = 0$ for $i \to \infty$, but it does not explain the behavior of these zeros for fixed i on the paths $\psi^{(4)}_{m_l(i),-1}(\alpha)$ for $\alpha \in A^{(l)}_i$. It would be natural to assume that for a fixed i the values of $\varepsilon^{(l)}_i$ and $\delta^{(l)}_i$ in conclusion 8.2.17 are getting smaller with decreasing α. Indeed, in most cases we found this behavior, but in few cases we found the opposite behavior. To illustrate this difference we refer to the Figure 8.13. In this figure the paths $\{\psi^{(4)}_{m_l(i),-1}\}_{i\in\mathbb{Z}}$ converging to the zeros $\beta_1, \beta_2 \in \mathcal{Z}^{(4)}_{0,-1}$ with $\beta_1 \approx \frac{1}{2} + 5.41733i$ and $\beta_2 \approx \frac{1}{2} + 5.87935i$ are shown. The plots on the left show the dependence on α of the imaginary parts of the paths $\psi^{(4)}_{m_l(i),-1}$, while the right plots show the distance $|\Im\beta_l - \Im\psi^{(4)}_{m_l(i),-1}(\alpha)|$ for $l = 1, 2$ depending on α, all in logarithmic scales. The paths $\psi^{(4)}_{m_l(i),-1}(\alpha)$ are shown not only on the intervals $A^{(l)}_i$ but for the whole range of α. As we can see, the zeros on the paths $\psi^{(4)}_{m_2(i),-1}$ converging to β_2 move closer towards β_2 on every interval $A^{(2)}_i$ as α decreases. Indeed, in the right plot the zeros on the different paths $\psi^{(4)}_{m_2(i),-1}$ on the intervals $A^{(2)}_i$ form a continuous line towards β_2. On the other hand, the zeros on the paths $\psi^{(4)}_{m_1(i),-1}$ converging to β_1 do not move closer towards β_1 on the individual intervals $A^{(1)}_i$ as α decreases, instead the zeros on the paths $\psi^{(4)}_{m_1(i),-1}$ converge towards β_1 by jumps between the values of $\Im\psi^{(4)}_{m_1(i+1),-1}(b^{(1)}_{i+1})$ and $\Im\psi^{(4)}_{m_1(i),-1}(a^{(1)}_i)$. In the right plot these zeros do not form a line; instead they form a set of steps converging to β_1 in an non-continuous way.

Table 8.6: Coefficient $C_{0,l}$ and d_l of curve $C_l(\alpha)$ (Infinite Avoided Crossing)

l	$\Im\beta_l$	d_l	$C_{0,l}$	$C_{0,l}$ for $d_l := 2$	Type
1	5.417334806844678385	1.9638154460	-9.2341680671	-13.1430525070	2.
2	5.879354157758601464	1.9999936101	14.2804646966	14.2812233934	1.
3	7.220871975958052161	2.0943099084	-16.8594265893	-0.6803184384	2.
4	8.042477591683672004	1.9950321727	-30.7003039754	-31.5749972420	1.
5	8.273665889586057109	1.9820217092	26.7536540195	29.2889084088	1.
6	8.922876486991967371	1.8916641367	-0.2247494385	-0.3501403493	1.

"Type" as given in observation 8.2.18

Experimental Observation 8.2.18. *For a set of paths $\{\psi^{(4)}_{m_l(i),-1}\}_{i=1,2,\dots}$ which converge to a zero $\beta_l \in \mathcal{Z}^{(4)}_{0,-1}$ on $\Re\beta = \frac{1}{2}$ as described in conclusion 8.2.17, depending on β_l one of the following cases applies:*

1. *For $\Im\beta_l - \Im\psi^{(4)}_{m_l(i),-1}(\alpha) = \varepsilon^{(l)}_i(\alpha)$, $|\varepsilon^{(l)}_i(\alpha)|$ is decreasing with decreasing $\alpha \in A^{(l)}_i = [a^{(l)}_i, b^{(l)}_i]$ and $\lim_{\alpha\to a^{(l)}_i} \varepsilon^{(l)}_i(\alpha) = \varepsilon^{(l)}_{i+1}(b^{(l)}_{i+1})$. For $\frac{d\psi^{(4)}_{m_l(i),-1}(\alpha)}{d\alpha} = \delta^{(l)}_i(\alpha)$, $|\delta^{(l)}_i(\alpha)|$ is decreasing with decreasing $\alpha \in A^{(l)}_i$, and $\lim_{\alpha\to a^{(l)}_i} \delta^{(l)}_i(\alpha) = \delta^{(l)}_{i+1}(a^{(l)}_{i+1})$.*

2. *For $\Im\beta_l - \Im\psi^{(4)}_{m_l(i),-1}(\alpha) = \varepsilon^{(l)}_i(\alpha)$, $|\varepsilon^{(l)}_i(\alpha)|$ is* not *decreasing with decreasing $\alpha \in A^{(l)}_i = [a^{(l)}_i, b^{(l)}_i]$ and $\lim_{\alpha\to a^{(l)}_i} \varepsilon^{(l)}_i(\alpha) \neq \varepsilon^{(l)}_{i+1}(b^{(l)}_{i+1})$. For $\frac{d\psi^{(4)}_{m_l(i),-1}(\alpha)}{d\alpha} = \delta^{(l)}_i(\alpha)$, $|\delta^{(l)}_i(\alpha)|$ is* not *decreasing with decreasing $\alpha \in A^{(l)}_i$, and $\lim_{\alpha\to a^{(l)}_i} \delta^{(l)}_i(\alpha) \neq \delta^{(l)}_{i+1}(a^{(l)}_{i+1})$.*

In most cases we considered we found the behavior as described by case 1 in observation 8.2.18. Obviously, in case 1 in observation 8.2.18 we can connect the paths $\psi^{(4)}_{m_l(i),-1}(A^{(l)}_i)$ by a continuous curve, which converges to the zero at $\beta_l \in \mathcal{Z}^{(4)}_{0,-1}$ on the critical line $\Re\beta = \frac{1}{2}$. Indeed, we found such a continuous curve also for case 2 in observation 8.2.18, but the paths $\psi^{(4)}_{j,-1}(A^{(l)}_i)$ intersect this curve only at one point:

Conclusion 8.2.19. *The set of paths $\{\psi^{(4)}_{m_l(i),-1}\}_{i=1,2,\dots}$ which converge to a zero $\beta_l \in \mathcal{Z}^{(4)}_{0,-1}$ on $\Re\beta = \frac{1}{2}$ as described in conclusion 8.2.17, defines a curve $(\frac{1}{2} + iC_l(\alpha), \alpha)$ in the (β, α)-plane such that $C_l(0) = \Im\beta_l$ and $\frac{dC_l(\alpha)}{d\alpha}|_{\alpha=0} = 0$, given by*

$$C_l(\alpha) = C_{0,l}\alpha^{d_l} + \Im\beta_l,$$

with $C_{0,l}, d_l \in \mathbb{R}$. For the paths $\psi^{(4)}_{m_l(i),-1}$ of case 1 of observation 8.2.18 the curve $C_l(\alpha)$ coincides with all paths $\psi^{(4)}_{m_l(i),-1}(A^{(l)}_i)$, i.e.

$$\text{for all } i \in \mathbb{Z}_> \quad \text{and } \alpha \in A^{(l)}_i : \quad C_l(\alpha) = \Im\psi^{(4)}_{m_l(i),-1}(\alpha).$$

For the paths $\psi^{(4)}_{m_l(i),-1}$ of case 2 of observation 8.2.18 the curve $C_l(\alpha)$ intersects all paths $\psi^{(4)}_{m_l(i),-1}(A^{(l)}_i)$ in a single point, i.e.

$$\text{for all } i \in \mathbb{Z}_> \quad \exists!\alpha^{(l)}_i \in A^{(l)}_i : \quad C_l(\alpha^{(l)}_i) = \Im\psi^{(4)}_{m_l(i),-1}(\alpha^{(l)}_i).$$

We can determine the constants $C_{0,l}$ and d_l from our data sets by the formulas

$$d_l = \frac{\ln|\Im\beta_l - \Im\psi^{(4)}_{m_l(i),-1}(\alpha_1)| - \ln|\Im\beta_l - \Im\psi^{(4)}_{m_l(i+1),-1}(\alpha_2)|}{\ln|\alpha_1| - \ln|\alpha_2|}$$

and

$$C_{0,l} = \frac{\Im\psi^{(4)}_{m_l(i),-1}(\alpha_1) - \Im\beta_l}{\alpha_1^{d_l}}$$

with $\alpha_1 \in A_i^{(l)}$ and $\alpha_2 \in A_{i+1}^{(l)}$. If the curve C_l and the paths $\psi^{(4)}_{m_l(i),-1}$ coincide as described in conclusion 8.2.19 we can choose for α_1 and α_2 any point on the interval $A_i^{(l)}$ respectively $A_{i+1}^{(l)}$. On the other hand, if the curve C_l intersects with these intervals only in one point the choice for α_1 and α_2 is rather difficult, since for slightly different chosen α_1 and α_2 the constants d_l and $C_{0,l}$ become rather different. In Table 8.6 we list the constants $C_{0,l}$ and d_l determined for the first 6 zeros $\beta_l \in \mathcal{Z}^{(4)}_{0,-1}$, where in the column "Type" - the type of the paths $\psi^{(4)}_{m_l(i),-1}$ as described in observation 8.2.18 - is given. In Figure 8.13 the red lines are the curves C_1 and C_2 with the constants $C_{0,l}$ for $d_l := 2$ with $l = 1, 2$ as given in Table 8.6. As we can see the curve C_2 coincides with the paths $\psi^{(4)}_{m_2(i),-1}$ on the intervals $A_i^{(2)}$, while C_1 intersects the paths $\psi^{(4)}_{m_1(i),-1}$ on the intervals $A_i^{(1)}$. As we can see from Table 8.6, the value of d_l seems to be constant for every curve C_l:

Experimental Observation 8.2.20. *For the curves $C_l(\alpha) = C_{0,l}\alpha^{d_l} + \Im\beta_l$ converging to the zeros $\beta_l \in \mathcal{Z}^{(4)}_{0,-1}$ as described in conclusion 8.2.19 the value of d_l is given by $d_l = 2$ for $1 \le l \le 6$.*

It follows from conclusion 8.2.17 that for $\alpha \to 0$ there is a convergence of the perturbed eigenvalues $\lambda_i^{(l)}(\alpha)$ of the hyperbolic Laplacian belonging to τ-odd Maass wave forms towards the unperturbed eigenvalues λ_l for $\alpha = 0$. This convergence is rather complicated, instead of a single eigenvalue $\lambda_i^{(l)}(\alpha)$ converging to an unperturbed eigenvalue there is an infinite sequence of eigenvalues $\{\lambda_i^{(l)}(\alpha) = \frac{1}{4} + (\Im\psi^{(4)}_{m_l(i),-1}(\alpha))^2\}_{i=1,2,\ldots}$ which converge for $i \to \infty$ to $\lambda_l = \frac{1}{4} + (\Im\beta_l)^2$. Since $\lambda_i^{(l)}(\alpha) \to \frac{1}{4}$ for $\alpha \to 0$ a one to one correspondence between an eigenvalue $\lambda_i^{(l)}(\alpha)$ and an unperturbed eigenvalue λ_l does not exist. This reflects in a certain sense the survival of τ-odd Maass wave forms for $\alpha = 0$ when α is turning away from zero. On the other hand, the convergence of eigenvalues related to τ-even Maass wave forms for $\alpha \to 0$ is rather different, as we will see in the next section.

8.2.4 The zeros $\mathcal{Z}^{(4)}_{\alpha,+1}$ of the Selberg zeta function $Z^{(4)}\left(\beta, \chi^{(4)}_\alpha\right)$

Next we will discuss in detail the zeros $\mathcal{Z}^{(4)}_{\alpha,+1}$ of the Selberg zeta function $Z^{(4)}(\beta, \chi^{(4)}_\alpha)$ which correspond to the eigenvalues $+1$ of the transfer operator $\mathcal{P}_2\mathcal{L}^{(4)}_{\beta,\varepsilon,\alpha}$ for $(\Gamma_0(4), \chi^{(4)}_\alpha)$ and their paths $\psi^{(4)}_{i,+1}$ in (8.19) in the β-plane parametrized by $\alpha \in (0, \frac{1}{2}]$. These paths $\psi^{(4)}_{i,+1}$ define the sets $\mathcal{V}^{(4)}_{i,+1}$ in (8.20) of the zeros in the (β, α)-plane of the Selberg zeta function $Z^{(4)}(\beta, \chi^{(4)}_\alpha)$ corresponding to the eigenvalue $+1$ of the transfer operator $\mathcal{P}_2\mathcal{L}^{(4)}_{\beta,\varepsilon,\alpha}$. In the figures presented in this section we denote the numerically determined curves of zeros in the (β, α)-plane by $\mathrm{S}\,r$, with $r \in \mathbb{Z}_>$. As mentioned in section 8.2.1 the points in a set $\mathrm{S}\,r$ approximate discrete points on a curve $\mathcal{V}^{(4)}_{r,+1}$. In Figures 8.14 - 8.17 there are shown 24 curves $\mathrm{S}\,r$ of zeros which correspond to the eigenvalue $+1$ of the transfer operator $\mathcal{P}_2\mathcal{L}^{(4)}_{\beta,\varepsilon,\alpha}$ for $\alpha \in (0, \frac{1}{2}]$ and the zeros $\mathcal{Z}^{(4)}_{\alpha,\pm1}$ for $\alpha = 0$ on the critical line $\Re\beta = \frac{1}{2}$. Let us summarise our results for $\mathcal{Z}^{(4)}_{\alpha,+1}$ which we mentioned already in previous sections:

- Conclusion 8.2.9: for $\alpha \in (0, \frac{1}{2}]$ all zeros $\mathcal{Z}^{(4)}_{\alpha,+1}$ are located in $\Re\beta < \frac{1}{2}$ and $\Im\beta > 0$, except for certain discrete values of α where some of the zeros in $\mathcal{Z}^{(4)}_{\alpha,+1}$ are on the critical line $\Re\beta = \frac{1}{2}$.
- Conclusion 8.1.6: for $\alpha \in [0, \frac{1}{2}]$ the zeros $\beta \in \mathcal{Z}^{(4)}_{\alpha,+1}$ on $\Re\beta = \frac{1}{2}$ give eigenvalues $\beta(1-\beta)$ of the hyperbolic Laplacian Δ where the eigenfunctions are Maass wave forms $u(z)$ which are even with respect to the involution $\tau z = \frac{\bar{z}}{2\bar{z}-1}$.
- Conjecture 8.2.11: for $\alpha \in (0, \frac{1}{2}]$ the zeros $\mathcal{Z}^{(4)}_{\alpha,+1}$ in $\Im\beta > 0$ have multiplicity one.

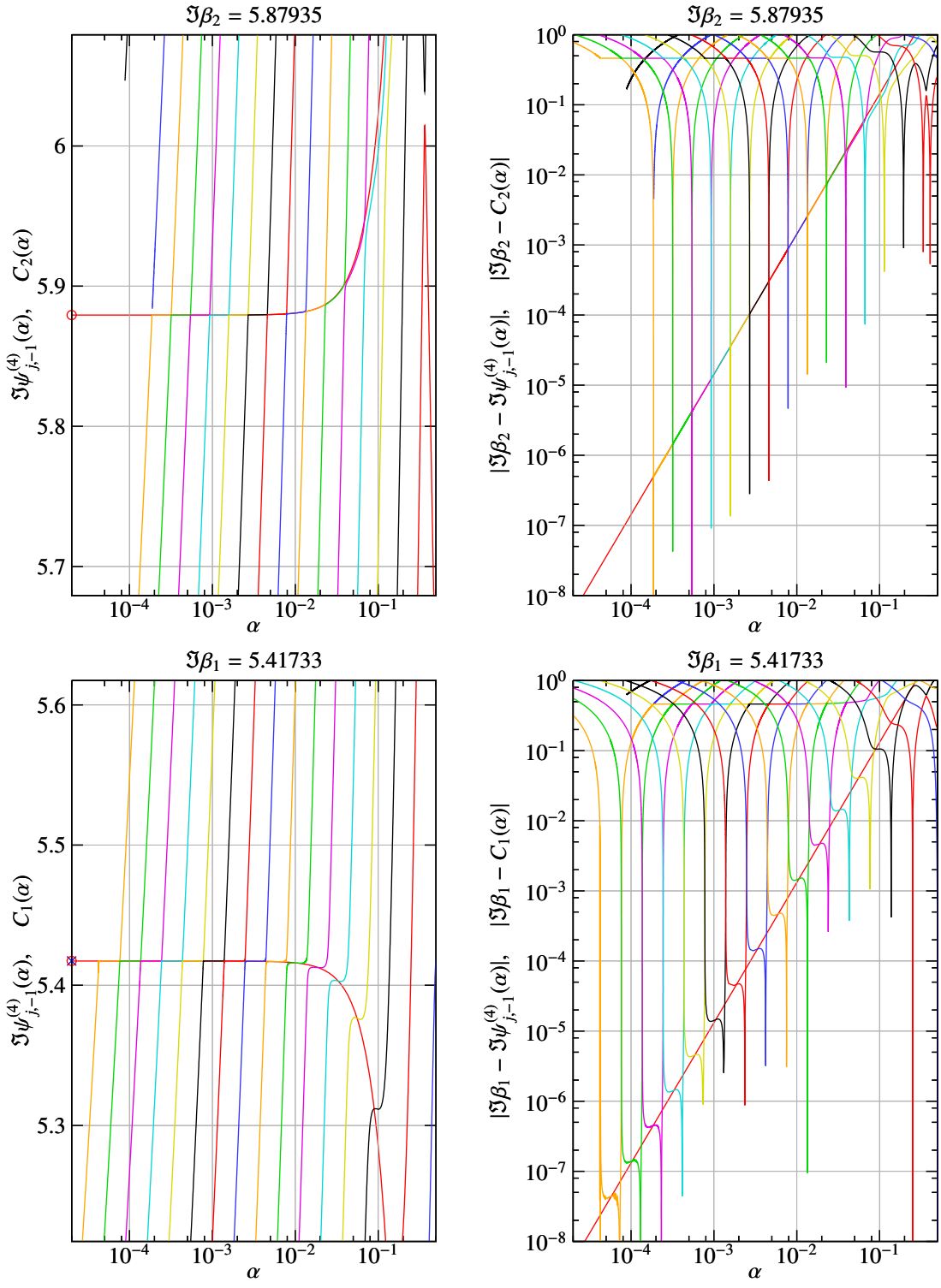

Figure 8.13: Infinite Avoided Crossing of the zeros $\mathcal{Z}^{(4)}_{\alpha,-1}$ on $\Re\beta = \frac{1}{2}$ for $\alpha \to 0$ (exponential law)

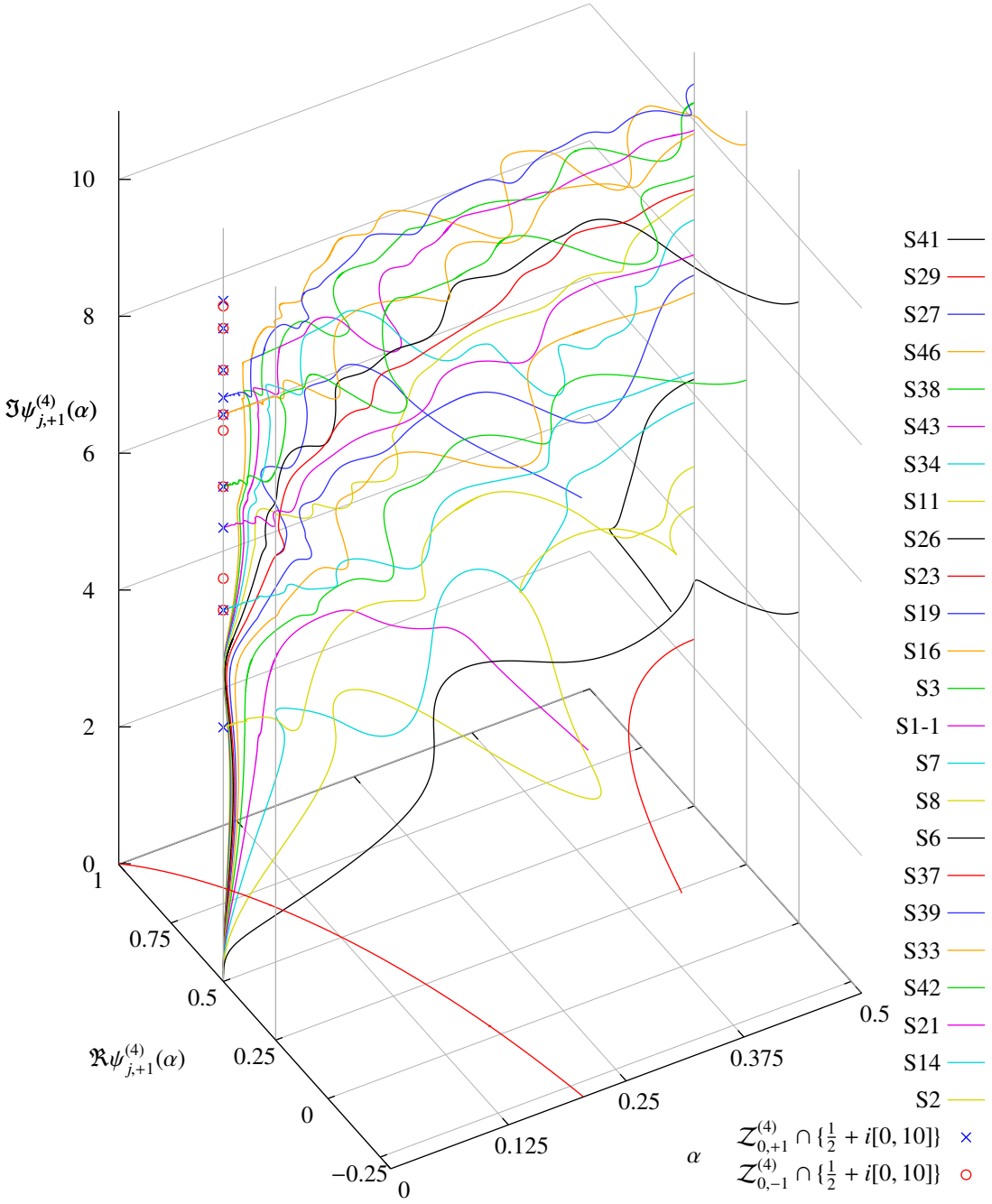

Figure 8.14: The zeros $\mathcal{Z}^{(4)}_{\alpha,+1}$ of the Selberg zeta function $Z^{(4)}\left(\beta, \chi^{(4)}_{\alpha}\right)$ in the (β, α)-plane

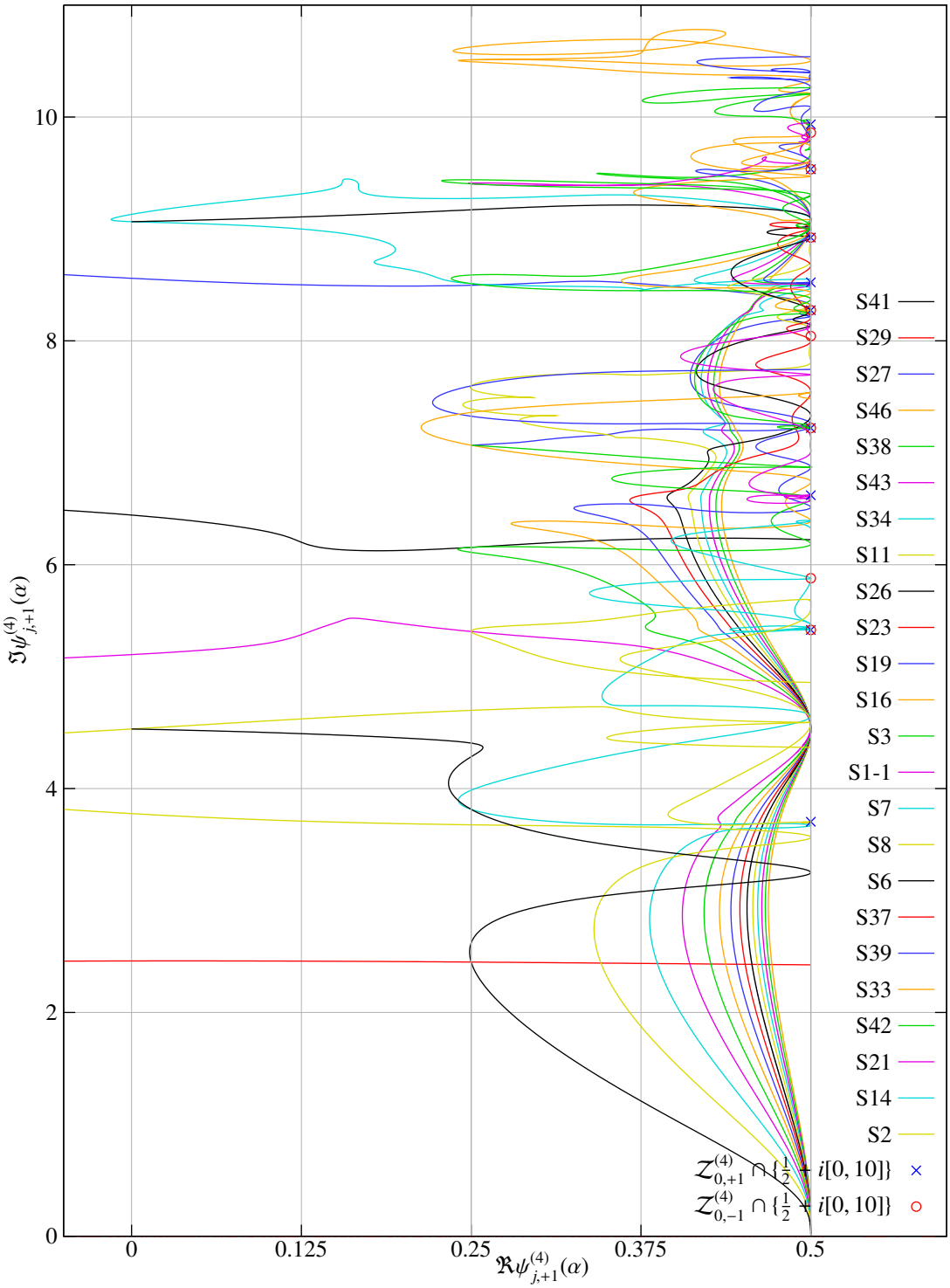

Figure 8.15: The zeros $\mathcal{Z}^{(4)}_{\alpha,+1}$ of the Selberg zeta function $Z^{(4)}\left(\beta, \chi^{(4)}_{\alpha}\right)$ in the β-plane for $\alpha \in (0, \frac{1}{2}]$

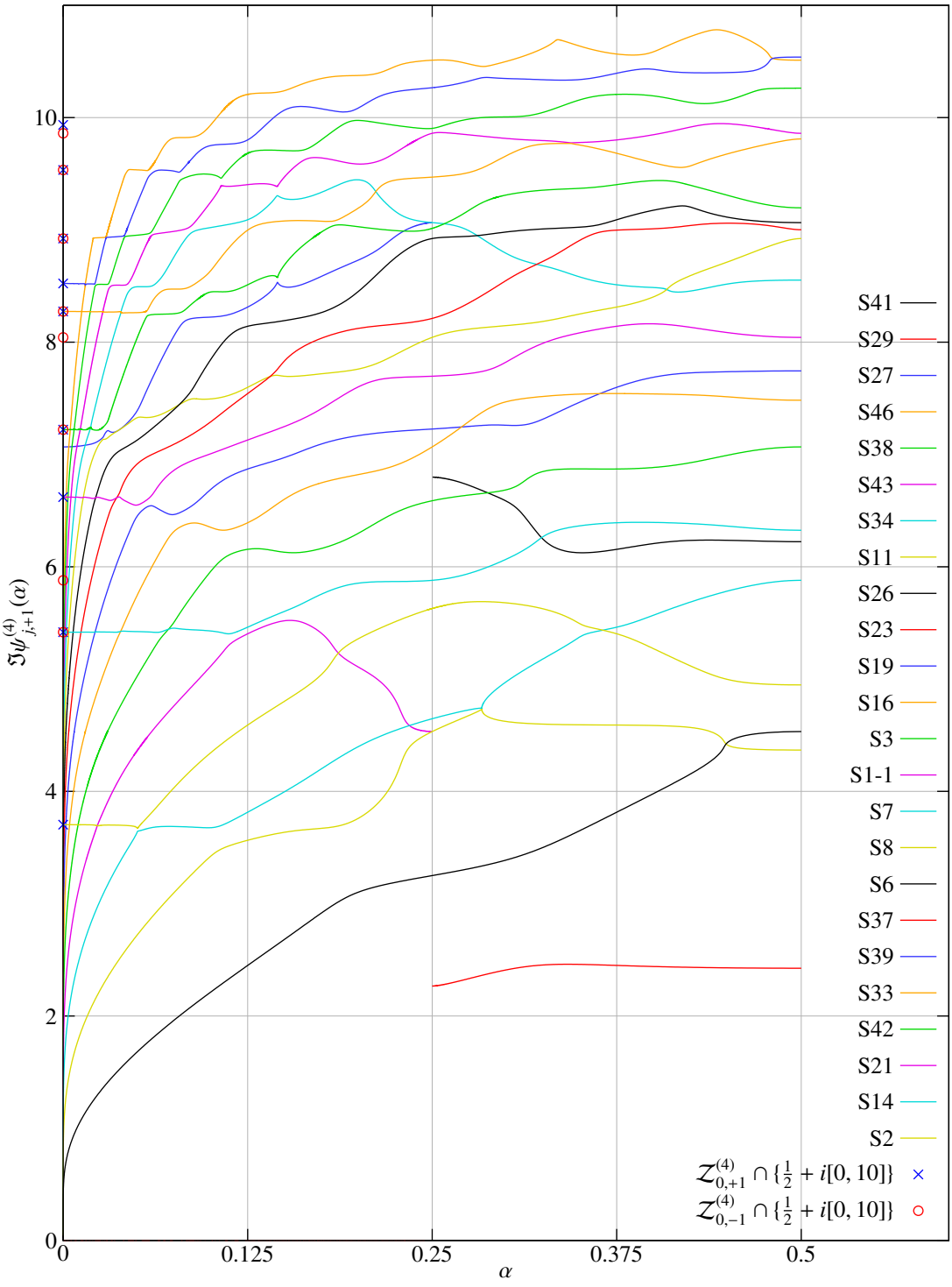

Figure 8.16: Imaginary parts of the zeros $\mathcal{Z}^{(4)}_{\alpha,+1}$ of the Selberg zeta function $Z^{(4)}\left(\beta, \chi^{(4)}_{\alpha}\right)$ for $\alpha \in (0, \frac{1}{2}]$

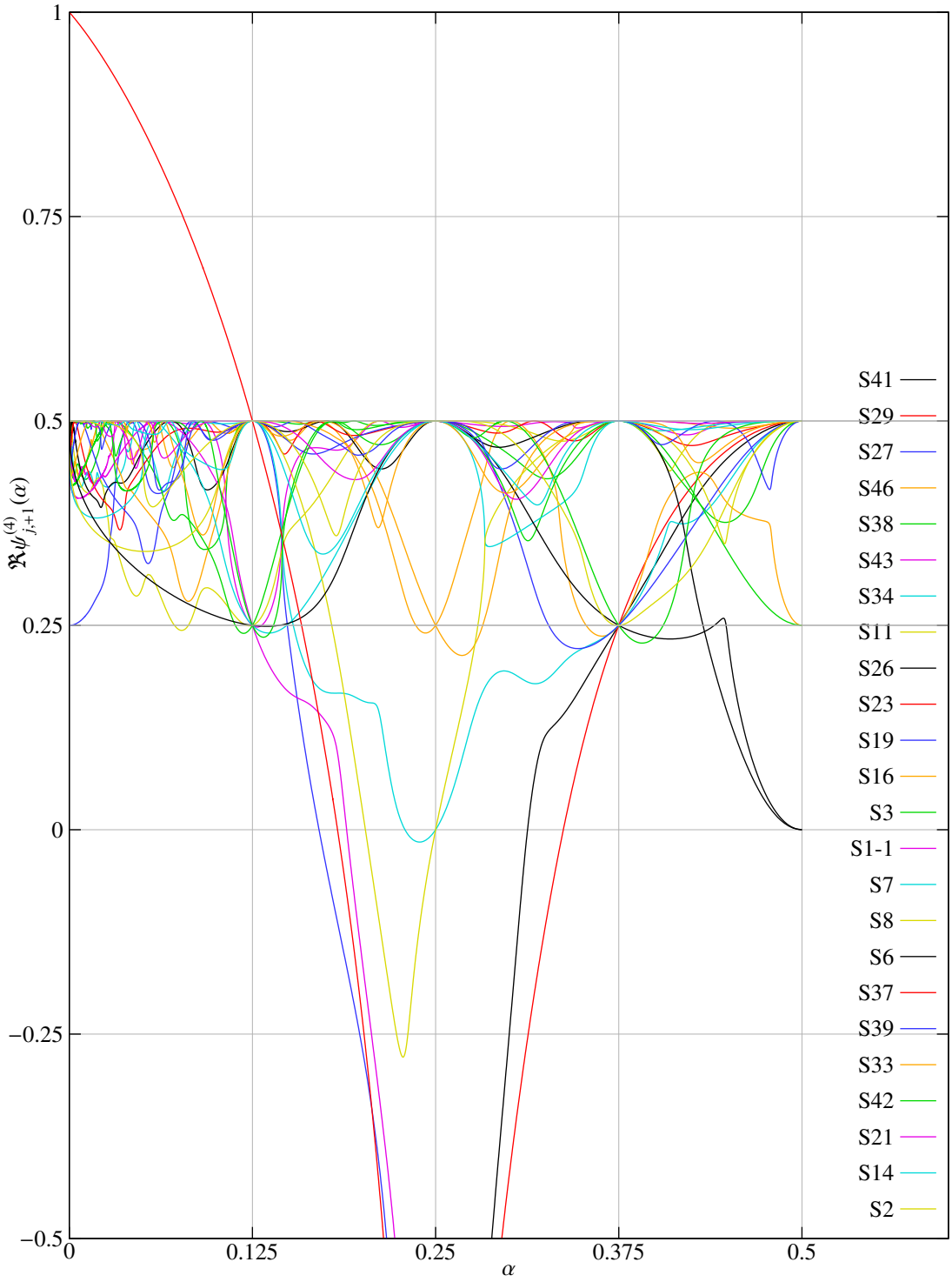

Figure 8.17: Real parts of the zeros $\mathcal{Z}^{(4)}_{\alpha,+1}$ of the Selberg zeta function $Z^{(4)}\left(\beta,\chi^{(4)}_{\alpha}\right)$ for $\alpha \in (0, \frac{1}{2}]$

- Experimental observation 8.2.8: for $\alpha_0 \in \{\frac{1}{8}, \frac{2}{8}, \frac{3}{8}, \frac{4}{8}\}$ the order of contact of the zeros $\mathcal{Z}^{(4)}_{\alpha,+1}$ for $\alpha \to \alpha_0$ with the critical line $\Re\beta = \frac{1}{2}$ is either 2 or 4.

Note that the multiplicity of $\mathcal{Z}^{(4)}_{\alpha,+1}$ for $\alpha = 0$ can be different from one.

The perturbation of the hyperbolic Laplacian for $\Gamma_0(4)$ by the character $\chi^{(4)}_\alpha$ is singular at $\alpha = 0$ since two cusps are closed as soon as α is set to a non-zero value. Observation 8.2.2 says that the Selberg zeta function $Z^{(4)}(\beta, \chi^{(4)}_\alpha)$ for $\Re\beta \leq \frac{1}{2}$ is non-analytic in $\alpha = 0$. In observation 8.2.13 we noticed that the curves of the zeros $\mathcal{Z}^{(4)}_{\alpha,-1}$ are also non-analytic in that case. It is not surprising that the curves of the zeros $\mathcal{Z}^{(4)}_{\alpha,+1}$ are non-analytic as well:

Experimental Observation 8.2.21. *For $(\Gamma_0(4), \chi^{(4)}_\alpha)$ even the smallest change of α away from zero leads to the following behavior of the zeros $\mathcal{Z}^{(4)}_{\alpha,+1}$ of the Selberg zeta function $Z^{(4)}(\beta, \chi^{(4)}_\alpha)$ corresponding to the eigenvalue $+1$ of the transfer operator $\mathcal{P}_2\mathcal{L}^{(4)}_{\beta,\varepsilon,\alpha}$:*

- *The multiplicity of the zeros $\mathcal{Z}^{(4)}_{\alpha,+1}$ for $\alpha = 0$ on the line $\Re\beta = \frac{1}{4}$ changes instantly to one for a non-zero value of α. (A zero $\beta \in \mathcal{Z}^{(4)}_{\alpha,+1}$ for $\alpha = 0$ on the line $\Re\beta = \frac{1}{4}$ with multiplicity greater than one does not just split up in several zeros in the β-plane for $\alpha \neq 0$; instead a single zero with multiplicity one remains.)*
- *(Selberg zeros) As predicted by Selberg in [Sel90] Theorem 3 we found that new zeros $\mathcal{Z}^{(4)}_{\alpha,+1}$ suddenly appear everywhere to the left of the critical line $\Re\beta = \frac{1}{2}$ for a non-zero value of α: near every point $\beta_0 = \frac{1}{2} + i\Im\beta_0$ on the critical line one can find a zero β with $\Re\beta < \frac{1}{2}$ of the Selberg zeta function, such that $|\Im\beta - \Im\beta_0| < \varepsilon$, with $\varepsilon = \varepsilon(\Im\beta_0, \alpha)$. The distance ε increases both with α and $\Im\beta_0$.*

We verified the instant change of multiplicity of the zeros on $\Re\beta = \frac{1}{4}$ by computation using the argument principle of the Selberg zeta function $Z^{(4)}(\beta, \chi^{(4)}_\alpha)$ for very small values of α. Observation 8.2.13 and conclusion 8.2.15 say that the zeros on the critical line $\Re\beta = \frac{1}{2}$ are getting dense for $\alpha \to 0$, and together with the zeros from observation 8.2.21 near the critical line $\Re\beta = \frac{1}{2}$ it seems impossible to track any zero $\mathcal{Z}^{(4)}_{\alpha,\pm1}$ on the critical line $\Re\beta = \frac{1}{2}$ starting with $\alpha = 0$. Since for the smallest change of α away from 0 many eigenvalues and resonances of the hyperbolic Laplacian are appearing it seems to us that in this case the application of perturbation theory is very difficult, if not impossible.

As we can see in Figures 8.15 and 8.17 most of the paths $\psi^{(4)}_{j,+1}$ of zeros are near to the critical line $\Re\beta = \frac{1}{2}$ and only a few of them are further away than $\Re\beta = \frac{1}{4}$. Figure 8.16 shows the dependence of the imaginary part of $\psi^{(4)}_{j,+1}$ on α, this plot has some similarity to Figure 8.9, which shows the paths $\psi^{(4)}_{j,-1}$ of zeros on the critical line $\Re\beta = \frac{1}{2}$. Although in Figures 8.15 - 8.17 the paths $\psi^{(4)}_{j,+1}$ of the zeros cross, one should keep in mind Figure 8.14 which shows that the curves of zeros $\mathcal{V}^{(4)}_{j,+1}$ are really in a three-dimensional space. Indeed, like in observation 8.2.14 for the zeros $\mathcal{Z}^{(4)}_{\alpha,-1}$ we found that the curves $\mathcal{V}^{(4)}_{j,+1}$ of zeros never cross:

Experimental Observation 8.2.22. *(Deflection) For $(\Gamma_0(4), \chi^{(4)}_\alpha)$ let $(\beta_1, \alpha_1) \in \mathcal{V}^{(4)}_{j,+1}$ and $(\beta_2, \alpha_2) \in \mathcal{V}^{(4)}_{k,+1}$ be zeros of the Selberg zeta function $Z^{(4)}(\beta, \chi^{(4)}_\alpha)$ on the curves $\mathcal{V}^{(4)}_{j,+1}$ and $\mathcal{V}^{(4)}_{k,+1}$. We found that the zeros (β_1, α_1) and (β_2, α_2) on the paths $\psi^{(4)}_{j,+1}$ and $\psi^{(4)}_{k,+1}$ deflect each other if $d((\beta_1, \alpha_1), (\beta_2, \alpha_2)) \ll 1$, i.e. the paths $\psi^{(4)}_{j,+1}$ and $\psi^{(4)}_{k,+1}$ do not cross but are deflected.*

This deflection is similar to the avoided crossing in observation 8.2.14, but it is more complicated, since the zeros move in a three dimensional space, while the avoided crossing is a phenomenon which exists in a two-dimensional space. We found the phenomenon of deflection every time when two zeros are close to each other, from this we conjectured in 8.2.11 that the multiplicity of the zeros $\mathcal{Z}^{(4)}_{\alpha,+1}$ for $0 < \alpha \leq \frac{1}{2}$ is always one.

In observation 8.2.21 we verified the existence of the Selberg zeros for $\alpha \to 0$. On the other hand, we also found zeros $\mathcal{Z}^{(4)}_{\alpha,+1}$ of the Selberg zeta function whose behavior for $\alpha \to 0$ is different from the Selberg zeros:

Experimental Observation 8.2.23. *In the limit $\alpha \to 0$ we found the following type of behavior of zeros $\mathcal{Z}^{(4)}_{\alpha,+1}$ of the Selberg zeta function $Z^{(4)}\left(\beta, \chi^{(4)}_\alpha\right)$ for $(\Gamma_0(4), \chi^{(4)}_\alpha)$ which are related to the eigenvalue $+1$ of the transfer operator $\mathcal{P}_2\mathcal{L}^{(4)}_{\beta,\varepsilon,\alpha}$:*

- *(Selberg zeros) See [Sel90] Theorem 3 and observation 8.2.21.*
- *(Convergence to Eigenvalues) There are zeros in $\mathcal{Z}^{(4)}_{\alpha,+1}$ which converge to the zeros $\mathcal{Z}^{(4)}_{0,+1}$ for $\alpha = 0$ on the critical line $\Re\beta = \frac{1}{2}$ with $\Im\beta > 0$. They approach these zeros in a rather complicated way, as we will see below.*
- *(Convergence to Resonances) There are zeros in $\mathcal{Z}^{(4)}_{\alpha,+1}$ which approach the zeros $\mathcal{Z}^{(4)}_{0,+1}$ for $\alpha = 0$ on the line $\Re\beta = \frac{1}{4}$ with $\Im\beta > 0$. The multiplicity of these zeros changes instantly at $\alpha = 0$, (see observation 8.2.21).*
- *(Convergence to Constant Eigenfunction) There is a zero in $\mathcal{Z}^{(4)}_{\alpha,+1}$ on the real line $\mathbb{R}$ which moves towards $\beta = 1$ for $\alpha \to 0$.*

For the path $\psi^{(4)}_{37,+1}$ of the zero on the real line which is curve S 37 in Figure 8.18 we have:

Experimental Observation 8.2.24. *(Real Zero) For the path $\psi^{(4)}_{37,+1}$ of the zero $\beta_0 = 1 \in \mathcal{Z}^{(4)}_{0,+1}$ of the Selberg zeta function $Z^{(4)}\left(\beta, \chi^{(4)}_0\right)$ related to the eigenvalue $+1$ of the transfer operator $\mathcal{P}_2\mathcal{L}^{(4)}_{\beta,\varepsilon,\alpha}$ we found the following behavior:*

- *The zero on the path $\psi^{(4)}_{37,+1}$ approaches $\beta_0 = 1$ for $\alpha = 0$ on a smooth curve, with $\lim_{\alpha\to 0}\psi^{(4)}_{37,+1}(\alpha) = 1$.*
- *As $\alpha \to \frac{2}{8}$ the zero on the path $\psi^{(4)}_{37,+1}$ moves faster and faster towards $-\infty$, i.e.*

$$\text{for } \alpha \to \frac{2}{8} \qquad \left|\frac{d\psi^{(4)}_{37,+1}(\alpha)}{d\alpha}\right| \to \infty \quad \text{together with} \quad \psi^{(4)}_{37,+1}(\alpha) \to -\infty.$$

- *The zero on the path $\psi^{(4)}_{37,+1}$ stays on the real line, i.e. $\psi^{(4)}_{37,+1}(\alpha) \in \mathbb{R}$ for all $\alpha \in [0, \frac{2}{8})$, moving in the negative direction for α growing monotonically, i.e. $\psi^{(4)}_{37,+1}(\alpha) \leq 1$ for all $\alpha \in [0, \frac{2}{8})$.*
- *The zero on the path $\psi^{(4)}_{37,+1}$ cancels the pole of the Selberg zeta function $Z^{(4)}\left(\beta, \chi^{(4)}_\alpha\right)$ at $\beta = \frac{1}{2}$ for $\alpha = \frac{1}{8}$, and both the pole and the zero disappear there.*

The fact, that this zero approaches $\beta = 1$ for $\alpha = 0$ smoothly is in agreement with our observation 8.2.2 namely that $\lim_{\alpha\to 0} Z^{(4)}\left(\beta, \chi^{(4)}_\alpha\right) = Z^{(4)}\left(\beta, \chi^{(4)}_0\right)$ exists for $\Re\beta > \frac{1}{2}$. Since this zero disappears at $\beta = \frac{1}{2}$ for $\alpha = \frac{1}{8}$ we had to compute a point for this curve shortly before, namely $\beta = 0.500125$ for $\alpha = 0.12498$, and continued the computations for a point shortly afterwards at the point $\beta = 0.499136$ for $\alpha = 0.12514$. Obviously, it can be asked if this is still the same zero which we are tracking, since it got destroyed at $\beta = \frac{1}{2}$. Since the curve S 37 of this zero in Figure 8.18 is smooth we assume that we are tracking the same zero. The same problem appears for all $\beta \in \mathbb{Z}_{\leq} \cup \frac{1}{2} + \mathbb{Z}_{\leq}$.

Besides the zero on the real line we also found other paths $\psi^{(4)}_{j,+1}$ of zeros with $\Re\psi^{(4)}_{j,+1}(\alpha) \to -\infty$ for $\alpha \to \frac{2}{8}$, as can be seen in Figure 8.18. Indeed, in [Sel90] section 3, Selberg predicted the existence of some such zeros. He proved the existence of a family of resonances, which for our character $\chi^{(4)}_\alpha$ move to

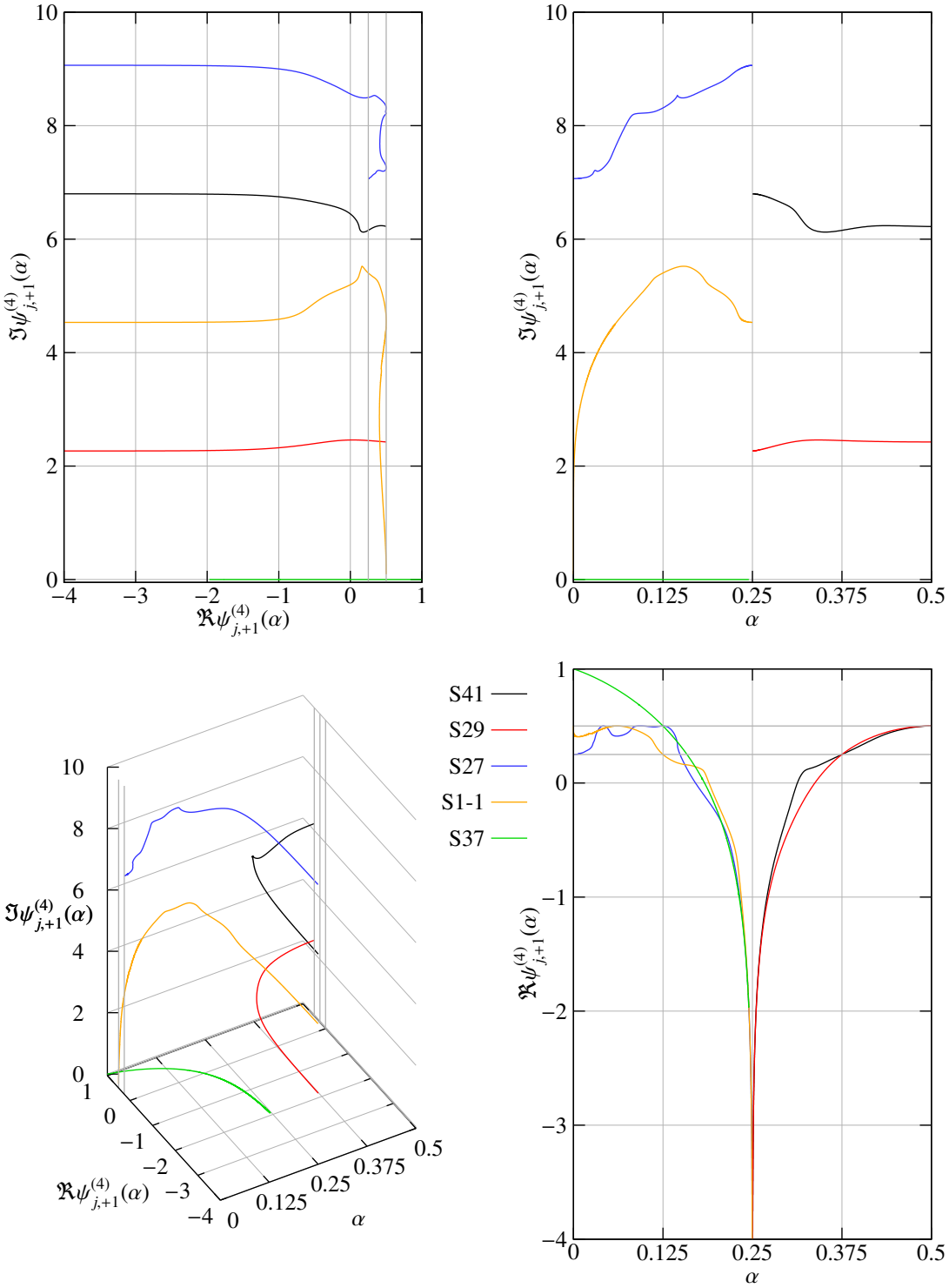

Figure 8.18: The zeros $\mathcal{Z}^{(4)}_{\alpha,+1}$ which are going to $\Re\beta \to -\infty$ for $\alpha \to \frac{2}{8}$

$\Re\beta \to -\infty$ for $\alpha \uparrow \frac{2}{8}$ respectively $\alpha \downarrow -\frac{2}{8}$ and disappear for $\alpha = \frac{2}{8}$ respectively $\alpha = -\frac{2}{8}$. It follows from our lemma 6.5.2 that $Z^{(4)}(\beta,\chi_\alpha^{(4)}) = Z^{(4)}(\beta,\chi_{-\alpha}^{(4)})$, and therefore the cases $\alpha \uparrow \frac{2}{8}$ and $\alpha \downarrow -\frac{2}{8}$ are equivalent. According to Selberg the number N of zeros which move to $\Re\beta \to -\infty$ with imaginary parts $|\Im\beta| < T$ is given by $N \approx \frac{\ln 4}{\pi} T$ for large T. Note that Selberg actually studied the zeros of a L-function which correspond to the zeros of the determinant of the scattering matrix for $\Re\beta > \frac{1}{2}$, these zeros are equivalent to our zeros of the Selberg zeta function for $\Re\beta < \frac{1}{2}$, see [Sel90]. Our numerical experiments show that there are also zeros with $\Re\beta \to -\infty$ for $\alpha \downarrow \frac{2}{8}$ (note that this is not the same case $\alpha \uparrow \frac{2}{8}$ or $\alpha \downarrow -\frac{2}{8}$ as considered by Selberg). We conclude from our numerical results that:

Conclusion 8.2.25. *(−∞-Zeros) There are paths $\psi_{j,+1}^{(4)}$ of zeros $\mathcal{Z}_{\alpha,+1}^{(4)}$ of the Selberg zeta function $Z^{(4)}(\beta,\chi_\alpha^{(4)})$ corresponding to the eigenvalue $+1$ of the transfer operator $\mathcal{P}_2\mathcal{L}_{\beta,\varepsilon,\alpha}^{(4)}$ which behave for $\alpha \to \frac{2}{8}$ in the following way:*

$$\left|\frac{d\Re\psi_{j,+1}^{(4)}(\alpha)}{d\alpha}\right| \to \infty \qquad \textit{and} \qquad \Re\psi_{j,+1}^{(4)}(\alpha) \to -\infty,$$

$$\left|\frac{d\Im\psi_{j,+1}^{(4)}(\alpha)}{d\alpha}\right| \to 0 \qquad \textit{and} \qquad \Im\psi_{j,+1}^{(4)}(\alpha) \to \frac{\pi}{\ln 2} m,$$

with

- *$m \in \mathbb{Z}$ for $\alpha \uparrow \frac{2}{8}$. These zeros on the paths $\psi_{j,+1}^{(4)}(\alpha)$ exist only for $\alpha \in (0, \frac{2}{8})$. The number N of such zeros with $|\Im\psi_{j,+1}^{(4)}(\alpha)| \le T$ for $\alpha \uparrow \frac{2}{8}$ is given by*

$$N = 2\left[\frac{\ln 2}{\pi} T\right] + 1.$$

- *$m \in \frac{1}{2} + \mathbb{Z}$ for $\alpha \downarrow \frac{2}{8}$. These zeros on the paths $\psi_{j,+1}^{(4)}(\alpha)$ exist only for $\alpha \in (\frac{2}{8}, \frac{4}{8}]$. The number N of such zeros with $|\Im\psi_{j,+1}^{(4)}(\alpha)| \le T$ for $\alpha \downarrow \frac{2}{8}$ is given by*

$$N = 2\left[\frac{\ln 2}{\pi} T + \frac{1}{2}\right].$$

Here $[\cdot]$ denotes the integer part.

Both of our formulas for N and Selberg's asymptotic formula $N \approx \frac{\ln 4}{\pi} T$ agree quite well for large T. The reason why we believe that these zeros disappear for $\alpha = \frac{2}{8}$ is that if these zeros would exist at $\Re\beta = -\infty$ for $\alpha = \frac{2}{8}$ they must also exists for $\alpha = \frac{4}{8}$, since the Selberg zeta functions for these two values of α are the same, (see conclusion 8.2.3). But if they would exists for $\alpha = \frac{4}{8}$, we would have also found zeros moving toward $\Re\beta \to -\infty$ for $\alpha \to \frac{4}{8}$, but we never saw such zeros.

In observation 8.2.21 we found the Selberg zeros near to the critical line $\Re\beta = \frac{1}{2}$ for $\alpha \to 0$ corresponding to the zeros of the scattering determinant as described by Selberg in [Sel90] theorem 3. Next we want to discuss more results about the Selberg zeros we obtained numerically: We can see in Figures 8.15 and 8.16 some paths $\psi_{j,+1}^{(4)}$ of zeros converging to $\beta = \frac{1}{2}$ for $\alpha \to 0$. Indeed, these are the paths of the Selberg zeros. The left plot in Figure 8.19 shows a close-up of these zeros in the β-plane, together with the zeros $\mathcal{Z}_{\alpha,-1}^{(4)}$ on the critical line $\Re\beta = \frac{1}{2}$ for two values of α. The right plot in Figure 8.19 shows the distance of the real parts of the paths $\psi_{j,+1}^{(4)}$ from $\Re\beta = \frac{1}{2}$ against the distance of the imaginary parts from $\Im\beta = 0$ scaled logarithmically. Figure 8.20 shows the dependence of the real and imaginary parts of $\psi_{j,+1}^{(4)}$ on α. In the left

plot also the curves of the zeros $\mathcal{Z}^{(4)}_{\alpha,-1}$ on the critical line $\Re\beta = \frac{1}{2}$ are shown as gray lines. We computed also the Selberg zeta function in the β-plane in the strip $0.45 \leq \Re\beta \leq 0.5$ and $0 \leq \Im\beta \leq 10$ for several different very small values of α. This way we could see the general behavior of the Selberg zeros and the zeros on the critical line:

Conclusion 8.2.26. *(Behavior of Selberg Zeros) Some zeros $\mathcal{Z}^{(4)}_{\alpha,+1}$ of the Selberg zeta function $Z^{(4)}\left(\beta, \chi^{(4)}_{\alpha}\right)$ corresponding to the eigenvalue $+1$ of the transfer operator $\mathcal{P}_2\mathcal{L}^{(4)}_{\beta,\varepsilon,\alpha}$ tend to $\beta = \frac{1}{2}$ for $\alpha \to 0$ and the paths $\psi^{(4)}_{j,+1}$ of these zeros approach the critical line $\Re\beta = \frac{1}{2}$. For small α the distance between two zeros on nearest neighbor paths $\psi^{(4)}_{j,+1}$ and $\psi^{(4)}_{k,+1}$ with $\Im\psi^{(4)}_{j,+1}(\alpha) < \Im\psi^{(4)}_{k,+1}(\alpha)$, is given by*

$$|\psi^{(4)}_{k,+1}(\alpha) - \psi^{(4)}_{j,+1}(\alpha)| = c_j(\alpha).$$

The value of $c_j(\alpha)$ depends on j such that $c_j(\alpha) > c_l(\alpha)$ for $\Im\psi^{(4)}_{j,+1}(\alpha) > \Im\psi^{(4)}_{l,+1}(\alpha)$. $c_j(\alpha)$ is decreasing as α is getting smaller.

- *These zeros on the paths $\psi^{(4)}_{j,+1}$ accumulate at the the critical line $\Re\beta = \frac{1}{2}$ for $\alpha \to 0$.*
- *For fixed small α these zeros can be connected by a smooth curve in the β-plane.*
- *(Eigenvalue-Resonance Pair): For every such zero on a path $\psi^{(4)}_{j,+1}$ there is another zero on a path $\psi^{(4)}_{k,-1}$ on the critical line $\Re\beta = \frac{1}{2}$ as described in conclusion 8.2.15, such that*

$$|\Im\psi^{(4)}_{j,+1}(\alpha) - \Im\psi^{(4)}_{k,-1}(\alpha)| \to 0 \quad \text{for } \alpha \to 0.$$

The main difference between the zeros $\mathcal{Z}^{(4)}_{\alpha,+1}$ and the zeros $\mathcal{Z}^{(4)}_{\alpha,-1}$ on the critical line $\Re\beta = \frac{1}{2}$ is that *all* the zeros $\mathcal{Z}^{(4)}_{\alpha,-1}$ behave as described in conclusion 8.2.15 for $\alpha \to 0$, while for the zeros $\mathcal{Z}^{(4)}_{\alpha,+1}$ we found different behaviors for $\alpha \to 0$ as described in observation 8.2.23. In observation 8.2.2 we found that the Selberg zeta function $Z^{(4)}\left(\beta, \chi^{(4)}_{\alpha}\right)$ shows strong oscillations for $\Re\beta \leq \frac{1}{2}$ as $\alpha \to 0$. We can see these oscillations in Figure 8.8. These oscillations seem to be related to the zeros in conclusion 8.2.26 and conclusion 8.2.15: It seems that these zeros are located at the end of every "wave crest" of such oscillations of the Selberg zeta function.

We have seen in conclusions 8.2.15 and 8.2.26 that the zeros on the critical line $\Re\beta = \frac{1}{2}$ respectively left of it move to $\beta = \frac{1}{2}$ for $\alpha \to 0$ and at the same time are becoming dense on the critical line. The question then is what happens to these zeros for $\alpha = 0$. Obviously, they disappear as zeros of the Selberg zeta function $Z^{(4)}(\beta, \chi^{(4)}_{\alpha})$ for $\alpha = 0$. On the other hand, the continuous spectrum of the hyperbolic Laplacian changes it multiplicity from one for $\alpha \neq 0$ to three for $\alpha = 0$. Therefore, we conclude that:

Conclusion 8.2.27. *(Continuous Spectrum Breakdown) As α moves away from the value 0 and the multiplicity of the continuous spectrum of the hyperbolic Laplacian for $(\Gamma_0(4), \chi^{(4)}_{\alpha})$ changes from three to one, a part of the continuous spectrum turns into discrete eigenvalues of the hyperbolic Laplacian which manifest themselves as zeros $\mathcal{Z}^{(4)}_{\alpha,-1}$ of the Selberg zeta function $Z^{(4)}(\beta, \chi^{(4)}_{\alpha})$ on the critical line $\Re\beta = \frac{1}{2}$ as described in conclusion 8.2.15. And at the same time a part of the continuous spectrum turns into resonances of the hyperbolic Laplacian which manifest themselves as zeros $\mathcal{Z}^{(4)}_{\alpha,+1}$ of the Selberg zeta function $Z^{(4)}(\beta, \chi^{(4)}_{\alpha})$ in the immediate neighborhood of the critical line $\Re\beta = \frac{1}{2}$ as described in conclusion 8.2.26.*

Next we want to discuss the zeros $\mathcal{Z}^{(4)}_{\alpha,+1}$ which converge for $\alpha \to 0$ towards zeros on the critical line $\Re\beta = \frac{1}{2}$. In Figure 8.21 one can see the first 6 of such zeros. At a first glance it looks as if these zeros just move onto the critical line $\Re\beta = \frac{1}{2}$ for $\alpha = 0$; however, a more detailed analysis shows that this approach is much more complicated. In Figure 8.22 we can see two close-ups of the curves S 2 and S 14 of zeros in the β-plane. The plots on the left show that these curves touch the critical line $\Re\beta = \frac{1}{2}$ for certain values

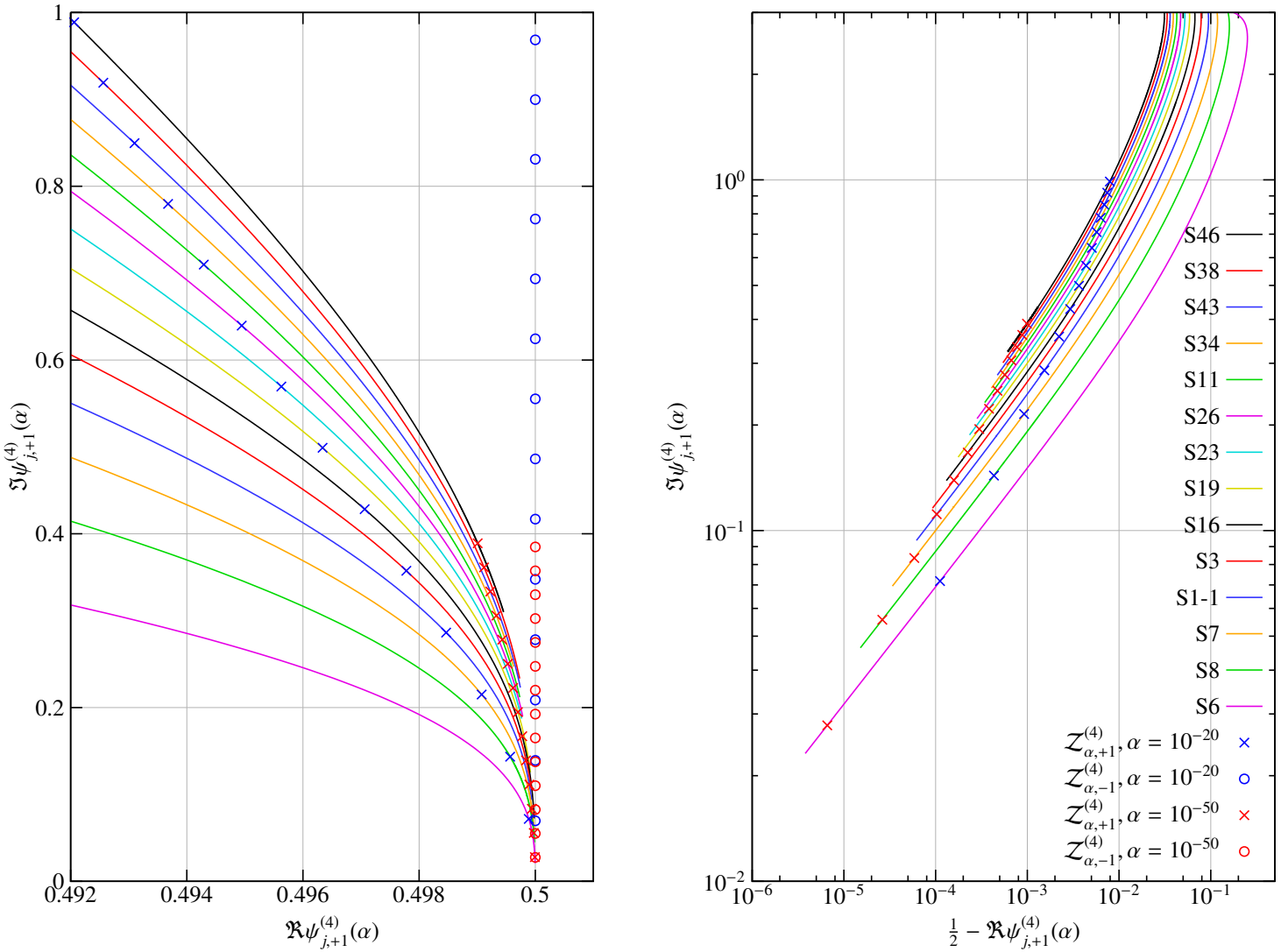

Figure 8.19: The zeros $\mathcal{Z}^{(4)}_{\alpha,+1}$ which are going to $\beta = \frac{1}{2}$ for $\alpha \to 0$ in the β-plane for $\alpha \in [10^{-60}, 0.5]$

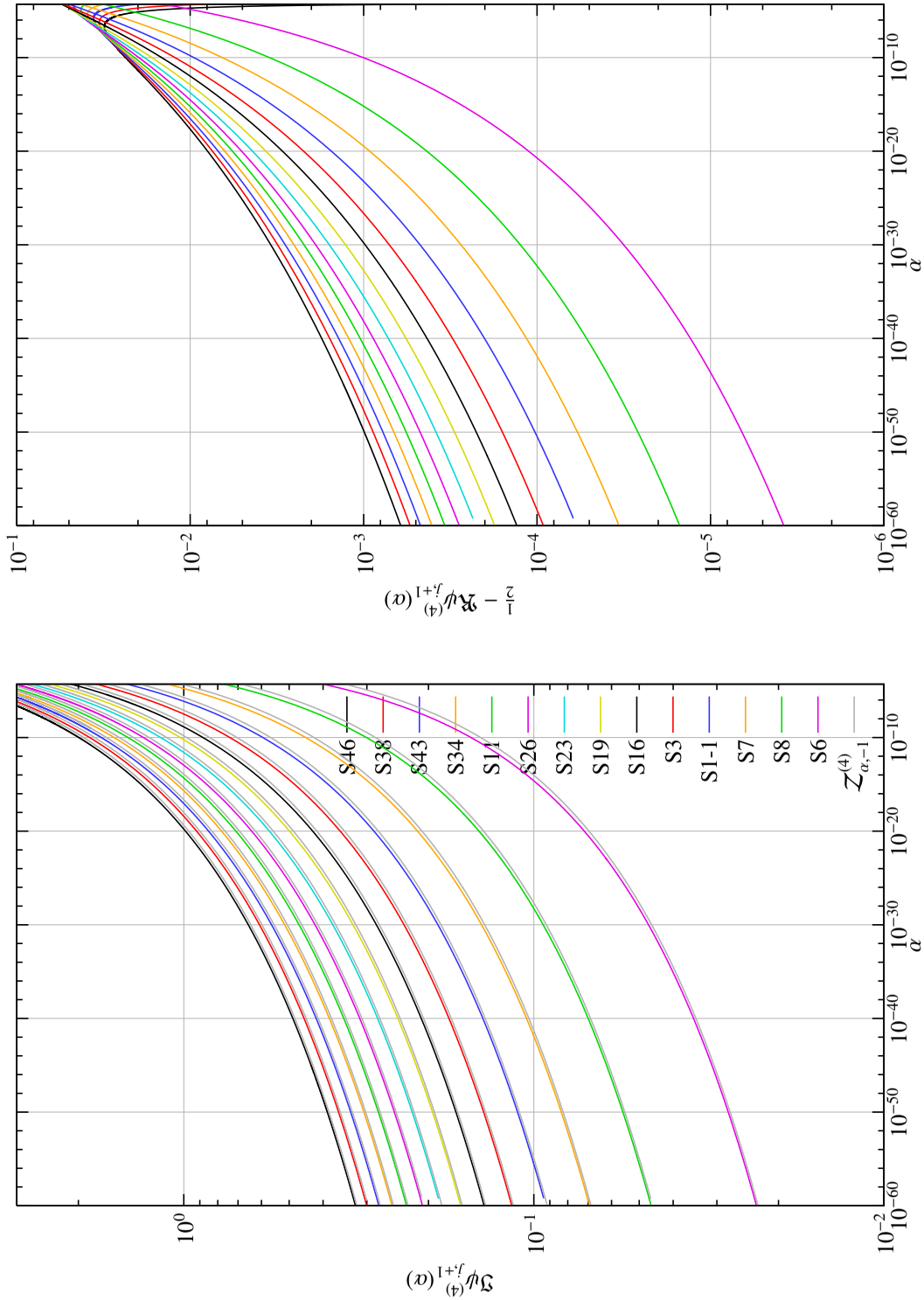

Figure 8.20: Imaginary and real parts of the zeros $\mathcal{Z}^{(4)}_{\alpha,+1}$ which are going to $\beta = \frac{1}{2}$ for $\alpha \to 0$

of α, these values are given to the right of the orange crosses. In the right plot the area in the β-plane close to the zeros for $\alpha = 0$ is magnified, even at this huge magnification we can see that both curves still touch the critical line for certain values of α. Although we found this behavior for all zeros $\mathcal{Z}^{(4)}_{\alpha,+1}$ converging to the zeros $\mathcal{Z}^{(4)}_{0,+1}$ on the critical line $\Re\beta = \frac{1}{2}$ which we track in the β-plane for $\Im\beta < 8.6$, other results for $\Im\beta > 8.6$ indicate, however, that there might be also a different kind of convergence of the zeros $\mathcal{Z}^{(4)}_{\alpha,+1}$ for $\alpha \to 0$ to the zeros $\mathcal{Z}^{(4)}_{0,+1}$ on the critical line $\Re\beta = \frac{1}{2}$, we discuss this issue later. Therefore, it is not certain if the following conclusion is true for every zero in $\mathcal{Z}^{(4)}_{0,+1}$ on the critical line $\Re\beta = \frac{1}{2}$:

Conclusion 8.2.28. *(Infinite Resonance-Eigenvalue Convergence) For a zero $\beta_l \in \mathcal{Z}^{(4)}_{0,+1}$ of the Selberg zeta function $Z^{(4)}(\beta, \chi^{(4)}_\alpha)$ on the critical line $\Re\beta = \frac{1}{2}$ corresponding to the eigenvalue $+1$ of the transfer operator $\mathcal{P}_2\mathcal{L}^{(4)}_{\beta,\varepsilon,\alpha}$, there is the following one-to-one correspondence between β_l and the path $\psi^{(4)}_{j(l),+1}$ converging to β_l for $\alpha \to 0$:*

- *The path $\psi^{(4)}_{j,+1}$ touches the critical line $\Re\beta = \frac{1}{2}$ tangentially for infinitely many discrete values of $\alpha^{(l)}_k$, with $k \in \mathbb{Z}_>$, i.e.*

$$\Re\psi^{(4)}_{j,+1}(\alpha^{(l)}_k) = \frac{1}{2} \quad \text{with } \alpha^{(l)}_k \in A_j \quad \text{for all } k \in \mathbb{Z}_>.$$

  For $\alpha^{(l)}_k > \alpha > \alpha^{(l)}_{k+1}$ the zero on the path $\psi^{(4)}_{j,+1}$ stays left of the critical line $\Re\beta = \frac{1}{2}$, i.e.

$$\Re\psi^{(4)}_{j,+1}(\alpha) < \frac{1}{2} \quad \text{with } \alpha \in (\alpha^{(l)}_{k+1}, \alpha^{(l)}_k) \quad \text{for all } k \in \mathbb{Z}_>.$$

  The distance $\alpha^{(l)}_k - \alpha^{(l)}_{k+1}$ decreases exponentially with $k \to \infty$, and $\alpha^{(l)}_k \to 0$ for $k \to \infty$.

- *The zero $\psi^{(4)}_{j,+1}(\alpha^{(l)}_k)$ converges towards the zero β_l:*

$$\lim_{k\to\infty} |\beta_l - \psi^{(4)}_{j,+1}(\alpha^{(l)}_k)| = 0.$$

- *When the zero on the path $\psi^{(4)}_{j,+1}(\alpha)$ goes down from the critical line, i.e. $\alpha \in (\alpha^{(l)}_{k+1}, \alpha^{(l)}_k)$, exactly one zero on a path $\psi^{(4)}_{m,-1}$ with $m = m(k)$ passes by on the critical line $\Re\beta = \frac{1}{2}$, i.e.*

$$\Im\psi^{(4)}_{j,+1}(\alpha^{(l)}_k) < \Im\psi^{(4)}_{m(k),-1}(\alpha^{(l)}_k) \text{ and } \Im\psi^{(4)}_{j,+1}(\alpha^{(l)}_{k+1}) > \Im\psi^{(4)}_{m(k),-1}(\alpha^{(l)}_{k+1}) \quad \text{for all } k \in \mathbb{Z}_>.$$

As in the case of the infinite avoided crossing sequence on the critical line (see conclusion 8.2.17) we can only compute a finite number of the values of $\alpha^{(l)}_k$ where the path $\psi^{(4)}_{j(l),+1}$ touches the critical line. But since the distance between $\alpha^{(l)}_k$ and $\alpha^{(l)}_{k+1}$ decreases exponentially it means that infinitely many points $\alpha^{(l)}_k$ will appear. In contrast to the infinite avoided crossing convergence described in conclusion 8.2.28 we can find here exactly one zero in $\mathcal{Z}^{(4)}_{\alpha,+1}$ which corresponds to a zero in $\mathcal{Z}^{(4)}_{0,+1}$ on the critical line $\Re\beta = \frac{1}{2}$. We can see in Figure 8.22 that the paths $\psi^{(4)}_{2,+1}$ and $\psi^{(4)}_{14,+1}$ form loops in the β-plane. Indeed, for all paths $\psi^{(4)}_{j,+1}$ of zeros with a behavior as described in conclusion 8.2.28, and which we investigated, we found that loops, which always rotate clockwise in the β-plane for $\alpha \to 0$. We cannot rule out that other shapes than loops are possible as well. We see also in the close-up on the right of Figure 8.22 that the shape of the loops is more or less preserved.

The last point in conclusion 8.2.28 shows that there is a close relation between the infinite resonance-eigenvalue convergence sequence and the zeros $\mathcal{Z}^{(4)}_{\alpha,-1}$ on the critical line $\Re\beta = \frac{1}{2}$ described in conclusion 8.2.15 which move to $\beta = \frac{1}{2}$ for $\alpha \to 0$. This is not surprising, since in 8.2.11 we conjectured that all zeros of the Selberg zeta function $Z^{(4)}(\beta, \chi^{(4)}_\alpha)$ have multiplicity one for $\alpha \in (0, \frac{1}{2}]$; therefore, the curves of zeros

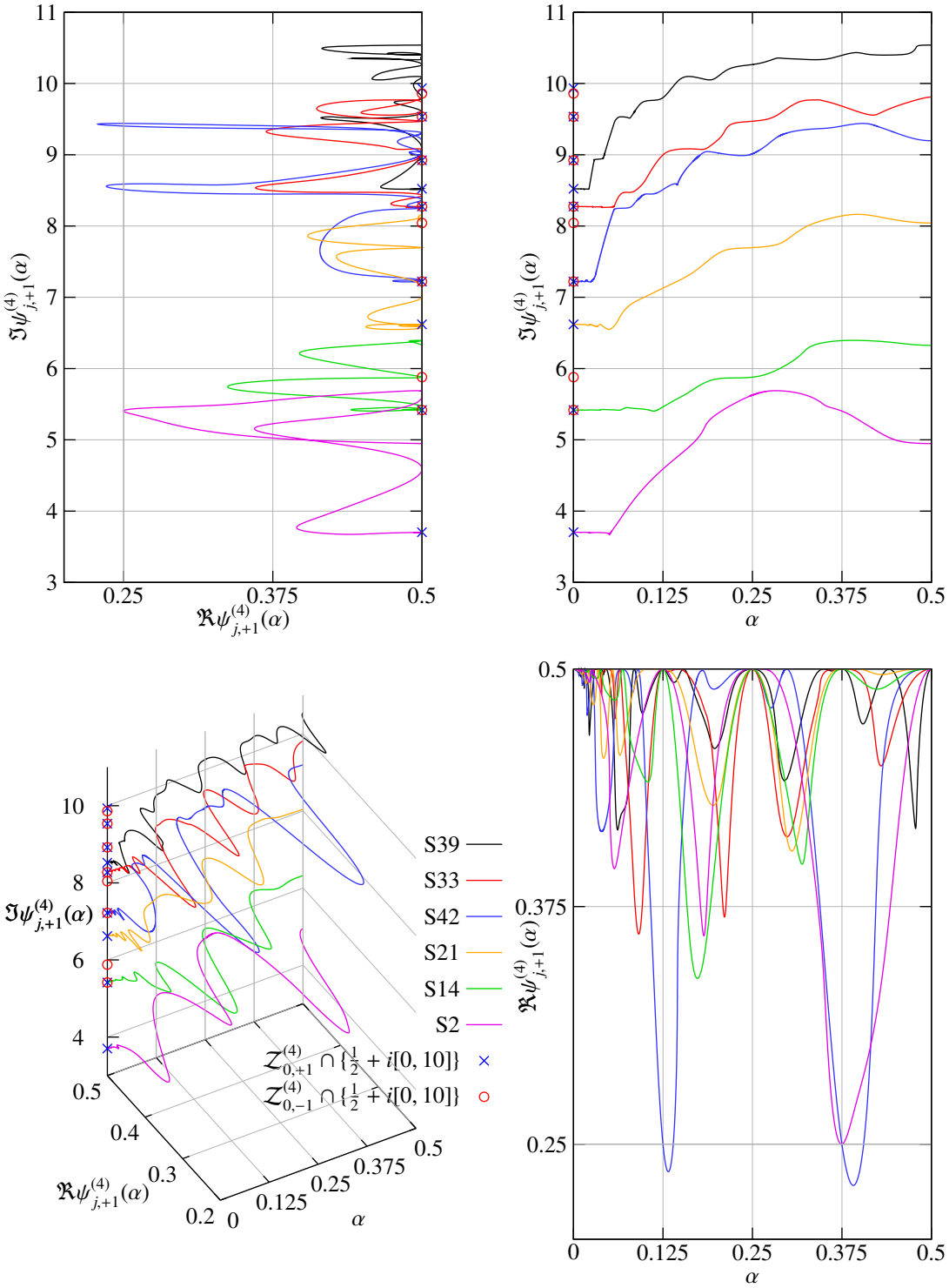

Figure 8.21: The zeros $\mathcal{Z}^{(4)}_{\alpha,+1}$ which converge to the zeros $\mathcal{Z}^{(4)}_{0,+1}$ on $\Re\beta = \frac{1}{2}$ for $\alpha = 0$

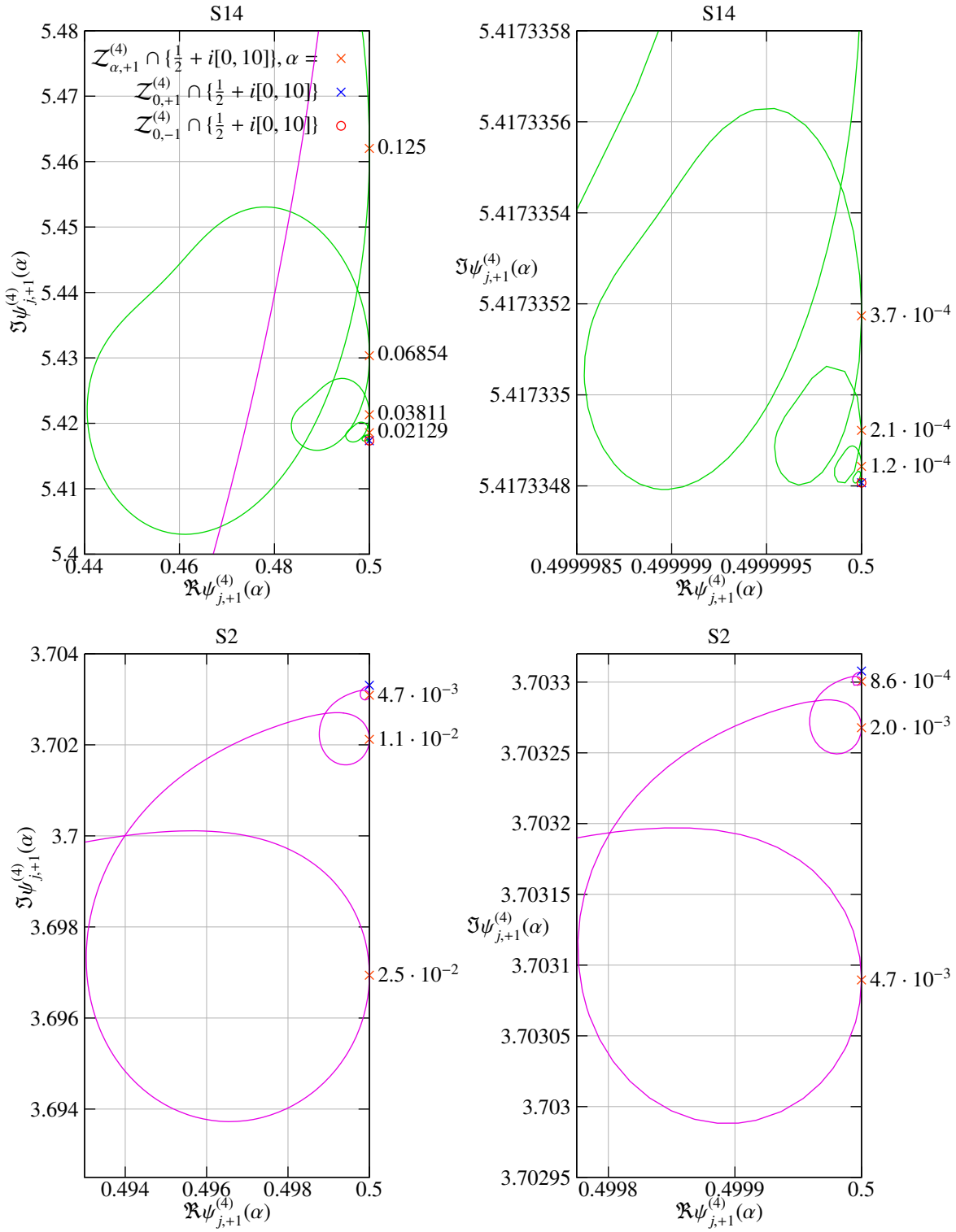

Figure 8.22: Infinite Resonance-Eigenvalue Convergence of the zeros $\mathcal{Z}^{(4)}_{\alpha,+1}$ in the β-plane for $\alpha \to 0$

Table 8.7: Coefficient $C_{0,l}$ and d_l of curve $C_l(\alpha)$ (Infinite Resonance-Eigenvalue Convergence)

l	$\Im\beta_l$	d_l	$C_{0,l}$	$C_{0,l}$ for $d_l := 2$
1	3.703307801219027665	1.99997147864	-9.94247613631	-9.94447820978
2	5.417334806844678385	1.99999204396	2.72453783969	2.72474702344

in $\mathcal{Z}^{(4)}_{\alpha,+1}$ which touch the critical line $\Re\beta = \frac{1}{2}$ must avoid the zeros $\mathcal{Z}^{(4)}_{\alpha,-1}$ on the critical line. In the left Figure 8.23 are shown the dependence on α of the imaginary parts of the paths $\psi^{(4)}_{j,+1}$ of zeros, which tend to the zeros $\beta_1 \approx \frac{1}{2} + 3.7033078i$ and $\beta_2 \approx \frac{1}{2} + 5.4173348i$. These are the paths $\psi^{(4)}_{j,+1}$ which form the loops in Figure 8.22. The right plots show the dependence on α of the distance $|\Im\beta_l - \Im\psi^{(4)}_{j+1}(\alpha)|$ for $l = 1, 2$. The points where the paths $\psi^{(4)}_{j,+1}$ touch the critical line, i.e. $\Re\psi^{(4)}_{j,+1}(\alpha) = \frac{1}{2}$, are marked by orange crosses. In the background are also shown as gray lines the paths $\psi^{(4)}_{j,-1}$ of the zeros which are always on the critical line. As we can clearly see, the paths $\psi^{(4)}_{j,+1}$ which converge to the zeros β_l for $l = 1, 2$ touch the critical line in between two zeros on the paths $\psi^{(4)}_{j,-1}$ on the critical line. Note that the zero β_2 has multiplicity two, indeed one can see there is also an infinite avoided crossing sequence converging to this zero, (see also the two plots on the bottom in Figure 8.13). The relation between the points $\psi^{(4)}_{j(l),+1}(\alpha^{(l)}_k)$ which touch the critical line and the values of $\alpha^{(l)}_k$ is described by the following curve:

Conclusion 8.2.29. *The points $\psi^{(4)}_{j(l),+1}(\alpha^{(l)}_k)$ which converge to a zero $\beta_l \in \mathcal{Z}^{(4)}_{0,+1}$ as described in conclusion 8.2.28 define a curve $(\frac{1}{2} + iC_l(\alpha), \alpha)$ in the (β, α)-plane such that $C_l(0) = \Im\beta_l$ and $\frac{dC_l(\alpha)}{d\alpha}|_{\alpha=0} = 0$, given by*

$$C_l(\alpha) = C_{0,l}\alpha^{d_l} + \Im\beta_l,$$

with $C_{0,l}, d_l \in \mathbb{R}$, and such that the points $\psi^{(4)}_{j(l),+1}(\alpha^{(l)}_k)$ lie on this curve, i.e.

$$\Im\psi^{(4)}_{j(l),+1}(\alpha^{(l)}_k) = C_l(\alpha^{(l)}_k) \quad \textit{for all } k \in \mathbb{Z}_>.$$

We can determine the constants $C_{0,l}$ and d_l from our data sets by the formulas

$$d_l = \frac{\ln|\Im\beta_l - \Im\psi^{(4)}_{j,+1}(\alpha_{k,l})| - \ln|\Im\beta_l - \Im\psi^{(4)}_{j,+1}(\alpha_{k+1,l})|}{\ln|\alpha_{k,l}| - \ln|\alpha_{k+1,l}|}$$

and

$$C_{0,l} = \frac{\Im\psi^{(4)}_{j,+1}(\alpha_{k,l}) - \Im\beta_l}{\alpha^{d_l}_{k,l}}.$$

In Table 8.7 the constants $C_{0,l}$ and d_l are given for the first two zeros $\beta_l \in \mathcal{Z}^{(4)}_{0,+1}$ on the critical line $\Re\beta_l = \frac{1}{2}$.

Experimental Observation 8.2.30. *For the curves $C_l(\alpha) = C_{0,l}\alpha^{d_l} + \Im\beta_l$ converging to the zeros $\beta_l \in \mathcal{Z}^{(4)}_{0,+1}$ as described in conclusion 8.2.29 we find $d_l = 2$ for $l \in \{1, 2\}$.*

We expect this observation to be true at least for most of the zeros $\beta_l \in \mathcal{Z}^{(4)}_{0,+1}$ on the critical line. In Figure 8.23 also the curves C_l for $l = 1, 2$ from conclusion 8.2.29 are shown as blue lines, the parameters $C_{0,l}$ for $d_l := 2$ are given in Table 8.7. As one can see the blue curves C_l in Figure 8.23 coincide with the orange points of the paths $\psi^{(4)}_{j,+1}$ touching the critical line and converging to the zero β_l. Surprisingly, one can also see in this figure that the blue curves C_l coincide, respectively are very near to the orange points of paths $\psi^{(4)}_{i,+1}$ which do not converge to the zero β_l, e.g., in the bottom plots in Figure 8.23 the curve S 2 converges to the zero β_1; as we can see the curve S 7 touches the critical line $\Re\beta = \frac{1}{2}$ almost exactly on the curve C_1:

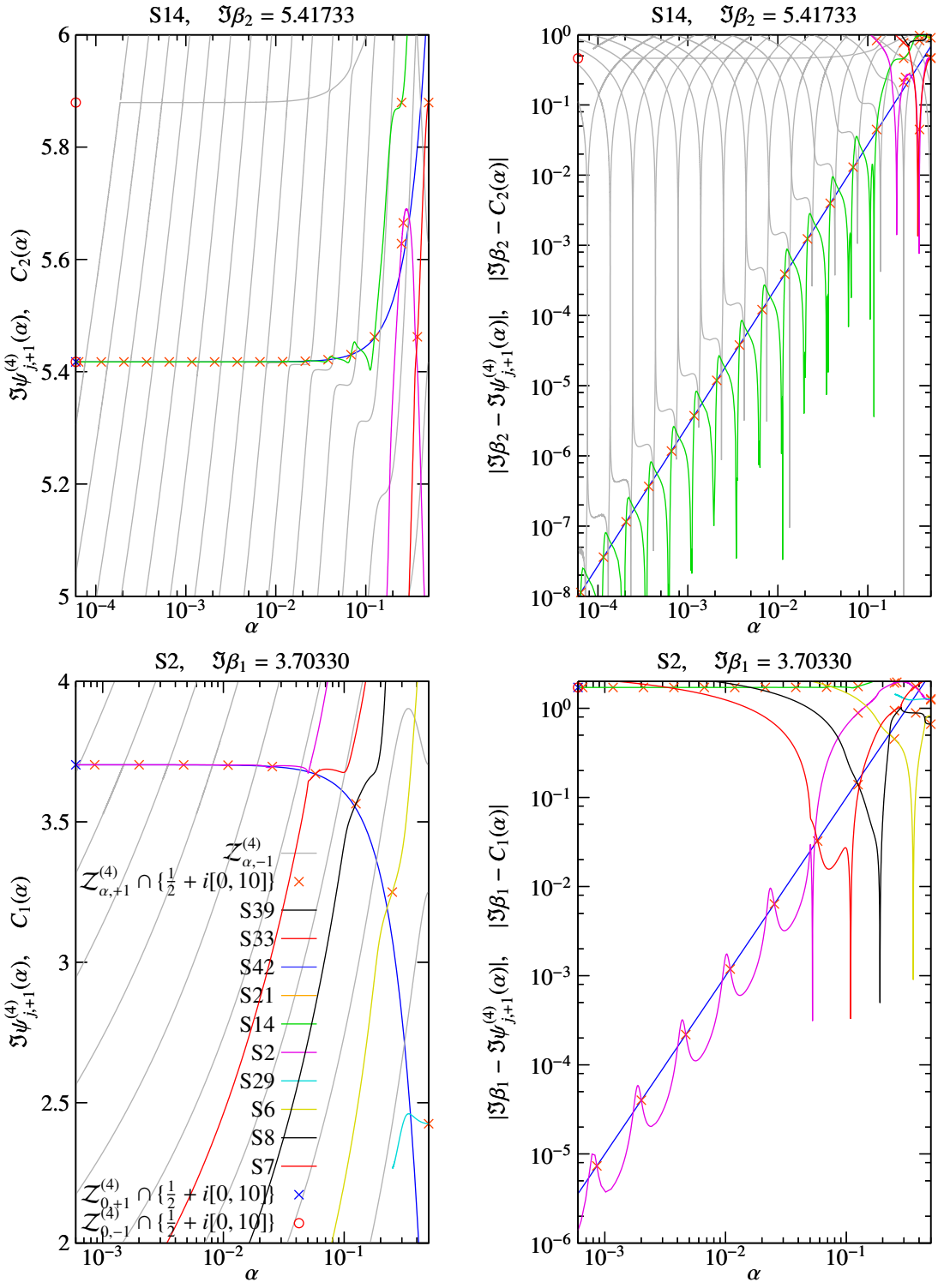

Figure 8.23: Infinite Resonance-Eigenvalue Convergence of the zeros $\mathcal{Z}^{(4)}_{\alpha,+1}$ (exponential law)

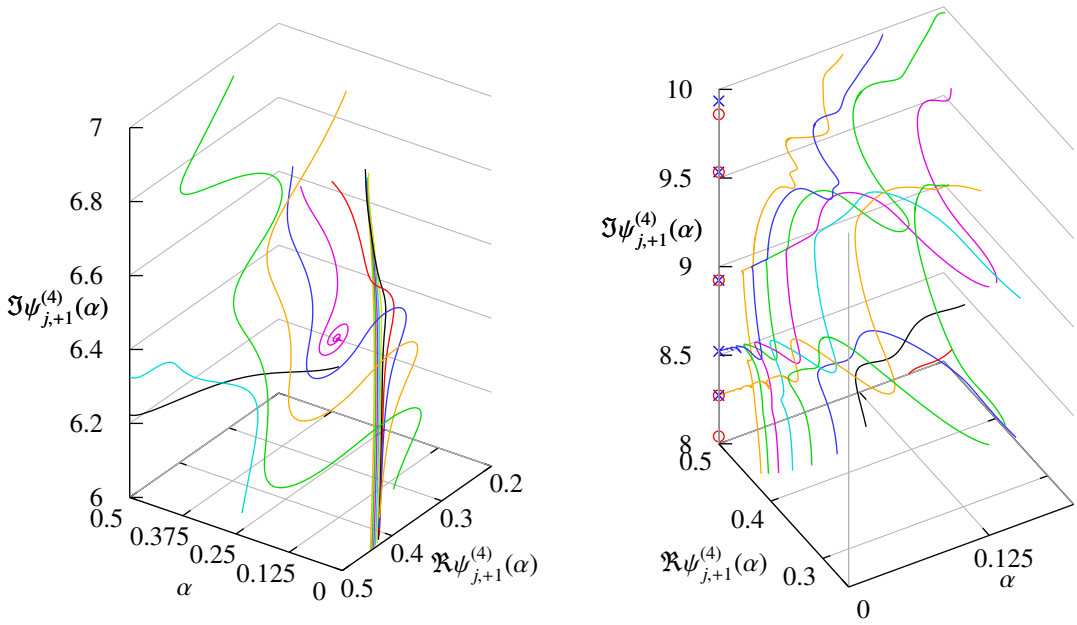

Figure 8.24: Infinite Resonance-Eigenvalue Convergence of the zeros $\mathcal{Z}^{(4)}_{\alpha,+1}$ in the (β,α)-plane

Experimental Observation 8.2.31. *For a path $\psi^{(4)}_{j(l),+1}$ and $\{\alpha^{(l)}_k\}_{k\in\mathbb{Z}_>}$ such that $\psi^{(4)}_{j(l),+1}(\alpha^{(l)}_k)$ converges towards a zero $\beta_l \in \mathcal{Z}^{(4)}_{0,+1}$ on the critical line as described by conclusion 8.2.28 and the corresponding curve C_l as given by conclusion 8.2.29, there is a finite sequence of points $\{\psi^{(4)}_{n_l(k),+1}(\tilde{\alpha}^{(l)}_k)\}_{k=1,2,\ldots,r_l}$, with $\tilde{\alpha}^{(l)}_k < \tilde{\alpha}^{(l)}_{k+1}$ for all k and $\alpha^{(l)}_1 < \tilde{\alpha}^{(l)}_1$, on different paths $\psi^{(4)}_{n_l(k),+1}$, where n_l maps the index k to the corresponding index of a path. The paths $\psi^{(4)}_{n_l(k),+1}$ touch the critical line $\Re\beta = \frac{1}{2}$ tangentially for the values of $\tilde{\alpha}^{(l)}_k$ i.e. $\Im\psi^{(4)}_{n_l(k),+1}(\tilde{\alpha}^{(l)}_k) = \frac{1}{2}$. These points $\psi^{(4)}_{n_l(k),+1}(\tilde{\alpha}^{(l)}_k)$ lie on the curve C_l respectively very near to it, i.e. $\Im\psi^{(4)}_{n_l(k),+1}(\tilde{\alpha}^{(l)}_k) = C_l(\tilde{\alpha}^{(l)}_k)$ or $|\Im\psi^{(4)}_{n_l(k),+1}(\tilde{\alpha}^{(l)}_k) - C_l(\tilde{\alpha}^{(l)}_k)| \ll 1$.*

On the left of Figure 8.24 a plot is shown of an infinite resonance-eigenvalue convergence in the (β,α)-plane, which is the spiral in the middle of that plot. As we can see there are other paths of zeros which wind around this spiral; these are the paths which touch the critical line $\Re\beta = \frac{1}{2}$ as described by observation 8.2.31. We mentioned that we cannot rule out that besides the convergence towards the zeros $\mathcal{Z}^{(4)}_{0,+1}$ on the critical line as described by conclusion 8.2.28 there are other types of convergence as well. Indeed, in the right plot of Figure 8.24 we can see two infinite resonance-eigenvalue convergence sequences at $\Im\beta \approx 8.25$ and $\Im\beta \approx 8.5$, but at $\Im\beta$ slightly below 9 we can see a sequence of zeros on different paths which remind us of the infinite avoided crossing phenomenon. The question which remains to be answered is whether this is actually an infinite avoided crossing of resonances or if this sequence will be taken over by an infinite resonance-eigenvalue convergence. Because this phenomenon occurs rather high at $\Im\beta \approx 9$, we did not compute many curves of zeros which belong to this sequence. Further investigations are necessary to resolve this issue.

According to conclusion 8.2.28 there is for $\alpha \to 0$ a convergence of perturbed eigenvalues $\lambda_l(\alpha)$ of the hyperbolic Laplacian related to τ-even Maass wave forms towards the unperturbed eigenvalues $\lambda_l(0)$. There is no smooth curve, since these eigenvalues $\lambda_l(\alpha^{(l)}_k) = \frac{1}{4} + (\Im\psi^{(4)}_{j(l),+1}(\alpha^l_k))^2$ exist only for special values $\alpha = \alpha^{(l)}_k$, when $\alpha \neq \alpha^{(l)}_k$ the eigenvalue $\lambda_l(\alpha^{(l)}_k)$ is destroyed and becomes a resonance. In contrast to the infinite avoided crossing convergence of the τ-odd Maass wave forms presented in the last section, there is a one-to-one correspondence between the eigenvalue $\lambda_l(\alpha^{(l)}_k)$ and the unperturbed eigenvalue $\lambda_l(0)$, since we

Table 8.8: Convergence to the phantom eigenvalue $\beta_1 = \frac{1}{2} + i\frac{\pi}{\ln 2} \approx \frac{1}{2} + 4.5323601418i$

k	$n_1(k)$	$\alpha_k^{(1)}$	$\Im\psi^{(4)}_{n_1(k),+1}(\alpha_k^{(1)})$	$\nu_1(k)$	$\Im\psi^{(4)}_{n_1(k),+1}(\alpha_k^{(1)}) - \Im\psi^{(4)}_{\nu_1(k),-1}(\alpha_k^{(1)})$
1	7	0.25	4.64659164296	9	0.278572102735
2	2	0.125	4.5904296289	10	0.0632088209629
3	1-1	0.0610248431740724114	4.54938888723	12	0.0135903761751
4	3	0.0302151410610085845	4.53676305828	13	0.00300594616914
5	16	0.0150610001203967288	4.5334687776	15	0.000684719160843
6	19	0.00752366773497756095	4.53263777533	18	0.000161023902675
7	23	0.00376085811779208181	4.53242955745	17	$< 10^{-4}$
8	26	0.00188029211776059531	4.53237749705	20	$< 10^{-4}$
9	11	0.000940127219202592837	4.53236456343	22	$< 10^{-4}$
10	34	0.000470060925477776997	4.53236122558	24	$< 10^{-4}$
11	43	0.000235030108209926727	4.5323604134	25	$< 10^{-4}$
12	38	0.000117515005782038248	4.53236020905	28	$< 10^{-4}$
13	46	0.0000587574964664974835	4.5323601585	30	$< 10^{-4}$

can associate both eigenvalues to a single path $\psi^{(4)}_{j(l),+1}$.

In Figure 8.15 it looks like if there would be a lot of curves of zeros that touch the critical line at $\beta = \frac{1}{2} + i\frac{\pi}{\ln 2} \approx \frac{1}{2} + 4.53236i$. Two close-ups of this point are shown in the bottom plots of Figure 8.25. As we can see in the plot at the bottom's right hand side these curves do not touch the critical line at the point $\beta = \frac{1}{2} + i\frac{\pi}{\ln 2}$, but get very near to it and converge towards it. Another point at $\beta = \frac{1}{2} + i2\frac{\pi}{\ln 2} \approx \frac{1}{2} + 9.06472i$ is shown in the top plots of Figure 8.25. Note, however, that we computed only a few curves around this point. Nevertheless we draw the following:

Conclusion 8.2.32. *(Phantom Eigenvalues) For any point $\beta_m = \frac{1}{2} + m\frac{\pi}{\ln 2}i$, $m \in \mathbb{Z}_>$, which does not belong to the zeros $\mathcal{Z}_0^{(4)}$ of the Selberg zeta function $Z^{(4)}(\beta, \chi_0^{(4)})$ there is an infinite sequence of points $\{\psi^{(4)}_{n_m(k),+1}(\alpha_k^{(m)})\}_{k\in\mathbb{Z}_>}$ such that:*

- *The zeros on the paths $\psi^{(4)}_{n_m(k),+1}$ touch the critical line $\Re\beta = \frac{1}{2}$ tangentially for the values of $\alpha_k^{(m)}$, i.e.*

$$\Re\psi^{(4)}_{n_m(k),+1}(\alpha_k^{(m)}) = \frac{1}{2}.$$

  The distance $\alpha_k^{(m)} - \alpha_{k+1}^{(m)}$ decreases exponentially with $k \to \infty$, and $\alpha_k^{(m)} \to 0$ for $k \to \infty$.

- *The zeros $\psi^{(4)}_{n_m(k),+1}(\alpha_k^{(m)})$ converge towards β_m:*

$$\lim_{k\to\infty} |\beta_m - \psi^{(4)}_{n_m(k),+1}(\alpha_k^{(m)})| = 0.$$

- *For every path $\psi^{(4)}_{n_m(k),+1}$ there is another path $\psi^{(4)}_{\nu_m(k),-1}$ on the critical line $\Re\beta = \frac{1}{2}$, such that*

$$\lim_{k\to\infty} |\psi^{(4)}_{\nu_m(k),-1}(\alpha_k^{(m)}) - \psi^{(4)}_{n_m(k),+1}(\alpha_k^{(m)})| = 0.$$

The fact that the $\alpha_k^{(m)}$ are decreasing exponentially suggests that there exist infinitely many $\alpha_k^{(m)}$, and therefore this sequence is infinite. From the point of view of the hyperbolic Laplacian it means that there is a sequence of eigenvalues $\lambda_m(\alpha_k^{(m)}) = \frac{1}{4} + (\Im\psi^{(4)}_{n_m(k),+1}(\alpha_k^{(m)}))^2$ belonging to τ-even Maass wave forms, with

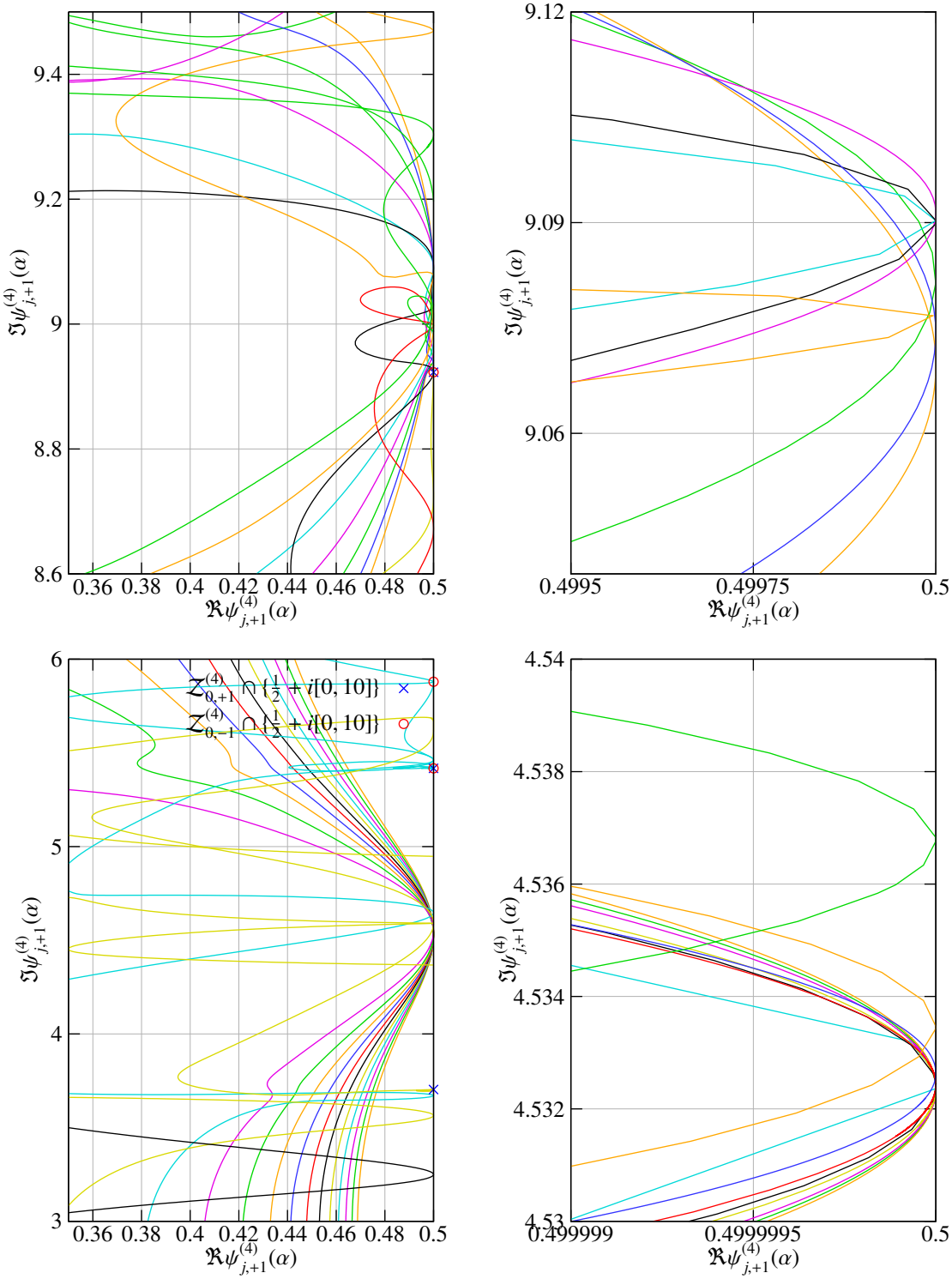

Figure 8.25: Convergence to Phantom Eigenvalues of the zeros $\mathcal{Z}^{(4)}_{\alpha,+1}$ in the β-plane for $\alpha \in (0, \frac{1}{2}]$

$\lim_{k\to\infty}\lambda_m(\alpha_k^{(m)}) = \frac{1}{4} + (m\frac{\pi}{\ln 2})^2$ and $\lim_{k\to\infty}\alpha_k^{(m)} = 0$. However, the limit $\frac{1}{4} + (m\frac{\pi}{\ln 2})^2$ is not an eigenvalue of the hyperbolic Laplacian for $\alpha = 0$; therefore, we call them *Phantom Eigenvalues*. The last point in conclusion 8.2.32 suggests that the zeros $\mathcal{Z}^{(4)}_{\alpha,-1}$ related to the eigenvalue -1 of the transfer operator $\mathcal{P}_2\mathcal{L}^{(4)}_{\beta,\varepsilon,\alpha}$ which are on the critical line $\Re\beta = \frac{1}{2}$ are as well related to these phantom eigenvalues for $\alpha \to 0$. In Table 8.8 the first 13 values of $\alpha_k^{(m)}$, $\psi^{(4)}_{n_m(k),+1}(\alpha_k^{(m)})$ and the corresponding $\psi^{(4)}_{\nu_m(k),-1}(\alpha_k^{(m)})$ on the critical line are given for $m = 1$. We can see the convergence as described by conclusion 8.2.32. In Figure 8.26 the dependence of the imaginary parts of $\psi^{(4)}_{j,+1}$ on α are shown. The points where these paths touch the critical line $\Re\beta = \frac{1}{2}$ are marked by orange crosses. As we can see there is a sequence of such crosses which converges to $\Im\beta_1 = \frac{\pi}{\ln 2} \approx 4.5323601418$. While the right plot shows the distance $|\Im\beta_1 - \Im\psi^{(4)}_{j,+1}(\alpha)|$ depending on α. In the background the paths $\psi^{(4)}_{k,-1}$ of the zeros which are always on the critical line are shown as gray lines. We see that the paths $\psi^{(4)}_{j,+1}$ touch the critical line near to the paths $\psi^{(4)}_{k,-1}$ on the critical line. Again, we can find a curve which describes the relation between the values of $\Im\psi^{(4)}_{n_m(k),+1}(\alpha_k^{(m)})$ and $\alpha_k^{(m)}$:

Conclusion 8.2.33. *The sequence of points $\psi^{(4)}_{n_m(k),+1}(\alpha_k^{(m)})$ which converge to the points $\beta_m = \frac{1}{2} + m\frac{\pi}{\ln 2}i$ as described in conclusion 8.2.32 defines a curve $(\frac{1}{2} + iC_m(\alpha), \alpha)$ such that $C_m(0) = \Im\beta_m$ and $\frac{dC_m(\alpha)}{d\alpha}|_{\alpha=0} = 0$, given by*

$$C_m(\alpha) = C_{0,m}\alpha^{d_m} + \Im\beta_m,$$

with $C_{0,m}, d_m \in \mathbb{R}$, and such that the points $\psi^{(4)}_{n_m(k),+1}(\alpha_k^{(m)})$ lie on this curve, i.e.

$$\Im\psi^{(4)}_{n_m(k),+1}(\alpha_k^{(m)}) = C_m(\alpha_k^{(m)}) \quad \textit{for all } k \in \mathbb{Z}_>.$$

We expect that $d_m = 2$ at least in most cases.

8.2.5 Results for $(\Gamma_0(8), \chi^{(8)}_\alpha)$ and $(\Gamma_0(4), \chi^{(4)}_{\alpha_1,\alpha_2})$

Next we want to compare our numerical results for $(\Gamma_0(8), \chi^{(8)}_\alpha)$ and $(\Gamma_0(4), \chi^{(4)}_{\alpha_1,\alpha_2})$ to the results for $(\Gamma_0(4), \chi^{(4)}_\alpha)$ presented in the previous sections. In contrast to $(\Gamma_0(4), \chi^{(4)}_\alpha)$ we have only a few results for $(\Gamma_0(8), \chi^{(8)}_\alpha)$ and $(\Gamma_0(4), \chi^{(4)}_{\alpha_1,\alpha_2})$, mostly because the computation time is dramatically larger in these cases.

First, let us recapitulate the results for $(\Gamma_0(8), \chi^{(8)}_\alpha)$ so far:

- Conclusion 8.2.6: $(\Gamma_0(8), \chi^{(8)}_\alpha)$ is arithmetic only for $\alpha \in \{0, \frac{1}{2}\}$.
- Conjecture 8.2.12: the multiplicity of the zeros $\mathcal{Z}^{(8)}_\alpha$ of the Selberg zeta function $Z^{(8)}(\beta, \chi^{(8)}_\alpha)$ is one for $\alpha \in (0, \frac{1}{2})$, and one or two for $\alpha = \frac{1}{2}$.
- Experimental observation 8.2.8: for $\alpha_0 = \frac{1}{2}$ the order of contact of the zeros $\mathcal{Z}^{(8)}_\alpha$ for $\alpha \to \alpha_0$ with the critical line $\Re\beta = \frac{1}{2}$ is either 2 or 4.

The Selberg zeta function $Z^{(8)}(\beta, \chi^{(8)}_\alpha)$ was evaluated by computing the spectrum of the transfer operator $\mathcal{L}^{(8)}_{\beta,+1,\alpha}\mathcal{L}^{(8)}_{\beta,-1,\alpha}$. Since all symmetries $\mathcal{P}_k$ are destroyed by the deformation with $\chi^{(8)}_\alpha$ we cannot use the operators $\mathcal{P}_k\mathcal{L}^{(8)}_{\beta,+1,\alpha}$ in our computations, and therefore unlike in the case of $(\Gamma_0(4), \chi^{(4)}_\alpha)$ we cannot split up the zeros $\mathcal{Z}^{(8)}_\alpha$ in zeros which are related to the eigenvalues $+1$ and -1 of some transfer operator. In Figure 8.27 the curves of the fist 8 zeros starting on the critical line $\Re\beta = \frac{1}{2}$ for $\alpha = \frac{1}{2}$ are shown. As we can see, all of these zeros leave the critical line $\Re\beta = \frac{1}{2}$. Obviously, the deformation by $\chi^{(8)}_\alpha$ for α away from zero closes two cusps; therefore, also the multiplicity of the pole $\beta = \frac{1}{2}$ of the Selberg zeta function changes as well:

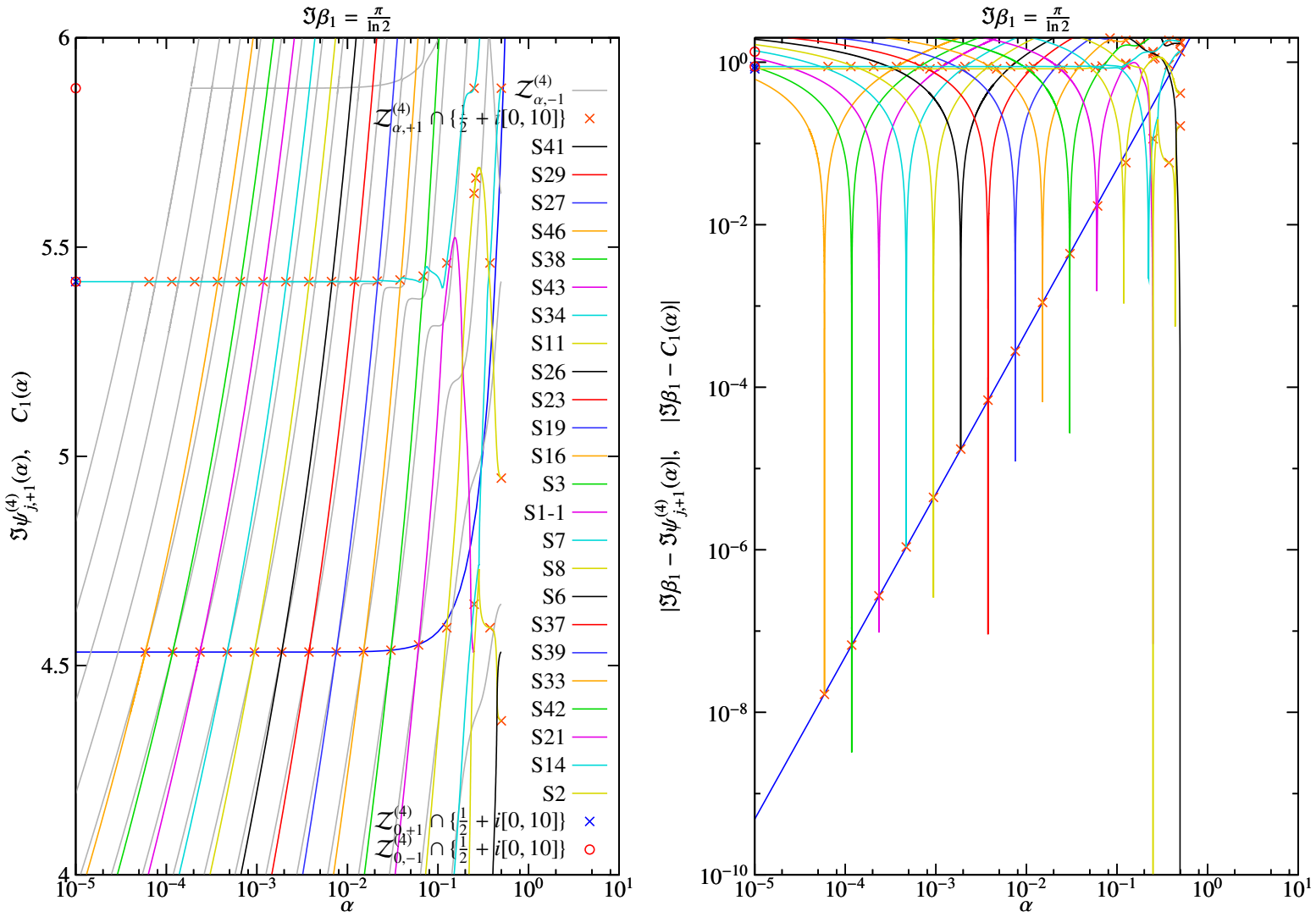

Figure 8.26: Convergence to Phantom Eigenvalues of the zeros $\mathcal{Z}^{(4)}_{\alpha,+1}$ (exponential law)

Conclusion 8.2.34. *The multiplicity of the pole at $\beta = \frac{1}{2}$ of the Selberg zeta function $Z^{(8)}(\beta, \chi_\alpha^{(8)})$ is:*

- *four for $\alpha = 0$.*
- *two for $\alpha \in (0, \frac{1}{2})$.*
- *one for $\alpha = \frac{1}{2}$.*

The change of the multiplicity of this pole from four for $\alpha = 0$ to two for $\alpha \in (0, \frac{1}{2})$ is obvious. On the other hand, the multiplicity one for $\alpha = \frac{1}{2}$ means that a zero of the Selberg zeta function moves to $\beta = \frac{1}{2}$ and cancels an order of this pole. Indeed, our experimental results show that:

Experimental Observation 8.2.35. *(Real Zero) For the path $\psi_j^{(8)}$ of the zero $\beta_0 = 1 \in \mathcal{Z}_0^{(8)}$ of the Selberg zeta function $Z^{(8)}(\beta, \chi_\alpha^{(8)})$ we found:*

- *The zero on the path $\psi_j^{(8)}$ is always real, i.e. $\psi_j^{(8)}(\alpha) \in \mathbb{R}$ for all α.*
- *The zero on the path $\psi_j^{(8)}$ approaches $\beta = 1$ for $\alpha = 0$ on a smooth curve.*
- *The zero on the path $\psi_j^{(8)}$ reduces the order of the pole of the Selberg zeta function $Z^{(8)}(\beta, \chi_\alpha^{(8)})$ with multiplicity two at $\beta = \frac{1}{2}$ for $\alpha = \frac{1}{2}$, where the zero disappears and a pole with multiplicity one remains.*

Hence the behavior of the real zero for $(\Gamma_0(8), \chi_\alpha^{(8)})$ is quite different from the one for $(\Gamma_0(4), \chi_\alpha^{(4)})$. As we tracked the zeros $\mathcal{Z}_\alpha^{(8)}$ from $\alpha = \frac{1}{2}$ to $\alpha \to 0$, we found the following behavior:

Experimental Observation 8.2.36. *The zeros $\mathcal{Z}_\alpha^{(8)}$ of the Selberg zeta function $Z^{(8)}(\beta, \chi_\alpha^{(8)})$ show for $\alpha \to 0$ the following types of behavior:*

- *There are zeros $\mathcal{Z}_\alpha^{(8)}$ left to the critical line $\Re\beta = \frac{1}{2}$ which tend to $\beta = \frac{1}{2}$ for $\alpha \to 0$. Their behavior is similar to the zeros $\mathcal{Z}_{\alpha,+1}^{(4)}$ as described in conclusion 8.2.26.*
- *There are zeros $\mathcal{Z}_\alpha^{(8)}$ left to the critical line $\Re\beta = \frac{1}{2}$ which tend to zeros $\mathcal{Z}_0^{(8)}$ on the critical line $\Re\beta = \frac{1}{2}$. Their approach to these zeros is an Infinite Resonance-Eigenvalue Convergence as described in conclusion 8.2.28.*

In both cases we do not know if there are also zeros on the critical line $\Re\beta = \frac{1}{2}$ which interact which the zeros as described in conclusions 8.2.26 and 8.2.28. We also found shapes other than loops for the Infinite Resonance-Eigenvalue Convergence for $(\Gamma_0(8), \chi_\alpha^{(8)})$. There should be other types of zeros than those described by observation 8.2.36, but we did not study them.

We also performed a few computations for $(\Gamma_0(4), \chi_{\alpha_1,\alpha_2}^{(4)})$. From a theoretical point of view, this is the easiest case since all cusps are closed, and there is no continuous spectrum for $\alpha_1, \alpha_2 \notin \mathbb{Z}$. On the other hand, for numerical computations this case is more complicated, since the evaluation of this character is more difficult. Since symmetries $\mathcal{P}_k$ in these cases do not exist we had to use the transfer operator $\mathcal{L}_{\beta,+1,\alpha_1,\alpha_2}^{(4)} \mathcal{L}_{\beta,-1,\alpha_1,\alpha_2}^{(4)}$ to evaluate the Selberg zeta function $Z^{(4)}(\beta, \chi_{\alpha_1,\alpha_2}^{(4)})$. Obviously, the Selberg zeta function $Z^{(4)}(\beta, \chi_{\alpha_1,\alpha_2}^{(4)})$ has no pole at $\beta = \frac{1}{2}$ and no zeros in $\Re\beta < \frac{1}{2}$, $\Im\beta > 0$ for $\alpha_1 \neq 0, \alpha_2 \neq 0$, which is in agreement with our numerical observations. If one of the parameters α_1 or α_2 goes to zero while the other remains constant we have again a singular situation, since one cusp will be opened. We tracked a few zeros $\mathcal{Z}_{(\alpha_1,\alpha_2)}^{(4)}$ on the critical line $\Re\beta = \frac{1}{2}$, and the results suggest that for $\alpha_1 \to 0$ or $\alpha_2 \to 0$ all zeros tend to $\beta = \frac{1}{2}$ in a similar way as in conclusion 8.2.15 described. Also the infinite avoided crossing phenomenon as described in conclusion 8.2.17 seems likely to occur. But we performed computations for $(\Gamma_0(4), \chi_{\alpha_1,\alpha_2}^{(4)})$ mainly to verify our implementation of the Selberg zeta function and not to obtain new results.

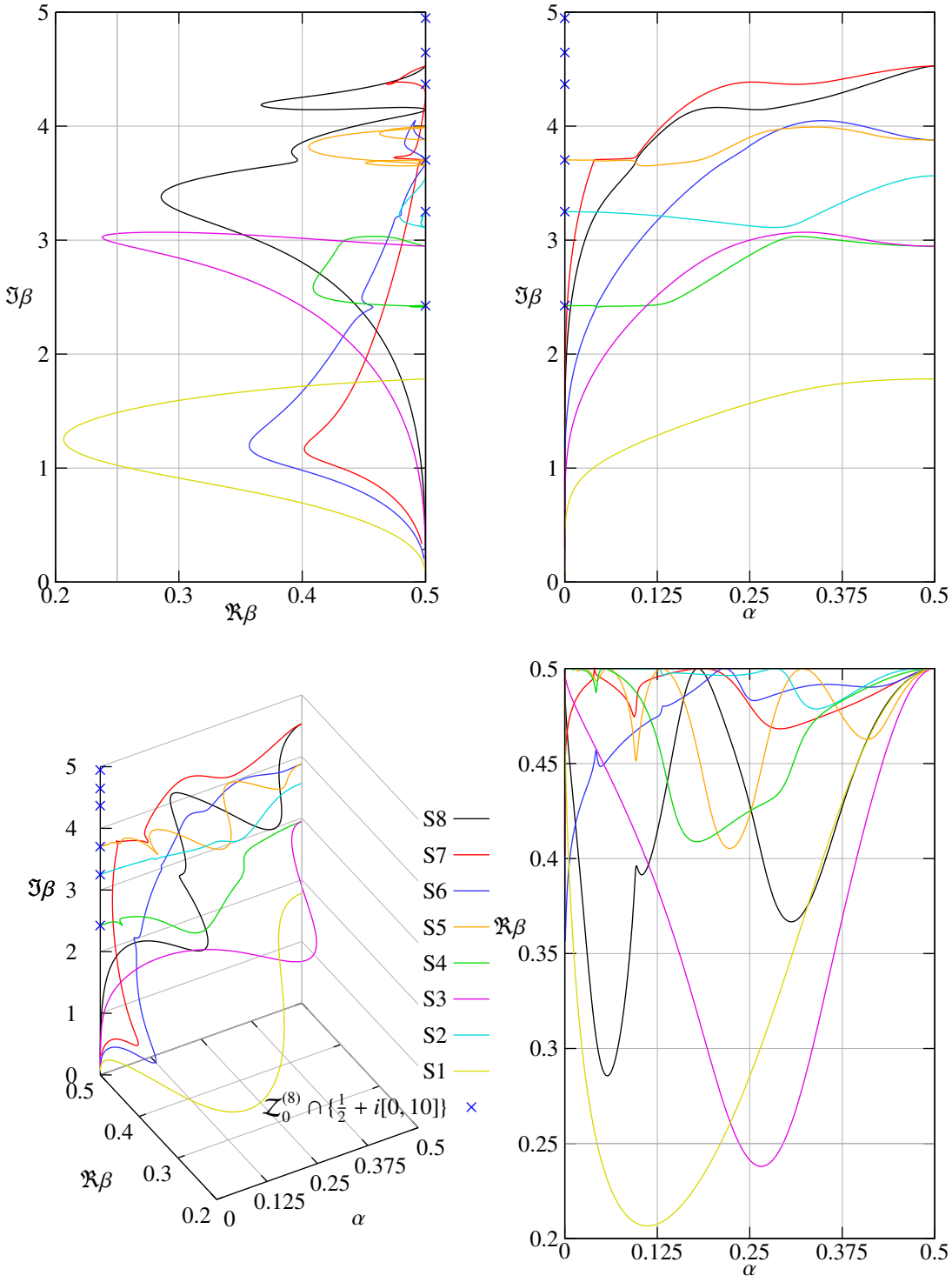

Figure 8.27: The zeros $\mathcal{Z}_\alpha^{(8)}$ of the Selberg zeta function $Z^{(8)}\left(\beta, \chi_\alpha^{(8)}\right)$ in the (β, α)-plane

8.3 Concluding remarks

The results in this chapter describe several phenomena for the transfer operator and the Selberg zeta function $Z^{(n)}(\beta,\chi)$ which seem thus far to be unknown even to the experts. Clearly, one of our basic results is the symmetries of the transfer operator in section 8.1.3, whose existence we found by investigating a new form of the transfer operator that we derived in lemma 7.4.5. This form allows us to write down explicitly the action of the transfer operator on every component of a vector valued function for any given group $\Gamma_0(n)$ with a character χ, (see, e.g., Appendix C for the form of the transfer operator for $\Gamma_0(8)$). All other results were influenced by the discovery of these symmetries since they allowed us to obtain more information about the zeros of the Selberg zeta function by relating them to the eigenvalue ± 1 of the transfer operator and to even/odd symmetries of Maass wave forms with respect to certain involutions. For $\Gamma_0(4)$ this result together with the fact that all odd Maass wave forms survive a deformation, allowed us to predict if a zero of the Selberg zeta function will stay on the critical line $\Re\beta = \frac{1}{2}$ or not. The symmetries improved also the computation time, since only "one half" of the original transfer operator has to be computed.

Little is known analytically about the spectrum of the transfer operator, but in section 8.1.4 we were able to obtain numerically many results which help us to understand its spectrum much better. Since there are no other results with which we could compare our numerical results, we also implemented the trace formula for the analytic continuation of the transfer operator we found in proposition 7.4.7 to have to some extent an independent numerical verification of the implementation of the transfer operator. Probably the most surprising result in observation 8.1.22 is that the spectrum of the transfer operator $\mathcal{P}_2\mathcal{L}^{(4)}_{\beta,\varepsilon,\alpha}$ is non-analytic for $\alpha \to 0$ and $\Re\beta \leq \frac{1}{2}$, which one cannot see immediately from the definition of the transfer operator. The result that the spectrum of the transfer operator $\mathcal{P}_2\mathcal{L}^{(4)}_{\beta,\varepsilon,\alpha}$ for varying $\alpha \to 0$ and fixed β with $\Re\beta = \frac{1}{2}$ consists of closed orbits, where several eigenvalues rotate in one orbit which goes through -1 is quite unexpected, and shows that a kind of "phase transition" happens between $\alpha \gg 0$ and $\alpha \to 0$, see also Figure 8.7. Also the result in observation 8.1.21 that the spectrum of the transfer operator for any $\Gamma_0(n)$ is located on concentric circles for large fixed $\Re\beta$, rotating with $\Im\beta$ was not known, (see top left plot in Figure 8.4). Another interesting result is that for $\Re\beta < 0$ some eigenvalues start to cluster around ± 1, and outweigh to some extent the large eigenvalues in the Fredholm determinant of the transfer operator, (see lower left plot in Figure 8.4). A theoretical explanation for this clustering would be very interesting.

The general properties of the Selberg zeta function in the β-plane for a tivial character are well understood. On the other hand, the Selberg zeta function with a character, especially a non-arithmetic one, was not yet studied theoretically nor numerically to our knowledge. The result in conclusion 8.2.3 that the Selberg zeta functions for $(\Gamma_0(4),\chi^{(4)}_\alpha)$ with $\alpha = \frac{2}{8}$ and $\alpha = \frac{4}{8}$ coincide is theoretically still not understood. The result in conclusion 8.2.7 that the zeros of the Selberg zeta function for $\alpha = 0$ are among those for $\alpha = \frac{2}{8}$, respectively that the zeros for $\alpha = \frac{3}{8}$ are among those for $\alpha = \frac{1}{8}$, is also not yet understood. A theoretical explanation for this should shed some light on the relation between the Selberg zeta functions for $(\Gamma_0(4),\chi^{(4)}_\alpha)$ for different values of α for which $\chi^{(4)}_\alpha$ is arithmetic. We also found two relations between the Selberg zeta functions for $\Gamma_0(8)$ with the character $\chi^{(8)}_{\alpha_1,\alpha_2,\alpha_3}$ and $\Gamma_0(4)$ with the character $\chi^{(4)}_{\alpha_1,\alpha_2}$: relation (8.12) is easy to understand since it follows almost immediately from the relation of both characters in lemma 6.5.4. On the other hand, for the relation given in conclusion 8.2.5 we could not find an explanation. Like for the spectrum of the transfer operator for $\alpha \to 0$, we observed in 8.2.2 that the Selberg zeta function $Z^{(4)}(\beta,\chi^{(4)}_\alpha)$ for $(\Gamma_0(4),\chi^{(4)}_\alpha)$ with $\Re\beta \leq \frac{1}{2}$ and $\alpha \to 0$ is a completely different function from the one for $\alpha = 0$, i.e. $Z^{(4)}(\beta,\chi^{(4)}_\alpha)$ is also non-analytic in this case. For the spectrum of the transfer operator, as well for the Selberg zeta function the limit $\alpha \to 0$ exists only for $\Re\beta > \frac{1}{2}$.

Our main numerical results are the curves of zeros of the Selberg zeta function $Z^{(4)}(\beta,\chi^{(4)}_\alpha)$ in the β-plane for $\alpha \in [0,\frac{1}{2}]$ in sections 8.2.3 and 8.2.4. Probably the most important results concern their behavior for $\alpha \to 0$, since this limit corresponds to a singular perturbation of the hyperbolic Laplacian. We found two different kinds of behavior in the approach of the perturbed eigenvalues of the Laplacian for $\alpha \neq 0$ to the non-perturbed ones for $\alpha = 0$: the infinite avoided crossing sequence on the critical line in conclusion

8.2.17 and the Infinite Eigenvalue-Resonance Convergence in conclusion 8.2.28, where for infinitely many values of α_k an eigenvalue of the Laplacian exists, which becomes a resonance for $\alpha \neq \alpha_k$. We also found phantom eigenvalues in conclusion 8.2.32, with a similar sequence of eigenvalues of the Laplacian existing only for α_k without an unperturbed limit eigenvalue for $\alpha = 0$. These results provide a better understanding of eigenvalues perturbed by a singular perturbation. Our calculations also confirm the zeros predicted by Selberg for $\alpha \to 0$ very near to the critical line in observation 8.2.21 and we describe their behavior further in conclusion 8.2.26. Moreover, we found that they are accompanied by similar zeros of opposite symmetry on the critical line $\Re\beta = \frac{1}{2}$ in conclusion 8.2.15, both families of zeros are getting dense on the critical line for $\alpha \to 0$. In all our computations we started with a value of $\alpha \neq 0$ and let $\alpha \to 0$: given all the zeros which move on or to the critical line $\Re\beta = \frac{1}{2}$ for $\alpha \to 0$ it seems that a perturbation of the hyperbolic Laplacian starting from $\alpha = 0$ is very difficult to carry out, since for the smallest change of α we can find in principle everywhere near and on the critical line zeros of the Selberg zeta function. So far our results are in agreement with the conjecture of Phillips and Sarnak. We can confirm the second- and fourth-order contact of zeros with the critical line found numerically in [Ave07] for $\Gamma_0(5)$, see also [PR10] for a theoretical discussion.

In this chapter we described new results, which presently remain unproven and are also without an independent numerical confirmation. Unfortunately, for most of the results there is no great hope for an analytic approach. So far we were able to prove the existence of the symmetries of the transfer operator and their relation to involutions of the Maass wave forms [FM11]. Also, thanks to the expertise of R. Bruggeman, we are working [BFM12] on an analytic verification of some of the results presented in this chapter for $(\Gamma_0(4), \chi_\alpha^{(4)})$ mainly for $\alpha \to 0$. So far, these results have been in agreement with the numerical ones.

We also want to mention some problems and limitations of the method we have used in this thesis to evaluate the Selberg zeta function: one problem is that this method is very slow for numerical computations. The source of this problem is the definition of the transfer operator, which is acting on vector-valued functions. If we approximate the operator for a group $\Gamma_0(n)$ by using 50 Taylor coefficient, the approximation is not just a 50×50 matrix, but the actual size is $50 \cdot \mu_n \times 50 \cdot \mu_n$, where μ_n is the index of $\Gamma_0(n)$ in $\mathrm{SL}(2,\mathbb{Z})$. For $\Gamma_0(4)$ we have $\mu_4 = 6$, and therefore we have to compute the eigenvalues of a 300×300 matrix. The only solution for this problem would be to find a transfer operator which acts on scalar functions instead of vector-valued ones. Because of this, computations for $\Gamma_0(n)$ of higher level n are practically impossible. Another problem is related to the Selberg zeta function and its computation via the transfer operator. One knows that the Selberg zeta function grows exponentially with $\Im\beta$ for $\Re\beta \leq \frac{1}{2}$ and also with negative $\Re\beta$, and numerical experiments show that this corresponds to eigenvalues of the transfer operator growing exponentially. This large eigenvalues force us to increase the precision in our computations to obtain reliable results for larger values of $\Im\beta$ and negative $\Re\beta$. Also the oscillations of the Selberg zeta function for $\alpha \to 0$ in the half plane $\Re\beta < \frac{1}{2}$ make the tracking of zeros very difficult. Nevertheless, although up to now the transfer operator method cannot provide new analytic results for the Selberg zeta function, one should keep in mind that right now it is one of the very few methods enabling the evaluation of the Selberg zeta function, which shows that the transfer operator method has an important application in experimental mathematics, granting access to numerical results which cannot be obtained by other analytical and numerical methods up to now.

Finally, we would like to mention that during the computations performed for the spectrum of the transfer operator and the Selberg zeta function so far we did not find any disagreement between our numerical results and known analytical results. Furthermore, all computations performed for $\Re\beta \leq \frac{1}{2}$ also support our conjecture 7.4.10 that the form of the transfer operator in proposition 7.4.9 is an analytic continuation of the transfer operator to the entire complex β-plane.

Chapter 9

Computational aspects of the transfer operator for the Kac-Baker model

In [May80b] Mayer introduced the transfer operator for the Kac-Baker model (see, e.g., [Kac59]). This model was created for a better understanding of phase transitions in systems with weak long-range interactions like the van der Waals gas. The transfer operator $\mathcal{L}_{\beta,\lambda} : B(D_R) \to B(D_R)$, given by

$$\mathcal{L}_{\beta,\lambda} f(z) = e^{\beta z} f(\lambda + \lambda z) + e^{-\beta z} f(-\lambda + \lambda z) \tag{9.1}$$

acts on the Banach space $B(D_R) = \left\{ f : D_R \to \mathbb{C} : f \text{ holomorphic in } D_R \text{ and continuous on } \bar{D}_R \right\}$ with the supremum norm $\|f\| = \sup_{z \in D_R} |f(z)|$ on the disk $D_R = \left\{ z \in \mathbb{C} : |z| < R \text{ and } R > \frac{\lambda}{1-\lambda} \right\}$. The parameter β can be interpreted as the "inverse temperature", which can be complex valued. The parameter $\lambda = \exp -\gamma$, with $0 < \gamma < 1$ determines the decay rate of the interaction as a function of distance. In [HM04] Hilgert and Mayer have shown, that the transfer operator $\mathcal{L}_{\beta,\lambda}$ has the same spectrum as the operator which was introduced by Kac in [Kac66] for this model. In this way, they could also show that the spectrum of $\mathcal{L}_{\beta,\lambda}$ is real for $\beta \in \mathbb{R}$. For the special value $\beta = 0$ the spectrum of this operator is given by $\sigma(\mathcal{L}_{0,\lambda}) = \{2\lambda^n : n \in \mathbb{Z}_{\geq}\}$. By using the trace formula (7.12) one can easily verify that the trace of this operator is given by

$$\operatorname{tr} \mathcal{L}_{\beta,\lambda} = \frac{2}{1-\lambda} \exp \frac{\beta\lambda}{1-\lambda}. \tag{9.2}$$

Like in the case of the transfer operator for Hecke congruence subgroups one can relate the Fredholm determinant of this operator to a zeta function. The Ruelle zeta function (7.4) for the Kac-Baker model has the representation

$$Z_R(z,\beta) = \frac{\det\left(1 - z\lambda\mathcal{L}_{\beta,\lambda}\right)}{\det\left(1 - z\mathcal{L}_{\beta,\lambda}\right)} \qquad \text{for } z, \beta \in \mathbb{C}. \tag{9.3}$$

This is an example of a dynamical zeta function. In [HM04] Hilgert and Mayer have shown that for $0 < \lambda < 1$ the Fredholm determinants $\det\left(1 - \lambda\mathcal{L}_{\beta,\lambda}\right)$ and $\det\left(1 - \mathcal{L}_{\beta,\lambda}\right)$ have infinitely many zeros on the real line $\beta \in \mathbb{R}$. Furthermore, the Fredholm determinant $\det\left(1 - \lambda\mathcal{L}_{\beta,\lambda}\right)$ also has infinitely many zeros on the line $\Re\beta = \ln 2$ for $\lambda = \frac{1}{2}$. Indeed, the zeros on the line $\Re\beta = \ln 2$ are equally spaced and given by $\beta = \ln 2 + i2\pi n$ with $n \in \mathbb{Z}$. They concluded that the Ruelle zeta function $Z_R(\beta) := Z_R(1,\beta)$ has infinitely many zeros and poles on the real line, and for the special value $\lambda = \frac{1}{2}$ infinitely many trivial zeros on the line $\Re\beta = \ln 2$. Accidental cancellations of the zeros of $\det(1 - \lambda\mathcal{L}_{\beta,\lambda})$ with the zeros of $\det(1 - \mathcal{L}_{\beta,\lambda})$ could destroy some of these zeros in $Z_R(\beta)$. Hilgert and Mayer raised two questions:

1. Does the Ruelle zeta function $Z_R(\beta)$ also have zeros on a line parallel to the imaginary β-axis for $0 < \lambda < 1$ different to $\lambda = \frac{1}{2}$?

2. Are there any other zeros of the Ruelle zeta function $Z_R(\beta)$ which are neither on the line $\Re\beta = \ln 2$ nor on the real line $\beta \in \mathbb{R}$ for $\lambda = \frac{1}{2}$?

It is expected that there are zeros on lines parallel to the imaginary β-axis for all values for λ. On the other hand, if at least for $\lambda = \frac{1}{2}$ there are only zeros on the line $\Re\beta = \ln 2$ and on the real axis, then some general Riemann hypothesis would also hold for the zeta function $Z_R(\beta)$. Indeed, there is no obvious connection of this zeta function to any arithmetic zeta function for which such a general Riemann hypothesis is known to hold.

9.1 A nuclear representation of the transfer operator for the Kac-Baker model

We want to investigate the spectrum of the transfer operator $\mathcal{L}_{\beta,\lambda}$ numerically. As soon as the eigenvalues $\rho_i = \rho_i(\beta, \lambda)$ of this operator are known, we can evaluate the Ruelle zeta function by

$$Z_R(\beta) = \frac{\prod_{i=0}^{\infty} 1 - \lambda\rho_i}{\prod_{i=0}^{\infty} 1 - \rho_i}.$$

To determine these eigenvalues we need to find a form of the transfer operator $\mathcal{L}_{\beta,\lambda}$ which is suitable for numerical computations, such as the nuclear representation (7.6):

Proposition 9.1.1. *The transfer operator in (9.1) can be written as*

$$\mathcal{L}_{\beta,\lambda} f(z) = \sum_{k=0}^{\infty} \sum_{l=0}^{\infty} \frac{f^{(l)}(0)}{l!} \lambda^l \left(1 + (-1)^{k+l}\right) \sum_{r=0}^{\min(k,l)} \binom{l}{r} \frac{\beta^{k-r}}{(k-r)!} z^k. \tag{9.4}$$

Proof. Obviously the Taylor expansions of $e^{\beta z}$ and $e^{-\beta z}$ in z at the point 0 are uniformly convergent:

$$\begin{aligned} \mathcal{L}_{\beta,\lambda} f(z) &= \sum_{n=0}^{\infty} \frac{\beta^n}{n!} z^n f(\lambda + \lambda z) + \sum_{n=0}^{\infty} \frac{(-1)^n \beta^n}{n!} z^n f(-\lambda + \lambda z) \\ &= \sum_{n=0}^{\infty} \frac{\beta^n}{n!} \left(f(\lambda + \lambda z) + (-1)^n f(-\lambda + \lambda z)\right) z^n. \end{aligned}$$

The Taylor expansion of $f(z)$ at the point 0 is uniformly convergent in $\bar{D}_R$:

$$\begin{aligned} \mathcal{L}_{\beta,\lambda} f(z) &= \sum_{n=0}^{\infty} \frac{\beta^n}{n!} \left(\sum_{l=0}^{\infty} \frac{f^{(l)}(0)}{l!} (\lambda + \lambda z)^l + (-1)^n \sum_{l=0}^{\infty} \frac{f^{(l)}(0)}{l!} (-\lambda + \lambda z)^l \right) z^n \\ &= \sum_{n=0}^{\infty} \frac{\beta^n}{n!} \sum_{l=0}^{\infty} \frac{f^{(l)}(0)}{l!} \left((\lambda + \lambda z)^l + (-1)^n (-\lambda + \lambda z)^l \right) z^n. \end{aligned}$$

With $(\lambda + \lambda z)^l = \lambda^l (1 + z)^l$ and $(-\lambda + \lambda z)^l = \lambda^l (-1 + z)^l$ we can write

$$\lambda^l (1 + z)^l = \lambda^l \sum_{r=0}^{l} \binom{l}{r} z^r \quad \text{and} \quad \lambda^l (-1 + z)^l = \lambda^l \sum_{r=0}^{l} (-1)^{l-r} \binom{l}{r} z^r.$$

Hence we arrive at

$$\begin{aligned}\mathcal{L}_{\beta,\lambda}f(z) &= \sum_{n=0}^{\infty}\frac{\beta^n}{n!}\sum_{l=0}^{\infty}\frac{f^{(l)}(0)}{l!}\left(\lambda^l\sum_{r=0}^{l}\binom{l}{r}z^r+(-1)^n\lambda^l\sum_{r=0}^{l}(-1)^{l-r}\binom{l}{r}z^r\right)z^n\\ &= \sum_{n=0}^{\infty}\frac{\beta^n}{n!}\sum_{l=0}^{\infty}\frac{f^{(l)}(0)}{l!}\lambda^l\sum_{r=0}^{l}\binom{l}{r}\left(1+(-1)^{n+l-r}\right)z^{n+r}.\end{aligned}$$

Setting $k := n + r$ we get

$$\frac{\beta^n}{n!}\left(1+(-1)^{l+n-r}\right)z^{n+r}=\frac{\beta^{k-r}}{(k-r)!}\left(1+(-1)^{l+k}\right)z^k.$$

Finally we have to rearrange the summations over n and r; since $0 \le n$ one has $r \le k$, and since $0 \le r \le l$ we get $0 \le k \le \infty$ and $0 \le r \le \min(k, l)$. This leads to formula (9.4). □

It is known (see, e.g., [Fri96]) that since the transfer operator in (9.4) is nuclear, one can approximate it by a finite rank operator. We proceed as in the case of the transfer operator for Hecke congruence subgroups to approximate the transfer operator for the Kac-Baker model.

Proposition 9.1.2. *We can approximate the transfer operator in (9.4) by the following matrix*

$$\left[\mathcal{M}_{\beta,\lambda}\right]_{k,l}=\lambda^l\left(1+(-1)^{k+l}\right)\sum_{r=0}^{\min(k,l)}\binom{l}{r}\frac{\beta^{k-r}}{(k-r)!} \tag{9.5}$$

with $0 \le k, l \le N$, in the limit of large $N \in \mathbb{Z}_>$. Note that if $k + l$ is an odd number then the entry $\left[\mathcal{M}_{\beta,\lambda}\right]_{k,l}$ is zero, i.e. this matrix has a checkerboard pattern. This fact is related to the odd and even symmetry of the eigenfunctions of this operator.

Proof. We consider the eigenvalue equation for the transfer operator in (9.4) and expand f in a Taylor series around $z = 0$

$$\begin{aligned}\mathcal{L}_{\beta,\lambda}f(z) &= \rho f(z)\\ &= \rho\sum_{q=0}^{\infty}\frac{f^{(q)}(0)}{q!}z^q.\end{aligned} \tag{9.6}$$

To determine the coefficients $\frac{f^{(q)}(0)}{q!}$ we have to compare the rhs of (9.6) and the rhs of (9.4). This leads to

$$\rho\frac{f^{(k)}(0)}{k!}=\sum_{l=0}^{\infty}\lambda^l\left(1+(-1)^{k+l}\right)\sum_{r=0}^{\min(k,l)}\binom{l}{r}\frac{\beta^{k-r}}{(k-r)!}\frac{f^{(l)}(0)}{l!}.$$

We define the matrix $\mathcal{M}_{\beta,\lambda}$ by

$$\left[\mathcal{M}_{\beta,\lambda}\right]_{k,l}=\lambda^l\left(1+(-1)^{k+l}\right)\sum_{r=0}^{\min(k,l)}\binom{l}{r}\frac{\beta^{k-r}}{(k-r)!}.$$

The dimension of this matrix is infinite. For numerical computations we have to truncate the Taylor expansions such that $0 \le k, l \le N$. □

Lemma 9.1.3. *For $\beta = 0$ the matrix $\mathcal{M}_{\beta,\lambda}$ is upper triangular. Its spectrum is given by $\sigma(\mathcal{M}_{0,\lambda}) = \left\{2\lambda^k : 0 \le k \le N\right\}$.*

Proof. The matrix $\mathcal{M}_{0,\lambda}$ is given by

$$[\mathcal{M}_{0,\lambda}]_{k,l} = \lambda^l \left(1 + (-1)^{k+l}\right) \sum_{r=0}^{\min(k,l)} \binom{l}{r} \frac{\delta_{k,r}}{(k-r)!} = \lambda^l \left(1 + (-1)^{k+l}\right) \cdot \begin{cases} \binom{l}{k} & \text{for } k \le l \\ 0 & \text{else.} \end{cases}$$

Its diagonal entries are given by $[\mathcal{M}_{0,\lambda}]_{k,k} = 2\lambda^k$ for $0 \le k \le N$. □

The following lemma is useful for numerical computations of the matrix $\mathcal{M}_{\beta,\lambda}$ in (9.5):

Lemma 9.1.4. *For $\beta \neq 0$ the expression $\sum_{r=0}^{\min(k,l)} \binom{l}{r} \frac{\beta^{k-r}}{(k-r)!}$ can be written as*

$$\frac{\beta^k}{k!} \left(1 + p_1 \left(1 + p_2 \left(1 + \cdots + p_{\min(k,l)-1} \left(1 + p_{\min(k,l)}\right)\right)\right)\right)$$

with $p_r = \frac{(l-r+1)(k-r+1)}{\beta\, r}$.

Proof. Put $a_r = \frac{l!}{r!(l-r)!} \frac{\beta^{k-r}}{(k-r)!}$. Then we get

$$\begin{aligned} a_{r-1} &= \frac{l!}{(r-1)!\,(l-r+1)!} \frac{\beta^{k-r+1}}{(k-r+1)!} = \frac{l!}{r!\,(l-r)!} \frac{\beta^{k-r}}{(k-r)!} \frac{r\beta}{(l-r+1)\,(k-r+1)} \\ &= a_r \frac{r\beta}{(l-r+1)\,(k-r+1)}. \end{aligned}$$

Define next $p_r = \frac{a_r}{a_{r-1}} = \frac{(l-r+1)(k-r+1)}{r\beta}$ then $\sum_{r=0}^{\min(k,l)} a_r = a_0(1 + p_1(1 + p_2(1 + \cdots + p_{\min(k,l)-1}(1 + p_{\min(k,l)}))))$ for $a_0 = \frac{\beta^k}{k!}$. □

9.2 A verification of the implementation of the approximation of the transfer operator

We have implemented the computation of the approximation of the transfer operator $\mathcal{L}_{\beta,\lambda}$ and its spectrum in our computer program package Morpheus. In this section we want to give a brief overview of the methods we have used to verified this implementation:

- First, we have verified that the spectrum of the matrix $\mathcal{M}_{\beta,\lambda}$ for the special case $\beta = 0$ is given by $\{2\lambda^n : n \in \mathbb{Z}_{\ge}\}$. Indeed, the results for several randomly chosen values for λ have shown that spectrum of $\mathcal{M}_{\beta,\lambda}$ is always given by $\{2\lambda^n : 0 \le n \le N\}$. E.g., for $\lambda = 0.37$ and $N = 100$ the smallest eigenvalue is given by the formula $2\lambda^N = 2 \cdot 0.37^{99} \approx 3.57273396153722 \cdot 10^{-43}$, comparing it to the smallest eigenvalue $3.572733961537225283 \cdot 10^{-43}$ of $\mathcal{M}_{\beta,\lambda}$ shows that both values are virtually the same.

- It is known [HM04] that the spectrum of $\mathcal{L}_{\beta,\lambda}$ is real for $\beta \in \mathbb{R}$. We have computed the spectrum of $\mathcal{M}_{\beta,\lambda}$ on the real line $-10 \le \beta \le 10$ in intervals of length 0.1. We have done this for $\lambda = 0.1, 0.2, \ldots, 0.7$. Indeed, the results have shown that the spectrum of $\mathcal{M}_{\beta,\lambda}$ is real in all these cases. See also Table 9.1, which shows that the trace of $\mathcal{M}_{\beta,\lambda}$ is also real for $\beta \in \mathbb{R}$.

- In [HM04] Hilger and Mayer proved that the Fredholm determinant $\det(1 - \lambda\mathcal{L}_{\beta,\lambda})$ for $\lambda = \frac{1}{2}$ has zeros at $\beta = \ln 2 + i2\pi n$, with $n \in \mathbb{Z}$, and that for a general λ the Fredholm determinants $\det(1 - \lambda\mathcal{L}_{\beta,\lambda})$ and $\det(1 - \mathcal{L}_{\beta,\lambda})$ have zeros on the real line $\beta \in \mathbb{R}$. They did not specify the exact locations of the zeros on the real line. We have determined the zeros of $\det(1 - \lambda\mathcal{M}_{\beta,\lambda})$ and $\det(1 - \mathcal{M}_{\beta,\lambda})$ on the real line for $-10 \le \beta \le 10$ and $\lambda = 0.1, 0.2, \ldots, 0.7$ and also the zeros of $\det(1 - \lambda\mathcal{M}_{\beta,\lambda})$ on the line $\Re\beta = \ln 2$ for $0 \le \Im\beta \le 15$ and $\lambda = \frac{1}{2}$. Indeed, we have found the zeros on the real line and the zeros on the line $\Re\beta = \ln 2$ at the expected locations at $\beta = \ln 2 + i2\pi n$. See also Figures 9.1 to 9.3 in the next section.

- One can compute the trace of $\mathcal{L}_{\beta,\lambda}$ by using the formula (9.2). This way we have compared the trace of $\mathcal{L}_{\beta,\lambda}$ to the trace of the matrix $\mathcal{M}_{\beta,\lambda}$. Some of the results are given in Table 9.1 for different values of β and λ. tr $\mathcal{M}_{\beta,\lambda}$ denotes the trace of $\mathcal{M}_{\beta,\lambda}$ calculated by the sum tr $\mathcal{M}_{\beta,\lambda} = \sum_{k=0}^{N} \left[\mathcal{M}_{\beta,\lambda}\right]_{k,k}$ and $\mathrm{tr}_\sigma\, \mathcal{M}_{\beta,\lambda}$ denotes the trace calculated by the sum $\mathrm{tr}_\sigma\, \mathcal{M}_{\beta,\lambda} = \sum_{k=0}^{N} \rho_k$ over the eigenvalues $\rho_k = \rho_k(\beta,\lambda) \in \sigma\left(\mathcal{M}_{\beta,\lambda}\right)$. tr $\mathcal{L}_{\beta,\lambda}$ denotes the trace of $\mathcal{L}_{\beta,\lambda}$ determined by the formula (9.2). The time to compute the matrix $\mathcal{M}_{\beta,\lambda}$ and its spectrum is also given. Indeed, the results for the traces are remarkably close to each other.

Table 9.1: Performance and accuracy of the approximation of $\mathcal{L}_{\beta,\lambda}$

args.	impl.	trace	time
$N = 150$	tr $\mathcal{M}_{\beta,\lambda}$	4.60289484066107E-1+4.08877216096480E-1I	
$\beta = -4.6 + 2.3I$	$\mathrm{tr}_\sigma\, \mathcal{M}_{\beta,\lambda}$	4.60289484066107E-1+4.08877216096480E-1I	3.955s
$\lambda = 0.24$	tr $\mathcal{L}_{\beta,\lambda}$	4.60289484066107E-1+4.08877216096480E-1I	
	$\lvert\mathrm{tr}_\sigma\, \mathcal{M}_{\beta,\lambda} - \mathrm{tr}\, \mathcal{L}_{\beta,\lambda}\rvert$	3.684679284362124120E-48	
$N = 250$	tr $\mathcal{M}_{\beta,\lambda}$	8.64390588395796E7-1.01707097328686E8I	
$\beta = 11.4 + 7.8I$	$\mathrm{tr}_\sigma\, \mathcal{M}_{\beta,\lambda}$	8.64390588395796E7-1.01707097328686E8I	19.305s
$\lambda = 0.6$	tr $\mathcal{L}_{\beta,\lambda}$	8.64390588395796E7-1.01707097328686E8I	
	$\lvert\mathrm{tr}_\sigma\, \mathcal{M}_{\beta,\lambda} - \mathrm{tr}\, \mathcal{L}_{\beta,\lambda}\rvert$	2.514285749322825345E-10	
$N = 100$	tr $\mathcal{M}_{\beta,\lambda}$	2.38559835601709+4.5604976964454E-1I	
$\beta = 0.8 + 1.7I$	$\mathrm{tr}_\sigma\, \mathcal{M}_{\beta,\lambda}$	2.38559835601709+4.5604976964454E-1I	1.336s
$\lambda = 0.1$	tr $\mathcal{L}_{\beta,\lambda}$	2.38559835601709+4.5604976964454E-1I	
	$\lvert\mathrm{tr}_\sigma\, \mathcal{M}_{\beta,\lambda} - \mathrm{tr}\, \mathcal{L}_{\beta,\lambda}\rvert$	1.371128296277296366E-48	
$N = 100$	tr $\mathcal{M}_{\beta,\lambda}$	8.902163713969870418	
$\beta = 0.8$	$\mathrm{tr}_\sigma\, \mathcal{M}_{\beta,\lambda}$	8.902163713969870418	0.440s
$\lambda = 0.5$	tr $\mathcal{L}_{\beta,\lambda}$	8.902163713969870418	
	$\lvert\mathrm{tr}_\sigma\, \mathcal{M}_{\beta,\lambda} - \mathrm{tr}\, \mathcal{L}_{\beta,\lambda}\rvert$	1.361664891462003177E-23	
$N = 100$	tr $\mathcal{M}_{\beta,\lambda}$	3.174603174603174603	
$\beta = 0$	$\mathrm{tr}_\sigma\, \mathcal{M}_{\beta,\lambda}$	3.174603174603174603	0.044s
$\lambda = 0.37$	tr $\mathcal{L}_{\beta,\lambda}$	3.174603174603174603	
	$\lvert\mathrm{tr}_\sigma\, \mathcal{M}_{\beta,\lambda} - \mathrm{tr}\, \mathcal{L}_{\beta,\lambda}\rvert$	2.098280021841448691E-43	
$N = 100$	tr $\mathcal{M}_{\beta,\lambda}$	3.628718131576500135E-1	
$\beta = -2.4$	$\mathrm{tr}_\sigma\, \mathcal{M}_{\beta,\lambda}$	3.628718131576500135E-1-1.347405855E-70I	0.580s
$\lambda = 0.5$	tr $\mathcal{L}_{\beta,\lambda}$	3.628718131576500135E-1	
	$\lvert\mathrm{tr}_\sigma\, \mathcal{M}_{\beta,\lambda} - \mathrm{tr}\, \mathcal{L}_{\beta,\lambda}\rvert$	7.596674397398449375E-31	

Results from widmo version *6.4.1*. Precision 160 bits (49 digits).

9.3 Numerical results for the transfer operator

To investigate the structure of the zeros and the poles of the Ruelle zeta function $Z_R(\beta) := Z_R(1,\beta)$ in (9.3) in the complex β-plane for a fixed value of λ we compute the spectrum of the matrix $\mathcal{M}_{\beta,\lambda}$ in (9.5) which approximates the spectrum of the transfer operator $\mathcal{L}_{\beta,\lambda}$ in (9.1). Obviously, one can approximate the Ruelle zeta function by

$$Z_R(\beta) = \prod_{i=0}^{N} \frac{1-\lambda\rho_i}{1-\rho_i}, \quad \text{for } N \to \infty$$

with $\rho_i = \rho_i(\beta,\lambda)$ the eigenvalues of $\mathcal{M}_{\beta,\lambda}$. For practical reasons we have to choose a finite N. Of course, preferably N should be chosen as small as possible in order to reduce the computation time. To ensure

that the matrix $\mathcal{M}_{\beta,\lambda}$ approximates the transfer operator $\mathcal{L}_{\beta,\lambda}$ well enough for a chosen N, we compare the spectral trace of $\mathcal{M}_{\beta,\lambda}$ with the trace formula (9.2) for $\mathcal{L}_{\beta,\lambda}$. It turned out that for $\lambda \leq 0.5$ the value $N = 150$ gives excellent results for $-10 \leq \Re\beta \leq 10$ and $0 \leq \Im\beta \leq 15$. Unfortunately, for values of λ larger than 0.5 one has to increase N extremely, e.g., for $\lambda = 0.6$ we set $N = 250$ and for $\lambda = 0.7$ even the value $N = 500$ does not give satisfying results in the whole part of the β-plane mentioned above. (See also Table 9.1 in the foregoing section.)

Since the poles and the zeros of the function $Z_R(\beta)$ are determined by the zeros of the Fredholm determinant $\det(1 - \mathcal{L}_{\beta,\lambda})$ resp. $\det(1 - \lambda\mathcal{L}_{\beta,\lambda})$, here we will only present figures which show the zeros of these determinants in the β-plane for a fixed value of λ. Obviously, these Fredholm determinants are zero if the transfer operator $\mathcal{L}_{\beta,\lambda}$ has an eigenvalue equal to 1 resp. equal to λ^{-1}. So we have to look for these eigenvalues in the spectrum of the matrix $\mathcal{M}_{\beta,\lambda}$. We have computed the spectrum of $\mathcal{M}_{\beta,\lambda}$ for $-10 \leq \Re\beta \leq 10$ and $0 \leq \Im\beta \leq 15$ in intervals of length 0.1 and a fixed value of λ. We performed these computations for the values $\lambda = 0.1, 0.2, \ldots, 0.8$, but we will present here only results for $\lambda = 0.1, 0.2, \ldots, 0.6$, since the results for the other values are not reliable enough. To display the results graphically we define the function $m_q(\beta, \lambda)$ by

$$m_q(\beta, \lambda) = \min_{0 \leq i \leq N} |q - \rho_i|, \quad \text{with } \rho_i = \rho_i(\beta, \lambda) \in \sigma\left(\mathcal{M}_{\beta,\lambda}\right).$$

Obviously, this function is just the smallest absolute difference between the eigenvalues of $\mathcal{M}_{\beta,\lambda}$ and the value of q, so if the matrix $\mathcal{M}_{\beta,\lambda}$ has the eigenvalue q this function becomes zero. Figures 9.1 to 9.3 show $m_{\lambda^{-1}}(\beta, \lambda)$ and $m_1(\beta, \lambda)$ in the β-plane for different values of $\lambda = 0.1, 0.2, \ldots, 0.6$. The colors red to yellow indicate a potential zero resp. pole of $Z_R(\beta)$ in this area.

Note, that since we have done our computations within fixed intervals of length 0.1 in the β-plane, it is possible, yet unlikely, that we have missed some of the zeros or poles of $Z_R(\beta)$. Also, in order to derive additional information our results cannot provide, further numerical investigations are necessary: To verify for instance if a point is indeed a zero resp. a pole of $Z_R(\beta)$ one should use the argument principle. To compute the exact location of the zeros and the poles of $Z_R(\beta)$ one should compute the zeros of the Fredholm determinants $\det\left(1 - \lambda\mathcal{M}_{\beta,\lambda}\right)$ and $\det\left(1 - \mathcal{M}_{\beta,\lambda}\right)$ in the β-plane by Newton's method.

9.3.1 Concluding discussion of the numerical results

Based on the results we obtained by numerical investigations, we will try to answer the two questions posed by Hilgert and Mayer, from the beginning of this chapter.

1. It seems that there are lines of zeros for the Ruelle zeta function $Z_R(\beta)$ parallel to the imaginary β-axis for every $0 < \lambda < 1$. Indeed, probably there is even an infinite number of these lines for every $0 < \lambda < 1$. Like the zeros on the line $\Re\beta = \ln 2$ for $\lambda = \frac{1}{2}$, the zeros on the other lines seem to be at least approximately equidistant.

2. There are also zeros of $Z_R(\beta)$ in the β-plane which are neither on the line $\Re\beta = \frac{1}{2}$ nor on the real line $\beta \in \mathbb{R}$ for $\lambda = \frac{1}{2}$. It seems that for any value of λ there are always zeros in the β-plane which are not on any line parallel to the imaginary β-axis. We believe that it is very unlikely that a general Riemann hypothesis holds for the Ruelle zeta function $Z_R(\beta)$.

It is not easy to answer the first question, since we can see only up to four zeros on a potential line of zeros in the part of the β-plane we have investigated. We did not spend more time to clarify if all zeros are in fact on straight lines, because the exact answer would be only relevant if there would not exist any other zeros which appear to be clearly not on any line. The answer to the second question is easier, since there are many zeros distributed over the entire β-plane. Still it seems likely that there is a more complicated pattern in the β-plane for the zeros which are off the lines.

Also, note that the pattern of the zeros and the poles is often quite similar. It gives the impression that the zeros and poles are somehow related to each other. This is especially true for the zeros and also the poles in

the half plane $\Re\beta < 0$, which seem to be located on diagonal lines. On the other hand, the zeros and poles in the half-plane $\Re\beta \geq 0$ which look to be on lines parallel to the imaginary β-axis appear to be also on some horizontal lines. These horizontal lines, however, are not straight lines. Presumably the zeros become dense for $\lambda \to 1.0$ on these horizontal lines. And also the distance between the different lines themselves becomes smaller as $\lambda \to 1.0$, maybe the lines become even dense. The real line $\mathbb{R}_>$ appears to be just a special case of these horizontal lines. We can also see that the zeros on the positive real line are equidistant. The distribution of the poles on the positive real line look to be more complicated, but obviously there is also some kind of pattern.

From formula (9.2) we can see that the trace of $\mathcal{L}_{\beta,\lambda}$ becomes large for $\lambda \to 1.0$ and also for $\Re\beta \to \infty$. This suggest that some of the eigenvalues becomes very large. Indeed, this is in agreement with the fact from our numerical results that the eigenvalues are getting larger. Actually, the eigenvalues are getting also larger for $|\beta| \to \infty$, but the trace remains small for $\Re\beta \leq 0$ since the eigenvalues cancel each other out in this case. These large eigenvalues also appear to be the reason why the absolute value of $Z_R(\beta)$ is in general rather small. Obviously, for large eigenvalues ρ_i the terms of this zeta function are just $\frac{1-\lambda\rho_i}{1-\rho_i} \sim \frac{\lambda\rho_i}{\rho_i} \sim \lambda$, and since $\lambda < 1$ the zeta function becomes rather small. Another consequence of the large eigenvalues for $\lambda \to 1.0$ and $|\beta| \to \infty$ is that we have to increase N quite dramatically in these cases to obtain reliable results for the relative small eigenvalues around 1 resp. λ^{-1} that we are looking for. Indeed, the reason why we do not present here the results for $\lambda > 0.6$ is that we cannot guarantee that these are precise enough. But it seems that these results just confirm the phenomena and the behavior we saw already for the smaller values of λ.

Another phenomenon we found is that in some cases the zeros resp. the poles appear in pairs. This phenomenon seems to show up for all kind of zeros or poles. Perhaps more computations with interim values of λ could shed some light on this issue.

Our implementation of the approximation of $\mathcal{L}_{\beta,\lambda}$ works for complex values of λ. Indeed, the transfer operator $\mathcal{L}_{\beta,\lambda}$ is also well defined if λ is a complex number with $|\lambda| < 1$. The trace formula (9.2) is also still valid in this case.

Comparing the Ruelle zeta function $Z_R(\beta)$ to other zeta functions we have computed during other numerical investigations in this thesis, shows that this zeta function is somehow different from the others: The absolute value of $Z_R(\beta)$ is rather small and we do not see any strong oscillation of the real part and the imaginary part of $Z_R(\beta)$ which seems to be typical for all other zeta functions. The zeta function $Z_R(\beta)$ appears to be quite regular in the β plane. Furthermore, the zeros and poles of $Z_R(\beta)$ have some pattern in the β-plane which is not very striking, and the parameter λ acts almost just as a scaling parameter of the β-plane. Also, the zeros and the poles have presumably not any deep interpretation like in the case of, e.g., Selberg zeta function. Moreover, there is a vast amount of information encoded in the Selberg zeta function; this seems not to be the case for the function $Z_R(\beta)$. Indeed, it might be that the Ruelle zeta function $Z_R(\beta)$ and maybe even general dynamical zeta functions are somehow different to the "classical" arithmetic zeta functions.

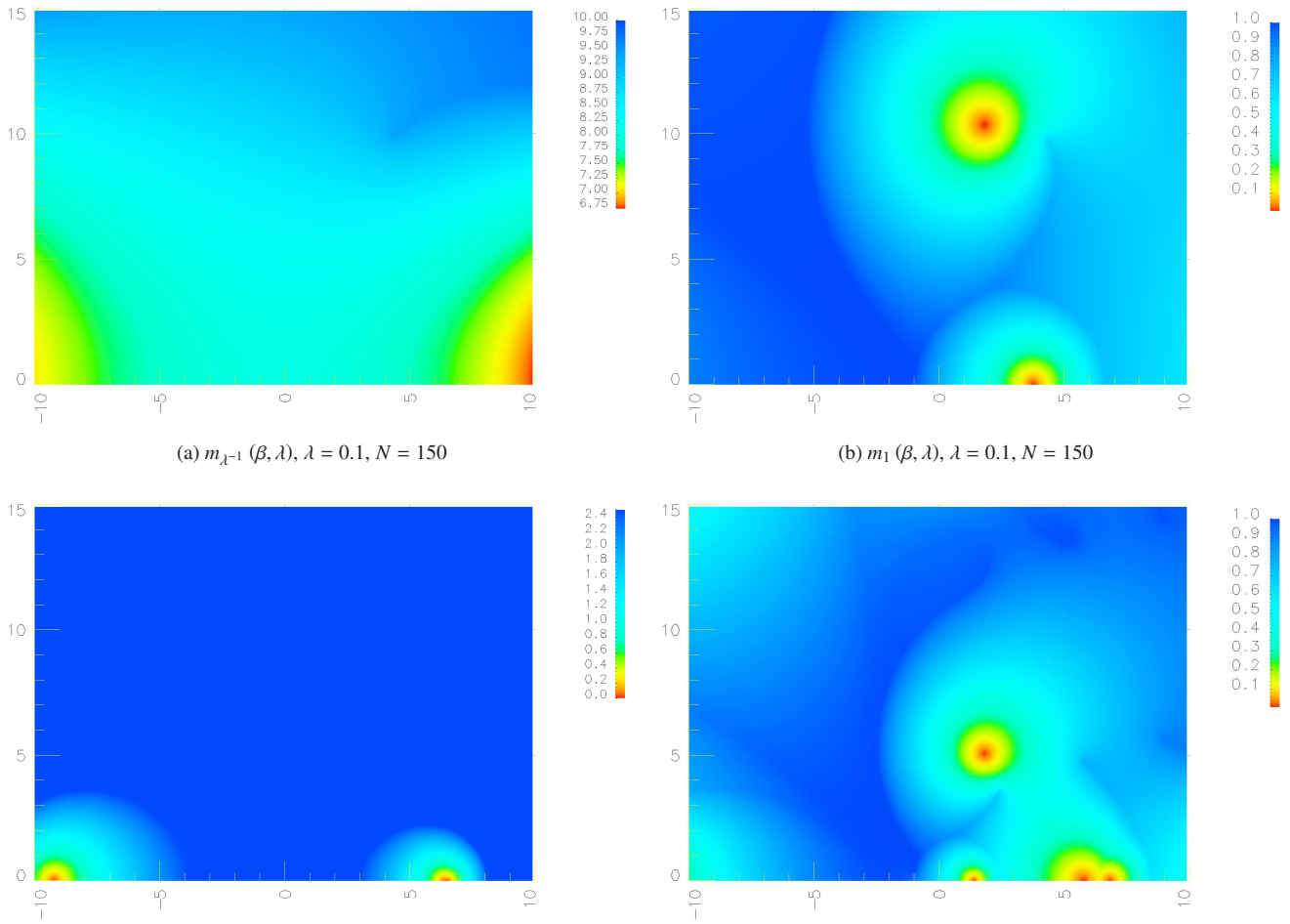

(a) $m_{\lambda^{-1}}(\beta, \lambda)$, $\lambda = 0.1$, $N = 150$

(b) $m_1(\beta, \lambda)$, $\lambda = 0.1$, $N = 150$

(c) $m_{\lambda^{-1}}(\beta, \lambda)$, $\lambda = 0.2$, $N = 150$

(d) $m_1(\beta, \lambda)$, $\lambda = 0.2$, $N = 150$

Figure 9.1: The zero $m_{\lambda^{-1}}(\beta, \lambda)$ and pole $m_1(\beta, \lambda)$ structure of $Z_R(\beta)$ in β-plane for $\lambda = 0.1$ and $\lambda = 0.2$

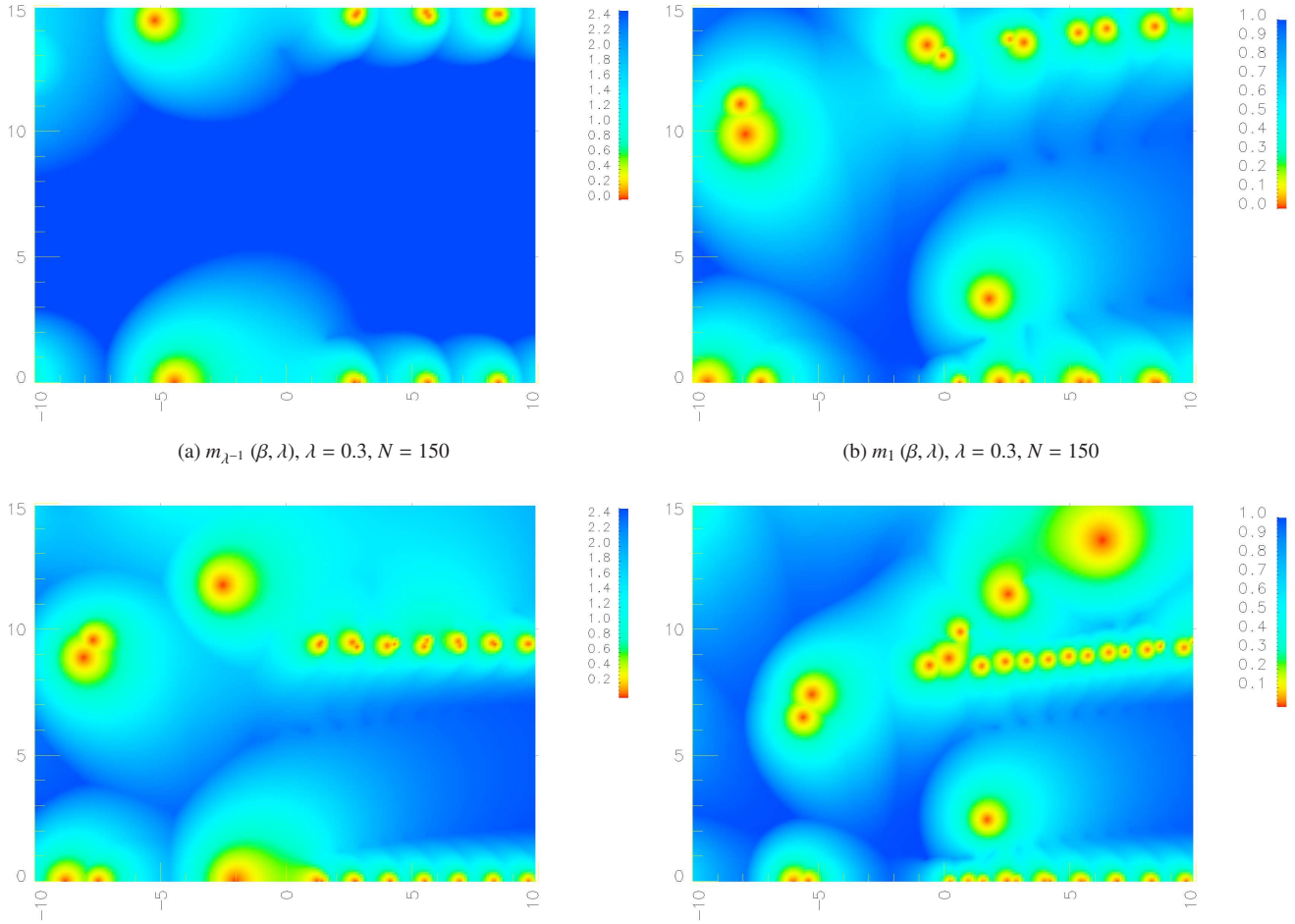

(a) $m_{\lambda^{-1}}(\beta, \lambda)$, $\lambda = 0.3$, $N = 150$

(b) $m_1(\beta, \lambda)$, $\lambda = 0.3$, $N = 150$

(c) $m_{\lambda^{-1}}(\beta, \lambda)$, $\lambda = 0.4$, $N = 150$

(d) $m_1(\beta, \lambda)$, $\lambda = 0.4$, $N = 150$

Figure 9.2: The zero $m_{\lambda^{-1}}(\beta, \lambda)$ and pole $m_1(\beta, \lambda)$ structure of $Z_R(\beta)$ in β-plane for $\lambda = 0.3$ and $\lambda = 0.4$

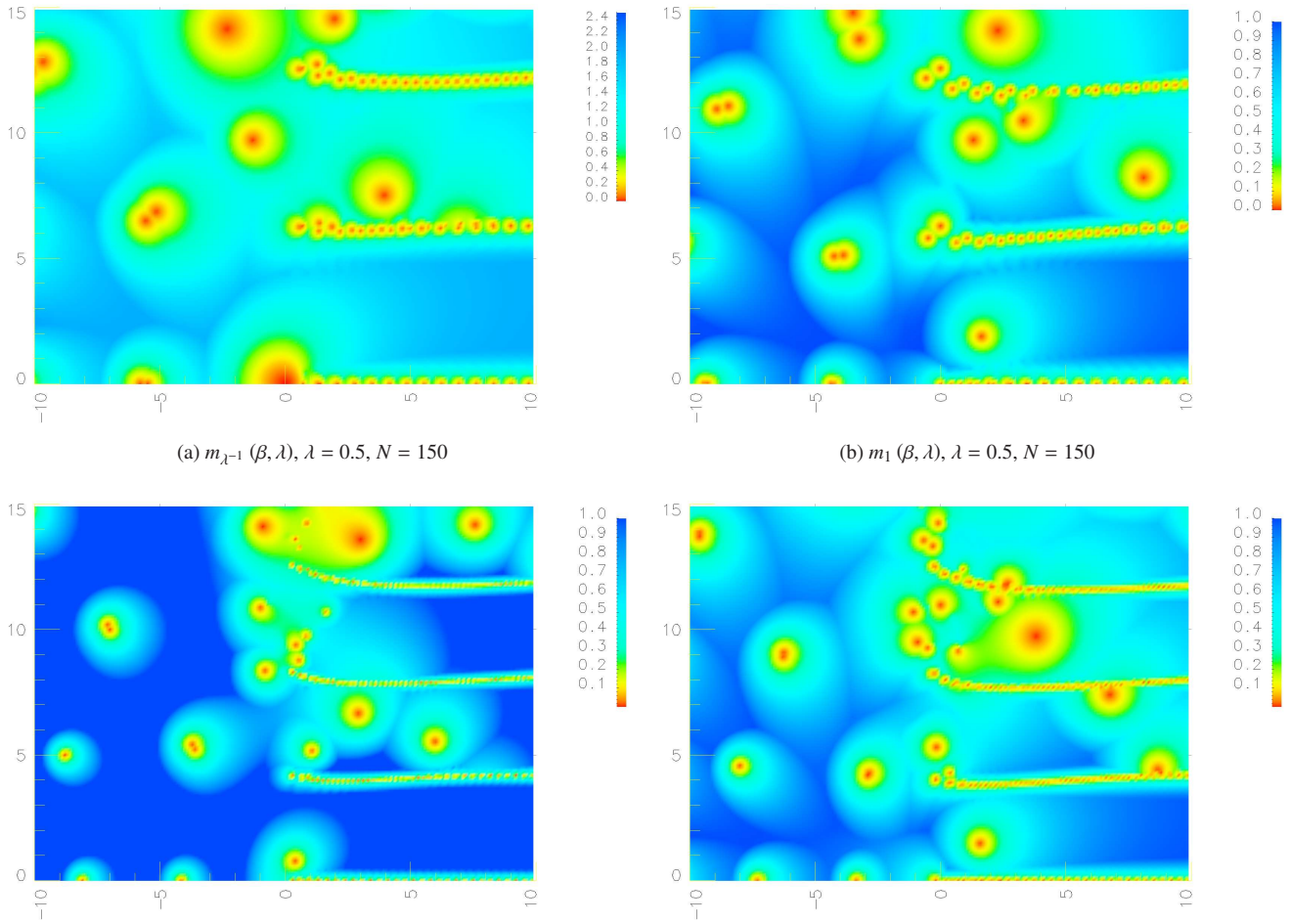

(a) $m_{\lambda^{-1}}(\beta,\lambda)$, $\lambda = 0.5$, $N = 150$

(b) $m_1(\beta,\lambda)$, $\lambda = 0.5$, $N = 150$

(c) $m_{\lambda^{-1}}(\beta,\lambda)$, $\lambda = 0.6$, $N = 250$

(d) $m_1(\beta,\lambda)$, $\lambda = 0.6$, $N = 250$

Figure 9.3: The zero $m_{\lambda^{-1}}(\beta,\lambda)$ and pole $m_1(\beta,\lambda)$ structure of $Z_R(\beta)$ in β-plane for $\lambda = 0.5$ and $\lambda = 0.6$

Appendix A

Project Morpheus

We developed the computer program package Morpheus to perform computations related to the transfer operator and Selberg zeta function for Hecke congruence subgroups $\Gamma_0(n)$ with a character χ. This package consists of the computer program CGF, which stands for *Compute Groups Fast*, the computer program widmo, which is Polish for *spectrum*, and the library CGF-lib. In short, the program CGF performs all integer and symbolic computations, while the program widmo carries out high-precision floating-point computations. The library CGF-lib provides an interface to the functions of CGF, making them available for widmo and any other computer program. We developed CGF and widmo with the objectives that the computations should be performed in high precision, the results should be reliable and the computation should be done reasonably fast. We use the GNU MPFR C library [MPF09] to perform high-precision arithmetic in our program widmo. To verify our computations we implemented a number of different tests in our programs in order to check if the computations fulfill certain criteria, e.g., if some functions have to fulfill certain functional equation etc. Furthermore, we also implemented sanity checks in our programs, to see if a result of a computation is in an expected range. Some of these tests are done during the computations, while for others we implemented special test runs. Since we want to evaluate the Selberg zeta function for many arguments by computing the spectrum of the transfer operator, we need to carry out the computations inside our programs rather fast. One of the main proposes of our program is to track the zeros of the Selberg zeta function $Z^{(n)}(\beta, \chi_\alpha^{(n)})$ in the β-plane when α is changing. The computation for $\Gamma_0(4)$ with $0 \leq \alpha \leq 0.5$ takes usually between 2 and 4 months. To reduce this time we optimized our programs by analysing the runtime with tools like *gprof*. We also compared different algorithms for the various tasks to check which one is faster and produces more precise results. A prominent example is the algorithm for computing the eigenvalues in Chapter 5. Furthermore, we used different techniques like look-up tables to improve the performance of our programs. Both programs CGF and widmo can be compiled and run on a personal computer under any Unix-like operating system, including Linux and Mac OS X. They can also run on large computer clusters by using the Message Passing Interface (MPI) application programming interface. This way we performed computations with up to 2048 CPU's on the HLRN[1] cluster. The latest version of CGF is 2.3.1 and of widmo is 6.5.0. CGF, widmo and CGF-lib are written in the C programming language and their complete source code is over 30 000 lines long.

We started the development of the computer program CGF during our diploma thesis [Fra06] and used it for computing the solutions of the Lewis equation for the Hecke congruence subgroup $\Gamma_0(mn)$ related to solutions for $\Gamma_0(n)$. We called these solutions "old" period functions, for which two different approaches exist: the first approach relies on the work of Hilgert, Mayer and Movasati in [HMM05], who derived the vector-valued period functions as special eigenfunctions of the transfer operator for $\Gamma_0(n)$. Another approach is the one by Mühlenbruch in [Müh06], who determined the period functions for $\Gamma_0(n)$ via a certain integral

[1] The North-German Supercomputing Alliance: Norddeutscher Verbund zur Förderung des Hoch- und Höchstleistungsrechnens

transform from Maass wave forms. His approach was used in [Fra06] to write down an explicit formula for the period functions for $\Gamma_0(mn)$ given the period functions for $\Gamma_0(n)$. It was also shown in [Fra06] that the constructions of the period functions of Mühlenbruch in [Müh06] and of Hilgert, Mayer and Movasati in [HMM05] coincide. We could also use our computer program to determine the explicit form of the Hecke-*like* operators acting on period functions for $\Gamma_0(n)$ introduced by Hilgert, Mayer and Movasati in [HMM05]. Furthermore, in [Fra06] the Fricke element acting on the space of Maass wave forms has been transferred to a Fricke operator for $\Gamma_0(n)$ acting on the space of vector-valued period functions. The explicit form of this operator could also be determined by our program.

During the preparation of our thesis we extended the program CGF to compute the character $\chi_{\alpha_1,\ldots,\alpha_k}$ (6.16) in section 6.5, namely

$$\chi_{\alpha_1,\ldots,\alpha_k}(\gamma) = \exp 2\pi i \sum_{i=1}^{k} \alpha_i \Omega_i(\gamma)$$

for any freely and finitely generated subgroup of $\mathrm{SL}(2,\mathbb{Z})$, whose system of generators $\{G_i\}$ is given. Currently we implemented the computation of the character $\chi^{(4)}_{\alpha_1,\alpha_2}$ for $\Gamma_0(4)$ the character $\chi^{(8)}_{\alpha_1,\alpha_2,\alpha_3}$ for $\Gamma_0(8)$. Our program determines the function $\Omega_i(\gamma)$ given in (6.17) by computing the representation of γ in terms of the generators $\{G_i\}$, then $\Omega_i(\gamma)$ is the sum of the exponents of the generator G_i in this representation. Since our program CGF can determine the representatives $\{r_i^{(n)}\}$ of the rest classes of $\Gamma_0(n)$ in $\mathrm{SL}(2,\mathbb{Z})$, we also can compute the explicit form of the representation U^χ in (7.22) for every element in $\Gamma_0(n)$

$$[U^\chi(g)]_{i,j} = \delta_{\Gamma_0(n)}\left(r_i^{(n)} g \left(r_j^{(n)}\right)^{-1}\right)\chi\left(r_i^{(n)} g \left(r_j^{(n)}\right)^{-1}\right),$$

where the character χ can be trivial or defined by (6.16). In Appendix B the representatives of $\Gamma_0(4)$ and $\Gamma_0(8)$ in $\mathrm{SL}(2,\mathbb{Z})$ are given. As an example the representation $U^{\chi^{(4)}_{\alpha_1,\alpha_2}}\begin{pmatrix} 0 & -1 \\ 1 & 3 \end{pmatrix}$ is given in section 7.4. By computing the representation U^χ our program CGF can also determine the explicit form of the transfer operator in lemma 7.4.5

$$\left[\mathcal{L}^{(n)}_{\beta,\varepsilon,\chi}\vec{f}(z)\right]_i = \sum_{q=0}^{\infty}\sum_{m=1}^{n}\sum_{j=1}^{\mu_n}[U^\chi(S T^{m\varepsilon})]_{i,j}\chi\left(r_j^{(n)} T^{n\varepsilon}\left(r_j^{(n)}\right)^{-1}\right)^q f_j|_{2\beta}\tilde{S}T^{m+nq}z,$$

and determine the operators $\mathcal{P}_k$ intertwining the transfer operators $\mathcal{L}^{(n)}_{\beta,+1,\chi}$ and $\mathcal{L}^{(n)}_{\beta,-1,\chi}$, which means

$$\mathcal{P}_k\mathcal{L}^{(n)}_{\beta,+1,\chi} = \mathcal{L}^{(n)}_{\beta,-1,\chi}\mathcal{P}_k,$$

using the algorithm given in section 8.1.3. In section 7.4.2 an output of CGF is given for the form of the transfer operators $\mathcal{L}^{(4)}_{\beta,+1,\chi^{(4)}_{\alpha_1,\alpha_2}}$ and $\mathcal{L}^{(4)}_{\beta,-1,\chi^{(4)}_{\alpha_1,\alpha_2}}$ and the operators $\mathcal{P}_k$ for $(\Gamma_0(4),\chi^{(4)}_{\alpha_1,\alpha_2})$, and in Appendix C an output for the form of the transfer operators $\mathcal{L}^{(8)}_{\beta,+1,\chi^{(8)}_{\alpha_1,\alpha_2,\alpha_3}}$ and $\mathcal{L}^{(8)}_{\beta,-1,\chi^{(8)}_{\alpha_1,\alpha_2,\alpha_3}}$ and the operators $\mathcal{P}_k$ for $(\Gamma_0(8),\chi^{(8)}_{\alpha_1,\alpha_2,\alpha_3})$ is given.

The computation of an approximation of the transfer operator, its eigenvalues and the Selberg zeta function have to be performed by using high-precision representations of complex numbers. To handle this kind of floating-point computations in widmo we implemented the complex numbers based on the implementation of arbitrary precision real numbers in the MPFR library [MPF09]. The formulas used in this implementation are given in section 2.1. The precision of the numbers used in our program widmo can be chosen for every computation. The default precision of the numbers we used was 160 bits, which is about 50 significant decimal digits. When necessary, we performed certain computations with a much higher precision of 256 bits and higher. The program widmo can determine numerically the approximation of the transfer operator

$\mathcal{L}^{(n)}_{\beta,\varepsilon,\chi}$ given by the matrix $\mathcal{M}^{(n)}_{\beta,\varepsilon,\chi}$ in proposition 7.4.11, namely

$$\begin{aligned}\left[\left(\mathcal{M}^{(n)}_{\beta,\varepsilon,\chi}\right)_{s,k}\right]_{i,j} &= \frac{1}{s!}\sum_{t=0}^{k}\binom{k}{t}\frac{(-1)^{k-t+s}}{n^{2\beta+t+s}}\frac{\Gamma(2\beta+t+s)}{\Gamma(2\beta+t)}\sum_{m=1}^{n}\left[U^{\chi}\left(S\,T^{m\varepsilon}\right)\right]_{i,j}\\ &\quad \Phi\left(\chi\left(r_j^{(n)}T^{n\varepsilon}\left(r_j^{(n)}\right)^{-1}\right), 2\beta+t+s, \frac{m+1}{n}\right),\end{aligned}$$

by using the representation U^{χ} and the character χ as computed in CGF. For this we implemented the approximation of the gamma function $\Gamma(s)$ of Chapter 3 and our approximation for the Lerch transcendent $\Phi(\chi, s, z)$ in Chapter 4. Furthermore, the program widmo is also able to compute the incomplete gamma functions $\Gamma(s,z)$ and $\gamma(s,z)$ given in Chapter 3, as well as the Hurwitz zeta function $\zeta(s,z)$ using our approximation given in Chapter 4. All of these special functions are involved in the computations of the approximation $\mathcal{M}^{(n)}_{\beta,\varepsilon,\chi}$. Next, we can compute the matrix $\mathcal{P}_k\mathcal{M}^{(n)}_{\beta,\varepsilon,\chi}$ given in (8.5) in section 8.1.4, where $\mathcal{P}_k$ is determined symbolically by CGF. To obtain the approximation of the Selberg zeta function

$$Z^{(n)}_{\mathcal{M}}(\beta,\chi) = \det(1-\mathcal{M}^{(n)}_{\beta,+1,\chi}\mathcal{M}^{(n)}_{\beta,-1,\chi}) = \prod_{i=1}^{\mu_n N}(1-\lambda_i)$$

respectively

$$Z^{(n)}_{\mathcal{M}}(\beta,\chi) = \det(1-\mathcal{P}_k\mathcal{M}^{(n)}_{\beta,+1,\chi})\det(1+\mathcal{P}_k\mathcal{M}^{(n)}_{\beta,+1,\chi}) = \prod_{i=1}^{\mu_n N}(1-\lambda_i)\,(1+\lambda_i)$$

we use the algorithm introduced in Chapter 5 to compute the eigenvalues λ_i of the matrices $\mathcal{M}^{(n)}_{\beta,+1,\chi}\mathcal{M}^{(n)}_{\beta,-1,\chi}$ respectively $\mathcal{P}_k\mathcal{M}^{(n)}_{\beta,+1,\chi}$. The results of this computation are saved in a .top file, which contains the entries of the matrices $\mathcal{M}^{(n)}_{\beta,+1,\chi}\mathcal{M}^{(n)}_{\beta,-1,\chi}$ respectively $\mathcal{P}_k\mathcal{M}^{(n)}_{\beta,+1,\chi}$, their eigenvalues and traces, as well as their Fredholm determinants of these matrices, together with additional information about the computation. To compute the determinant $\varphi(\beta,\chi)$ of the scattering matrix we use the functional equation (6.7)

$$\varphi(\beta,\chi) = \eta(\beta)\,\frac{Z^{(n)}(1-\beta,\chi)}{Z^{(n)}(\beta,\chi)}.$$

The function η can be determined by the formula (6.9) for any $(\Gamma_0(n),\chi)$ with $4\,|\,n$. Currently we implemented the computation of the function η for $(\Gamma_0(4),\chi^{(4)}_{\alpha})$ using (6.28) and (6.29)

$$\begin{aligned}\eta(\beta) &= \eta\left(\frac{1}{2}\right)\left(2^{2\beta-1}\frac{\Gamma\left(\frac{1}{2}+\beta\right)}{\Gamma\left(\frac{3}{2}-\beta\right)}\right)^3\exp\left\{2\pi\int_0^{\beta-\frac{1}{2}}\tau\tan(\pi\tau)d\tau\right\} \quad \text{for } \alpha=0\\ \eta(\beta) &= \eta\left(\frac{1}{2}\right)2^{2\beta-1}\frac{\Gamma\left(\frac{1}{2}+\beta\right)}{\Gamma\left(\frac{3}{2}-\beta\right)}\exp\left\{2\pi\int_0^{\beta-\frac{1}{2}}\tau\tan(\pi\tau)d\tau\right\}\left(|1-e^{2\pi i\alpha}|\,|1-e^{-2\pi i\alpha}|\right)^{2\beta-1} \quad \text{for } \alpha\neq 0.\end{aligned}$$

Our program can also find the zeros of the Selberg zeta function $Z^{(n)}\left(\beta,\chi^{(n)}_{\alpha}\right)$ and track them in the β-plane for varying α, where the computations are based on Newton's method and the procedure described in section 8.2. The results of this computation are saved in a .min file, which contains the set of points $\{(\beta_i,\alpha_i)\}_{i\in\mathbb{Z}_>}$ for which $Z^{(n)}\left(\beta_i,\chi^{(n)}_{\alpha_i}\right)$ is zero, together with additional information about the computation. We can also determine the point where a zero of $Z^{(n)}\left(\beta,\chi^{(n)}_{\alpha}\right)$ touches the critical line $\Re\beta=\frac{1}{2}$ by a procedure described also in section 8.2. To determine the number N and P of zeros, respectively poles in the β-plane of the Selberg zeta function $Z^{(n)}(\beta,\chi)$ and the determinant $\varphi(\beta,\chi)$ of the scattering matrix we use an implementation of the argument principle

$$\frac{1}{2\pi}\left[\arg f(\beta)\right]_C = N-P$$

where $[\arg f(\beta)]_C$ denotes the change in the argument of $f(\beta)$ along the contour C. Our computer program widmo can determine the change in the argument of the Selberg zeta function respectively the determinant of the scattering matrix along a given curve C, and thereby compute the number of zeros minus the number of poles $N - P$ in the region inside of C. Finally, our computer program widmo can calculate the trace of the analytic continuation of the transfer operator by the trace formula in proposition 7.4.7

$$\operatorname{tr} \mathcal{L}^{(n)}_{\beta,\varepsilon,\chi} = \operatorname{tr} \mathcal{N}^{(n)}_{\beta,\varepsilon,\chi,N} + \operatorname{tr} \mathcal{A}^{(n)}_{\beta,\varepsilon,\chi,N},$$

with

$$\begin{aligned}\operatorname{tr} \mathcal{N}^{(n)}_{\beta,\varepsilon,\chi,N} &= \sum_{q=0}^{\infty} \sum_{m=1}^{n} \sum_{i=1}^{\mu_n} [U^\chi(ST^{m\varepsilon})]_{i,i} \chi\left(r_i^{(n)} T^{n\varepsilon} \left(r_i^{(n)}\right)^{-1}\right)^q \\ &\quad \left(\frac{\left(z^*_{q,m} + m + nq\right)^{-2\beta}}{1 + \left(z^*_{q,m} + m + nq\right)^{-2}} - \sum_{k=0}^{N} \frac{(-1)^k}{k!} \frac{\Gamma(2\beta + 2k)}{\Gamma(2\beta + k)} (m + nq)^{-2\beta - 2k} \right) \\ \text{and} \\ \operatorname{tr} \mathcal{A}^{(n)}_{\beta,\varepsilon,\chi,N} &= \sum_{k=0}^{N} \sum_{m=1}^{n} \sum_{i=1}^{\mu_n} [U^\chi(ST^{m\varepsilon})]_{i,i} \frac{(-1)^k}{n^{2\beta+2k} k!} \frac{\Gamma(2\beta + 2k)}{\Gamma(2\beta + k)} \\ &\quad \Phi\left(\chi\left(r_i^{(n)} T^{n\varepsilon} \left(r_i^{(n)}\right)^{-1}\right), 2\beta + 2k, \frac{m}{n}\right).\end{aligned}$$

To verify our computations we compared this trace of the analytic continued transfer operator with the trace of the matrix $\mathcal{M}^{(n)}_{\beta,\varepsilon,\chi}$ which approximates the transfer operator.

Finally, our computer program widmo can perform the above-described computations also for the transfer operator for the Kac-Baker model in Chapter 9, where an approximation of this operator is given by the matrix

$$\left[\mathcal{M}_{\beta,\lambda}\right]_{k,l} = \lambda^l \left(1 + (-1)^{k+l}\right) \sum_{r=0}^{\min(k,l)} \binom{l}{r} \frac{\beta^{k-r}}{(k-r)!},$$

given in (9.5).

A.1 CGF options

The program CGF is executed from a command line. Example: to compute the representation $U^\chi\begin{pmatrix} 1 & 3 \\ 0 & 1 \end{pmatrix}$ for $\Gamma_0(4)$ we type in a terminal:

```
> cgf -S 4,1,3,0,1
```

The output is written in the file "output.tex". Usually the output of a computation is written in a LaTeX file, which can be included in a document. The following text is an output from the program CGF which shows all possible options, indicating what can be computed by this program:

```
/Users/marek/bin/cgf options
version 2.3.1

options:
  -A, --lang=arg        set language to english (default) or german
  -C, --sigma=arg       canonical projection map sigma between the sets of
```

```
                        representatives for Gamma_0(NM) and Gamma_0(N), arg=N,M
  -c, --sigma2=arg      canonical projection map sigma between the index sets
                        I_nm and I_n, arg=n,m
  -S, --indRep=arg      representation of SL(2,Z) induced by a character
                        for Gamma_0(N), for the matrix (a,b;c,d)
                        arg=[i]N,a,b,c,d
                        if arg starts with 'i' invert matrix (a,b;c,d)
                        or string of ST's e.g: arg=4,ST3
  -U, --indRepI=arg     like -S but with representatives from Index set I_n
  -F, --farey=arg       Farey-sequence of level N, arg=N
  -f, --fricke=arg      the Fricke operator on the space of period functions
                        for Gamma_0(N), arg=N
  -g, --group=arg       Hecke congruence subgroup Gamma_0(N):
                        index of Gamma_0(N) in SL(2,Z),
                        representatives of Gamma_0(N) in SL(2,Z),
                        set of matrices X_m,
                        maps sigma:X_m -> X_m
                        and Phi:rep. of Gamma_0(N) -> rep. of Gamma_0(N)
                        arg=N,m or arg=N (m is set to N)
  -h, --help            display this help message and exit
  -I, --part=arg        the index set I_n, the set P_n, set of matrices X_n^*,
                        map between I_n and X_n^*,
                        representatives of Gamma_0(n) in SL(2,Z) associated
                        with I_n, arg=n
  -i, --index=arg       index of Gamma_0(N) in SL(2,Z), arg=N
  -K, --opK=arg         action of operator K on matrix (a,b;c,d), arg=a,b,c,d
  -l, --lewis=arg       solutions of the Lewis equation for Gamma_0(NM) from
                        solutions of the Lewis equation for Gamma_0(N),
                        from eigenfunctions of the transfer operator,
                        arg=N,M
  -L, --Lewis=arg       solutions of the Lewis equation for Gamma_0(NM) from
                        solutions of the Lewis equation for Gamma_0(N),
                        from integral transform of Maass wave forms,
                        arg=N,M
  -M, --matsum=arg      sum of matrices for M(p/q) constructed from some
                        Farey-sequence, arg=p,q
  -P, --perm            print induced representations of SL(2,Z) used
                        in internal calculations
  -p, --prime=arg       prime numbers smaller then n
                        or the first n prime numbers, arg=n or arg=+n
  -s, --stat            print some internal calculations:
                        prime numbers, Farey-sequences and sums of matrices M
  -T, --opT=arg         the Hecke operator T_n,m on the space of period
                        functions for Gamma_0(n), arg=n,m
  -o, --out=arg         set output file [Default output.tex]
  -V, --version         version
  -x, --xmat=arg        the set of matrices X_m or the set of matrices X_m^*
                        arg=m or arg=*m
  -z, --rep=arg         index and representatives of Gamma_0(N) in SL(2,Z)
                        arg=N
```

```
  -Z, --maprep=arg      index and representatives of Gamma_0(N) in SL(2,Z)
                        with representatives from Index set I_n, arg=N
  -t, --trans=arg       transfer operator and symmetries P for Gamma_0(N)
                        alpha_i can be set to 0 or 1 (default)
                        arg=N[,alpha_1,alpha_2...]
  -D, --symtryP=arg     multiplication of symmetries P of transfer operator
                        for Gamma_0(N), P_str=P1P3 arg=N,P_str
  -R, --transI=arg      like -t, but with representatives from Index set I_n
                        arg=N
  -k, --char=arg        character of matrix (a,b;c,d) for Gamma_0(N)
                        arg=N,a,b,c,d

Author: Markus Fraczek, markus.fraczek@tu-clausthal.de

Use \include{file} or \input{file} in your TeX file to add the output
file to your project. You need also to include the package "packgroup.sty",
with \usepackage{packgroup}, which you can find in the "tex" directory of
this distribution. (See the file "example.tex" in directory "tex".)
```

A.2 widmo options

Like CGF the program widmo is executed from a command line. Example: to compute the Selberg zeta function for $(\Gamma_0(4), \chi_\alpha^{(4)})$ with $\alpha = 0.3$ by the Fredholm determinant of the operator $\mathcal{P}_2\mathcal{L}^{(4)}_{\beta,+1,\alpha}$ for $\beta = 0.4 + 2.5i$ with 50 Taylor coefficients used in the approximation, we type in a terminal:

```
> widmo -P P2 -A 0.3 -t 4,50,0.4+2.5I
```

The output is written in a .top file. The .top files are text files containing all the information about the computation and the results. The following text is the help output of widmo which shows all possible options:

```
/Users/marek/bin/widmo options
version 6.5.0
compiled with gcc version 4.2.1

using libraries:
cgf     2.3.1
mpfr    2.4.1 (complied with 2.4.1)

default precision: 160 bits (49 digits)
internal bits: 20 (7 digits)

options:
  -t, --transG=arg      Transfer operator approximation for Gauss Map:
                        Compute Eigenvalues and Selberg zeta function
                        with matrix M_beta
```

```
                    level of congruence subgroup = n,
                    number of Taylor coefficients = N,
                    arg=n,N,beta
-P, --Symetry=arg   Use only with Transfer operator for Gauss Map:
                    Use symmetry P, compute Selberg Zeta function
                    by det(1-PL_+)det(1+PL_-)
                    P_string="P1P2..PN" or P_string=I for identity
                    arg=P_string
-C, --Cheby         Use only with Transfer operator for Gauss Map:
                    Use Chebyshev polynomials instead of Taylor expansion
-k, --transK=arg    Transfer operator approximation for Kac Model:
                    Compute Eigenvalues
                    with matrix M_beta
                    number of Taylor coefficients = N,
                    arg=N,beta,lambda
-B, --transT=arg    Transfer operator (test) for SL(2,Z):
                    constructed from symmetry z <--> -1/z
                    Compute Eigenvalues
                    with matrix M_beta
                    number of Taylor coefficients = N,
                    parameter lambda;
                    arg=N,beta
-A, --alpha=arg     Set deformation parameters alpha_i in character:
                    alpha_i corresponds to generator G_i
                    arg=alpha_1,alpha_2,alpha_3
-v, --change=arg    Set which deformation parameter alpha_i should be vary
                    in computations, arg=i
-S, --detS=arg      Determinant of the scattering matrix,
                    arguments like -t
-i, --iterG=arg     like -t, iteration between beta_start upto beta_end
                    arg = n,N,beta_start,step,beta_end
-l, --iterK=arg     like -k, iteration between beta_start upto beta_end
                    arg=N,beta_start,step,beta_end,lambda
-I, --iterA=arg     like -t, iteration between alpha upto alpha_end
                    alpha = alpha_start * exp(alpha_step)
                    arg = n,N,beta,alpha_step,alpha_end
-z, --zeta=arg      Zeta function - Hurwitz or Lerch, arg=s,z[,l]
                    z can be a complex or rational number
                    eg. z=0.4+2.21I or z=2/53
                    (eg. -z 4+2.3I,6+7I,0.43)
-R, --Rzeta=arg     Zeta function with Rest- Hurwitz or Lerch
                    a,p parameter of approximation
                    arg=a,p,s,z[,l]
-g, --gamma=arg     upper incomplete gamma function , arg=a,z
-o, --out=arg       set output file
-p, --prec=arg      set precision, digits = p'd' or bits = p, arg=p[d]
                    computing with numbers of p bits
                    internal computations (e.g. zeta function) are done in
                    precision of p - internal bits
-h, --help          display this help message and exit
```

```
-V, --version         version
-T, --test=arg        -T help for list of all possible tests
-D, --dataZ=arg       Output Selberg zeta function from .top files,
                      Selberg zeta function
                      arg=[n,N,P,beta_start,beta_end,alpha,]dir
-E, --dataE=arg       Output Eigenvalues of transfer operator from .top file,
                      arg=filename
-W, --EVp=arg         Output 1-EV from .top file,
                      EV is the closest eigenvalue to one
                      arg's like -D
-X, --EVm=arg         Output 1+EV from .top file
                      EV is the closest eigenvalue to minus one
                      arg's like -D
-Y, --EVl=arg         Output 1/lambda-EV from .top file
                      EV is the closest eigenvalue to 1/lambda
                      lambda is the parameter in Kac model
                      arg's like -D
-e, --opendx          set output format of data to opendx, default is gnuplot
-m, --minG=arg        search for eigenvalue one by using Newton's method,
                      arguments same as -t
                      P: search for eigenvalue one till it's P digits exact
                      alpha_delta: maximal difference between old and new alpha
                      max_d: step size, i.e. sqrt(delta beta^2+delta alpha^2)
                      arg=n,N,P,beta[,alpha_delta,alpha_end[,max_d]]
-G, --vmaxd           decrease max_d if other eigenvalue one appears
                      use with -m etc
-O, --lmaxd           decrease max_d if zero gets near to the critical line 0.5
                      use with -m etc
-n, --minK=arg        search for eigenvalue one by using Newton's method,
                      arguments same as -k
                      P: search for eigenvalue one till it's P digits exact
                      max_d: maximal difference between old and new beta
                      arg=N,P,beta,lambda[,max_d]
-M, --minZ=arg        search for zeros of Selberg's Zeta Function
                      by using Newton's method,
                      arguments same as -m
-N, --minZ2=arg       search for zeros of Selberg's Zeta Function
                      by using Newton's method,
                      fix Re(beta), modify alpha and Im(beta)
                      arguments same as -M
-K, --online=arg      search for the point where zero of
                      the Selberg's Zeta Function
                      go on the critical line 0.5 (CL):
                      Starts with a point off the CL
                      and try to find the local minimum to CL.
                      Useful to search where resonances touch CL
                      arguments same as -M
-L, --line=arg        search in .min file for values near a line
                      line is parallel to imaginary axis
                      output only the local minimum
```

```
                        args=line,max_d,file.min
  -J, --ialpha=arg      search in .min file for a specific value of alpha
                        and output corresponding beta value
                        if alpha value does not exist interpolate the beta value
                        args=alpha,file.min
  -s, --kappa=arg       compute k_E,phi
                        args=alpha,Im(beta)
  -a, --zeroZ=arg       argument principle of Selberg's Zeta Function
                        like -t
                        ds: side length of a box surrounding point beta
                        delta: step size when going around this box
                        e.g.: 1,50,0.5+9.5336I,0.1+0.1I,0.02
                        arg=n,N,beta,ds,delta
  -b, --zeroS=arg       argument principle of the Determinant
                        of the scattering matrix
                        like -a
                        arg=n,N,beta,ds,p
  -j, --jobs=arg        number of jobs, parallel computing mode
                        only for fork(), for mpi use mpiexec with flag -n
  -F, --trace=arg       Trace of the Transfer operator: the trace of the
                        approximation of the operator L_+ (resp. L_-)
                        and trace by the trace formula for the analytic cont.
                        level of congruence subgroup = n,
                        number of Taylor coefficients = N (for approx. only),
                        number of terms in trace = N2,
                        arg=n,N,N2,beta
  -q, --quiet           quite mode

Author: Markus Fraczek  markus.fraczek@tu-clausthal.de
```

Appendix B

The representatives of $\Gamma_0(4)$ and $\Gamma_0(8)$ in $\mathrm{SL}(2,\mathbb{Z})$

The following is an output of our program CGF for the group $\Gamma_0(4)$, where we use the following system of representatives for our numerical computations:

Index of $\Gamma_0(4)$ in $\mathrm{SL}(2,\mathbb{Z})$:

$$\mu_4 = [\ \mathrm{SL}(2,\mathbb{Z}) : \Gamma_0(4)\ ] = 6$$

Representatives of the rest classes of $\Gamma_0(4)$ in $\mathrm{SL}(2,\mathbb{Z})$:

$$r_1^{(4)} = I = \begin{pmatrix} 1 & 0 \\ 0 & 1 \end{pmatrix} \quad r_2^{(4)} = S = \begin{pmatrix} 0 & -1 \\ 1 & 0 \end{pmatrix}$$

$$r_3^{(4)} = ST = \begin{pmatrix} 0 & -1 \\ 1 & 1 \end{pmatrix} \quad r_4^{(4)} = ST^2 = \begin{pmatrix} 0 & -1 \\ 1 & 2 \end{pmatrix}$$

$$r_5^{(4)} = ST^3 = \begin{pmatrix} 0 & -1 \\ 1 & 3 \end{pmatrix} \quad r_6^{(4)} = ST^2S = \begin{pmatrix} -1 & 0 \\ 2 & -1 \end{pmatrix}$$

with $\begin{pmatrix} 1 & 0 \\ 0 & 1 \end{pmatrix} \in \Gamma_0(4)$, $S = \begin{pmatrix} 0 & -1 \\ 1 & 0 \end{pmatrix}$ and $T = \begin{pmatrix} 1 & 1 \\ 0 & 1 \end{pmatrix}$

The following is an output of our program CGF, for the representatives we use for our numerical computations:

Index of $\Gamma_0(8)$ in $\mathrm{SL}(2,\mathbb{Z})$:

$$\mu_8 = [\,\mathrm{SL}(2,\mathbb{Z}) : \Gamma_0(8)\,] = 12$$

Representatives of the rest classes of $\Gamma_0(8)$ in $\mathrm{SL}(2,\mathbb{Z})$:

$$\begin{aligned}
r_1^{(8)} &= I = \begin{pmatrix} 1 & 0 \\ 0 & 1 \end{pmatrix} & r_2^{(8)} &= S = \begin{pmatrix} 0 & -1 \\ 1 & 0 \end{pmatrix} \\
r_3^{(8)} &= ST = \begin{pmatrix} 0 & -1 \\ 1 & 1 \end{pmatrix} & r_4^{(8)} &= ST^2 = \begin{pmatrix} 0 & -1 \\ 1 & 2 \end{pmatrix} \\
r_5^{(8)} &= ST^3 = \begin{pmatrix} 0 & -1 \\ 1 & 3 \end{pmatrix} & r_6^{(8)} &= ST^4 = \begin{pmatrix} 0 & -1 \\ 1 & 4 \end{pmatrix} \\
r_7^{(8)} &= ST^5 = \begin{pmatrix} 0 & -1 \\ 1 & 5 \end{pmatrix} & r_8^{(8)} &= ST^6 = \begin{pmatrix} 0 & -1 \\ 1 & 6 \end{pmatrix} \\
r_9^{(8)} &= ST^7 = \begin{pmatrix} 0 & -1 \\ 1 & 7 \end{pmatrix} & r_{10}^{(8)} &= ST^2S = \begin{pmatrix} -1 & 0 \\ 2 & -1 \end{pmatrix} \\
r_{11}^{(8)} &= ST^4S = \begin{pmatrix} -1 & 0 \\ 4 & -1 \end{pmatrix} & r_{12}^{(8)} &= ST^6S = \begin{pmatrix} -1 & 0 \\ 6 & -1 \end{pmatrix}
\end{aligned}$$

with $\begin{pmatrix} 1 & 0 \\ 0 & 1 \end{pmatrix} \in \Gamma_0(8)$, $S = \begin{pmatrix} 0 & -1 \\ 1 & 0 \end{pmatrix}$ and $T = \begin{pmatrix} 1 & 1 \\ 0 & 1 \end{pmatrix}$

Appendix C

The transfer operator for $(\Gamma_0(8), \chi^{(8)}_{\alpha_1,\alpha_2,\alpha_3})$

The following is an output from our program CGF for the form of the transfer operator for $(\Gamma_0(8), \chi^{(8)}_{\alpha_1,\alpha_2,\alpha_3})$ as given in lemma 7.4.5 and the permutations which define the symmetries $\mathcal{P}_1$ and $\mathcal{P}_2$ for this operator. The system of representatives of $\Gamma_0(8)$ in $\mathrm{SL}(2,\mathbb{Z})$ used in this computation is given in Appendix B.

The transfer operator for $\Gamma_0(8)$ reads as

$$
\begin{aligned}
\left[\mathcal{L}^{\Gamma_0(8)}_{\beta,+1}\vec{f}\right]_1 = \sum_{q=0}^{\infty} \quad & e^{2\pi i(q\alpha_1)} f_3|_\beta \tilde{S} T^{1+8q} \\
+ \quad & e^{2\pi i(q\alpha_1)} f_4|_\beta \tilde{S} T^{2+8q} \\
+ \quad & e^{2\pi i(q\alpha_1)} f_5|_\beta \tilde{S} T^{3+8q} \\
+ \quad & e^{2\pi i(q\alpha_1)} f_6|_\beta \tilde{S} T^{4+8q} \\
+ \quad & e^{2\pi i(q\alpha_1)} f_7|_\beta \tilde{S} T^{5+8q} \\
+ \quad & e^{2\pi i(q\alpha_1)} f_8|_\beta \tilde{S} T^{6+8q} \\
+ \quad & e^{2\pi i(q\alpha_1)} f_9|_\beta \tilde{S} T^{7+8q} \\
+ \quad & e^{2\pi i((1+q)\alpha_1)} f_2|_\beta \tilde{S} T^{8+8q} \\
\left[\mathcal{L}^{\Gamma_0(8)}_{\beta,+1}\vec{f}\right]_2 = \sum_{q=0}^{\infty} \quad & e^{2\pi i((1+8q)\alpha_3)} f_1|_\beta \tilde{S} T^{1+8q} \\
+ \quad & e^{2\pi i((2+8q)\alpha_3)} f_1|_\beta \tilde{S} T^{2+8q} \\
+ \quad & e^{2\pi i((3+8q)\alpha_3)} f_1|_\beta \tilde{S} T^{3+8q} \\
+ \quad & e^{2\pi i((4+8q)\alpha_3)} f_1|_\beta \tilde{S} T^{4+8q}
\end{aligned}
$$

$$
\begin{aligned}
&+ && e^{2\pi i((5+8q)\alpha_3)} f_1|_\beta \tilde{S} T^{5+8q} \\
&+ && e^{2\pi i((6+8q)\alpha_3)} f_1|_\beta \tilde{S} T^{6+8q} \\
&+ && e^{2\pi i((7+8q)\alpha_3)} f_1|_\beta \tilde{S} T^{7+8q} \\
&+ && e^{2\pi i((8+8q)\alpha_3)} f_1|_\beta \tilde{S} T^{8+8q} \\
\left[\mathcal{L}^{\Gamma_0(8)}_{\beta,+1} \vec{f}\right]_3 &= \textstyle\sum_{q=0}^{\infty} && e^{2\pi i(q\alpha_1-\alpha_3)} f_2|_\beta \tilde{S} T^{1+8q} \\
&+ && e^{2\pi i(q\alpha_1-\alpha_3)} f_3|_\beta \tilde{S} T^{2+8q} \\
&+ && e^{2\pi i(q\alpha_1-\alpha_3)} f_4|_\beta \tilde{S} T^{3+8q} \\
&+ && e^{2\pi i(q\alpha_1-\alpha_3)} f_5|_\beta \tilde{S} T^{4+8q} \\
&+ && e^{2\pi i(q\alpha_1-\alpha_3)} f_6|_\beta \tilde{S} T^{5+8q} \\
&+ && e^{2\pi i(q\alpha_1-\alpha_3)} f_7|_\beta \tilde{S} T^{6+8q} \\
&+ && e^{2\pi i(q\alpha_1-\alpha_3)} f_8|_\beta \tilde{S} T^{7+8q} \\
&+ && e^{2\pi i(q\alpha_1-\alpha_3)} f_9|_\beta \tilde{S} T^{8+8q} \\
\left[\mathcal{L}^{\Gamma_0(8)}_{\beta,+1} \vec{f}\right]_4 &= \textstyle\sum_{q=0}^{\infty} && e^{2\pi i((-1-4q)\alpha_1-4q\alpha_2+(-1-4q)\alpha_3)} f_{12}|_\beta \tilde{S} T^{1+8q} \\
&+ && e^{2\pi i((-1-4q)\alpha_1+(-1-4q)\alpha_2+(-1-4q)\alpha_3)} f_{10}|_\beta \tilde{S} T^{2+8q} \\
&+ && e^{2\pi i((-2-4q)\alpha_1+(-1-4q)\alpha_2+(-2-4q)\alpha_3)} f_{12}|_\beta \tilde{S} T^{3+8q} \\
&+ && e^{2\pi i((-2-4q)\alpha_1+(-2-4q)\alpha_2+(-2-4q)\alpha_3)} f_{10}|_\beta \tilde{S} T^{4+8q} \\
&+ && e^{2\pi i((-3-4q)\alpha_1+(-2-4q)\alpha_2+(-3-4q)\alpha_3)} f_{12}|_\beta \tilde{S} T^{5+8q} \\
&+ && e^{2\pi i((-3-4q)\alpha_1+(-3-4q)\alpha_2+(-3-4q)\alpha_3)} f_{10}|_\beta \tilde{S} T^{6+8q} \\
&+ && e^{2\pi i((-4-4q)\alpha_1+(-3-4q)\alpha_2+(-4-4q)\alpha_3)} f_{12}|_\beta \tilde{S} T^{7+8q} \\
&+ && e^{2\pi i((-4-4q)\alpha_1+(-4-4q)\alpha_2+(-4-4q)\alpha_3)} f_{10}|_\beta \tilde{S} T^{8+8q} \\
\left[\mathcal{L}^{\Gamma_0(8)}_{\beta,+1} \vec{f}\right]_5 &= \textstyle\sum_{q=0}^{\infty} && e^{2\pi i(q\alpha_1+\alpha_2)} f_8|_\beta \tilde{S} T^{1+8q} \\
&+ && e^{2\pi i(q\alpha_1+\alpha_2)} f_9|_\beta \tilde{S} T^{2+8q} \\
&+ && e^{2\pi i((1+q)\alpha_1+\alpha_2)} f_2|_\beta \tilde{S} T^{3+8q} \\
&+ && e^{2\pi i((1+q)\alpha_1+\alpha_2)} f_3|_\beta \tilde{S} T^{4+8q} \\
&+ && e^{2\pi i((1+q)\alpha_1+\alpha_2)} f_4|_\beta \tilde{S} T^{5+8q}
\end{aligned}
$$

$$
\begin{aligned}
&+ \quad e^{2\pi i((1+q)\alpha_1+\alpha_2)} f_5|_\beta \tilde{S} T^{6+8q} \\
&+ \quad e^{2\pi i((1+q)\alpha_1+\alpha_2)} f_6|_\beta \tilde{S} T^{7+8q} \\
&+ \quad e^{2\pi i((1+q)\alpha_1+\alpha_2)} f_7|_\beta \tilde{S} T^{8+8q} \\
\left[\mathcal{L}^{\Gamma_0(8)}_{\beta,+1} \vec{f}\right]_6 = \sum_{q=0}^{\infty} \quad & e^{2\pi i((1+8q)\alpha_2)} f_{11}|_\beta \tilde{S} T^{1+8q} \\
&+ \quad e^{2\pi i((2+8q)\alpha_2)} f_{11}|_\beta \tilde{S} T^{2+8q} \\
&+ \quad e^{2\pi i((3+8q)\alpha_2)} f_{11}|_\beta \tilde{S} T^{3+8q} \\
&+ \quad e^{2\pi i((4+8q)\alpha_2)} f_{11}|_\beta \tilde{S} T^{4+8q} \\
&+ \quad e^{2\pi i((5+8q)\alpha_2)} f_{11}|_\beta \tilde{S} T^{5+8q} \\
&+ \quad e^{2\pi i((6+8q)\alpha_2)} f_{11}|_\beta \tilde{S} T^{6+8q} \\
&+ \quad e^{2\pi i((7+8q)\alpha_2)} f_{11}|_\beta \tilde{S} T^{7+8q} \\
&+ \quad e^{2\pi i((8+8q)\alpha_2)} f_{11}|_\beta \tilde{S} T^{8+8q} \\
\left[\mathcal{L}^{\Gamma_0(8)}_{\beta,+1} \vec{f}\right]_7 = \sum_{q=0}^{\infty} \quad & e^{2\pi i(q\alpha_1-\alpha_2)} f_6|_\beta \tilde{S} T^{1+8q} \\
&+ \quad e^{2\pi i(q\alpha_1-\alpha_2)} f_7|_\beta \tilde{S} T^{2+8q} \\
&+ \quad e^{2\pi i(q\alpha_1-\alpha_2)} f_8|_\beta \tilde{S} T^{3+8q} \\
&+ \quad e^{2\pi i(q\alpha_1-\alpha_2)} f_9|_\beta \tilde{S} T^{4+8q} \\
&+ \quad e^{2\pi i((1+q)\alpha_1-\alpha_2)} f_2|_\beta \tilde{S} T^{5+8q} \\
&+ \quad e^{2\pi i((1+q)\alpha_1-\alpha_2)} f_3|_\beta \tilde{S} T^{6+8q} \\
&+ \quad e^{2\pi i((1+q)\alpha_1-\alpha_2)} f_4|_\beta \tilde{S} T^{7+8q} \\
&+ \quad e^{2\pi i((1+q)\alpha_1-\alpha_2)} f_5|_\beta \tilde{S} T^{8+8q} \\
\left[\mathcal{L}^{\Gamma_0(8)}_{\beta,+1} \vec{f}\right]_8 = \sum_{q=0}^{\infty} \quad & e^{2\pi i(-4q\alpha_1+(-1-4q)\alpha_2-4q\alpha_3)} f_{10}|_\beta \tilde{S} T^{1+8q} \\
&+ \quad e^{2\pi i((-1-4q)\alpha_1+(-1-4q)\alpha_2+(-1-4q)\alpha_3)} f_{12}|_\beta \tilde{S} T^{2+8q} \\
&+ \quad e^{2\pi i((-1-4q)\alpha_1+(-2-4q)\alpha_2+(-1-4q)\alpha_3)} f_{10}|_\beta \tilde{S} T^{3+8q} \\
&+ \quad e^{2\pi i((-2-4q)\alpha_1+(-2-4q)\alpha_2+(-2-4q)\alpha_3)} f_{12}|_\beta \tilde{S} T^{4+8q} \\
&+ \quad e^{2\pi i((-2-4q)\alpha_1+(-3-4q)\alpha_2+(-2-4q)\alpha_3)} f_{10}|_\beta \tilde{S} T^{5+8q} \\
&+ \quad e^{2\pi i((-3-4q)\alpha_1+(-3-4q)\alpha_2+(-3-4q)\alpha_3)} f_{12}|_\beta \tilde{S} T^{6+8q}
\end{aligned}
$$

$$
\begin{aligned}
&+ \quad e^{2\pi i((-3-4q)\alpha_1+(-4-4q)\alpha_2+(-3-4q)\alpha_3)} f_{10}|_\beta \tilde{S} T^{7+8q} \\
&+ \quad e^{2\pi i((-4-4q)\alpha_1+(-4-4q)\alpha_2+(-4-4q)\alpha_3)} f_{12}|_\beta \tilde{S} T^{8+8q}
\end{aligned}
$$

$$
\begin{aligned}
\left[\mathcal{L}^{\Gamma_0(8)}_{\beta,+1} \vec{f}\right]_9 = \sum_{q=0}^{\infty} \quad & e^{2\pi i((1+q)\alpha_1+\alpha_3)} f_4|_\beta \tilde{S} T^{1+8q} \\
+ \quad & e^{2\pi i((1+q)\alpha_1+\alpha_3)} f_5|_\beta \tilde{S} T^{2+8q} \\
+ \quad & e^{2\pi i((1+q)\alpha_1+\alpha_3)} f_6|_\beta \tilde{S} T^{3+8q} \\
+ \quad & e^{2\pi i((1+q)\alpha_1+\alpha_3)} f_7|_\beta \tilde{S} T^{4+8q} \\
+ \quad & e^{2\pi i((1+q)\alpha_1+\alpha_3)} f_8|_\beta \tilde{S} T^{5+8q} \\
+ \quad & e^{2\pi i((1+q)\alpha_1+\alpha_3)} f_9|_\beta \tilde{S} T^{6+8q} \\
+ \quad & e^{2\pi i((2+q)\alpha_1+\alpha_3)} f_2|_\beta \tilde{S} T^{7+8q} \\
+ \quad & e^{2\pi i((2+q)\alpha_1+\alpha_3)} f_3|_\beta \tilde{S} T^{8+8q}
\end{aligned}
$$

$$
\begin{aligned}
\left[\mathcal{L}^{\Gamma_0(8)}_{\beta,+1} \vec{f}\right]_{10} = \sum_{q=0}^{\infty} \quad & e^{2\pi i(q\alpha_1)} f_5|_\beta \tilde{S} T^{1+8q} \\
+ \quad & e^{2\pi i(q\alpha_1)} f_6|_\beta \tilde{S} T^{2+8q} \\
+ \quad & e^{2\pi i(q\alpha_1)} f_7|_\beta \tilde{S} T^{3+8q} \\
+ \quad & e^{2\pi i(q\alpha_1)} f_8|_\beta \tilde{S} T^{4+8q} \\
+ \quad & e^{2\pi i(q\alpha_1)} f_9|_\beta \tilde{S} T^{5+8q} \\
+ \quad & e^{2\pi i((1+q)\alpha_1)} f_2|_\beta \tilde{S} T^{6+8q} \\
+ \quad & e^{2\pi i((1+q)\alpha_1)} f_3|_\beta \tilde{S} T^{7+8q} \\
+ \quad & e^{2\pi i((1+q)\alpha_1)} f_4|_\beta \tilde{S} T^{8+8q}
\end{aligned}
$$

$$
\begin{aligned}
\left[\mathcal{L}^{\Gamma_0(8)}_{\beta,+1} \vec{f}\right]_{11} = \sum_{q=0}^{\infty} \quad & e^{2\pi i(q\alpha_1)} f_7|_\beta \tilde{S} T^{1+8q} \\
+ \quad & e^{2\pi i(q\alpha_1)} f_8|_\beta \tilde{S} T^{2+8q} \\
+ \quad & e^{2\pi i(q\alpha_1)} f_9|_\beta \tilde{S} T^{3+8q} \\
+ \quad & e^{2\pi i((1+q)\alpha_1)} f_2|_\beta \tilde{S} T^{4+8q} \\
+ \quad & e^{2\pi i((1+q)\alpha_1)} f_3|_\beta \tilde{S} T^{5+8q} \\
+ \quad & e^{2\pi i((1+q)\alpha_1)} f_4|_\beta \tilde{S} T^{6+8q} \\
+ \quad & e^{2\pi i((1+q)\alpha_1)} f_5|_\beta \tilde{S} T^{7+8q}
\end{aligned}
$$

$$
\begin{aligned}
&+ && e^{2\pi i((1+q)\alpha_1)} f_6|_\beta \tilde{S} T^{8+8q} \\
\left[\mathcal{L}^{\Gamma_0(8)}_{\beta,+1} \vec{f}\right]_{12} &= \textstyle\sum_{q=0}^{\infty} && e^{2\pi i(q\alpha_1)} f_9|_\beta \tilde{S} T^{1+8q} \\
&+ && e^{2\pi i((1+q)\alpha_1)} f_2|_\beta \tilde{S} T^{2+8q} \\
&+ && e^{2\pi i((1+q)\alpha_1)} f_3|_\beta \tilde{S} T^{3+8q} \\
&+ && e^{2\pi i((1+q)\alpha_1)} f_4|_\beta \tilde{S} T^{4+8q} \\
&+ && e^{2\pi i((1+q)\alpha_1)} f_5|_\beta \tilde{S} T^{5+8q} \\
&+ && e^{2\pi i((1+q)\alpha_1)} f_6|_\beta \tilde{S} T^{6+8q} \\
&+ && e^{2\pi i((1+q)\alpha_1)} f_7|_\beta \tilde{S} T^{7+8q} \\
&+ && e^{2\pi i((1+q)\alpha_1)} f_8|_\beta \tilde{S} T^{8+8q} \\
\left[\mathcal{L}^{\Gamma_0(8)}_{\beta,-1} \vec{f}\right]_{1} &= \textstyle\sum_{q=0}^{\infty} && e^{2\pi i((-1-q)\alpha_1)} f_9|_\beta \tilde{S} T^{1+8q} \\
&+ && e^{2\pi i((-1-q)\alpha_1)} f_8|_\beta \tilde{S} T^{2+8q} \\
&+ && e^{2\pi i((-1-q)\alpha_1)} f_7|_\beta \tilde{S} T^{3+8q} \\
&+ && e^{2\pi i((-1-q)\alpha_1)} f_6|_\beta \tilde{S} T^{4+8q} \\
&+ && e^{2\pi i((-1-q)\alpha_1)} f_5|_\beta \tilde{S} T^{5+8q} \\
&+ && e^{2\pi i((-1-q)\alpha_1)} f_4|_\beta \tilde{S} T^{6+8q} \\
&+ && e^{2\pi i((-1-q)\alpha_1)} f_3|_\beta \tilde{S} T^{7+8q} \\
&+ && e^{2\pi i((-1-q)\alpha_1)} f_2|_\beta \tilde{S} T^{8+8q} \\
\left[\mathcal{L}^{\Gamma_0(8)}_{\beta,-1} \vec{f}\right]_{2} &= \textstyle\sum_{q=0}^{\infty} && e^{2\pi i((-1-8q)\alpha_3)} f_1|_\beta \tilde{S} T^{1+8q} \\
&+ && e^{2\pi i((-2-8q)\alpha_3)} f_1|_\beta \tilde{S} T^{2+8q} \\
&+ && e^{2\pi i((-3-8q)\alpha_3)} f_1|_\beta \tilde{S} T^{3+8q} \\
&+ && e^{2\pi i((-4-8q)\alpha_3)} f_1|_\beta \tilde{S} T^{4+8q} \\
&+ && e^{2\pi i((-5-8q)\alpha_3)} f_1|_\beta \tilde{S} T^{5+8q} \\
&+ && e^{2\pi i((-6-8q)\alpha_3)} f_1|_\beta \tilde{S} T^{6+8q} \\
&+ && e^{2\pi i((-7-8q)\alpha_3)} f_1|_\beta \tilde{S} T^{7+8q} \\
&+ && e^{2\pi i((-8-8q)\alpha_3)} f_1|_\beta \tilde{S} T^{8+8q}
\end{aligned}
$$

$$\begin{aligned}
\left[\mathcal{L}^{\Gamma_0(8)}_{\beta,-1}\vec{f}\right]_3 &= \sum_{q=0}^{\infty} && e^{2\pi i((-1-q)\alpha_1-\alpha_3)} f_8|_\beta \tilde{S} T^{1+8q} \\
&+ && e^{2\pi i((-1-q)\alpha_1-\alpha_3)} f_7|_\beta \tilde{S} T^{2+8q} \\
&+ && e^{2\pi i((-1-q)\alpha_1-\alpha_3)} f_6|_\beta \tilde{S} T^{3+8q} \\
&+ && e^{2\pi i((-1-q)\alpha_1-\alpha_3)} f_5|_\beta \tilde{S} T^{4+8q} \\
&+ && e^{2\pi i((-1-q)\alpha_1-\alpha_3)} f_4|_\beta \tilde{S} T^{5+8q} \\
&+ && e^{2\pi i((-1-q)\alpha_1-\alpha_3)} f_3|_\beta \tilde{S} T^{6+8q} \\
&+ && e^{2\pi i((-1-q)\alpha_1-\alpha_3)} f_2|_\beta \tilde{S} T^{7+8q} \\
&+ && e^{2\pi i((-2-q)\alpha_1-\alpha_3)} f_9|_\beta \tilde{S} T^{8+8q} \\
\left[\mathcal{L}^{\Gamma_0(8)}_{\beta,-1}\vec{f}\right]_4 &= \sum_{q=0}^{\infty} && e^{2\pi i(4q\alpha_1+(1+4q)\alpha_2+4q\alpha_3)} f_{12}|_\beta \tilde{S} T^{1+8q} \\
&+ && e^{2\pi i((1+4q)\alpha_1+(1+4q)\alpha_2+(1+4q)\alpha_3)} f_{10}|_\beta \tilde{S} T^{2+8q} \\
&+ && e^{2\pi i((1+4q)\alpha_1+(2+4q)\alpha_2+(1+4q)\alpha_3)} f_{12}|_\beta \tilde{S} T^{3+8q} \\
&+ && e^{2\pi i((2+4q)\alpha_1+(2+4q)\alpha_2+(2+4q)\alpha_3)} f_{10}|_\beta \tilde{S} T^{4+8q} \\
&+ && e^{2\pi i((2+4q)\alpha_1+(3+4q)\alpha_2+(2+4q)\alpha_3)} f_{12}|_\beta \tilde{S} T^{5+8q} \\
&+ && e^{2\pi i((3+4q)\alpha_1+(3+4q)\alpha_2+(3+4q)\alpha_3)} f_{10}|_\beta \tilde{S} T^{6+8q} \\
&+ && e^{2\pi i((3+4q)\alpha_1+(4+4q)\alpha_2+(3+4q)\alpha_3)} f_{12}|_\beta \tilde{S} T^{7+8q} \\
&+ && e^{2\pi i((4+4q)\alpha_1+(4+4q)\alpha_2+(4+4q)\alpha_3)} f_{10}|_\beta \tilde{S} T^{8+8q} \\
\left[\mathcal{L}^{\Gamma_0(8)}_{\beta,-1}\vec{f}\right]_5 &= \sum_{q=0}^{\infty} && e^{2\pi i(-q\alpha_1+\alpha_2)} f_6|_\beta \tilde{S} T^{1+8q} \\
&+ && e^{2\pi i(-q\alpha_1+\alpha_2)} f_5|_\beta \tilde{S} T^{2+8q} \\
&+ && e^{2\pi i(-q\alpha_1+\alpha_2)} f_4|_\beta \tilde{S} T^{3+8q} \\
&+ && e^{2\pi i(-q\alpha_1+\alpha_2)} f_3|_\beta \tilde{S} T^{4+8q} \\
&+ && e^{2\pi i(-q\alpha_1+\alpha_2)} f_2|_\beta \tilde{S} T^{5+8q} \\
&+ && e^{2\pi i((-1-q)\alpha_1+\alpha_2)} f_9|_\beta \tilde{S} T^{6+8q} \\
&+ && e^{2\pi i((-1-q)\alpha_1+\alpha_2)} f_8|_\beta \tilde{S} T^{7+8q} \\
&+ && e^{2\pi i((-1-q)\alpha_1+\alpha_2)} f_7|_\beta \tilde{S} T^{8+8q} \\
\left[\mathcal{L}^{\Gamma_0(8)}_{\beta,-1}\vec{f}\right]_6 &= \sum_{q=0}^{\infty} && e^{2\pi i((-1-8q)\alpha_2)} f_{11}|_\beta \tilde{S} T^{1+8q}
\end{aligned}$$

$$
\begin{aligned}
&+ && e^{2\pi i((-2-8q)\alpha_2)} f_{11}|_\beta \tilde{S} T^{2+8q} \\
&+ && e^{2\pi i((-3-8q)\alpha_2)} f_{11}|_\beta \tilde{S} T^{3+8q} \\
&+ && e^{2\pi i((-4-8q)\alpha_2)} f_{11}|_\beta \tilde{S} T^{4+8q} \\
&+ && e^{2\pi i((-5-8q)\alpha_2)} f_{11}|_\beta \tilde{S} T^{5+8q} \\
&+ && e^{2\pi i((-6-8q)\alpha_2)} f_{11}|_\beta \tilde{S} T^{6+8q} \\
&+ && e^{2\pi i((-7-8q)\alpha_2)} f_{11}|_\beta \tilde{S} T^{7+8q} \\
&+ && e^{2\pi i((-8-8q)\alpha_2)} f_{11}|_\beta \tilde{S} T^{8+8q} \\
\left[\mathcal{L}^{\Gamma_0(8)}_{\beta,-1} \vec{f}\right]_7 &= \textstyle\sum_{q=0}^{\infty} && e^{2\pi i(-q\alpha_1-\alpha_2)} f_4|_\beta \tilde{S} T^{1+8q} \\
&+ && e^{2\pi i(-q\alpha_1-\alpha_2)} f_3|_\beta \tilde{S} T^{2+8q} \\
&+ && e^{2\pi i(-q\alpha_1-\alpha_2)} f_2|_\beta \tilde{S} T^{3+8q} \\
&+ && e^{2\pi i((-1-q)\alpha_1-\alpha_2)} f_9|_\beta \tilde{S} T^{4+8q} \\
&+ && e^{2\pi i((-1-q)\alpha_1-\alpha_2)} f_8|_\beta \tilde{S} T^{5+8q} \\
&+ && e^{2\pi i((-1-q)\alpha_1-\alpha_2)} f_7|_\beta \tilde{S} T^{6+8q} \\
&+ && e^{2\pi i((-1-q)\alpha_1-\alpha_2)} f_6|_\beta \tilde{S} T^{7+8q} \\
&+ && e^{2\pi i((-1-q)\alpha_1-\alpha_2)} f_5|_\beta \tilde{S} T^{8+8q} \\
\left[\mathcal{L}^{\Gamma_0(8)}_{\beta,-1} \vec{f}\right]_8 &= \textstyle\sum_{q=0}^{\infty} && e^{2\pi i((1+4q)\alpha_1+4q\alpha_2+(1+4q)\alpha_3)} f_{10}|_\beta \tilde{S} T^{1+8q} \\
&+ && e^{2\pi i((1+4q)\alpha_1+(1+4q)\alpha_2+(1+4q)\alpha_3)} f_{12}|_\beta \tilde{S} T^{2+8q} \\
&+ && e^{2\pi i((2+4q)\alpha_1+(1+4q)\alpha_2+(2+4q)\alpha_3)} f_{10}|_\beta \tilde{S} T^{3+8q} \\
&+ && e^{2\pi i((2+4q)\alpha_1+(2+4q)\alpha_2+(2+4q)\alpha_3)} f_{12}|_\beta \tilde{S} T^{4+8q} \\
&+ && e^{2\pi i((3+4q)\alpha_1+(2+4q)\alpha_2+(3+4q)\alpha_3)} f_{10}|_\beta \tilde{S} T^{5+8q} \\
&+ && e^{2\pi i((3+4q)\alpha_1+(3+4q)\alpha_2+(3+4q)\alpha_3)} f_{12}|_\beta \tilde{S} T^{6+8q} \\
&+ && e^{2\pi i((4+4q)\alpha_1+(3+4q)\alpha_2+(4+4q)\alpha_3)} f_{10}|_\beta \tilde{S} T^{7+8q} \\
&+ && e^{2\pi i((4+4q)\alpha_1+(4+4q)\alpha_2+(4+4q)\alpha_3)} f_{12}|_\beta \tilde{S} T^{8+8q} \\
\left[\mathcal{L}^{\Gamma_0(8)}_{\beta,-1} \vec{f}\right]_9 &= \textstyle\sum_{q=0}^{\infty} && e^{2\pi i((1-q)\alpha_1+\alpha_3)} f_2|_\beta \tilde{S} T^{1+8q} \\
&+ && e^{2\pi i(-q\alpha_1+\alpha_3)} f_9|_\beta \tilde{S} T^{2+8q}
\end{aligned}
$$

$$
\begin{aligned}
&+ && e^{2\pi i(-q\alpha_1+\alpha_3)} f_8|_\beta \tilde{S} T^{3+8q}\\
&+ && e^{2\pi i(-q\alpha_1+\alpha_3)} f_7|_\beta \tilde{S} T^{4+8q}\\
&+ && e^{2\pi i(-q\alpha_1+\alpha_3)} f_6|_\beta \tilde{S} T^{5+8q}\\
&+ && e^{2\pi i(-q\alpha_1+\alpha_3)} f_5|_\beta \tilde{S} T^{6+8q}\\
&+ && e^{2\pi i(-q\alpha_1+\alpha_3)} f_4|_\beta \tilde{S} T^{7+8q}\\
&+ && e^{2\pi i(-q\alpha_1+\alpha_3)} f_3|_\beta \tilde{S} T^{8+8q}\\
\left[\mathcal{L}^{\Gamma_0(8)}_{\beta,-1} \vec{f}\right]_{10} &= \textstyle\sum_{q=0}^{\infty} && e^{2\pi i(-q\alpha_1)} f_3|_\beta \tilde{S} T^{1+8q}\\
&+ && e^{2\pi i(-q\alpha_1)} f_2|_\beta \tilde{S} T^{2+8q}\\
&+ && e^{2\pi i((-1-q)\alpha_1)} f_9|_\beta \tilde{S} T^{3+8q}\\
&+ && e^{2\pi i((-1-q)\alpha_1)} f_8|_\beta \tilde{S} T^{4+8q}\\
&+ && e^{2\pi i((-1-q)\alpha_1)} f_7|_\beta \tilde{S} T^{5+8q}\\
&+ && e^{2\pi i((-1-q)\alpha_1)} f_6|_\beta \tilde{S} T^{6+8q}\\
&+ && e^{2\pi i((-1-q)\alpha_1)} f_5|_\beta \tilde{S} T^{7+8q}\\
&+ && e^{2\pi i((-1-q)\alpha_1)} f_4|_\beta \tilde{S} T^{8+8q}\\
\left[\mathcal{L}^{\Gamma_0(8)}_{\beta,-1} \vec{f}\right]_{11} &= \textstyle\sum_{q=0}^{\infty} && e^{2\pi i(-q\alpha_1)} f_5|_\beta \tilde{S} T^{1+8q}\\
&+ && e^{2\pi i(-q\alpha_1)} f_4|_\beta \tilde{S} T^{2+8q}\\
&+ && e^{2\pi i(-q\alpha_1)} f_3|_\beta \tilde{S} T^{3+8q}\\
&+ && e^{2\pi i(-q\alpha_1)} f_2|_\beta \tilde{S} T^{4+8q}\\
&+ && e^{2\pi i((-1-q)\alpha_1)} f_9|_\beta \tilde{S} T^{5+8q}\\
&+ && e^{2\pi i((-1-q)\alpha_1)} f_8|_\beta \tilde{S} T^{6+8q}\\
&+ && e^{2\pi i((-1-q)\alpha_1)} f_7|_\beta \tilde{S} T^{7+8q}\\
&+ && e^{2\pi i((-1-q)\alpha_1)} f_6|_\beta \tilde{S} T^{8+8q}\\
\left[\mathcal{L}^{\Gamma_0(8)}_{\beta,-1} \vec{f}\right]_{12} &= \textstyle\sum_{q=0}^{\infty} && e^{2\pi i(-q\alpha_1)} f_7|_\beta \tilde{S} T^{1+8q}\\
&+ && e^{2\pi i(-q\alpha_1)} f_6|_\beta \tilde{S} T^{2+8q}\\
&+ && e^{2\pi i(-q\alpha_1)} f_5|_\beta \tilde{S} T^{3+8q}
\end{aligned}
$$

$$+ \quad e^{2\pi i(-q\alpha_1)} f_4|_\beta \tilde{S} T^{4+8q}$$

$$+ \quad e^{2\pi i(-q\alpha_1)} f_3|_\beta \tilde{S} T^{5+8q}$$

$$+ \quad e^{2\pi i(-q\alpha_1)} f_2|_\beta \tilde{S} T^{6+8q}$$

$$+ \quad e^{2\pi i((-1-q)\alpha_1)} f_9|_\beta \tilde{S} T^{7+8q}$$

$$+ \quad e^{2\pi i((-1-q)\alpha_1)} f_8|_\beta \tilde{S} T^{8+8q}$$

i	1	2	3	4	5	6	7	8	9	10	11	12
$p_1(i)$	1	2	9	8	7	6	5	4	3	12	11	10

i	1	2	3	4	5	6	7	8	9	10	11	12
$p_2(i)$	11	6	5	4	3	2	9	8	7	10	1	12

The symmetries $\mathcal{P}_1$ and $\mathcal{P}_2$ commute since $p_1 \circ p_2(i) = p_2 \circ p_1(i)$ for $1 \leq i \leq 12$.

Appendix D

The zeros and poles of the Selberg zeta function for arithmetic $(\Gamma_0(4), \chi_\alpha^{(4)})$ and arithmetic $(\Gamma_0(8), \chi_\alpha^{(8)})$

The zeros and poles of the Selberg zeta function $Z^{(4)}(\beta, \chi_\alpha^{(4)})$ for arithmetic $(\Gamma_0(4), \chi_\alpha^{(4)})$, $\alpha \in \{0, \frac{1}{8}, \frac{2}{8}, \frac{3}{8}, \frac{4}{8}\}$, in the region $0 \leq \Re\beta \leq 1$ and $0 \leq \Im\beta \leq 10$ are listed in Tables D.1 - D.5. Furthermore, the zeros and poles on the critical line $\Re\beta = \frac{1}{2}$ with $0 < \Im\beta \leq 10$ for arithmetic $(\Gamma_0(8), \chi_\alpha^{(8)})$, $\alpha \in \{0, \frac{1}{2}\}$, are given in Tables D.6 and D.7. The Selberg zeta function $Z^{(n)}(\beta, \chi)$ can be expressed by the Fredholm determinant of the transfer operator $\mathcal{L}_{\beta,\varepsilon,\chi}^{(n)}$ given in section 7.4:

$$Z^{(n)}(\beta, \chi) = \det\left(1 - \mathcal{L}_{\beta,+1,\chi}^{(n)} \mathcal{L}_{\beta,-1,\chi}^{(n)}\right) = \det\left(1 - \mathcal{L}_{\beta,-1,\chi}^{(n)} \mathcal{L}_{\beta,+1,\chi}^{(n)}\right).$$

Using the operators $\mathcal{P}_k$ introduced in section 8.1.3 $Z^{(n)}(\beta, \chi)$ can be written as

$$Z^{(n)}(\beta, \chi) = \det\left(1 - \mathcal{P}_k \mathcal{L}_{\beta,\varepsilon,\chi}^{(n)}\right) \det\left(1 + \mathcal{P}_k \mathcal{L}_{\beta,\varepsilon,\chi}^{(n)}\right).$$

Obviously the zeros of the Selberg zeta function can therefore be related to eigenvalues ± 1 of the operator $\mathcal{P}_k \mathcal{L}_{\beta,\varepsilon,\chi}^{(n)}$. To determine the spectrum of the transfer operator we approximate it by the matrix $\mathcal{M}_{\beta,\varepsilon,\chi}^{(n)}$ in proposition 7.4.11 and its spectrum. The zeros of the Selberg zeta function were determined in the β-plane for fixed values of α by the Newton method described in section 2.5. We verified the zeros and poles using the argument principle. For this, we evaluated the Selberg zeta function at certain points on the contour of a square with side length 10^{-4} and centered around a zero or pole, where the distance between the computed points was $5 \cdot 10^{-6}$. Then the argument principle is given by the change of the argument of the Selberg zeta function along these points.

The following information is included in the table:

- $\Re\beta$ and $\Im\beta$ denote the real, respectively imaginary part of a zero or a pole of the Selberg zeta function $Z^{(n)}(\beta, \chi_\alpha^{(n)})$.
- The value of α for which this zero or pole was found.
- #+1 respectively #-1 denote the number of $+1$ respectively -1 eigenvalues of the corresponding transfer operator for this zero of the Selberg zeta function. A value in brackets indicates that we computed the spectrum of the approximating matrix for $\beta' = \beta + 10^{-5}$, where β is the corresponding pole or zero of the Selberg zeta function.

- AP denotes the result derived from the argument principle around this zero or pole. A positive value, respectively negative value indicates the multiplicity of a zero respectively a pole.
- $Z^{(n)}(\beta, \chi_\alpha^{(n)})$ is the numerical value of the Selberg zeta function obtained from the last iteration of Newtons method when determining this zero.
- p denotes the number of bits used for the representation of numbers on the computer during the computations.
- N denotes the number of Taylor coefficients used in the approximating matrix $\mathcal{M}_{\beta,\varepsilon,\chi}^{(n)}$.
- DF denotes the name of the file which contains this zero. These files contain β values of a zero for $0 \leq \alpha \leq 0.5$. See section 8.2.1 for details.
- $\alpha' = \frac{x}{8}$ with $x \in \{0, 1, 2, 3, 4\}$ and $\chi_{\alpha'}^{(n)}$ denotes the values for which the corresponding zero, respectively pole exists. Note that the zeros, respectively poles may have a different multiplicity for different α'.
- T denotes the type of convergence for $\alpha \to 0$ to this zero: "L" indicates an Infinite Resonance-Eigenvalue Convergence (see conclusion 8.2.28), and "C" indicates an Infinite Avoided Crossings sequence (see conclusion 8.2.17).
- O denotes the order of contact of this zero for $\alpha \neq 0$ with the critical line $\Re\beta = \frac{1}{2}$, see (8.32). If the zero stays on the critical line we indicate this by the letter "E".

Table D.1: The zeros and poles of $Z^{(4)}(\beta,\chi_\alpha^{(4)})$ with $0 \le \Re\beta \le 1$, $0 \le \Im\beta \le 10$ and $\alpha = 0$

$\Re\beta$	$\Im\beta$	α	$\mathcal{P}_2\mathcal{L}^{(4)}_{\beta,+1,\alpha}$ #+1	#-1	AP	$Z^{(4)}(\beta,\chi_\alpha^{(4)})$	p	N	DF	$\alpha' = \frac{x}{8}$	T	$\mathcal{L}^{(4)}_{\beta,+1,\alpha}\mathcal{L}^{(4)}_{\beta,-1,\alpha}$ #+1	$\mathcal{L}^{(4)}_{\beta,+1,\alpha}$ #+1	#-1	$\mathcal{P}_1\mathcal{L}^{(4)}_{\beta,+1,\alpha}$ #+1	#-1
0	0	0	(3)	(2)	1	-	160	50		0,1,2,3,4		(5)	(3)	(2)	(3)	(2)
0	4.532360141827193809	0	1	1	2	-4E-41-6E-41I	192	70	(P13)	0,2,4		2	1	1	2	
0	9.064720283654387634	0	1	1	2	1E-47+2E-48I	192	70	(P14)	0,2,4		2	1	1	2	
1/4	7.067362570867346896	0	2	1	3	-9E-42-5E-42I	160	50	S27	0,2,4		3	2	1	3	
1/2	0	0	(1)	(2)	-3	-	160	50		0,2,3,4		(3)	(1)	(2)		(3)
1/2	3.703307801219027665	0	1		1	3E-47-1E-46I	160	50	S2	0,2,4	L	1	1			1
1/2	5.417334806844678385	0	1	1	2	3E-41+1E-41I	160	50	S14	0,2,4	LC	2	1	1		2
1/2	5.879354157758601464	0		1	1	1E-44+6E-44I	160	50	(P1)	0,2,4	C	1		1	1	
1/2	6.620422873842205998	0	1		1	1E-42+6E-43I	160	50	S21	0,2,4	L	1	1			1
1/2	7.220871975958052161	0	1	1	2	-1E-49+1E-49I	160	50	S42	0,2,4	LC	2	1	1		2
1/2	8.042477591683672004	0		1	1	-3E-41-6E-41I	160	50	(P2)	0,2,4	C	1		1	1	
1/2	8.273665889586057109	0	1	1	2	1E-45-1E-45I	160	50	S33	0,2,4	LC	2	1	1		2
1/2	8.522503016868544791	0	1		1	-4E-41+2E-41I	160	50	S39	0,2,4	L	1	1			1
1/2	8.922876486991967371	0	1	1	2	-1E-50+4E-50I	160	50	(P3)	0,2,4	C	2	1	1	2	
1/2	9.533695261353561224	0	1	2	3	-9E-42-3E-41I	192	70	(P4)	0,2,4		3	1	2		3
1/2	9.859896162238452828	0		1	1	-1E-48+9E-49I	192	70	(P5)	0,2,4		1		1	1	
1/2	9.934919959369116405	0	1		1	-5E-46+2E-45I	192	70	(P6)	0,2,4		1	1			1
1	0	0	1		1	-1E-45-2E-58I	160	50	S37	0		1	1		1	

Table D.2: The zeros and poles of $Z^{(4)}(\beta, \chi_\alpha^{(4)})$ with $0 \le \Re\beta \le 1$, $0 \le \Im\beta \le 10$ and $\alpha = 1/8$

$\Re\beta$	$\Im\beta$	α	$\mathcal{P}_2\mathcal{L}^{(4)}_{\beta,+1,\alpha}$ #+1	#-1	AP	$Z^{(4)}(\beta, \chi_\alpha^{(4)})$	p	N	DF	$\alpha' = \frac{x}{8}$	O
0	0	1/8	(1)	(1)	1	-	160	50		0,1,2,3,4	
1/4	2.449986998503518252	1/8	1		1	2E-43-2E-43I	160	50	S6	1,3	
1/4	3.814214420884698858	1/8	1		1	-7E-42-8E-42I	160	50	S7	1,3	
1/4	5.403294081930856007	1/8	1		1	1E-48+3E-52I	192	70	S1-1	1,3	
1/4	6.155271497118264841	1/8	1		1	2E-48+2E-50I	192	70	S3	1,3	
1/4	7.597877125322561389	1/8	1		1	2E-46-1E-46I	192	70	S11	1,3	
1/4	8.511142987154173628	1/8	1		1	-2E-45-2E-45I	192	70	S42	1,3	
1/4	9.402979453853571250	1/8	1		1	-6E-44+1E-43I	192	70	S43	1,3	
1/2	0	1/8	(1)	(1)	0	-	160	50	(S37)		
1/2	1.782213978191369112	1/8		1	1	-7E-44-8E-45I	160	50	S5	1	E
1/2	2.946441970575437918	1/8		1	1	7E-43-8E-43I	160	50	S4-2	1,3	E
1/2	3.564427956382738234	1/8	1		1	8E-46-1E-46I	160	50	S8	1	2
1/2	3.879328713546061516	1/8		1	1	2E-42+1E-42I	160	50	S9	1,3	E
1/2	4.527220808156573476	1/8		1	1	-8E-46+3E-45I	160	50	S10	1,3	E
1/2	4.590429629234487105	1/8	1		1	-5E-45-5E-45I	160	50	S2	1,3	2
1/2	5.126324398828679926	1/8		1	1	-1E-44-1E-43I	160	50	S12	1,3	E
1/2	5.346641934574103869	1/8		1	1	5E-44-3E-44I	160	50	S13	1	E
1/2	5.462015080446370362	1/8	1		1	1E-41-5E-42I	160	50	S14	1,3	2
1/2	5.991432640140732809	1/8		1	1	4E-43+2E-44I	160	50	S15	1,3	E
1/2	6.078238108570858251	1/8		1	1	-4E-41+6E-41I	160	50	S18	1,3	E
1/2	6.391958602015716352	1/8	1		1	-2E-42-3E-43I	160	50	S16	1,3	2
1/2	6.698857003565354647	1/8		1	1	-4E-42+7E-42I	160	50	S17	1,3	E
1/2	6.870505381182096125	1/8	1		1	-1E-51+4E-52I	192	70	S19	1,3	2
1/2	6.992646678257929964	1/8		1	1	2E-42+7E-43I	192	70	S20	1,3	E
1/2	7.128855912765476448	1/8	1		1	1E-51-1E-51I	192	70	S21	1	2
1/2	7.360734345217853149	1/8		1	1	9E-52+2E-51I	192	70	S22	1,3	E
1/2	7.542485324108996653	1/8	1		1	6E-47-1E-45I	192	70	S23	1,3	2
1/2	7.794134053288051745	1/8		1	1	-2E-49+1E-49I	192	70	S24	1,3	E
1/2	7.819671962802205995	1/8		1	1	-1E-49+4E-49I	192	70	S25	1,3	E
1/2	8.141853572885032452	1/8	1		1	6E-46+2E-47I	192	70	S26	1,3	2
1/2	8.312638564688989946	1/8	1		1	-2E-41+7E-42I	192	70	S27	1,3	2
1/2	8.447199030243931547	1/8		1	1	-1E-49+5E-49	192	70	S28	1,3	E
1/2	8.479324427814975479	1/8		1	1	-4E-50-1E-50I	192	70	S30	1,3	E
1/2	8.911069890956845407	1/8		1	1	8E-43+4E-42I	192	70	S31	1	E
1/2	8.939925305864625431	1/8		1	1	-1E-45-2E-47I	192	70	S32	1,3	E
1/2	8.997747473708370012	1/8	1		1	-1E-49+5E-50I	192	70	S33	1,3	2
1/2	9.090290630504841981	1/8	1		1	-4E-49-1E-49I	192	70	S34	1,3	2
1/2	9.252661337903369108	1/8		1	1	-3E-49+3E-48I	192	70	S35	1,3	E
1/2	9.521284422337261783	1/8		1	1	-2E-48-6E-48I	192	70	S36	1,3	E
1/2	9.682096277368199221	1/8	1		1	-1E-49+2E-49I	192	70	S38	1,3	2
1/2	9.684932577050462800	1/8		1	1	1E-49+2E-49I	192	70	S40	1,3	E
1/2	9.801070122016401792	1/8	1		1	-8E-48+2E-47I	192	70	S39	1,3	2
1/2	10.072369378536320625	1/8		1	1	-2E-47-3E-47I	192	70	S44		E
1/2	10.204038419612264408	1/8		1	1	1E-48-4E-50I	192	70	S45		E
1/2	10.206479022778734443	1/8	1		1	1E-48+2E-49I	192	70	S46		2
1/2	10.394868513015148678	1/8	1		1	-1E-48+2E-49I	192	70	(P7)		
1/2	10.438414941339101440	1/8		1	1	-2E-47+7E-48I	192	70	(P8)		
1/2	10.647378684127939622	1/8		1	1	4E-46+6E-45I	192	70	(P9)		
1/2	10.693283869148149258	1/8	1		1	-2E-47-1E-48I	192	70	(P10)		
1/2	10.877871155967807921	1/8	1		1	1E-46+2E-46I	192	70	(P11)		
1/2	10.949493302792528271	1/8		1	1	-1E-46-3E-46I	192	70	(P12)		

Table D.3: The zeros and poles of $Z^{(4)}(\beta, \chi_\alpha^{(4)})$ with $0 \leq \Re\beta \leq 1$, $0 \leq \Im\beta \leq 10$ and $\alpha = 2/8$

$\Re\beta$	$\Im\beta$	α	$\mathcal{P}_2\mathcal{L}^{(4)}_{\beta,+1,\alpha}$ #+1	#-1	AP	$Z^{(4)}(\beta, \chi_\alpha^{(4)})$	p	N	DF	$\alpha' = \frac{\gamma}{8}$	O
0	0	2/8	(1)	(1)	1	-	160	50		0,1,2,3,4	
0	4.532360141827193749	2/8	1		1	5E-41+1E-41I	160	50	S8	0,2,4	
0	9.064720283654387634	2/8	1		1	-1E-37+3E-37I	192	70	S34	0,2,4	
1/4	7.067362570867346895	2/8	1		1	-5E-48-2E-48I	192	70	S16	0,2,4	
1/4	10.511019819385790636	2/8	1		1	7E-42-4E-42I	192	70	S46		
1/2	0	2/8		(1)	-1	-	160	50		0,2,3,4	
1/2	2.425056827091418202	2/8		1	1	-1E-47+2E-48I	160	50	S5	2,4	E
1/2	3.249976963537702231	2/8	1		1	1E-46+8E-47I	160	50	S6	2,4	2
1/2	3.703307801219027665	2/8		1	1	-5E-46-5E-46I	160	50	S4-2	0,2,4	E
1/2	4.368019540226407989	2/8		1	1	2E-46+3E-47I	160	50	S9	2,4	E
1/2	4.646591642961023179	2/8	1		1	6E-46-3E-45I	160	50	S7	2,4	2
1/2	4.947831677133491175	2/8		1	1	1E-44+5E-45I	160	50	S10	2,4	E
1/2	5.417334806844680152	2/8		1	1	-9E-44+9E-45I	160	50	S12	0,2,4	E
1/2	5.628120929419301028	2/8	1		1	-7E-44-3E-44I	160	50	S2	2,4	2
1/2	5.879354157758601464	2/8	1		1	3E-44+1E-43I	160	50	S14	0,2,4	2
1/2	6.223180825323994226	2/8		1	1	-3E-43+1E-43I	160	50	S13	2,4	E
1/2	6.325314061989612026	2/8		1	1	-6E-45-1E-43I	160	50	S15	2,4	E
1/2	6.587692853147737071	2/8	1		1	8E-44-5E-43I	160	50	S3	2,4	2
1/2	6.620422873842205998	2/8		1	1	3E-43-1E-43I	160	50	S18	0,2,4	E
1/2	7.220871975958791160	2/8		1	1	7E-42-7E-41I	160	50	S17	0,2,4	E
1/2	7.226569067061128031	2/8	1		1	4E-44-2E-43I	160	50	S19	2,4	2
1/2	7.483018117504385669	2/8		1	1	1E-43-1E-41I	160	50	S20	2,4	E
1/2	7.696847806432627715	2/8	1		1	-1E-42+4E-42I	160	50	S21	2,4	2
1/2	7.744447737020311651	2/8		1	1	-9E-43-1E-41I	160	50	S22	2,4	E
1/2	8.042477591691602154	2/8	1		1	-1E-50-3E-50I	192	70	S11	0,2,4	2
1/2	8.211711182460681491	2/8	1		1	-4E-46-2E-47I	192	70	S23	2,4	2
1/2	8.273665889586095522	2/8		1	1	4E-51+1E-50I	192	70	S24	0,2,4	E
1/2	8.522503016868544791	2/8		1	1	-2E-41-9E-41I	160	50	S25	0,2,4	E
1/2	8.552880329050080905	2/8		1	1	2E-51-1E-50I	192	70	S28	2,4	E
1/2	8.922876486991746922	2/8	1		1	6E-50-1E-49I	192	70	S26	0,2,4	2
1/2	9.001205809650663151	2/8		1	1	-1E-51-1E-50I	192	70	S30	2,4	E
1/2	9.013228492064441121	2/8	1		1	1E-51+2E-50I	192	70	S42	2,4	2
1/2	9.196526852556367326	2/8		1	1	6E-49-5E-49I	192	70	S31	2,4	E
1/2	9.470083134201299174	2/8	1		1	4E-43-4E-43I	192	70	S33	2,4	2
1/2	9.533695261353557372	2/8		1	1	-3E-48+3E-48I	192	70	S32	0,2,4	E
1/2	9.810018121325218118	2/8		1	1	-7E-50+1E-49I	192	70	S35	2,4	E
1/2	9.859896162238452828	2/8	1		1	1E-42+5E-43I	192	70	S43	0,2,4	2
1/2	9.903977703803958939	2/8	1		1	-4E-50-9E-50I	192	70	S38	2,4	2
1/2	9.934919959369116405	2/8		1	1	-2E-49+4E-49I	192	70	S36	0,2,4	E
1/2	10.261814252511740214	2/8		1	1	-2E-48-2E-48I	192	70	S40		E
1/2	10.265915116762014474	2/8	1		1	7E-49-7E-49I	192	70	S39		2
1/2	10.538808057912809353	2/8		1	1	2E-47-1E-47I	192	70	S44		E
1/2	10.712706900697778989	2/8		1	1	-5E-48-1E-48I	192	70	S45		E

Table D.4: The zeros and poles of $Z^{(4)}(\beta, \chi_\alpha^{(4)})$ with $0 \le \Re\beta \le 1$, $0 \le \Im\beta \le 10$ and $\alpha = 3/8$

$\Re\beta$	$\Im\beta$	α	$\mathcal{P}_2\mathcal{L}^{(4)}_{\beta,+1,\alpha}$ #+1	#-1	AP	$Z^{(4)}(\beta, \chi_\alpha^{(4)})$	p	N	DF	$\alpha' = \frac{\alpha}{8}$	O
0	0	3/8	(1)	(1)	1	-	160	50		0,1,2,3,4	
1/4	2.449986998503518251	3/8	1		1	-2E-53+6E-53I	192	70	S29	1,3	
1/4	3.814214420884698917	3/8	1		1	3E-42-1E-41I	160	50	S6	1,3	
1/4	5.403294081930856007	3/8	1		1	-4E-47+5E-48I	192	70	S2	1,3	
1/4	6.155271497118264841	3/8	1		1	1E-48+2E49I	192	70	S41	1,3	
1/4	7.597877125322561384	3/8	1		1	7E-46+2E-46I	192	70	S19	1,3	
1/4	8.511142987154173669	3/8	1		1	-2E-46+2E-45I	192	70	S34	1,3	
1/4	9.402979453853574191	3/8	1		1	-1E-46+4E-45I	192	70	S42	1,3	
1/4	10.565822981110667270	3/8	1		1	-1E-42-1E-42I	192	70	S46		
1/2	0	3/8		(1)	-1	-	160	50			
1/2	2.946441970575437918	3/8		1	1	-7E-44+1E-43I	160	50	S5	1,3	E
1/2	3.879328713546061546	3/8		1	1	1E-42-1E-42I	160	50	S4-2	1,3	E
1/2	4.527220808156574058	3/8		1	1	-1E-46-1E-46I	160	50	S9	1,3	E
1/2	4.590429629234487405	3/8	1		1	2E-46+1E-45I	160	50	S8	1,3	2
1/2	5.126324398828679789	3/8		1	1	-4E-45+5E-45I	160	50	S10	1,3	E
1/2	5.462015080446355425	3/8	1		1	-5E-41+5E-41I	160	50	S7	1,3	2
1/2	5.991432640140644578	3/8		1	1	2E-41+5E-42I	160	50	S12	1,3	E
1/2	6.078238108570872078	3/8		1	1	-1E-41+3E-41I	160	50	S13	1,3	E
1/2	6.391958602016011556	3/8	1		1	8E-41+4E-41I	160	50	S14	1,3	2
1/2	6.698857003563950799	3/8		1	1	1E-43+1E-42I	160	50	S15	1,3	E
1/2	6.870503811821015 33	3/8	1		1	2E-43+2E-43I	160	50	S3	1,3	2
1/2	6.992646678257876321	3/8		1	1	-1E-42+2E-42I	160	50	S18	1,3	E
1/2	7.360734345217754475	3/8		1	1	7E-42-5E-42I	160	50	S17	1,3	E
1/2	7.542485324108996652	3/8	1		1	-3E-50+5E-50I	192	70	S16	1,3	2
1/2	7.794134053288051735	3/8		1	1	-1E-50-1E-50I	192	70	S20	1,3	E
1/2	7.819671962801902589	3/8		1	1	1E-41+8E-42I	160	50	S22	1,3	E
1/2	8.141853572885032463	3/8	1		1	-2E-49-2E-49I	192	70	S21	1,3	2
1/2	8.312638564688989949	3/8	1		1	-1E-47-1E-46I	192	70	S11	1,3	2
1/2	8.447199030243931489	3/8		1	1	4E-41-1E-41I	192	70	S24	1,3	E
1/2	8.479324427813371146	3/8		1	1	1E-41-3E-42I	160	50	S25	1,3	E
1/2	8.939925305864625388	3/8		1	1	3E-43+1E-43I	192	70	S28	1,3	E
1/2	8.997747473708370016	3/8	1		1	1E-49-7E-49I	192	70	S23	1,3	2
1/2	9.090290630504841927	3/8	1		1	-6E-50+4E-50I	192	70	S26	1,3	2
1/2	9.252661337903368494	3/8		1	1	-4E-41-7E-41I	192	70	S30	1,3	E
1/2	9.521284422337264263	3/8		1	1	8E-49+1E-48I	192	70	S31	1,3	E
1/2	9.682096277368197537	3/8	1		1	1E-50+7E-51I	192	70	S33	1,3	2
1/2	9.684932577050463673	3/8		1	1	-1E-49+5E-50I	192	70	S32	1,3	E
1/2	9.801070122016401727	3/8	1		1	-7E-48+5E-48I	192	70	S43	1,3	2
1/2	10.072369378536331299	3/8		1	1	-1E-48-5E-49I	192	70	S35		E
1/2	10.204038419612279107	3/8		1	1	5E-50+2E-50I	192	70	S36		E
1/2	10.206479022778743101	3/8	1		1	5E-50+2E-51I	192	70	S38		2
1/2	10.394868513015151137	3/8	1		1	-3E-48-4E-49I	192	70	S39		2
1/2	10.438414941339094626	3/8		1	1	-2E-48+6E-49I	192	70	S40		E
1/2	10.647378684127942490	3/8		1	1	-6E-47-4E-47I	192	70	S44		E
1/2	10.949493302792630531	3/8		1	1	2E-48+1E-47I	192	70	S45		E

Table D.5: The zeros and poles of $Z^{(4)}(\beta,\chi_\alpha^{(4)})$ with $0 \le \Re\beta \le 1$, $0 \le \Im\beta \le 10$ and $\alpha = 4/8$

$\Re\beta$	$\Im\beta$	α	$\mathcal{P}_2\mathcal{L}^{(4)}_{\beta,+1,\alpha}$ #+1	#-1	AP	$Z^{(4)}(\beta,\chi_\alpha^{(4)})$	p	N	DF	$\alpha' = \frac{\alpha}{8}$	O
0	0	4/8	(1)	(1)	1	-	160	50		0,1,2,3,4	
0	4.532360141827193809	4/8	1		1	-1E-41-1E-42I	160	50	S6	0,2,4	
0	9.064720283654387619	4/8	1		1	5E-41-9E-42I	192	70	S26	0,2,4	
1/4	7.067362570867346895	4/8	1		1	4E-47-1E-47I	192	70	S3	0,2,4	
1/4	10.511019819385777488	4/8	1		1	-1E-43-4E-43I	192	70	S46		
1/2	0	4/8		(1)	-1	-	160	50		0,2,3,4	
1/2	2.425056827091418202	4/8	1		1	-5E-47-1E-47I	160	50	S29	2,4	2
1/2	3.249976963537702231	4/8		1	1	9E-48-1E-46I	160	50	S5	2,4	E
1/2	3.703307801219027665	4/8		1	1	-1E-41-1E-41I	160	50	S4-2	0,2,4	E
1/2	4.368019540226407989	4/8	1		1	8E-46-1E-45I	160	50	S8	2,4	2
1/2	4.646591642961023179	4/8		1	1	5E-45+1E-45I	160	50	S9	2,4	E
1/2	4.947831677133491175	4/8	1		1	9E-42-2E-41I	160	50	S2	2,4	2
1/2	5.417334806844678385	4/8		1	1	1E-44-8E-45I	160	50	S10	0,2,4	E
1/2	5.628120929419301028	4/8		1	1	1E-43+3E-44I	160	50	S12	2,4	E
1/2	5.879354157758599655	4/8	1		1	1E-44+1E-43I	160	50	S7	0,2,4	4
1/2	6.223180825323977644	4/8	1		1	1E-42+5E-42I	192	70	S41	2,4	2
1/2	6.325314061989612026	4/8	1		1	9E-44-1E-43I	160	50	S14	2,4	2
1/2	6.587692853147737071	4/8		1	1	3E-43-1E-43I	160	50	S13	2,4	E
1/2	6.620422873842281516	4/8		1	1	7E-45+9E-44I	160	50	S15	0,2,4	E
1/2	7.220871975958052161	4/8		1	1	8E-44-6E-44I	160	50	S18	0,2,4	E
1/2	7.226569067061128031	4/8		1	1	-9E-44-1E-43I	160	50	S17	2,4	E
1/2	7.483018117505630832	4/8	1		1	1E-51+2E-51I	192	70	S16	2,4	2
1/2	7.696847806432627715	4/8		1	1	-4E-43+3E-42I	160	50	S20	2,4	E
1/2	7.744447737020311651	4/8	1		1	-4E-42+9E-42I	160	50	S19	2,4	2
1/2	8.042477591691655725	4/8	1		1	2E-41-3E-41I	160	50	S21	0,2,4	4
1/2	8.211711182480059028	4/8		1	1	3E-42+2E-41I	160	50	S22	2,4	E
1/2	8.273665889586095525	4/8		1	1	2E-51-1E-51I	192	70	S24	0,2,4	E
1/2	8.522503016884216497	4/8		1	1	-1E-41+8E-46I	160	50	S25	0,2,4	E
1/2	8.552880329050080905	4/8	1		1	-7E-51+6E-51I	192	70	S34	2,4	2
1/2	8.922876486991746892	4/8	1		1	5E-41+3E-41I	192	70	S11	0,2,4	4
1/2	9.001205809650663151	4/8	1		1	6E-51+4E-51I	192	70	S23	2,4	2
1/2	9.013228492064441121	4/8		1	1	1E-43+2E-44I	192	70	S28	2,4	E
1/2	9.196526852556367326	4/8	1		1	-4E-47+9E-48I	192	70	S42	2,4	2
1/2	9.470083134201299174	4/8		1	1	4E-43-4E-43I	192	70	S30	2,4	E
1/2	9.533695261353557555	4/8		1	1	6E-44-4E-44I	192	70	S31	0,2,4	E
1/2	9.810018121325218118	4/8	1		1	-1E-49+2E-49I	192	70	S33	2,4	2
1/2	9.859896162238453467	4/8	1		1	1E-42+5E-43I	192	70	S43	0,2,4	4
1/2	9.903977703803958939	4/8		1	1	7E-50+1E-49I	192	70	S32	2,4	E
1/2	9.934919959369116830	4/8		1	1	-3E-50+8E-50I	192	70	S35	0,2,4	E
1/2	10.261814252511740214	4/8	1		1	-2E-48-2E-48I	192	70	S38		2
1/2	10.265915116762014474	4/8		1	1	7E-49-7E-49I	192	70	S36		E
1/2	10.538808057912809353	4/8	1		1	-2E-47+7E-48I	192	70	S39		2
1/2	10.681798843078321027	4/8		1	1	4E-48-1E-48I	192	70	S40		E
1/2	10.712706900697770951	4/8		1	1	-4E-49+6E-50I	192	70	S44		E
1/2	10.764710683186371974	4/8		1	1	-1E-48+2E-48I	192	70	S45		E

Table D.6: The zeros and poles of $Z^{(8)}(\beta, \chi_\alpha^{(8)})$ with $\Re\beta = \frac{1}{2}$, $0 < \Im\beta \leq 10$ and $\alpha = 0$

$\Re\beta$	$\Im\beta$	α	$\mathcal{L}^{(8)}_{\beta,+1,\alpha}\mathcal{L}^{(8)}_{\beta,-1,\alpha}$ #+1	AP	$Z^{(8)}(\beta, \chi_\alpha^{(8)})$	p	N	DF	T	$\mathcal{P}_1\mathcal{L}^{(8)}_{\beta,+1,\alpha}$ #+1	#-1	$\mathcal{P}_2\mathcal{L}^{(8)}_{\beta,+1,\alpha}$ #+1	#-1
1/2	2.425056827091418202	0	1	1	2E-47+2E-48I	160	50	S4	L		1	1	
1/2	3.249976963537702230	0	1	1	4E-48-9E-47I	160	50	S2	L	1			1
1/2	3.703307801219027664	0	2	2	-4E-42-1E-42I	160	50	S5	L		2	1	1
1/2	4.368019540226407939	0	1	1	1E-45+1E-45I	160	50				1	1	
1/2	4.646591642961023079	0	1	1	5E-45-5E-45I	160	50			1			1
1/2	4.947831677133491433	0	1	1	-8E-45+3E-44I	160	50				1	1	
1/2	5.417334806844683869	0	3	3	-3E-41-3E-41I	160	50				3	1	2
1/2	5.628120929419300691	0	1	1	-1E-41+4E-42I	160	50			1			1
1/2	5.879354157758601464	0	2	2	3E-45-2E-45I	160	50			2		1	1
1/2	6.223180825323988997	0	1	1	-2E-43+1E-43I	160	50				1	1	
1/2	6.325314061989568234	0	1	1	-4E-43-1E-42I	160	50				1	1	
1/2	6.587692853147743397	0	1	1	6E-44+2E-44I	160	50			1			1
1/2	6.620422873842205998	0	2	2	6E-41+1E-41I	160	50				2	1	1
1/2	7.220871975958052161	0	3	3	-1E-44+2E-44I	160	50				3	1	2
1/2	7.226569067062127488	0	1	1	-4E-47-2E-47I	160	50			1			1
1/2	7.483018117502053659	0	1	1	2E-41-2E-41I	160	50				1	1	
1/2	7.696847806428616516	0	1	1	-1E-41-4E-41I	160	50			1			1
1/2	7.744447737022791325	0	1	1	3E-41+3E-42I	160	50				1	1	
1/2	8.042477591691083118	0	2	2	3E-42-2E-42I	160	50			2		1	1
1/2	8.211711182462191568	0	1	1	-1E-41+8E-43I	160	50			1			1
1/2	8.273665889562946076	0	3	3	3E-43-3E-43I	160	50				3	1	2
1/2	8.522503016842951638	0	2	2	1E-49+1E-49I	160	50				2	1	1
1/2	8.552880329020826542	0	1	1	4E-41-8E-41I	160	50				1	1	
1/2	8.922876486797633648	0	3	3	6E-44-8E-43I	160	50			3		2	1
1/2	9.001205809359216576	0	1	1	1E-41+1E-41I	160	50				1	1	
1/2	9.013228492093346810	0	1	1	7E-41+5E-41I	160	50			1			1
1/2	9.196526852228834921	0	1	1	1E-48-1E-50I	192	50				1	1	
1/2	9.470083134796074504	0	1	1	1E-49+8E-50I	192	50			1			1
1/2	9.533695260321753372	0	4	4	-3E-46-9E-47I	192	50				4	1	3
1/2	9.810018119330442828	0	1	1	6E-49-2E-48I	192	50				1	1	
1/2	9.859896160679748741	0	2	2	-1E-51-1E-51I	192	50			2		1	1
1/2	9.903977702401437611	0	1	1	4E-50-3E-50I	192	50			1			1
1/2	9.934919958350126398	0	2	2	-2E-41+3E-41I	192	50				2	1	1

Table D.7: The zeros and poles of $Z^{(8)}(\beta,\chi_\alpha^{(8)})$ with $\Re\beta = \frac{1}{2}$, $0 < \Im\beta \leq 10$ and $\alpha = 1/2$

$\Re\beta$	$\Im\beta$	α	$\mathcal{L}^{(8)}_{\beta,+1,\alpha}\mathcal{L}^{(8)}_{\beta,-1,\alpha}$ #+1	AP	$Z^{(8)}(\beta,\chi_\alpha^{(8)})$	p	N	DF	O
1/2	1.782213978191369112	1/2	1	1	2E-47-1E-47I	160	50	S1	2
1/2	2.946441970575437918	1/2	2	2	5E-46+5E-47I	160	50	S3,4	2,2
1/2	3.564427956382738234	1/2	1	1	2E-42-1E-42I	160	50	S2	4
1/2	3.879328713546061546	1/2	2	2	1E-42+3E-43I	160	50	S5,6	2,2
1/2	4.527220808156573476	1/2	2	2	6E-47+4E-47I	160	50	S7,8	2,2
1/2	4.590429629234487105	1/2	2	2	1E-41-4E-41I	160	50		
1/2	5.126324398828679789	1/2	2	2	3E-50-2E-49I	160	50		
1/2	5.346641934574103869	1/2	1	1	-6E-44-4E-44I	160	50		
1/2	5.462015080446355425	1/2	2	2	2E-52+9E-53I	160	50		
1/2	5.991432640140644578	1/2	2	2	-1E-51+1E-51I	160	50		
1/2	6.078238108570872078	1/2	2	2	4E-42-1E-41I	160	50		
1/2	6.391958602015716352	1/2	2	2	3E-41-6E-41I	160	50		
1/2	6.698857003565354647	1/2	2	2	1E-53+3E-53I	160	50		
1/2	6.870505381182101533	1/2	2	2	2E-53+6E-55I	160	50		
1/2	6.992646678257876321	1/2	2	2	1E-52-4E-52I	160	50		
1/2	7.128855912768139413	1/2	1	1	2E-41+2E-41I	160	50		
1/2	7.360734345217754475	1/2	2	2	8E-50-4E-49I	160	50		
1/2	7.542485324107354997	1/2	2	2	4E-42-2E-43I	160	50		
1/2	7.794134053287582310	1/2	2	2	2E-53+2E-52I	160	50		
1/2	7.819671962803166441	1/2	2	2	7E-49+2E-49I	160	50		
1/2	8.141853572890553020	1/2	2	2	2E-49-6E-50I	160	50		
1/2	8.312638564690151364	1/2	2	2	-1E-49-4E-50I	160	50		
1/2	8.447199030245365380	1/2	2	2	2E-44-4E-45I	160	50		
1/2	8.479324427813371146	1/2	2	2	-1E-50+5E-52I	160	50		
1/2	8.911069890387360163	1/2	1	1	-4E-51+4E-50I	192	50		
1/2	8.939925305978208869	1/2	2	2	1E-56+7E-57I	192	50		
1/2	8.997747473537935196	1/2	2	2	-9E-58+6E-58I	192	50		
1/2	9.090290630326135029	1/2	2	2	3E-45+6E-45I	192	50		
1/2	9.252661337774319740	1/2	2	2	-1E-46+8E-47I	192	50		
1/2	9.521284416180150564	1/2	2	2	4E-48-1E-47I	192	50		
1/2	9.682096277480911098	1/2	2	2	-5E-42-7E-41I	192	50		
1/2	9.684932578054138307	1/2	2	2	4E-59+1E-59I	192	50		
1/2	9.801070123030508742	1/2	2	2	-5E-55-3E-55I	192	50		

Bibliography

[AF84] R. Adler and L. Flatto, *Cross section map for the geodesic flow on the modular surface*, Contemporary Math. **26** (1984), 9–24.

[AF03] M. Ablowitz and A. Fokas, *Complex variables*, Cambridge University Press, 2003.

[AL70] A. O. L. Atkin and J. Lehner, *Hecke operators on* $\Gamma_0(m)$, Math. Ann. **185** (1970), no. 2, 134–160.

[Art24] E. Artin, *Ein mechanisches System mit quasi-ergodischen Bahnen*, Abh. Math. Sem. d. Hamburgischen Universität **3** (1924), 170–175, (also in Collected Papers, Addison-Wesley, (1965), 499-501).

[AS64] M. Abramowitz and I. Stegun, *Handbook of Mathematical Functions*, Dover, 1964.

[Ave07] H. Avelin, *Deformation of* $\Gamma_0(5)$*-cusp forms*, Math. Comp. **76** (2007), 361–384.

[Bal00] V. Baladi, *Positive transfer operators and decay of correlations*, World Scientific, 2000.

[Ban32] S. Banach, *Théorie des opérations linéaires*, Ed. S. Banach, B. Knaster, K. Kuratowski, S. Mazurkiewicz, W. Sierpiński i H. Steinhaus, Monografie Matematyczne, vol. 1, Instytut Matematyczny Polskiej Akademi Nauk, 1932.

[BBM02] K. Braman, R. Byers, and R. Mathias, *The multishift qr algorithm. part i and ii: Maintaining well-focused shifts and level 3 performance and aggressive early deflation*, SIAM J. MATRIX ANAL. APPL. **23** (2002), no. 4, 929–973.

[BDKM02] D. Bindel, J. Demmel, W. Kahan, and O. Marques, *On Computing Givens Rotations Reliably and Efficiently*, ACM Transactions on Mathematical Software **28** (2002), 206–238.

[BFM12] R. Bruggeman, M. Fraczek, and D. Mayer, *Perturbation of zeros of the Selberg zeta-function for* $\Gamma_0(4)$, preprint, arXiv:1201.2324v1 (2012).

[BH99] V. Baladi and M. Holschneider, *Approximation of nonessential spectrum of transfer operators*, Nonlinearity **12** (1999), 525–538.

[BJ08] O. Bandtlow and O. Jenkinson, *Explicit eigenvalue estimates for transfer operators acting on spaces of holomorphic functions*, Advances in Mathematics **218** (2008), 902–925.

[Bow73] R. Bowen, *Symbolic Dynamics for Hyperbolic Flows*, American Journal of Mathematics **95** (1973), no. 2, 429–460.

[Bow08] ———, *Equilibrium States and the Ergodic Theory of Anosov Diffeomorphisms, Second Edition*, Ed. J. Chazottes, Springer-Verlag, 2008.

[Bru94] R. Bruggeman, *Families of Automorphic Forms*, Birkhäuser, 1994.

[BS79] R. Bowen and C. Series, *Markov maps associated with Fuchsian groups*, Publications Mathématiques de L'IHÉS **50** (1979), no. 1, 153–170.

[Bum98] D. Bump, *Automorphic Forms and Representations*, Cambridge University Press, 1998.

[Car92] P. Cartier, *An Introduction to Zeta Functions*, ch. 1, Springer-Verlag, 1992, in From Number Theroy to Phyiscs, Eds.: M. Waldschmidt and P. Moussa and J.-M. Luck and C. Itzykson.

[Cha99] C.-H. Chang, *Die Transferoperator-Methode für Quantenchaos auf den Modulflächen* $\Gamma \setminus \mathbb{H}$, Ph.D. thesis, 1999, Papierflieger, Clausthal-Zellerfeld.

[CM99] C.-H. Chang and D. Mayer, *The Transfer Operator approach to Selberg's zeta function and modular and Maass wave forms for* $\mathrm{PSL}(2,\mathbb{Z})$, pp. 72–142, Springer-Verlag, 1999, in Emerging applications of number theory, Eds.: D. Hejhal, M. Gutzwiller, et al.

[CM01] ———, *An Extension of the Thermodynamic Formalism Approach to Selberg's Zeta Function for General Modular Groups*, pp. 523–562, Springer-Verlag, 2001, in Ergodic Theory, Analysis, and Efficient Simulation of Dynamical Systems, Eds.: B. Fiedler.

[CS99] B. Carl and C. Schiebold, *Nonlinear equations in soliton physics and operator ideals*, Nonlinearity **12** (1999), no. 2, 333–364.

[Dev03] R. Devaney, *An Introduction To Chaotic Dynamical Systems, Second Edition*, Westview Pres, 2003.

[DGLR94] B. Diu, C. Guthmann, D. Lederer, and B. Roulet, *Grundlagen der Statistischen Physik*, de Gruyter, 1994.

[DIPS85] J. Deshouillers, H. Iwaniec, R. Phillips, and P. Sarnak, *Maass cusp forms*, Proc. Natl. Acad. Sci. USA **82** (1985), 3533–3534.

[Efr93] I. Efrat, *Dynamics of the continued fraction map and the spectral theory of* $\mathrm{SL}(2,\mathbb{Z})$, Inventiones math. **114** (1993), 207–218.

[EH70] C.J. Earle and R.S. Hamilton, *A fixed point theorem for holomorphic mappings*, vol. 16, pp. 61–65, Proc. Symp. Pure Math., Amer. Math. Soc., Providence, R.I., 1970, in Global Analysis.

[ER85] J. Eckmann and D. Ruelle, *Ergodic theory of chaos and strange attractors*, Rev. Mod. Phys. **57** (1985), 617–656.

[Erd53] A. Erdelyi, *Higher transcendental functions*, vol. 1, McGraw-Hill, 1953.

[FL05] D. Farmer and S. Lemurell, *Deformations of Maass forms*, Math. Comp. **74** (2005), no. 252, 1967–1982.

[FM11] M. Fraczek and D. Mayer, *Symmetries of the transfer operator for* $\Gamma_0(n)$ *and a character deformation of the Selberg zeta function for* $\Gamma_0(4)$, preprint, arXiv:1011.4441v3 (2011).

[FMM07] M. Fraczek, D. Mayer, and T. Mühlenbruch, *A realization of the Hecke algebra on the space of period functions for* $\Gamma_0(n)$, J. reine angew. Math. **603** (2007), 133–163.

[Fra05] M. Fraczek, *Transfer Operatoren*, Clausthal University, 2005.

[Fra06] ———, *Spezielle Eigenfunktionen des Transfer-Operators für Hecke Kongruenz Untergruppen*, Diploma Thesis, Clausthal University, 2006.

[Fr61] J. Francis, *The QR Transformation A Unitary Analogue to the LR Transformation Part 1*, The Computer Journal **4** (1961), no. 3, 265–271.

[Fr62] ———, *The QR Transformation Part 2*, The Computer Journal **4** (1962), no. 4, 332–345.

[Fri86] D. Fried, *The zeta functions of Ruelle and Selberg*, Ann. Sci. Ec. Norm. Sup. **19** (1986), 491–517.

[Fri96] ———, *Symbolic dynamics for triangle groups*, Invent. Math. **125** (1996), 487–521.

[Giv58] W. Givens, *Computation of Plane Unitary Rotations Transforming a General Matrix to Triangular Form*, Journal of the Society for Industrial and Applied Mathematics **6** (1958), no. 1, 26–50.

[GL96] G. Golub and C. Van Loan, *Matrix computations*, Johns Hopkins University Press, 1996.

[GLZ04] L. Guillope, K. Lin, and M. Zworski, *The Selberg zeta function for convex co-compact Schottky groups*, Comm. Math. Phys. **245** (2004), no. 1, 149–175.

[Gro52] A. Grothendieck, *Résumé des résultats essentiels dans la théorie des produits tensoriels topologiques et des espaces nucléaires*, Annales de l'institut Fourier **4** (1952), 73–143.

[Gro55] ———, *Produits tensoriels topologiques et espaces nucléaires*, Mem. Am. Math. Soc. **16** (1955).

[Gro56] ———, *La théorie de Fredholm*, Math. France **84** (1956), 319–384.

[GS97] D. Gottlieb and C. Shu, *On the gibbs phenomenon and its resolution*, SIAM Review **39** (1997), no. 4, 644–668.

[Had98] J. Hadamard, *Les surfaces à courbures opposées et leurs lignes géodésique*, J. Math. Pures Appl. **4** (1898), 27–73.

[Hej76] D. Hejhal, *The Selberg trace formula for* PSL$(2,\mathbb{R})$*, Volume 1*, Springer-Verlag, 1976.

[Hej83] ———, *The Selberg trace formula for* PSL$(2,\mathbb{R})$*, Volume 2*, Springer-Verlag, 1983.

[Hej92] ———, *Eigenvalues of the Laplacian for Hecke triangle groups*, Mem. Amer. Math. Soc. **97** (1992), no. 496.

[Hej08] ———, *Selberg zeta function*, 2008, Personal Communication.

[HM04] J. Hilgert and D. Mayer, *The dynamical zeta function and transfer operator for the Kac-Baker model*, Contemporary Mathematics **364** (2004), 67–92.

[HMM05] J. Hilgert, D. Mayer, and H. Movasati, *Transfer operators for* $\Gamma_0(n)$ *and the Hecke operators for period functions of* PSL$(2,\mathbb{Z})$, Math. Proc. Camb. Phil. Soc. **139** (2005), 81–116.

[Hov50] L. Van Hove, *Sur L'intégrale de Configuration Pour Les Systèmes De Particules À Une Dimension*, Physica **16** (1950), no. 2, 137–143.

[Hur82] A. Hurwitz, *Einige Eigenschaften der Dirichlet'schen Funktionen* $F(s) = \sum \frac{D}{n} \cdot \frac{1}{n^s}$*, die bei der Bestimmung der Klassenanzahlen Binärer quadratischer Formen auftreten*, Z. für Math. und Physik **27** (1882), 86–101.

[Hux84] M. Huxley, *Scattering Matrices for Congruence Subgroups*, Modular Forms (1984), 141–156.

[Isi25] E. Ising, *Beitrag zur Theorie des Ferromagnetismus*, Zeitschrift für Physik A Hadrons and Nuclei **31** (1925), no. 1, 253–258.

[Iwa02] H. Iwaniec, *Spectral Methods of Automorphic Forms*, American Mathematical Society, 2002.

[Jud95] C. Judge, *On the existence of maass cusp forms on hyperbolic surfaces with cone points*, Journal of the American Mathematical Society **8** (1995), no. 3, 715–759.

[Kac59] M. Kac, *On the partition function of a one-dimensinal lattice gas*, Phys. Fluids **2** (1959), 8–12.

[Kac66] ———, *The mathematical mechanism of phase transitions*, pp. 245–305, Gordon & Breach, New York, 1966, in Brandeis University Summer Institute in Theoretical Physics, vol. 1, Eds.: H. Chretien et al.

[Kam75] H. Kamowitz, *The spectra of composition operators on H^p*, Journal of Functional Analysis **18** (1975), no. 2, 132–150.

[Kat80] T. Kato, *Perturbation Theory for Linear Operators*, Springer, 1980.

[Kön80] H. König, *s-numbers, eigenvalues and the trace theorem in Banach spaces*, Studia Math. **67** (1980), 157–172.

[Len20] W. Lenz, *Beitrag zum Verständnis der magnetischen Eigenschaften in festen Körpern*, Physikalische Zeitschrift **21** (1920), 613–615.

[Ler87] M. Lerch, *Note sur la fonction $K(w, x, s) = \sum_{n\geq 1} \exp\{2\pi inx\}(n+w)^{-s}$*, Acta Math. **11** (1887), 19–24.

[Lid59] V.B. Lidskii, *Non-self-adjoint operators with a trace*, Dokl. Akad. Nauk SSSR **125** (1959), 485–488.

[LM66] E. Lieb and D. Mattis, *Mathematical Physics in One Dimension: Exactly Soluble Models of Interacting Particles (Perspectives in Physics : a Series of Reprint Collections)*, Academic Press, 1966.

[LM94] A. Lasota and M. Mackey, *Chaos, fractals, and noise: Stochastic aspects of dynamics*, Springer, 1994.

[LZ01] J. Lewis and D. Zagier, *Period functions for Maass wave forms, I*, Ann. Math. **153** (2001), 191–258.

[May76] D. Mayer, *On a ζ function related to the continued fraction transformation*, Bulletin de la S.M.F. **104** (1976), 195–203.

[May80a] ———, *On composition operators on Banach spaces of holomorphic functions* , Journal of Functional Analysis **35** (1980), no. 2, 191–206.

[May80b] ———, *The Ruelle-Araki transfer operator in classical statistical mechanics*, Lect. Notes in Physics, Springer Verlag, Berlin **123** (1980).

[May90] ———, *On the thermodynamic formalism for the gauss map*, Commun. Math. Phys. **130** (1990), no. 2, 311–333.

[May91a] ———, *Continued fractions and related transformations*, ch. 7, pp. 175–222, Oxford University Press, 1991, in Ergodic theory, symbolic dynamics and hyperbolic spaces, Eds.: T. Bedford et al.

[May91b] ———, *The thermodynamic formalism approach to Selberg's zeta function for* $\mathrm{PSL}(2,\mathbb{Z})$, Bull. Amer. Math. Soc. (N.S.) **25** (1991), no. 1, 55–60.

[May11] ———, *A factorization of the Selberg zeta function for* $\Gamma_0(8)$, 2011, Personal Communication.

[Miy06] T. Miyake, *Modular Forms*, Springer Monographs in Mathematics, 2006.

[MM02] Yu. Manin and M. Marcolli, *Continued fractions, modular symbols and non commutative geometry*, Selecta Math. (N.S.) **8** (2002), 475–520.

[MMS11] D. Mayer, T. Mühlenbruch, and F. Strömberg, *The transfer operator for the Hecke triangle groups*, Proceedings of International Conference Dynamical Systems II, Denton, UNT 2009, To appear in Discrete and Continuous Dynamical Systems (2011).

[Mor97] T. Morita, *Markov systems and transfer operators associated with cofinite fuchsian groups*, Ergodic Theory and Dynamical Systems **17** (1997), no. 5, 1147–1181.

[MPF09] *GNU MPFR, The Multiple Precision Floating-Point Reliable Library*, 2.4.1 ed., 2009.

[MR87] D. Mayer and G. Roepstorff, *On the relaxation time of Gauss's continued-fraction map I. The Hilbert space approach (Koopmanism)*, Journal of Statistical Physics **47** (1987), no. 1–2, 149–171.

[MS91] C. Matthies and F. Steiner, *Selberg's ζ function and the quantization of chaos*, Phys. Rev. A **44** (1991), no. 12.

[MS08] D. Mayer and F. Strömberg, *Symbolic dynamics for the geodesic flow on Hecke surfaces*, Journal of Modern Dynamics **2** (2008), no. 4, 581–627.

[Müh03] T. Mühlenbruch, *Hecke operators on period functions for the full modular group*, Ph.D. thesis, 2003, Cuvillier Verlag, Germany.

[Müh06] ———, *Hecke operators on period functions for* $\Gamma_0(n)$, J. Number Th. **118** (2006), 208–235.

[Ons44] L. Onsager, *Crystal Statistics. I. A Two-Dimensional Model with an Order-Disorder Transition*, Phys. Rev. **65** (1944), 117–149.

[Pie86] A. Pietsch, *Eigenvalues and s-numbers*, Cambridge University Press, 1986.

[Pie91] ———, *Approximation numbers of nuclear operators and geometry of Banach spaces*, Arch. Math. **57** (1991), no. 2, 155–168.

[Pol91] M. Pollicott, *Some applications of thermodynamic formalism to manifolds with constant negative curvature*, Advances in mathematics **85** (1991), no. 2, 161–192.

[PR10] Y. Petridis and M. Risager, *Dissolving cusp forms: Higher order Fermi's Golden Rules*, preprint, arXiv:1003.2820 (2010).

[PS85] R. Phillips and P. Sarnak, *On cusp forms for co-finite subgroups of* $\mathrm{PSL}(2,\mathbb{Z})$, Invent. Math. **80** (1985), 339–364.

[PS91] ———, *The spectrum of fermat curves*, Geometric and Functional Analysis **1** (1991), 80–146.

[PS94] ———, *Cusp forms for character varieties*, Geom. Funct. Anal. **4** (1994), 93–118.

[Pug04] G. Pugh, *An analysis of the Lanczos gamma approximation*, Ph.D. thesis, University of British Columbia, 2004.

[Rue76a] D. Ruelle, *Generalized zeta-functions for Axiom A basic sets*, Bulletin of the American Mathematical Society **82** (1976), no. 1, 153–156.

[Rue76b] ———, *Zeta-functions for expanding maps and Anosov flows*, Inventiones Mathematicae **34** (1976), no. 3, 231–242.

[Rue04] ———, *Thermodynamic Formalism: The Mathematical Structures of Equilibrium Statistical Mechanics, Second Edition*, Cambridge University Press, 2004.

[Rus51] A. F. Ruston, *On the Fredholm Theory of Integral Equations for Operators Belonging to the Trace Class of a General Banach Space*, Proc. London Math. Soc. **2** (1951), no. 2, 109–124.

[Sch97] H. Schwarz, *Numerische Mathematik*, B.G. Teubner Stuttgart, 1997.

[Sel56] A. Selberg, *Harmonic analysis and discontinuous groups in weakly symmetric Riemannian spaces with applications to Dirichlet series*, J. Indian Math. Soc. **20** (1956), 47–87.

[Sel89] ———, *Atle Selberg Collected Papers*, vol. 1, ch. Harmonic analysis (Göttingen lectures), 1954, pp. 626–674, Springer, 1989.

[Sel90] ———, *Remarks on the distribution of poles of Eisenstein series*, Festschrift in honor of I.I. Piatetski-Shapiro, vol. 2, 1990, (also in Collected Papers, vol. 2, Springer, (1991), 15-45), pp. 251–278.

[Ser85] C. Series, *The modular surface and continued fractions*, J. London Math. Soc. (2) **31** (1985), 69–80.

[Sin77] Y. Sinai, *Introduction to ergodic theory*, Princeton Univ. Press, 1977.

[Sma67] S. Smale, *Differentiable dynamical systems*, Bull. Amer. Math. Soc. **73** (1967), no. 6, 747–817.

[Str04] F. Strömberg, *Computational aspects of maass waveforms*, Ph.D. thesis, Uppsala University, 2004.

[Str07] ———, *Notes on Hurwitz zeta function*, 2007, Personal Communication.

[Str08] ———, *Computation of Selberg Zeta Functions on Hecke Triangle Groups* , preprint, arXiv:0804.4837v1 (2008).

[Str09a] ———, *Approximate transfer operator using chebyshev polynomials*, 2009, Personal Communication.

[Str09b] ———, *List of all eigenvalues* $\lambda = \frac{1}{4} + R^2$ *of the hyperbolic Laplacian for* $\Gamma_0(n)$ *for* $R \leq 10$ *and* $1 \leq n \leq 30$, 2009, Personal Communication.

[Tem94] N. M. Temme, *Computational aspects of incomplete gamma functions with large complex parameters*, Proceedings of the conference on Approximation and computation : a Festschrift in honor of Walter Gautschi (Cambridge, MA, USA), Birkhauser Boston Inc., 1994, pp. 551–562.

[Wat08] D. Watkins, *The QR Algorithm Revisited*, SIAM Review **50** (2008), no. 1, 133–145.

[Whi96] M. White, *Analytic multivalued functions and spectral trace*, Mathematische Annalen **304** (1996), no. 1, 669–683.

[Win88] A. Winkler, *Cusp forms and Hecke groups*, Journal für die reine und angewandte Mathematik (Crelles Journal) (1988), no. 386, 187–204.

[Win03] S. Winitzki, *Computing the incomplete Gamma function to arbitrary precision*, LNCS **2667** (2003).

[Wol94] S. Wolpert, *Disappearance of cusp forms in special families*, Annals of Mathematics **139** (1994), no. 2, 239–291.

Index of Notations

$M^\dagger$	the conjugate transposition of matrix M
$M_{i,j}$	entry i, j of matrix M
$M_{i:j,k:l}$	submatrix of matrix M, rows i to j and columns k to l of matrix M
$[x]$	the integer part of x
$\bar{z}$	complex conjugation of z
$\bigsqcup_{i\in I} S_i$	a disjoint union of S_i's
$\emptyset$	a empty set
$\|\|f\|\|$	the norm of f
$f\|_s g$	the slash action of g on f with weight s, page 69
$\|s\|$	the absolute value of s
$\mathcal{A}^{(n)}_{\beta,\pm 1,\chi,N}$	part of an analytic continuation of the transfer operator $\mathcal{L}^{(n)}_{\beta,\varepsilon,\chi}$, page 72
$\arg(s)$	the argument of s
$B(D)$	the Banach space of holomorphic and continuous functions on the disk D
B_j	the Bernoulli numbers, page 18
$\mathbb{C}$	the set of complex numbers, page 9
$\chi(\gamma)$	the character of γ, page 54
$\bar{D}$	the closure of D
$\delta_{i,j}$	$\delta_{i,j} = 1$ if $i = j$ and $\delta_{i,j} = 0$ if $i \neq j$
$\det(M)$	the determinant of M

$\mathrm{diag}(a_1, \ldots, a_n)$	diagonal matrix with entries a_i
D	the disk in $\mathbb{C}$ with center at 1 and radius smaller $3/2$
D_R	the disk in $\mathbb{C}$ with center at 0 and radius larger $\lambda/(1-\lambda)$
$\delta_\Gamma(g)$	the characteristic function, page 65
F_Γ	a fundamental domain of Γ
$\Gamma(s,z)$	the upper incomplete gamma function of s and z, page 13
$\gamma(s,z)$	the lower incomplete gamma function of s and z, page 13
$\Gamma(s)$	the gamma function of s, page 13
$\Gamma_0(n)$	the Hecke congruence subgroup
h	the number of cusps of F_Γ
h_0	the number of open cusps of F_Γ
I	identity matrix
$\Im s$	the imaginary part of s
$\mathrm{int}\, S$	the interior of set S
κ_i	a cuspidal point of F_Γ
$\tilde{\mathcal{L}}_\beta$	the transfer operator $(0, \mathcal{L}_{\beta,+}; \mathcal{L}_{\beta,-}, 0)$ for finite index subgroups of $\mathrm{SL}(2,\mathbb{Z})$, page 64
$\mathcal{L}_A$	the transfer operator, page 60
$\mathcal{L}_{\beta,\lambda}$	the transfer operator for the Kac-Baker model, page 159
$\mathcal{L}_{\beta,\pm 1}$	the transfer operator for finite index subgroups of $\mathrm{SL}(2,\mathbb{Z})$, page 64
$\mathcal{L}^{(n)}_{\beta,\pm 1,\chi}$	the transfer operator for $\Gamma_0(n) \subset \mathrm{SL}(2,\mathbb{Z})$ with character χ, page 69
$\mathcal{M}_{\beta,\lambda}$	the matrix which approximates the transfer operator for the Kac-Baker model, page 161
$\mathcal{M}^{(n)}_{\beta,\varepsilon,\chi}$	the matrix which approximates the transfer operator for $\Gamma_0(n)$, page 81
μ_n	the index of $\Gamma_0(n)$ in $\mathrm{SL}(2,\mathbb{Z})$

$\mathcal{N}^{(n)}_{\beta,\pm1,\chi,N}$ part of an analytic continuation of the transfer operator $\mathcal{L}^{(n)}_{\beta,\varepsilon,\chi}$, page 72

$\psi^{(n)}_i$ the path of a zero of $Z^{(n)}(\beta,\chi^{(n)}_\alpha)$ in the β-plane parametrized by α, page 115

$\psi^{(4)}_{i,\pm1}$ the path of a zero of $Z^{(4)}(\beta,\chi^{(4)}_\alpha)$ related to the eigenvalue $+1$ respectively -1 of the transfer operator $\mathcal{P}_2\mathcal{L}^{(4)}_{\beta,\varepsilon,\alpha}$ in the β-plane parametrized by α, page 115

$\Phi(\alpha, s, z)$ the Lerch transcendent of α, s and z, page 24

$\mathcal{P}_k$ symmetries of the transfer operator $\mathcal{L}^{(n)}_{\beta,\pm1,\chi}$, page 92

$\varphi(\beta,\chi)$ the determinant of the automorphic scattering matrix

$P(A)$ the topological pressure, page 60

$\mathbb{Q}$ the set of rational numbers

$\Re s$ the real part of s

r^Γ_i the right coset representatives of Γ in $\mathrm{SL}(2,\mathbb{Z})$

$r^{(n)}_i$ the right coset representatives of $\Gamma_0(n)$ in $\mathrm{SL}(2,\mathbb{Z})$

$\mathbb{R}$ the set of real numbers

$\mathbb{R}_>$ the set of positive real numbers

$R(p,q,c,s)$ the Givens rotation matrix, page 37

$\sigma(M)$ the spectrum of M

$\mathrm{SL}(2,\mathbb{Z})$ the full modular group

$\sup_S(f)$ the supremum of f in S

$\mathrm{S}\,r$ the set of points (β_i,α_i) approximating points the curve $\mathcal{V}^{(n)}_x$, page 118

$\tilde{S}$ the matrix $(0,1;1,0)$

S the matrix $(0,-1;1,0)$

Θ the automorphic scattering matrix, page 50

$\mathrm{tr}\,(M)$ the trace of M

$\mathrm{tr}_\sigma\,(M)$ the spectral trace of M

T the matrix $(1,1;0,1)$

$T_G(x)$ the Gauss map, page 63

$U^{\chi}(g)$ the representation of g induced by χ, page 67

$U^{\Gamma}(g)$ the representation of g induced by δ_{Γ}, page 65

$\mathcal{V}_i^{(n)}$ the set of all points on the path $\psi_i^{(n)}$, page 115

$\mathcal{V}_{i,\pm 1}^{(4)}$ the set of all points on the path $\psi_{i,\pm 1}^{(4)}$, page 115

$\mathcal{W}^{(n)}$ the set of zeros of $Z^{(n)}(\beta, \chi_\alpha^{(n)})$ in the (β, α)-plane, page 115

$\mathcal{W}_{\pm 1}^{(4)}$ the set of zeros of $Z^{(4)}(\beta, \chi_\alpha^{(4)})$ in the (β, α)-plane related to the eigenvalue $+1$ respectively -1 of the transfer operator $\mathcal{P}_2 \mathcal{L}_{\beta,\varepsilon,\alpha}^{(4)}$, page 115

$Z^{(n)}(\beta, \chi)$ the Selberg zeta function for $\Gamma_0(n)$, page 51

$Z_{\mathcal{M}}^{(n)}(\beta, \chi)$ an approximation of the Selberg zeta function $Z^{(n)}$ for $\Gamma_0(n)$, page 110

$\mathcal{Z}_\alpha^{(n)}$ the set of zeros of $Z^{(n)}(\beta, \chi_\alpha^{(n)})$ in the β-plane for fixed α, page 110

$\mathcal{Z}_\chi^{(n)}$ the set of zeros of $Z^{(n)}(\beta, \chi)$ in the β-plane for fixed χ, page 110

$\mathcal{Z}_{\alpha,\pm 1}^{(4)}$ the set of zeros of $Z^{(4)}(\beta, \chi_\alpha^{(4)})$ in the β-plane for fixed α, related to the eigenvalue $+1$ respectively -1 of the transfer operator $\mathcal{P}_2 \mathcal{L}_{\beta,\varepsilon,\alpha}^{(4)}$, page 110

$\zeta(s, z)$ the Hurwitz zeta function of s and z, page 18

$\zeta_L(\lambda, s, z)$ the Lerch zeta function of λ, s and z, page 24

$\zeta_R(s)$ the Riemann zeta function of s, page 17

$\mathbb{Z}$ the set of integers

$\mathbb{Z}_<$ the set of negative integers

$\mathbb{Z}_\leq$ the set of non-positive integers

$\mathbb{Z}_>$ the set of positive integers

$\mathbb{Z}_\geq$ the set of non-negative integers

$Z(\beta, \chi)$ the Selberg zeta function, page 51

$Z_n(A)$ the generalized partitions functions for dynamical systems, page 60

$Z_R(z, A)$ the Ruelle zeta function, page 60